

# UC Berkeley

## UC Berkeley Electronic Theses and Dissertations

### Title

New Reactions and Synthetic Strategies toward Indolizidine Alkaloids and Pallavicinia Diterpenes

### Permalink

<https://escholarship.org/uc/item/2618703k>

### Author

Narayan, Alison Rae Hardin

### Publication Date

2011

Peer reviewed|Thesis/dissertation

New Reactions and Synthetic Strategies Toward Indolizidine Alkaloids and Pallavicinia  
Diterpenes

by

Alison Rae Hardin Narayan

A dissertation submitted in partial satisfaction of the

requirements for the degree of

Doctor of Philosophy

in

Chemistry

in the

GRADUATE DIVISION

of the

UNIVERSITY OF CALIFORNIA, BERKELEY

Committee in charge:

Professor Richmond Sarpong, Chair

Professor F. Dean Toste

Professor Mary Wildermuth

Spring 2011



## Abstract

New Reactions and Synthetic Strategies toward Indolizidine Alkaloids and Pallavicinia  
Diterpenes

by

Alison Rae Hardin Narayan

Doctor of Philosophy in Chemistry

University of California, Berkeley

Professor Richmond Sarpong, Chair

Strategies toward indolizidine alkaloids and pallavicinia diterpenes have been established. The first six chapters of this thesis are devoted to the development and execution of approaches toward *N*-fused bicycles and their application to the synthesis of indolizidine alkaloids. The final chapter details efforts toward the synthesis of pallavicinin and related diterpenes.

An overview of the indolizidine alkaloids is provided, including the major structural distinctions of the subclasses of these alkaloids as well as their known biological activity. This sets the stage for a discussion of our synthetic approach toward this class of natural products, aiming to build these molecules from indolizine and indolizinone precursors.

Several methods were developed to rapidly access indolizines and indolizinones. Specifically, the platinum-catalyzed cycloisomerization of propargylic esters to 2,3-disubstituted indolizines was realized. The nuances of the effect of the substrate's electronic properties on the reaction pathway were studied and this knowledge was utilized to develop a reaction selective for the formation of 2,3-disubstituted indolizines over the 1,3-disubstituted products. Subsequently, a metal-free version of a previously established metal-catalyzed cyclization was identified for the formation of 1,3-disubstituted indolizines and indolizinones.

With methods in place to form substituted indolizines and indolizinones, these bicycles were employed in the synthesis of indolizidine alkaloids. First, indolizine precursors were used to accomplish a five-step total synthesis of indolizidine 209D and a formal synthesis of securinine. Next, the innate reactivity of indolizinones was explored and applied to the synthesis of tricyclic marine alkaloids. From indolizinone building blocks, two routes were established to the tricyclic cylindricine core. The first approach toward the cylindricines featured a ring-opening/ring-closing metathesis to assemble the *cis*-6,6-ring fusion conserved throughout this family of natural products. The second approach toward the cylindricines employed a ring-contractive cyclization to form a tricyclic indolizinone, which served as a common intermediate to both the

cylindricine and the closely related lepadiformine alkaloids. The ring-contractive cyclization approach led to the synthesis of the cylindricine core in eight steps. Additionally, progress toward lepadiformine C from an intermediate accessed in the cylindricine synthesis has been achieved.

Finally, a strategy toward pallavicinin and related diterpenes has been tested. The approach features a gold-catalyzed cyclization to construct the [3.2.1]bicycle of pallavicinin and an Eschenmoser-Claisen rearrangement to form a key carbon-carbon bond. This strategy has been successful for the formation of the 8,9-*epi,epi*-pallavicinin tetracycle.

To Rishi, for all of  
his support and encouragement.

## Table of Contents

|   |    |
|---|----|
| Acknowledgments   | v  |
| <b><i>Chapter One: Indolizidine Alkaloids: Introduction and Approach</i></b>  |    |
| <hr/>   |    |
| 1.1 Introduction  | 1  |
| 1.2 Major Classes of Indolizidine Alkaloids   | 1  |
| 1.3 Approach toward indolizidine alkaloids from indolizines and indolizinones   | 6  |
| 1.4 References and Notes  | 8  |
| <br>  |    |
| <b><i>Chapter Two: Development of a Platinum-Catalyzed Cyclization of Propargylic Esters to 2,3-Disubstituted Indolizines</i></b> |    |
| <hr/>   |    |
| 2.1 Introduction  | 11 |
| 2.2 Substrate Synthesis   | 13 |
| 2.3 Reaction optimization   | 14 |
| 2.4 Substrate Scope   | 18 |
| 2.5 Mechanistic Questions   | 23 |
| 2.6 Future Directions   | 26 |
| 2.7 Experimental Contributions  | 26 |
| 2.8 Experimental Methods  | 26 |
| 2.9 References and Notes  | 47 |
| <br>  |    |
| <i>Appendix One: Spectra Relevant to Chapter Two</i>  | 48 |

***Chapter Three: Development of a Metal-Free Cyclization for the Formation of 1,3-Disubstituted Indolizines and Indolizinones***

---

|   |     |
|---|-----|
| 3.1 Introduction  | 97  |
| 3.2 Metal-Mediated Cyclizations   | 97  |
| 3.3 Considerations for a Metal-Free Cyclization   | 102 |
| 3.4 Metal-Free Cyclization to Form 1,3-disubstituted Indolizines                          | 103 |
| 3.5 Exploring the Effect of Solvent, Temperature, and pH                                  | 104 |
| 3.6 Substrate Scope of the Metal-Free Indolizine Forming Cyclization                      | 106 |
| 3.7 Mechanistic Insights  | 109 |
| 3.8 Extension to the Metal-Free Formation of Indolizinones                                | 109 |
| 3.9 Potential Mechanistic Pathways for Indolizinone Formation                             | 110 |
| 3.10 Similarities and differences between the metal-catalyzed and metal-free cyclizations | 111 |
| 3.11 Conclusions  | 112 |
| 3.12 Experimental Contributions   | 113 |
| 3.13 Experimental Methods   | 113 |
| 3.14 References and Notes   | 117 |
| <i>Appendix Two: Spectra Relevant to Chapter Three</i>                                    | 119 |

***Chapter Four: Synthetic Studies Toward Type I Indolizidine Alkaloids from Indolizines***

---

|  |     |
|--|-----|
| 4.1 Selection of targeted indolizidine alkaloids | 130 |
| 4.2 Synthesis of indolizidine alkaloid 209D      | 130 |
| 4.3 Securinine                                   | 134 |
| 4.4 Conclusions and Future Directions            | 149 |



|   |     |
|---|-----|
| 4.5 Experimental Contributions                          | 149 |
| 4.6 Experimental Methods                                | 150 |
| 4.7 References and Notes                                | 156 |
| <i>Appendix Three: Spectra Relevant to Chapter Four</i> | 159 |

***Chapter Five: The Chemistry of Indolizinones***

---

|  |     |
|--|-----|
| 5.1 Introduction                                       | 171 |
| 5.2 Indolizine Reactive Sites                          | 172 |
| 5.3 Bromination  | 173 |
| 5.4 Hydrogenation                                      | 175 |
| 5.5 Diels-Alder Cycloaddition                          | 177 |
| 5.6 Chemistry of the Vinylogous Amide                  | 183 |
| 5.7 Conclusions  | 186 |
| 5.8 Experimental Contributions                         | 187 |
| 5.9 Experimental Methods                               | 187 |
| 5.10 References and Notes                              | 201 |
| <i>Appendix Four: Spectra Relevant to Chapter Five</i> | 202 |

***Chapter Six: Synthetic Studies Toward Type II Indolizidine Alkaloids***

---

|   |     |
|---|-----|
| 6.1 Selection of Type II Indolizidine Targets                           | 230 |
| 6.2 Tricyclic Marine Alkaloids: The Cylindricines and Lepadiformines    | 230 |
| 6.3 Toward Cylindricine K   | 233 |
| 6.4 A Consolidated Approach Toward the Lepadiformines and Cylindricines |     |

|  |     |
|--|-----|
| via a Ring-Contractive Cyclization   | 246 |
| 6.5 Conclusions and Future Directions  | 256 |
| 6.6 Experimental Contributions   | 256 |
| 6.7 Experimental Methods   | 256 |
| 6.8 References and Notes   | 276 |
| <i>Appendix Five: Spectra Relevant to Chapter Six</i>                                  | 278 |
| <br>   |     |
| <b><i>Chapter 7. Synthetic Endeavors Toward Pallavicinia subciliata Diterpenes</i></b> |     |
| <hr/>  |     |
| 7.1 Introduction to the Pallavicinia subciliata Diterpenes                             | 312 |
| 7.2 Previous Synthetic Work Toward Pallavicinin and Neopallavicinin                    | 314 |
| 7.3 First-Generation Approach Toward Pallavicinin                                      | 317 |
| 7.4 Forward from Amide 7.66: Correcting the Stereochemistry at C-9                     | 324 |
| 7.5 Alternative Approaches Toward Pallavicinin   | 327 |
| 7.6 Toward 8,9-epi-epi-Pallavicinin  | 334 |
| 7.7 Conclusions and Future Directions  | 335 |
| 7.8 Experimental Contributions   | 336 |
| 7.9 Experimental Methods   | 336 |
| 7.10 References and Notes  | 354 |
| <i>Appendix Six: Spectra Relevant to Chapter Seven</i>                                 | 355 |

## Acknowledgments

My experience at Berkeley has been filled with individuals that have been generous with their time, knowledge and friendship. I can only begin to express my gratitude to my mentors, colleagues, friends and family.

I am grateful to my advisor, Professor Richmond Sarpong for welcoming me into his research group five years ago and providing me with the tools to develop as a chemist, teacher and leader. Richmond's work ethic and enthusiasm are contagious and have provided a rich environment for research and collaboration. He has taught me many lessons over the years beyond chemistry that I will carry with me for years to come. I must also acknowledge those who cultivated my interest in chemistry before arriving at Berkeley including Professor John P. Wolfe, my research advisor at the University of Michigan and Dr. Filisaty Vounatsos, my mentor at Amgen.

The students and post-doctoral researchers in the Sarpong group have created a place that I truly look forward to going to everyday. The first class of Sarpong students (Doctors Kimberly Larson, Eric Bunnelle, Andrew Marcus and Eric Simmons) invested their energy and time to build a solid group infrastructure from which I have greatly benefitted. I am also grateful to, Jesse Cortez, my classmate in the Sarpong group for being my compadre through classes, qualifying exams and the thesis writing process.

Everyday, I learn something from my labmates. They are some of the smartest, most hard working, and quirky people in my life. Dr. Eric Simmons and Dr. Laura Miller mentored me during my first years of graduate school. I do not know if I could have accomplished half as much (...or survived) without their guidance. Since their departure, I have been fortunate to share 844 Latimer with Jessica Kisunzu, Gary Gallego, and most recently Dr. Terry Lebold, all who continue to provide a lively and engaging research environment.

Other members of the Sarpong group, Scott West, Brian Pujanauski, Jessica Wood and Steve Heller have endured countless sessions of good idea/bad idea. I am thankful for their input and friendship.

During my five years at Berkeley, I have had the opportunity of work with several talented students on collaborative projects. Dr. Eric Simmons taught me the power of collaboration in our efforts together toward the cortistatin family of natural products. I am grateful to Steve Heller who has recently joined the efforts toward understanding the metal-free indolizinone formation and the synthesis indolizidine alkaloids. I had the privilege of working with two motivated undergraduate students, Vishal Vashistha and Michael Delong. Both Vishal and Michael are currently attending medical school, but the multi-gram quantities of pallavicinin intermediates remain in the Sarpong group and will most definitely be put to use by Dr. Andre Isaacs, a post doctoral research who has recently, enthusiastically continued the work toward pallavicinin.

Many individuals from the department have provided me with guidance and assistance. I am grateful to Professors Dean Toste, Bob Bergman, Chris Chang and Mary Wildermuth for serving on my qualifying exam and thesis committees. I have benefitted from the mentorship of Professor Bob Bergman, who always made time for research discussions and worked with me as the faculty sponsor for the Green Chemistry and Sustainable Design seminar series. I would also like to thank Rudi Nunlist and Dr. Chris Canlas for assistance in the NMR facility as well as Dr. Antonio Dipasquale for his enthusiasm and skill in X-ray crystallography.

I would like to acknowledge Dr. Eric Simmons, Jessica Wood, Steve Heller, and Dr. Terry Lebold for the time and effort they put into reading and providing feedback on thesis chapters. Additionally, I am also grateful to Dr. Pablo Garcia, Rebecca Murphy and Jessica Kisunzu for proofreading the experimental methods sections of this thesis. Their suggestions have greatly improved this document.

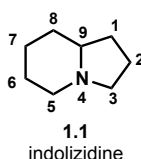
Finally, I would like to thank my friends and family for their unending support and encouragement. I am fortunate to have parents and siblings that have always nurtured my passions and served as my cheerleaders. I am grateful for the strong friendships I have developed while at Berkeley and the support system they have provided. Specifically, Kimberly Sogi and Ellen Sletten have played an important role in my graduate school life, and I will treasure the times we have enjoyed together on the 8<sup>th</sup> floor and at the RSF. Additionally, I would like to thank the book club girls for their friendship and perspectives as women in science. Most of all, I am eternally grateful to my husband, Rishi, for his unconditional support and encouragement throughout graduate school and also for supplying the Sarpong group with custom softball shirts.

## Chapter 1. Indolizidine Alkaloids: Introduction and Approach

### 1.1. Introduction

Indolizidine alkaloids are an extraordinarily large and diverse class of natural products. Thousands of compounds have been isolated from natural sources that contain the indolizidine core (**1.1**), which is a [4.3.0]bicycle with a nitrogen atom at one of the ring-fusion positions (Figure 1.1.1). The sheer number of compounds in this class has warranted the nearly annual publication of reviews focused on indolizidine alkaloids (1982-2008).<sup>1-23</sup> These manuscripts detail the isolation and structural characterization of new indolizidine alkaloids as well as synthetic efforts toward these natural products.

**Figure 1.1.1.** The indolizidine core and numbering.



The indolizidine alkaloids have been categorized into subgroups reflecting their structural diversity. The structural features of these molecules are often an important part of the narrative of the biological activity as well as the source of the compound. These facets of each sub-class are briefly discussed herein.

Ultimately, our interest in indolizidine alkaloids stems from our ability to rapidly access the nitrogen-containing 6,5-fused ring system in the form of an indolizine or an indolizinone, and the potential application of these *N*-heterocycles as building blocks in the total synthesis of indolizidine natural products. Our synthetic strategy toward this end is articulated in the final section of this chapter.

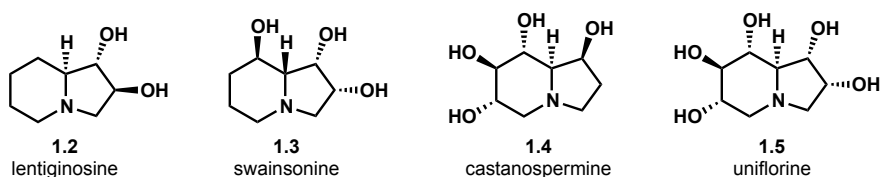
### 1.2. Major Classes of Indolizidine Alkaloids

#### *Hydroxylated indolizidine alkaloids:*

Polyhydroxylated indolizidine alkaloids are some of the most famous molecules in the indolizidine family due to their biological activity and the synthetic attention that they have attracted (Figure 1.2.1). These molecules were also among the first indolizidine alkaloids to be characterized, preceded only by salframine (**1.13**, Scheme 1.2.1), 5,8-dimethylindolizidine, and a handful of elaeocarpus alkaloids.<sup>24,25</sup> One of the most well-known polyhydroxylated indolizidine alkaloids, swainsonine (**1.3**) was isolated in the 1970's and gained attention for its adverse effects on livestock. During this time period, large numbers of cattle in North America, as well as in Australia, were found to exhibit the symptoms of mannosidosis, which is a neurological disease that afflicts both cattle and humans. Mannosidosis is a genetic deficiency of the lysosomal hydrolase  $\alpha$ -mannosidase that leads to build up of mannose-rich oligosaccharides in the lysosomes of cells.<sup>26</sup> This lysosomal accumulation subsequently causes organ dysfunction and various neurological problems. The root of this disease in the affected cattle herds was

ultimately traced back to their diet. Specifically, extracts of a plant native to Australia, commonly referred to as “poison peas,” were tested in an assay for  $\alpha$ -mannosidase and exhibited inhibition of the enzyme. The compound responsible for this activity was identified as swainsonine (**1.3**).<sup>27</sup> The same trihydroxyindolizidine was isolated in North America from certain species of *Astragalus* and *Oxytropis*, known locally as locoweed.<sup>26</sup>

**Figure 1.2.1.** Polyhydroxylated indolizidine alkaloids.

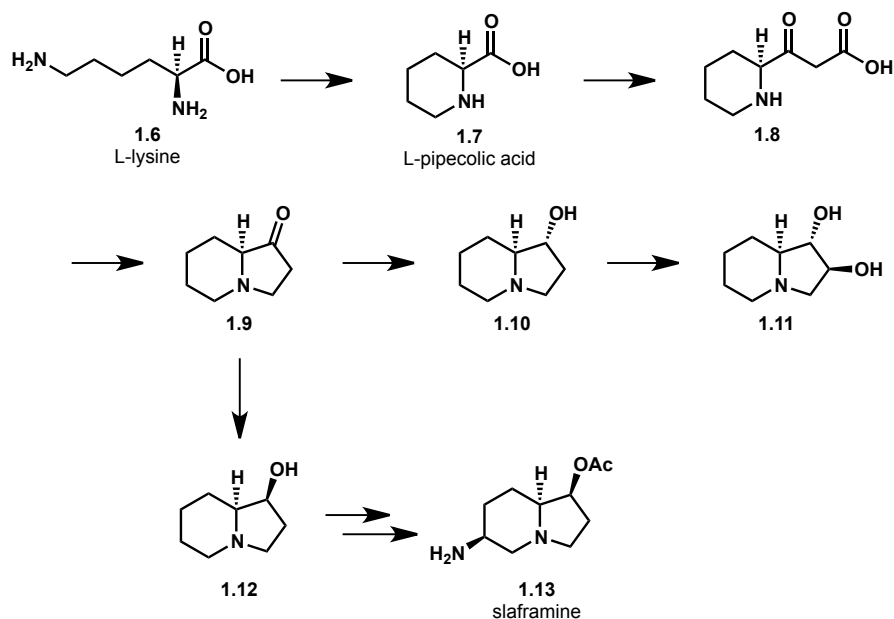


Other polyhydroxylated indolizidine alkaloids are also potent inhibitors of specific glucosidases. This biological activity can be attributed to their structural resemblance to naturally occurring sugars and has earned them the name “iminosugars”. For example, lentiginosine (**1.2**) inhibits amyloglucosidase, but interestingly demonstrates no activity toward  $\alpha$ -mannosidase. The activity of these compounds is closely tied to both the stereochemistry and location of the hydroxyl groups on the indolizidine core, since 2-*epi*-lentiginosine displays no inhibition of amyloglucosidase. This combination of potency and selectivity has made hydroxylated indolizidines drug candidates for a variety of diseases, including cancer, in which glycoprotein processing plays an integral role.<sup>28</sup>

Biosynthetically, hydroxylated indolizidines are thought to arise from the cyclization of lysine (**1.6**) to form pipercolic acid (**1.7**), which constitutes the six-membered ring portion of the indolizidine core. From pipercolic acid (**1.7**), feeding studies provide evidence that the final two carbon atoms necessary to form the five-membered ring are incorporated through a Claisen condensation with malonate. Cyclization of **1.8** to form the five-membered ring followed by reduction gives indolizidinone (**1.9**), which serves as a precursor to the polyhydroxylated indolizidines, as well as to other indolizidine alkaloids such as slaframine (**1.13**).

Hydroxylated indolizidines have enjoyed status as popular synthetic targets over the last four decades. Both naturally occurring congeners of these iminosugars as well as non-natural stereo- and regioisomers have been prepared synthetically and studied in various biological assays. These efforts have led to a greater understanding of the parameters responsible for the selective activity of this class of compounds toward specific glucosidases.

**Scheme 1.2.1.** Proposed biosynthetic pathway for production of hydroxylated indolizidine alkaloids.



*Polyalkyl indolizidine alkaloids:*

Although the hydroxylated indolizidine alkaloids were the first subclass of indolizidine alkaloids to be widely isolated and studied, alkylated indolizidines greatly outnumber all other types of indolizidine natural products (Figure 1.2.2). These compounds are so great in number that when they are isolated, they are not given a common name, but instead are assigned a code that consists of the molecular weight of the molecule followed by a letter (For example, indolizidine 167B, **1.14**). The vast majority of these compounds were first isolated from the skin of frogs and other amphibians,<sup>29</sup> a consequence of the lipophilic nature of these alkaloids, which causes them to localize in amphibian skin. The potent toxicity of mono- and dialkylated indolizidines suggests that these compounds could function as a defense mechanism to deter predators. Many have hypothesized that these alkaloids also possess antimicrobial properties and can protect against skin infections, since frogs with high alkaloid levels in their skin often lack the antimicrobial peptides produced by other species of frogs. Recent studies have provided support for this hypothesis.<sup>30</sup>

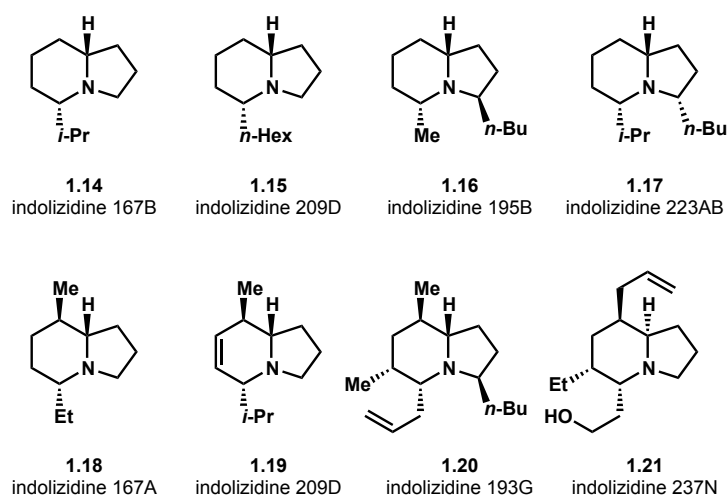
Regardless of the number of alkyl substituents about the indolizidine core, a majority of the molecules isolated to date possess an alkyl group at C-5. Proposed structures of monosubstituted indolizidines, such as indolizidine 167B (**1.14**) and indolizidine 209D (**1.15**), place the alkyl substituent at the C-5 position. Structure-activity studies of these 5-alkylindolizidines illustrate the importance of the alkyl chain on the biological activity. The length of the alkyl chain is correlated with the affinity of these compounds to ion channels, with longer chains providing superior binding.<sup>31</sup>

Over thirty 3,5-disubstituted indolizidines, which possess a substituent at C-5 have been isolated from anurans.<sup>29</sup> Alkyl chains of up to five carbons in length with various levels of

unsaturation and oxygenation are appended to the C-3 and C-5 positions of these molecules. Even though 3,5-disubstituted indolizidines have not undergone extensive biological testing, preliminary studies suggest that this class of indolizidines is not as toxic as other alkylated indolizidines, and have LD<sub>50</sub> values of greater than 200 µg per mouse.<sup>29</sup>

There are over eighty 5,8-disubstituted indolizidines (e.g., indolizidine 167A, **1.18**), which are regioisomeric to the 3,5-disubstituted alkaloids, and an additional thirty 6,7-dehydro-5,8-disubstituted indolizidines (e.g., indolizidine 209D, **1.19**). These indolizidines are commonly found in dendrobatid and mantellid frogs and are less frequently isolated from bufonid toads.<sup>29</sup> Evidence reported in the literature suggests that these compounds are not synthesized by the frogs themselves, but are rather acquired from their diet of ants.<sup>29</sup>

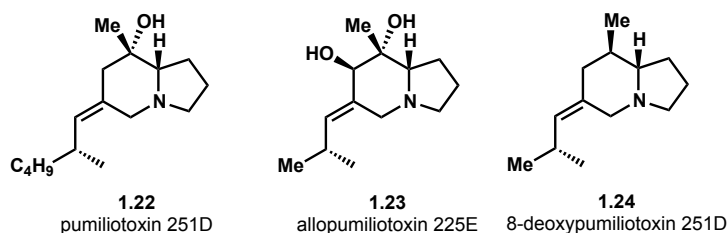
**Figure 1.2.2.** Select polyalkyl indolizidine alkaloids.



The pumiliotoxin subclass is unique both structurally as well as biosynthetically. First, the pumiliotoxins do not possess a C-5 substituent, and in addition to having alkyl groups about the indolizidine core, their six-membered ring is often decorated with hydroxyl groups (Figure 1.2.3). The pumiliotoxins and derivatives are common to frogs from the neotropics, South America, Madagascar and Australia. As in the case of dialkyl indolizidines (*vide supra*), frogs are thought to acquire pumiliotoxins through the consumption of ants, which in turn acquire these compounds from their mite-rich diet. Dendrobatid frogs possess a pumiliotoxin 7-hydroxylase enzyme that can convert dietary pumiliotoxins to the corresponding allopumiliotoxin, which possess an additional hydroxyl group at C-7.<sup>32</sup> This is the only example of a dietary indolizidine alkaloid being metabolically derivatized by a frog. The C-7 hydroxyl group present in the allopumiliotoxins has been shown to increase toxicity levels by five-fold as compared to the parent pumiliotoxin.



**Figure 1.2.3.** Select members of the pumiliotoxin family.

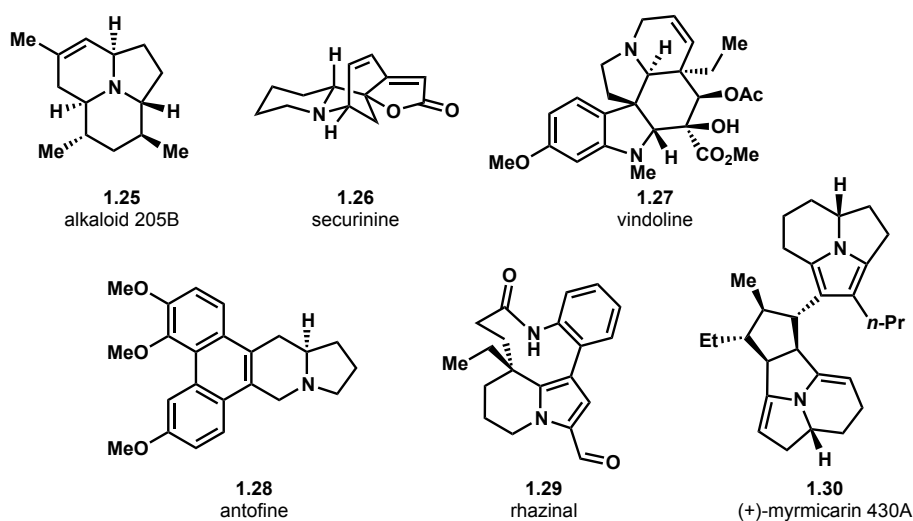


The molecules illustrated in Figures 1.2.2 and 1.2.3 only represent a sample of the alkylated indolizidine alkaloids that have been isolated from amphibians and other natural sources. From frogs alone, over eight-hundred alkaloids have been isolated and characterized to date.<sup>29</sup>

### *Polycyclic indolizidine alkaloids*

Although the hydroxylated and alkylated indolizidine alkaloids have a rich history and huge potential for medicinal applications, their simple bicyclic structure can leave something to be desired by the modern synthetic organic chemist. Highly complex indolizidine alkaloids have also been isolated with polycyclic skeletons that display a plethora of functional groups and offer more of a synthetic challenge (Figure 1.2.4). Like the structurally less complex molecules discussed earlier in this chapter, many of the more complex indolizidine alkaloids demonstrate important biological properties, which have only begun to be exploited.

**Figure 1.2.4.** Examples of polycyclic indolizidine alkaloids.



Polycyclic indolizidine alkaloids have been isolated from a variety of natural sources of both terrestrial and marine origin. Some polycyclic indolizidines have been isolated from the same organisms that produce simple alkylated indolizidines. For example, tricyclic alkaloid

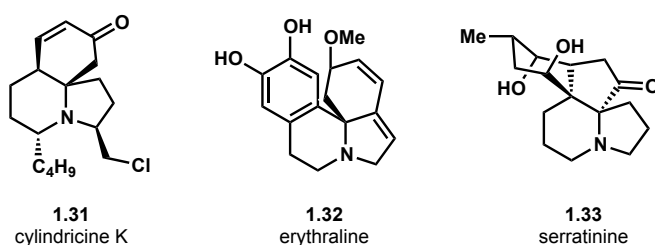
205B (**1.25**) has been found in the skin of frogs<sup>29</sup> and myrmicarin 430A (**1.30**) was isolated from the poison glands of myrmicara ants<sup>33</sup> (Figure 1.2.4). These toxins have garnered attention from the chemical community on the basis of their interesting structures and questions surrounding their biosynthetic origins.<sup>34,35</sup>

Other indolizidine alkaloids, such as securinine (**1.26**), have earned the spotlight based on their biological activity. Initially, this compound was shown to be extremely toxic to cells and induce convulsions in animals.<sup>36,37</sup> However, later studies revealed that at lower doses, securinine is a GABA receptor antagonist with potential as a treatment for neurological disorders.<sup>38</sup> More recently, securinine has been investigated as a possible therapy for colon cancer<sup>39</sup> and leukemia.<sup>40</sup> The potential of antofine (**1.28**) as a treatment for cancer has also been explored, specifically targeting cancer cells that display multidrug resistance.<sup>41</sup>

One of the more complex indolizidine alkaloids is vindoline (**1.27**), which has gained fame because of the biological activity of molecules in its family, as well as its highly oxygenated pentacyclic core that excites and at the same time humbles the synthetic organic chemist. Although vindoline is often referred to as an indole alkaloid, it also possesses the isoindole, indolizidine bicycle in its pentacyclic core.

Until this point, all of the indolizidine alkaloids discussed in this chapter share a hydrogen atom substituent on the ring-fusion carbon. This structural feature is common to the vast majority of indolizidine natural products. However, a subset of these alkaloids possess a carbon substituent at the ring-fusion carbon. For example, the cylindricine family of marine alkaloids (e.g., cylindricine K, **1.31**, Figure 1.2.5) contains a second six-membered ring, which is fused with respect to the indolizidine six-membered ring and is spirocyclic to the indolizidine five-membered ring. The ring-fusion carbon-carbon bond is also conserved throughout the *Erythrina* alkaloids (e.g., erythraline, **1.32**) and the *Lycopodium* alkaloid, serratinine (**1.33**).

**Figure 1.2.5.** Additional examples of polycyclic indolizidine alkaloids.



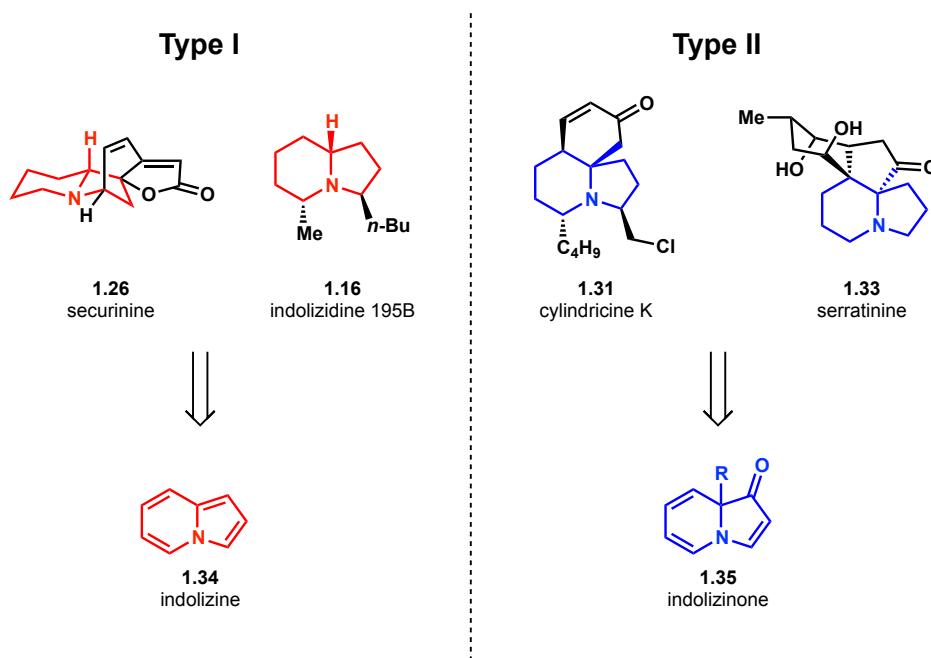
Indolizidine alkaloids come from many sources and have varied biological activities. The molecules described in this chapter constitute only a small fraction of the indolizidine alkaloids that have been characterized to date, but are included to provide a sense of the structural diversity that this class of natural products offers to the synthetic chemist.

### 1.3. Approach toward indolizidine alkaloids from indolizines and indolizinsones

After considering several indolizidine alkaloids as synthetic targets and developing preliminary strategies, we began to divide these alkaloids into two distinct categories. The first group (Type I, Figure 1.3.2) encompasses those compounds that possess a hydrogen atom at the

ring fusion (e.g., securinine, **1.26**, and indolizidine 195B, **1.16**), or molecules with a unit of unsaturation to the ring-fusion carbon (e.g., rhazinal, **1.29**). The remaining indolizidines are those that bear a quaternary carbon at the ring fusion (e.g., cylindricine K, **1.31**, and serratinine, **1.33**), which constitute the second category (Type II). We envisioned accessing Type I indolizidines from *indolizine* (**1.34**) precursors, whereas the Type II indolizidines could be elaborated from *indolizinone* (**1.35**) building blocks, which already contain the ring-fusion quaternary carbon present in these natural products (Figure 1.3.1).

**Figure 1.3.1.** General strategy for the synthesis of Type I and Type II indolizidine alkaloids from indolizines and indolizinones.



For a number of years, we have been interested in developing methods for the synthesis of indolizines (**1.34**, see Chapters 2 and 3) and indolizinones (**1.35**, see Chapter 3). These heterocycles share the [4.3.0]azabicyclic core common to indolizidine alkaloids, but exist at a higher oxidation level. The structural diversity within the indolizidine class of natural products provides an opportunity to exploit our established access to the 6,5-azabicyclo. With cycloisomerization strategies in place to construct 2,3-disubstituted indolizines (see Chapter 2), as well as 1,3-disubstituted indolizidines and indolizinones (see Chapter 3), we were eager to test the potential for using these heterocycles as building blocks in the total synthesis of natural products.

At the onset of this project, we anticipated that employing indolizines and indolizinones as intermediates toward the synthesis of natural products would test the utility of these heterocycles as well as expand the chemistry known for each of these cores. We were also cognizant of the potential challenges for synthesis including (1) the ease with which the indolizine nucleus could be reduced to the fully saturated indolizidine and also (2) whether the stereochemistry of the quaternary ring-fusion carbon could be successfully translated to the

formation of subsequent stereocenters in the desired natural products. The outcome of these endeavors is disclosed in Chapters 4-6.

#### ***1.4 References and Notes***

- (1) Gellert, E. *J. Nat. Prod.* **1982**, *45*, 50.
- (2) Lamberton, J. A. *Nat. Prod. Rep.* **1984**, *1*, 245.
- (3) Grundon, M. F. *Nat. Prod. Rep.* **1985**, *2*, 235.
- (4) Grundon, M. F. *Nat. Prod. Rep.* **1987**, *4*, 415.
- (5) Rajeswari, S.; Chandrasekharan, S.; Govindachari, T. R. *Heterocycles* **1987**, *25*, 659.
- (6) Grundon, M. F. *Nat. Prod. Rep.* **1989**, *6*, 523.
- (7) Michael, J. P. *Nat. Prod. Rep.* **1990**, *7*, 485.
- (8) Michael, J. P. *Nat. Prod. Rep.* **1991**, *8*, 553.
- (9) Michael, J. P. *Nat. Prod. Rep.* **1994**, *11*, 17.
- (10) Michael, J. P. *Nat. Prod. Rep.* **1994**, *11*, 639.
- (11) Michael, J. P. *Nat. Prod. Rep.* **1995**, *12*, 535.
- (12) Michael, J. P. *Nat. Prod. Rep.* **1997**, *14*, 619.
- (13) Michael, J. P. *Nat. Prod. Rep.* **1997**, *14*, 21.
- (14) Michael, J. P. *Nat. Prod. Rep.* **1998**, *15*, 571.
- (15) Michael, J. P. *Nat. Prod. Rep.* **1999**, *16*, 675.
- (16) Michael, J. P. *Nat. Prod. Rep.* **2000**, *17*, 579.
- (17) Michael, J. P. *Nat. Prod. Rep.* **2001**, *18*, 520.
- (18) Michael, J. P. *Nat. Prod. Rep.* **2002**, *19*, 719.

- (19) Michael, J. P. *Nat. Prod. Rep.* **2003**, *20*, 458.
- (20) Michael, J. P. *Nat. Prod. Rep.* **2004**, *21*, 625.
- (21) Michael, J. P. *Nat. Prod. Rep.* **2005**, *22*, 603.
- (22) Michael, J. P. *Nat. Prod. Rep.* **2007**, *24*, 191.
- (23) Michael, J. P. *Nat. Prod. Rep.* **2008**, *25*, 139.
- (24) Johns, S. R.; Lamberto, J. A.; Sioumis, A. A.; Willing, R. I. *Aust. J. Chem.* **1969**, *22*, 775.
- (25) Johns, S. R.; Lamberto, J. A.; Sioumis, A. A. *Aust. J. Chem.* **1969**, *22*, 793.
- (26) Molyneux, R. J.; Lee, S. T.; Gardner, D. R.; Panter, K. E.; James, L. F. *Phytochemistry* **2007**, *68*, 2973.
- (27) Colegate, S. M.; Dorling, P. R.; Huxtable, C. R. *Aust. J. Chem.* **1979**, *32*, 2257.
- (28) Olden, K.; Breton, P.; Grzegorzewski, K.; Yasuda, Y.; Gause, B. L.; Oredipe, O. A.; Newton, S. A.; White, S. L. *Pharmacol. Ther.* **1991**, *50*, 285.
- (29) Daly, J. W.; Spande, T. F.; Garraffo, H. M. *J. Nat. Prod.* **2005**, *68*, 1556.
- (30) Macfoy, C.; Danosus, D.; Sandit, R.; Jones, T. H.; Garraffo, H. M.; Spande, T. F.; Daly, J. W. *Z. Naturforsch., C* **2005**, *60*, 932.
- (31) Sauviat, M. P.; Vercauteren, J.; Grimaud, N.; Juge, M.; Nabil, M.; Petit, J. Y.; Biard, J. F. *J. Nat. Prod.* **2006**, *69*, 558.
- (32) Daly, J. W.; Garraffo, H. M.; Spande, T. F.; Clark, V. C.; Ma, J. Y.; Ziffer, H.; Cover, J. F. *Proc. Natl. Acad. Sci. U.S.A.* **2003**, *100*, 11092.
- (33) Schroder, F.; Sinnwell, V.; Baumann, H.; Kaib, M. *Chem. Commun.* **1996**, 2139.
- (34) Snyder, S. A.; Elsohly, A. M.; Kontes, F. *Angew. Chem. Int. Ed.* **2010**, *49*, 9693.
- (35) Ondrus, A. E.; Kaniskan, H. U.; Movassaghi, M. *Tetrahedron* **2010**, *66*, 4784.
- (36) Chang, H. Y. *Chin. Med. J.* **1974**, 234.
- (37) Tao, S. C.; Peng, J. Z.; Lu, M. W. *Acta Pharmacol. Sin.* **1986**, *7*, 9.
- (38) Beutler, J. A.; Karbon, E. W.; Brubaker, A. N.; Malik, R.; Curtis, D. R.; Enna, S. J. *Brain Res.* **1985**, *330*, 135.

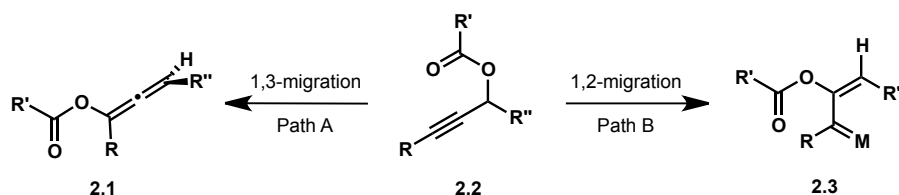
- (39) Rana, S.; Gupta, K.; Gomez, J.; Matsuyama, S.; Chakrabarti, A.; Agarwal, M. L.; Agarwal, A.; Agarwal, M. K.; Wald, D. N. *Faseb J.* **2010**, *24*, 2126.
- (40) Dong, N. Z.; Gu, Z. L.; Chou, W. H.; Kwok, C. Y. *Acta Pharmacol. Sin.* **1999**, *20*, 267.
- (41) Min, H. Y.; Chung, H. J.; Kim, E. H.; Kim, S.; Park, E. J.; Lee, S. K. *Biochem. Pharmacol.* **2010**, *80*, 1356.

## Chapter 2. Development of a Platinum-Catalyzed Cyclization of Propargylic Esters to 2,3-Disubstituted Indolizines

### 2.1 Introduction

The chemistry of propargylic esters (e.g., **2.2**, Scheme 2.1.1) has become an area of active research during the past ten years.<sup>1</sup> Propargylic esters serve as precursors to a variety of compounds using reactions that proceed through allenyl ester (e.g., **2.1**) or metallocarbenoid intermediates (e.g., **2.3**). In one mechanistic scenario, a 1,3-migration of the acyl group in **2.2**, initiated via 6-*endo*-dig cyclization (Path A), generates an allenyl ester (**2.1**), which upon further activation with a metal can proceed to a plethora of products.<sup>2</sup> Alternatively, the corresponding 1,2-acyl migration (Path B) was first proposed by Rautenstrauch in 1984 to explain the observation of an unexpected product when a propargylic ester was treated with a catalytic amount of PdCl<sub>2</sub>(MeCN)<sub>2</sub>.<sup>3</sup> This 1,2-acyl migration remained unexplored for nearly twenty years until a study was reported by Marco-Contelles in which substrates intended for cycloisomerization reactions with a free hydroxyl group at the propargylic position were found to give dramatically different products when the hydroxyl group was acylated.<sup>4</sup>

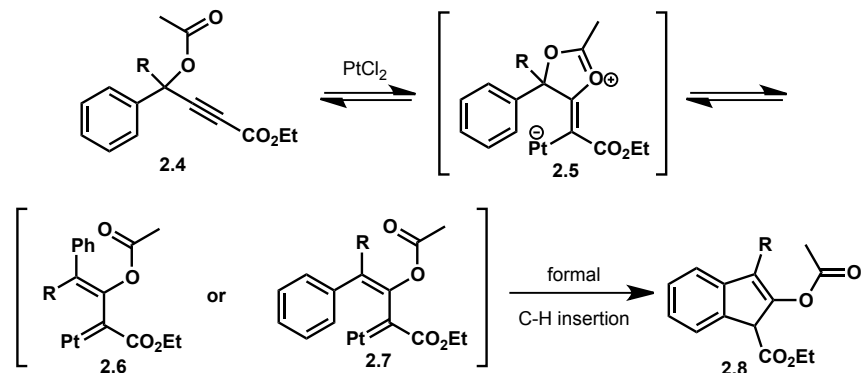
Scheme 2.1.1. Acyl migration pathways.



Although metal-catalyzed reactions of propargylic esters have been used by numerous groups to generate products that arise from both 1,2- and 1,3-acyl migration in synthetically useful yields, the factors that control 1,2- versus 1,3-migration are not completely understood. Often, the application of either transformation begins with empirical optimization of the reaction conditions to favor one pathway over the other. Terminal alkynes typically favor 1,2-acyl migration, whereas internal alkynes tend to undergo competing 1,3-acyl migration.<sup>5,6</sup> In some cases, alkyl substitution at the terminus of the alkyne leads to 1,2-migration whereas aryl substitution results only in non-specific decomposition.<sup>7</sup> However, there are exceptions to this trend as reported by Malacria *et al.*,<sup>8</sup> who have demonstrated that substrates that possess an ester at the alkyne terminus proceed through a 1,2-acyl migration. Conversely, terminal alkynes led exclusively to allenyl esters, which arise through 1,3-migration.

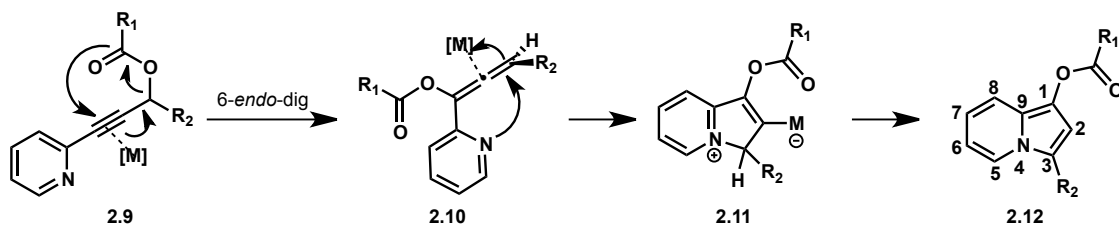
A previous observation in the Sarpong group supports the hypothesis that the electronics of the alkyne substituent influence the mode of acyl migration. With an ester group at the terminus of the alkyne, exclusive 1,2-migration is observed.<sup>9</sup> For example, with **2.4** (Scheme 2.1.2) as a substrate, initial platinum-catalyzed 1,2-acyl migration leads to a platinum carbenoid (**2.6** or **2.7**), which can go on to form interesting products such as functionalized indenenes (**2.8**). Replacing the ester with a phenyl group at the alkyne terminus leads to 6-*endo*-dig cyclization of the acetate onto the alkyne, giving an allenyl ester as the major product.<sup>10</sup>

**Scheme 2.1.2.** Platinum-catalyzed acyl migration and indene formation.

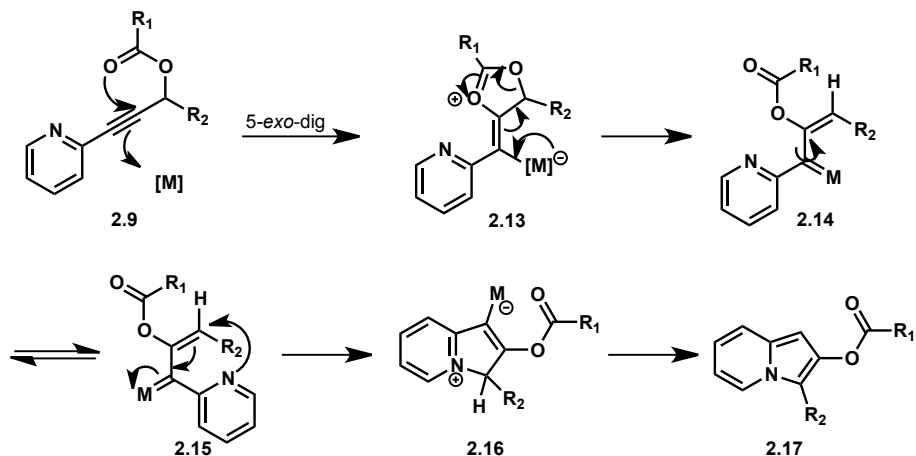


Intrigued by the observed electronic influence of the alkyne substituent and the possibility of accessing synthetically important products, a variant of this reaction, that incorporates a pyridine at the alkyne terminus, was explored as a route to disubstituted indolizines. If 6-*endo*-dig cyclization was the preferred path (Scheme 2.1.3), allene formation (see **2.10**) followed by metal activation could lead to nucleophilic attack of the pyridine nitrogen to form a five-membered ring zwitterion (**2.11**), which upon proton transfer would provide 1,3-disubstituted indolizine **2.12**. However, if 5-*exo*-dig cyclization was the favored mode (Scheme 2.1.4), metallocarbenoid **2.14** would be formed, which could proceed via **2.15** and **2.16** to provide 2,3-disubstituted indolizine **2.17**.

**Scheme 2.1.3.** Formation of a 1,3-disubstituted indolizine via 6-*endo*-dig cyclization.



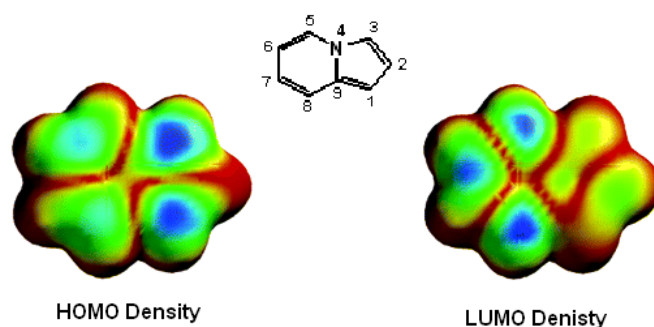
**Scheme 2.1.4.** Formation of a 2,3-disubstituted indolizine via 5-*exo*-dig cyclization.





In addition to assessing the cyclization pathway that would be favored with a pyridinyl alkyne substrate, we were interested in biasing the reaction toward 5-*exo*-dig cyclization through the use of exogenous additives and substrate design. Although either 6-*endo*-dig or 5-*exo*-dig cyclization could give rise to disubstituted indolizines, the 5-*exo*-dig pathway would provide a 2,3-disubstituted indolizine (see for example **2.17**, Scheme 2.1.4), which has historically been synthetically challenging to access as compared to 1,3-disubstituted indolizines (see for example **2.12**, Scheme 2.1.3). This is especially important since functionalization of the C-2 position of indolizines is difficult once the indolizine core has been formed. According to DFT calculations performed by Gevorgyan *et al.*, the site with the least electron density in both the HOMO and the LUMO is the C-2 position, making it difficult to functionalize (Figure 2.1.1).<sup>11</sup> Thus our initial goal was to prepare a series of propargylic ester substrates (**2.9**) with varying electronic properties to examine the effect of substrate electronics on the preferred cyclization pathway.

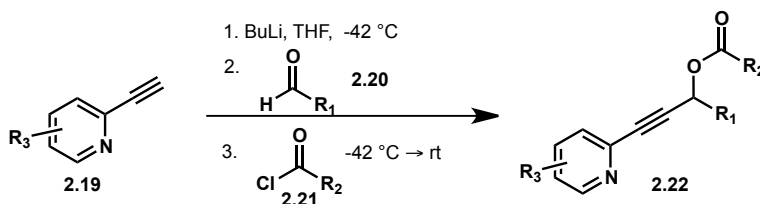
**Figure 2.1.1.** HOMO and LUMO electron density of indolizines, where blue corresponds to the highest levels of electron density.



## 2.2. Substrate Synthesis

The pyridinyl alkyne substrates for this project were accessible in one to three steps from commercially available materials. To obtain substrates with various substituents at the propargylic position, the acetylide anion of 2-ethynylpyridine was treated with the corresponding aldehyde. The resultant alkoxide was trapped *in situ* with an acid chloride to provide an assortment of substrates in 55 to 93% overall yield (Scheme 2.2.1).

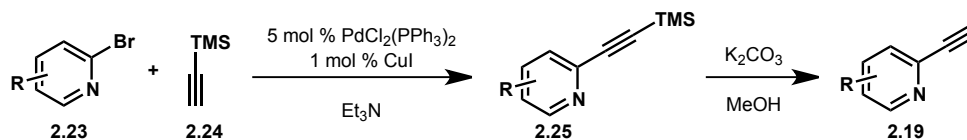
**Scheme 2.2.1.** Synthesis of substrates.



To construct substrates with substitution on the pyridine ring (e.g., **2.22**, Scheme 2.2.1), substituted 2-ethynylpyridines (**2.19**, Scheme 2.2.2) were synthesized via a Sonogashira coupling

of the corresponding 2-bromopyridine (**2.23**) and trimethylsilylacetylene (**2.24**), followed by cleavage of the trimethylsilyl group with potassium carbonate in methanol.

**Scheme 2.2.2.** Synthesis of substituted ethynylpyridine (**2.19**).

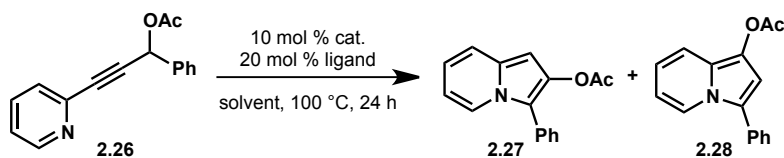


### 2.3. Reaction optimization

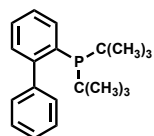
Initial attempts to effect the desired transformation began by screening metal catalysts and solvents. On the basis of precedent from our group, ruthenium(II), platinum(IV) or platinum(II) catalysts were heated with the substrate in toluene (entries 1-3, Table 2.3.1). Only platinum(II) chloride provided trace amounts of indolizine product (4% yield), so further studies were conducted with this catalyst to optimize reaction yields. Changing the solvent to dioxane resulted in no product formation (entry 4), whereas tetrahydrofuran and benzene led to a slight increase in yield (entries 5-6). On the basis of the success of other Sarpong group members using bulky phosphine additives to effect related transformations, Johnphos, Davephos, and triphenylphosphine were surveyed;<sup>12</sup> unfortunately, no product was observed in the presence of these ligands (entries 7-9). However switching to an electron-deficient phosphine (tris(pentafluorophenyl)phosphine) gave a significant increase in yield (entry 10). We hypothesized that the use of an electron-deficient ligand would in turn lead to a more deficient metal-center and a more strongly activating  $\pi$ -Lewis acid.

Characterization of the products obtained in Table 2.3.1, entry 10 revealed a 3:1 mixture of 2,3- and 1,3-disubstituted indolizines, which were inseparable by column chromatography. The major isomer was identified as the 2,3-disubstituted indolizine (**2.237**) through nOe studies that indicated an nOe relationship between the C-1 and C-8 hydrogen atoms (see **2.27**, Figure 2.3.1).

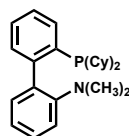
**Table 2.3.1.** Optimization of reaction conditions.



| entry | catalyst  | solvent | ligand   | yield             |
|-------|---|---------|--|-------------------|
| 1     | [RuCl <sub>2</sub> (CO) <sub>3</sub> ] <sub>2</sub> | PhMe    | None   | Starting Material |
| 2     | PtCl <sub>4</sub>                                   | PhMe    | None   | Starting Material |
| 3     | PtCl <sub>2</sub>                                   | PhMe    | None   | 4%                |
| 4     | PtCl <sub>2</sub>                                   | Dioxane | None   | Starting Material |
| 5     | PtCl <sub>2</sub>                                   | THF     | None   | 8%                |
| 6     | PtCl <sub>2</sub>                                   | PhH     | None   | 10%               |
| 7     | PtCl <sub>2</sub>                                   | PhH     | JohnPhos                                       | Starting Material |
| 8     | PtCl <sub>2</sub>                                   | PhH     | DavePhos                                       | Starting Material |
| 9     | PtCl <sub>2</sub>                                   | PhH     | PPh <sub>3</sub>                               | Starting Material |
| 10    | PtCl <sub>2</sub>                                   | PhH     | P(C <sub>6</sub> F <sub>5</sub> ) <sub>3</sub> | 42%               |

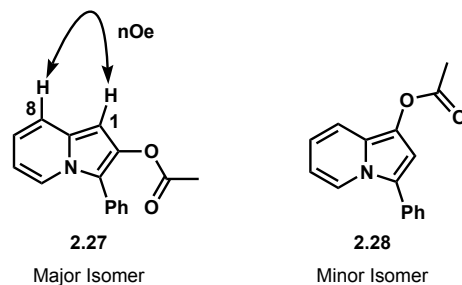


JohnPhos  
2.29



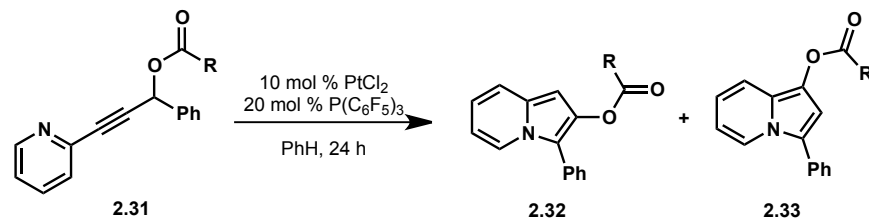
DavePhos  
2.30

**Figure 2.3.1.** Identification of the major indolizine isomer through nOe.



With the knowledge that both 2,3- and 1,3-disubstituted indolizines were being formed, the focus of the reaction optimization evolved from improving the combined yield to include maximizing the ratio of 2,3- to 1,3-disubstituted indolizine product. Increasing the steric bulk of the acyl group from an acetate to a pivalate group provided an increase in yield and also improved the ratio of **2.32:2.33** from 3:1 to 5:1 (Table 2.3.2, entry 2). Additionally, decreasing the temperature at which the reaction was conducted further improved the ratio of **2.32:2.33** to 9:1. However, the improved ratio came at the cost of the reaction yield (entry 3).

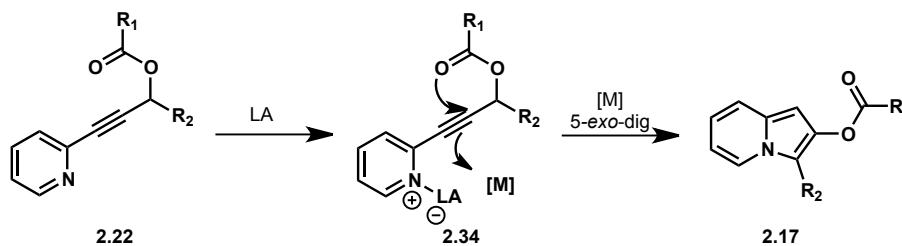
**Table 2.3.2.** Optimization of acyl group and temperature.



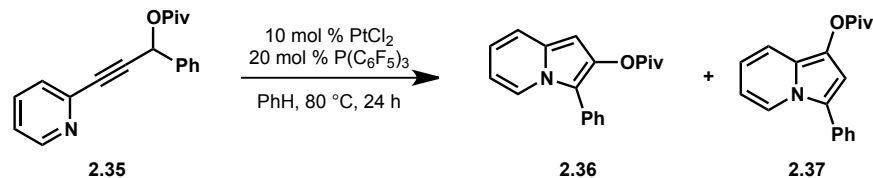
| entry | R            | temperature (°C) | yield | ratio (2.32:2.33) |
|-------|--------------|------------------|-------|-------------------|
| 1     | Me           | 100              | 42%   | 3:1               |
| 2     | <i>t</i> -Bu | 100              | 64%   | 5:1               |
| 3     | <i>t</i> -Bu | 80               | 45%   | 9:1               |

We hypothesized that reducing the electron density of the pyridine moiety would favor 1,2-acyl migration and the formation of 2,3-disubstituted indolizine products over 1,3-acyl migration and formation of 1,3-disubstituted indolizines. This idea stemmed from our initial observation that having an ester at the terminus of the alkyne gives exclusively 1,2-acyl migration whereas a phenyl group at the terminus leads to 1,3-acyl migration. In theory, a Lewis acid could accept electron density from the pyridine nitrogen, making the pyridine ring a more electron-deficient substituent.

**Scheme 2.3.1.** Proposed action of a Lewis acid.



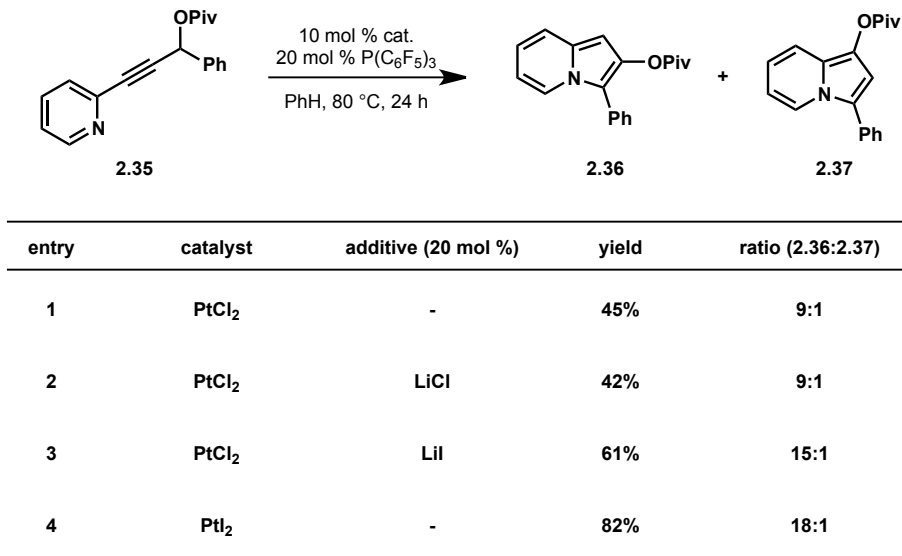
With this goal in mind, a screen of Lewis acids and other additives was undertaken (Table 2.3.3). A variety of Lewis acids led to complex mixtures, which did not contain starting material or indolizine product (entries 1-6). Upon addition of lithium iodide, the yield of the reaction increased to 61% and the ratio of **2.36** to **2.37** improved to 15:1 (entry 7). Encouraged by this result, other lithium salts were investigated as additives in this reaction. However, lithium chloride and lithium tetrafluoroborate did not show the same yield or product ratio enhancement as lithium iodide (entries 8-9).

**Table 2.3.3.** Screen of Lewis acids.

| entry | additive (20 mol %)  | yield         | ratio (2.36:2.37) |
|-------|----------------------|---------------|-------------------|
| 1     | InCl <sub>3</sub>    | decomposition | -                 |
| 2     | Yb(OTf) <sub>3</sub> | decomposition | -                 |
| 3     | TMSCl                | decomposition | -                 |
| 4     | TMSBr                | decomposition | -                 |
| 5     | AlCl <sub>3</sub>    | decomposition | -                 |
| 6     | 5% HCl               | decomposition | -                 |
| 7     | LiI                  | 61%           | 15:1              |
| 8     | LiCl                 | 42%           | 9:1               |
| 9     | LiBF <sub>4</sub>    | 43%           | 9:1               |

Although at the outset it was anticipated that the coordination of lithium to the pyridine nitrogen (see **2.34**, Scheme 2.3.1) could enhance formation of 2,3-disubstituted indolizine, the data suggest that the counteranion was in fact responsible for the increased yield and product ratio. It seemed plausible that a halide metathesis to form platinum(II) iodide occurs, *in situ*. To test this hypothesis, PtCl<sub>2</sub> was replaced by PtI<sub>2</sub> as the catalyst. With PtI<sub>2</sub> as the catalyst, the reaction afforded an 82% yield of the indolizine products in an 18:1 ratio for **2.36:2.37** (Table 2.3.4, entry 4).

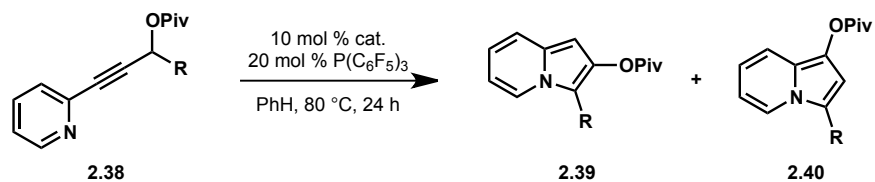
In summary, a systematic screening of catalysts, solvents, phosphines, additives and temperature identified the optimal reaction conditions to be 10 mol % PtI<sub>2</sub> with 20 mol % tris(pentafluorophenyl)phosphine in benzene at 80 °C for 24 h. These conditions gave an 18:1 mixture of 2,3- to 1,3-disubstituted indolizine in 82% yield.

**Table 2.3.4.** Platinum(II) chloride versus platinum(II) iodide.

## 2.4 Substrate Scope

A series of substrates possessing different substituents at the propargylic position were synthesized and subjected to the reaction conditions (Table 2.4.1). A trend quickly emerged: while a cyclohexyl-substituted substrate gave no indolizine product (entry 2), the corresponding cyclohexenyl derivative provided a yield and product ratio, which matched the phenyl substrate (entry 3). Similarly, an isobutyl substituent at the alkyne terminus resulted in no indolizine product (entry 4) whereas an isobutenyl containing substrate gave the desired product in a 14:1 ratio and a 54% yield (entry 5). As a general trend, aryl and vinyl substituents are tolerated by the reaction whereas sp<sup>3</sup> hybridization adjacent to the propargylic position is not. However, there are examples that strayed from this rule; an isopropenyl group gives no indolizine product (entry 6) whereas a *tert*-butyl at the propargylic position forms a trace amount of product (entry 7).

**Table 2.4.1.** Effect of substitution at the propargylic position.



| entry | R            | yield (%) | ratio (2.39:2.40) |
|-------|--------------|-----------|-------------------|
| 1     | Ph           | 45        | 9:1               |
| 2     |              | 0         | -                 |
| 3     |              | 74        | 14:1              |
| 4     |              | 0         | -                 |
| 5     |              | 54        | 14:1              |
| 6     |              | 0         | -                 |
| 7     | <i>t</i> -Bu | 11        | 4:1               |
| 8     |              | 49        | 3:1               |
| 9     |              | 73        | 11:1              |
| 10    |              | 34        | >20:1             |
| 11    |              | 56        | >20:1             |

**Table 2.4.2.** Aryl groups with varying electronic and steric properties at the propargylic position.

Reaction scheme: 2.38 (propargyl pyridine with OPiv and R groups) reacts with 10 mol % PtI<sub>2</sub> and 20 mol % P(C<sub>6</sub>F<sub>5</sub>)<sub>3</sub> in PhH at 80 °C for 24 h to yield a mixture of indoles 2.39 and 2.40.

| entry | R  | yield (%) | ratio (2.39:2.40) |
|-------|----|-----------|-------------------|
| 1     | Ph | 45        | 9:1               |
| 2     |    | 74        | 13:1              |
| 3     |    | 67        | 13:1              |
| 4     |    | 76        | 7:1               |
| 5     |    | 58        | 2:1               |
| 6     |    | 78        | 6:1               |
| 7     |    | 31        | 3:1               |
| 8     |    | 0         | -                 |
| 9     |    | 72        | 10:1              |
| 10    |    | 91        | >20:1             |

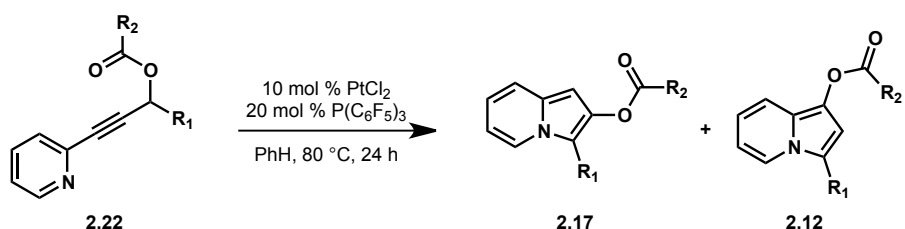
After identifying the important role played by the propargylic substituent, the impact of the electronic and steric properties of this substituent was probed further. Several substrates were synthesized containing substituted aryl groups, and the electronic properties of the aryl group



proved to be important with respect to both the overall yield of the reaction and the ratio of products obtained (Table 2.4.2). The presence of electron-donating groups on the phenyl ring led to yields and product ratios comparable to those obtained with an unsubstituted phenyl group (entries 1-4). However, the presence of electron-withdrawing groups at the *para*-position of the phenyl ring led to lower overall yields and a reduced selectivity for the 2,3-disubstituted indolizine product (entries 5-7). Notably, the presence of a nitro group at the *para*-position resulted in consumption of the starting material but no identifiable product formation (entry 8). Additionally substitution at the *ortho*-position of the aryl substituent was tolerated in this reaction and provided good to excellent product yields and ratios (entries 9-10).

This initial study indicated that the presence of an electron-withdrawing aryl substituent led to a greater amount of 1,3-acyl migration than what was observed with more electron-donating substituents. In an attempt to balance the effect of an electron-withdrawing propargylic substituent, the acyl group was changed from pivaloyl to the more electron-rich *p*-methoxybenzoyl. This alteration improved the ratio of **2.17**:**2.12** for the substrate bearing a phenyl group at the propargylic position from 13:1 to >20:1 (Table 2.4.3, entry 2), and for the substrate bearing a *para*-trifluoromethylphenyl there was a dramatic improvement from 2:1 to 13:1 (entry 4). This observed effect of the electronic properties of the acyl group suggests an additional means to control the 1,2 versus 1,3 selectivity of the cyclization process.

**Table 2.4.3.** Effects of altering the electronics of the acyl group.



| entry | R <sub>1</sub>   | R <sub>2</sub>                                | yield (%) | ratio (2.17:2.12) |
|-------|--|---|-----------|-------------------|
| 1     | Ph   | <i>t</i> -Bu                                  | 75        | 13:1              |
| 2     | Ph   | <i>p</i> -OMe(C <sub>6</sub> H <sub>4</sub> ) | 67        | >20:1             |
| 3     | <i>p</i> -CF <sub>3</sub> (C <sub>6</sub> H <sub>4</sub> ) | <i>t</i> -Bu                                  | 58        | 2:1               |
| 4     | <i>p</i> -CF <sub>3</sub> (C <sub>6</sub> H <sub>4</sub> ) | <i>p</i> -OMe(C <sub>6</sub> H <sub>4</sub> ) | 56        | 13:1              |

Although the initial attempt to favor 1,2-acyl migration via coordination of a Lewis acid to the pyridine was not fruitful, the concept of altering the electronic properties of the pyridine ring and tracking the effect on 1,2- versus 1,3-acyl migration was still intriguing. Placing a methoxy group on the pyridine ring led to a poor ratio of **2.42**:**2.43** and low overall yield (Table 2.4.4, entry 2). However, introduction of a trifluoromethyl group on the pyridine ring produced the desired indolizine product in >20:1 ratio (entry 3). These results align with the trend defined by the cases with an ester or a phenyl group at the terminus of the alkyne, which lead to 1,2- and 1,3-acyl migration, respectively.

**Table 2.4.4.** Substituted pyridine substrates.

Reaction scheme: Substrate 2.41 (a pyridine ring with an R group at the 2-position and a propargyl ester group at the 3-position) reacts with 10 mol % PtCl<sub>2</sub> and 20 mol % P(C<sub>6</sub>F<sub>5</sub>)<sub>3</sub> in PhH at 80 °C for 24 h to yield a mixture of 2,3-disubstituted indolizine (2.42) and 1,3-disubstituted indolizine (2.43).

| entry | substrate | yield (%) | ratio (2.42:2.43) |
|-------|-----------|-----------|-------------------|
| 1     |           | 75        | 13:1              |
| 2     |           | 26        | 2:1               |
| 3     |           | 82        | >20:1             |
| 4     |           | 76        | 10:1              |

### *Summary of Substrate Scope Observations*

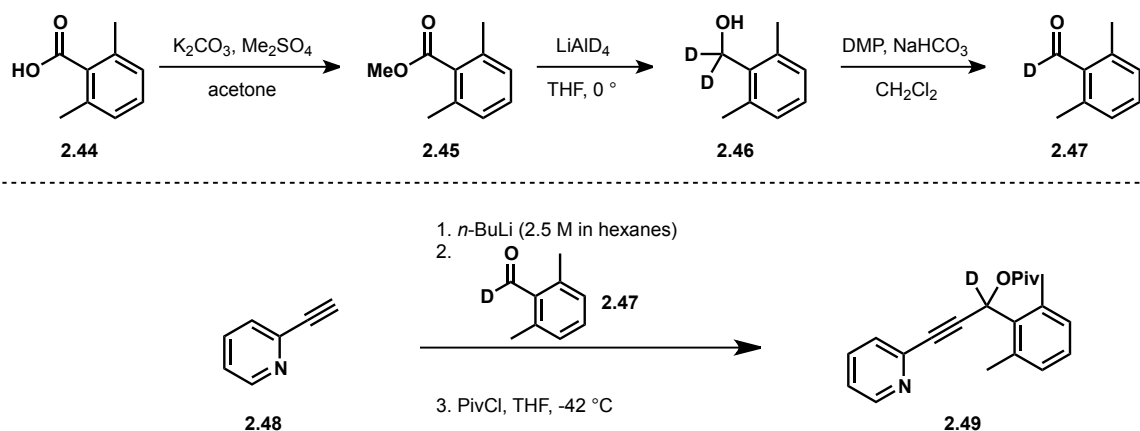
Exploration of the substrate scope, for the cycloisomerization of pyridinyl propargylic esters to afford indolizines, revealed the importance of the propargylic substituent, the electronic properties of the acyl group and the electronic properties of the pyridine ring on the ratio of the 2,3- and 1,3-disubstituted indolizine product obtained in the cyclization reaction. Only vinyl and aryl propargylic substituents led to synthetically useful yields. Electron-rich and neutral propargylic substituents gave acceptable 2,3- versus 1,3-disubstituted indolizine ratios whereas electron-deficient substituents led to increased amounts of 1,3-acyl migration and lower ratios of the 2,3- versus 1,3-disubstituted products. A more electron-rich acyl group favors 1,2-acyl migration and improves the product ratio. Finally, adding an electron-donating group to the pyridine ring increases the amount of 1,3-disubstituted indolizine, whereas placing an electron-withdrawing group on the pyridine ring leads to increased amounts of 2,3-disubstituted indolizine product.

## 2.5 Mechanistic Questions

Three experiments were designed to gain insight into the mechanism of this reaction: (1) a labeling experiment incorporating a deuterium atom at the propargylic position of the substrate; (2) a crossover experiment to determine whether an *intra* or *intermolecular* proton transfer occurs and (3) subjecting a tertiary alcohol-derived substrate to the reaction conditions to support our hypothesis that 1,2-acyl migration to form a metallocarbenoid is an operative mechanistic pathway.

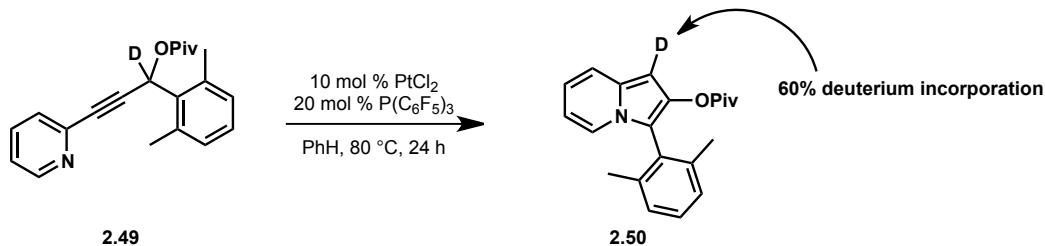
A substrate bearing a deuterium atom at the propargylic position was synthesized from 2,6-dimethylbenzoic acid (Scheme 2.5.1). The synthetic sequence commenced with conversion of the acid (**2.44**) to the corresponding methyl ester (**2.45**) with dimethylsulfate and potassium carbonate in acetone. The methyl ester was then reduced with lithium aluminum deuteride, and the resulting alcohol (**2.46**) was oxidized to deuterated aldehyde **2.47** with Dess Martin periodinane.<sup>13</sup> To complete the synthesis of the deuterated substrate, deuterated 2,6-dimethylbenzaldehyde (**2.47**) was coupled with the acetylide anion of **2.48** followed by *in situ* acylation to give deuterated substrate **2.49** with 90% deuterium incorporation, as determined by <sup>1</sup>H NMR (Scheme 2.5.1).

**Scheme 2.5.1.** Synthesis of deuterated substrate.



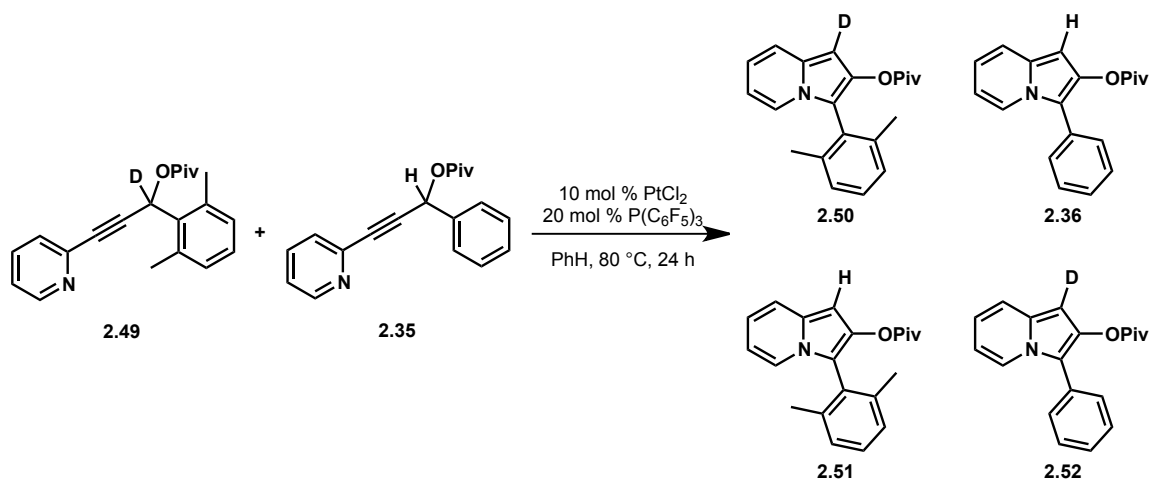
Under our optimized conditions, propargylic ester **2.49** gave 2,3-disubstituted indolizine **2.50** with 60% deuterium incorporation at the C-1 position of the crude product (Scheme 2.5.2). Unfortunately, following purification by flash chromatography, no deuterium remained in the product, indicating that proton exchange at the C-1 position of the indolizine occurred readily.

### Scheme 2.5.2. Deuterium labeling experiment.



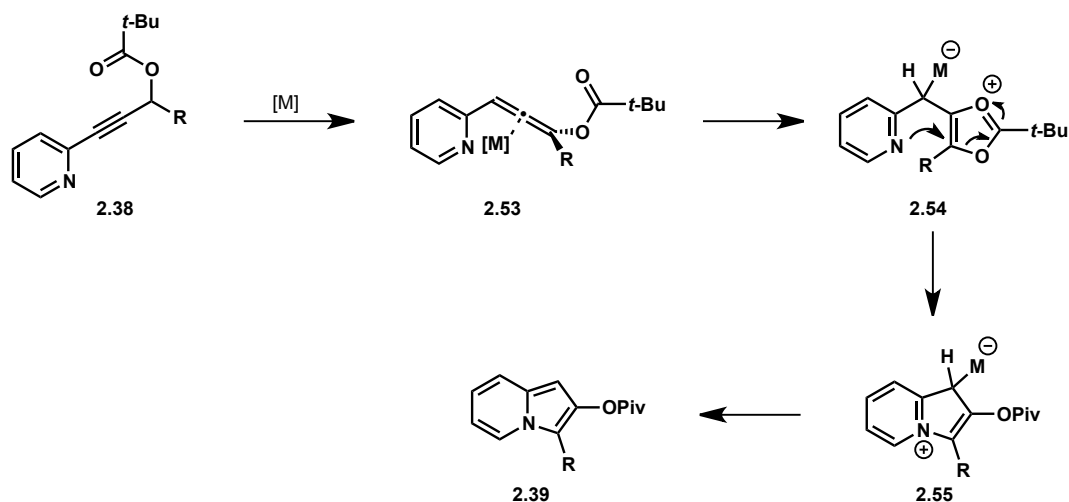
To determine whether proton transfer occurred in an intra or intermolecular fashion, a 1:1 mixture of deuterated and undeuterated substrates (**2.49** and **2.35**, respectively) were subjected to the reaction conditions (Scheme 2.5.3). If proton transfer occurred by an intramolecular process, then **2.50** and **2.36** should be the only observed products. However, all possible products (i.e., **2.50**, **2.36**, **2.51**, **2.52**) were obtained, consistent with an *intermolecular* proton transfer process.

### Scheme 2.5.3. Crossover experiment.



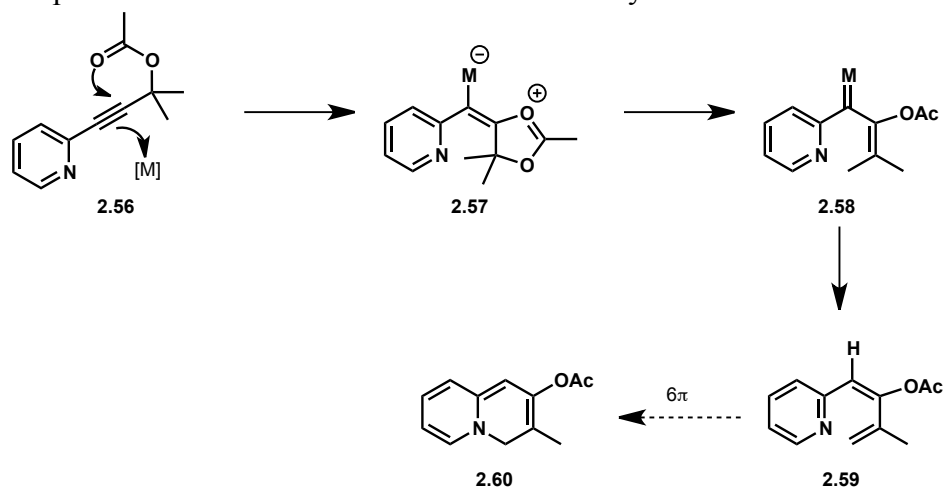
Furthermore, to test our proposed mechanism, it was necessary to determine whether metalcarbenoid formation was an operative pathway. Although we envisioned arriving at the 2,3-disubstituted indolizine through the 1,2-acyl migration mechanism (see Scheme 2.1.4), it is also conceivable that the reaction could proceed via initial isomerization of the propargylic ester to an allene (**2.53**, Scheme 2.5.4).<sup>14</sup>

**Scheme 2.5.4.** Alternative mechanism involving initial isomerization to allene.



A tertiary alcohol-derived substrate, which eliminated the opportunity for isomerization to an allene (see **2.38**→**2.53**), was synthesized and subjected to the reaction conditions. With **2.56** as the substrate, the diene pyridine **2.59** was the only isolated product, which could be accounted for by a formal hydride shift resulting from an initially formed metallocarbenoid (**2.58**). The diene pyridine (**2.59**) was isolated in 8% yield when 10 mol % of the catalyst was used and the majority of the mass balance was accounted for by recovered starting material. In an attempt to increase the amount of diene formed, the catalyst loading was increased to 50 mol %. Still, only 8% of the diene was isolated, but the mass balance could not be accounted for by the remaining starting material. A polar compound was isolated via column chromatography, and analysis by mass spectrometry indicated that the complex contains the platinum salt, one phosphine ligand, and one equivalent of the starting material (**2.56**). The structure of this complex was not elucidated.

**Scheme 2.5.5.** Proposed mechanism for isomerization of tertiary substrate **2.56**.



## 2.6 Future Directions

Future efforts on this project will be focused on optimizing the transformation of tertiary propargylic ester substrates as well as conducting comprehensive kinetic studies of the indolizine formation to gain insight into the mechanism of the cycloisomerization. The first priority is the elucidation of the organoplatinum complex formed from **2.56** via X-ray crystallography. Identification of this complex should provide information to help elucidate the mechanistic puzzle of this reaction and aid in the optimization of the reaction. Additionally, we will search for conditions to effect the  $6\pi$  electrocycloization of the diene (**2.59**) to the 6,6-fused ring system (e.g., **2.60**), which form the core of quinolizidine compounds.

To better quantify the electronic effects of substituents at the propargylic position, kinetic studies will be conducted to determine how electron-withdrawing and electron-donating substituents affect the rate of indolizine formation. Additionally, deuterated versions of substrates with electron-withdrawing and electron-donating propargylic substituents will be synthesized and used to determine (1) whether a kinetic isotope effect is observed in this reaction and (2) if the results of the kinetic isotope studies are the same with electron-withdrawing and electron-donating substituents. This will give an indication as to whether a mechanism change occurs with a change in the electronic properties of the substrate.

## 2.7 Experimental Contributions

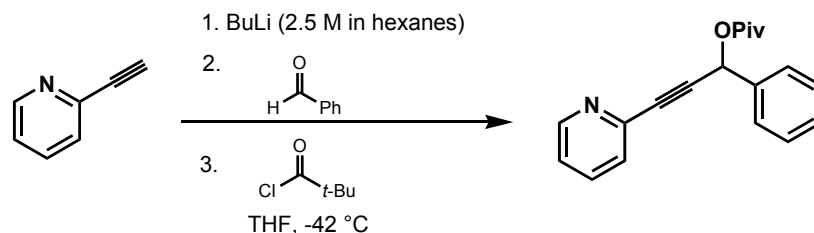
Alison Hardin Narayan carried out the research detailed in Chapter 2.

## 2.8 Experimental Methods

### Materials and Methods

Unless otherwise stated, reactions were performed in flame-dried glassware fitted with rubber septa under a nitrogen atmosphere. Liquid reagents and solvents were transferred via syringe under nitrogen. THF was distilled over sodium/benzophenone ketyl; dichloromethane, benzene and toluene were distilled over calcium hydride. All other solvents were used as received unless otherwise noted. Reaction temperatures above 23 °C were controlled by an IKA<sup>®</sup> temperature modulator. Reactions were monitored by thin layer chromatography using SiliCycle silica gel 60 F254 precoated plates (0.25 mm) which were visualized using UV irradiation, anisaldehyde stain or KMnO<sub>4</sub> stain. SiliCycle Silica-P silica gel (particle size 40-63  $\mu\text{m}$ ) was used for flash chromatography. <sup>1</sup>H and <sup>13</sup>C NMR were recorded on Bruker AVB-400 or DRX-500 MHz spectrometers with <sup>13</sup>C operating frequencies of 100 and 125 MHz, respectively, in benzene-*d*<sub>6</sub> at 23 °C. Chemical shifts ( $\delta$ ) are reported in ppm relative to the residual solvent signal ( $\delta = 7.15$  for <sup>1</sup>H NMR and  $\delta = 128.02$  <sup>13</sup>C NMR). Data for <sup>1</sup>H NMR are reported as follows: chemical shift (multiplicity, coupling constant, number of hydrogens). Multiplicity is abbreviated as follows: s (singlet), d (doublet), t (triplet), q (quartet), m (multiplet). IR spectra were recorded on a Nicolet MAGNA-IR 850 spectrometer and are reported in frequency of absorption ( $\text{cm}^{-1}$ ). Mass spectral data were obtained from the Mass Spectral Facility at the University of California, Berkeley.

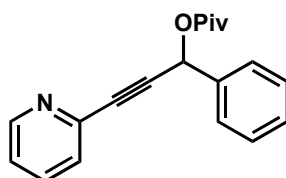
### Scheme 2.7.1.



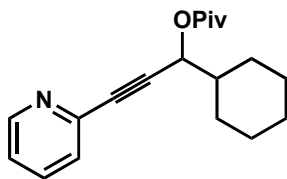
### Representative Procedure for the Synthesis of Substrates

A flame-dried, round-bottom flask was charged with anhydrous THF (50 mL) and 2-ethynylpyridine (490  $\mu\text{L}$ , 4.85 mmol). The solution was cooled to  $-42\text{ }^\circ\text{C}$  and *n*-BuLi (2.5 M in hexanes, 2.3 mL, 5.82 mmol) was added dropwise. The solution was allowed to stir at  $-42\text{ }^\circ\text{C}$  for 90 min, and then benzaldehyde (700  $\mu\text{L}$ , 6.79 mmol) was added dropwise to the reaction mixture at  $-42\text{ }^\circ\text{C}$ . The mixture was stirred for at  $-42\text{ }^\circ\text{C}$  for 2 h, then pivaloyl chloride (900  $\mu\text{L}$ , 7.28 mmol) was added dropwise at  $-42\text{ }^\circ\text{C}$ . The mixture was stirred for at  $-42\text{ }^\circ\text{C}$  for an additional 45 min, then the mixture was allowed to warm to rt. After 3 h, sat. aqueous  $\text{NH}_4\text{Cl}$  solution (30 mL) was added slowly and stirring continued for 10 min. The mixture was diluted with EtOAc (50 mL). The aqueous layer was extracted with EtOAc (3 x 30 mL). The organic layers were combined, washed with brine (60 mL) and dried over  $\text{MgSO}_4$ . The solvent was removed under reduced pressure and the crude mixture was purified by flash chromatography (4:1 hexanes/EtOAc) to obtain a yellow crystalline solid (1.18 g, 83% yield).

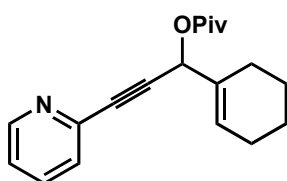
### Spectral Data for Substrates



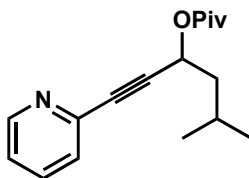
**1-Phenyl-3-(pyridin-2-yl)prop-2-ynyl pivalate:** Yellow oil, 83% yield;  $R_f$  (3:1 hexanes/EtOAc) 0.24;  $^1\text{H NMR}$  (300 MHz,  $\text{C}_6\text{D}_6$ )  $\delta$  8.32 (d,  $J = 4.8$  Hz, 1H), 7.58 (dd,  $J = 7.9, 1.2$  Hz, 2H), 7.12-6.96 (m, 4H), 6.93 (s, 1H), 6.75 (dt,  $J = 7.8, 1.7$  Hz, 1H), 6.47-6.39 (m, 1H), 1.10 (s, 9H);  $^{13}\text{C NMR}$  (125 MHz,  $\text{C}_6\text{D}_6$ )  $\delta$  176.6, 150.3, 143.2, 137.7, 135.5, 129.0, 128.9, 128.3, 127.3, 123.0, 87.0, 85.9, 66.0, 38.8, 27.0; **IR** (film)  $\nu_{\text{max}}$  2974, 1734, 1583, 1464, 1428, 1275, 1138, 697  $\text{cm}^{-1}$ ; **MS** ( $\text{EI}^+$ ):  $m/z$  293 ( $\text{M}^+$ ); **HRMS** ( $\text{EI}^+$ ) calcd for  $[\text{C}_{19}\text{H}_{19}\text{NO}_2]^+$ :  $m/z$  293.1416, found 293.1411.



**1-Cyclohexyl-3-(pyridin-2-yl)prop-2-ynyl pivalate:** Yellow oil, 55% yield;  $R_f$  (3:1 hexanes/EtOAc) 0.30;  $^1\text{H NMR}$  (400 MHz,  $\text{C}_6\text{D}_6$ )  $\delta$  8.41-8.30 (m, 1H), 7.04 (td,  $J = 7.8, 1.0$  Hz, 1H), 6.80-6.72 (m, 1H), 6.43 (ddd,  $J = 7.62, 4.9, 1.1$  Hz, 1H), 5.68 (d,  $J = 6.1$  Hz, 1H), 1.90 (dd,  $J = 45.6, 12.5$  Hz, 2H), 1.67-1.40 (m, 4H), 1.18 (s, 9H), 1.13-0.94 (m, 4H);  $^{13}\text{C NMR}$  (125 MHz,  $\text{C}_6\text{D}_6$ )  $\delta$  176.8, 150.2, 143.4, 135.5, 127.3, 122.8, 86.4, 85.9, 68.4, 42.4, 39.0, 28.7, 27.2, 26.4, 26.1; **IR** (film)  $\nu_{\text{max}}$  2931, 2855, 1734, 1583, 1464, 1428, 1281, 1151, 976, 779  $\text{cm}^{-1}$ ; **MS** ( $\text{EI}^+$ ):  $m/z$  299 ( $\text{M}^+$ ); **HRMS** ( $\text{EI}^+$ ) calcd for  $[\text{C}_{19}\text{H}_{25}\text{NO}_2]^+$ :  $m/z$  299.1885, found 299.1884.

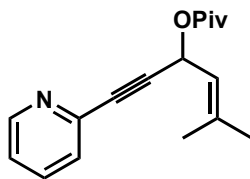


**1-Cyclohexenyl-30(pyridine-2-yl)prop-2-ynyl pivalate:** Yellow oil, 72% yield;  $R_f$  (3:1 hexanes/EtOAc) 0.28;  $^1\text{H NMR}$  (400 MHz,  $\text{C}_6\text{D}_6$ )  $\delta$  8.36-8.32 (m, 1H), 7.04 (td,  $J = 7.8, 1.0$  Hz, 1H), 6.75 (dt,  $J = 7.8, 1.8$  Hz, 1H), 6.42 (ddd,  $J = 7.6, 4.9, 1.2$  Hz, 1H), 6.34 (s, 1H), 6.04 (d,  $J = 1.0$  Hz, 1H), 2.42-2.01 (m, 2H), 1.86-1.73 (m, 2H), 1.54-1.41 (m, 2H), 1.39-1.27 (m, 2H), 1.16 (s, 9H);  $^{13}\text{C NMR}$  (100 MHz,  $\text{C}_6\text{D}_6$ )  $\delta$  176.6, 150.2, 143.4, 135.5, 133.7, 127.3, 122.8, 86.2, 85.8, 68.2, 39.0, 27.3, 27.2, 25.2, 24.9, 22.7, 22.3; **IR** (film)  $\nu_{\text{max}}$  2932, 1733, 1582, 1463, 1428, 1274, 1143, 1030, 779  $\text{cm}^{-1}$ ; **MS** ( $\text{EI}^+$ ):  $m/z$  297 ( $\text{M}^+$ ); **HRMS** ( $\text{EI}^+$ ) calcd for  $[\text{C}_{19}\text{H}_{23}\text{NO}_2]^+$ :  $m/z$  297.1729, found 297.1733.

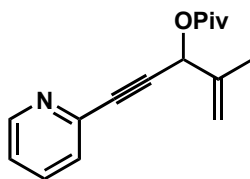


**5-Methyl-1-(pyridine-2-yl)hex-1-yn-3-yl pivalate:** Yellow oil, 53% yield;  $R_f$  (3:1 hexanes/EtOAc) 0.37;  $^1\text{H NMR}$  (400 MHz,  $\text{C}_6\text{D}_6$ )  $\delta$  8.35 (d,  $J = 4.8$  Hz, 1H), 7.05 (d,  $J = 7.8$  Hz, 1H), 6.77 (dt,  $J = 7.7, 1.6$  Hz, 1H), 6.43 (dd,  $J = 7.5, 4.9$  Hz, 1H), 5.90 (t,  $J = 7.1$  Hz, 1H), 1.93-1.72 (m, 2H), 1.70-1.61 (m, 1H), 1.17 (s, 9H), 0.80 (d,  $J = 6.6$  Hz, 6H);  $^{13}\text{C NMR}$  (100 MHz,  $\text{C}_6\text{D}_6$ )  $\delta$  176.8, 150.3, 143.4, 135.5, 122.8, 87.3, 85.3, 63.1, 43.7, 38.8, 27.1, 25.1, 22.5, 22.3; **IR** (film)  $\nu_{\text{max}}$  2960, 1732, 1583, 1464, 1428, 1368, 1281, 1151, 780  $\text{cm}^{-1}$ ; **MS** ( $\text{EI}^+$ ):  $m/z$  273 ( $\text{M}^+$ ); **HRMS** ( $\text{EI}^+$ ) calcd for  $[\text{C}_{17}\text{H}_{23}\text{NO}_2]^+$ :  $m/z$  273.1729, found 273.1731.

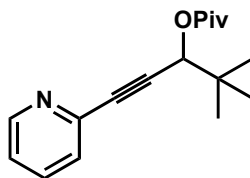




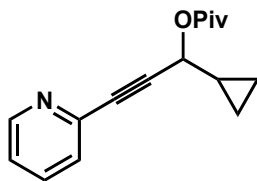
**5-Methyl-1-(pyridine-2-yl)hex-4-en-1-yn-3-yl pivalate:** Yellow oil, 82% yield;  $R_f$  (3:1 hexanes/EtOAc) 0.40;  $^1\text{H NMR}$  (400 MHz,  $\text{C}_6\text{D}_6$ )  $\delta$  8.33 (dd,  $J = 4.8, 0.7$  Hz, 1H), 7.06 (d,  $J = 7.8$  Hz, 1H), 6.76 (dt,  $J = 7.7, 1.8$  Hz, 1H), 6.63 (d,  $J = 9.0$  Hz, 1H), 6.43 (ddd,  $J = 7.6, 4.8, 1.1$  Hz, 1H), 5.58-5.53 (m, 1H), 1.54 (d,  $J = 1.2$  Hz, 3H), 1.41 (d,  $J = 1.2$  Hz, 3H), 1.16 (s, 9H);  $^{13}\text{C NMR}$  (100 MHz,  $\text{C}_6\text{D}_6$ )  $\delta$  176.7, 150.3, 143.5, 139.3, 135.5, 127.3, 122.8, 121.2, 86.8, 85.2, 61.6, 38.9, 27.2, 25.5, 18.2; **IR** (film)  $\nu_{\text{max}}$  2973, 1730, 1582, 1463, 1428, 1275, 1145, 924, 778  $\text{cm}^{-1}$ ; **MS** ( $\text{EI}^+$ ):  $m/z$  271 ( $\text{M}^+$ ); **HRMS** ( $\text{EI}^+$ ) calcd for  $[\text{C}_{17}\text{H}_{21}\text{NO}_2]^+$ :  $m/z$  271.1572, found 271.1573.



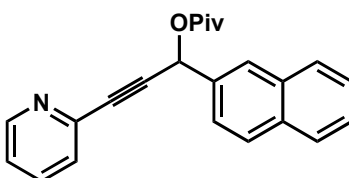
**4-Methyl-1-(pyridin-2-yl)pent-4-en-1-yn-3-yl pivalate:** Yellow oil, 76%;  $R_f$  (3:1 hexanes/EtOAc) 0.38;  $^1\text{H NMR}$  (400 MHz,  $\text{C}_6\text{D}_6$ )  $\delta$  8.32 (d,  $J = 4.0$  Hz, 1H), 7.00 (td,  $J = 7.8, 1.0$  Hz, 1H), 6.77 (dt,  $J = 7.7, 1.8$  Hz, 1H), 6.44 (ddd,  $J = 7.6, 4.8, 1.1$  Hz, 1H), 6.30 (s, 1H), 5.30 (d,  $J = 0.9$  Hz, 1H), 4.84 (s, 1H), 1.79 (s, 3H), 1.13 (s, 9H);  $^{13}\text{C NMR}$  (100 MHz,  $\text{C}_6\text{D}_6$ )  $\delta$  176.4, 150.3, 143.2, 140.7, 135.5, 127.3, 122.9, 115.0, 86.3, 85.2, 67.4, 38.9, 27.1, 18.5; **IR** (film)  $\nu_{\text{max}}$  2976, 1735, 1582, 1464, 1429, 1276, 1142, 976, 933, 780  $\text{cm}^{-1}$ ; **MS** ( $\text{EI}^+$ ):  $m/z$  257 ( $\text{M}^+$ ); **HRMS** ( $\text{EI}^+$ ) calcd for  $[\text{C}_{16}\text{H}_{19}\text{NO}_2]^+$ :  $m/z$  257.1416, found 257.1419.



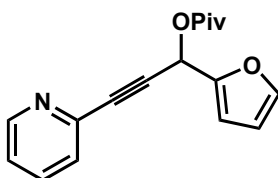
**4,4-Dimethyl-1-(pyridin-2-yl)pent-1-yn-3-yl pivalate:** Yellow oil, 69% yield;  $R_f$  (3:1 hexanes/EtOAc) 0.36;  $^1\text{H NMR}$  (400 MHz,  $\text{C}_6\text{D}_6$ )  $\delta$  8.32 (d,  $J = 4.14$  Hz, 1H), 7.02 (d,  $J = 7.8$  Hz, 1H), 6.77 (dt,  $J = 7.7, 1.8$  Hz, 1H), 6.44 (ddd,  $J = 7.6, 4.8, 1.1$  Hz, 1H), 5.58 (s, 1H), 1.16 (s, 9H), 1.03 (s, 9H);  $^{13}\text{C NMR}$  (100 MHz,  $\text{C}_6\text{D}_6$ )  $\delta$  176.6, 150.2, 143.4, 135.5, 128.3, 127.3, 122.8, 85.9, 72.0, 35.7, 27.2, 25.7; **IR** (film)  $\nu_{\text{max}}$  2971, 1735, 1583, 1464, 1428, 1278, 1147, 973, 780  $\text{cm}^{-1}$ ; **MS** ( $\text{EI}^+$ ):  $m/z$  273 ( $\text{M}^+$ ); **HRMS** ( $\text{EI}^+$ ) calcd for  $[\text{C}_{17}\text{H}_{23}\text{NO}_2]^+$ :  $m/z$  273.1729, found 273.1725.



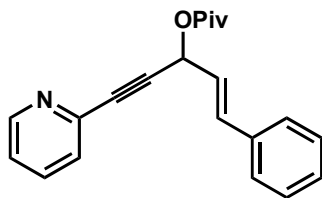
**1-Cyclopropyl-3-(pyridin-2-yl)prop-2-ynyl pivalate:** Yellow oil, 56% yield;  $R_f$  (3:1 hexanes/EtOAc) 0.33;  $^1\text{H NMR}$  (500 MHz,  $\text{C}_6\text{D}_6$ )  $\delta$  8.32 (d,  $J = 4.4$  Hz, 1H), 7.02 (d,  $J = 7.8$  Hz, 1H), 6.76 (dt,  $J = 7.7, 1.8$  Hz, 1H), 6.43 (ddd,  $J = 7.6, 4.8, 1.1$  Hz, 1H), 5.59 (d,  $J = 7.2$  Hz, 1H), 1.28-1.21 (m, 1H), 1.18 (s, 9H), 0.51-0.47 (m, 2H), 0.35-0.25 (m, 2H);  $^{13}\text{C NMR}$  (125 MHz,  $\text{C}_6\text{D}_6$ )  $\delta$  176.9, 150.3, 143.3, 135.5, 127.3, 122.8, 85.4, 67.6, 38.9, 27.2, 15.1, 3.7, 2.6; **IR** (film)  $\nu_{\text{max}}$  2974, 1731, 1582, 1464, 1429, 1278, 1148, 1031, 968, 780  $\text{cm}^{-1}$ .



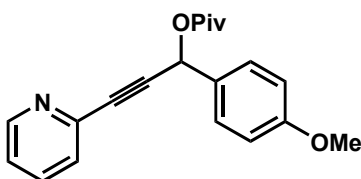
**1-(Naphthalen-3-yl)-3-(pyridine-2-yl)prop-2-ynyl pivalate:** Yellow oil, 68% yield;  $R_f$  (3:1 hexanes/EtOAc) 0.27;  $^1\text{H NMR}$  (400 MHz,  $\text{C}_6\text{D}_6$ )  $\delta$  8.34 (dd,  $J = 4.8, 0.8$  Hz, 1H), 8.00 (d,  $J = 0.5$  Hz, 1H), 7.72 (dd,  $J = 8.5, 1.7$  Hz, 1H), 7.58 (d,  $J = 8.6$  Hz, 1H), 7.53 (dd,  $J = 5.9, 3.3$  Hz, 2H), 7.21-7.17 (m, 2H), 7.09 (s, 1H), 7.04 (td,  $J = 7.8, 1.0, 1.0$  Hz, 1H), 6.75 (dt,  $J = 7.7, 1.8$  Hz, 1H), 6.43 (ddd,  $J = 7.6, 4.8, 1.2$  Hz, 1H), 1.13 (s, 9H);  $^{13}\text{C NMR}$  (125 MHz,  $\text{C}_6\text{D}_6$ )  $\delta$  176.6, 150.3, 143.2, 135.5, 135.0, 133.9, 133.6, 129.0, 128.7, 128.3, 127.6, 127.4, 126.7, 126.5, 125.4, 123.0, 87.3, 86.0, 66.3, 38.9, 27.0; **IR** (film)  $\nu_{\text{max}}$  2973, 1732, 1582, 1463, 1428, 1274, 1138  $\text{cm}^{-1}$ ; **MS** ( $\text{EI}^+$ ):  $m/z$  343 ( $\text{M}^+$ ); **HRMS** ( $\text{EI}^+$ ) calcd for  $[\text{C}_{23}\text{H}_{21}\text{NO}_2]^+$ :  $m/z$  343.1572, found 343.1577.



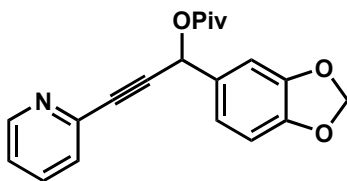
**1-(Furan-2-yl)-3-(pyridin-2-yl)prop-2-ynyl pivalate:** Orange oil, 70% yield;  $R_f$  (3:1 hexanes/EtOAc) 0.23;  $^1\text{H NMR}$  (400 MHz,  $\text{C}_6\text{D}_6$ )  $\delta$  8.32 (d,  $J = 4.2$  Hz, 1H), 7.04-6.95 (m, 3H), 6.76 (dt,  $J = 7.8, 1.7$  Hz, 1H), 6.49 (d,  $J = 3.3$  Hz, 1H), 6.44 (dd,  $J = 7.6, 4.9$  Hz, 1H), 5.93 (dd,  $J = 3.2, 1.9$  Hz, 1H), 1.10 (s, 9H);  $^{13}\text{C NMR}$  (100 MHz,  $\text{C}_6\text{D}_6$ )  $\delta$  176.6, 150.3, 149.9, 143.7, 142.9, 135.5, 127.5, 123.1, 110.8, 110.5, 86.1, 83.5, 59.2, 38.9, 27.0; **IR** (film)  $\nu_{\text{max}}$  2974, 1737, 1583, 1464, 1429, 1273, 1135, 1008, 919, 779, 741  $\text{cm}^{-1}$ ; **MS** ( $\text{EI}^+$ ):  $m/z$  283 ( $\text{M}^+$ ); **HRMS** ( $\text{EI}^+$ ) calcd for  $[\text{C}_{17}\text{H}_{17}\text{NO}_3]^+$ :  $m/z$  283.1208, found 283.1205.



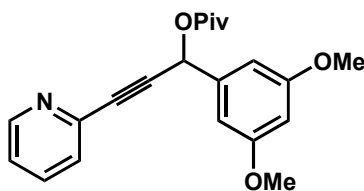
**(E)-5-Phenyl-1-(pyridin-2-yl)pent-4-en-1-yn-3-yl pivalate:** Yellow oil, 56% yield;  $R_f$  (3:1 hexanes/EtOAc) 0.36;  $^1\text{H NMR}$  (500 MHz,  $\text{C}_6\text{D}_6$ )  $\delta$  8.34 (d,  $J = 4.2$  Hz, 1H), 7.11-7.05 (m, 3H), 7.04-6.97 (m, 3H), 6.87 (d,  $J = 15.7$  Hz, 1H), 6.77 (dt,  $J = 7.7, 1.8$  Hz, 1H), 6.48 (dd,  $J = 6.7, 0.9$  Hz, 1H), 6.44 (ddd,  $J = 7.6, 4.8, 1.0$  Hz, 1H), 6.29 (dd,  $J = 15.8, 6.7$  Hz, 1H), 1.17 (s, 9H);  $^{13}\text{C NMR}$  (125 MHz,  $\text{C}_6\text{D}_6$ )  $\delta$  176.7, 150.4, 143.3, 136.2, 135.5, 135.1, 128.7, 128.5, 128.3, 127.3, 124.1, 123.0, 86.9, 85.2, 64.9, 38.9, 27.1; **IR** (film)  $\nu_{\text{max}}$  2973, 1732, 1582, 1464, 1428, 1273, 1140, 965, 779, 693  $\text{cm}^{-1}$ ; **MS** ( $\text{EI}^+$ ):  $m/z$  319 ( $\text{M}^+$ ); **HRMS** ( $\text{EI}^+$ ) calcd for  $[\text{C}_{21}\text{H}_{21}\text{NO}_2]^+$ :  $m/z$  319.1572, found 319.1573.



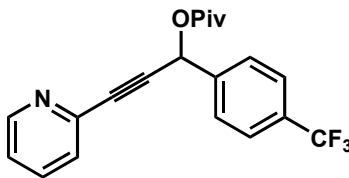
**1-(4-Methoxyphenyl)-3-(pyridine-2-yl)prop-2-ynyl pivalate:** Yellow oil, 81% yield;  $R_f$  (3:1 hexanes/EtOAc) 0.33;  $^1\text{H NMR}$  (400 MHz,  $\text{C}_6\text{D}_6$ )  $\delta$  8.33 (d,  $J = 4.3$  Hz, 1H), 7.54 (d,  $J = 8.7$  Hz, 2H), 7.04 (d,  $J = 7.8$  Hz, 1H), 6.94 (s, 1H), 6.78 (dt,  $J = 7.7, 1.8$  Hz, 1H), 6.68 (d,  $J = 8.7$  Hz, 2H), 6.45 (ddd,  $J = 7.6, 4.8, 1.1$  Hz, 1H), 3.21 (s, 3H), 1.12 (s, 9H);  $^{13}\text{C NMR}$  (125 MHz,  $\text{C}_6\text{D}_6$ )  $\delta$  176.7, 160.5, 150.3, 143.3, 135.5, 129.8, 129.6, 127.3, 122.9, 114.3, 86.9, 86.3, 65.8, 54.7, 38.8, 27.0; **IR** (film)  $\nu_{\text{max}}$  2972, 1732, 1582, 1464, 1251, 1140, 1032, 833, 779  $\text{cm}^{-1}$ ; **MS** ( $\text{EI}^+$ ):  $m/z$  323 ( $\text{M}^+$ ); **HRMS** ( $\text{EI}^+$ ) calcd for  $[\text{C}_{20}\text{H}_{21}\text{NO}_3]^+$ :  $m/z$  323.1521, found 323.1517.



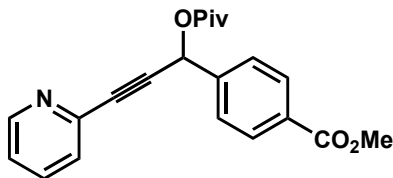
**1-(Benzo[d][1,3]dioxol-5-yl)-3-(pyridine-2-yl)prop-2-ynyl pivalate:** Yellow oil, 92% yield;  $R_f$  (3:1 hexanes/EtOAc) 0.23;  $^1\text{H NMR}$  (400 MHz,  $\text{C}_6\text{D}_6$ )  $\delta$  8.33 (d,  $J = 3.3$  Hz, 1H), 7.18 (d,  $J = 1.7$  Hz, 1H), 7.03-6.97 (m, 2H), 6.83 (s, 1H), 6.75 (dt,  $J = 7.7, 1.6$  Hz, 1H), 6.52 (d,  $J = 8.0$  Hz, 1H), 6.43 (dd,  $J = 7.4, 4.9$  Hz, 1H), 5.20 (d,  $J = 3.6$  Hz, 2H), 1.10 (s, 9H);  $^{13}\text{C NMR}$  (125 MHz,  $\text{C}_6\text{D}_6$ )  $\delta$  176.6, 150.3, 148.6, 148.4, 143.2, 135.5, 131.5, 127.3, 123.0, 122.1, 108.5, 108.4, 101.2, 86.9, 86.0, 65.9, 38.8, 27.0; **IR** (film)  $\nu_{\text{max}}$  2974, 1732, 1582, 1489, 1464, 1249, 1140, 1038, 936, 779  $\text{cm}^{-1}$ ; **MS** ( $\text{EI}^+$ ):  $m/z$  337 ( $\text{M}^+$ ); **HRMS** ( $\text{EI}^+$ ) calcd for  $[\text{C}_{20}\text{H}_{19}\text{NO}_4]^+$ :  $m/z$  337.1314, found 337.1311.



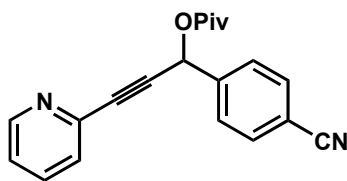
**1-(3,5-dimethoxyphenyl)-3-(pyridin-2-yl)prop-2-ynyl pivalate:** Yellow oil, 90% yield;  $R_f$  (3:1 hexanes/EtOAc) 0.15;  $^1\text{H NMR}$  (400 MHz,  $\text{C}_6\text{D}_6$ )  $\delta$  8.31 (d,  $J = 4.8$  Hz, 1H), 7.00 (d,  $J = 7.8$  Hz, 1H), 6.97-6.94 (m, 3H), 6.75 (dt,  $J = 7.7, 1.6$  Hz, 1H), 6.49 (t,  $J = 2.2$  Hz, 1H), 6.43 (dd,  $J = 7.1, 5.3$  Hz, 1H), 3.27 (s, 6H), 1.13 (s, 9H);  $^{13}\text{C NMR}$  (125 MHz,  $\text{C}_6\text{D}_6$ )  $\delta$  176.6, 161.7, 150.3, 143.2, 140.0, 135.5, 128.6, 127.4, 122.9, 105.8, 101.5, 86.0, 66.0, 54.9, 38.9, 27.1.; **IR** (film)  $\nu_{\text{max}}$  2971, 1735, 1598, 1464, 1429, 1274, 1206, 1139, 1068, 779  $\text{cm}^{-1}$ ; **MS** ( $\text{EI}^+$ ):  $m/z$  353 ( $\text{M}^+$ ); **HRMS** ( $\text{EI}^+$ ) calcd for  $[\text{C}_{21}\text{H}_{23}\text{NO}_4]^+$ :  $m/z$  353, 1627, found 353.1628.



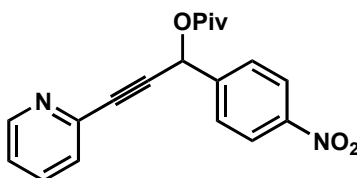
**1-(4-(trifluoromethyl)phenyl)-3-(pyridine-2-yl)prop-2-ynyl pivalate:** Yellow oil, 78% yield;  $R_f$  (3:1 hexanes:EtOAc) 0.27;  $^1\text{H NMR}$  (400 MHz,  $\text{C}_6\text{D}_6$ )  $\delta$  8.33 (d,  $J = 4.6$  Hz, 1H), 7.36 (d,  $J = 8.2$  Hz, 2H), 7.24 (d,  $J = 8.2$  Hz, 2H), 7.02 (d,  $J = 7.8$  Hz, 1H), 6.80-6.73 (m, 2H), 6.50-6.38 (m, 1H), 1.10 (s, 9H);  $^{13}\text{C NMR}$  (100 MHz,  $\text{C}_6\text{D}_6$ )  $\delta$  176.3, 150.3, 142.7, 141.1, 135.5, 128.0, 127.8, 127.2, 125.7, 125.7, 123.1, 87.3, 84.9, 65.0, 38.7, 26.8; **IR** (film)  $\nu_{\text{max}}$  2976, 1737, 1583, 1464, 1429, 1326, 1132, 1068, 1019, 779  $\text{cm}^{-1}$ ; **MS** ( $\text{EI}^+$ ):  $m/z$  361 ( $\text{M}^+$ ); **HRMS** ( $\text{EI}^+$ ) calcd for  $[\text{C}_{20}\text{H}_{18}\text{F}_3\text{NO}_2]^+$ :  $m/z$  361.1299, found 361.1302.



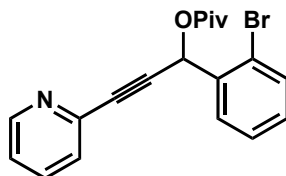
**Methyl 4-(1-(pivaloyloxy)-3-(pyridin-2-yl)prop-2-ynyl)benzoate:** White solid, 73% yield;  $R_f$  (3:1 hexanes/EtOAc) 0.17;  $^1\text{H NMR}$  (500 MHz,  $\text{C}_6\text{D}_6$ )  $\delta$  8.31 (d,  $J = 4.1$  Hz, 1H), 8.03 (d,  $J = 8.4$  Hz, 2H), 7.49 (d,  $J = 8.2$  Hz, 2H), 7.00 (d,  $J = 7.8$  Hz, 1H), 6.82 (s, 1H), 6.76 (dt,  $J = 7.7, 1.8$  Hz, 1H), 6.44 (ddd,  $J = 7.6, 4.8, 1.1$  Hz, 1H), 3.44 (s, 3H), 1.09 (s, 9H);  $^{13}\text{C NMR}$  (125 MHz,  $\text{C}_6\text{D}_6$ )  $\delta$  176.4, 166.1, 150.4, 143.0, 142.1, 135.5, 131.1, 130.3, 127.3, 123.1, 87.4, 85.2, 65.4, 51.6, 38.8, 27.0; **IR** (film)  $\nu_{\text{max}}$  2974, 1727, 1582, 1464, 1429, 1278, 1137, 1021, 779, 704  $\text{cm}^{-1}$ ; **MS** ( $\text{EI}^+$ ):  $m/z$  351 ( $\text{M}^+$ ); **HRMS** ( $\text{EI}^+$ ) calcd for  $[\text{C}_{21}\text{H}_{21}\text{NO}_4]^+$ :  $m/z$  351.1471, found 351.1470.



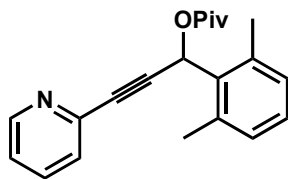
**1-(4-Cyanophenyl)-3-(pyridin-2-yl)prop-2-ynyl pivalate:** Yellow solid, 77% yield;  $R_f$  (3:1 hexanes/EtOAc) 0.20;  $^1\text{H NMR}$  (500 MHz,  $\text{C}_6\text{D}_6$ )  $\delta$  8.30 (d,  $J = 4.8$  Hz, 1H), 7.16 (d,  $J = 8.3$  Hz, 2H), 7.01 (d,  $J = 7.8$  Hz, 1H), 6.92 (d,  $J = 8.3$  Hz, 2H), 6.78 (dt,  $J = 7.7, 1.7$  Hz, 1H), 6.63 (s, 1H), 6.45 (ddd,  $J = 7.6, 4.8, 0.8$  Hz, 1H), 1.08 (s, 9H);  $^{13}\text{C NMR}$  (125 MHz,  $\text{C}_6\text{D}_6$ )  $\delta$  176.3, 150.5, 142.7, 141.7, 135.6, 132.4, 128.3, 127.3, 123.3, 118.3, 113.2, 87.6, 84.5, 65.1, 38.8, 26.9; **IR** (film)  $\nu_{\text{max}}$  2974, 2230, 1737, 1582, 1464, 1429, 1276, 1135, 1032, 780  $\text{cm}^{-1}$ ; **MS** ( $\text{EI}^+$ ):  $m/z$  318 ( $\text{M}^+$ ); **HRMS** ( $\text{EI}^+$ ) calcd for  $[\text{C}_{20}\text{H}_{18}\text{N}_2\text{O}_2]^+$ :  $m/z$  318.1368, found 318.1368.



**1-(4-Nitrophenyl)-3-(pyridin-2-yl)prop-2-ynyl pivalate:** Orange oil, 80% yield;  $R_f$  (3:1 hexanes/EtOAc) 0.25;  $^1\text{H NMR}$  (400 MHz,  $\text{C}_6\text{D}_6$ )  $\delta$  8.31 (d,  $J = 4.1$  Hz, 1H), 7.69 (d,  $J = 8.8$  Hz, 2H), 7.18 (d,  $J = 8.6$  Hz, 2H), 7.03 (d,  $J = 7.8$  Hz, 1H), 6.77 (dt,  $J = 7.8, 1.8$  Hz, 1H), 6.65 (s, 1H), 6.44 (ddd,  $J = 7.6, 4.8, 1.1$  Hz, 1H), 1.10 (s, 9H);  $^{13}\text{C NMR}$  (100 MHz,  $\text{C}_6\text{D}_6$ )  $\delta$  176.3, 150.5, 148.3, 143.5, 142.6, 135.7, 128.3, 127.3, 123.9, 123.4, 87.8, 84.4, 64.8, 38.8, 26.9; **IR** (film)  $\nu_{\text{max}}$  2974, 1747, 1595, 1519, 1480, 1345, 1269, 1098, 855, 738  $\text{cm}^{-1}$ ; **MS** ( $\text{EI}^+$ ):  $m/z$  338 ( $\text{M}^+$ ); **HRMS** ( $\text{EI}^+$ ) calcd for  $[\text{C}_{19}\text{H}_{18}\text{N}_2\text{O}_4]^+$ :  $m/z$  338.1267, found 338.1260.

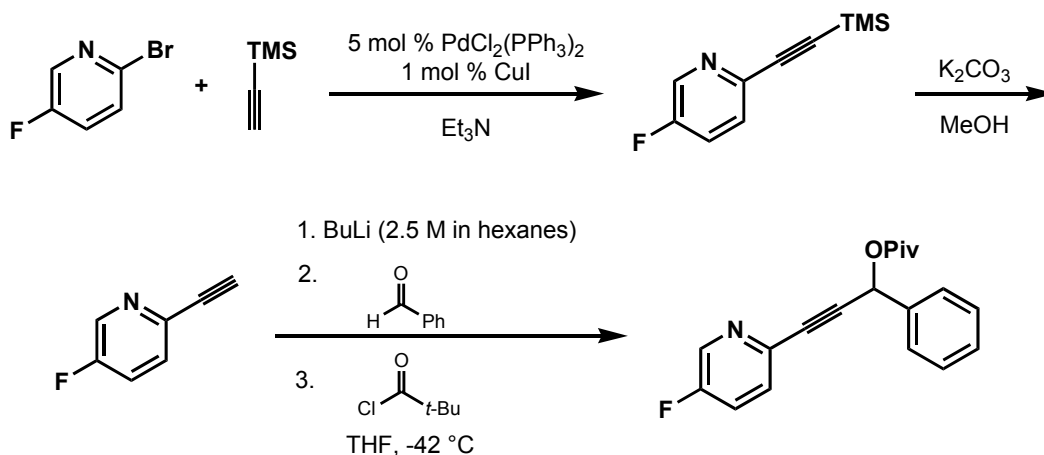


**1-(2-Bromophenyl)-3-(pyridin-2-yl)prop-2-ynyl pivalate:** Yellow oil, 83% yield;  $R_f$  (3:1 hexanes/EtOAc) 0.23;  $^1\text{H NMR}$  (400 MHz,  $\text{C}_6\text{D}_6$ )  $\delta$  8.32 (d,  $J = 4.1$  Hz, 1H), 7.95 (d,  $J = 7.7$  Hz, 1H), 7.29 (s, 1H), 7.24 (dd,  $J = 8.0, 1.1$  Hz, 1H), 7.00 (d,  $J = 7.8$  Hz, 1H), 6.87 (dt,  $J = 7.7, 1.1$  Hz, 1H), 6.74 (dt,  $J = 7.8, 1.6$  Hz, 1H), 6.62 (dt,  $J = 7.9, 1.6$  Hz, 1H), 6.46-6.40 (m, 1H), 1.14 (s, 9H);  $^{13}\text{C NMR}$  (100 MHz,  $\text{C}_6\text{D}_6$ )  $\delta$  176.2, 150.2, 136.6, 135.5, 133.3, 130.5, 130.2, 123.8, 123.0, 87.4, 85.0, 65.8, 60.0, 38.9, 27.1, 20.5, 14.2; **IR** (film)  $\nu_{\text{max}}$  2973, 1737, 1582, 1464, 1429, 1275, 1135, 1028, 779  $\text{cm}^{-1}$ ; **MS** ( $\text{EI}^+$ ):  $m/z$  371 ( $\text{M}^+$ ); **HRMS** ( $\text{EI}^+$ ) calcd for  $[\text{C}_{19}\text{H}_{18}\text{BrNO}_2]^+$ :  $m/z$  371.0520, found 371.0511.



**1-(2,6-dimethylphenyl)-3-(pyridin-2-yl)prop-2-ynyl pivalate:** Yellow oil, 80% yield;  $R_f$  (3:1 hexanes/EtOAc) 0.23;  $^1\text{H NMR}$  (400 MHz,  $\text{C}_6\text{D}_6$ )  $\delta$  8.30 (d,  $J = 4.8$  Hz, 1H), 7.44 (s, 1H), 6.99-6.91 (m, 2H), 6.89-6.84 (m, 2H), 6.74 (dt,  $J = 7.7, 1.8$  Hz, 1H), 6.42 (ddd,  $J = 7.6, 4.8, 1.1$  Hz, 1H), 2.65 (s, 6H), 1.07 (s, 9H);  $^{13}\text{C NMR}$  (100 MHz,  $\text{C}_6\text{D}_6$ )  $\delta$  176.6, 150.3, 143.3, 137.8, 135.5, 134.1, 129.5, 129.0, 127.2, 122.8, 86.4, 85.7, 62.4, 38.9, 27.1, 20.5; **IR** (film)  $\nu_{\text{max}}$  2974, 1732, 1582, 1463, 1428, 1275, 1141, 1032, 938, 777  $\text{cm}^{-1}$ ; **MS** ( $\text{EI}^+$ ):  $m/z$  321 ( $\text{M}^+$ ); **HRMS** ( $\text{EI}^+$ ) calcd for  $[\text{C}_{21}\text{H}_{23}\text{NO}_2]^+$ :  $m/z$  321.1729, found 321.1724.

### Scheme 2.7.2



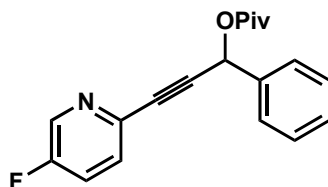
### Representative Procedure for Substituted Pyridine Substrates:

$\text{PdCl}_2(\text{PPh}_3)_2$  (123 mg, 0.180 mmol),  $\text{CuI}$  (7 mg, 0.04 mmol), 2-bromo-5-fluoropyridine (616 mg, 3.5 mmol), and  $\text{Et}_3\text{N}$  (18 mL) were combined in a flame-dried round-bottom flask equipped with a stir bar. The mixture was sparged with nitrogen for 10 min. The nitrogen line was removed and trimethylsilylacetylene (600  $\mu\text{L}$ , 4.03 mmol) was added via syringe. The rubber septum was removed and replaced with a plastic cap. The reaction mixture turned from cloudy yellow to cloudy green then cloudy brown over a 3 min period. The reaction mixture was stirred at room temperature for 12 h. The mixture was concentrated under reduced pressure and the remaining residue was dissolved in dichloromethane (20 mL). The solution was diluted with water (30 mL). The aqueous layer was extracted with dichloromethane (3 x 20 mL). The combined organic layers were washed with brine (40 mL), dried over  $\text{MgSO}_4$  and concentrated under reduced pressure. The crude mixture was purified via flash chromatography (9:1 hexanes/EtOAc) to obtain a yellow oil (559 mg, 91% yield).

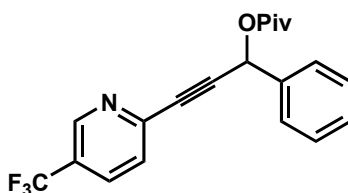
The trimethylsilyl alkyne (559 mg, 3.2 mmol) was combined with potassium carbonate (885 mg, 6.4 mmol) and methanol (30 mL) in a round-bottom flask. The mixture was stirred under a nitrogen atmosphere at rt for 2 h. The mixture was diluted with water (30 mL). The aqueous layer was extracted with dichloromethane (3 x 20 mL). The organic layers were combined and washed with brine (40 mL) and dried over MgSO<sub>4</sub>. The solvent was removed under reduced pressure to provide a light yellow oil (357 mg, 94% yield).

The ethynyl pyridine was added into benzaldehyde and acylated as previously described.

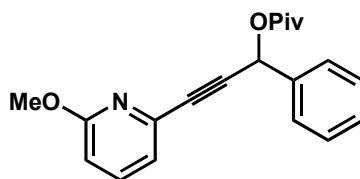
### Spectral Data for Substituted Pyridine Substrates



**3-(5-fluoropyridin-2-yl)-1-phenylprop-2-ynyl pivalate:** Colorless oil, 75%; **R<sub>f</sub>** (3:1 hexanes/EtOAc) 0.56; **<sup>1</sup>H NMR** (500 MHz, C<sub>6</sub>D<sub>6</sub>) δ 8.09 (d, *J* = 2.6 Hz, 1H), 7.56 (d, *J* = 7.4 Hz, 2H), 7.08 (t, *J* = 7.8 Hz, 2H), 7.05-7.00 (m, 1H), 6.90 (s, 1H), 6.75-6.70 (m, 1H), 6.37-6.30 (m, 1H), 1.11 (s, 9H); **<sup>13</sup>C NMR** (125 MHz, C<sub>6</sub>D<sub>6</sub>) δ 176.6, 159.9, 157.8, 138.8, 138.6, 137.6, 129.0, 128.9, 128.3, 127.9, 122.5, 85.9, 65.9, 38.8, 27.0; **IR** (film)  $\nu_{\max}$  2974, 1735, 1578, 1474, 1383, 1271, 1224, 1139, 1031, 839, 698 cm<sup>-1</sup>.

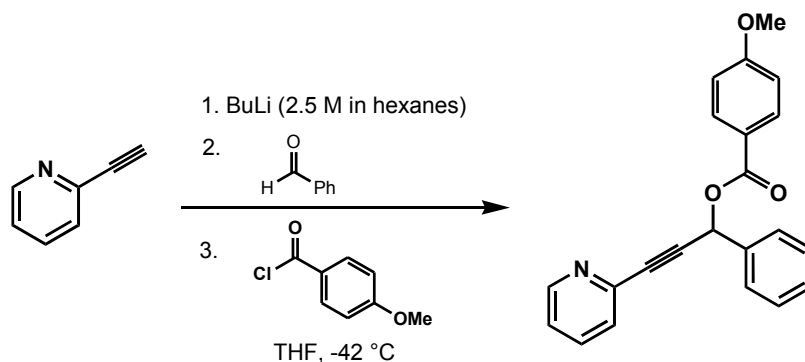


**3-(5-(Trifluoromethyl)pyridin-2-yl)-1-phenylprop-2-ynyl pivalate:** Yellow oil, 61% yield; **R<sub>f</sub>** (3:1 hexanes/EtOAc) 0.71; **<sup>1</sup>H NMR** (500 MHz, C<sub>6</sub>D<sub>6</sub>) δ 8.58 (s, 1H), 7.54 (d, *J* = 8.6 Hz, 2H), 7.13-7.07 (m, 2H), 7.07-7.02 (m, 1H), 6.94 (dd, *J* = 8.2, 2.0 Hz, 1H), 6.86 (s, 1H), 6.74 (d, *J* = 8.2 Hz, 1H), 1.11 (s, 9H); **<sup>13</sup>C NMR** (125 MHz, C<sub>6</sub>D<sub>6</sub>) δ 176.570, 146.91 (q, *J* = 4.13 Hz, 1C), 146.927, 146.895, 146.863, 146.188, 137.182, 132.890, 132.862, 129.205, 129.006, 127.879, 126.841, 88.539, 85.772, 65.794, 38.843, 26.984, 26.377; **IR** (film)  $\nu_{\max}$  2974, 1736, 1600, 1481, 1327, 1136, 1082, 1012, 697 cm<sup>-1</sup>.



**3-(6-Methoxypyridin-2-yl)-1-phenylprop-2-ynyl pivalate:** Yellow oil, 79% yield;  $R_f$  (2:1 hexanes/EtOAc) 0.66;  $^1\text{H NMR}$  (400 MHz,  $\text{C}_6\text{D}_6$ )  $\delta$  7.56 (d,  $J = 7.0$  Hz, 2H), 7.11-7.05 (m, 2H), 7.05-7.00 (m, 1H), 6.94 (s, 1H), 6.78-6.73 (m, 2H), 6.44-6.38 (m, 1H), 3.68 (s, 3H), 1.10 (s, 9H);  $^{13}\text{C NMR}$  (100 MHz,  $\text{C}_6\text{D}_6$ )  $\delta$  176.5, 164.2, 140.0, 138.4, 137.8, 128.9, 128.9, 127.9, 121.0, 111.7, 86.9, 85.6, 66.0, 53.4, 38.8, 27.0; **IR** (film)  $\nu_{\text{max}}$  2976, 1735, 1570, 1464, 1429, 1260, 1138, 1020, 803, 699  $\text{cm}^{-1}$ ; **MS** ( $\text{EI}^+$ ):  $m/z$  323 ( $\text{M}^+$ ); **HRMS** ( $\text{EI}^+$ ) calcd for  $[\text{C}_{20}\text{H}_{21}\text{NO}_3]^+$ :  $m/z$  323.1521, found 323.1521.

### Scheme 2.7.3.

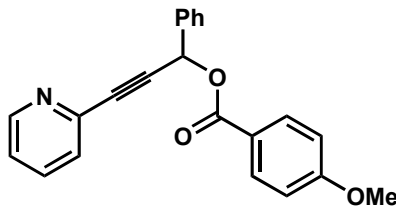


### Representative Procedure for 4-Methoxybenzoate Substrates

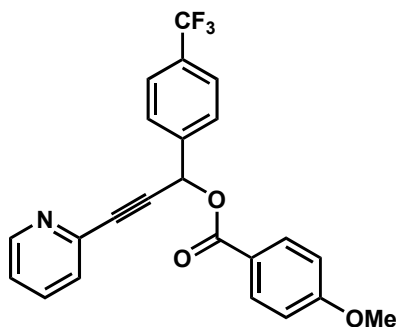
A flame-dried, round-bottom flask was charged with anhydrous THF (27 mL) and 2-ethynylpyridine (280  $\mu\text{L}$ , 2.75 mmol). The solution was cooled to  $-42$   $^\circ\text{C}$  and *n*-BuLi (1.21 mL, 3.03 mmol, 2.5 M in hexanes) was added dropwise. The solution was allowed to stir at  $-42$   $^\circ\text{C}$  for 90 min, and then benzaldehyde (335  $\mu\text{L}$ , 3.30 mmol) was added dropwise to the reaction mixture at  $-42$   $^\circ\text{C}$ . The mixture was stirred at  $-42$   $^\circ\text{C}$  for 2 h, then 4-methoxybenzoyl chloride (521  $\mu\text{L}$ , 3.85 mmol) was added dropwise at  $-42$   $^\circ\text{C}$ . The mixture was stirred at  $-42$   $^\circ\text{C}$  for an additional 90 min, then the mixture was allowed to warm to rt. After 3 h, sat. aqueous  $\text{NH}_4\text{Cl}$  solution (25 mL) was added slowly and stirring continued for 10 min. The mixture was diluted with EtOAc (20 mL). The aqueous layer was extracted with EtOAc (3 x 20 mL). The organic layers were combined, washed with brine (30 mL) and dried over  $\text{MgSO}_4$ . The solvent was removed under reduced pressure and the crude mixture was purified via flash chromatography (4:1 hexanes/EtOAc) to obtain a yellow oil (724.6 mg, 77% yield).



## Spectral Data for 4-Methoxybenzoate Substrates

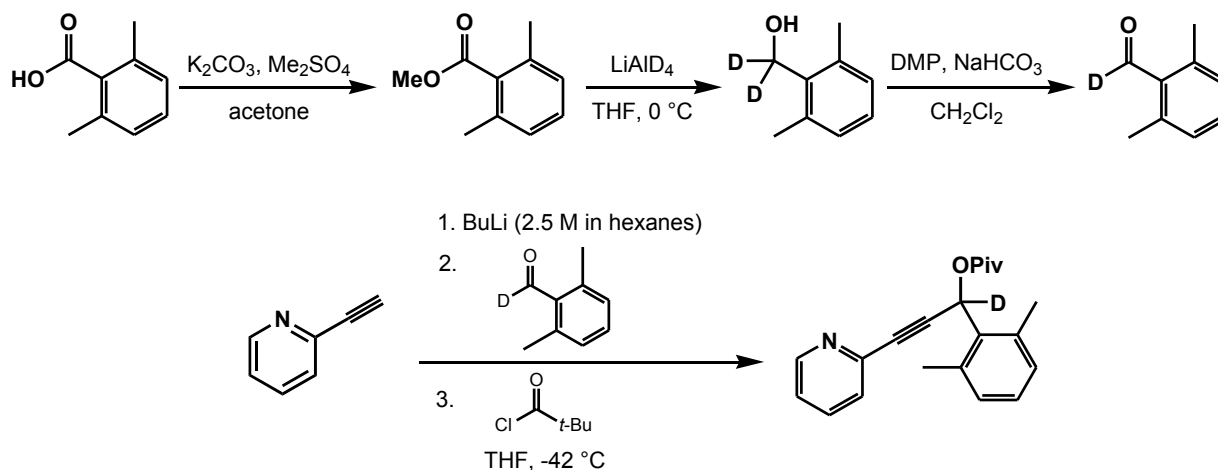


**1-Phenyl-3-(pyridin-2-yl)prop-2-ynyl 4-methoxybenzoate:** Yellow oil, 77% yield;  $R_f$  (3:1 hexanes/EtOAc) 0.10;  $^1\text{H NMR}$  (400 MHz,  $\text{C}_6\text{D}_6$ )  $\delta$  8.34 (d,  $J = 4.1$  Hz, 1H), 8.10 (d,  $J = 9.0$  Hz, 2H), 7.69 (d,  $J = 7.1$  Hz, 2H), 7.20 (s, 1H), 7.12-7.01 (m, 3H), 6.98 (td,  $J = 7.8, 1.0$  Hz, 1H), 6.75 (dt,  $J = 7.8, 1.8$  Hz, 1H), 6.56-6.51 (m, 2H), 6.43 (ddd,  $J = 7.6, 4.9, 1.1$  Hz, 1H), 3.08 (s, 3H);  $^{13}\text{C NMR}$  (100 MHz,  $\text{C}_6\text{D}_6$ )  $\delta$  165.1, 163.9, 150.2, 143.2, 137.6, 135.5, 132.4, 129.0, 128.9, 127.9, 127.4, 123.0, 122.6, 113.9, 87.3, 86.1, 66.5, 54.8; **IR** (film)  $\nu_{\text{max}}$  2974, 1716, 1606, 1582, 1511, 1463, 1253, 1167, 1091, 768  $\text{cm}^{-1}$ ; **MS** ( $\text{EI}^+$ ):  $m/z$  343 ( $\text{M}^+$ ); **HRMS** ( $\text{EI}^+$ ) calcd for  $[\text{C}_{22}\text{H}_{17}\text{NO}_3]^+$ :  $m/z$  343.1208, found 343.1205.



**1-(4-(trifluoromethyl)phenyl)-3-(pyridin-2-yl)prop-2-ynyl 4-methoxybenzoate:** Yellow oil, 91% yield;  $R_f$  (3:1 hexanes/EtOAc) 0.15;  $^1\text{H NMR}$  (500 MHz,  $\text{C}_6\text{D}_6$ )  $\delta$  8.33 (d,  $J = 4.7$  Hz, 1H), 8.11 (d,  $J = 8.5$  Hz, 2H), 7.46 (d,  $J = 8.0$  Hz, 2H), 7.24 (d,  $J = 8.1$  Hz, 2H), 7.05-7.00 (m, 2H), 6.77 (t,  $J = 7.7$  Hz, 1H), 6.58 (d,  $J = 8.5$  Hz, 2H), 6.45 (dd,  $J = 7.5, 4.9$  Hz, 1H), 3.09 (s, 3H);  $^{13}\text{C NMR}$  (125 MHz,  $\text{C}_6\text{D}_6$ )  $\delta$  164.9, 164.1, 150.4, 142.9, 141.2, 135.6, 132.380, 128.4, 128.3, 127.9, 127.4, 125.9, 123.2, 122.2, 114.1, 87.7, 85.1, 65.6, 54.8; **IR** (film)  $\nu_{\text{max}}$  2937, 2841, 1719, 1606, 1511, 1464, 1326, 1254, 1168, 1091, 1020, 846, 771  $\text{cm}^{-1}$ ; **MS** ( $\text{EI}^+$ ):  $m/z$  411 ( $\text{M}^+$ ); **HRMS** ( $\text{EI}^+$ ) calcd for  $[\text{C}_{23}\text{H}_{16}\text{F}_3\text{NO}_3]^+$ :  $m/z$  411.1082, found 411.1079.

### Scheme 2.7.4.



### Synthesis of the Deuterated Substrate

2,6-dimethylbenzoic acid (1.00 g, 6.7 mmol), potassium carbonate (1.40 g, 10.1 mmol), dimethyl sulfate (700  $\mu$ L, 7.4 mmol) and acetone (33 mL) were combined in a round-bottom flask. The mixture was stirred under a nitrogen atmosphere at rt for 4 h. The solvent was removed under reduced pressure and the resulting residue was taken up in ethyl acetate (20 mL). The solution was diluted with water (20 mL). The aqueous layer was extracted with ethyl acetate (3 x 15 mL). The organic layers were combined, washed with brine (30 mL), and dried over  $MgSO_4$ . The solvent was removed under reduced pressure to yield a peach oil. The crude product was purified via flash chromatography (9:1 hexanes/EtOAc) to give a light peach oil (1.02 g, 93% yield).

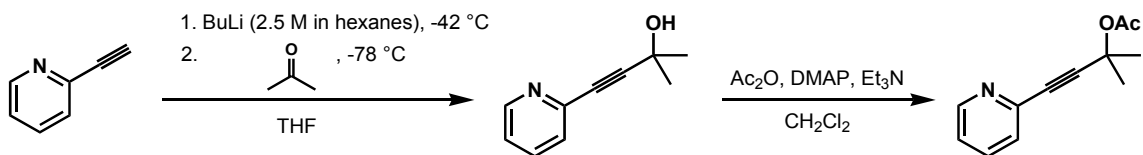
Lithium aluminum deuteride (51.2 mg, 1.22 mmol) was added in portions to a round-bottom flask containing methyl ester (200 mg, 1.22 mmol) in THF (6 mL) at 0 °C. The mixture was stirred at 0 °C for 2 h under a nitrogen atmosphere. Water (51  $\mu$ L) was added dropwise over 1 min followed by 10% sodium hydroxide aqueous solution (51  $\mu$ L). Then, an additional 153  $\mu$ L of water was added dropwise. The salts were removed via vacuum filtration. The solvent was removed under reduced pressure and a white crystalline solid was obtained (144.9 mg, 86% yield).

The deuterated alcohol (441.9 mg, 3.2 mmol), sodium bicarbonate (806.5 mg, 9.6 mmol) and dichloromethane (16 mL) were combined in a flame-dried round-bottom flask. Dess Martin periodinane (1.612 g, 3.8 mmol) was added to the mixture in portions over 5 min. The mixture was stirred at rt under a nitrogen atmosphere for 1 h. Sat. aqueous sodium sulfite solution (20 mL) was added. The aqueous layer was extracted with dichloromethane (3 x 20 mL). The organic layers were combined and washed with sat. aqueous sodium bicarbonate solution (1 x 30 mL), brine (1 x 30 mL) and dried over  $MgSO_4$ . The solvent was removed under reduced pressure. The crude aldehyde was purified via flash chromatography (4:1 hexanes/EtOAc). The deuterated aldehyde was obtained as a colorless oil (315.3 mg, 73% yield).

2-ethynylpyridine was added into the deuterated aldehyde using the previously described protocol to give the deuterated substrate as a colorless oil (306.2 mg, 63% yield).  $^1H$  NMR (500 MHz,  $C_6D_6$ )  $\delta$  8.32 (d,  $J$  = 4.8 Hz, 1H), 6.97-6.92 (m, 2H), 6.87 (d,  $J$  = 7.5 Hz, 2H), 6.74 (dt,  $J$  = 7.7, 1.4 Hz, 1H), 6.45-6.41 (m, 1H), 2.65 (s, 6H), 1.07 (s, 9H);  $^{13}C$  NMR (125 MHz,  $C_6D_6$ )  $\delta$

176.6, 150.2, 143.2, 137.8, 135.5, 134.0, 129.8, 129.0, 128.3, 127.3, 122.9, 86.4, 85.7, 38.9, 27.1, 20.5; **IR** (film)  $\nu_{\max}$  2973, 1732, 1582, 1463, 1276, 1149, 1084, 778  $\text{cm}^{-1}$ ; **MS** ( $\text{EI}^+$ ):  $m/z$  322 ( $\text{M}^+$ ); **HRMS** ( $\text{EI}^+$ ) calcd for  $[\text{C}_{21}\text{H}_{22}\text{DNO}_2]^+$ :  $m/z$  322.1792, found 322.1789.

### Scheme 2.7.5.

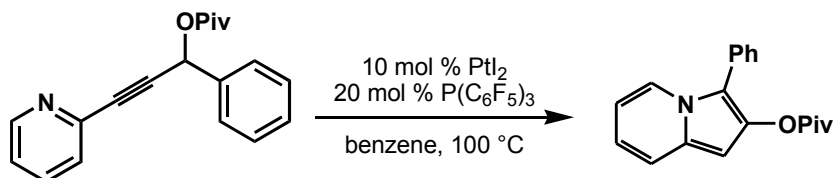


### Synthesis of Tertiary Substrate

**2-Methyl-4-(pyridin-2-yl)but-3-yn-2-yl acetate:** A flame-dried, round-bottom flask was charged with anhydrous THF (20 mL) and 2-ethynylpyridine (202  $\mu\text{L}$ , 2.0 mmol). The solution was cooled to  $-42\text{ }^\circ\text{C}$  and *n*-BuLi (880  $\mu\text{L}$ , 2.2 mmol, 2.5 M in hexanes) was added dropwise. The solution was allowed to stir at  $-42\text{ }^\circ\text{C}$  for 90 min, and then was cooled to  $-78\text{ }^\circ\text{C}$ . Acetone (177  $\mu\text{L}$ , 2.4 mmol) was added dropwise at  $-78\text{ }^\circ\text{C}$ . The mixture was stirred at  $-78\text{ }^\circ\text{C}$  for 4 h and then the mixture was allowed to warm to rt. After 3 h, sat. aqueous  $\text{NH}_4\text{Cl}$  solution (20 mL) was added slowly and stirring continued for 10 min. The mixture was diluted with EtOAc (15 mL). The aqueous layer was extracted with EtOAc (3 x 15 mL). The organic layers were combined, washed with brine (30 mL) and dried over  $\text{MgSO}_4$ . The solvent was removed under reduced pressure and the crude mixture was purified via flash chromatography (1:1 hexanes/EtOAc) to obtain a yellow oil (258.8 mg, 80% yield).

The propargylic alcohol (258 mg, 1.6 mmol), acetic anhydride (190  $\mu\text{L}$ , 2.0 mmol), *N,N*-4-dimethylaminopyridine (9.8 mg, 0.1 mmol), triethylamine (670  $\mu\text{L}$ , 3.0 mmol) and dichloromethane (16 mL) were combined in a flame-dried round-bottom flask and stirred under an nitrogen atmosphere at  $23\text{ }^\circ\text{C}$  for 4 d. Sat. aqueous ammonium chloride solution (15 mL) was added. The aqueous layer was extracted with dichloromethane (3 x 15 mL). The organic layers were combined, washed with brine (30 mL) and dried over  $\text{MgSO}_4$ . The solvent was removed under reduced pressure. The crude oil was purified via flash chromatography (2:1 hexanes/EtOAc) and a light yellow oil was obtained (212.9 mg, 66% yield).  $^1\text{H NMR}$  (400 MHz,  $\text{C}_6\text{D}_6$ )  $\delta$  8.33 (d,  $J = 4.8\text{ Hz}$ , 1H), 7.17 (d,  $J = 8.2\text{ Hz}$ , 1H), 6.81-6.74 (m, 1H), 6.45-6.41 (m, 1H), 1.63-1.62 (m, 9H);  $^{13}\text{C NMR}$  (125 MHz,  $\text{C}_6\text{D}_6$ )  $\delta$  168.6, 150.2, 143.8, 135.4, 127.3, 122.6, 90.3, 84.6, 72.0, 28.8, 21.4; **IR** (film)  $\nu_{\max}$  2989, 1739, 1582, 1464, 1428, 1281, 1245, 1135, 1016, 781  $\text{cm}^{-1}$ ; **MS** ( $\text{EI}^+$ ):  $m/z$  203 ( $\text{M}^+$ ); **HRMS** ( $\text{EI}^+$ ) calcd for  $[\text{C}_{12}\text{H}_{13}\text{NO}_2]^+$ :  $m/z$  203.0946, found 203.0952.

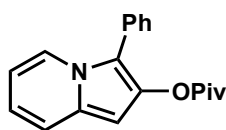
### Scheme 2.7.6.



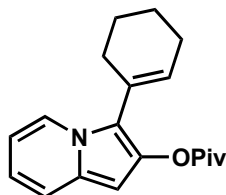
## Representative Procedure for the Formation of 2,3-Disubstituted Indolizines

1-Phenyl-3-(pyridin-2-yl)prop-2-ynyl pivalate (80 mg, 0.272 mmol), platinum(II) iodide (12 mg, 0.027 mmol) and tris(pentafluorophenyl) phosphine (28 mg, 0.054 mmol) were combined in an oven-dried 4 mL vial equipped with a stir bar. The vial was evacuated and backfilled with nitrogen (x 3). Benzene (2.0 mL) was added via syringe. The vial was capped with a Teflon cap and heated to 100 °C for 24 h. The vial was removed from heat and allowed to cool to 23 °C. The solvent was removed under reduced pressure. The crude product was purified using flash chromatography (9:1 hexanes/EtOAc) to yield a yellow oil (65.8 mg, 82% yield).

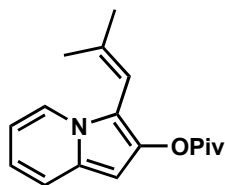
### Spectral Data for Indolizine Products



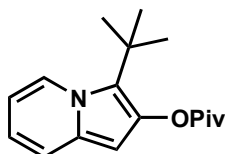
**3-Phenylindolizin-2-yl pivalate:** Yellow oil, 75% yield;  $R_f$  (3:1 hexanes/EtOAc) 0.61;  $^1\text{H NMR}$  (500 MHz,  $\text{C}_6\text{D}_6$ )  $\delta$  7.72 (d,  $J = 7.1$  Hz, 1H), 7.32 (dd,  $J = 8.0, 1.0$  Hz, 2H), 7.16-7.11 (m, 2H), 7.06-6.99 (m, 2H), 6.68 (s, 1H), 6.35 (ddd,  $J = 8.9, 6.6, 0.9$  Hz, 1H), 5.98 (dt,  $J = 7.1, 1.3$  Hz, 1H), 1.13 (s, 9H);  $^{13}\text{C NMR}$  (100 MHz,  $\text{C}_6\text{D}_6$ )  $\delta$  175.9, 140.0, 130.7, 129.9, 129.6, 129.0, 127.6, 122.2, 119.4, 117.7, 114.9, 110.7, 93.5, 39.1, 27.2; **IR** (film)  $\nu_{\text{max}}$  2974, 1751, 1479, 1432, 1351, 1312, 1275, 1110, 759, 700  $\text{cm}^{-1}$ ; **MS** ( $\text{EI}^+$ ):  $m/z$  293 ( $\text{M}^+$ ); **HRMS** ( $\text{EI}^+$ ) calcd for  $[\text{C}_{19}\text{H}_{19}\text{NO}_2]^+$ :  $m/z$  293.1416, found 293.1411.



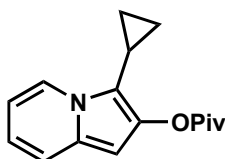
**3-Cyclohexenylindolizin-2-yl pivalate:** Yellow oil, 74% yield;  $R_f$  (3:1 hexanes/EtOAc) 0.66;  $^1\text{H NMR}$  (400 MHz,  $\text{C}_6\text{D}_6$ )  $\delta$  7.66 (dd,  $J = 7.1, 0.9$  Hz, 1H), 7.04 (dt,  $J = 9.0, 1.0$  Hz, 1H), 6.58 (s, 1H), 6.38 (ddd,  $J = 8.9, 6.5, 1.0$  Hz, 1H), 6.13 (td,  $J = 7.1, 1.3$  Hz, 1H), 5.84-5.80 (m, 1H), 2.25-2.19 (m, 2H), 2.01-1.94 (m, 2H), 1.61-1.46 (m, 4H), 1.28 (s, 9H);  $^{13}\text{C NMR}$  (100 MHz,  $\text{C}_6\text{D}_6$ )  $\delta$  175.9, 139.2, 131.0, 129.9, 127.5, 123.1, 119.3, 117.0, 116.7, 110.2, 92.9, 39.2, 27.7, 27.4, 25.8, 23.2, 22.5; **IR** (film)  $\nu_{\text{max}}$  2932, 1752, 1480, 1437, 1276, 1137, 1110  $\text{cm}^{-1}$ ; **MS** ( $\text{EI}^+$ ):  $m/z$  297 ( $\text{M}^+$ ); **HRMS** ( $\text{EI}^+$ ) calcd for  $[\text{C}_{19}\text{H}_{23}\text{NO}_2]^+$ :  $m/z$  297.1729, found 297.1730.



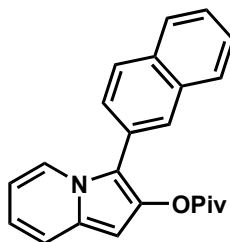
**3-(2-Methylprop-1-enyl)indolizin-2-yl pivalate:** Yellow oil, 54% yield;  $R_f$  (3:1 hexanes/EtOAc) 0.64;  $^1\text{H NMR}$  (500 MHz,  $\text{C}_6\text{D}_6$ )  $\delta$  7.31 (d,  $J = 7.0$  Hz, 1H), 7.06 (d,  $J = 8.9$  Hz, 1H), 6.67 (s, 1H), 6.43-6.38 (m, 1H), 6.13 (dt,  $J = 7.0, 6.9, 1.2$  Hz, 1H), 5.86 (s, 1H), 1.73 (s, 3H), 1.62 (s, 3H), 1.26 (s, 9H);  $^{13}\text{C NMR}$  (125 MHz,  $\text{C}_6\text{D}_6$ )  $\delta$  175.7, 141.0, 139.8, 130.1, 122.7, 119.0, 117.0, 112.3, 112.1, 110.2, 92.8, 39.2, 27.4, 25.4, 20.7; **IR** (film)  $\nu_{\text{max}}$  2973, 1752, 1480, 1455, 1351, 1275, 1143, 1109, 755  $\text{cm}^{-1}$ ; **MS** ( $\text{EI}^+$ ):  $m/z$  271 ( $\text{M}^+$ ); **HRMS** ( $\text{EI}^+$ ) calcd for  $[\text{C}_{17}\text{H}_{21}\text{NO}_2]$ :  $m/z$  271.1572, found 271.1567.



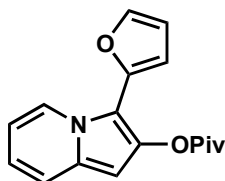
**3-tert-butylindolizin-2-yl pivalate:** Yellow oil, 11% yield;  $R_f$  (3:1 hexanes/EtOAc) 0.50;  $^1\text{H NMR}$  (500 MHz,  $\text{C}_6\text{D}_6$ )  $\delta$  7.61 (d,  $J = 7.4$  Hz, 1H), 7.34 (d,  $J = 9.0$  Hz, 1H), 6.85 (s, 1H), 6.38-6.30 (m, 1H), 6.10-6.06 (m, 1H), 1.29 (s, 9H), 1.15 (s, 9H); **IR** (film)  $\nu_{\text{max}}$  2969, 1750, 1479, 1417, 1366, 1343, 1278, 1120  $\text{cm}^{-1}$ ; **MS** ( $\text{EI}^+$ ):  $m/z$  273 ( $\text{M}^+$ ); **HRMS** ( $\text{EI}^+$ ) calcd for  $[\text{C}_{17}\text{H}_{23}\text{NO}_2]$ :  $m/z$  273.1729, found 273.1727.



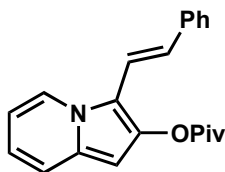
**3-Cyclopropylindolizin-2-yl pivalate:** Yellow oil, 49% yield;  $R_f$  (3:1 hexanes/EtOAc) 0.57;  $^1\text{H NMR}$  (500 MHz,  $\text{C}_6\text{D}_6$ )  $\delta$  7.66 (dd,  $J = 7.0, 0.8$  Hz, 1H), 7.07 (d,  $J = 8.9$  Hz, 1H), 6.52 (s, 1H), 6.47-6.42 (m, 1H), 6.23 (dt,  $J = 6.9, 1.2$  Hz, 1H), 1.40-1.33 (m, 1H), 1.31 (s, 9H), 0.60-0.54 (m, 2H), 0.46-0.41 (m, 2H);  $^{13}\text{C NMR}$  (125 MHz,  $\text{C}_6\text{D}_6$ )  $\delta$  175.7, 140.5, 129.4, 122.6, 119.0, 116.7, 110.0, 92.0, 39.2, 27.4, 5.1, 3.8; **IR** (film)  $\nu_{\text{max}}$  2974, 1751, 1455, 1439, 1341, 1277, 1143, 1111  $\text{cm}^{-1}$ ; **MS** ( $\text{EI}^+$ ):  $m/z$  257 ( $\text{M}^+$ ); **HRMS** ( $\text{EI}^+$ ) calcd for  $[\text{C}_{16}\text{H}_{19}\text{NO}_2]$ :  $m/z$  257.1416, found 257.1412.



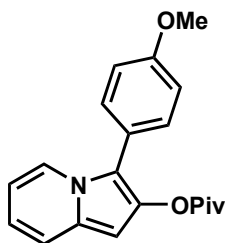
**3-(Naphthalen-2-yl)indolizin-2-yl pivalate:** Yellow oil; 73% yield;  $R_f$  (3:1 hexanes/EtOAc) 0.55;  $^1\text{H NMR}$  (500 MHz,  $\text{C}_6\text{D}_6$ )  $\delta$  7.85 (d,  $J = 7.1$  Hz, 1H), 7.77 (s, 1H), 7.64-7.54 (m, 3H), 7.47 (dd,  $J = 8.5, 1.5$  Hz, 1H), 7.28-7.21 (m, 2H), 7.09 (d,  $J = 9.0$  Hz, 1H), 6.78 (s, 1H), 6.41 (dd,  $J = 8.5, 6.8$  Hz, 1H), 6.06-6.01 (m, 1H), 1.15 (s, 9H);  $^{13}\text{C NMR}$  (125 MHz,  $\text{C}_6\text{D}_6$ )  $\delta$  175.9, 140.3, 134.1, 133.0, 130.9, 128.7, 128.5, 128.3, 127.3, 127.2, 126.6, 126.4, 122.2, 119.4, 117.9, 114.9, 110.8, 93.7, 39.2, 27.2; **IR** (film)  $\nu_{\text{max}}$  2973, 1754, 1466, 1310, 1110, 751  $\text{cm}^{-1}$ ; **MS** ( $\text{EI}^+$ ):  $m/z$  343 ( $\text{M}^+$ ); **HRMS** ( $\text{EI}^+$ ) calcd for  $[\text{C}_{23}\text{H}_{21}\text{NO}_2]$ :  $m/z$  343.1572, found 343.1572.



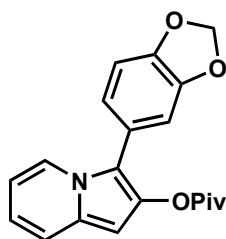
**3-(Furan-2-yl)indolizin-2-yl pivalate:** Brown oil, 34% yield;  $R_f$  (3:1 hexanes/EtOAc) 0.56;  $^1\text{H NMR}$  (500 MHz,  $\text{C}_6\text{D}_6$ )  $\delta$  8.24 (dd,  $J = 7.1, 0.7$  Hz, 1H), 7.11 (d,  $J = 1.2$  Hz, 1H), 6.97 (d,  $J = 8.9$  Hz, 1H), 6.74 (s, 1H), 6.51 (d,  $J = 3.3$  Hz, 1H), 6.36 (ddd,  $J = 8.8, 6.6, 0.8$  Hz, 1H), 6.23 (dd,  $J = 3.3, 1.9$  Hz, 1H), 6.10 (dt,  $J = 7.1, 1.3$  Hz, 1H), 1.24 (s, 9H);  $^{13}\text{C NMR}$  (125 MHz,  $\text{C}_6\text{D}_6$ )  $\delta$  175.4, 145.5, 141.2, 140.7, 131.3, 124.1, 119.1, 118.3, 111.4, 111.2, 107.7, 93.8, 39.3, 27.3; **IR** (film)  $\nu_{\text{max}}$  2973, 1754, 1479, 1431, 1311, 1275, 1139, 1108  $\text{cm}^{-1}$ ; **MS** ( $\text{EI}^+$ ):  $m/z$  283 ( $\text{M}^+$ ); **HRMS** ( $\text{EI}^+$ ) calcd for  $[\text{C}_{17}\text{H}_{17}\text{NO}_3]$ :  $m/z$  283.1208, found 283.1208.



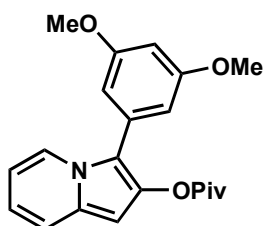
**3-Styrylindolizin-2-yl pivalate:** Yellow oil, 56% yield;  $R_f$  (3:1 hexanes/EtOAc) 0.55;  $^1\text{H NMR}$  (500 MHz,  $\text{C}_6\text{D}_6$ )  $\delta$  7.45-7.38 (m, 3H), 7.25-7.19 (m, 3H), 7.09 (t,  $J = 7.3$  Hz, 1H), 6.99-6.95 (m, 2H), 6.81 (s, 1H), 6.37 (td,  $J = 11.8, 5.9$  Hz, 1H), 6.12-6.07 (m, 1H), 1.27 (s, 9H);  $^{13}\text{C NMR}$  (125 MHz,  $\text{C}_6\text{D}_6$ )  $\delta$  175.3, 141.5, 138.8, 131.2, 129.0, 127.3, 126.8, 126.2, 122.4, 119.2, 118.0, 114.2, 113.1, 111.1, 94.5, 39.4, 27.4; **IR** (film)  $\nu_{\text{max}}$  2973, 1752, 1455, 1437, 1269, 1141, 1105  $\text{cm}^{-1}$ ; **MS** ( $\text{EI}^+$ ):  $m/z$  319 ( $\text{M}^+$ ); **HRMS** ( $\text{EI}^+$ ) calcd for  $[\text{C}_{21}\text{H}_{21}\text{NO}_2]$ :  $m/z$  319.1572, found 319.1573.



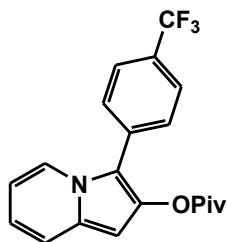
**3-(4-Methoxyphenyl)indolizin-2-yl pivalate:** Yellow oil, 74% yield;  $R_f$  (3:1 hexanes: EtOAc) 0.59;  $^1\text{H NMR}$  (400 MHz,  $\text{C}_6\text{D}_6$ )  $\delta$  7.76 (d,  $J = 6.3$  Hz, 1H), 7.27 (d,  $J = 8.8$  Hz, 2H), 7.08 (d,  $J = 9.0$  Hz, 1H), 6.78 (d,  $J = 8.8$  Hz, 2H), 6.73 (s, 1H), 6.42-6.36 (m, 1H), 6.08-6.02 (m, 1H), 3.28 (s, 3H), 1.19 (s, 9H);  $^{13}\text{C NMR}$  (100 MHz,  $\text{C}_6\text{D}_6$ )  $\delta$  176.0, 159.6, 139.8, 131.2, 130.3, 122.2, 122.1, 119.4, 117.4, 114.9, 114.6, 110.5, 93.3, 54.8, 39.2, 27.3; **IR** (film)  $\nu_{\text{max}}$  2968, 1751, 1602, 1494, 1349, 1248, 1177, 1111, 1031  $\text{cm}^{-1}$ ; **MS** ( $\text{EI}^+$ ):  $m/z$  323 ( $\text{M}^+$ ); **HRMS** ( $\text{EI}^+$ ) calcd for  $[\text{C}_{20}\text{H}_{21}\text{NO}_3]$ :  $m/z$  323.1521, found 323.1520.



**3-(Benzo[d][1,3]dioxol-6-yl)indolizin-2-yl pivalate:** Yellow oil, 67% yield;  $R_f$  (3:1 hexanes/EtOAc) 0.50;  $^1\text{H NMR}$  (500 MHz,  $\text{C}_6\text{D}_6$ )  $\delta$  7.72 (d,  $J = 7.1$  Hz, 1H), 7.05 (d,  $J = 8.9$  Hz, 1H), 6.86 (d,  $J = 1.3$  Hz, 1H), 6.78 (dd,  $J = 8.0, 1.5$  Hz, 1H), 6.70-6.63 (m, 2H), 6.38 (dd,  $J = 8.2, 7.2$  Hz, 1H), 6.05-6.01 (m, 1H), 5.32-5.28 (m, 2H), 1.19 (s, 9H);  $^{13}\text{C NMR}$  (125 MHz,  $\text{C}_6\text{D}_6$ )  $\delta$  176.0, 148.5, 147.5, 139.8, 130.4, 123.6, 123.4, 122.2, 119.3, 117.5, 114.6, 110.6, 110.0, 108.9, 101.2, 93.3, 39.2, 27.3; **IR** (film)  $\nu_{\text{max}}$  2974, 1751, 1481, 1237, 1142, 1110, 1038  $\text{cm}^{-1}$ ; **MS** ( $\text{EI}^+$ ):  $m/z$  337 ( $\text{M}^+$ ); **HRMS** ( $\text{EI}^+$ ) calcd for  $[\text{C}_{20}\text{H}_{19}\text{NO}_4]$ :  $m/z$  337.1314, found 337.1310.

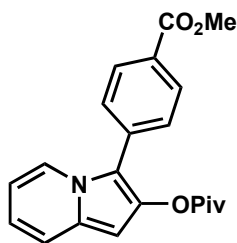


**3-(3,5-Dimethoxyphenyl)indolizin-2-yl pivalate:** Yellow oil, 76% yield;  $R_f$  (3:1 hexanes/EtOAc) 0.62;  $^1\text{H NMR}$  (500 MHz,  $\text{C}_6\text{D}_6$ )  $\delta$  7.91 (d,  $J = 7.1$  Hz, 1H), 7.06 (d,  $J = 8.9$  Hz, 1H), 6.72 (d,  $J = 2.2$  Hz, 2H), 6.70 (s, 1H), 6.56 (t,  $J = 2.1$  Hz, 1H), 6.38 (dd,  $J = 8.4, 7.1$  Hz, 1H), 6.04 (t,  $J = 6.8$  Hz, 1H), 3.32 (s, 6H), 1.21 (s, 9H);  $^{13}\text{C NMR}$  (125 MHz,  $\text{C}_6\text{D}_6$ )  $\delta$  176.0, 161.8, 140.0, 131.7, 130.7, 122.6, 119.3, 117.7, 110.7, 107.5, 100.7, 93.5, 54.9, 39.2, 27.3; **IR** (film)  $\nu_{\text{max}}$  2971, 1751, 1593, 1455, 1419, 1282, 1205, 1156, 1111  $\text{cm}^{-1}$ ; **MS** ( $\text{EI}^+$ ):  $m/z$  353 ( $\text{M}^+$ ); **HRMS** ( $\text{EI}^+$ ) calcd for  $[\text{C}_{21}\text{H}_{23}\text{NO}_4]$ :  $m/z$  353.1627, found 353.1620.

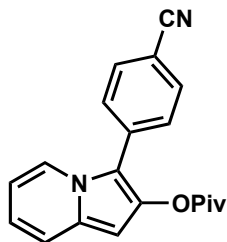


**3-(4-(Trifluoromethyl)phenyl)indolizin-2-yl pivalate:** Yellow solid, 58% yield;  $R_f$  (3:1 hexanes/EtOAc) 0.61;  $^1\text{H NMR}$  (500 MHz,  $\text{C}_6\text{D}_6$ )  $\delta$  7.59 (d,  $J = 7.2$  Hz, 1H), 7.37 (d,  $J = 8.1$  Hz, 2H), 7.30 (d,  $J = 8.5$  Hz, 1H), 7.20 (d,  $J = 8.0$  Hz, 2H), 6.67 (s, 1H), 6.40 (ddd,  $J = 8.9, 6.6, 0.8$  Hz, 1H), 6.04 (dt,  $J = 7.1, 1.3$  Hz, 1H), 1.13 (s, 9H);  $^{13}\text{C NMR}$  (125 MHz,  $\text{C}_6\text{D}_6$ )  $\delta$  175.9, 175.7, 140.5, 133.5, 133.5, 131.4, 129.2, 128.3, 127.9, 126.0, 126.0, 125.9, 125.9, 124.4, 121.9, 121.5, 119.5, 118.5, 117.0, 116.7, 113.3, 111.4, 111.2, 108.1, 93.9, 39.3, 39.1, 27.4, 27.1; **IR** (film)  $\nu_{\text{max}}$  2976, 1753, 1480, 1325, 1111, 1068, 761  $\text{cm}^{-1}$ ; **MS** ( $\text{EI}^+$ ):  $m/z$  361 ( $\text{M}^+$ ); **HRMS** ( $\text{EI}^+$ ) calcd for  $[\text{C}_{20}\text{H}_{18}\text{F}_3\text{NO}_2]$ :  $m/z$  361.1290, found 361.1285.

(\*\*Note: this is a 2:1 mixture of 2,3- and 1,3-disubstituted indolizine)



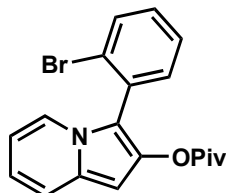
**Methyl 4-(2-pivaloyloxy)indolizin-3-yl)benzoate:** Green oil, 78% yield;  $R_f$  (3:1 hexanes/EtOAc) 0.44;  $^1\text{H NMR}$  (400 MHz,  $\text{C}_6\text{D}_6$ )  $\delta$  8.16 (d,  $J = 8.5$  Hz, 2H), 7.71 (dd,  $J = 7.1, 0.7$  Hz, 1H), 7.32 (d,  $J = 8.5$  Hz, 2H), 7.02 (d,  $J = 9.1$  Hz, 1H), 6.70 (s, 1H), 6.39 (ddd,  $J = 8.9, 6.7, 0.8$  Hz, 1H), 6.02 (dt,  $J = 7.1, 1.3$  Hz, 1H), 3.52 (s, 3H), 1.15 (s, 9H);  $^{13}\text{C NMR}$  (100 MHz,  $\text{C}_6\text{D}_6$ )  $\delta$  175.7, 166.4, 140.6, 134.4, 131.5, 130.3, 129.1, 128.6, 122.2, 119.4, 118.5, 113.8, 111.1, 94.0, 51.6, 39.2, 27.2; **IR** (film)  $\nu_{\text{max}}$  2974, 1753, 1721, 1607, 1438, 1276, 1140, 1108, 771  $\text{cm}^{-1}$ ; **MS** ( $\text{EI}^+$ ):  $m/z$  351 ( $\text{M}^+$ ); **HRMS** ( $\text{EI}^+$ ) calcd for  $[\text{C}_{21}\text{H}_{21}\text{NO}_4]$ :  $m/z$  351.1471, found 351.1466.



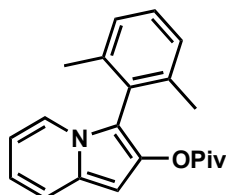
**3-(4-Cyanophenyl)indolizin-2-yl pivalate:** Green oil, 31% yield;  $R_f$  (3:1 hexanes/EtOAc) 0.47;  $^1\text{H NMR}$  (500 MHz,  $\text{C}_6\text{D}_6$ )  $\delta$  7.52 (d,  $J = 7.2$  Hz, 1H), 7.04-6.96 (m, 4H), 6.78 (d,  $J = 8.5$  Hz, 1H), 6.64 (s, 1H), 6.38 (ddd,  $J = 8.9, 6.7, 0.8$  Hz, 1H), 6.01 (dt,  $J = 7.1, 1.2$  Hz, 1H), 1.13 (s, 9H);  $^{13}\text{C NMR}$  (125 MHz,  $\text{C}_6\text{D}_6$ )  $\delta$  175.5, 140.7, 133.8, 132.4, 131.7, 128.7, 128.3, 127.4, 121.9,



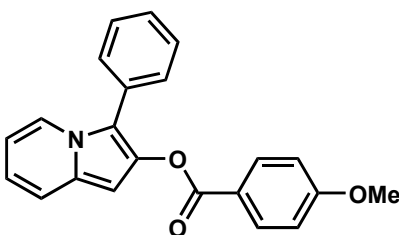
119.5, 118.9, 111.4, 110.8, 94.1, 39.1, 27.1; **IR** (film)  $\nu_{\max}$  2975, 2225, 1752, 1605, 1511, 1479, 1439, 1314, 1275, 1139, 1109  $\text{cm}^{-1}$ .



**3-(2-Bromophenyl)indolizin-2-yl pivalate:** Yellow oil, 72% yield; **R<sub>f</sub>** (3:1 hexanes/EtOAc) 0.50; **<sup>1</sup>H NMR** (500 MHz, C<sub>6</sub>D<sub>6</sub>)  $\delta$  7.44 (d,  $J$  = 8.8 Hz, 1H), 7.23 (d,  $J$  = 7.0 Hz, 1H), 7.18 (dd,  $J$  = 7.6, 1.5 Hz, 1H), 7.08 (d,  $J$  = 9.0 Hz, 1H), 6.91 (dt,  $J$  = 7.6, 1.1 Hz, 1H), 6.78-6.73 (m, 2H), 6.44-6.39 (m, 1H), 6.11-6.06 (m, 1H), 1.12 (s, 9H); **<sup>13</sup>C NMR** (125 MHz, C<sub>6</sub>D<sub>6</sub>)  $\delta$  175.8, 140.3, 134.1, 133.4, 131.1, 130.8, 130.2, 127.5, 126.5, 123.0, 119.2, 117.9, 113.8, 110.565, 93.0, 39.2, 27.2; **IR** (film)  $\nu_{\max}$  2973, 1752, 1463, 1431, 1313, 1111, 1028, 756  $\text{cm}^{-1}$ ; **MS** (EI<sup>+</sup>):  $m/z$  371 (M<sup>+</sup>); **HRMS** (EI<sup>+</sup>) calcd for [C<sub>19</sub>H<sub>18</sub>BrNO<sub>2</sub>]:  $m/z$  371.0521, found 371.0522.

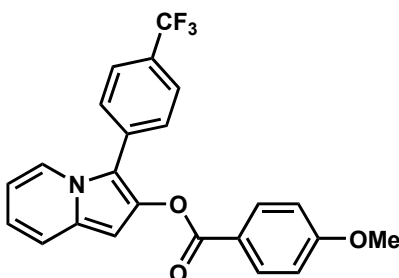


**3-(2,6-dimethylphenyl)indolizin-2-yl pivalate:** Yellow oil, 91% yield; **R<sub>f</sub>** (3:1 hexanes/EtOAc) 0.63; **<sup>1</sup>H NMR** (400 MHz, C<sub>6</sub>D<sub>6</sub>)  $\delta$  7.31-7.21 (m, 3H), 7.17-7.11 (m, 2H), 6.83 (s, 1H), 6.54 (ddd,  $J$  = 8.9, 6.6, 0.9 Hz, 1H), 6.18 (dt,  $J$  = 6.8, 1.2 Hz, 1H), 2.16 (s, 6H), 1.18 (s, 9H); **<sup>13</sup>C NMR** (100 MHz, C<sub>6</sub>D<sub>6</sub>)  $\delta$  175.9, 140.5, 139.7, 130.4, 129.3, 128.4, 122.2, 119.3, 117.0, 113.724, 110.7, 92.8, 39.0, 27.0, 19.8; **IR** (film)  $\nu_{\max}$  2973, 1754, 1461, 1347, 1276, 1138, 1110, 757  $\text{cm}^{-1}$ ; **MS** (EI<sup>+</sup>):  $m/z$  321 (M<sup>+</sup>); **HRMS** (EI<sup>+</sup>) calcd for [C<sub>21</sub>H<sub>23</sub>NO<sub>2</sub>]:  $m/z$  321.1729, found 321.1729.

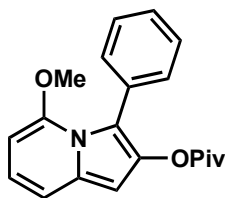


**3-Phenylindolizin-2-yl 4-methoxybenzoate:** Yellow oil, 67% yield; **R<sub>f</sub>** (3:1 hexanes/EtOAc) 0.60; **<sup>1</sup>H NMR** (500 MHz, C<sub>6</sub>D<sub>6</sub>)  $\delta$  8.17 (d,  $J$  = 8.7 Hz, 2H), 7.82 (d,  $J$  = 7.1 Hz, 1H), 7.45 (d,  $J$  = 7.6 Hz, 2H), 7.17-7.12 (m, 2H), 7.09 (d,  $J$  = 8.9 Hz, 1H), 7.03 (t,  $J$  = 7.5 Hz, 1H), 6.93 (s, 1H), 6.55 (d,  $J$  = 8.7 Hz, 2H), 6.40 (dd,  $J$  = 8.4, 7.0 Hz, 1H), 6.04 (t,  $J$  = 6.8 Hz, 1H), 3.10 (s, 3H); **<sup>13</sup>C NMR** (125 MHz, C<sub>6</sub>D<sub>6</sub>)  $\delta$  164.4, 163.9, 140.0, 132.6, 130.8, 130.1, 129.4, 129.1, 127.6, 122.5, 122.2, 119.5, 117.8, 115.0, 114.1, 110.7, 93.9, 54.8; **IR** (film)  $\nu_{\max}$  2360, 1732, 1606,

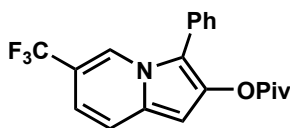
1510, 1254, 1167, 1070, 761  $\text{cm}^{-1}$ ; **MS** ( $\text{EI}^+$ ):  $m/z$  343 ( $\text{M}^+$ ); **HRMS** ( $\text{EI}^+$ ) calcd for  $[\text{C}_{22}\text{H}_{17}\text{NO}_3]$ :  $m/z$  343.1208, found 343.1206.



**3-(4-trifluoromethylphenyl)indolizin-2-yl 4-methoxybenzoate:** Yellow oil, 56% yield; **R<sub>f</sub>** (3:1 hexanes/EtOAc) 0.55; **<sup>1</sup>H NMR** (400 MHz,  $\text{C}_6\text{D}_6$ )  $\delta$  8.15 (d,  $J = 8.7$  Hz, 2H), 7.64 (d,  $J = 7.1$  Hz, 1H), 7.31 (q,  $J = 8.6$  Hz, 4H), 7.05 (d,  $J = 9.6$  Hz, 1H), 6.87 (s, 1H), 6.57 (d,  $J = 8.8$  Hz, 2H), 6.42 (dd,  $J = 8.9, 6.6$  Hz, 1H), 6.06 (t,  $J = 6.9$  Hz, 1H), 3.10 (s, 3H); **<sup>13</sup>C NMR** (100 MHz,  $\text{C}_6\text{D}_6$ )  $\delta$  163.9, 163.9, 140.2, 133.4, 132.2, 131.2, 128.7, 128.4, 125.7, 125.701, 121.8, 121.7, 119.3, 118.2, 113.9, 113.1, 110.9, 94.0, 54.5; **IR** (film)  $\nu_{\text{max}}$  2360, 1734, 1607, 1511, 1325, 1252, 1167, 1122, 1068, 763  $\text{cm}^{-1}$ ; **MS** ( $\text{EI}^+$ ):  $m/z$  411 ( $\text{M}^+$ ); **HRMS** ( $\text{EI}^+$ ) calcd for  $[\text{C}_{23}\text{H}_{16}\text{F}_3\text{NO}_3]$ :  $m/z$  411.1082, found 411.1084.

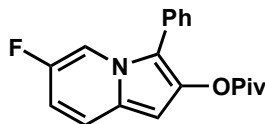


**5-Methoxy-3-phenylindolizin-2-yl pivalate:** Yellow oil, 26% yield; **R<sub>f</sub>** (3:1 hexanes/EtOAc) 0.55; **<sup>1</sup>H NMR** (500 MHz,  $\text{C}_6\text{D}_6$ )  $\delta$  7.35 (d,  $J = 6.8$  Hz, 2H), 7.24 (dd,  $J = 7.8, 1.6$  Hz, 1H), 7.14-7.09 (m, 2H), 6.89 (d,  $J = 8.3$  Hz, 1H), 6.72 (s, 1H), 6.46 (dd,  $J = 16.3, 7.7$  Hz, 1H), 5.23 (d,  $J = 6.8$  Hz, 1H), 2.88 (s, 3H), 1.13 (s, 9H); **<sup>13</sup>C NMR** (125 MHz,  $\text{C}_6\text{D}_6$ )  $\delta$  176.1, 151.5, 141.0, 135.9, 133.2, 133.0, 131.6, 130.5, 128.3, 126.9, 126.7, 126.3, 118.4, 117.2, 114.7, 111.9, 110.646 108.9, 93.8, 86.8, 54.8, 39.3, 39.1, 27.4, 27.2; **IR** (film)  $\nu_{\text{max}}$  2973, 1751, 1539, 1476, 1451, 1313, 1277, 1114  $\text{cm}^{-1}$ ; **MS** ( $\text{EI}^+$ ):  $m/z$  323 ( $\text{M}^+$ ); **HRMS** ( $\text{EI}^+$ ) calcd for  $[\text{C}_{20}\text{H}_{21}\text{NO}_3]$ :  $m/z$  323.1521, found 323.1523.



**6-(Trifluoromethyl)-3-phenylindolizin-2-yl pivalate:** Orange solid, 82% yield; **R<sub>f</sub>** (3:1 hexanes/EtOAc) 0.67; **<sup>1</sup>H NMR** (500 MHz,  $\text{C}_6\text{D}_6$ )  $\delta$  8.24 (s, 1H), 7.22 (d,  $J = 7.1$  Hz, 2H), 7.10 (t,  $J = 7.6$  Hz, 2H), 7.04-6.99 (m, 1H), 6.85 (d,  $J = 9.3$  Hz, 1H), 6.64 (s, 1H), 6.51 (dd,  $J = 9.3, 1.3$  Hz, 1H), 1.14 (s, 9H); **<sup>13</sup>C NMR** (125 MHz,  $\text{C}_6\text{D}_6$ )  $\delta$  175.8, 141.1, 130.1, 129.3, 129.2,

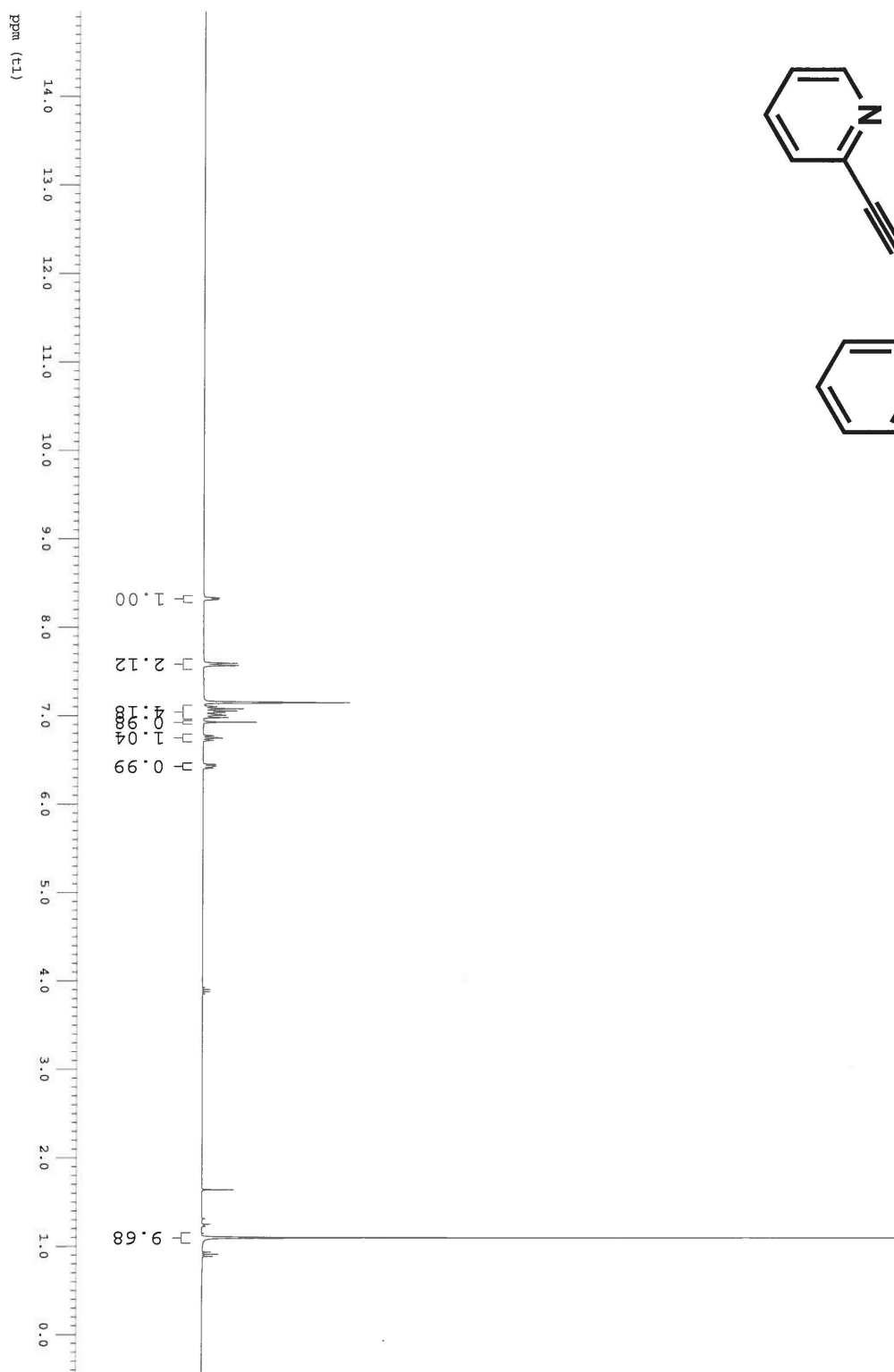
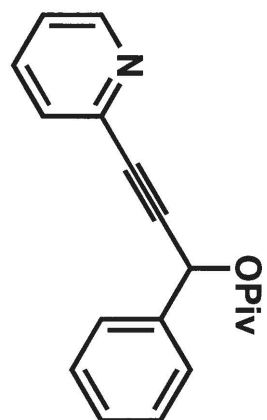
128.6, 128.4, 123.7, 121.3, 120.0, 116.8, 113.2, 113.2, 95.5, 39.2, 27.1; **IR** (film)  $\nu_{\max}$  2976, 1755, 1488, 1440, 1325, 1162, 1117, 1058, 798, 701  $\text{cm}^{-1}$ .

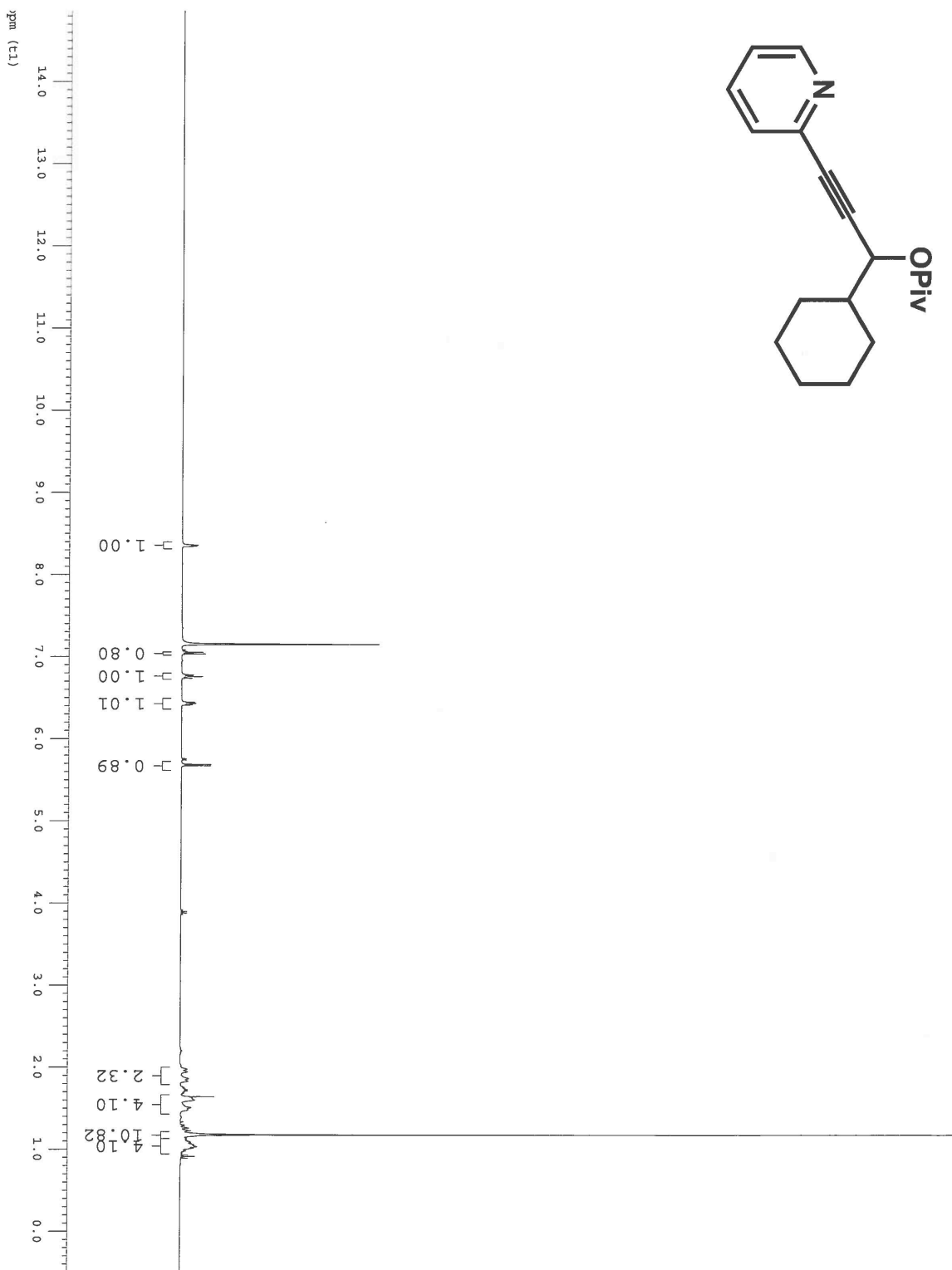
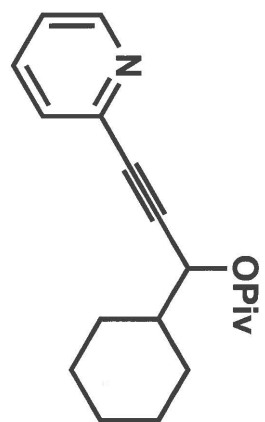


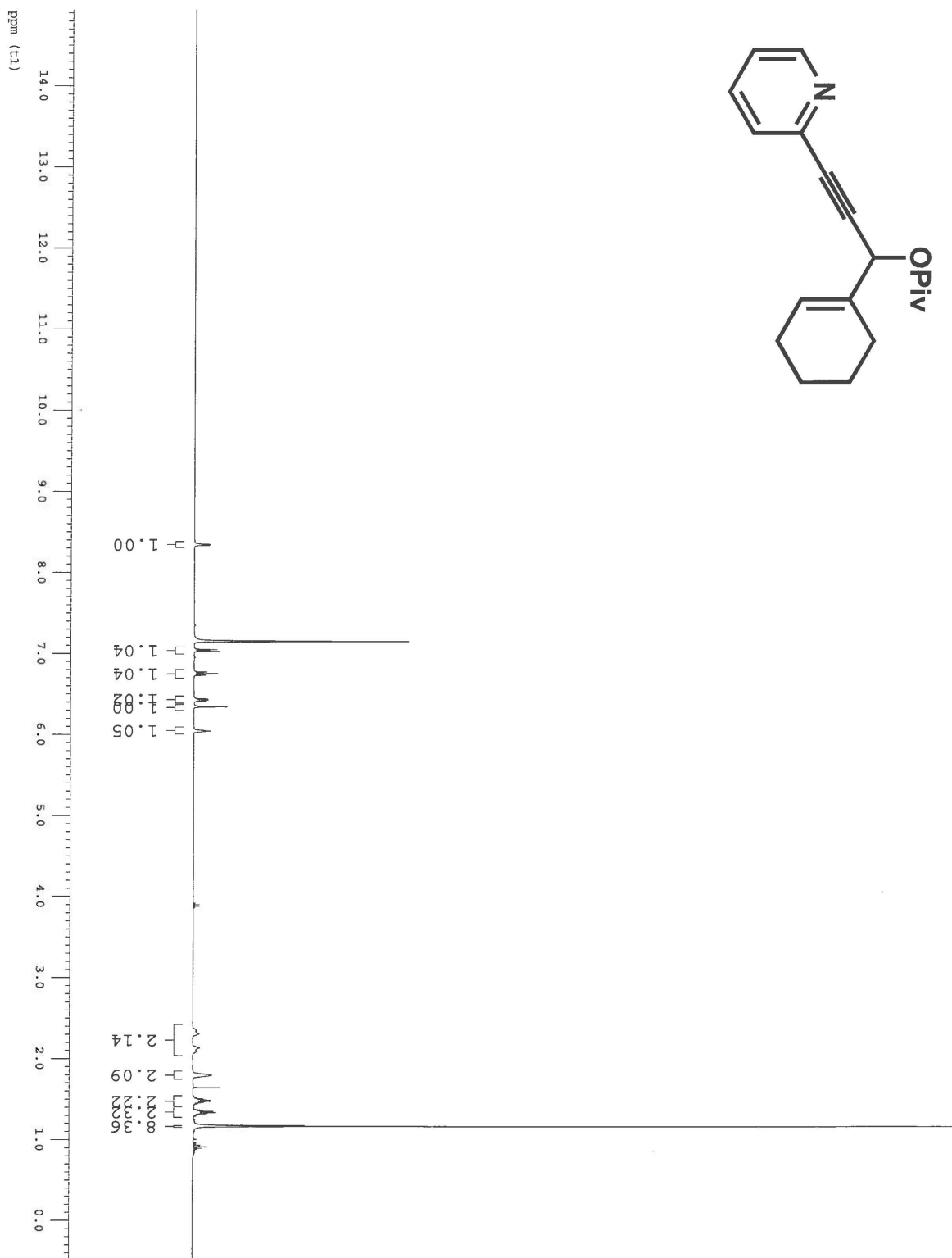
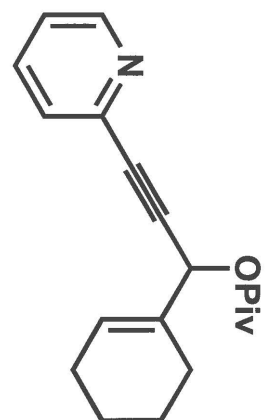
**6-Fluoro-3-phenylindoliz-2-yl pivalate:** Yellow oil, 76% yield;  $R_f$  (3:1 hexanes/EtOAc) 0.65;  $^1\text{H NMR}$  (500 MHz,  $\text{C}_6\text{D}_6$ )  $\delta$  7.76 (dd,  $J = 5.6, 2.1$  Hz, 1H), 7.26 (dd,  $J = 8.1, 1.0$  Hz, 2H), 7.17-7.10 (m, 2H), 7.07-7.02 (m, 1H), 6.78 (dd,  $J = 9.7, 5.7$  Hz, 1H), 6.68 (s, 1H), 6.29 (ddd,  $J = 9.9, 8.0, 2.2$  Hz, 1H), 1.15 (s, 9H);  $^{13}\text{C NMR}$  (125 MHz,  $\text{C}_6\text{D}_6$ )  $\delta$  175.812, 154.371, 152.522, 140.183, 140.164, 129.410, 129.14 (d,  $J = 14.2$  Hz, 1C), 120.12 (d,  $J = 9.19$  Hz, 1C), 116.545, 116.533, 109.98 (d,  $J = 25.80$  Hz, 1C), 108.57 (d,  $J = 41.83$  Hz, 1C), 94.567, 39.138, 27.184; **IR** (film)  $\nu_{\max}$  2975, 1753, 1551, 1479, 1369, 1255, 1103, 808, 760  $\text{cm}^{-1}$ .

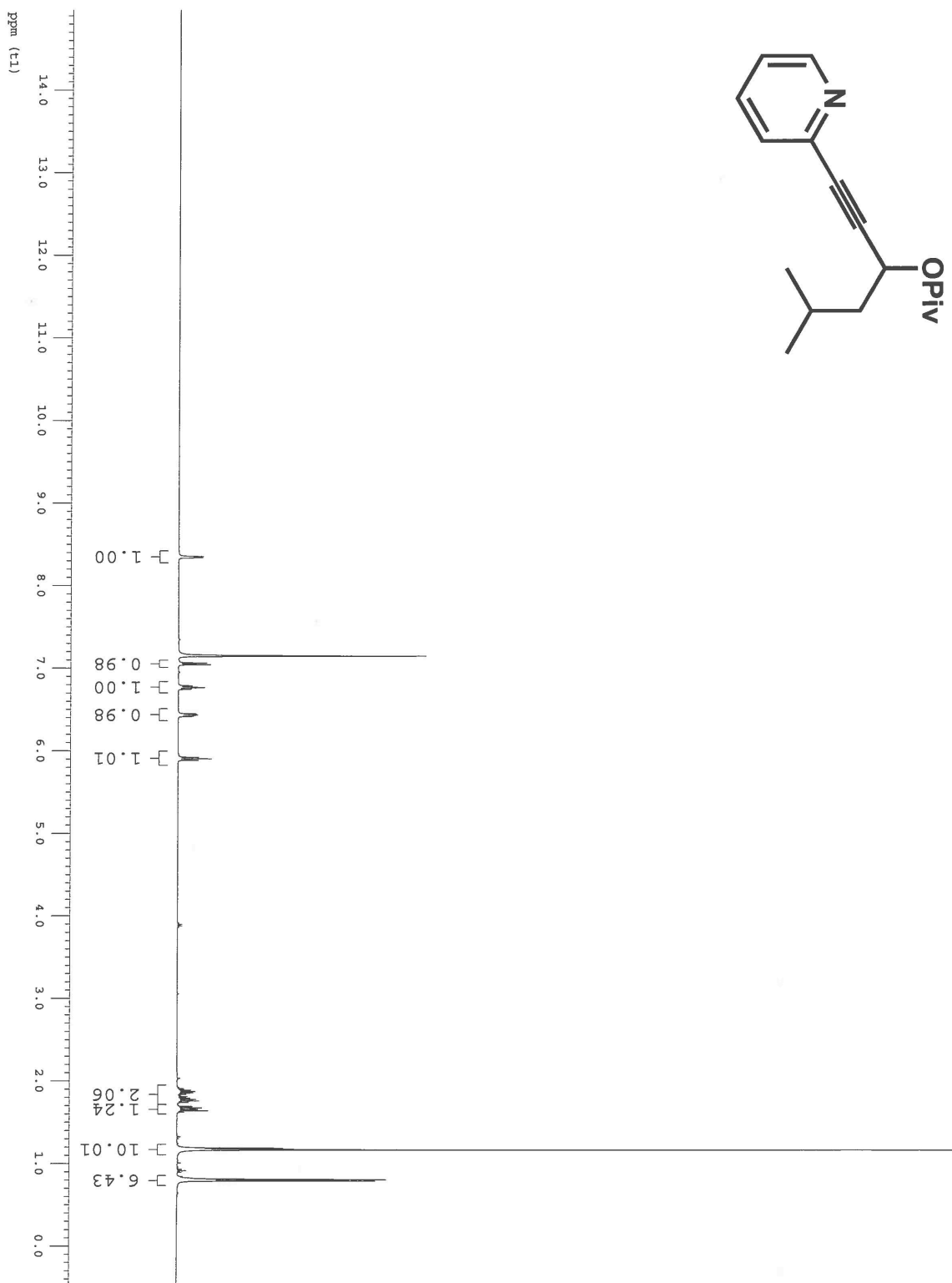
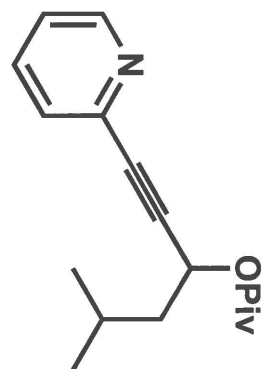
## 2.9 References and Notes

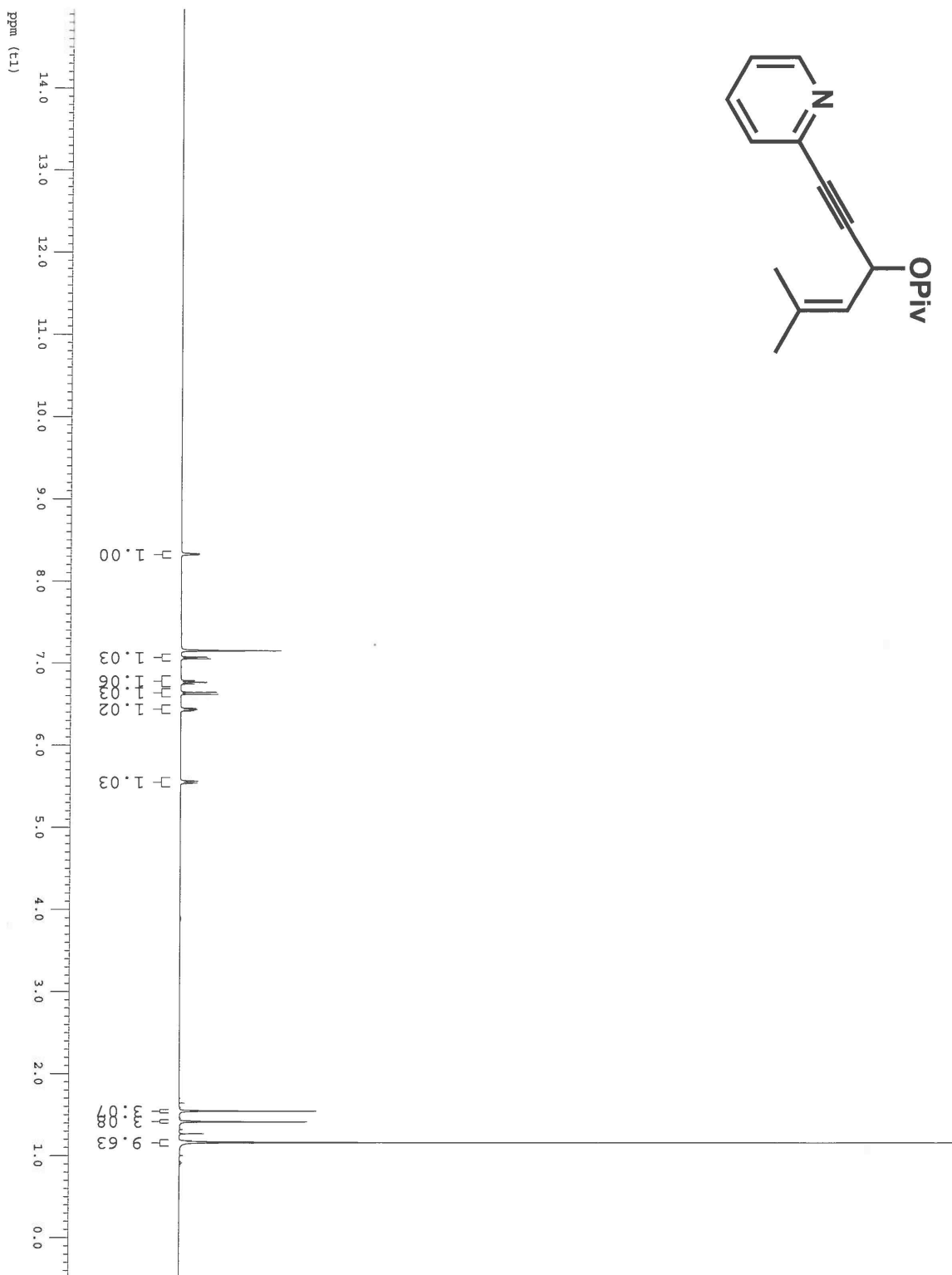
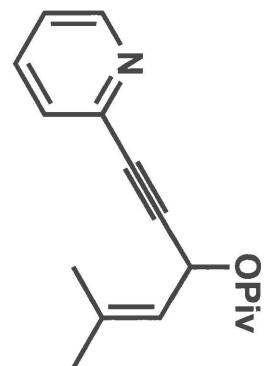
- (1) For reviews see (a) Marion, N.; Nolan, S. *Angew. Chem. Int. Ed.* **2007**, *46*, 2750. (b) Furstner, A.; Davies, P. W. *Angew. Chem. Int. Ed.* **2007**, *46*, 3099. (c) Bruneau, C. *Angew. Chem. Int. Ed.* **2005**, *44*, 2328. (d) Miki, K.; Uemura, S.; Ohe, K. *Chem. Lett.* **2005**, *34*, 1068.
- (2) (a) Schlosserczyk, H.; Sieber, W.; Hesse, M.; Hanson, H. J.; Schmidt, H. *Helv. Chim. Acta.* **1973**, *56*, 875. (b) Oelberg, D. G.; Schiavolli, M. D. *J. Org. Chem.* **1977**, *42*, 1804.
- (3) Rautenstrauch, V. *J. Org. Chem.* **1984**, *49*, 950.
- (4) Mainetti, E.; Mouries, V.; Fensterbank, L.; Malacria, M.; Marco-Contelles, J. *Angew. Chem. Int. Ed.* **2002**, *41*, 2132.
- (5) Cariou, K.; Mainetti, E.; Fensterbank, L. Malacria, M. *Tetrahedron* **2004**, *60*, 9745.
- (6) Cho, E. J.; Kim, M.; Lee, D. *Org. Lett.* **2006**, *8*, 5413.
- (7) Marion, N.; de Fremont, P.; Lemiere, G.; Stevenes, E. D.; Fensterbank, L.; Malacria, M.; Nolan, S. P. *Chem. Commun.* **2006**, 2048.
- (8) Marcos-Contelles, J.; Arroyo, N.; Anjum, S.; Mainetti, E.; Marion, N.; Cariou, K.; Lemiere, G.; Mouries, V.; Fensterbank, L.; Malacria, M. *Eur. J. Org. Chem.* **2006**, 4618.
- (9) (a) Bhanu Prasad, B. A.; Yoshimoto, F. K.; Sarpong R. *J. Am. Chem. Soc.* **2005**, *127*, 12468. (b) Pujanauski, B. G.; Bhanu Prasad, B. A.; Sarpong, R. *J. Am. Chem. Soc.* **2006**, *128*, 6786.
- (10) Bhanu Prasad, B. A. and Sarpong, R. unpublished results.
- (11) Park, C. H.; Ryabova, V.; Seregin, I.V.; Sromek, A. W.; Gevorgyan, V. *Org. Lett.* **2004**, *6*, 1159.
- (12) Smith, C. R.; Bunnelle, E. M.; Rhodes, A.; Sarpong, R. *Org. Lett.* **2007**, *9*, 1169.
- (13) Dess, D. B.; Martin, J. C. *J. Org. Chem.* **1983**, *48*, 4155.
- (14) Sromek, A. W.; Kelin, A.V.; Gevorgyan, V. *Angew. Chem. Int. Ed.* **2004**, *43*, 2280.



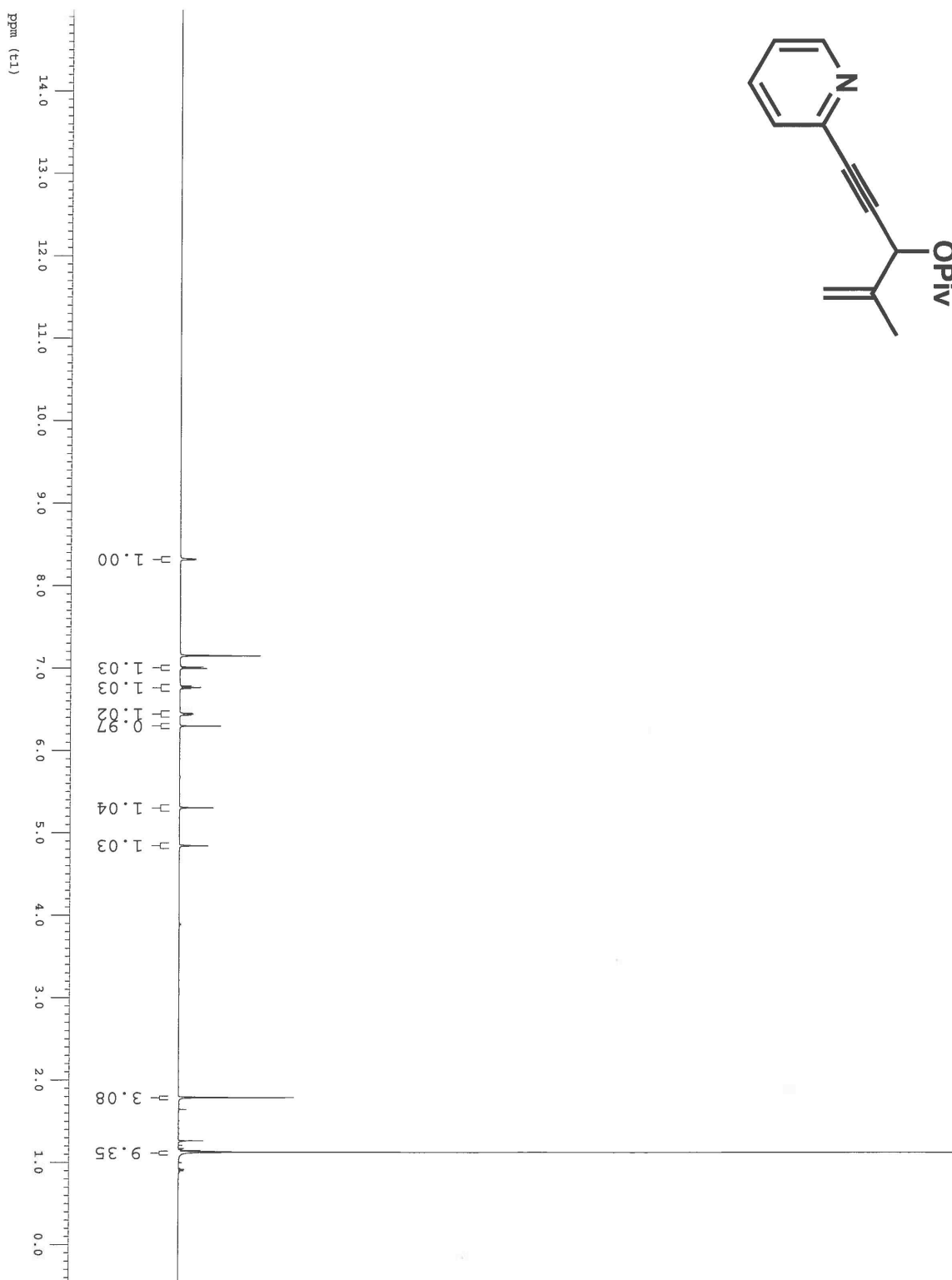
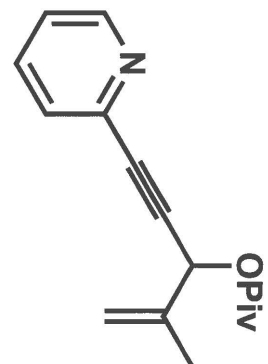


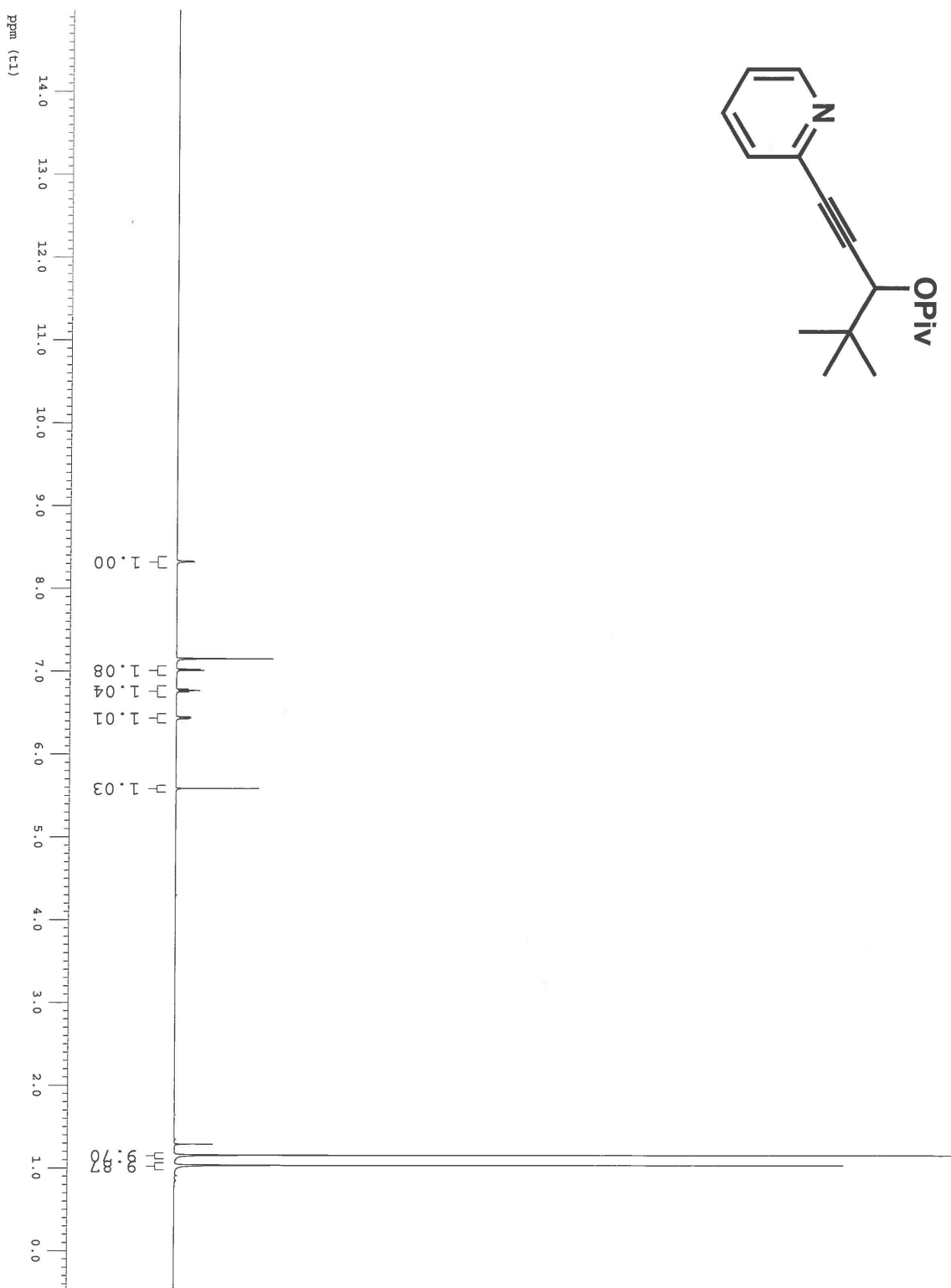
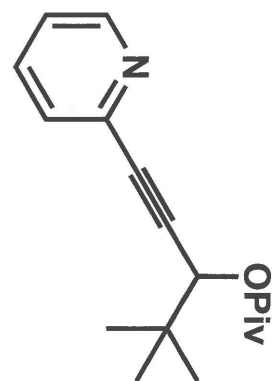


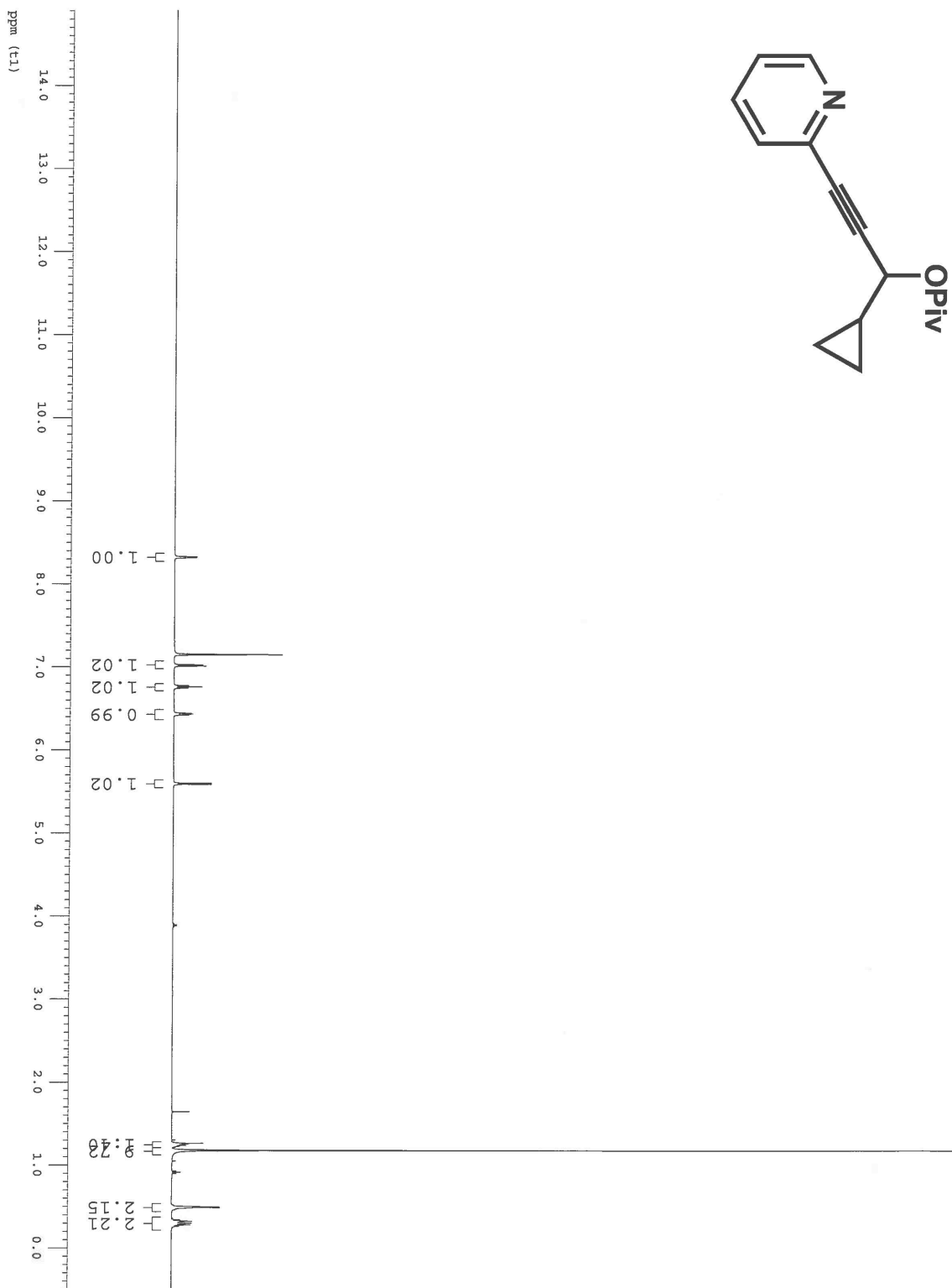
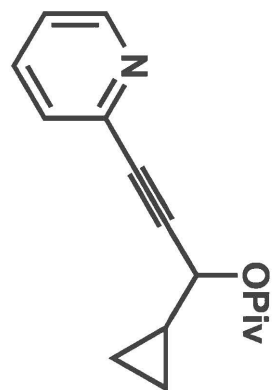


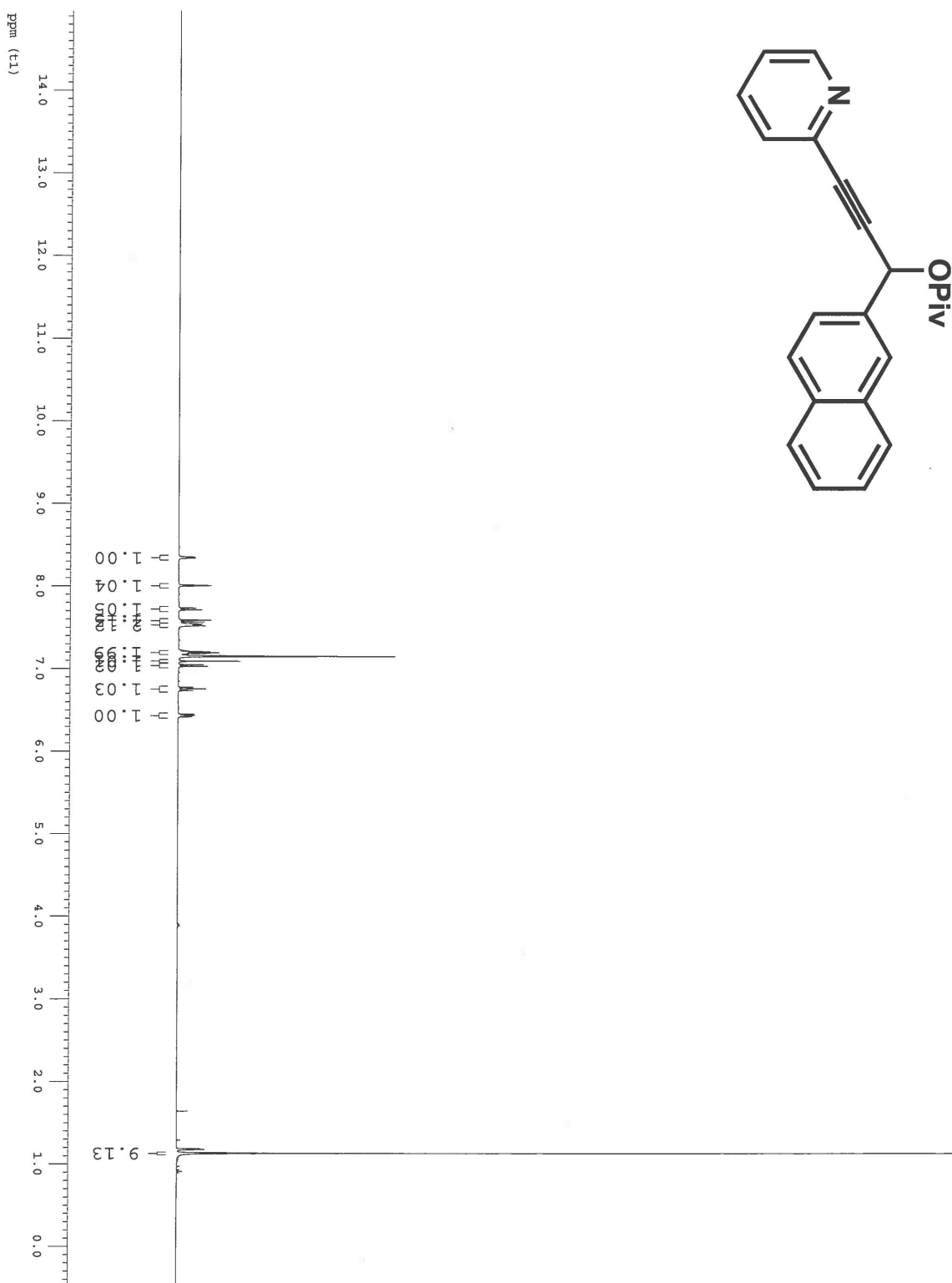
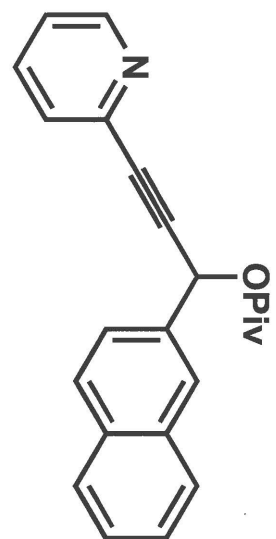


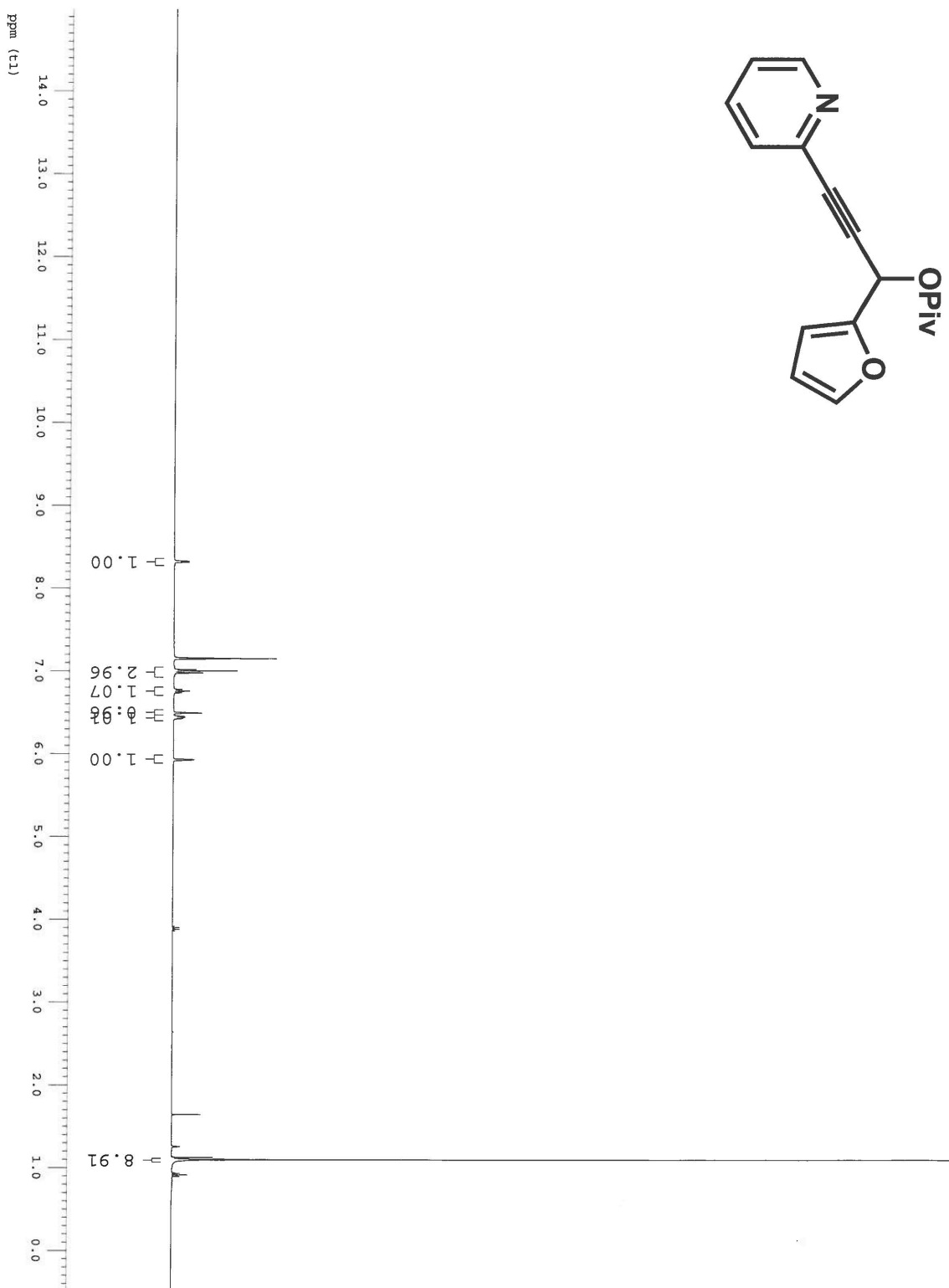
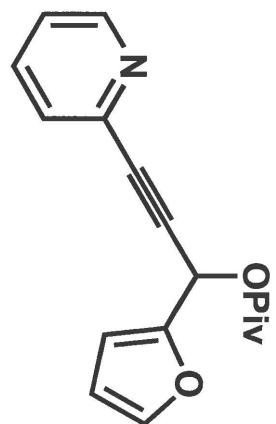


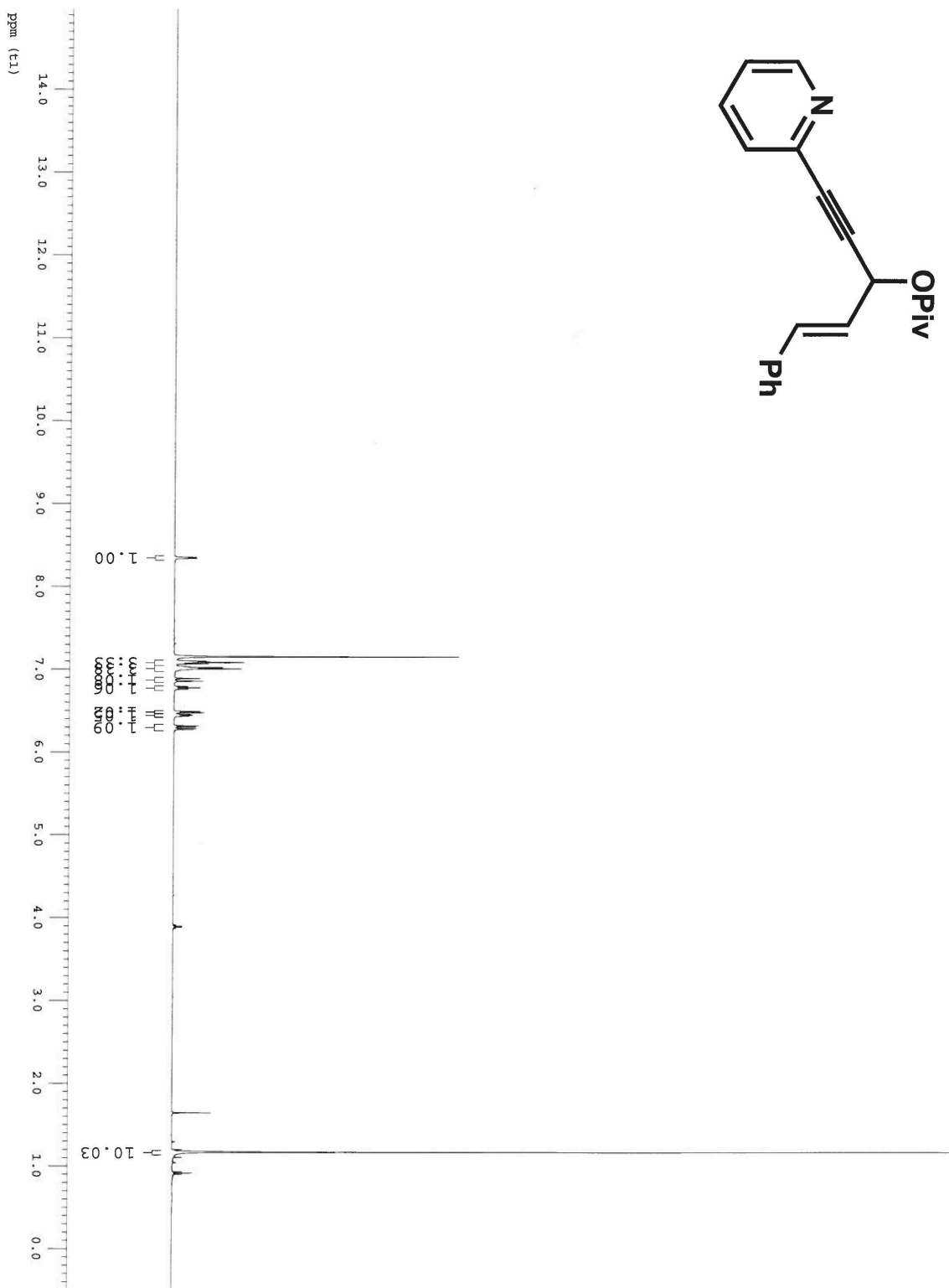
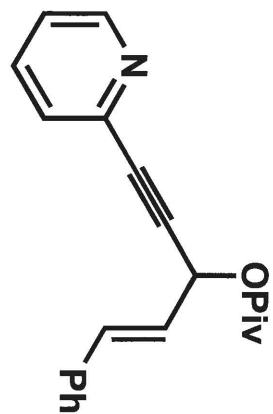


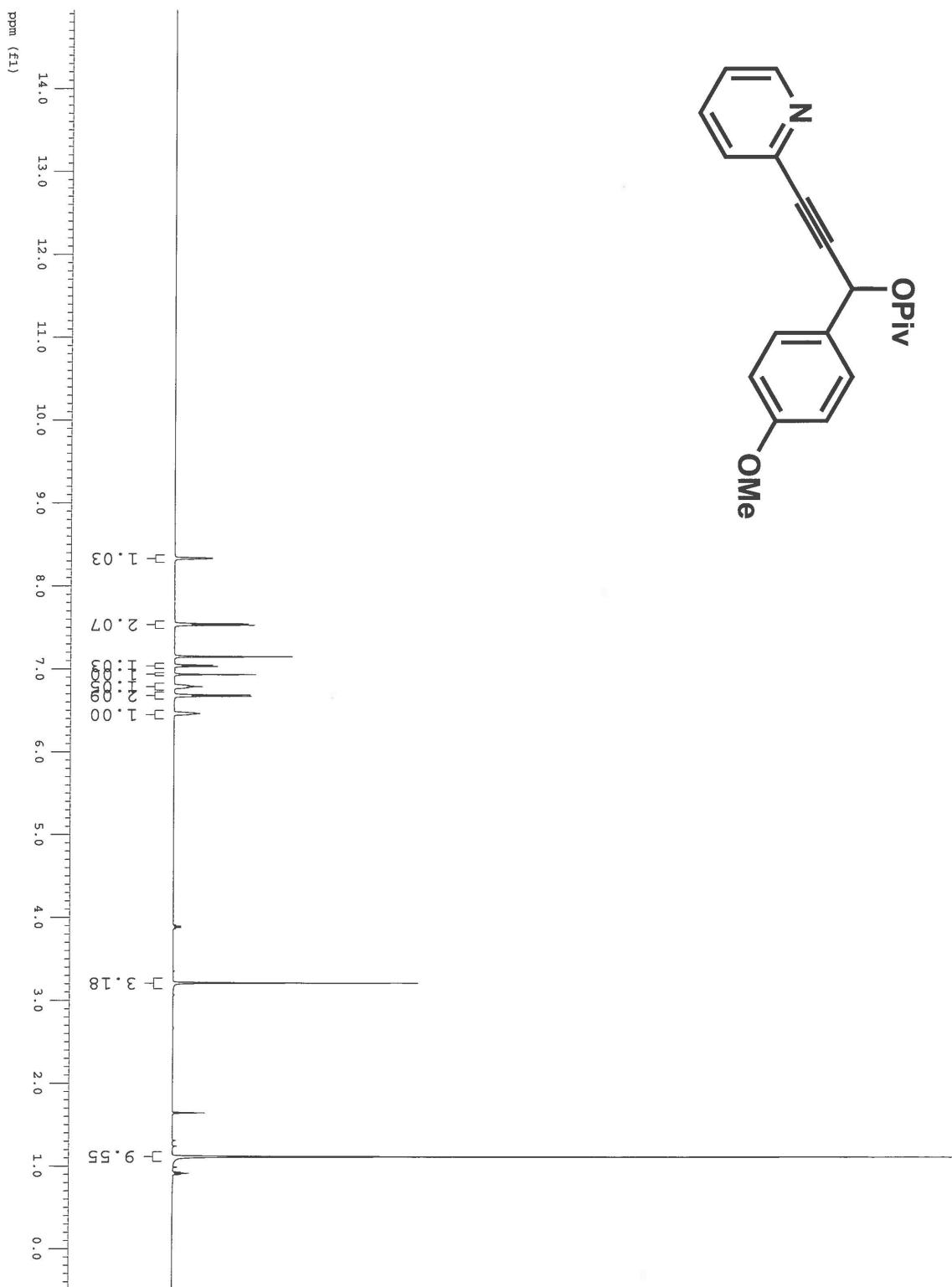
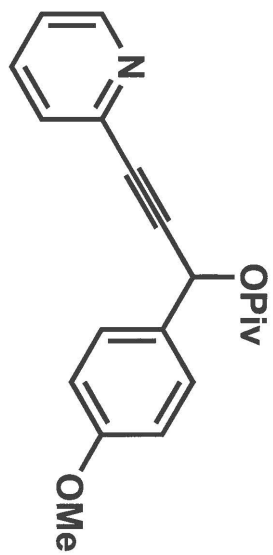


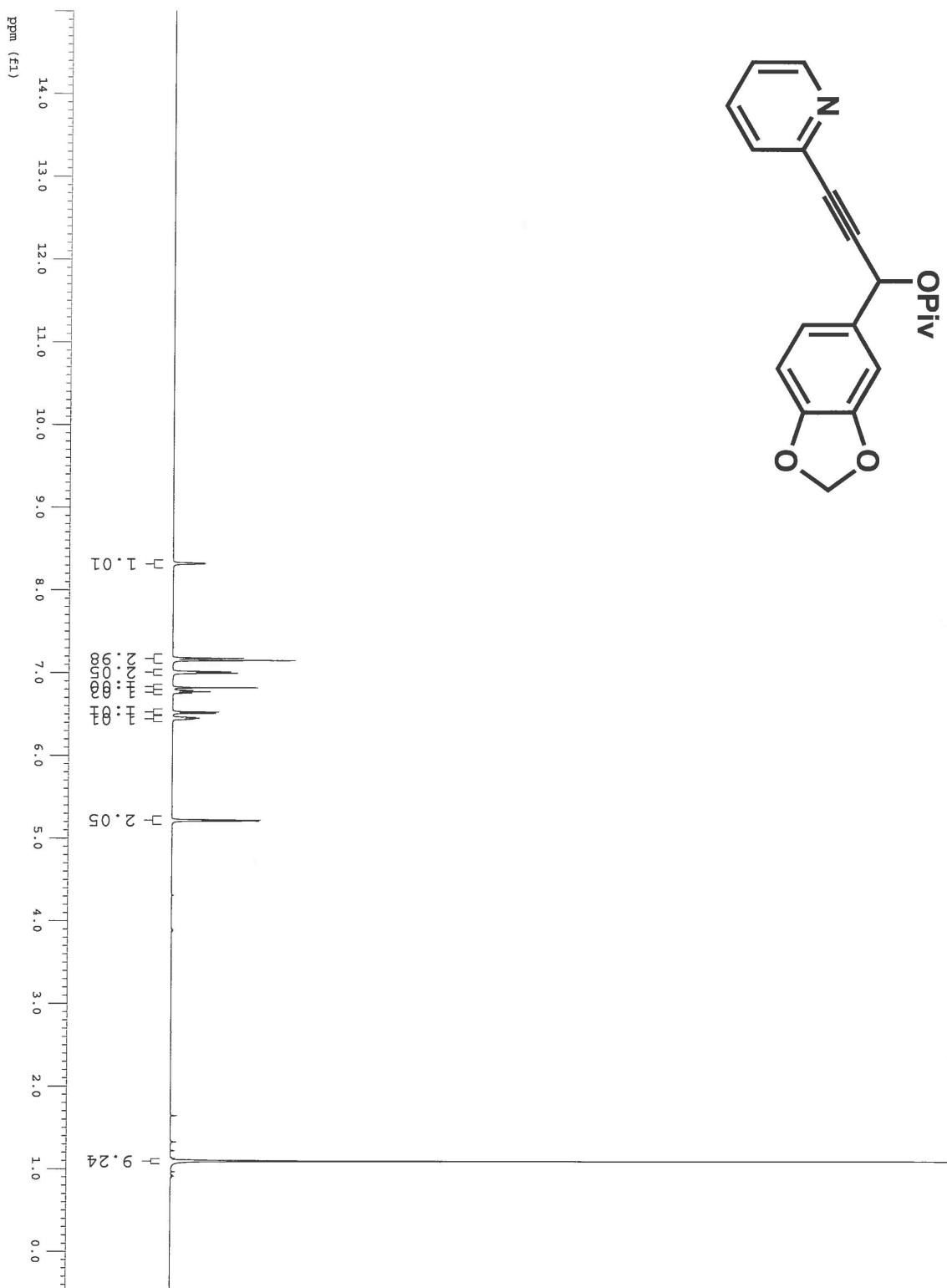
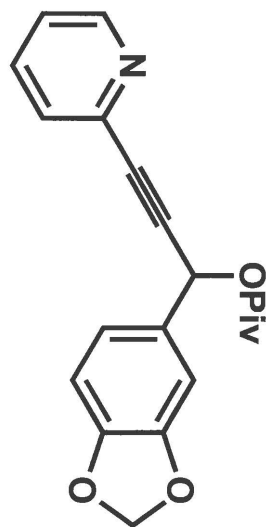




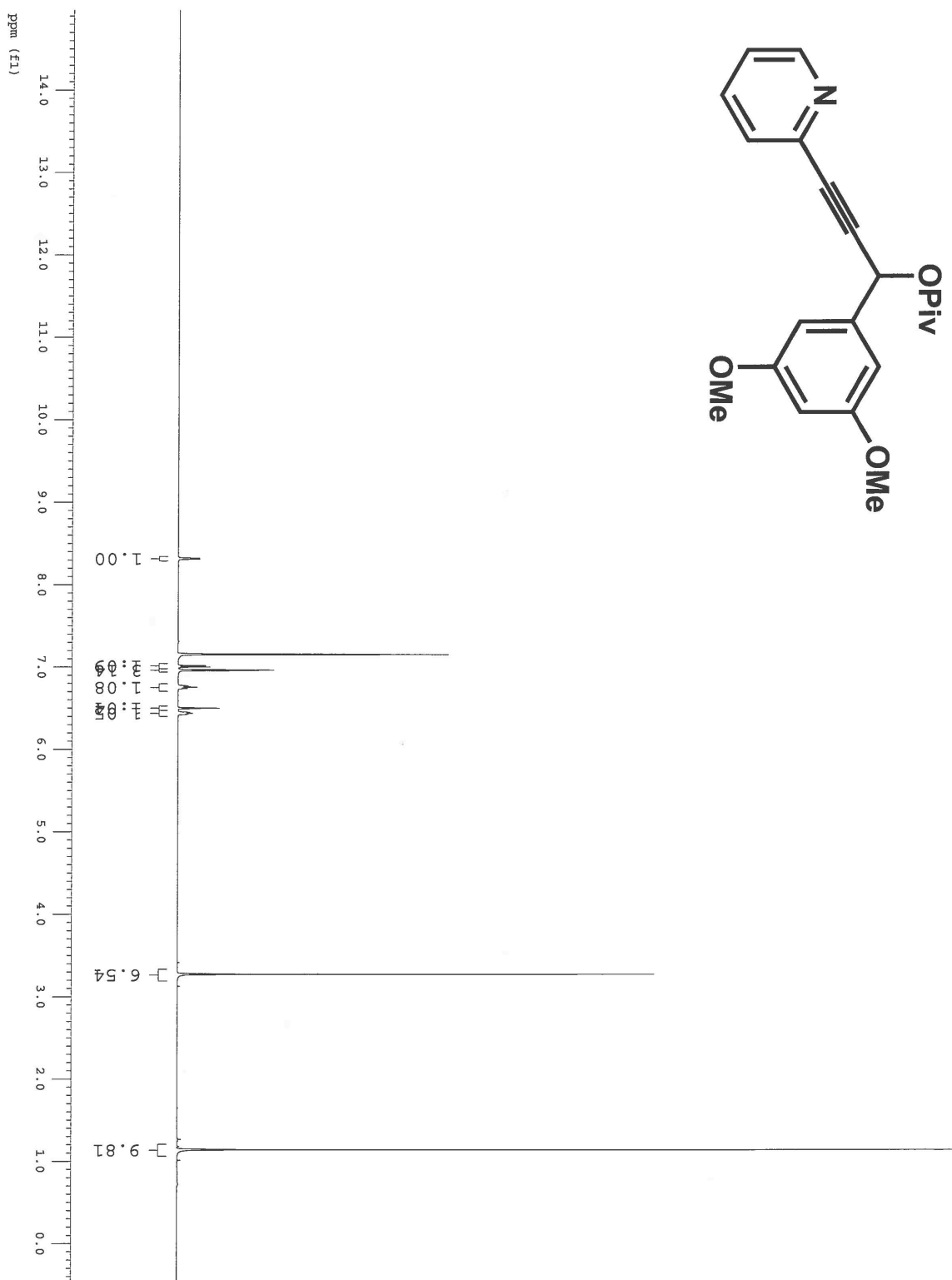
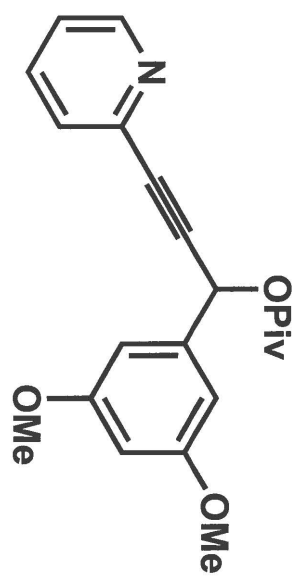


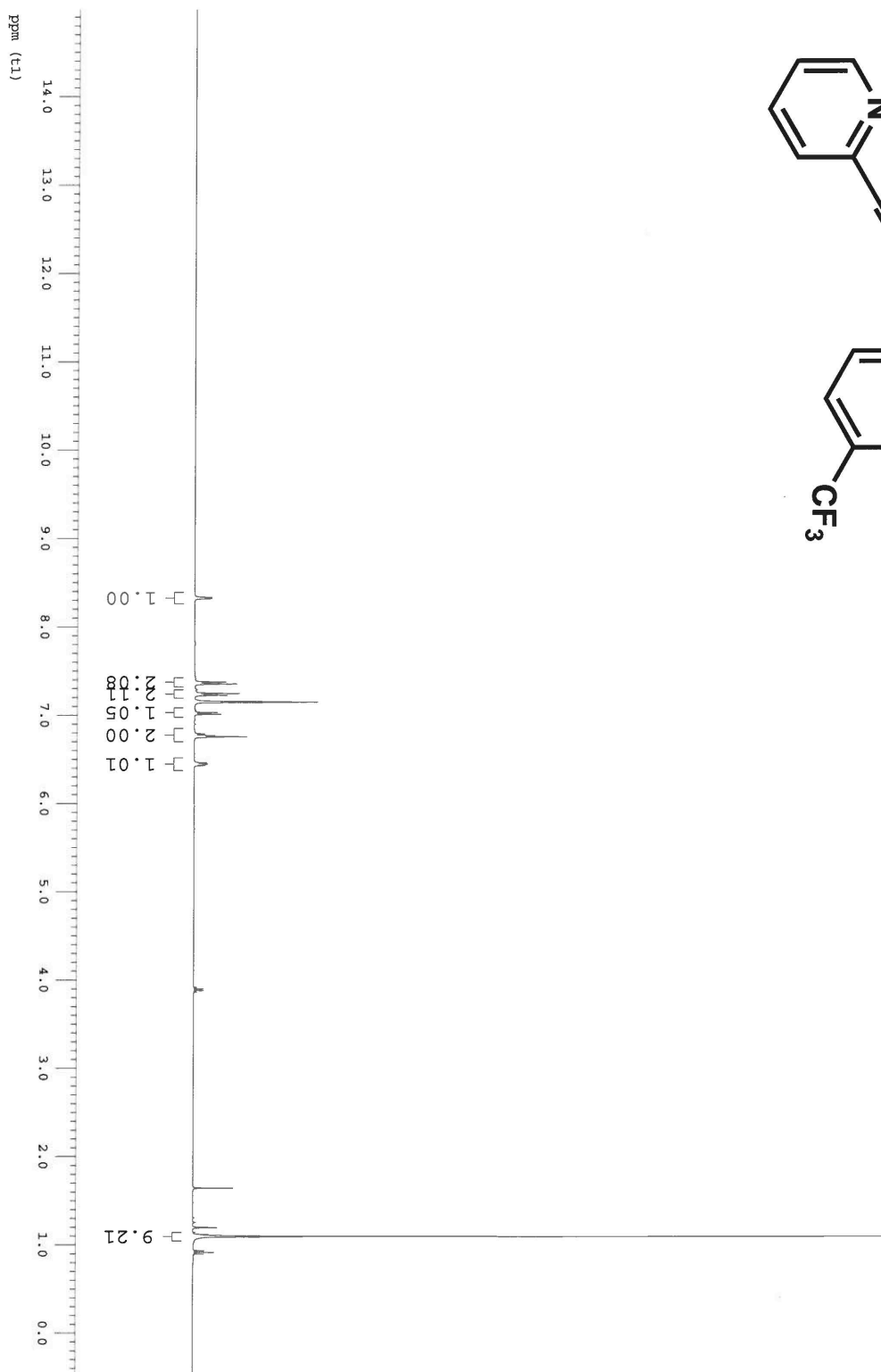
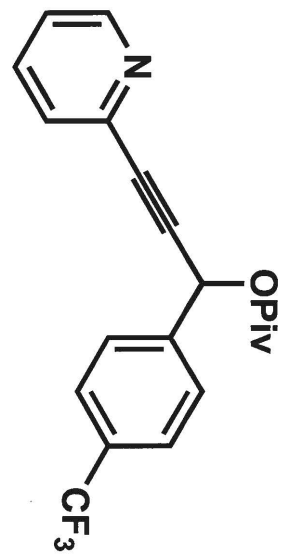


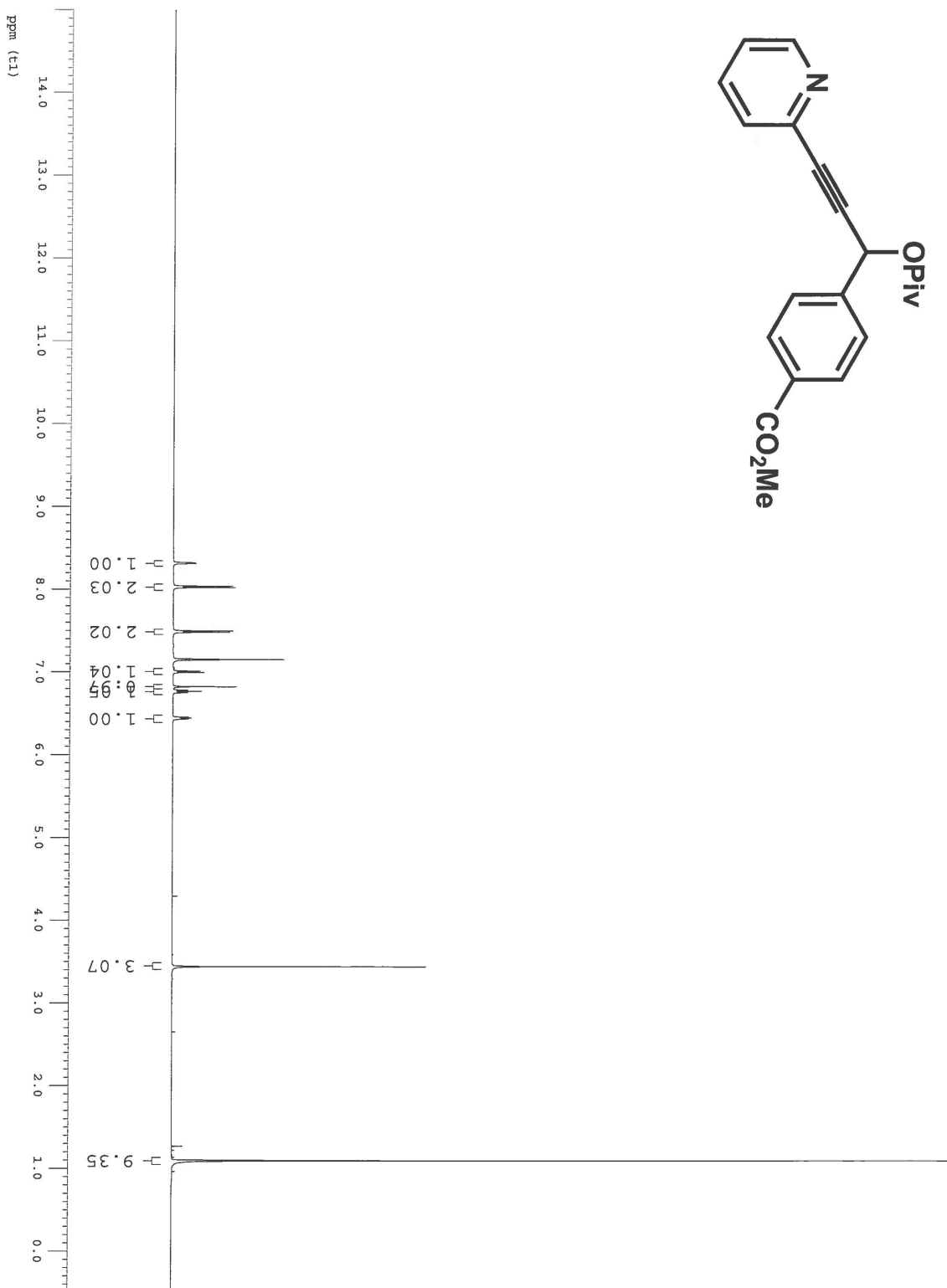
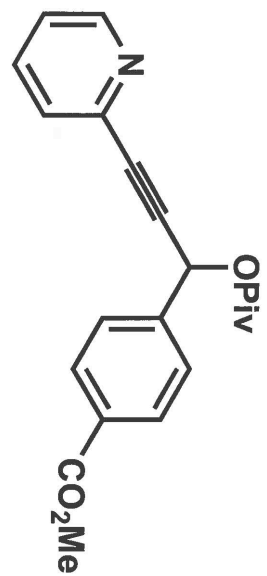


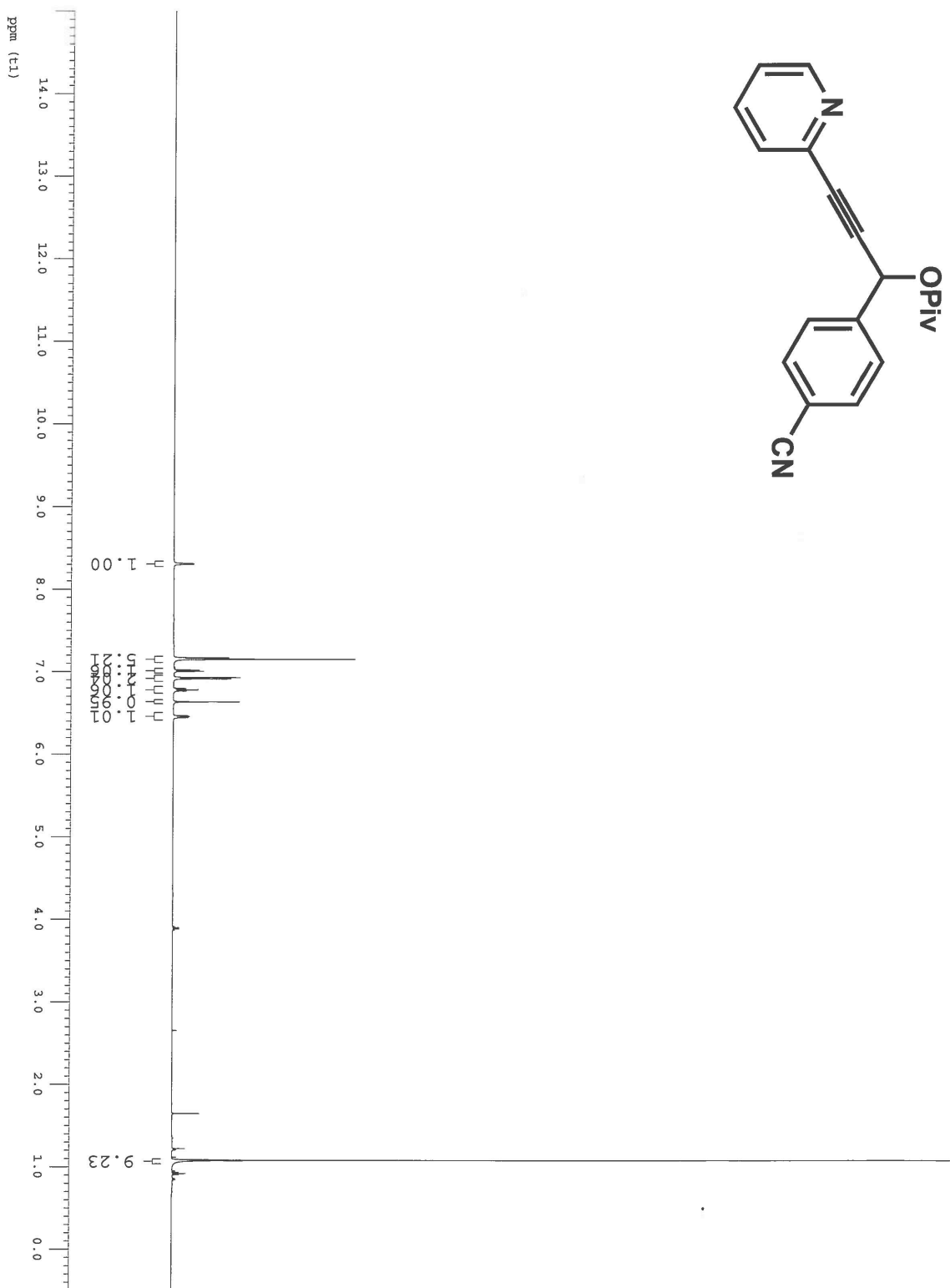
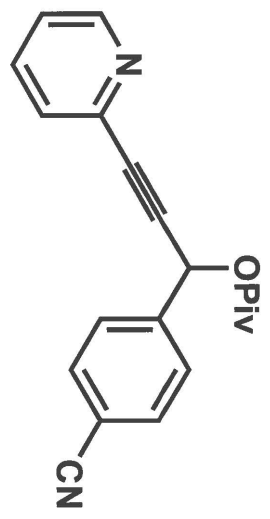


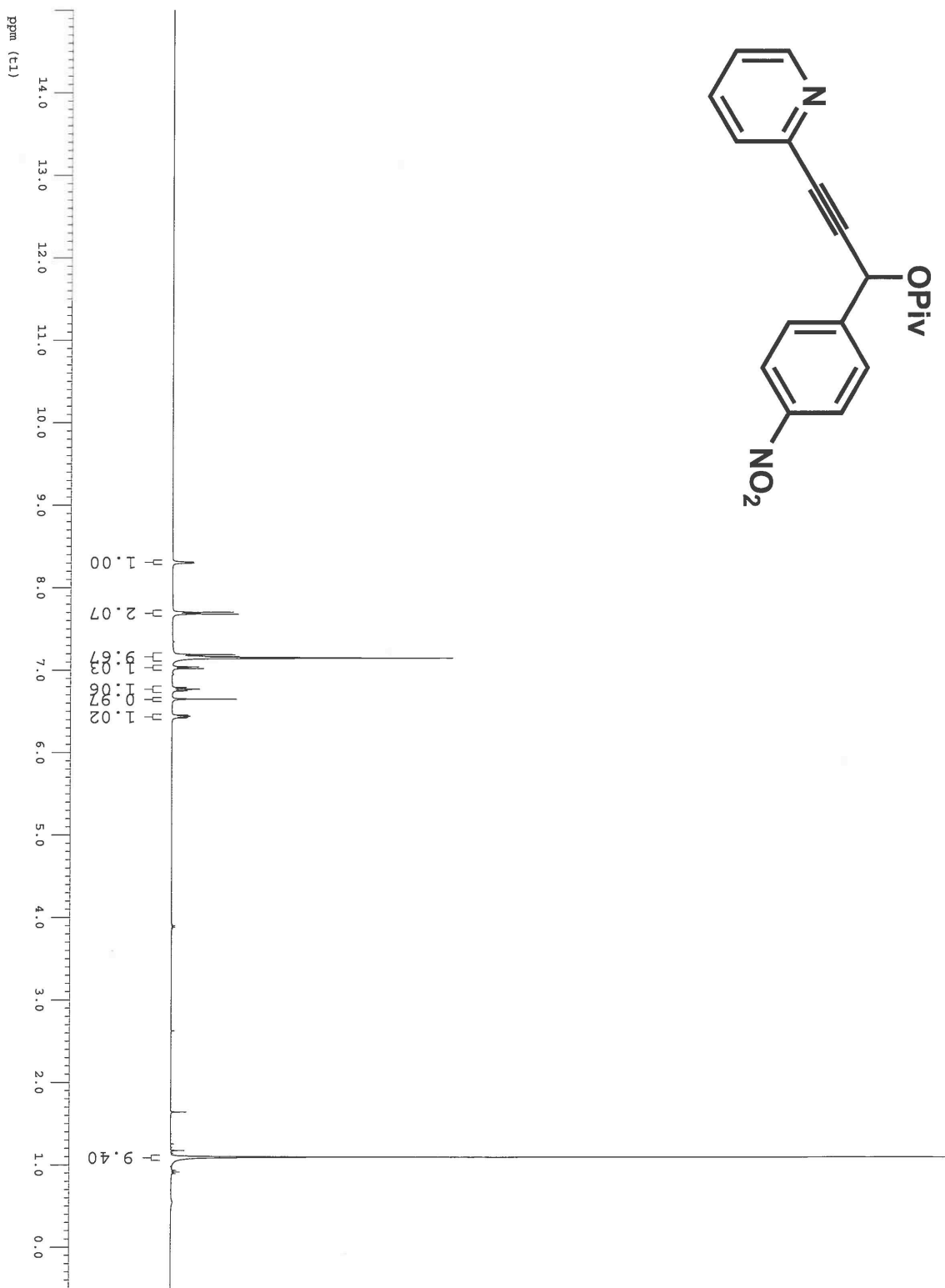
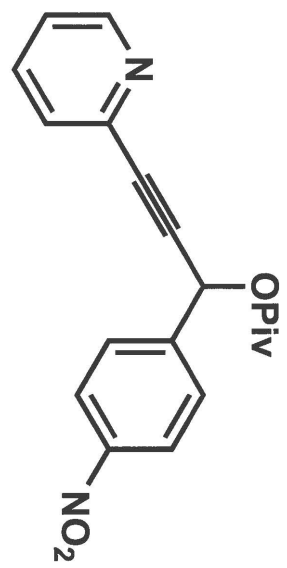


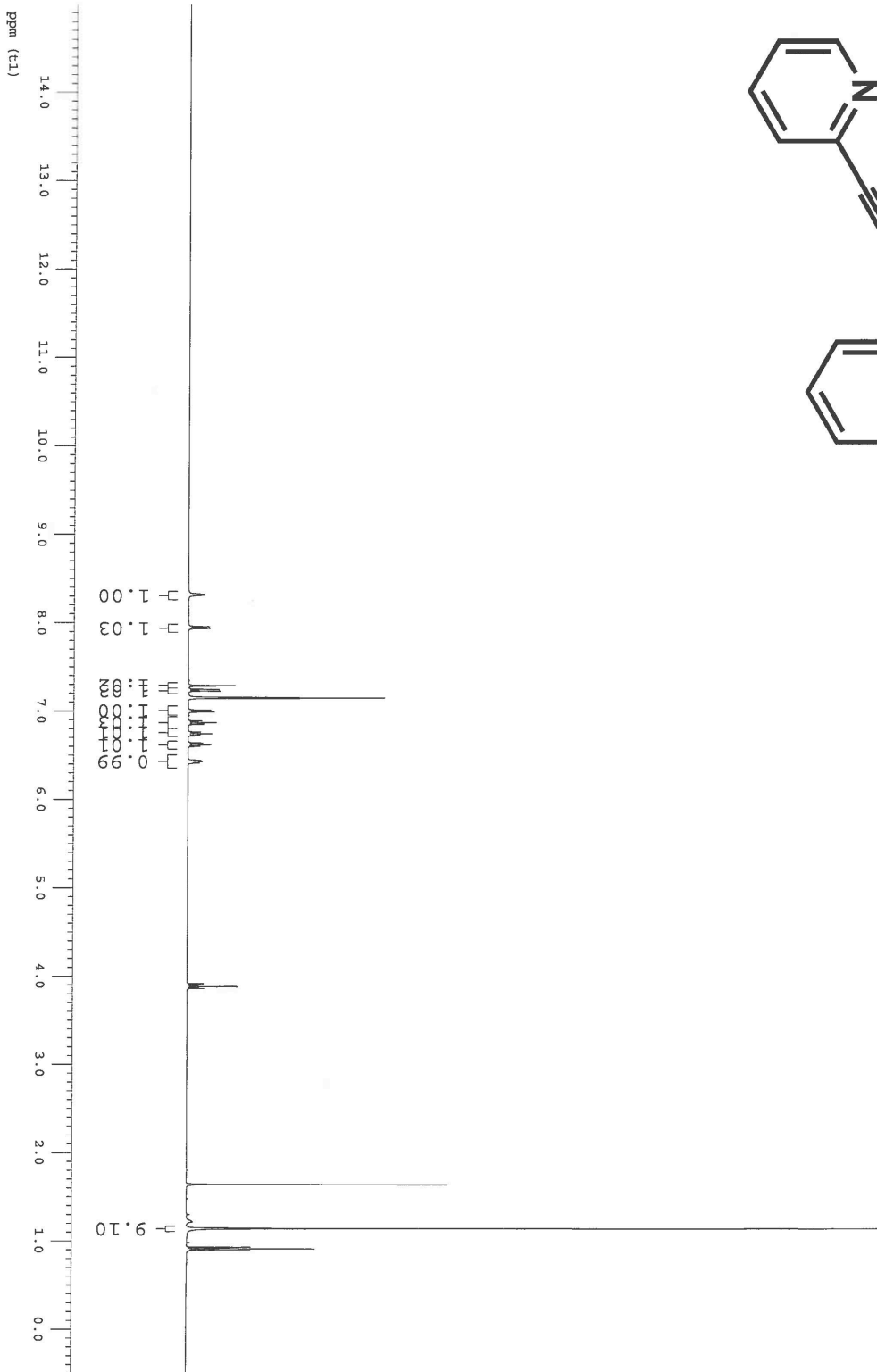
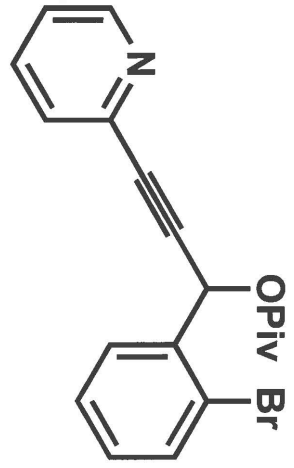


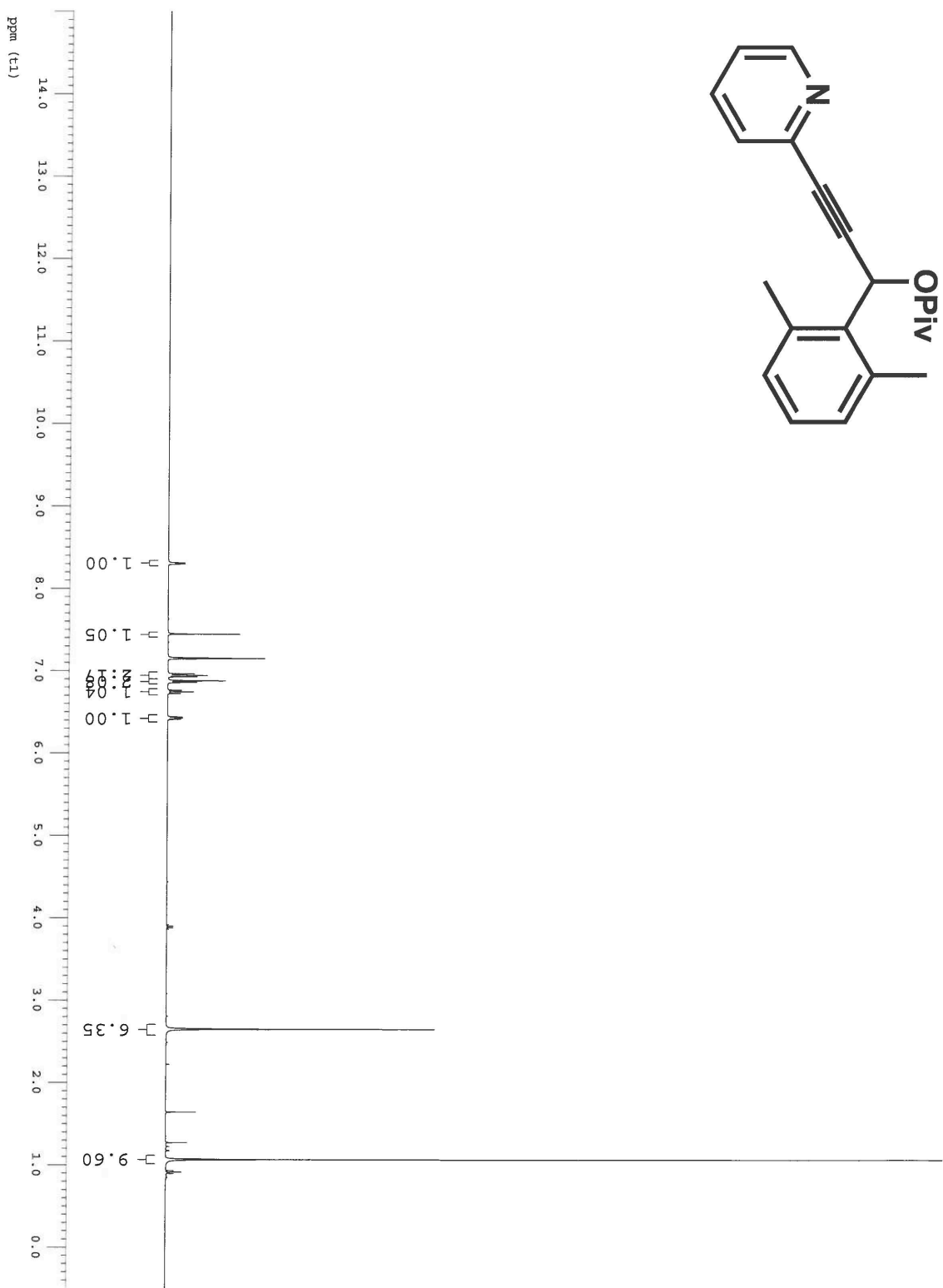
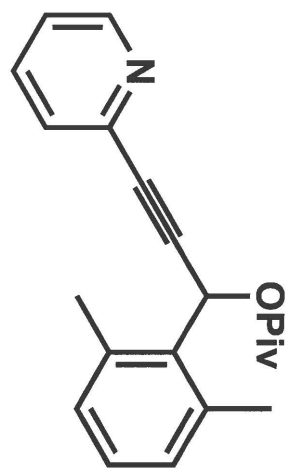


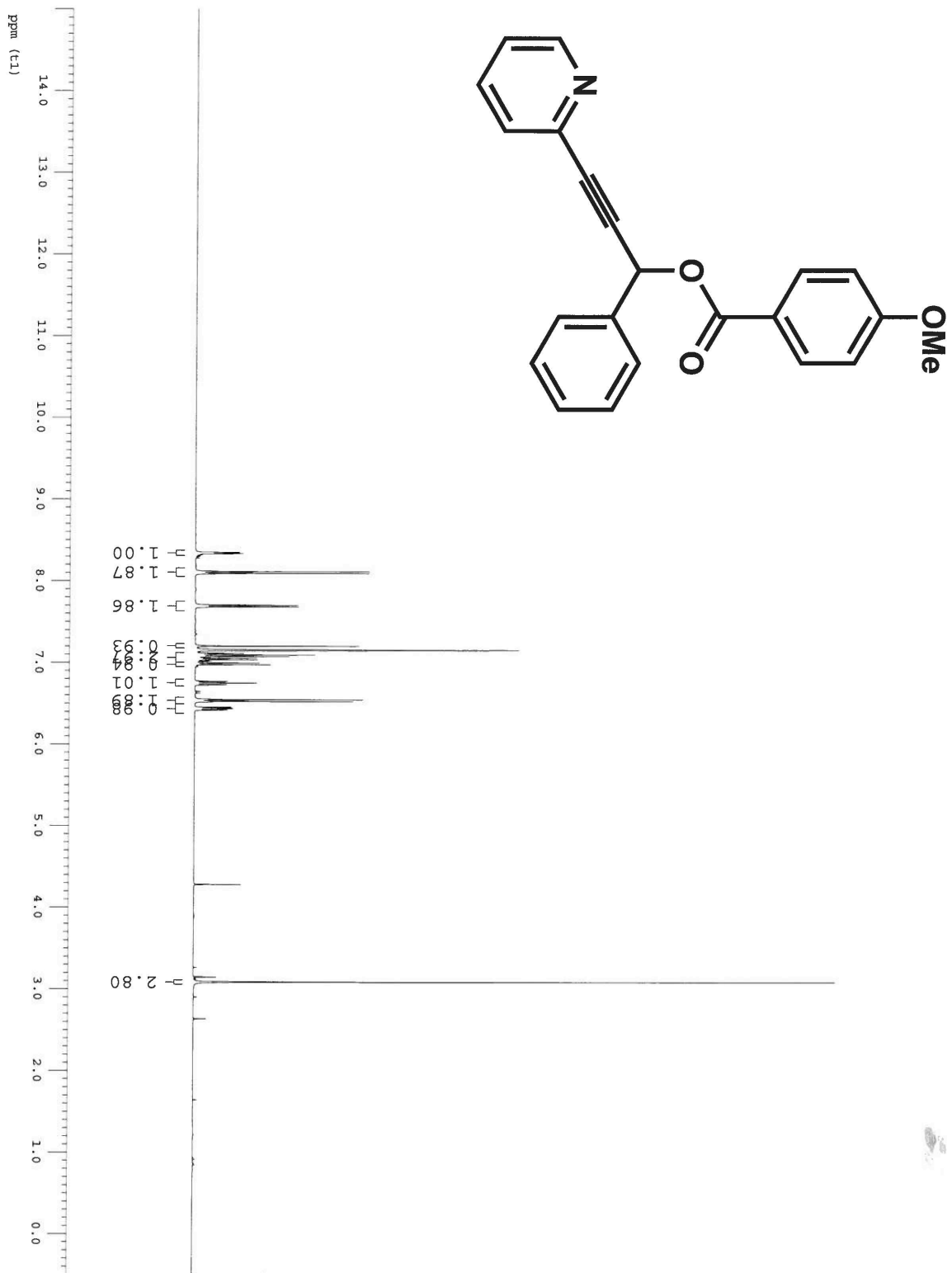




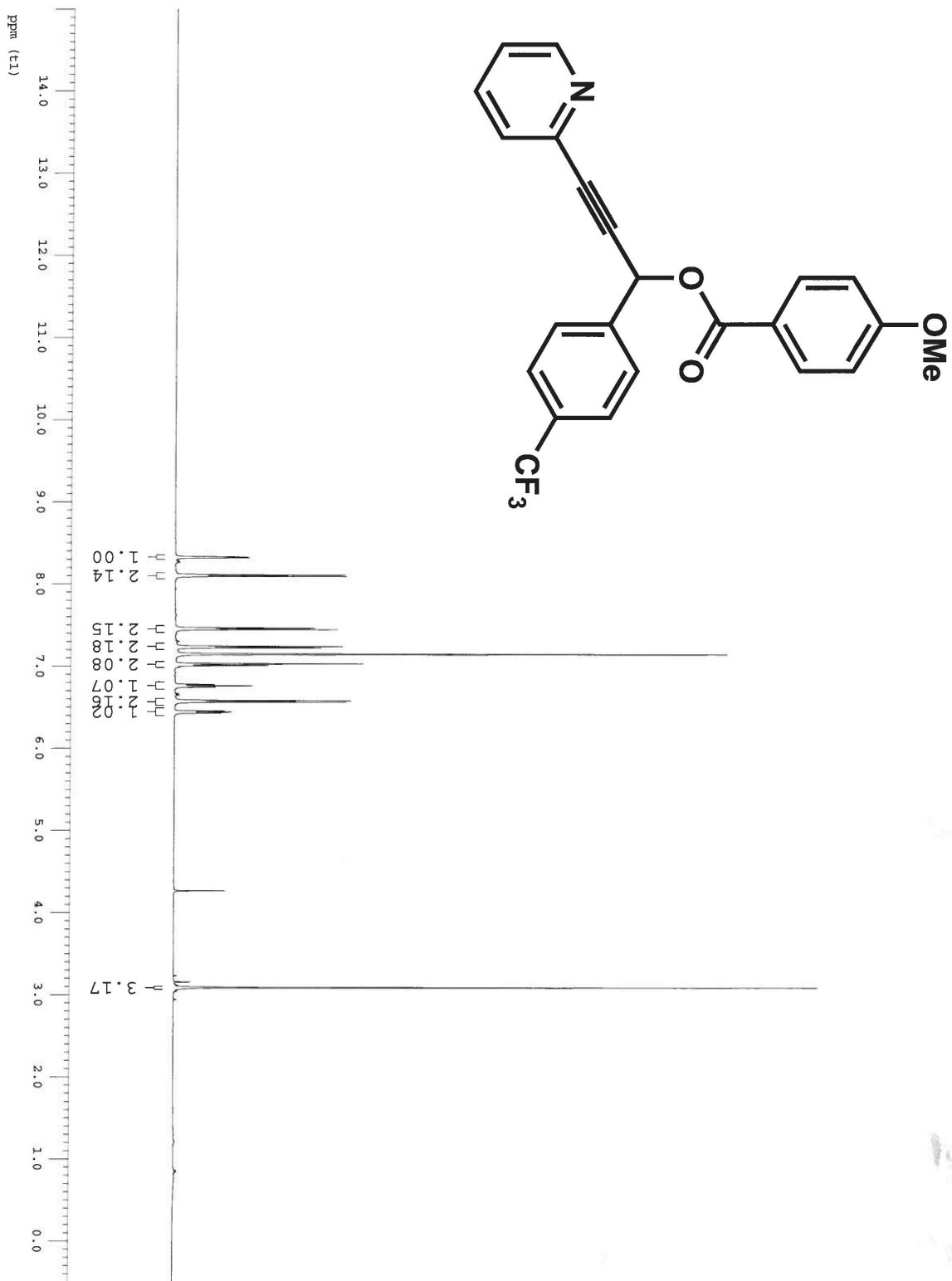


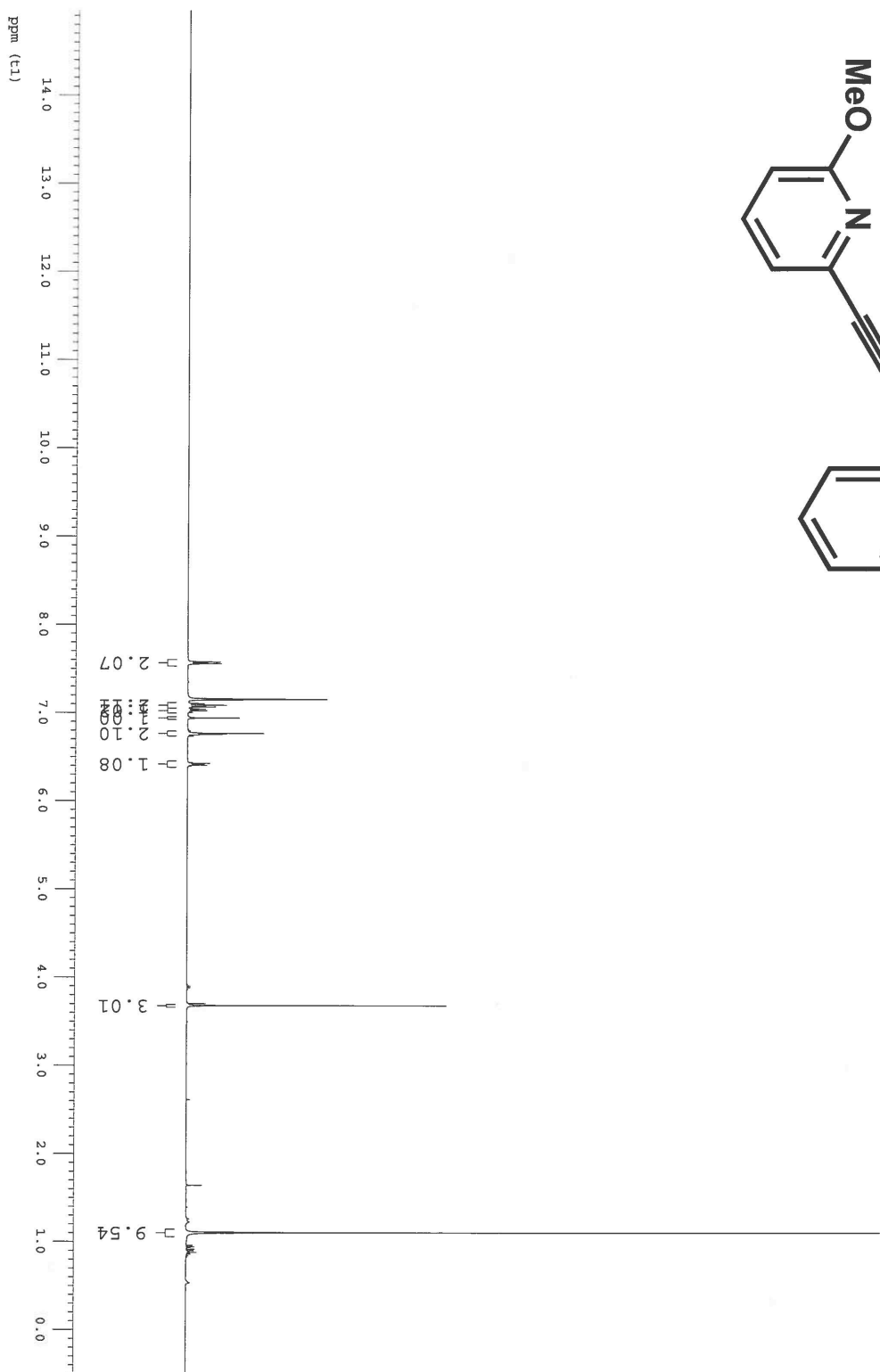
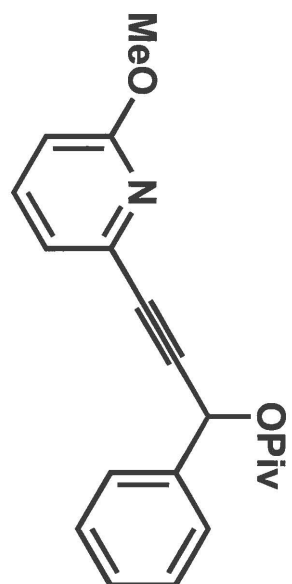


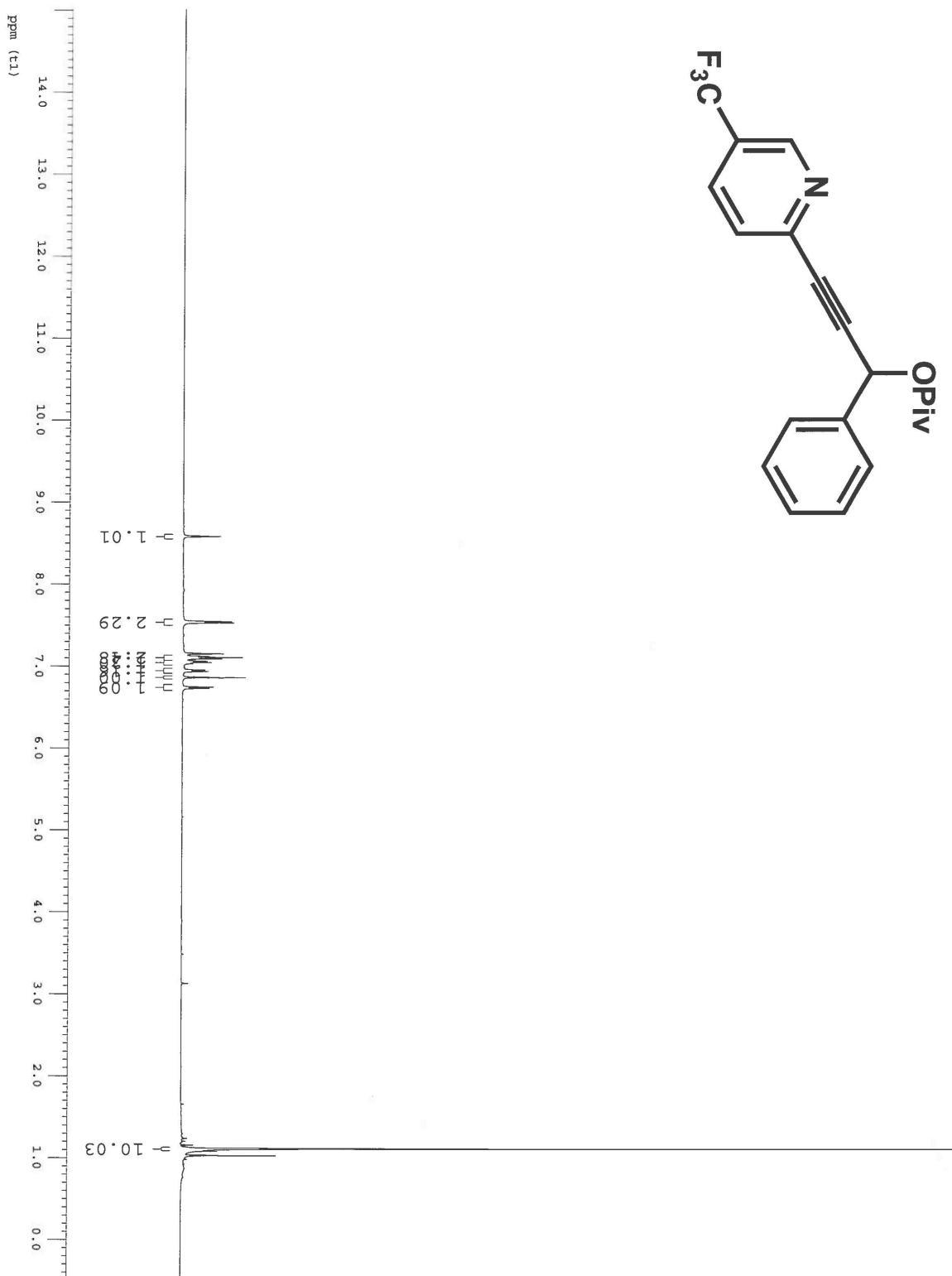
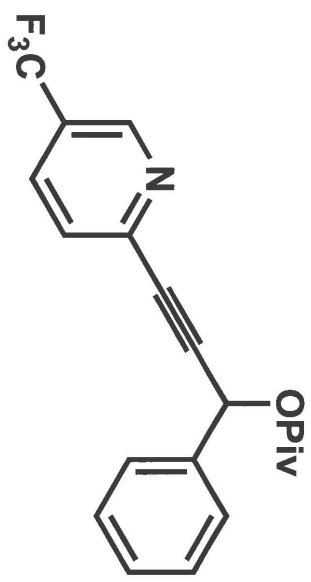


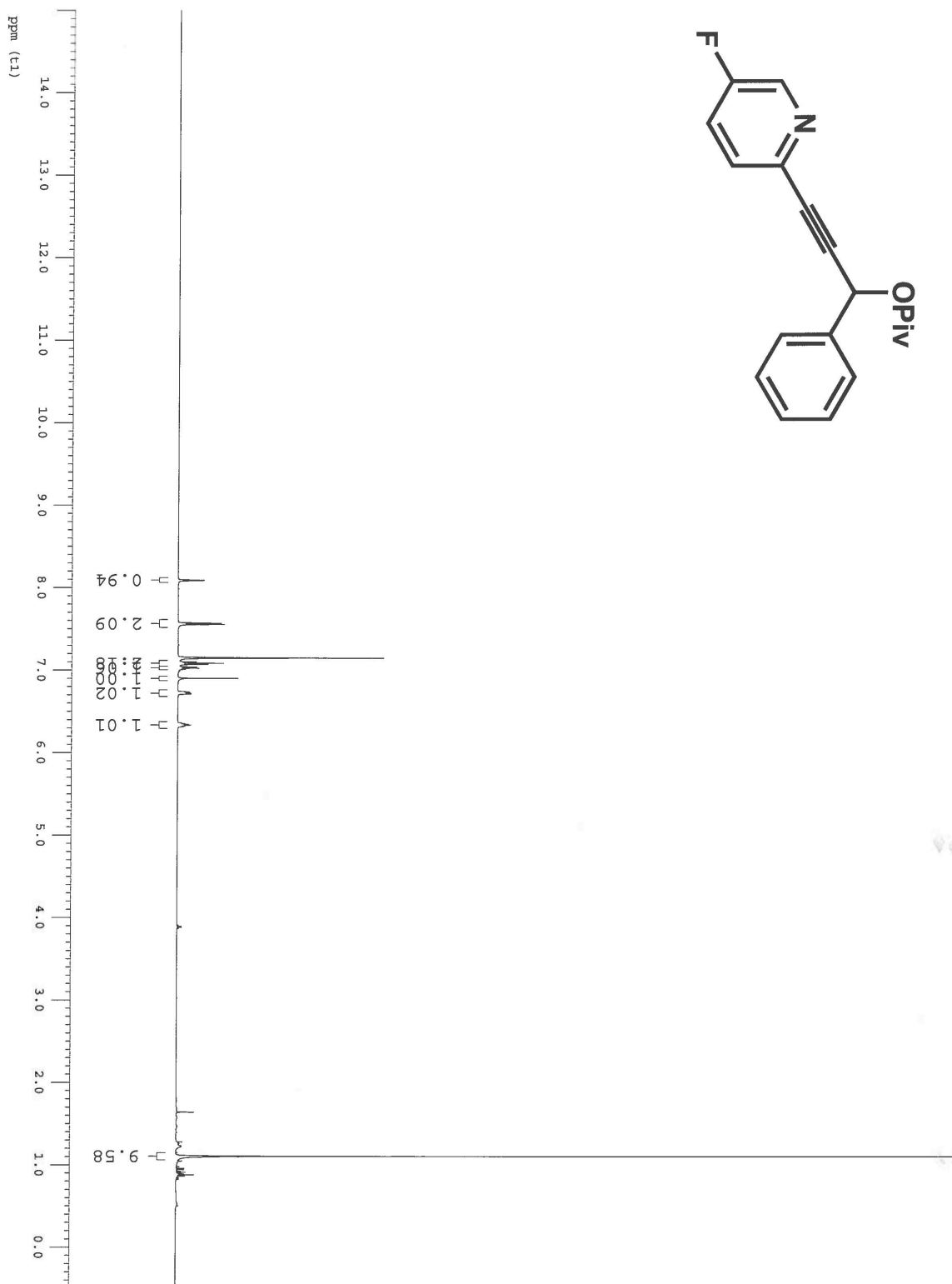
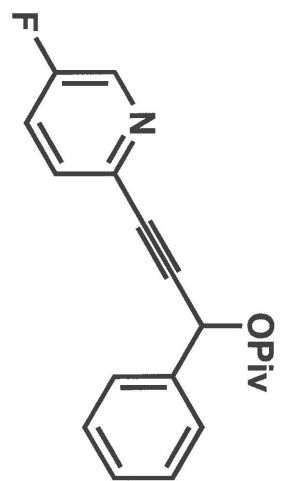


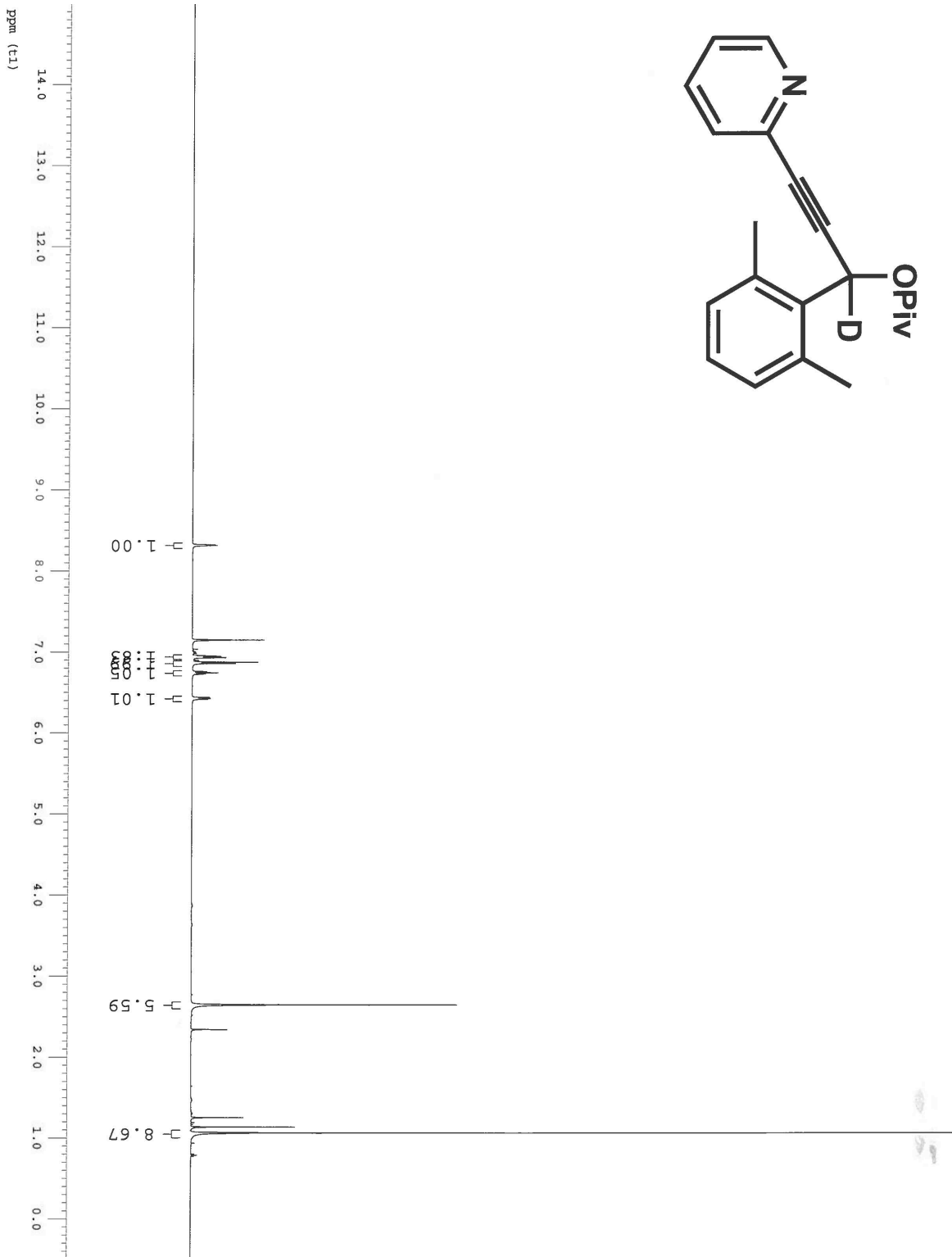
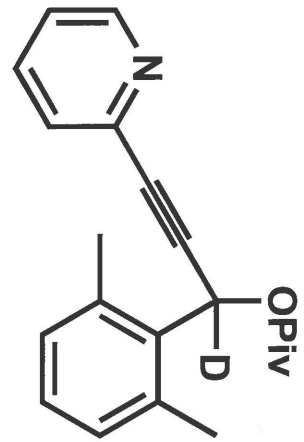


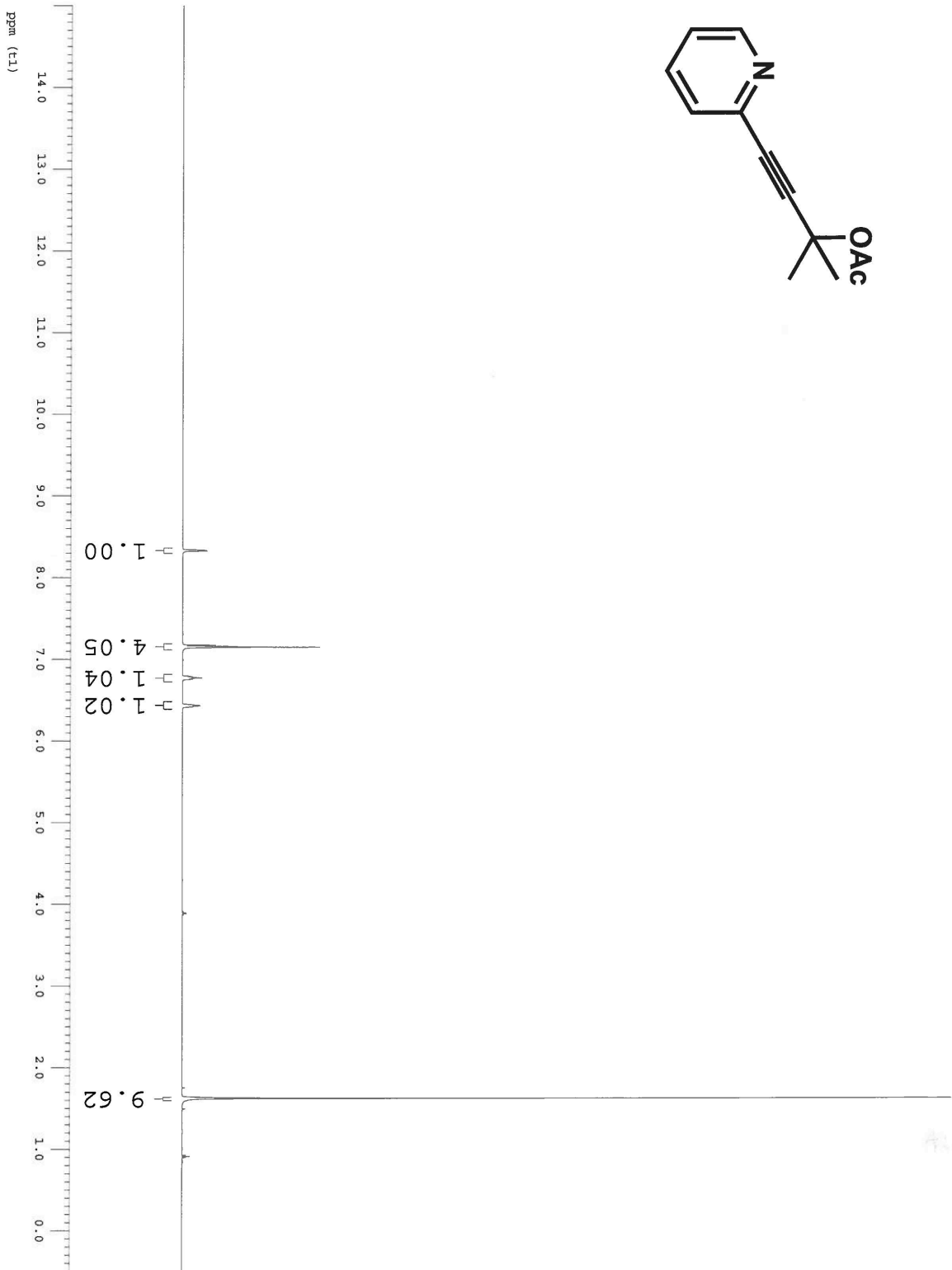
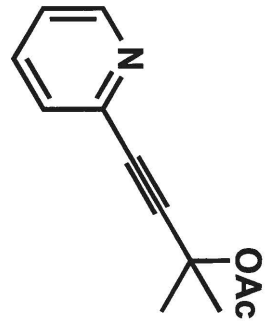


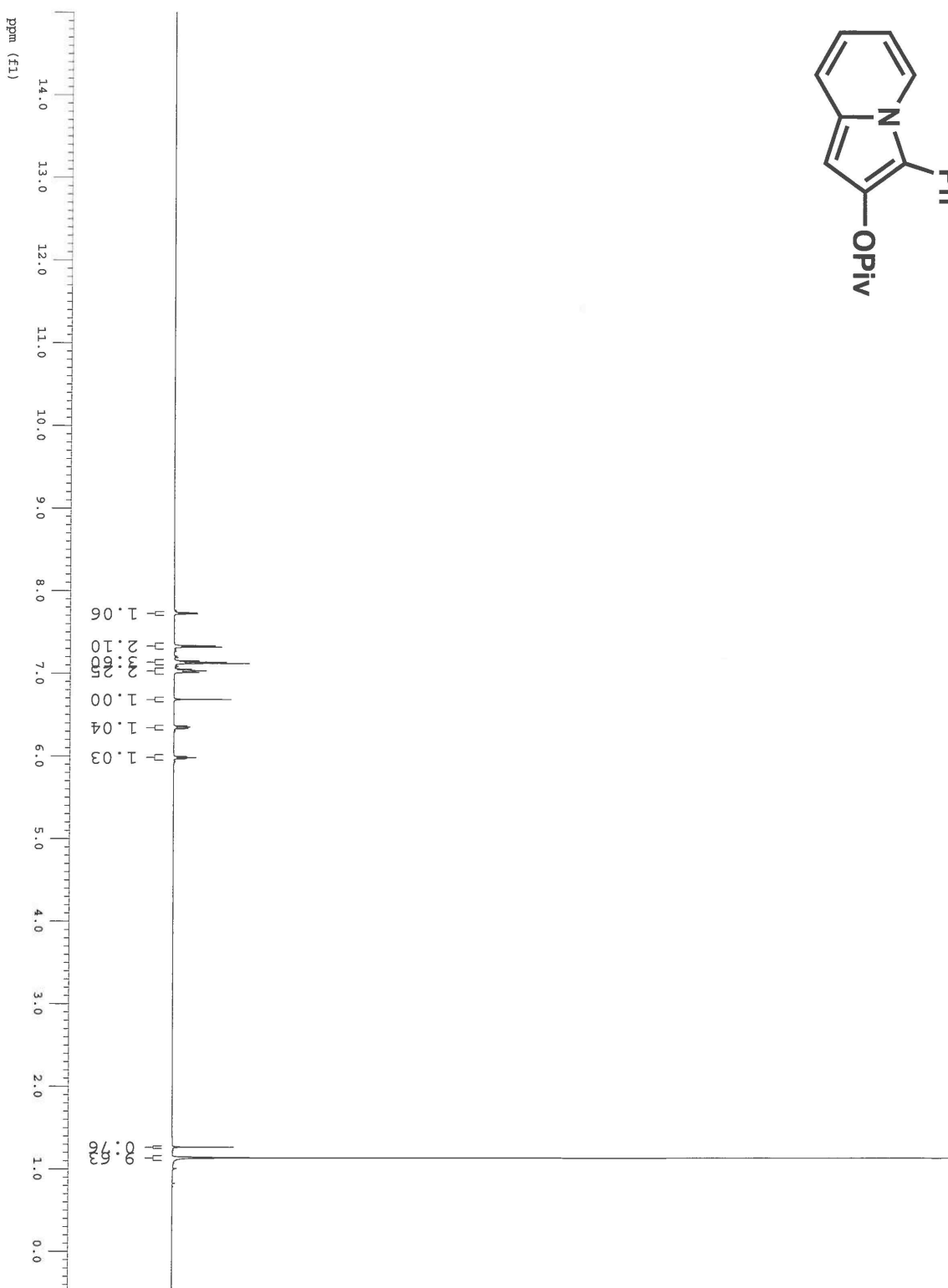
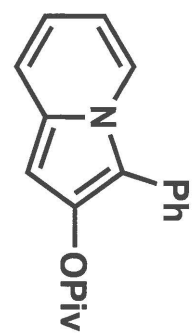


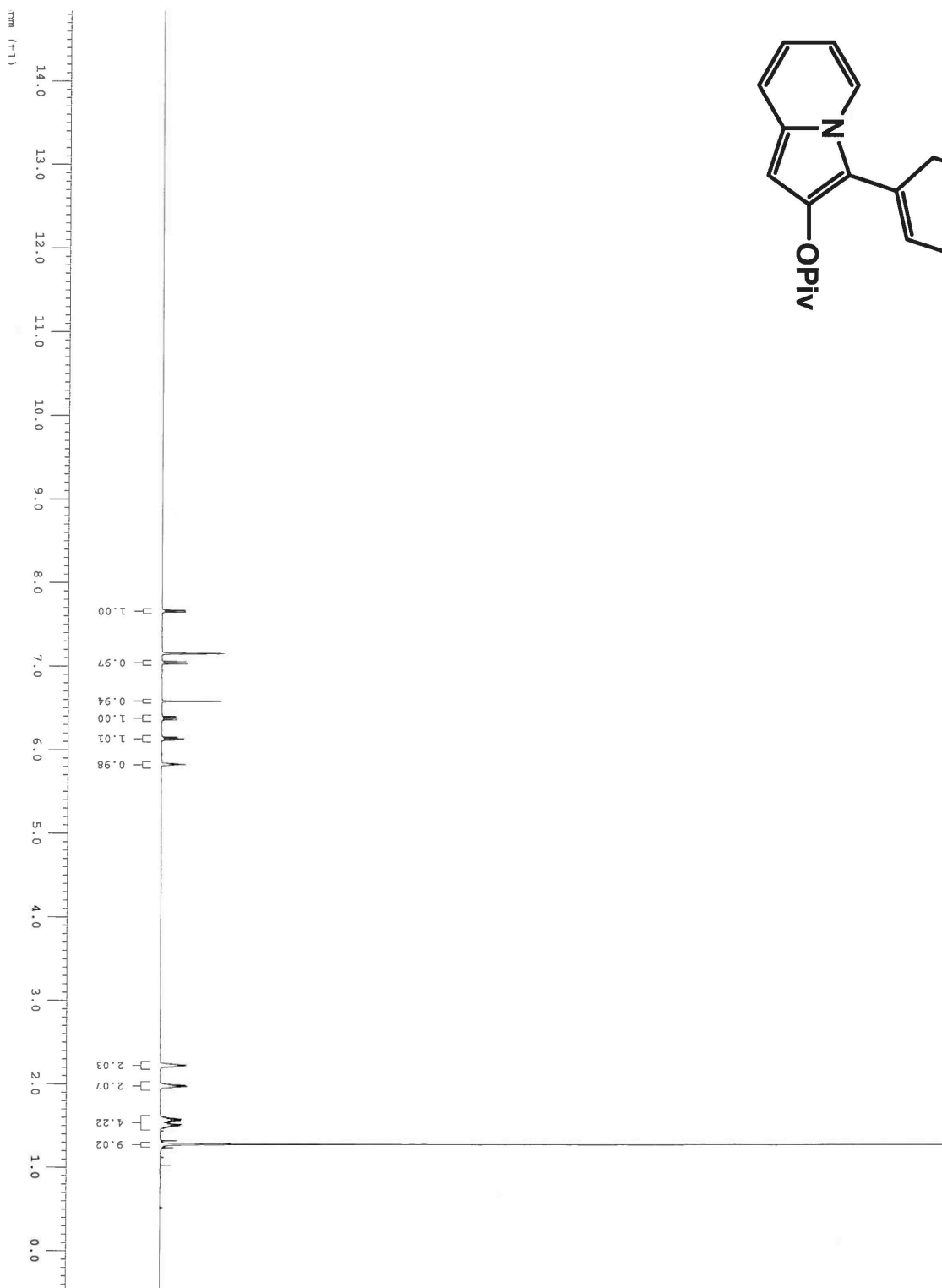
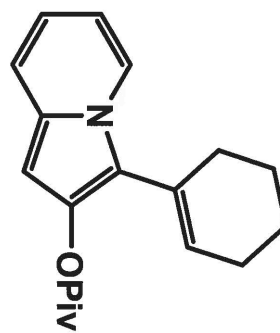




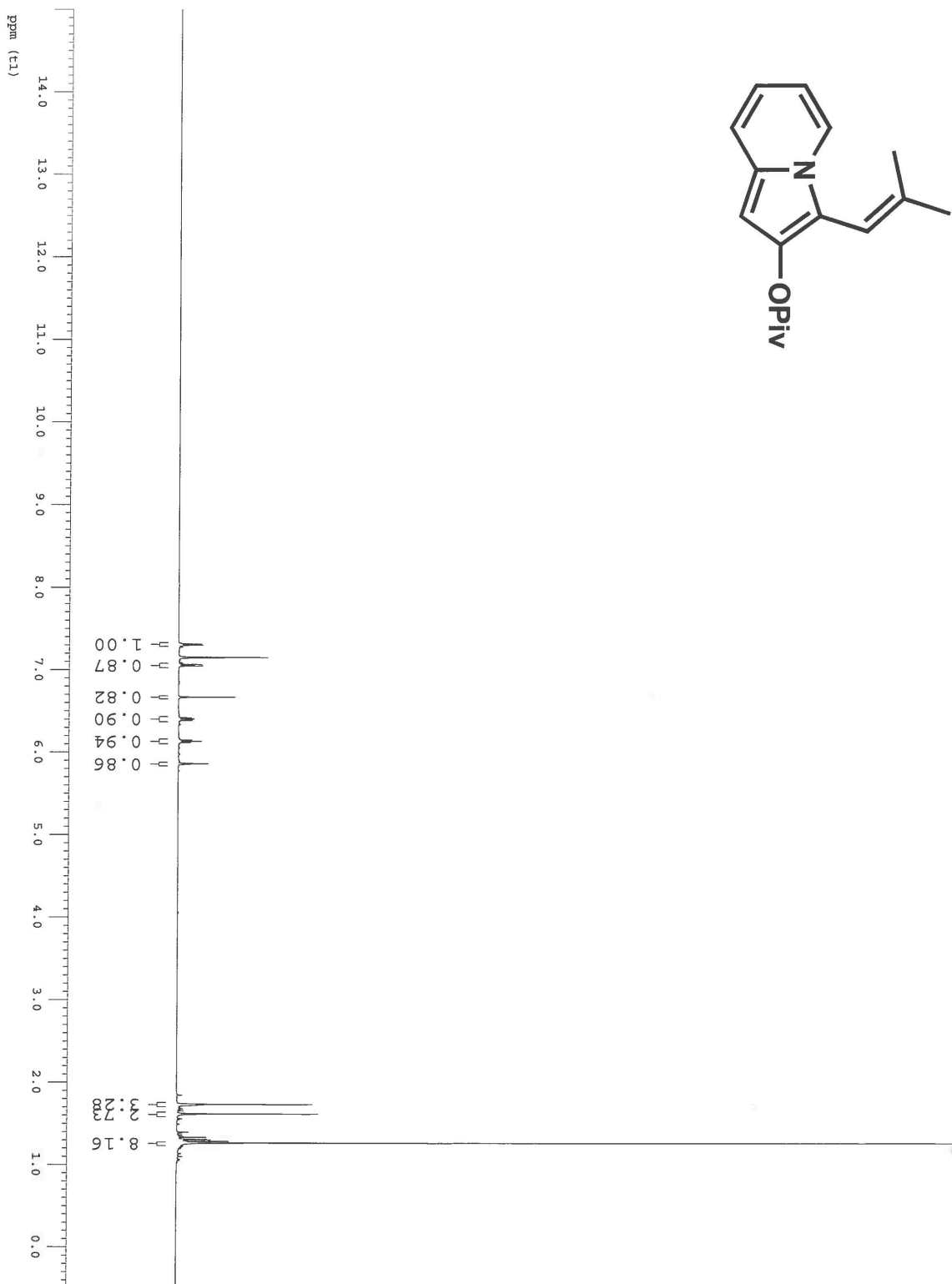
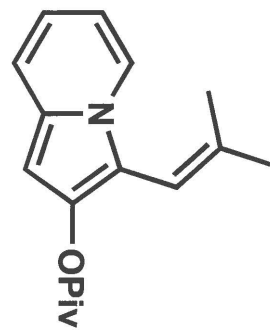


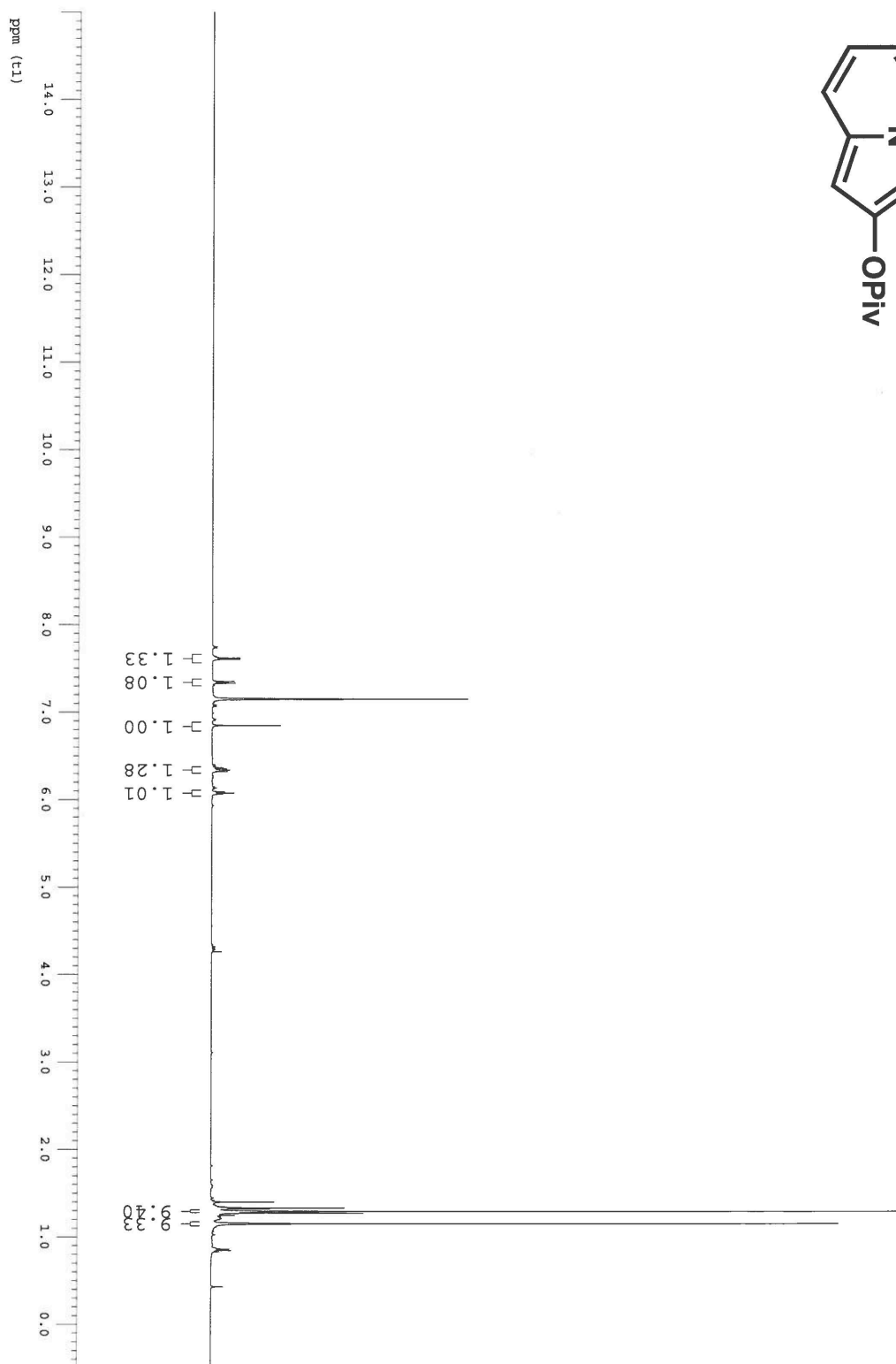
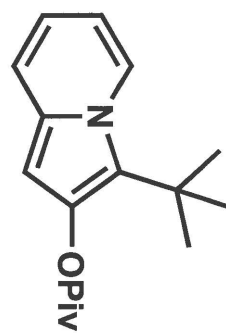


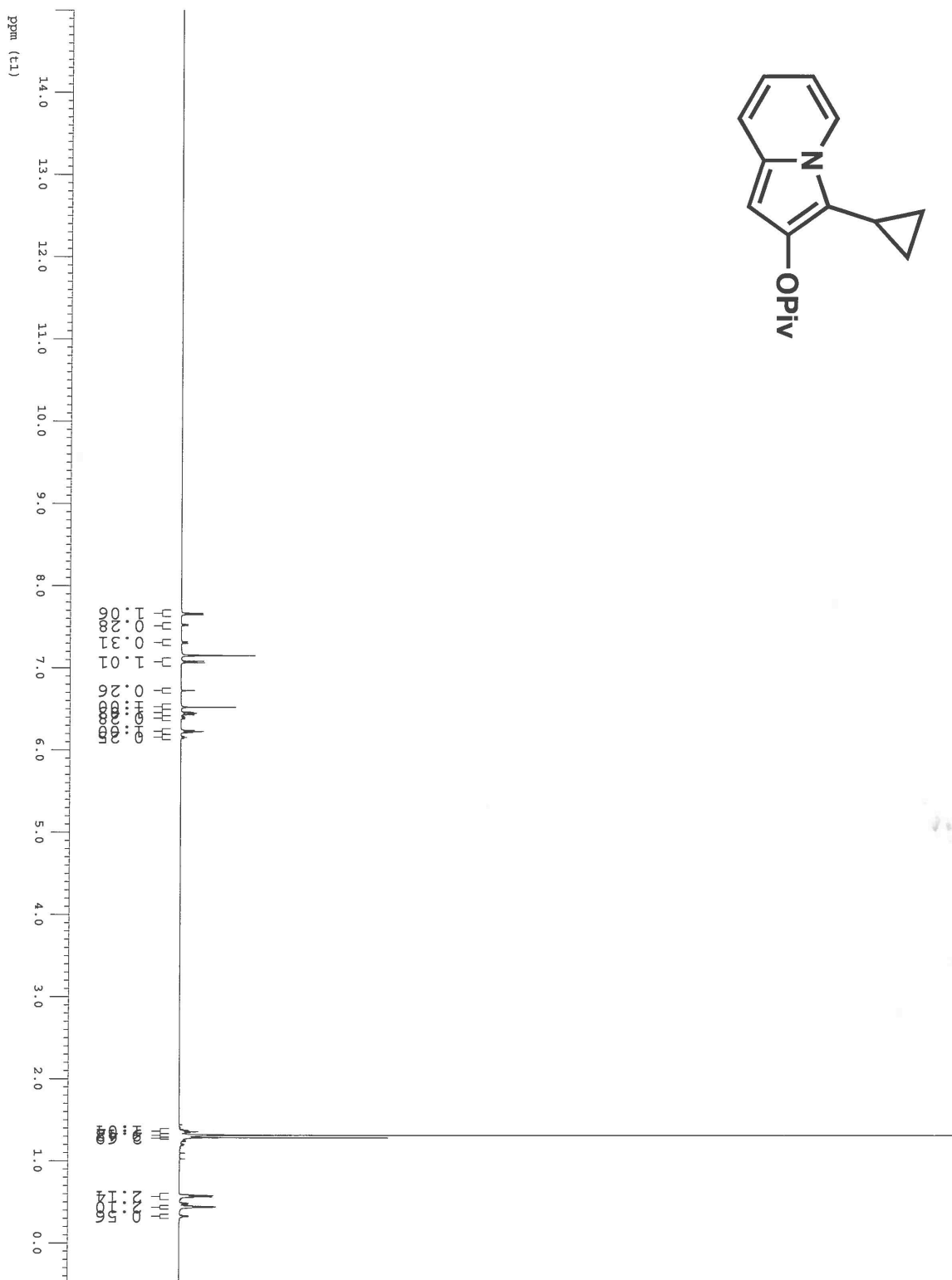
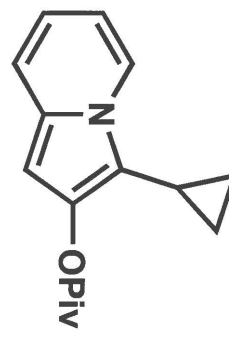


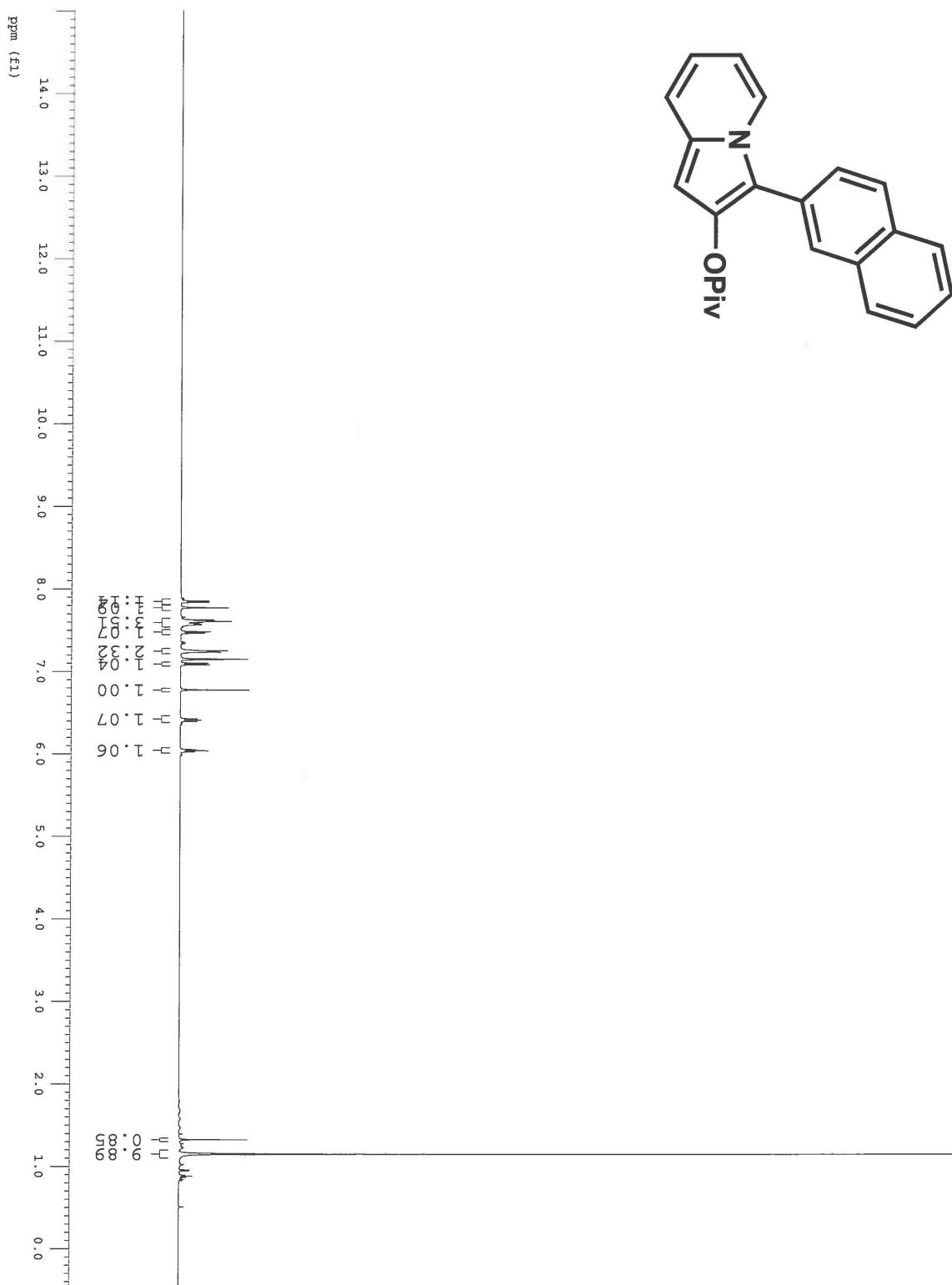
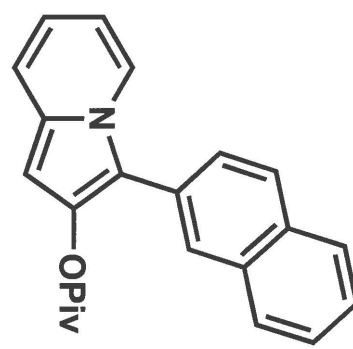


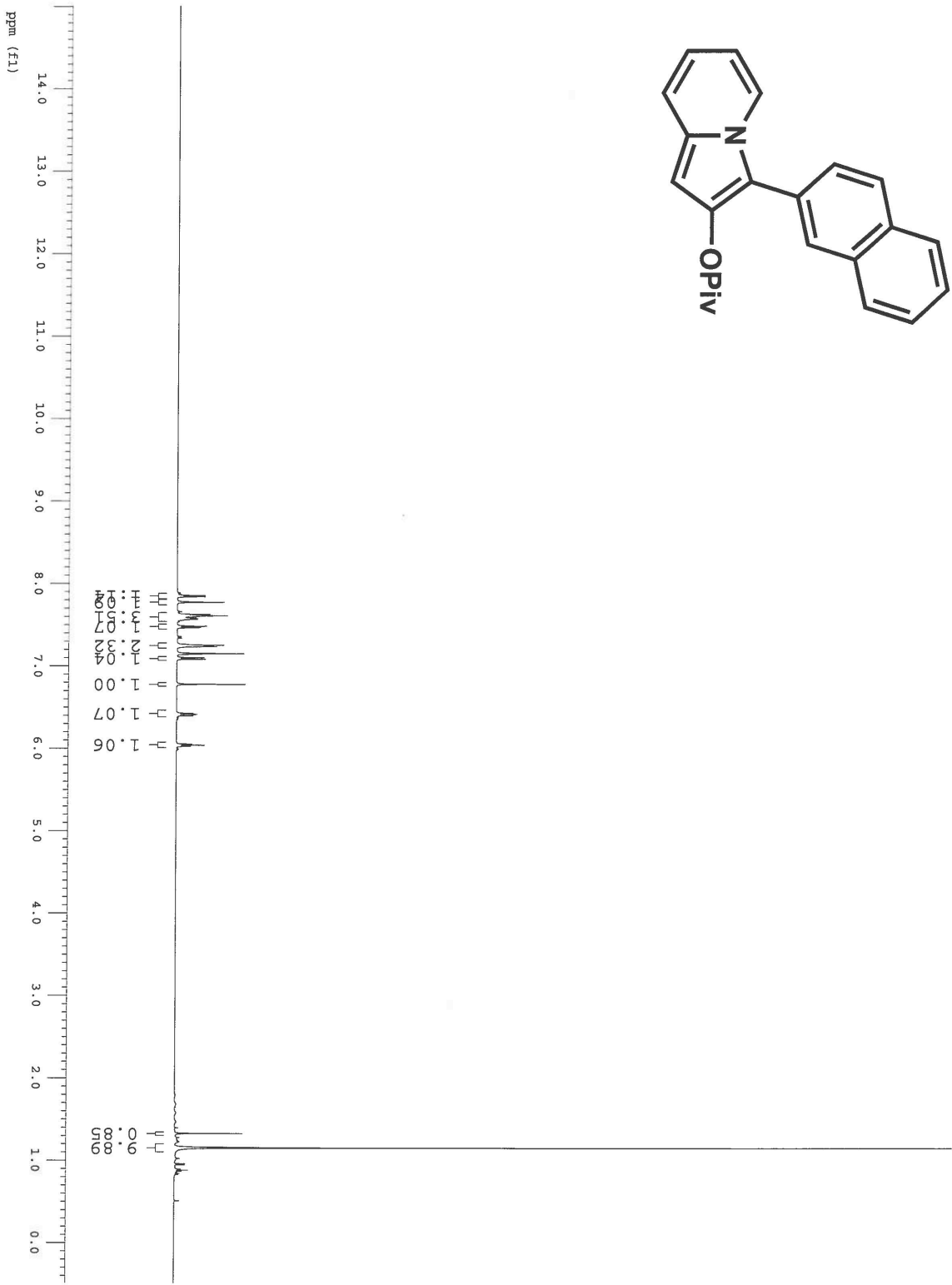
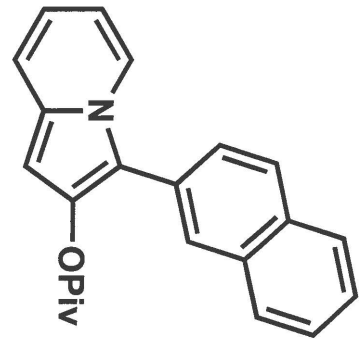


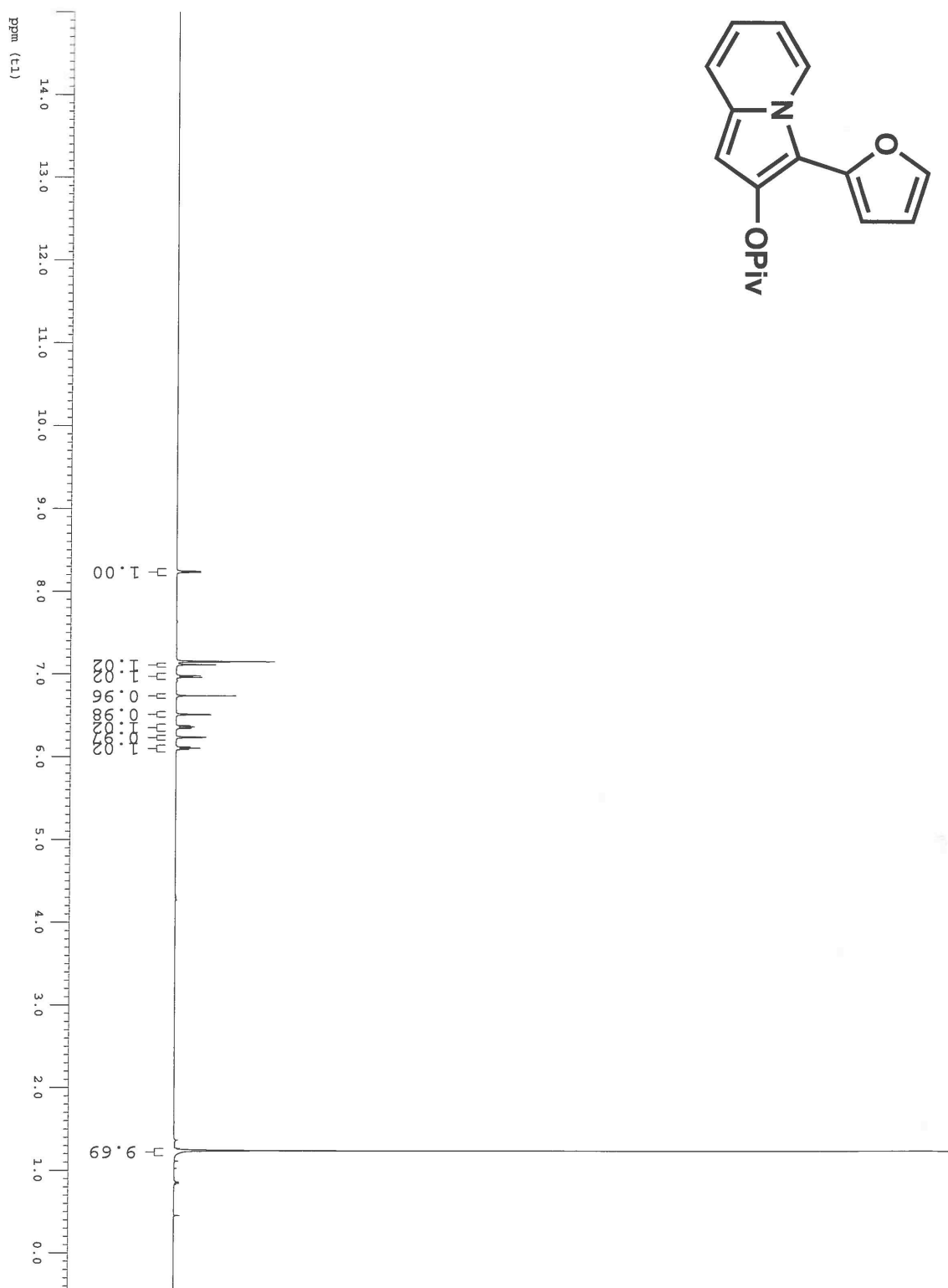
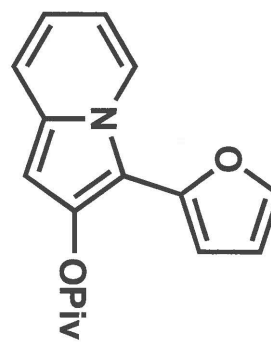




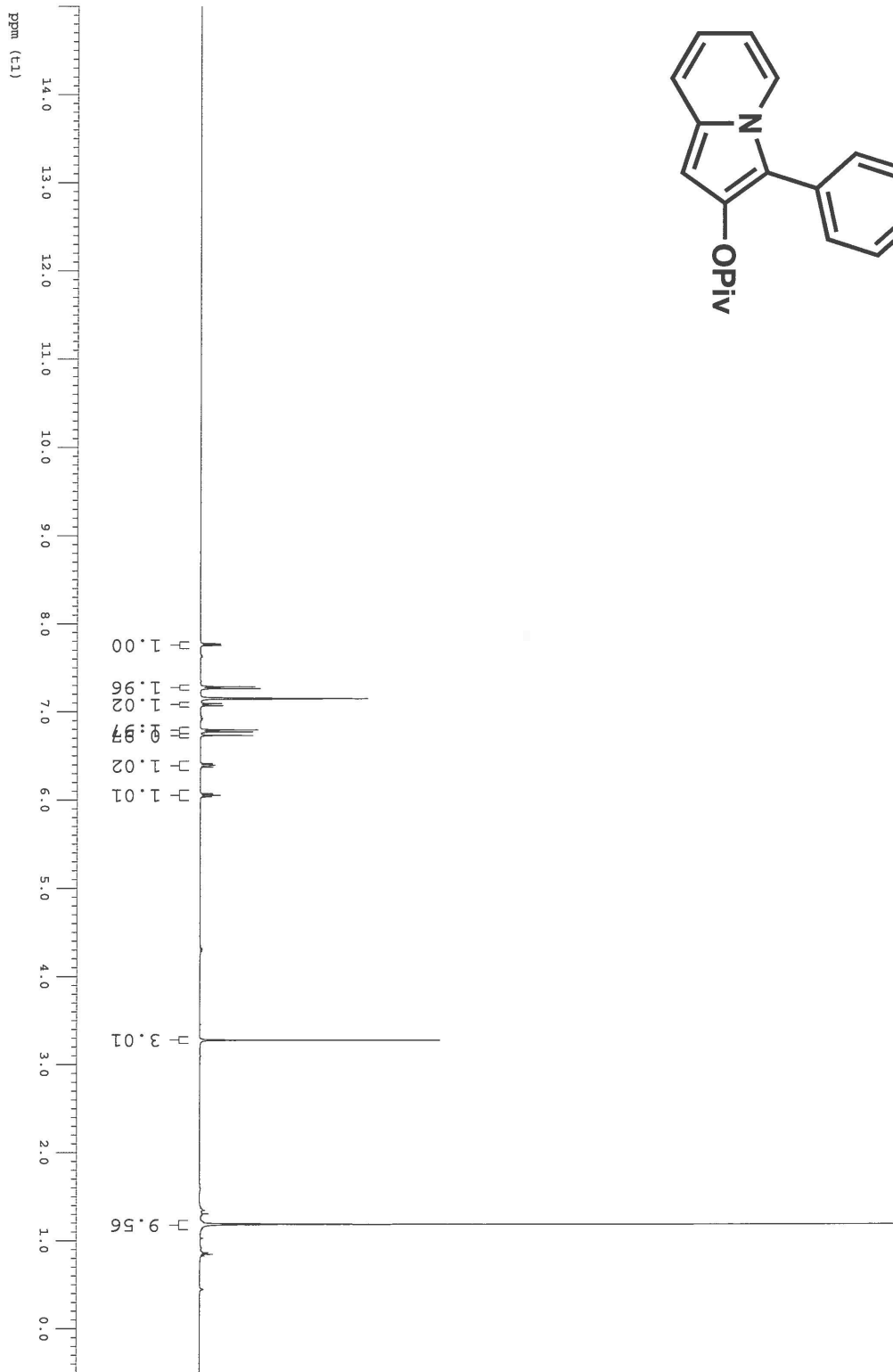
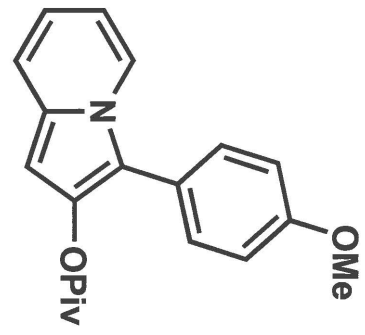




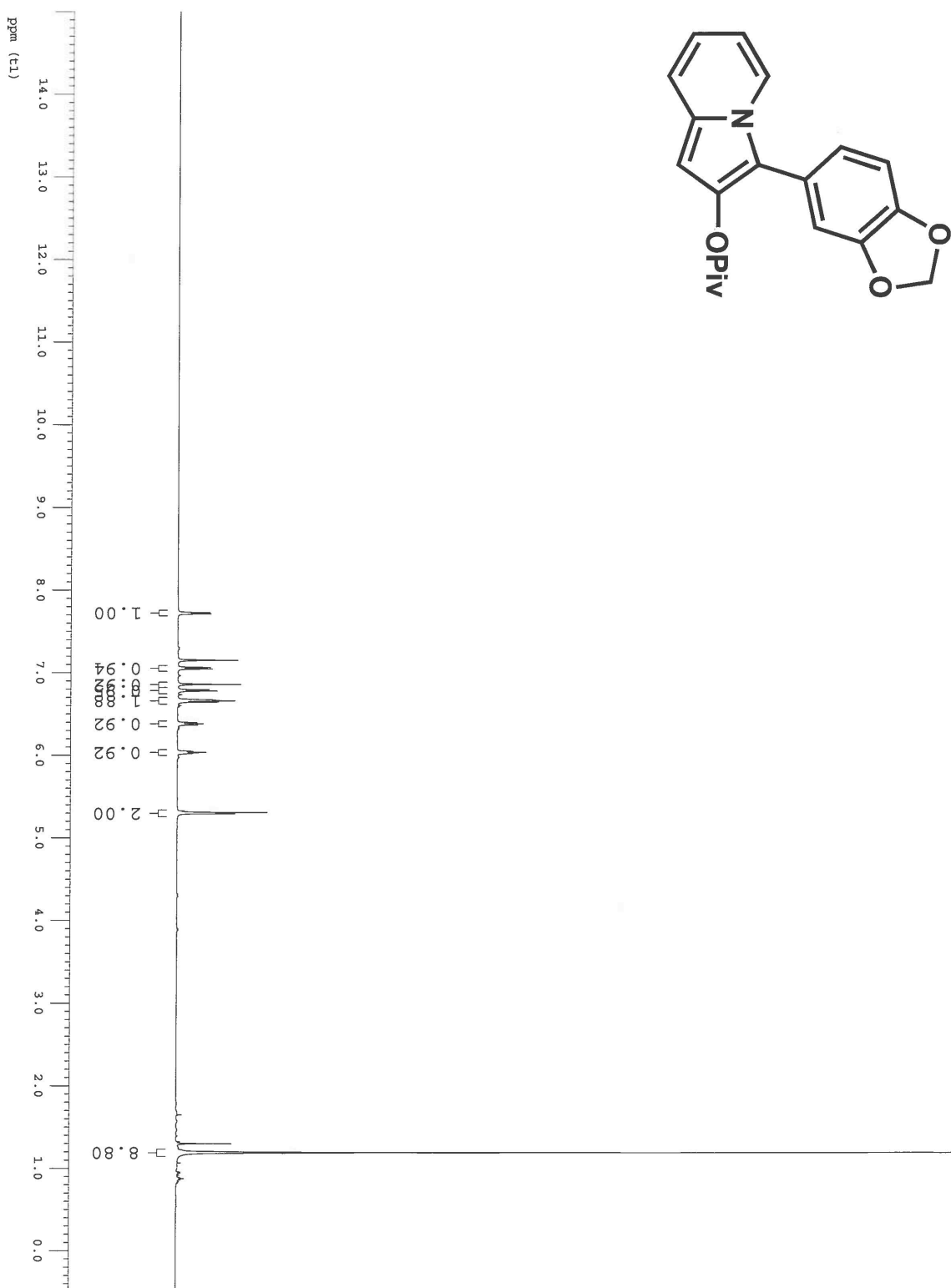
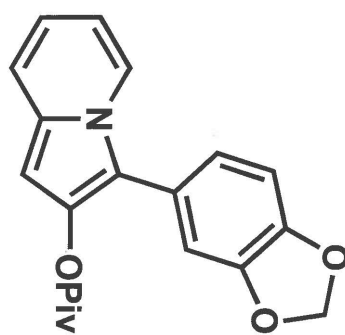


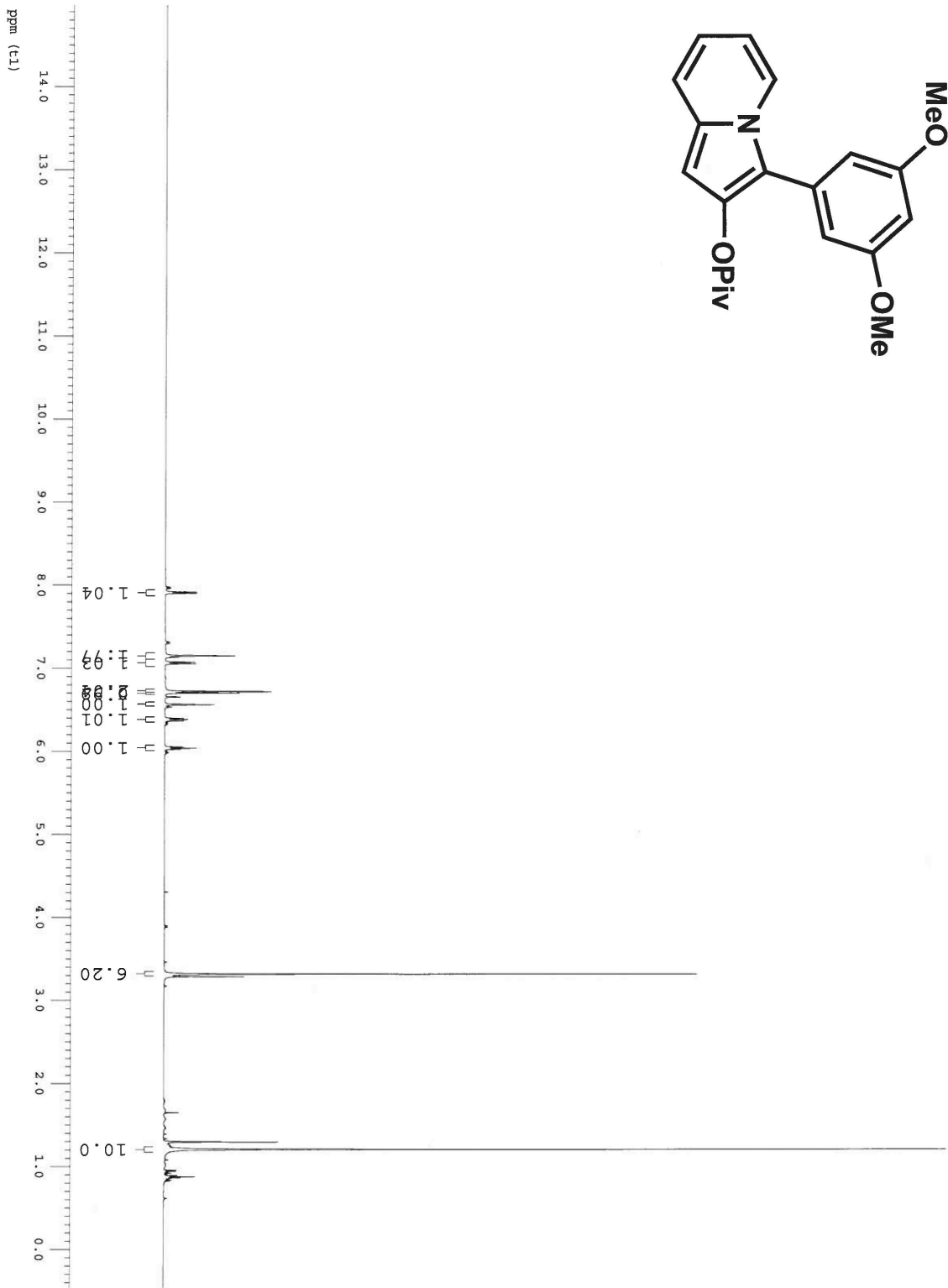
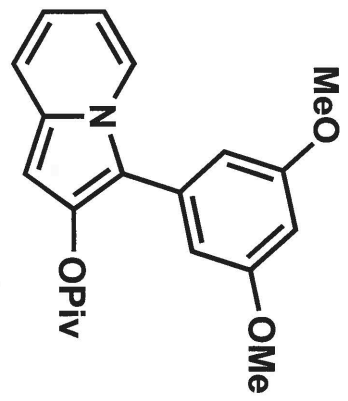


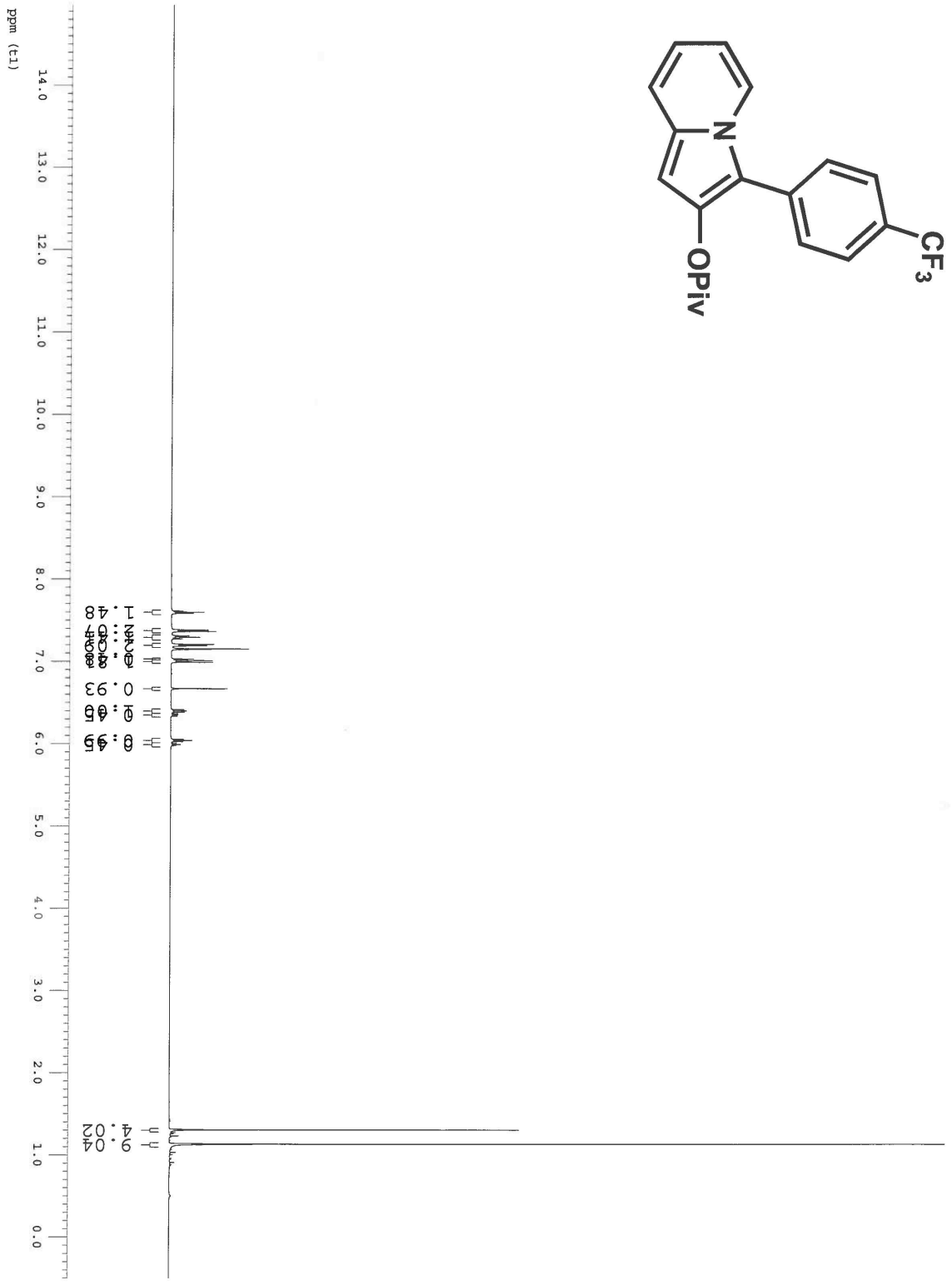
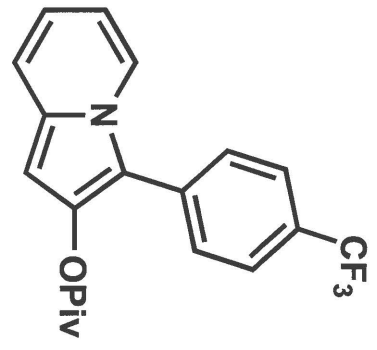


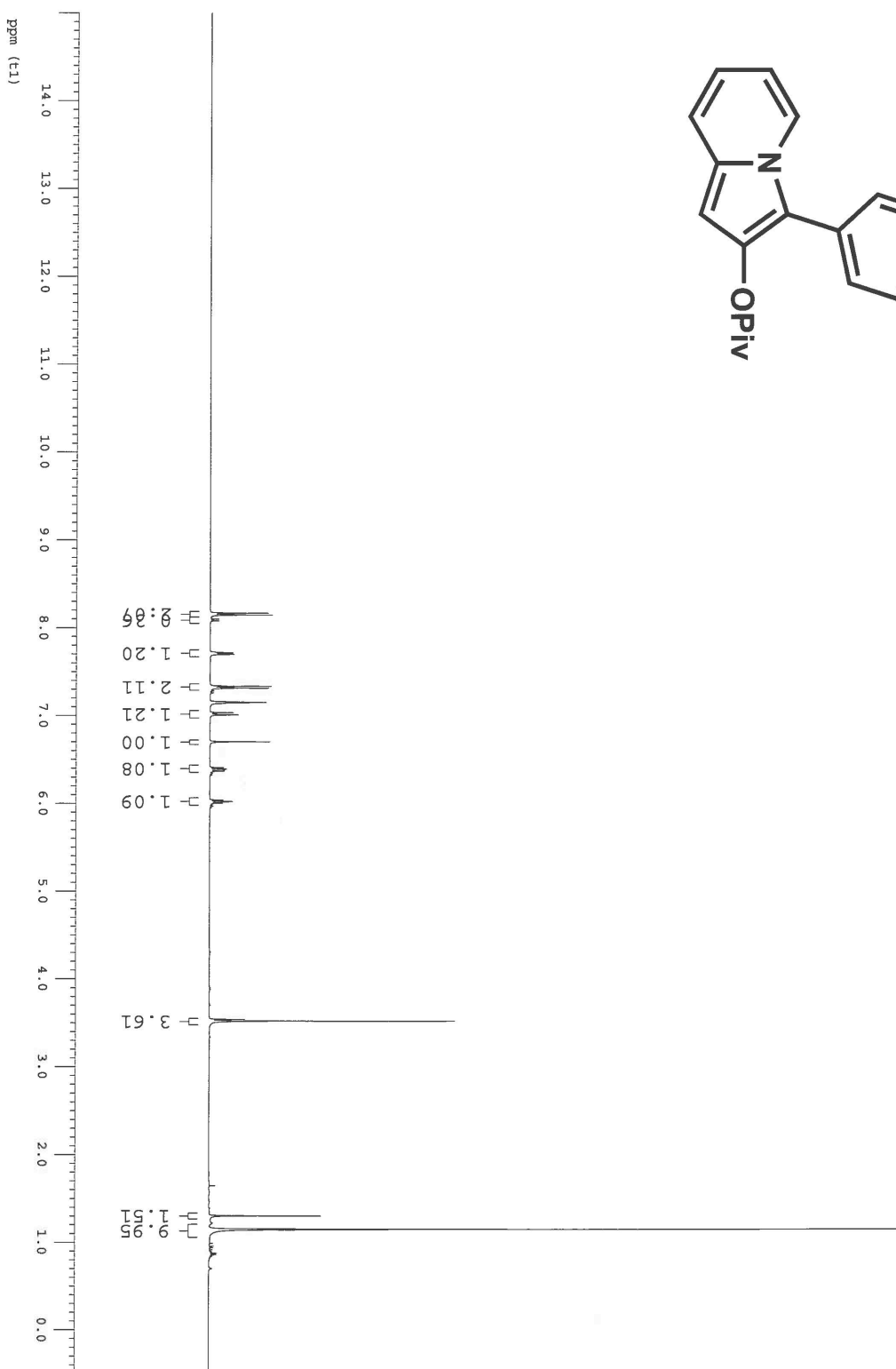
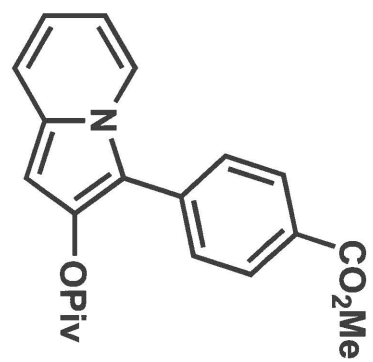


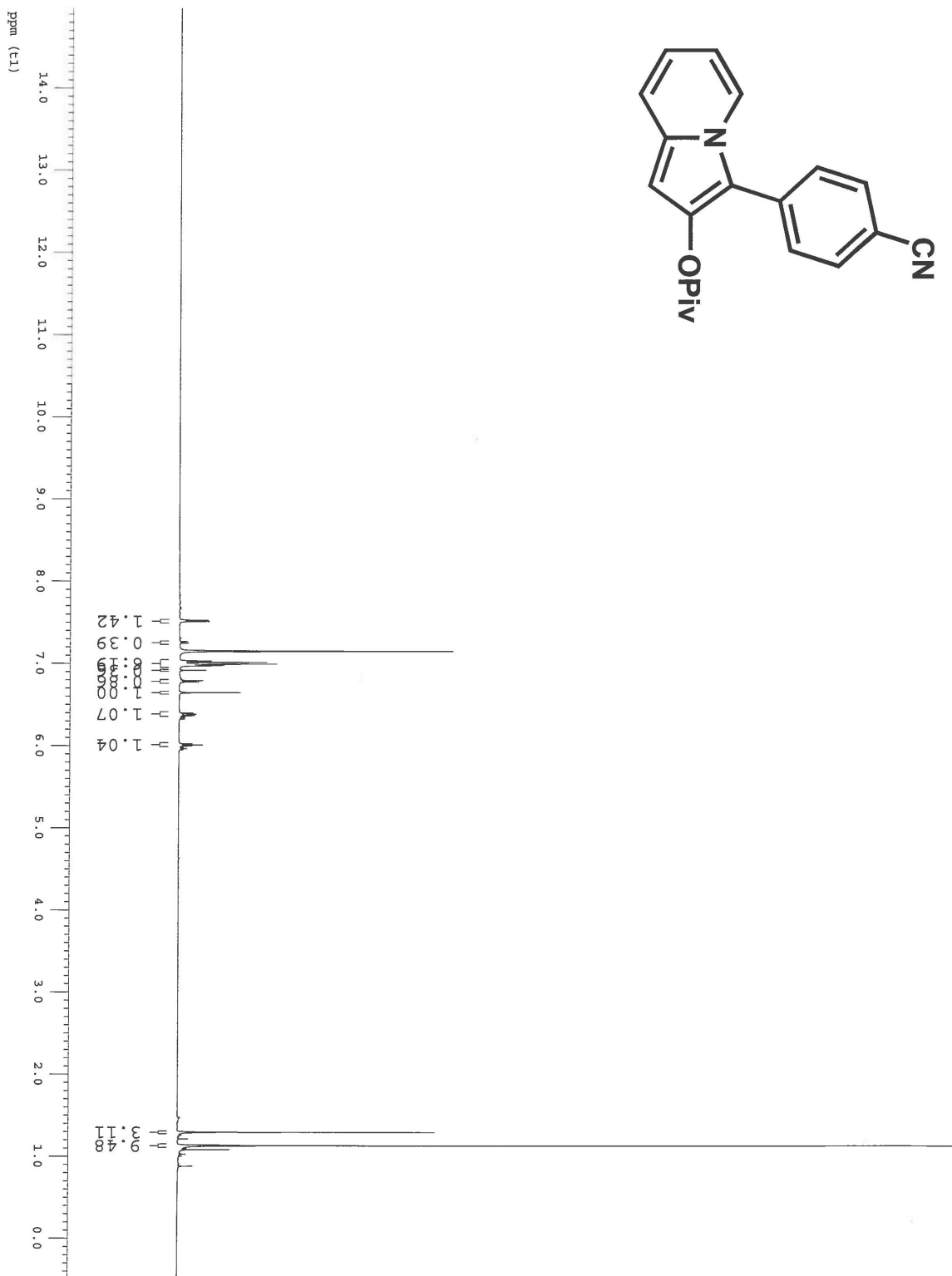
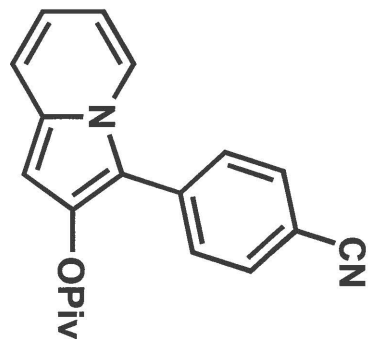


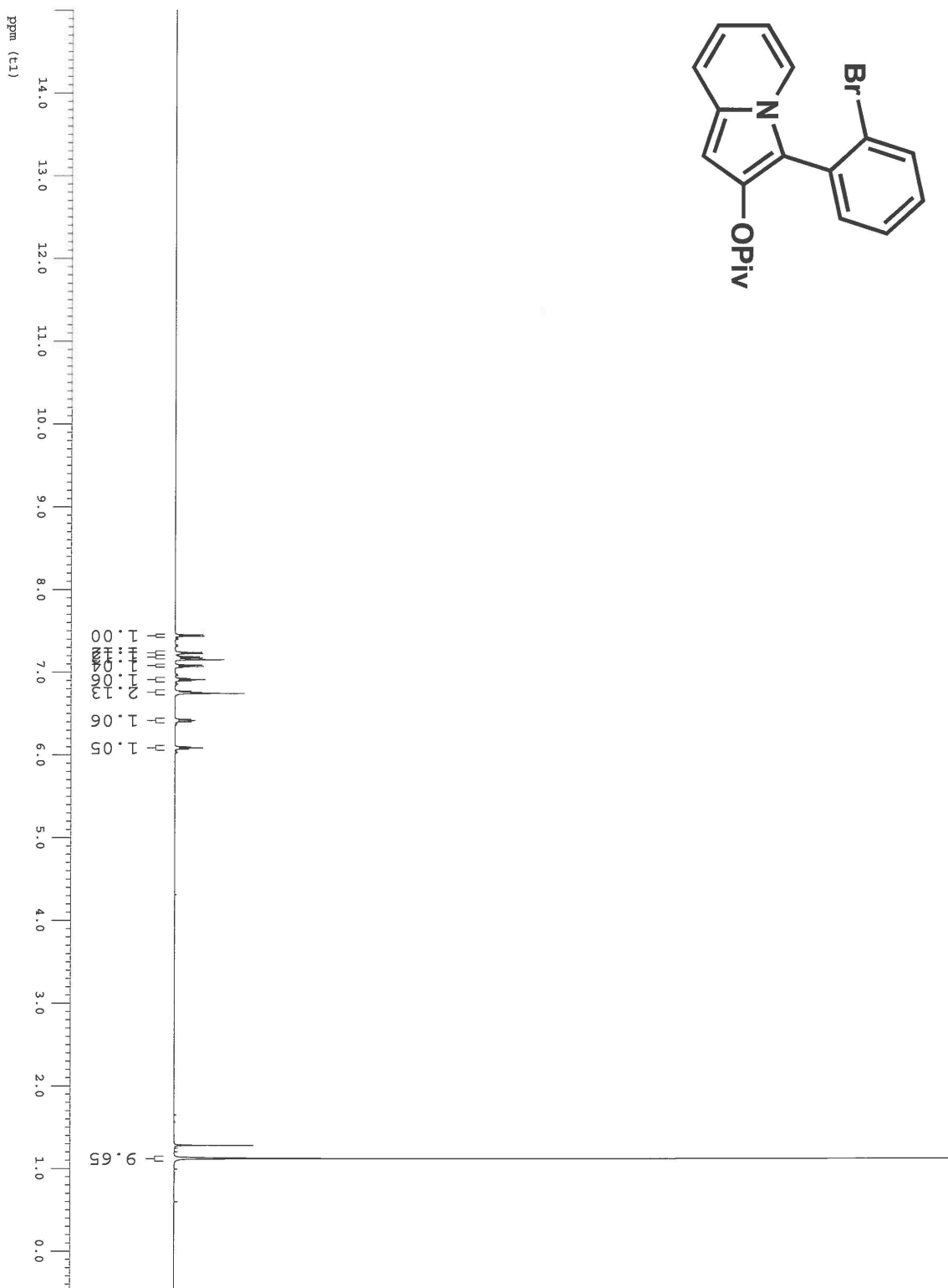
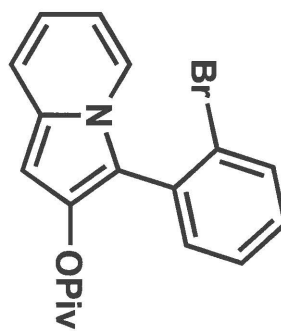


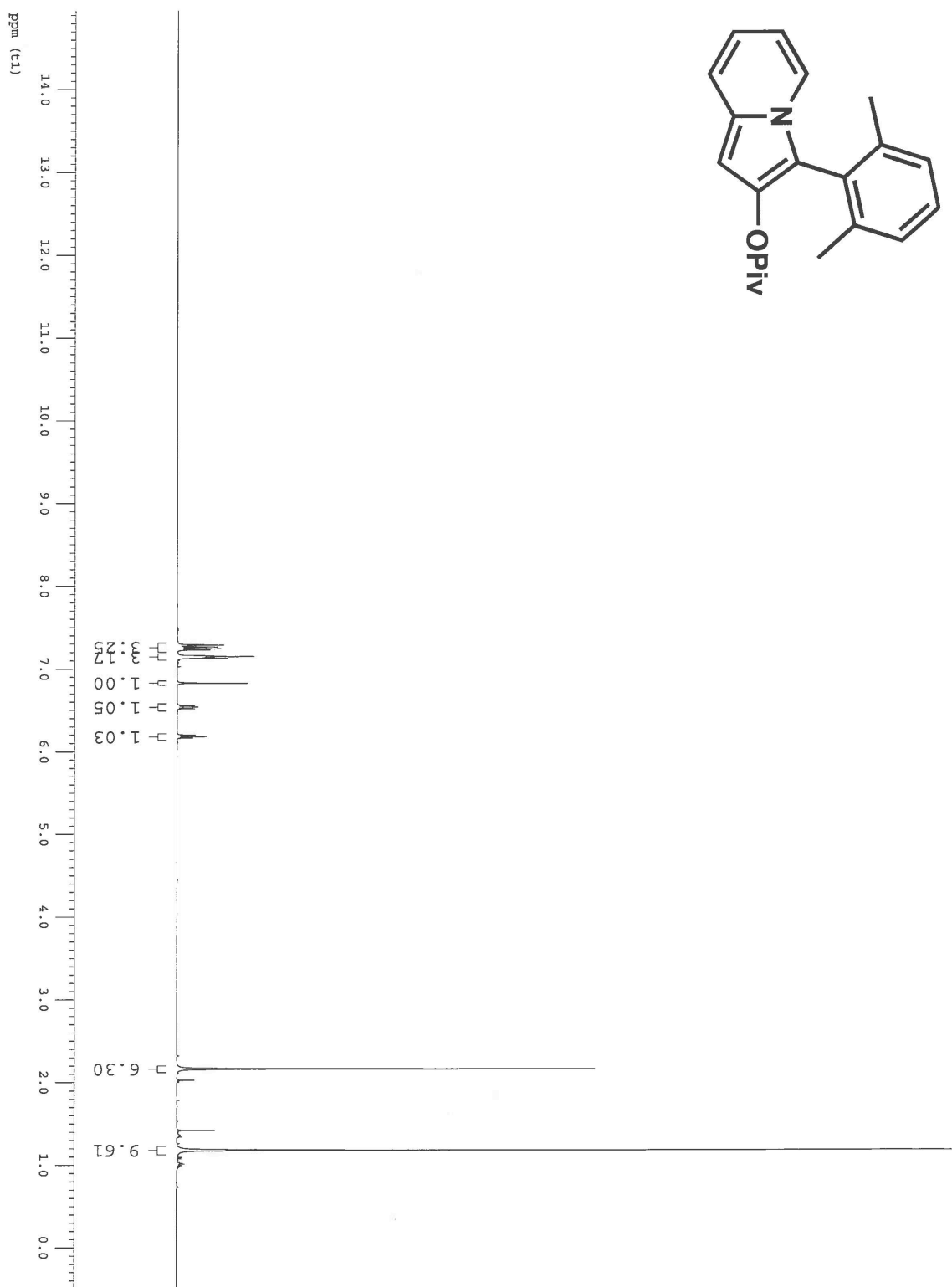
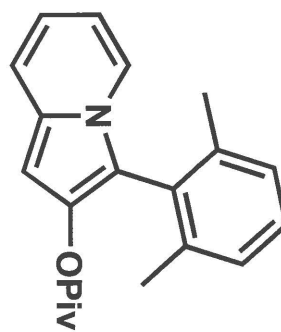


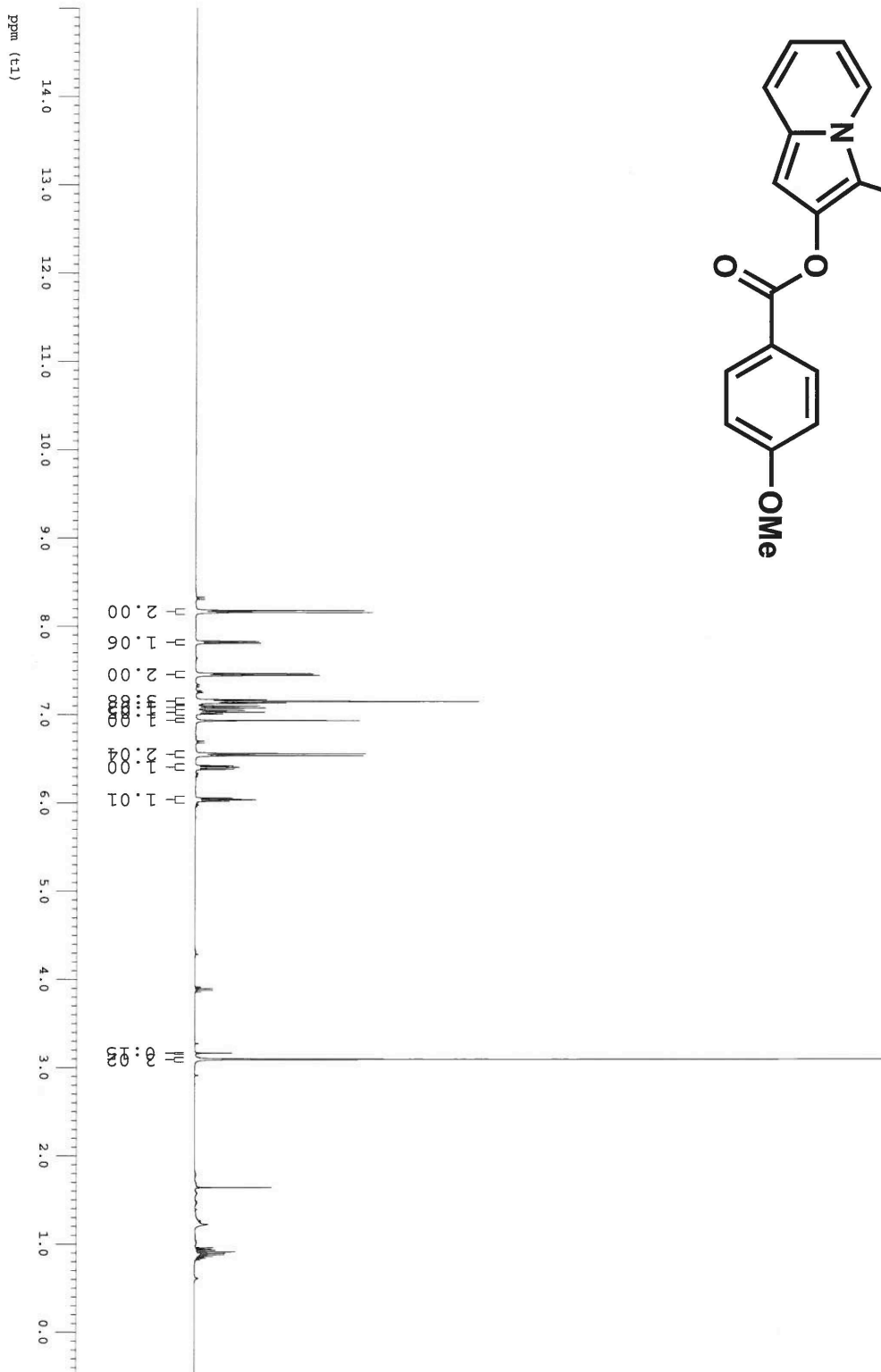
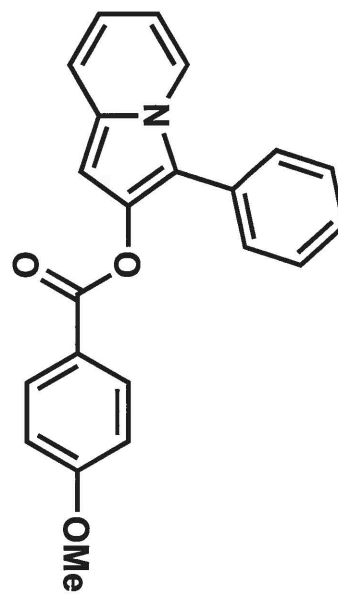




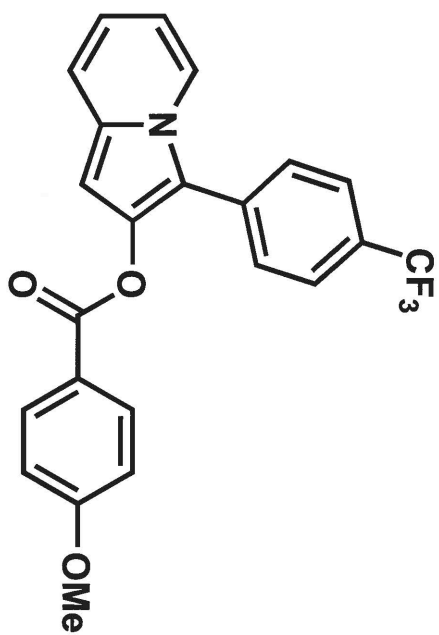






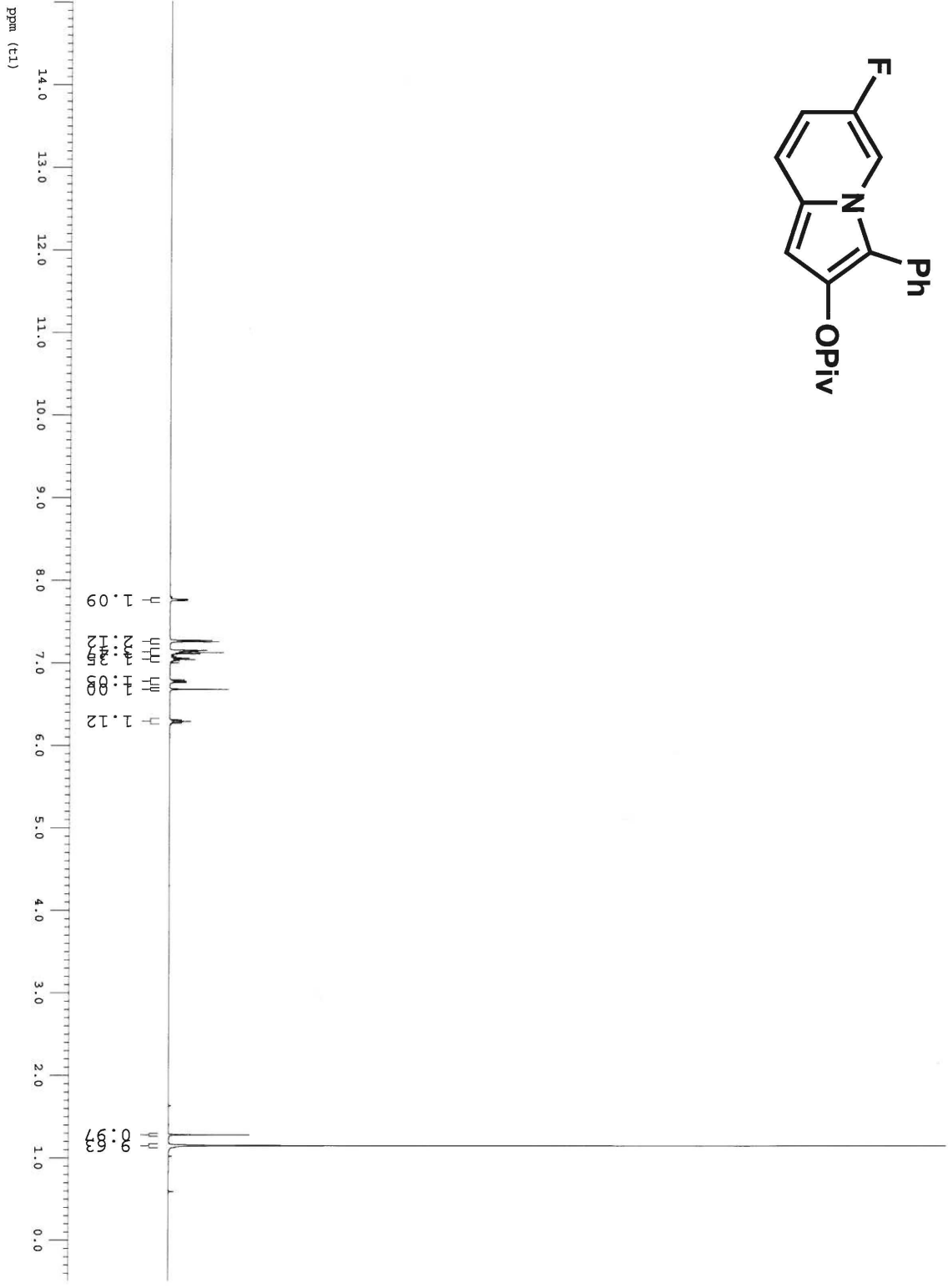
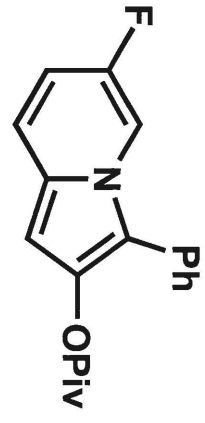












## Chapter 3. Development of a Metal-Free Cyclization for the Formation of 1,3-Disubstituted Indolizines and Indolizinones

### 3.1 Introduction

In the last decade, there has been an increasing focus on developing greener and more sustainable chemical processes and products. Nearly every type of chemist can connect with a number of the twelve principles of green chemistry, which were outlined by John Warner and Paul Anastas.<sup>1</sup> Synthetic organic chemists have begun to rise to the challenge of embodying the twelve principles of green chemistry in the design of new methods and synthetic strategies. This movement toward greener chemistry has included developing atom economical reactions,<sup>2</sup> minimizing the use of toxic reagents and switching to environmentally benign solvents.<sup>3</sup> These efforts represent important steps toward achieving the ideal chemical transformation.

Within the context of methods development and total synthesis, there are endless opportunities to make green choices. When devising a strategy to synthesize a complex molecule, one can choose a renewable starting material over a petroleum based feedstock and strive for a streamlined, high-yielding route that avoids excessively toxic reagents. Likewise, there are several critical choices made in the course of developing a new reaction. For example, the choice of solvent largely impacts the overall greenness of a reaction, as it accounts for the majority of the waste. Other factors that contribute to the sustainability of a reaction are the atom economy, amount of waste generated and toxicity of the chemicals employed and generated.

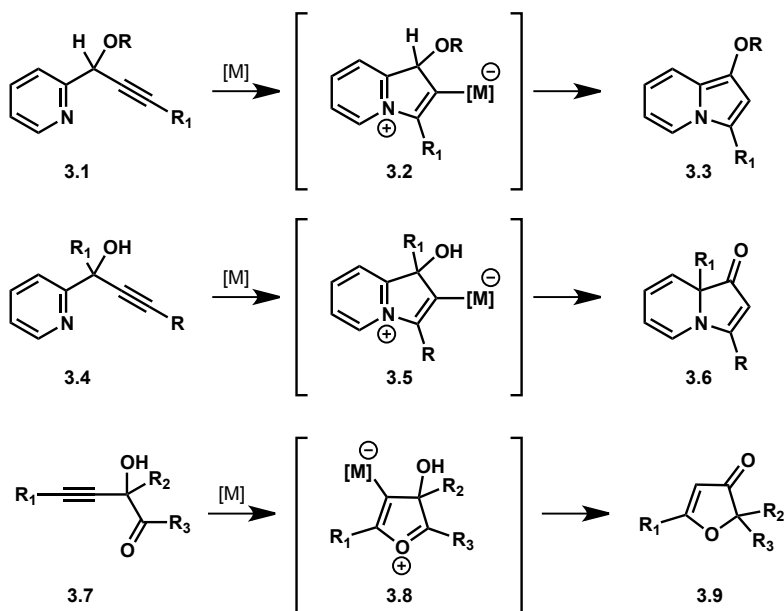
Cycloisomerizations are a class of reactions that have exploded under the green chemistry umbrella as they are inherently atom economical and are often promoted by catalysts, which in principle could be recovered and reused. The development of  $\pi$ -Lewis acid-mediated cycloisomerizations is currently an active area of research.<sup>4</sup> A variety of salts derived from metals including Cu, Hg, Ag, Au, Pt, In and Ga have proven to be very useful catalysts for these processes. Along these lines, our laboratory has developed several of these reactions mediated by Pt, Ga and In salts. For example, we and others have reported the hetero-cycloisomerization of pyridine propargylic alcohols (e.g., **3.1**, Figure 3.2.1) in the presence of  $\pi$ -Lewis acids to yield indolizines (**3.3**) via the presumed intermediacy of **3.2**.<sup>5</sup> Variants of this transformation utilizing **3.4** or **3.7** as substrates lead to indolizinones (**3.6**)<sup>5</sup> or furanones (**3.9**),<sup>6</sup> respectively. We became interested in devising new protocols to improve these transformations by eliminating the expensive  $\pi$ -Lewis acid catalysts as well as the organic solvents that have been traditionally utilized for these reactions. Commensurate with these considerations, if trace amounts of the heavy metals could be avoided in the reaction products, these processes would be more attractive to the pharmaceutical industry, where these types of heterocyclic motifs could find widespread utility. This chapter provides a detailed account of our initial results, which indicate that pure water, *without any additives*, as well as other polar protic solvents efficiently facilitate some of the cycloisomerizations depicted in Figure 3.2.1. We anticipate that this simple protocol may be readily extended to a range of other hetero-cycloisomerization reactions.

### 3.2 Metal-Mediated Cyclizations

The utility of highly-functionalized heterocycles spans the fields of medicine and biological research to materials and natural product total synthesis (see Chapter 1). The Sarpong

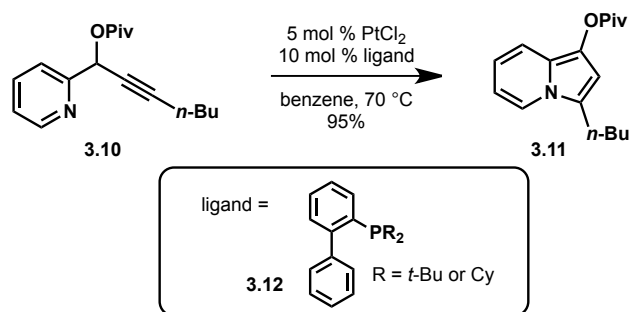
group has been particularly interested in constructing highly substituted heterocycles via cyclization of a heteroatom onto an activated alkyne. To this end, methods have been developed for the synthesis of 2,3-disubstituted indolizines (see Chapter 2),<sup>7</sup> 1,3-disubstituted indolizines (**3.1**→**3.3**),<sup>5</sup> indolizinones (**3.4**→**3.6**),<sup>5</sup> and furanones (**3.7**→**3.9**)<sup>6</sup> (Figure 3.2.1). These methods rely on activation of a carbon-carbon triple bond with a  $\pi$ -Lewis acid such as platinum(II) or indium(III) to induce cyclization of a tethered heteroatom to provide the heterocyclic product.

**Figure 3.2.1.** Select metal-catalyzed cycloisomerizations to form heterocycles.



The cyclization of propargylic alcohol derivatives such as **3.1** to form 1,3-disubstituted indolizines (e.g. **3.3**) was developed in our group using metal salts capable of acting as  $\pi$ -Lewis acids. A screen of catalysts indicated that platinum(IV) chloride, platinum(II) chloride and indium(III) chloride were all capable of inducing the indolizine-forming cyclization. Further optimization identified bulky, electron-rich phosphine ligands, such as 2-(di-*tert*-butylphosphino)biphenyl or 2-(dicyclohexylphosphino)biphenyl (**3.12**) in conjunction with catalytic amounts of PtCl<sub>2</sub> in benzene at 70 °C to be optimal in providing indolizine products in good yields (Scheme 3.2.1).

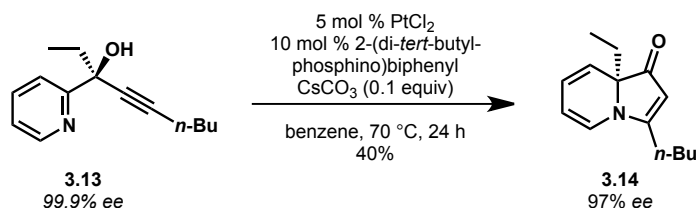
**Scheme 3.2.1.** Platinum catalyzed cycloisomerization to form 1,3-disubstituted indolizines.



The conditions shown in Scheme 3.2.1 proved to be general for a variety of pyridyl substrates. Internal alkynes substituted with alkyl, alkenyl and aryl groups behaved well in the cyclization. However, terminal alkynes proved to be problematic, providing modest yields of indolizine products. In addition to propargylic ester substrates, silyl ethers could also be used. This demonstrates the lack of participation of the pivaloyl ester in the transformation and also the tolerance of a range of substituents at the propargylic position with varying electronic properties.

Similar conditions were employed in a related reaction for the synthesis of indolizinone products (Scheme 3.2.2). This transformation requires a tertiary propargylic alcohol substrate, where R<sub>1</sub> is an alkyl or aryl group (see, 3.4, Figure 3.2.1) that undergoes a 1,2-migration. Unlike the indolizine formation, base was necessary to effect significant conversion of the propargylic alcohols to indolizinone products. It is possible that the base facilitates proton transfer events that precede the 1,2-shift. Importantly, enantio-pure alcohol **3.13** (99.9% *ee*) was converted to enriched indolizinone **3.14** in modest yield (40%), but with a high degree of chirality transfer (97% *ee*).

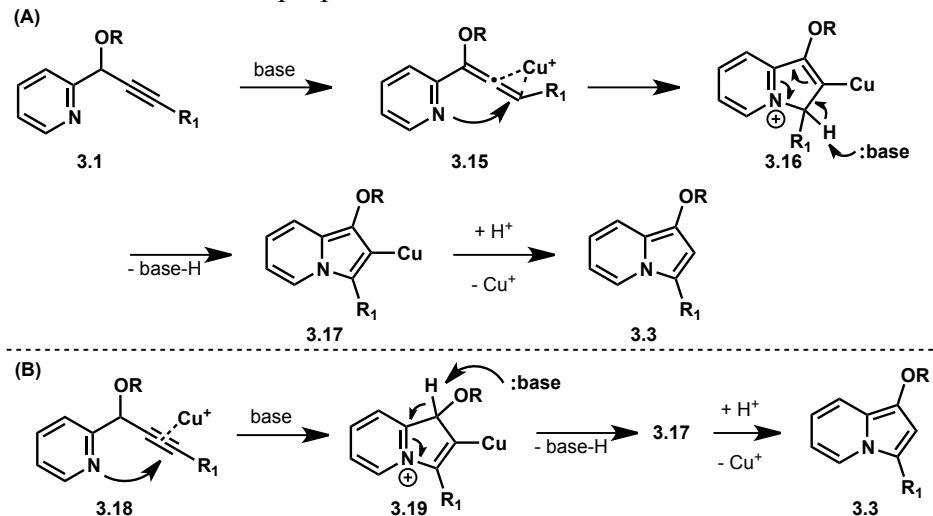
**Scheme 3.2.2.** Platinum catalyzed cycloisomerization to form indolizinones.



The platinum-catalyzed cycloisomerization of tertiary propargylic alcohols provided modest yields of indolizinone products with a variety of substrates. Notably, the cyclization worked well only with internal alkyne substrates, as terminal alkyne substrates led to ketone products that had undergone the loss of the alkyne moiety. A range of migrating groups were productive for the formation of indolizinone products including methyl, ethyl, 3,5-dimethoxyphenyl, phenyl, and cyclopropyl. The reaction times ranged from 2-7 days and provided yields from 36-70%.

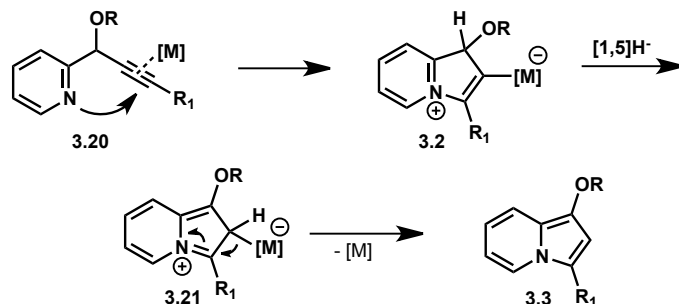
Following the report from our group on the Pt(II) and In(III) catalyzed reactions to form indolizines and indolizinones,<sup>5</sup> Liu and coworkers reported the catalysis of the same two transformations with Cu(I).<sup>8</sup> They reported that treatment of propargylic alcohol derivatives with catalytic CuI and one equivalent of triethylamine in acetonitrile was sufficient for the formation of indolizine products at ambient temperature and for the formation of indolizinone products at 80 °C. Notably, under copper-catalysis, the reaction times were significantly shorter, as brief as 15 minutes for the indolizine formation and one hour for indolizinones. Liu proposed two potential mechanisms for the copper-mediated process. The first proposed pathway commences with the isomerization of propargyl ester **3.1** to allene **3.15** which is activated by Cu(I) to undergo cyclization (Scheme 3.2.3A). Alternatively, cyclization of the pyridine moiety of **3.18** directly onto the activated triple bond could provide an intermediate such as **3.19** (Scheme 3.2.3B).

**Scheme 3.2.3.** Liu's mechanistic proposals.



Less than two months after the Liu report, Gevorgyan et al. demonstrated the efficiency of Au(I) and Ag(I) salts for the cyclization of propargylic ester substrates such as **3.1** to form indolizine products.<sup>9</sup> They found that 3 mol % of AuI or AgBF<sub>4</sub> led to near quantitative yields of product in 3 h or 30 min, respectively. When catalyzed by gold or silver, this cycloisomerization was facile at ambient temperatures with dichloromethane or toluene as the solvent. Under these conditions, the addition of a base was not necessary for the desired transformation to occur. Like Liu, Gevorgyan also proposed two potential mechanisms for this reaction, the first paralleling Liu's proposition for attack onto the metal-activated alkyne (see Scheme 3.2.3B). Gevorgyan's second mechanistic proposal is illustrated in Scheme 3.2.4. Although this mechanism commences with the same attack of the pyridine onto the activated triple bond, the product is proposed to arise through a [1,5]-hydride shift from **3.2** to **3.21**, which upon loss of the metal, rearomatizes to the indolizine product (Scheme 3.2.4).

**Scheme 3.2.4.** Gevorgyan's second mechanistic proposal.



Gevorgyan and coworkers attempted to discriminate between these two potential pathways via a deuterium-labeling experiment of silyl ether **3.22** (Scheme 3.2.5). Upon



cyclization catalyzed by  $\text{AgBF}_4$ , only 51% of the indolizine product retained the deuterium label at C2. This result was interpreted by the authors as evidence that a 1,5-hydride shift was not the operative mechanism due to loss of half of the deuterium from the starting material. They had anticipated the hydride shift mechanism would result in complete retention of the deuterium-label in the indolizine product (**3.23**). Our studies indicate that proton exchange occurs readily at the C-1 position and is possible at C-2 as well; however, exchange at C-2 is significantly slower and highly dependent on the indolizine substituents. To make a well-substantiated claim based on the loss of deuterium from **3.22**, a control experiment on the rate of H/D exchange at the C-2 position of **3.23** is required.

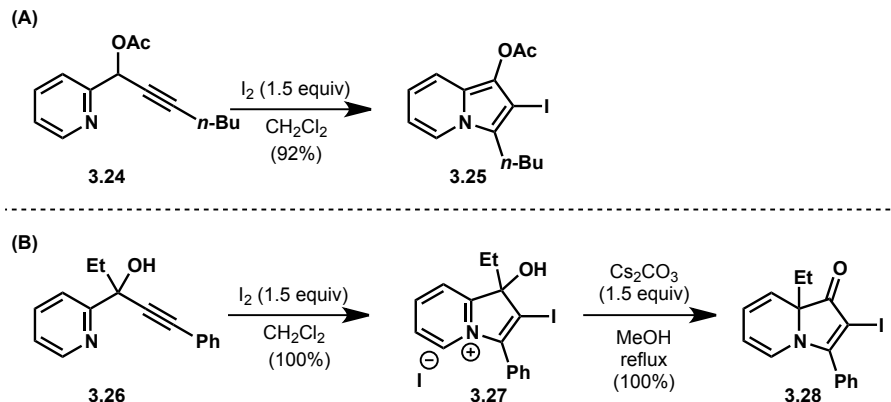
**Scheme 3.2.5.** Gevorgyan's deuterium-labeling experiment.



While Liu and Gevorgyan were demonstrating the potential for the cyclization of pyridyl propargylic alcohols and their derivatives catalyzed by a variety of metals, Kim and coworkers were developing a cyclization induced by iodine. In July of 2007, Kim reported the cyclization of propargylic esters (**3.24**) with super-stoichiometric amounts of iodine to form 1,2,3-trisubstituted indolizines (e.g., **3.25**) that bear an iodine atom at C2 (Scheme 3.2.6A).<sup>10</sup> This reaction proceeds in dichloromethane at room temperature and provides excellent yields of trisubstituted indolizine products. Interestingly, after screening a variety of electrophilic reagents (e.g., *N*-bromosuccinimide, bromine, and phenylselenium chloride), only iodine effected the desired transformation. Like many of the metal-catalyzed cyclizations, the iodine-mediated reaction is only productive for internal alkynes. Terminal alkynes led to what Kim described as a complex mixture.

This concept was extended to the synthesis of 2-iodoindolizinones through a two-step protocol (Scheme 3.2.6B).<sup>11</sup> Starting from tertiary propargylic alcohols, treatment with iodine provides the iodide salt **3.27**, which withstood an aqueous work-up and was routinely isolated. Exposure of indolizinium salt **3.27** to cesium carbonate in refluxing methanol affords 2-iodoindolizinone **3.28** (Scheme 3.2.6B).

**Scheme 3.2.6.** Iodine mediated synthesis of 2-iodoindolizines and indolizinones.



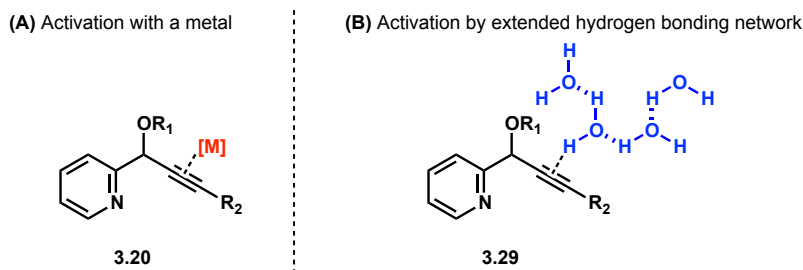
In addition to providing an alternative to the transition-metal catalyzed cycloisomerization, the iodine-mediated reaction introduces an additional functional handle onto the indolizine/indolizinone core. Kim<sup>10,12</sup> has subsequently demonstrated the utility of having a halogen atom at the C2-position by using these iodoazabicycles as coupling partners in a variety of cross-coupling reactions.

### 3.3 Considerations for a Metal-Free Cyclization

Given the broad spectrum of metals and other reagents capable of mediating the cyclization of pyridinyl propargylic alcohols and derivatives to form 1,3-disubstituted indolizines (3.3) and indolizinones (3.6), we began to ponder the minimum amount of activation necessary to induce cyclization.<sup>13</sup> Activation of the triple bond with a metal has proven to be a robust reaction for a class of propargylic alcohol derivatives; however, many substrates were not transformed to azabicyclic products in the metal-mediated reaction. For example, terminal alkynes often did not fare well under the metal-catalyzed conditions, and formed ketone products via the presumed ejection of a metal acetylide. Furthermore, the exploration of *N*-heterocycles beyond pyridine was in some cases plagued by sluggish reactions and low yields. We anticipated that an alternative form of alkyne activation could provide a complimentary method to the metal-mediated version of the reaction, providing access to new classes of indolizines and indolizinones.

Concomitant with these considerations, we were also interested in improving the “greenness” of this method by reducing the number of additives (such as ligands), eliminating the need for metals, and employing a more environmentally benign solvent. Toward these goals, we hypothesized that the extended hydrogen-bonding network in bulk water could suitably activate the alkyne moiety in an analogous manner to the metal-alkyne interaction (Scheme 3.3.1).

### Scheme 3.3.1. Alkyne activation modes.



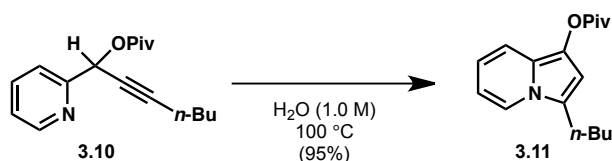
Despite the long recognized positive influence of water on the efficiency of select organic reactions such as the Diels-Alder reaction,<sup>13,14</sup> only relatively recently has it begun to be investigated heavily as a “green” solvent for a variety of transformations.<sup>15,16</sup> Along with the development of this field, important distinctions between reactions using water have also begun to emerge, and the terms “on water”<sup>17</sup> and “in water”<sup>18</sup> are sometimes applied to reactions that proceed as heterogeneous or homogeneous mixtures with water, respectively.

Several aspects of the hetero-cycloisomerization reactions shown in Scheme 3.2.1 made them attractive to study on/in water. First, because these reactions are thought to proceed via charged reactive intermediates, we hypothesized that the corresponding transition states would be stabilized by water, which has a relatively high static permittivity ( $\epsilon_T = 78.4$ ).<sup>19</sup> Additionally, our qualitative examination of these reactions suggested that they should have negative activation volumes,<sup>20</sup> and should therefore be accelerated in water as discussed by Lubineau and others.<sup>21,22</sup> Despite the potential for facilitation of the hetero-cycloisomerization reactions using water, several challenges were evident. For example, hydration of the alkyne fragment in **3.29**, as well as hydrolysis of the protecting group ( $R_1$ ) could be competitive with the desired transformation. Of more significant concern was the possible interception of the charged intermediates by a water molecule.

#### 3.4 Metal-Free Cyclization to Form 1,3-disubstituted Indolizines

In an initial experiment, pyridine propargylic ester **3.10** (Scheme 3.4.1), which had been previously used by our research group as a substrate in hetero-cycloisomerizations, was investigated. We were delighted to find that the desired transformation proceeded using pure water at 100 °C over 2 h to form the corresponding indolizine **3.11** in 95% yield. This yield compared favorably with the yield obtained in organic solvent using  $\text{PtCl}_2$  or  $\text{InCl}_3$  (as reported by us previously), or using  $\text{AgBF}_4$ <sup>[6a]</sup> or  $\text{CuI}$ <sup>[6b]</sup> as the catalyst, yet was procedurally more simple. The elimination of the metal catalyst, ligands, and additives such as a base, coupled with a switch to a less toxic, more environmentally benign solvent, significantly increase the green profile of this reaction.

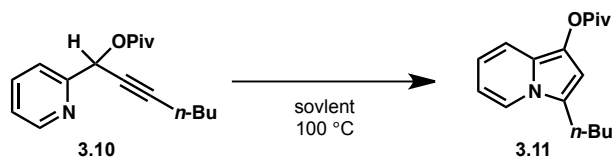
### Scheme 3.4.1. Proof of concept for the metal-free cyclization.



### 3.5 Exploring the Effect of Solvent, Temperature, and pH

In an effort to gain a better understanding of the origin of the positive effects of water on the hetero-cycloisomerization reactions, several experiments were performed using **3.10** as a substrate. Parallel reactions were conducted using H<sub>2</sub>O, D<sub>2</sub>O, benzene and no solvent (Table 3.5.1). Both the reaction with H<sub>2</sub>O as well as the reaction with D<sub>2</sub>O reached complete conversion and provided indolizine **3.11** in excellent yield. The reaction in D<sub>2</sub>O required three hours to reach complete conversion of the starting material to indolizine product **3.11** (entry 2). However, even after extended periods of heating at 100 °C, the reaction conducted in benzene and the reaction run neat contained significant starting material, a small amount of indolizine product, and substantial amounts of decomposition products.

Table 3.5.1. Preliminary solvent screen.



| entry | solvent          | mmol 3.10/mL H <sub>2</sub> O | time (h) | conversion of 3.10 (%) |
|-------|------------------|-------------------------------|----------|------------------------|
| 1     | H <sub>2</sub> O | 2                             | 2        | >95                    |
| 2     | D <sub>2</sub> O | 2                             | 3        | >95                    |
| 3     | benzene          | 2                             | 18       | 70                     |
| 4     | neat             | -                             | 18       | 55                     |

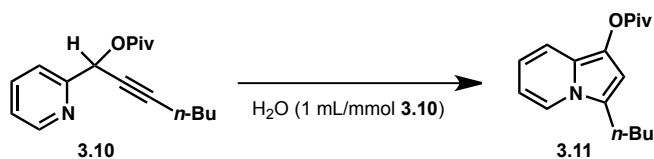
This preliminary study on the effect of a polar protic solvent versus a less polar aprotic solvent on the metal-free cyclization prompted a broader screen of solvents. Upon conducting the reaction in a variety of solvents, the initial trend of solvent effects that had been observed between water and benzene was reinforced. Polar protic solvents such as methanol, ethanol, and 2,2,2-trifluoroethanol led to near quantitative yields of indolizine product in 2-3 hours. However, polar aprotic solvents such as *N,N*-dimethylformamide and *N,N*-dimethylacetamide produced only trace amounts of indolizine in the same timeframe. The use of less polar solvents (e.g., benzene and toluene) led to low yields of indolizine, but this was accompanied by significant

quantities of extremely polar decomposition products. The formation of the indolizine products in trace amounts in benzene or under neat conditions suggests that a polar protic solvent is not an absolute requirement for cycloisomerization to occur; however, competing decomposition pathways apparently occur at a comparable rate under these conditions.

In order to maximize product formation on an acceptable time scale (<18 h) using **3.10**, it was important to heat the reaction mixture to 100 °C (Table 3.5.2). No product was detected when **3.10** was vigorously stirred with water at room temperature (entry 4). However, indolizine product **3.11** was detected in reactions conducted at both 50 °C and 75 °C (entries 3 and 2, respectively), although these reactions failed to reach completion after 18 h.

On the basis of the relatively rapid rate of cyclization in polar protic solvents versus the lack of cyclization in polar aprotic solvents, we hypothesized that the availability of protons in reaction media could impact the rate of cyclization. To this end, the progress of the cyclization was monitored in a set of parallel reactions where all factors except the pH were held constant. Two substrates, propargylic ester **3.30** and silyl ether **3.32**, displayed the same trend (Table 3.5.3 A and B). When the propargylic alcohol derivatives were heated in aqueous 1 M acetic acid, the light yellow reaction mixture turned opaque black within minutes of heating and subsequent analysis by <sup>1</sup>H NMR did not lead to the detection of identifiable starting material or indolizine product. This decomposition is not surprising given the acid sensitivity of both the propargylic alcohol derivatives as well as indolizines. However, in aqueous 1 M sodium bicarbonate and pure water, the starting material is cleanly converted to product. After two hours, the ratio of indolizine to starting material is higher for the reaction in pure water for both the propargylic ester **3.30** and silyl ether **3.32**. This result suggests that the rate of reaction is greater in pure water (pH measured to be 6.3) than under slightly basic conditions.

**Table 3.5.2.** Temperature study for the hetero-cycloisomerization of **3.10**.



| entry | temp (°C) | time (h) | ratio (3.11:3.10) |
|-------|-----------|----------|-------------------|
| 1     | 100       | 2        | >95:5             |
| 2     | 75        | 18       | 7:1               |
| 3     | 50        | 18       | 1:15              |
| 4     | 23        | 18       | <5:95             |

**Table 3.5.3.** pH study for the hetero-cycloisomerization of propargylic esters and ethers.

(A)

3.30  $\xrightarrow{\text{solvent, } 100\text{ }^\circ\text{C}}$  3.31

| entry | solvent                | time (h) | starting material:product |
|-------|------------------------|----------|---------------------------|
| 1     | 1 M AcOH               | 2        | decomposition             |
| 2     | 1 M NaHCO <sub>3</sub> | 2        | 2:1                       |
| 3     | H <sub>2</sub> O       | 2        | < 5 : > 95                |

(B)

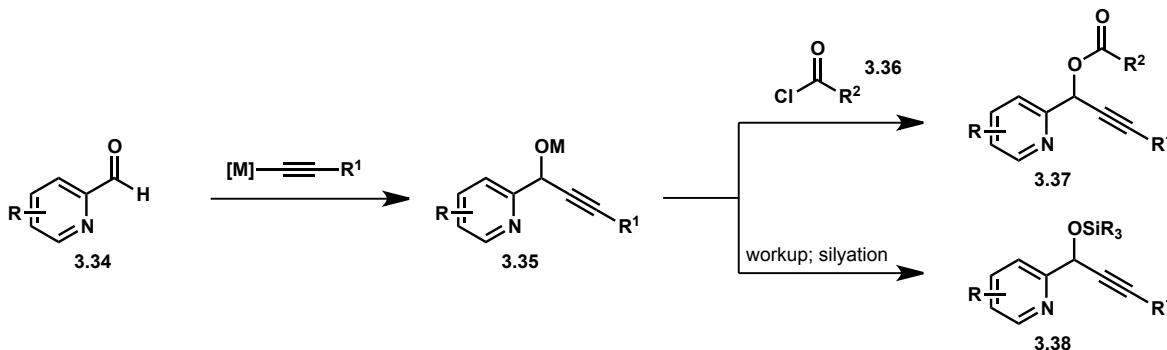
3.32  $\xrightarrow{\text{solvent, } 100\text{ }^\circ\text{C}}$  3.33

| entry | solvent                | time (h) | starting material:product |
|-------|------------------------|----------|---------------------------|
| 1     | 1 M AcOH               | 2        | decomposition             |
| 2     | 1 M NaHCO <sub>3</sub> | 2        | 15:1                      |
| 3     | H <sub>2</sub> O       | 2        | 7:1                       |

### 3.6 Substrate Scope of the Metal-Free Indolizine-Forming Cyclization

To determine the substrate scope of the metal-free cyclization to form 1,3-disubstituted indolizines, a range of substrates were synthesized in 1-3 steps starting from pyridine building blocks such as pyridine 2-carboxaldehyde (**3.34**). A representative substrate synthesis is outlined in Scheme 3.6.1, which begins with the addition of a lithium acetylide or ethynyl Grignard reagent to pyridine 2-carboxaldehyde (**3.34**). The newly formed alkoxide (**3.35**) can be trapped in the same pot to give a propargylic alcohol derivative. Alternatively, the reaction can be quenched to provide the propargylic alcohol, which can be derivatized in a second step. For the formation of propargylic ester substrates (e.g., **3.10** and **3.39**, Table 3.6.1) the single-pot procedure provides higher yields than isolation of the intermediate propargylic alcohol, which can in some instances isomerize to the allene or undergo other non-specific degradation pathways. Silyl ether cyclization substrates such as **3.41** were obtained in the highest yields by isolating the propargylic alcohol and carrying out the silylation in a second step.

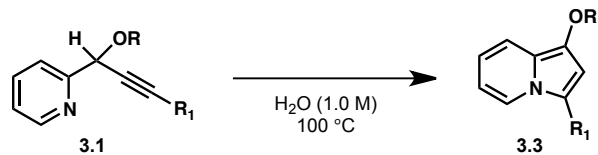
**Scheme 3.6.1.** Strategy for the synthesis of cyclization substrates.



As shown in Table 3.6.1, the scope of the hetero-cycloisomerization reaction of pyridine propargylic alcohol derivatives using water is comparable to that observed using metal salts as previously reported by us,<sup>5</sup> as well as by Gevorgyan<sup>9</sup> and Liu.<sup>8</sup> Of note, a silyl (TBS) protective group (entry 4) is tolerated as well. In addition to providing high yields of the indolizines that can also be formed in the metal-catalyzed reaction, the metal-free conditions are amenable to the cyclization of terminal alkyne substrates to give mono-substituted indolizines (entry 3). As discussed in Section 3.2, the treatment of terminal alkyne substrates with the metal-catalyzed conditions in most cases does not lead to the desired indolizines, but only ketone products. A second, important class of substrates that are more amenable to the metal-free conditions are pyridines that possess a substituent at the 6-position (entry 5).

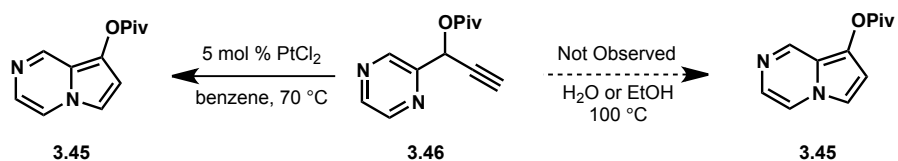
The metal-free cyclization proved to be a robust method for the synthesis of indolizines; however, deviation from pyridine-containing substrates highlighted a weakness in the metal-free protocol. For example, the addition of a second nitrogen atom to the aromatic ring is the only difference between pyridine substrate **3.30**, which provided high yields of indolizine product (Table 3.6.1, entry 3), and pyrazine substrate **3.46**, which did not undergo cyclization in either boiling water or ethanol (Scheme 3.6.2). However, pyrazine substrate **3.46** did undergo cyclization when subjected to the Pt(II) conditions to afford 7-azaindolizine **3.45** (Scheme 3.6.2). The key difference between the pyridine substrate **3.30** and the pyrazine analog **3.46** is likely the basicity/nucleophilicity of the nitrogen that ultimately cyclizes onto the alkyne. Because the pyrazine nitrogen is less basic than pyridine, we hypothesize that stronger activation of the alkyne is necessary for cyclization to occur, which is likely the case under the metal-catalyzed conditions.

**Table 3.6.1.** Substrate scope of the indolizine cyclization in water.



| entry | substrate | product | time (h) | yield (%) |
|-------|-----------|---------|----------|-----------|
| 1     |           |         | 2        | 95        |
| 2     |           |         | 15       | 85        |
| 3     |           |         | 2        | 97        |
| 4     |           |         | 8        | 97        |
| 5     |           |         | 15       | 99        |

**Scheme 3.6.2.** Superiority of platinumium-catalyzed conditions for pyrazine substrate **3.46**.



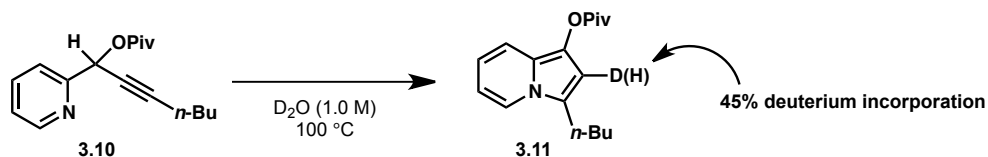


### 3.7 Mechanistic Insights

Although the benefits of conducting these transformations using water are clear (i.e., low cost, ease of operation and improved safety), the basis for the success of these reactions is not well understood at this time. We have carried out several preliminary experiments to gain some insight into the facilitation of the heterocyclization reactions presented in Table 3.6.1 by water. We note that even though a number of the substrates in neat form or as a solution in benzene undergo transformation to the corresponding indolizines in the absence of catalyst over prolonged heating (ca. 18 h), the yields are generally low and accompanied by significant decomposition. These observations suggest that the effect of water extends beyond simply creating a high effective substrate concentration based on the hydrophobic effect<sup>23</sup> and that hydrogen-bonding is likely important. This is further supported by the qualitative observation that the reactions proceed more slowly in D<sub>2</sub>O as compared to H<sub>2</sub>O (complete conversion of **3.10** to **3.11** in D<sub>2</sub>O after 3 h versus 2 h in H<sub>2</sub>O). This result is consistent with the observations of Sharpless et al.<sup>[10]</sup> for the cycloaddition of quadricyclane with dimethyl azodicarboxylate, which likely reflects a solvent isotope effect.<sup>19</sup>

When the cycloisomerization of **3.10** was carried out in D<sub>2</sub>O, 45% deuterium incorporation was observed at C-2 of the indolizine product (see, **3.11** in Scheme 3.7.1) as observed by <sup>1</sup>H NMR analysis. In an effort to determine if deuterium incorporation occurs during the cycloisomerization of **3.10** or after the indolizine product had formed, protio- (0% D) indolizine **3.11** was heated in D<sub>2</sub>O to 100 °C for 2 h and then submitted to work up by the same procedure used to isolate partially deuterated (45% D) indolizine **3.11**. No deuterium incorporation was observed as judged by <sup>1</sup>H NMR analysis, suggesting that deuterium incorporation takes place during indolizine formation.

**Scheme 3.7.1.** Hetero-cycloisomerization conducted in D<sub>2</sub>O.



### 3.8 Extension to the Metal-Free Formation of Indolizinones

Having established an efficient cycloisomerization protocol for the formation of indolizines using water, we were eager to determine if related reactions could also take place under metal-free conditions. We first turned our attention to the formation of indolizinones from propargylic alcohols (see **3.4** to **3.6**, Table 3.8.1). Although this transformation shares similar elements with the indolizine cyclization, the 1,2-migration of the propargylic substituent constitutes an extra challenge. We considered the possibility that addition of a molecule of solvent to the pyridinium intermediate **3.5** could outcompete the 1,2-migration pathway. However, these fears were not realized, and as shown in Figure 3.8.1, indolizinones are readily formed in good to excellent yields from tertiary propargylic alcohol substrates. Again, the efficiency of these reactions compare favorably with those performed in organic solvents using CuI,<sup>8</sup> and are superior to the PtCl<sub>2</sub>-catalyzed processes developed previously in our laboratory.<sup>5</sup>

**Table 3.8.1.** Metal-free cyclization to form indolizinones.

The reaction shows a pyridine ring (3.4) with a hydroxyl group and an alkyne group on the same carbon. The alkyne is substituted with an R group. This cyclizes to form an indolizinium cation intermediate (3.5), which is shown in brackets with a positive charge on the nitrogen atom. The intermediate then loses a proton to form the final indolizinone product (3.6).

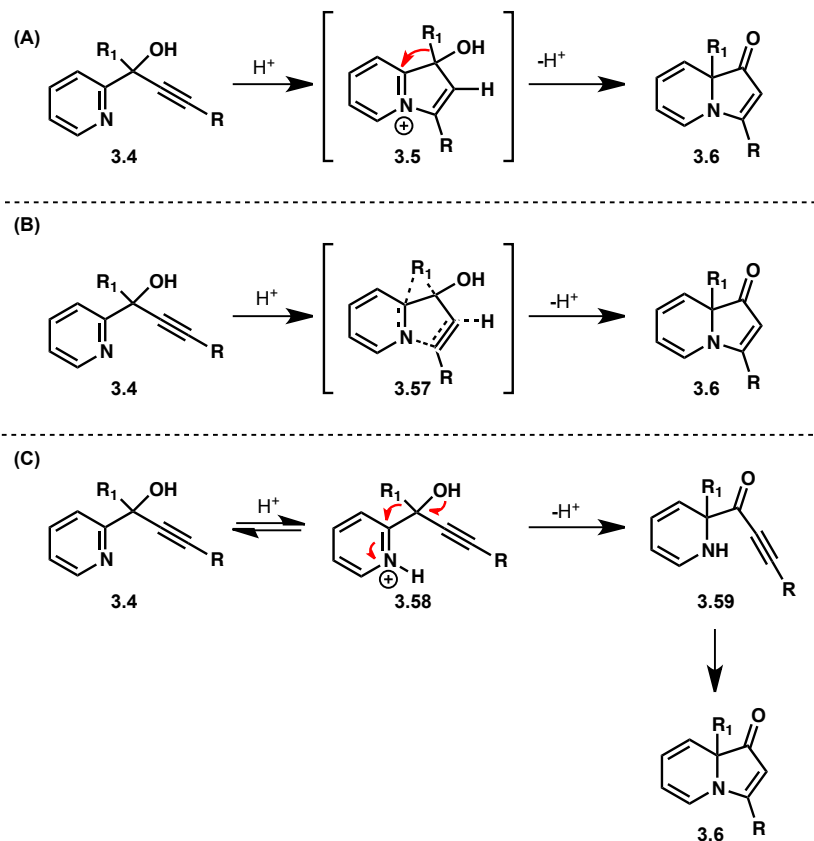
| entry | substrate | product | time (h) | yield (%) |
|-------|-----------|---------|----------|-----------|
| 1     |           |         | 15       | 78        |
| 2     |           |         | 10       | 58        |
| 3     |           |         | 15       | 92        |
| 4     |           |         | 3        | 97        |
| 5     |           |         | 3        | 88        |

### 3.9 Potential Mechanistic Pathways for Metal-Free Indolizinone Formation

Even though the indolizinone-forming cyclization has been characterized throughout this chapter as a two-step process that proceeds through an indolizinium intermediate (**3.5**, Figure 3.9.1A), we have also considered other potential mechanisms. For example, the cyclization and 1,2-shift could be concerted, proceeding through a transition state such as **3.57** (Figure 3.9.1B). Alternatively, one could imagine a pre-equilibrium between the pyridine **3.4** and pyridinium **3.58**

followed by a 1,2-shift to arrive at ynone **3.59**. This species could then undergo an intramolecular aza-Michael addition to yield indolizinone **3.6** (Figure 3.9.1C).

**Figure 3.9.1.** Potential mechanisms for metal-free indolizinone formation.



Evidence for a two-step process proceeding through indolizinium **3.5** exists in the context of the metal-catalyzed reaction. However, at this point we do not have any evidence to support intermediates such as indolizinium **3.5** or ynone **3.59** that would favor mechanisms A or C, respectively, in the metal-free reaction.

### 3.10 Similarities and differences between the metal-catalyzed and metal-free cyclizations

Both the metal-catalyzed and metal-free cyclization to form *N*-fused bicycles are sufficiently robust to generate gram-quantities of indolizinone building blocks. However, each method has unique advantages, which one must be cognizant of when selecting conditions for a given substrate. We have observed that the following factors impact the metal-catalyzed and metal-free reactions differently: (1) the nucleophilicity of the nitrogen, (2) the substitution of the alkyne moiety, and (3) the migrating group.

High nucleophilicity of the heterocyclic nitrogen atom is crucial in the metal-free reaction, where a less nucleophilic nitrogen can lead to a slower reaction or no cyclization. The general trend for qualitative rate of indolizinone formation correlates with the pKa of the protonated heterocycle: isoquinoline (pKa = 5.4) > pyridine (pKa = 5.2) > quinoline (pKa = 4.9)

> pyrazine (pKa = 0.7). As stated in Section 3.6, the pyrazine substrate **3.46** does not cyclize under the metal-free conditions. This trend does not manifest itself to a significant extent in the metal-catalyzed reaction.

Substitution at the alkyne terminus is beneficial in the metal-catalyzed reaction while it can retard the rate of reaction in the metal-free reaction. For example, alkynes with an *n*-butyl group at the terminus of the alkyne (see Table 3.8.1, entry 3) took five times as long to reach completion as otherwise similar substrates possessing a terminal alkyne moiety (entries 4 and 5). However, in some cases a higher temperature can accelerate the cyclization of internal alkyne substrates under metal-free conditions.

Although a terminal alkyne is an ideal substrate for the metal-free reaction, low yields are observed for substrates with terminal alkynes under conditions that employ  $\pi$ -Lewis acidic metals. Our original report on the use of Pt(II) as a catalyst only describes two substrates with terminal alkyne moieties, which led to 79% and 59% yields of the corresponding indolizine products. There were no examples of terminal alkyne substrates for the formation of indolizinones using metal catalysis.

The impact of the migrating group on the rate of cyclization is another interesting difference between the metal-catalyzed and metal-free reactions. On the basis of reports from the literature, the metal-catalyzed reaction rate appears to track with the migratory aptitude of the propargylic substituent (Ph > Et > Me). However, this type of rate dependence on migratory aptitude does not appear to manifest itself in the metal-free reaction.

Practically, these qualitative differences between the metal-free and metal-catalyzed reactions are important considerations that must be carefully considered when selecting conditions for the cyclization of a given substrate. Furthermore, these observations could point to different rate-determining steps for each of these reactions, with the metal-free reaction potentially having initial cyclization as the rate-determining step, and the metal-catalyzed reaction having the alkyl/aryl group migration as the rate-determining step. More detailed kinetic studies to further probe this hypothesis are currently ongoing in our laboratories.

### **3.11 Conclusions**

A method for the synthesis of indolizines and indolizinones has been developed which relies on substrate activation by water or other polar protic solvents for activation in place of a traditional metal catalyst. The parameters that govern the cyclization were explored as well as the substrate scope of the reaction. In the course of this investigation, it became clear that there are significant differences between the metal-catalyzed and metal-free versions of these cyclizations. Efforts are ongoing in our laboratory to understand the underlying mechanism of each of these transformations.

Given the number of metal catalysts, solvents and additives that have been investigated for the burgeoning number of  $\pi$ -Lewis acid-catalyzed isomerization reactions, it is remarkable that more attention has not been paid to water not only as a solvent, but as a catalyst for these reactions. We believe that our observations portend significant gains toward achieving ideal transformations. Although our initial studies have only explored a very small subset of cycloisomerization reactions, it is our anticipation that the use of water in place of expensive metal catalysts and organic solvents can be applied more broadly.

### 3.12 Experimental Contributions

Alison Hardin Narayan carried out the research detailed in Chapter 3.

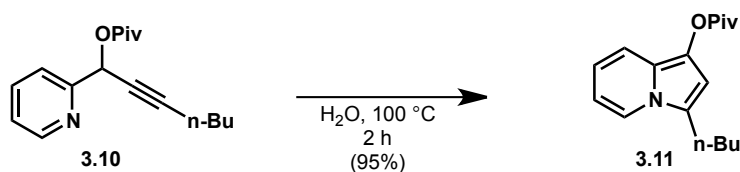
### 3.13 Experimental Methods

Unless otherwise stated, reactions were performed in flame-dried glassware fitted with rubber septa under a nitrogen atmosphere and were stirred with Teflon-coated magnetic stirring bars. Liquid reagents and solvents were transferred via syringe using standard Schlenk techniques. Tetrahydrofuran (THF), diethyl ether, benzene, toluene, and triethylamine were dried over alumina under a nitrogen atmosphere in a GlassContour solvent system. Dichloromethane (DCM) was distilled over calcium hydride. All other solvents and reagents were used as received unless otherwise noted. Reaction temperatures above 23 °C refer to oil or sand bath temperatures, which were controlled by an OptiCHEM temperature modulator. Thin layer chromatography was performed using SiliCycle silica gel 60 F-254 precoated plates (0.25 mm) and visualized by UV irradiation and anisaldehyde or potassium permanganate stain. SiliCycle Silica-P silica gel (particle size 40-63  $\mu\text{m}$ ) was used for flash chromatography.  $^1\text{H}$  and  $^{13}\text{C}$  NMR spectra were recorded on Bruker AVB-400, DRX-500, AV-500 and AV-600 MHz spectrometers with  $^{13}\text{C}$  operating frequencies of 100, 125, 125, and 150 MHz, respectively. Chemical shifts ( $\delta$ ) are reported in ppm relative to the residual solvent signal ( $\text{CDCl}_3$ ;  $\delta = 7.26$  for  $^1\text{H}$  NMR and  $\delta = 77.0$  for  $^{13}\text{C}$  NMR;  $\text{C}_6\text{D}_6$ ;  $\delta = 7.15$  for  $^1\text{H}$  NMR and  $\delta = 128.39$  for  $^{13}\text{C}$  NMR). Data for  $^1\text{H}$  NMR spectra are reported as follows: chemical shift (multiplicity, coupling constants, number of hydrogens). Abbreviations are as follows: s (singlet), d (doublet), t (triplet), dd (doublet of doublets), m (multiplet), br (broad). IR spectra were recorded on a Nicolet MAGNA-IR 850 spectrometer and are reported in frequency of absorption ( $\text{cm}^{-1}$ ). Only selected IR absorbencies are reported. High resolution mass spectral data were obtained from the Mass Spectral Facility at the University of California, Berkeley.

### General

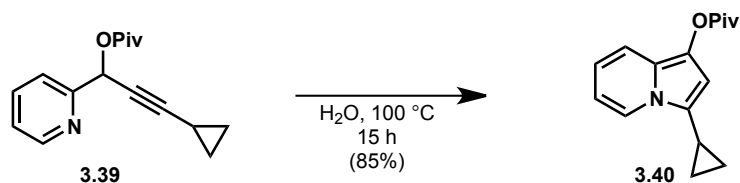
The majority of the compounds reported herein were prepared and characterized previously in our laboratory. For additional procedures describing the synthesis of substrates as well as full characterization data for both starting materials and heterocyclic products, see C. R. Smith, E. M. Bunnelle, A. J. Rhodes, R. Sarpong, *Org. Lett.* **2007**, *9*, 1169-1171.

### Representative Procedures for the Formation of Indolizines and Indolizinones

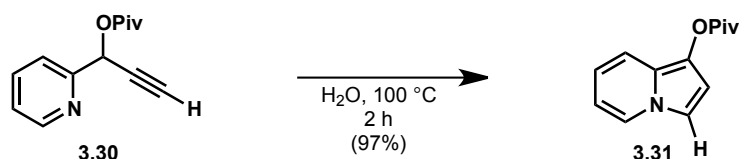


**Indolizine 3.11:** A heterogeneous mixture of pyridine propargylic ester **3.10** (54.7 mg, 0.200 mmol) and distilled deionized water or EtOH (200  $\mu\text{L}$ ) was heated at  $100\text{ }^\circ\text{C}$  for 2 h at which point TLC analysis indicated that the starting material had been consumed. The reaction mixture

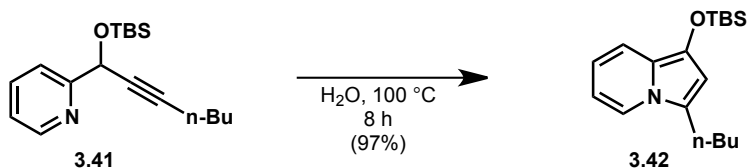
was cooled to 23 °C, and the solvent was removed under reduced pressure to provide indolizine **3.11** as a brown oil (52.0 mg, 95% yield). The crude product was >90% purity by <sup>1</sup>H NMR. <sup>1</sup>H NMR (500 MHz, C<sub>6</sub>D<sub>6</sub>) δ 7.30 (d, *J* = 9.01 Hz, 1H), 7.04 (d, *J* = 7.10 Hz, 1H), 6.76 (s, 1H), 6.32 (dd, *J* = 8.99, 6.42 Hz, 1H), 6.06 (t, *J* = 6.76 Hz, 1H), 2.26 (t, *J* = 7.65 Hz, 2H), 1.40-1.32 (m, 2H), 1.27 (s, 9H), 1.18-1.10 (m, 2H), 0.74 (t, *J* = 7.34 Hz, 3H); <sup>13</sup>C NMR (125 MHz, C<sub>6</sub>D<sub>6</sub>) δ 175.7, 127.1, 121.3, 120.9, 120.7, 116.1, 114.0, 109.6, 105.0, 38.9, 29.0, 27.0, 25.2, 22.4, 13.6; IR (film)  $\nu_{\max}$  2958, 2931, 2871, 1749, 1278, 1120, 728 cm<sup>-1</sup>; HRMS (EI) calcd for [C<sub>17</sub>H<sub>23</sub>NO<sub>2</sub>]<sup>+</sup>: *m/z* 273.1729, found 273.1732.



**Indolizine 3.40:** A heterogeneous mixture of pyridine propargylic ester **3.39** (51.5 mg, 0.200 mmol) and distilled deionized water or EtOH (200  $\mu$ L) was heated at 100 °C for 15 h at which point TLC analysis indicated that the starting material had been consumed. The reaction mixture was cooled to 23 °C, and the solvent was removed under reduced pressure to provide indolizine **3.40** as a green oil in 85% yield (43.8 mg). <sup>1</sup>H NMR (500 MHz, C<sub>6</sub>D<sub>6</sub>) δ 7.52 (d, *J* = 7.1 Hz, 1H), 7.31 (d, *J* = 9.0 Hz, 1H), 6.73 (s, 1H), 6.39 (dd, *J* = 9.0, 6.4 Hz, 1H), 6.15 (s, 1H), 1.28 (s, 9H), 0.49 – 0.45 (m, 2H), 0.32 (dd, *J* = 5.1, 2.0 Hz, 2H).

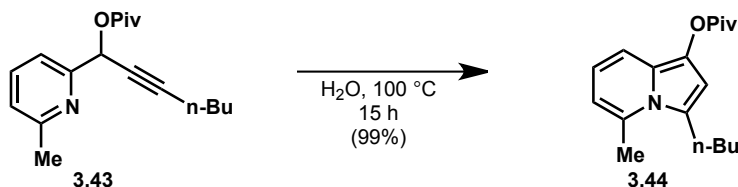


**Indolizine 3.31:** A heterogeneous mixture of pyridine propargylic ester **3.30** (43.5 mg, 0.200 mmol) and distilled deionized water or EtOH (200  $\mu$ L) was heated at 100 °C for 2 h at which point TLC analysis indicated that the starting material had been consumed. The reaction mixture was cooled to 23 °C, and the solvent was removed under reduced pressure to provide indolizine **3.31** as a brown oil in 97% yield (42.2 mg). <sup>1</sup>H NMR (500 MHz, C<sub>6</sub>D<sub>6</sub>) δ 7.22 (d, *J* = 9.1 Hz, 1H), 6.93 (d, *J* = 2.9 Hz, 1H), 6.91 (d, *J* = 7.0 Hz, 1H), 6.59 (d, *J* = 2.9 Hz, 1H), 6.26 (dd, *J* = 9.0, 6.5 Hz, 1H), 5.90 (s, 1H), 1.26 (s, 9H).

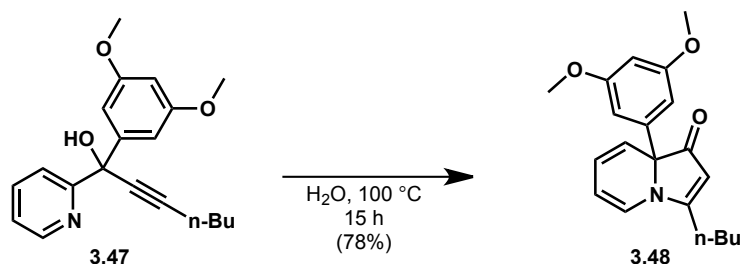


**Indolizine 3.42:** A heterogeneous mixture of pyridine propargylic ester **3.41** (60.7 mg, 0.200 mmol) and distilled deionized water or EtOH (200  $\mu$ L) was heated at 100 °C for 8 h at which point TLC analysis indicated that the starting material had been consumed. The reaction mixture

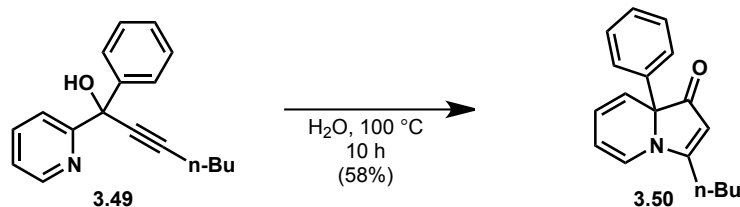
was cooled to 23 °C, and the solvent was removed under reduced pressure to provide indolizine **3.42** as a brown oil in 97% yield (58.9 mg). <sup>1</sup>H NMR (500 MHz, C<sub>6</sub>D<sub>6</sub>) δ 7.47 (d, *J* = 9.0 Hz, 1H), 7.10 (d, *J* = 7.2 Hz, 1H), 6.30 (s, 1H), 6.29 – 6.26 (m, 1H), 6.08 (s, 1H), 2.37 (s, 2H), 1.48 – 1.44 (m, 2H), 1.21 (dd, *J* = 13.9, 6.4 Hz, 2H), 1.09 (d, *J* = 2.8 Hz, 9H), 0.79 (d, *J* = 7.4 Hz, 3H).



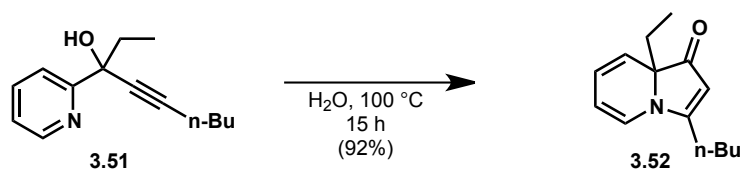
**Indolizine 3.44:** A heterogeneous mixture of pyridine propargylic ester **3.43** (31.0 mg, 0.108 mmol) and distilled deionized water or EtOH (200 μL) was heated at 100 °C for 8 h at which point TLC analysis indicated that the starting material had been consumed. The reaction mixture was cooled to 23 °C, and the solvent was removed under reduced pressure to provide indolizine **3.44** as a brown oil in 99% yield (30.7 mg). <sup>1</sup>H NMR (500 MHz, C<sub>6</sub>D<sub>6</sub>) δ 7.28 (d, *J* = 8.8 Hz, 1H), 6.83 (s, 1H), 6.31 (dd, *J* = 8.9, 6.5 Hz, 1H), 5.81 (d, *J* = 6.3 Hz, 1H), 2.74 (s, 2H), 2.17 (s, 3H), 1.39 (s, 2H), 1.30 (s, 9H), 1.16 (s, 2H), 0.78 (t, *J* = 7.3 Hz, 3H).



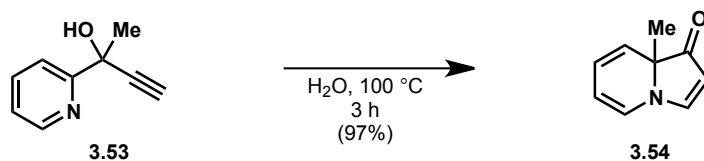
**Indolizinone 3.48:** A heterogeneous mixture of tertiary propargylic alcohol **3.47** (32.5 mg, 0.0999 mmol) and distilled deionized water or EtOH (200 μL) was heated at 100 °C for 15 h at which point TLC analysis indicated that the starting material had been consumed. The reaction mixture was cooled to 23 °C and concentrated under reduced pressure to provide indolizinone **3.48** as a brown oil in 78% yield (25.4 mg). The crude product was >90% purity by <sup>1</sup>H NMR. <sup>1</sup>H NMR (500 MHz, C<sub>6</sub>D<sub>6</sub>) δ 6.88 (d, *J* = 2.19 Hz, 2H), 6.40 (d, *J* = 2.19 Hz, 1H), 6.36 (t, *J* = 2.17 Hz, 1H), 5.99 (d, *J* = 7.07 Hz, 1H), 5.69 (dd, *J* = 9.19 Hz, 1H), 5.04-5.01 (m, 1H), 4.76 (s, 1H), 3.31 (s, 6H), 1.85-1.70 (m, 2H), 1.16-1.06 (m, 2H), 1.03-0.92 (m, 2H), 0.65 (t, *J* = 7.31 Hz, 3H); <sup>13</sup>C NMR (125 MHz, C<sub>6</sub>D<sub>6</sub>) δ 199.4, 175.6, 161.1, 143.2, 122.8, 122.8, 122.5, 108.6, 103.1, 99.2, 97.2, 71.1, 54.5, 28.3, 26.3, 22.1, 13.3; IR (film)  $\nu_{\max}$  2957, 2872, 1683, 1595, 1536, 1426, 1156, 1063, 725 cm<sup>-1</sup>; HRMS (EI) calcd for [C<sub>18</sub>H<sub>19</sub>NO]<sup>+</sup>: *m/z* 325.1678, found 325.1676.



**Indolizinone 3.50:** A heterogeneous mixture of tertiary propargylic alcohol **3.49** (53.1 mg, 0.200 mmol) and distilled deionized water or EtOH (200  $\mu$ L) was heated at 100  $^{\circ}$ C for 10 h at which point TLC analysis indicated that the starting material had been consumed. The reaction mixture was cooled to 23  $^{\circ}$ C and concentrated under reduced pressure to provide indolizinone **3.50** as a brown oil in 58% yield (30.9 mg).  $^1\text{H NMR}$  (500 MHz,  $\text{C}_6\text{D}_6$ )  $\delta$  7.56 (d,  $J = 7.4$  Hz, 2H), 7.17 (m, 2H), 7.03 (t,  $J = 7.4$  Hz, 1H), 6.43 (d,  $J = 9.2$  Hz, 1H), 5.97 (d,  $J = 7.0$  Hz, 1H), 5.68 (dd,  $J = 9.2, 5.4$  Hz, 1H), 5.00 (t,  $J = 6.0$  Hz, 1H), 4.77 (s, 1H), 1.79 (dd,  $J = 18.9, 8.8$  Hz, 2H), 1.12 (d,  $J = 6.8$  Hz, 2H), 0.99 (d,  $J = 7.4$  Hz, 2H), 0.68 (t,  $J = 7.3$  Hz, 3H).

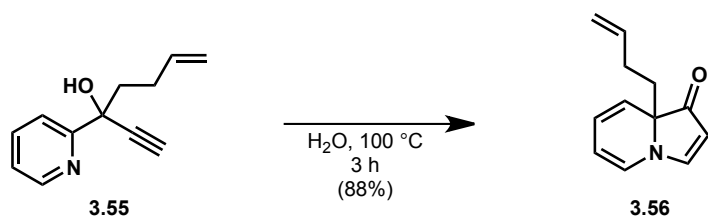


**Indolizinone 3.52:** A heterogeneous mixture of tertiary propargylic alcohol **3.51** (47.5 mg, 0.200 mmol) and distilled deionized water or EtOH (200  $\mu$ L) was heated at 100  $^{\circ}$ C for 15 h at which point TLC analysis indicated that the starting material had been consumed. The reaction mixture was cooled to 23  $^{\circ}$ C and concentrated under reduced pressure to provide indolizinone **3.52** as a brown oil in 92% yield (43.7 mg).  $^1\text{H NMR}$  (400 MHz,  $\text{C}_6\text{D}_6$ )  $\delta$  7.01 (d,  $J = 6.8$  Hz, 3H), 6.96 (d,  $J = 6.7$  Hz, 2H), 6.14 (d,  $J = 7.2$  Hz, 1H), 6.00 (d,  $J = 9.2$  Hz, 1H), 5.61 (dd,  $J = 9.2, 5.4$  Hz, 1H), 5.14 (s, 1H), 4.88 (t,  $J = 6.3$  Hz, 1H), 1.96 (d,  $J = 7.2$  Hz, 1H), 1.87 (d,  $J = 7.2$  Hz, 1H), 0.93 (t,  $J = 7.4$  Hz, 3H).



**Indolizinone 3.54:** A heterogeneous mixture of tertiary propargylic alcohol **3.53** (77.0 mg, 0.523 mmol) and distilled deionized water or EtOH (500  $\mu$ L) was heated at 100  $^{\circ}$ C for 3 h at which point TLC analysis indicated that the starting material had been consumed. The reaction mixture was cooled to 23  $^{\circ}$ C and concentrated under reduced pressure to provide indolizinone **3.54** as a yellow oil in 97% yield (74.7 mg).  $^1\text{H NMR}$  (600 MHz,  $\text{CDCl}_3$ )  $\delta$  7.75 (d,  $J = 3.6$  Hz, 1H), 6.36 (d,  $J = 7.0$  Hz, 1H), 5.86 (dt,  $J = 23.6, 7.3$  Hz, 2H), 5.40 (t,  $J = 6.2$  Hz, 1H), 5.05 (d,  $J = 3.6$  Hz, 1H), 1.31 (s, 3H);  $^{13}\text{C NMR}$  (151 MHz,  $\text{CDCl}_3$ )  $\delta$  204.5, 159.3, 124.5, 123.0, 122.0, 108.2, 97.6, 66.8, 24.3; **HRMS** (ESI+) calcd for  $[\text{C}_9\text{H}_{10}\text{ON}]^+$  (M-H) $^+$ :  $m/z$  148.0757, found 148.0757.





**Indolizinone 3.56:** A solution of tertiary alcohol **3.55** (300 mg, 0.803 mmol) in EtOH (5.0 mL) was sparged with N<sub>2</sub> for 5 min. The reaction vessel, a 20 mL vial, was equipped with a green Teflon-lined cap and Teflon tape and heated at 100 °C for 4 h. The reaction mixture was cooled to room temperature and concentrated to provide indolizinone **3.56** in 88% yield (264 mg). <sup>1</sup>H NMR (400 MHz, CDCl<sub>3</sub>) δ 6.48 (d, *J* = 7.2 Hz, 1H), 5.87 (dd, *J* = 17.9, 7.3 Hz, 2H), 5.69 (ddt, *J* = 16.8, 10.2, 6.5 Hz, 1H), 5.40 (s, 1H), 5.14 (s, 1H), 4.95 (dd, *J* = 17.1, 1.7 Hz, 1H), 4.90 (dd, *J* = 10.2, 1.6 Hz, 1H), 4.65 (d, *J* = 0.5 Hz, 2H), 2.04 (m, 4H), 1.80 (d, *J* = 5.7 Hz, 2H), 1.15 (dd, *J* = 14.3, 6.7 Hz, 3H), 1.08 (d, *J* = 6.2 Hz, 18H); <sup>13</sup>C NMR (101 MHz, CDCl<sub>3</sub>) δ 202.7, 137.717, 124.0, 123.0, 122.2, 114.8, 109.5, 97.7, 71.0, 58.6, 37.6, 26.5, 17.9, 11.9.

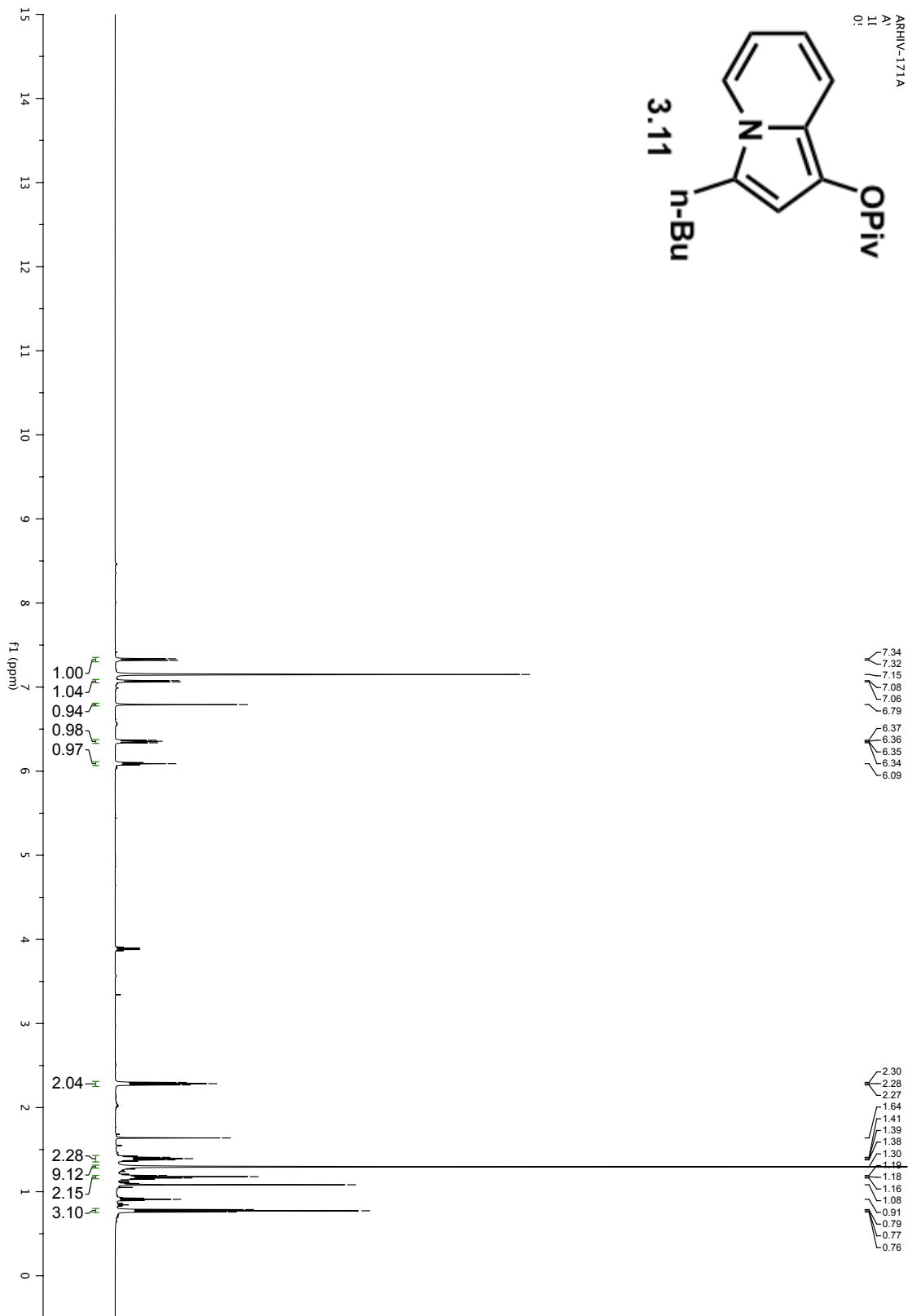
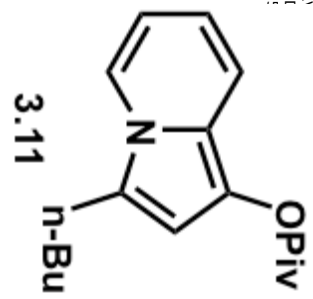
### 3.14 References and Notes

- (1) Anastas, P. T.; Warner, J. C. *Green Chemistry: Theory and Practice*; Oxford University Press: New York, **1998**.
- (2) Trost, B. M. *Acc. Chem. Res.* **2002**, *35*, 695.
- (3) Nelson, W. M. *Green Solvents in Chemistry, Perspectives and Practice*; Oxford University Press: New York, **2003**.
- (4) Furstner, A.; Davies, P. W. *Angew. Chem. Int. Ed.* **2007**, *46*, 3410.
- (5) Smith, C. R.; Bunnelle, E. M.; Rhodes, A. J.; Sarpong, R. *Org. Lett.* **2007**, *9*, 1169.
- (6) Bunnelle, E. M.; Smith, C. R.; Lee, S. K.; Singaram, S. W.; Rhodes, A. J.; Sarpong, R. *Tetrahedron* **2008**, *64*, 7008.
- (7) Hardin, A. R.; Sarpong, R. *Org. Lett.* **2007**, *9*, 4547.
- (8) Yan, B.; Zhou, Y. B.; Zhang, H.; Chen, J. J.; Liu, Y. H. *J. Org. Chem.* **2007**, *72*, 7783.
- (9) Seregin, I. V.; Schammel, A. W.; Gevorgyan, V. *Org. Lett.* **2007**, *9*, 3433.
- (10) Kim, I.; Choi, J.; Won, H. K.; Lee, G. H. *Tetrahedron Lett.* **2007**, *48*, 6863.
- (11) Choi, J.; Lee, G. H.; Kim, I. *Synlett* **2008**, 1243.
- (12) Kim, K.; Kim, I. *J. Comb. Chem.* **2010**, *12*, 379.

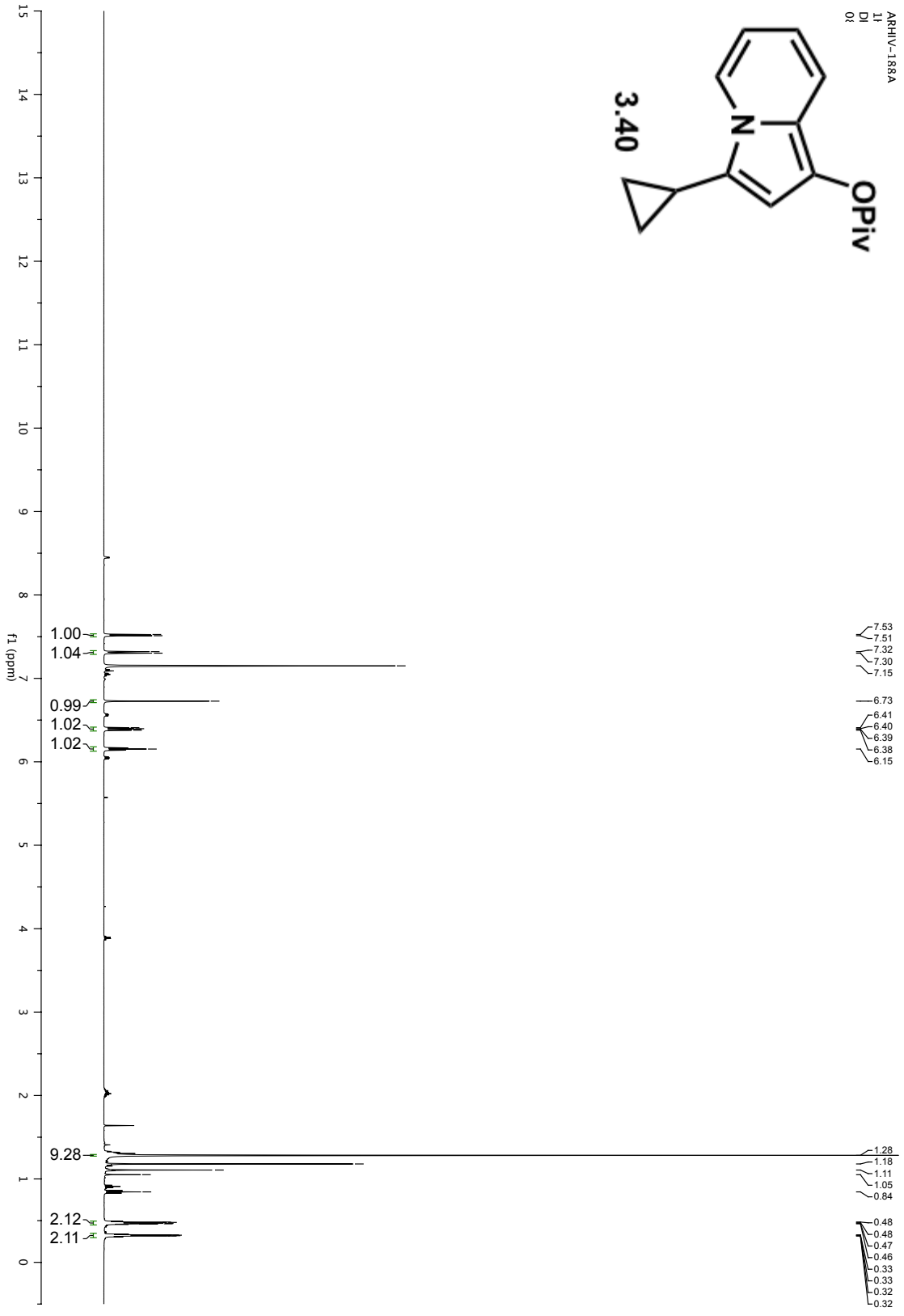
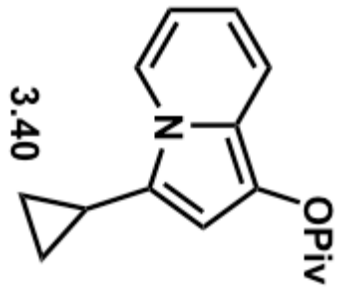
- (13) Rideout, D. C.; Breslow, R. *J. Am. Chem. Soc.* **1980**, *102*, 7816.
- (14) Breslow, R. *Acc. Chem. Res.* **1991**, *24*, 159.
- (15) Breslow, R.; Oxford University Press: New York, **1998**, p Ch. 13.
- (16) Vilotijevic, I.; Jamison, T. F. *Science* **2007**, *317*, 1189.
- (17) Narayan, S.; Muldoon, J.; Finn, M. G.; Fokin, V. V.; Kolb, H. C.; Sharpless, K. B. *Angew. Chem. Int. Ed.* **2005**, *44*, 3275.
- (18) Li, C. J. *Chem. Rev.* **2005**, *105*, 3095.
- (19) Pirrung, M. C. *Chem. Eur. J.* **2006**, *12*, 1312.
- (20) Brower, K. R. *J. Am. Chem. Soc.* **1961**, *83*, 4370.
- (21) Lubineau, A. *J. Org. Chem.* **1986**, *51*, 2142.
- (22) Lubineau, A.; Auge, J. *Modern Solvents in Organic Synthesis* **1999**, 206, 1.
- (23) Otto, S.; Engberts, J. *Org. Biomol. Chem.* **2003**, *1*, 2809.

*Appendix Two:  
Spectra Relevant to Chapter Three*

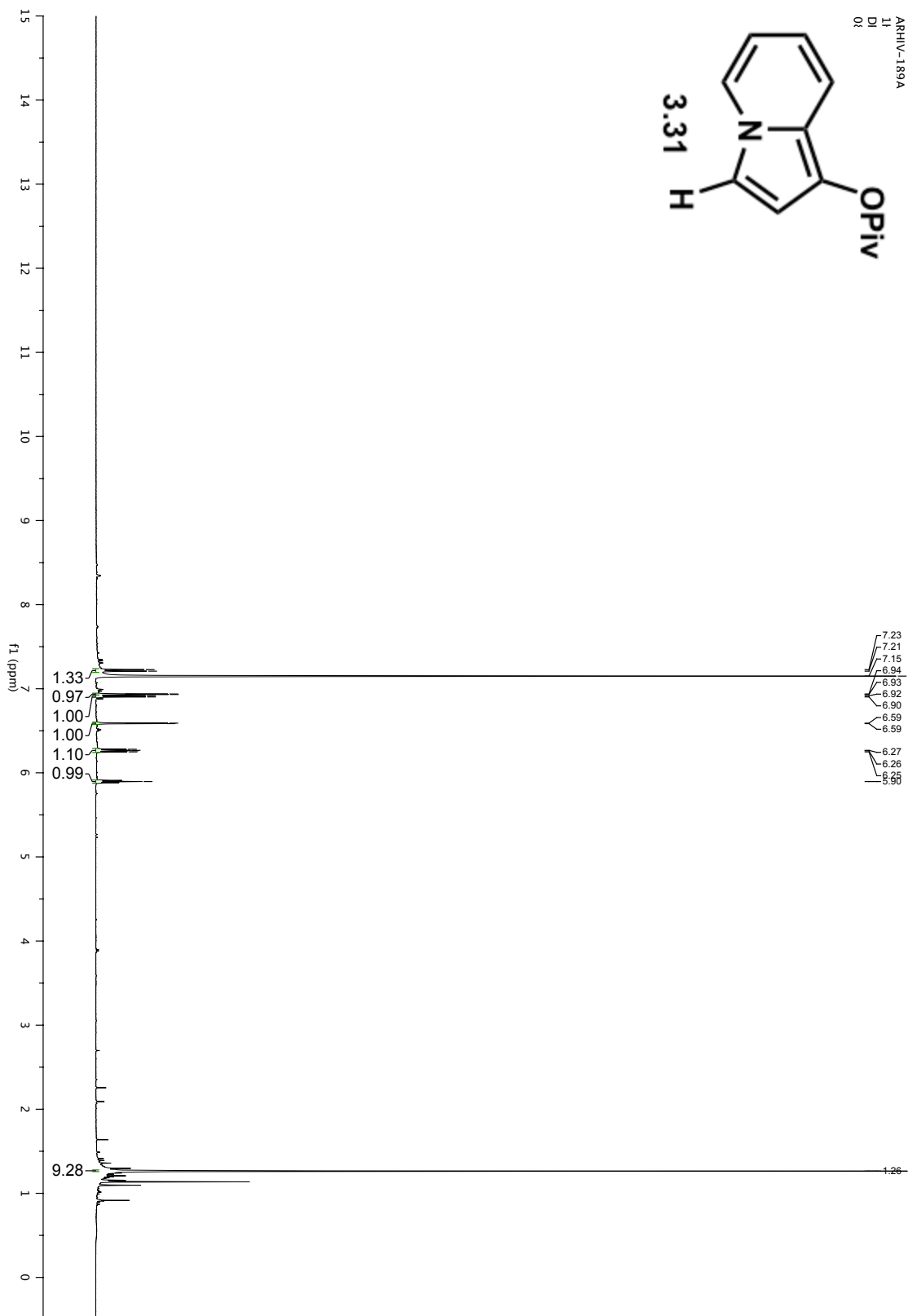
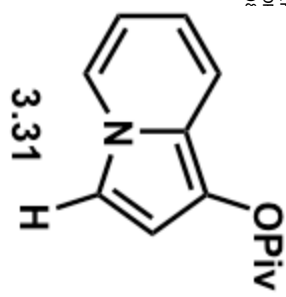
ARRIV-171A  
A:  
11:  
0:

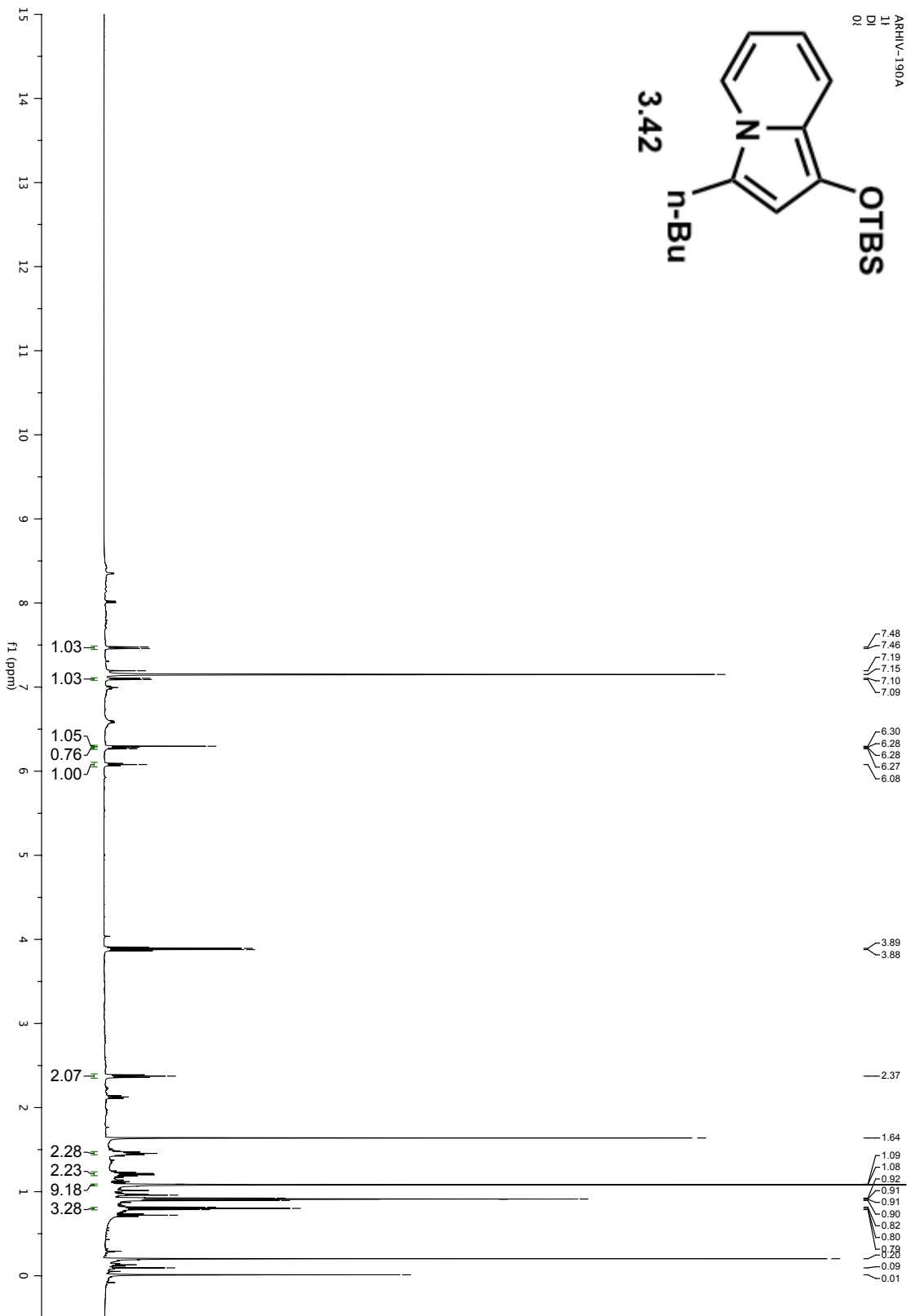


ARHIV-188A  
11  
DI  
01

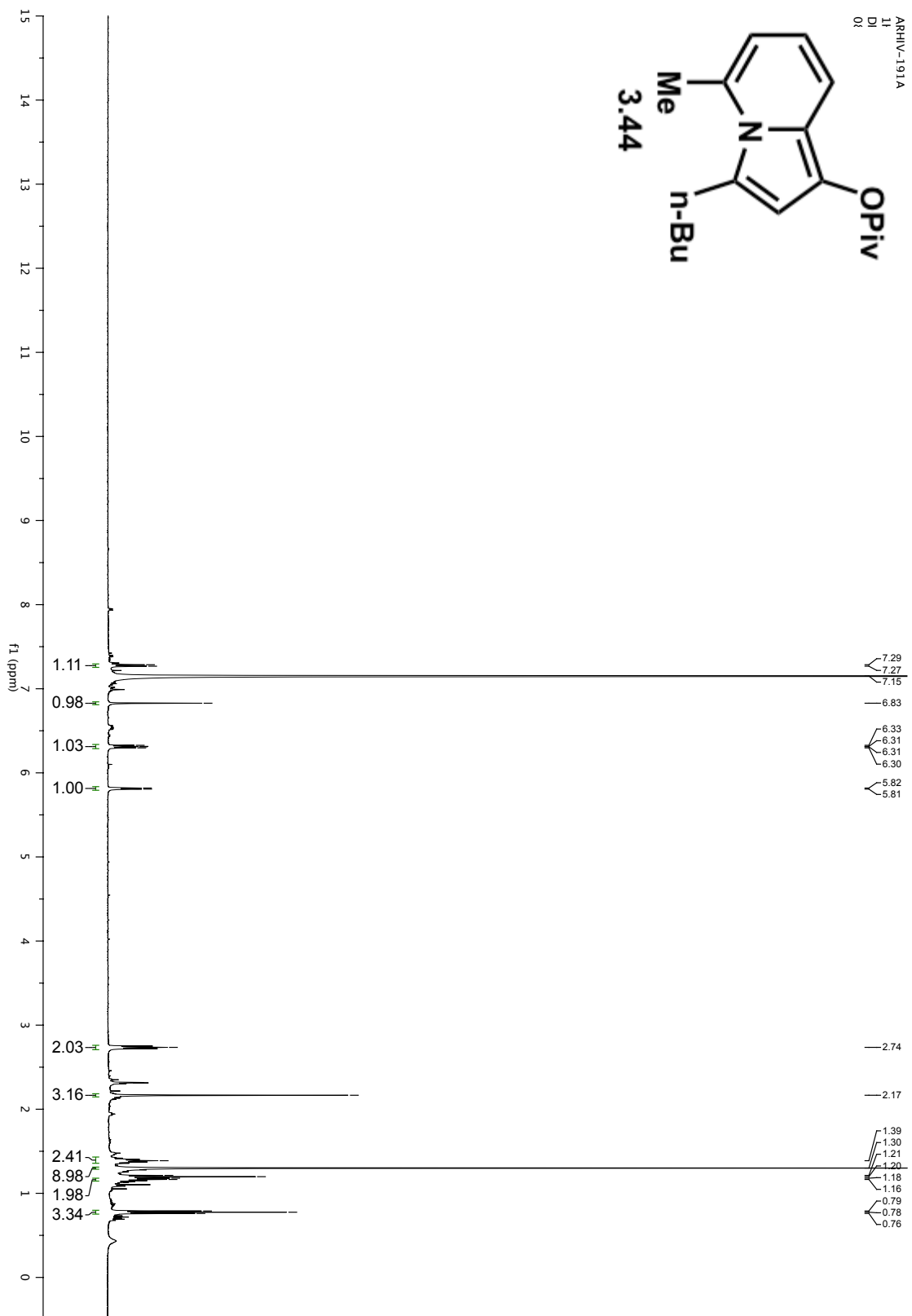
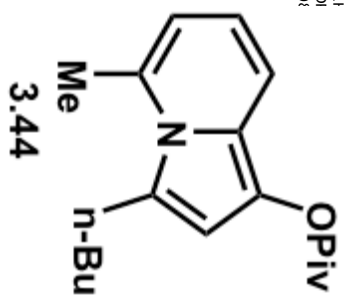


ARHIV-189A  
11  
DI  
01

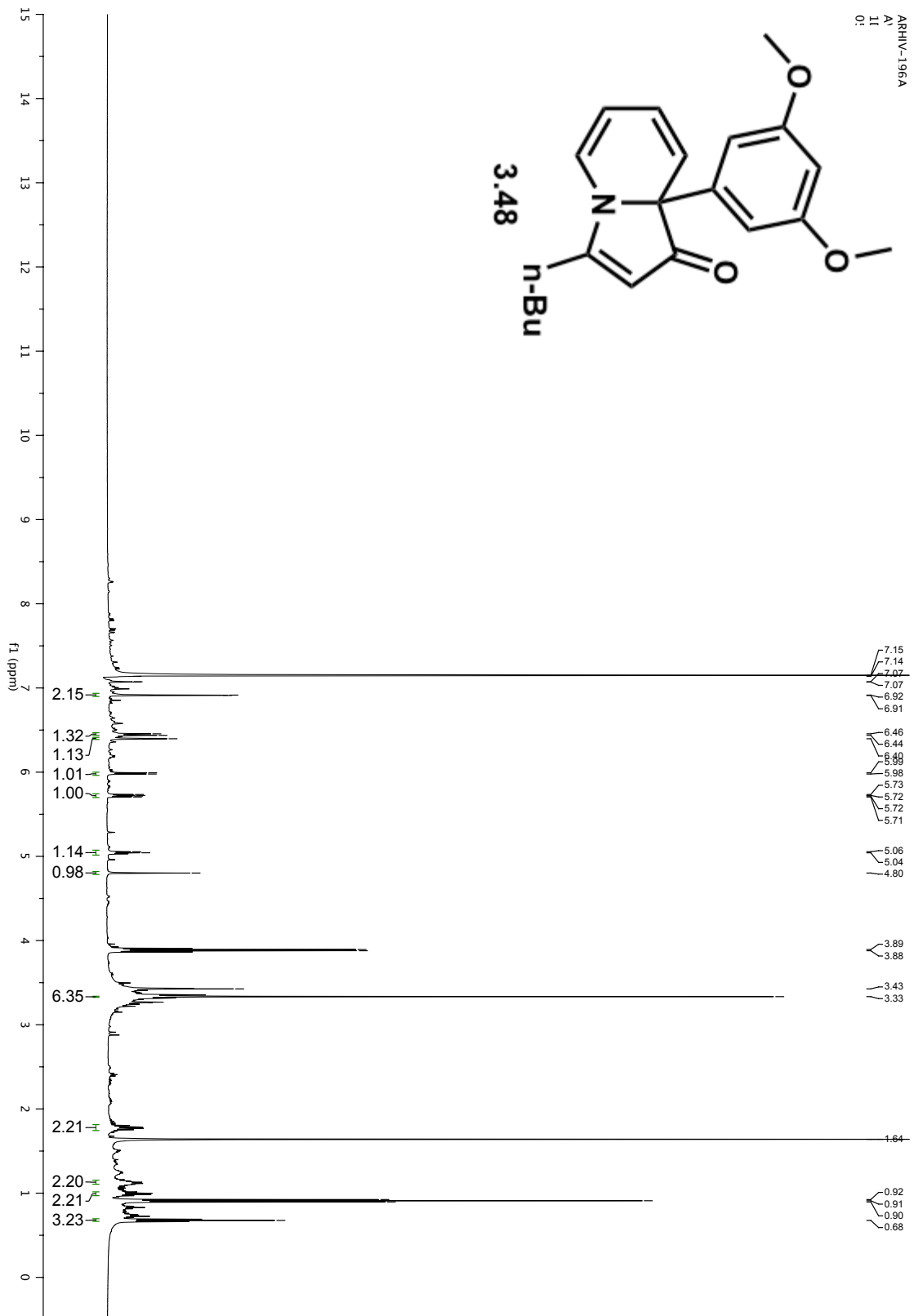


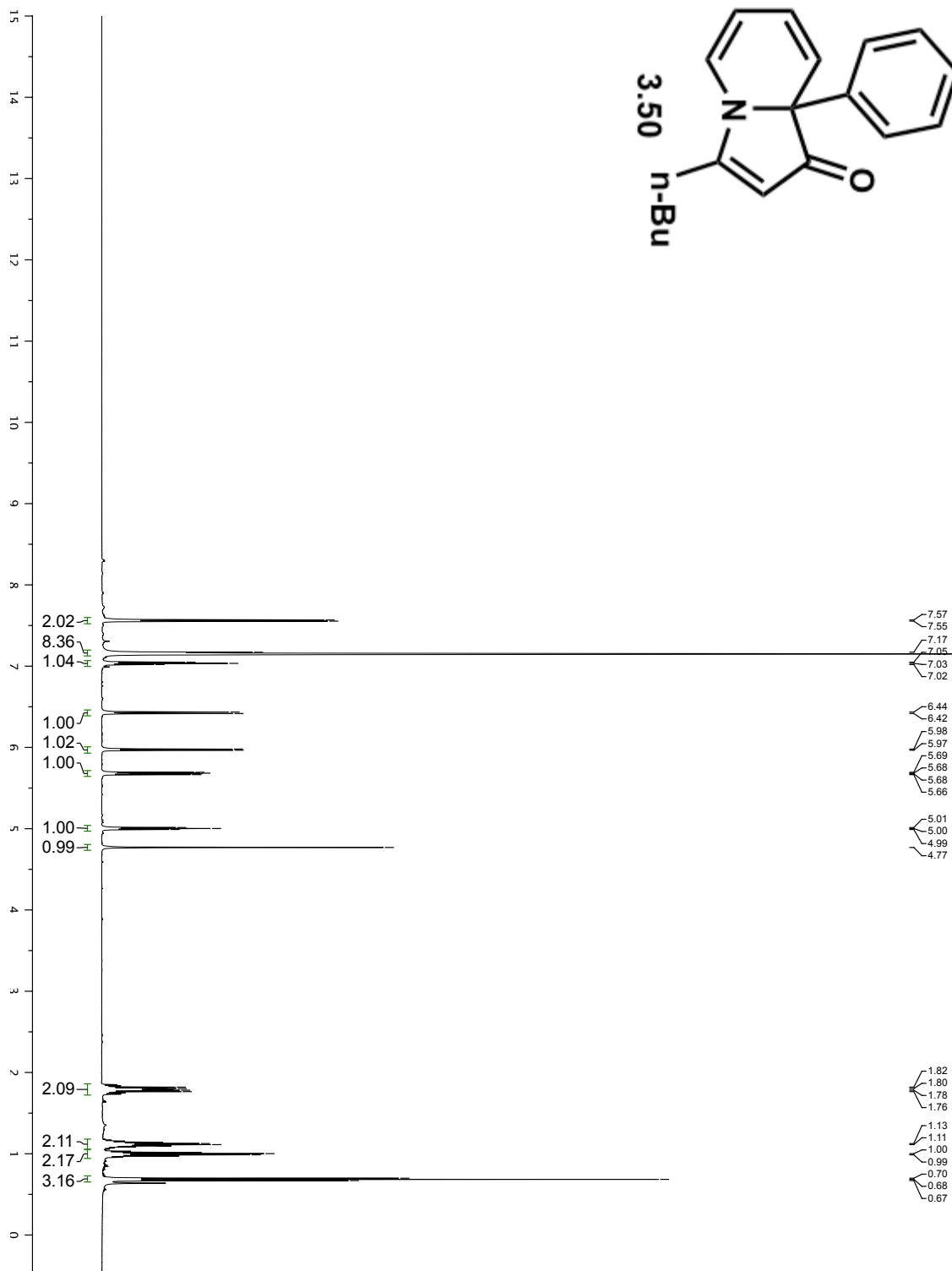
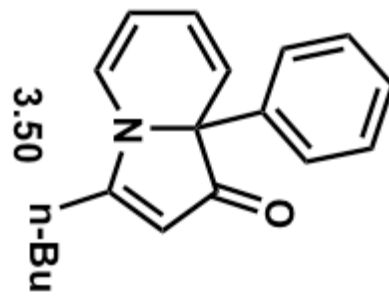


ARRIV-191A  
11  
DI  
01



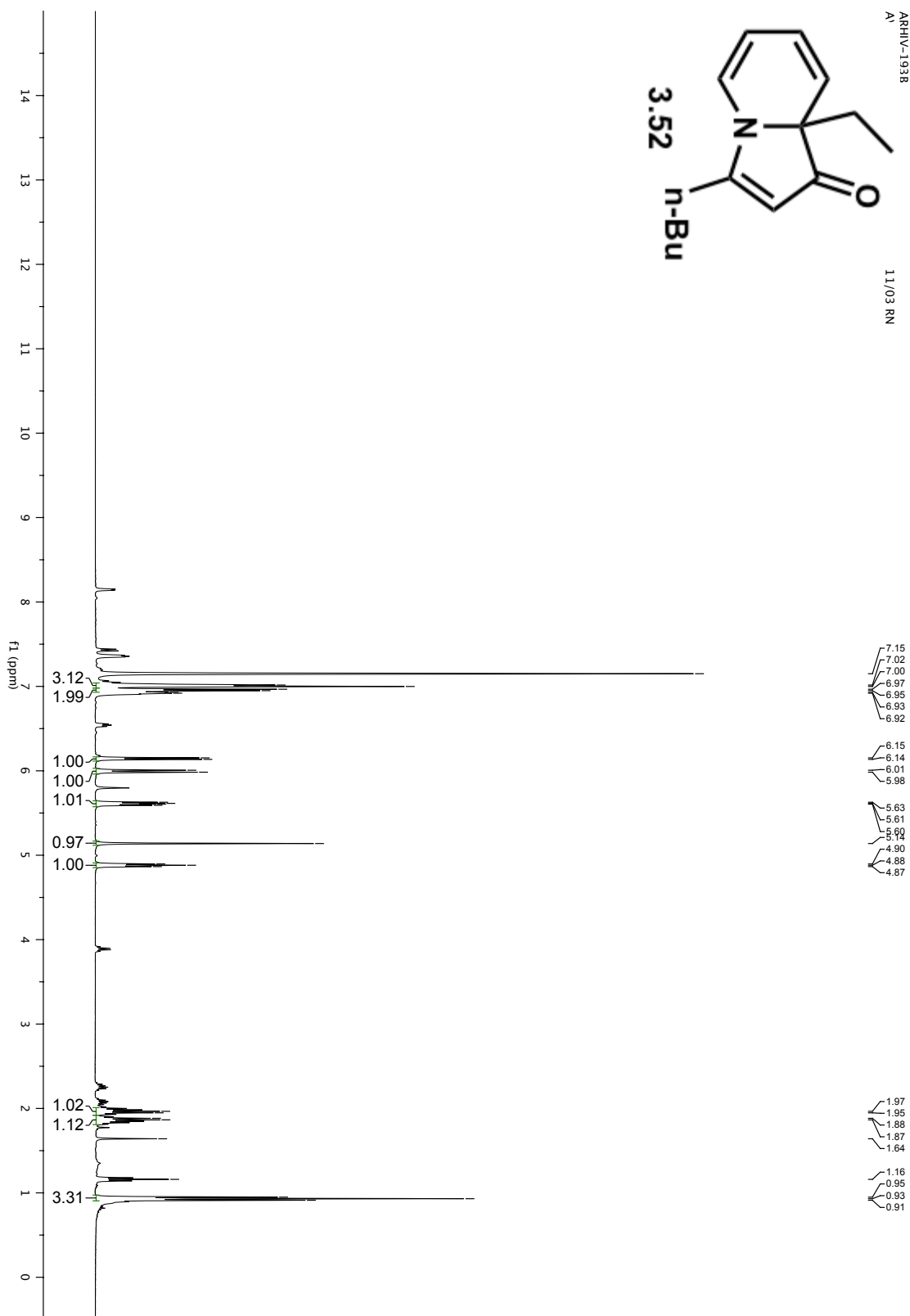
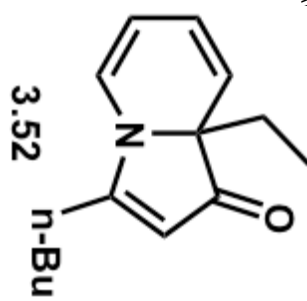




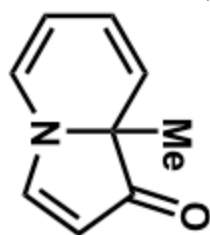


ARRIV-1938  
A'

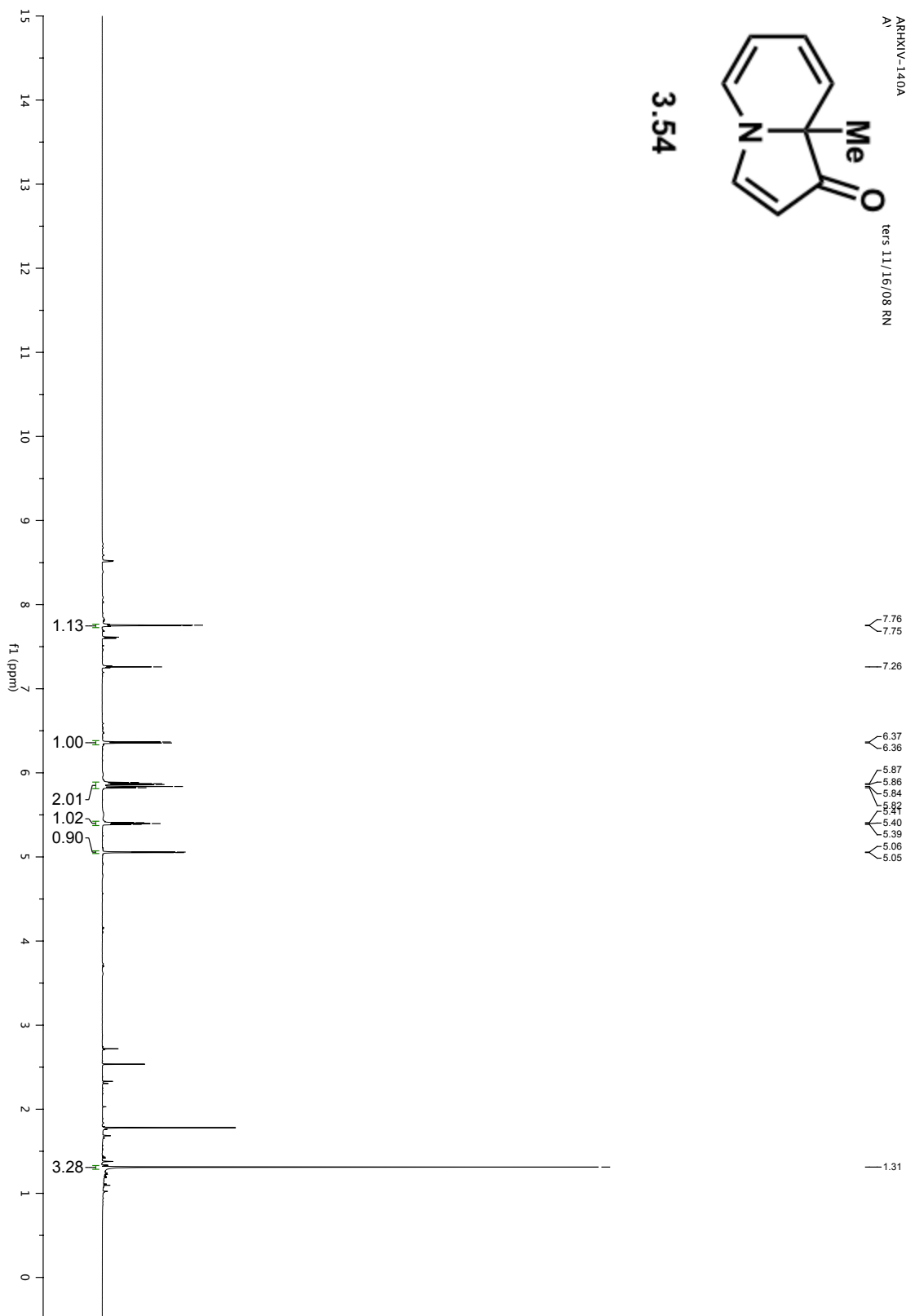
11/03 RN

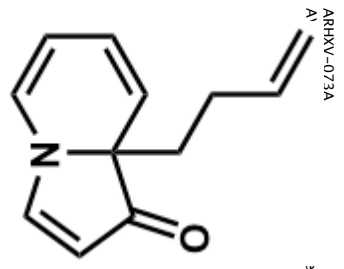


ARRXIV-140A  
A1  
terc 11/16/08 RN

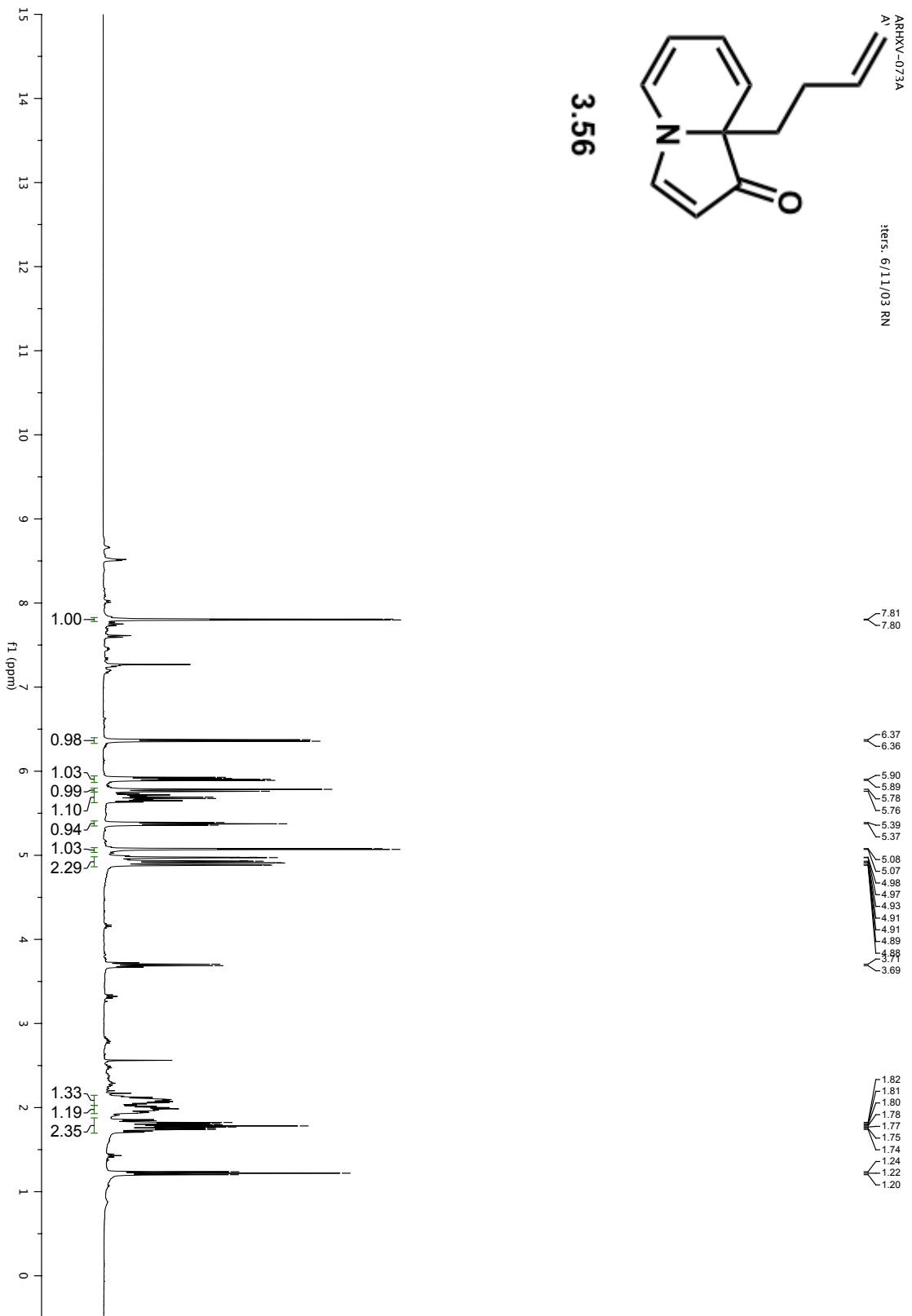


3.54





3.56



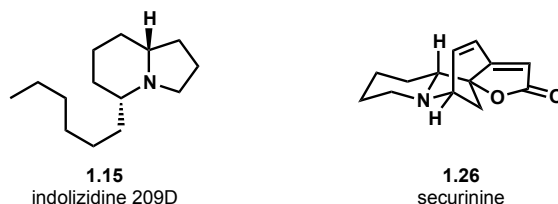
## Chapter 4. Synthetic Studies Toward Type I Indolizidine Alkaloids from Indolizines

### 4.1 Selection of Targeted Indolizidine Alkaloids

As outlined in Chapter 1, we became interested in exploiting substituted indolizines to synthesize type I indolizidine alkaloids. At the outset of this project, we anticipated that the challenges associated with this strategy would include (1) the ability to install the necessary functional groups about the indolizine core, (2) reduction of the indolizine to the fully saturated indolizidine, and (3) the ease with which indolizidines could be elaborated to more complex scaffolds.

Our initial synthetic targets were selected with these challenges, as well as the bioactivity of these natural products, in mind. To this end, we chose indolizidine 209D (**1.15**) and securinine (**1.26**) as the focus of our synthetic endeavors. The synthesis of indolizidine 209D, a mono-substituted indolizidine natural product, would require the installation of an *n*-hexyl chain onto the indolizidine framework as well as complete reduction to the indolizidine oxidation level. To access securinine, an appropriate indolizine precursor would need to be reduced to the corresponding indolizidine, which would be further elaborated to a tetracyclic skeleton. Additionally, both indolizidine 209D and securinine exhibit intriguing biological activity. The details of the biological properties of these molecules, as well as our efforts toward building these natural products, are detailed herein.

**Figure 4.1.1.** Indolizidine natural product targets.



### 4.2 Synthesis of indolizidine alkaloid 209D

#### Isolation and Biological Activity

Indolizidine 209D, like many alkylated indolizidines (see Chapter 1), has been isolated from the skin of neotropical frogs native to Central and South America. However, unlike most frog indolizidine alkaloids that are common to several species, indolizidine 209D has been isolated only once from an unidentified type of dedrobatid frog found on the Isla de Colon, Panama.<sup>1</sup> Following isolation, the structure was assigned based on mass spectral data. The inability of Daly and coworkers to isolate indolizidine 209D and other mono-alkylated indolizidine alkaloids, such as indolizidine 167B (**1.14**, see Figure 1.2.2), from other frog populations has led to some skepticism as to whether these molecules are indeed natural products.<sup>1</sup> The lack of continued access to these compounds from a natural source has also spurred the chemical synthesis of these natural products to understand their structure and also to explore their biological activity.

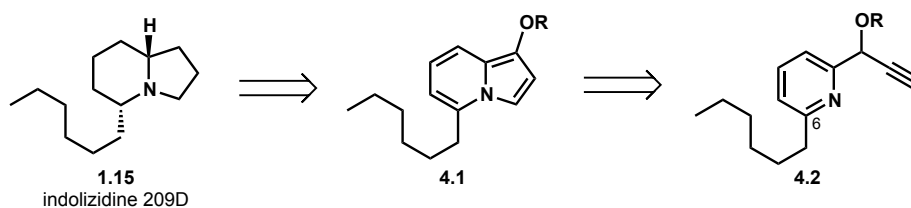
Among other potential biological functions, indolizidine 209D and related alkylated indolizidines have been identified as potent noncompetitive blockers for nicotinic receptor-channels.<sup>2</sup> Competitive inhibitors directly bind the same site as nicotinic agonists, whereas noncompetitive blockers bind to other sites on the receptor channel. When a noncompetitive blocker binds it can have the effect of physically blocking the receptor channel, impeding the opening of the channel, or enhancing the rate of channel closing. Noncompetitive blockers have been well studied and developed as local anesthetics.<sup>3</sup>

The potency of indolizidine alkaloids has been shown to correlate with the length of the alkyl chain attached to C-5.<sup>4</sup> It has been hypothesized that the chain anchors the molecule in the ion channel, and that an optimal chain length exists that is neither too short nor too long.<sup>5</sup> We sought to develop a flexible synthetic route to indolizidine 209D that would enable us to make a range of analogs containing alkyl chains of varying lengths.

### Retrosynthetic Analysis

Our plan was to rapidly access indolizidine 209D (**1.15**) from a 1,5-disubstituted indolizine such as **4.1** (Figure 4.2.1). Indolizine **4.1** could be prepared by metal-free cyclization of propargylic alcohol derivative **4.2** containing a pyridine with the requisite six-carbon chain already installed. We envisioned being able to construct a variety of analogs of **1.15** possessing alkyl chains of different lengths by simply varying the substituent at C-6 of the pyridine substrate. In addition, facile functionalization at the alkyne terminus of **4.2** would enable us to access other indolizidine natural products as well as their non-natural derivatives.

**Figure 4.2.1.** Retrosynthesis of indolizidine 209D.



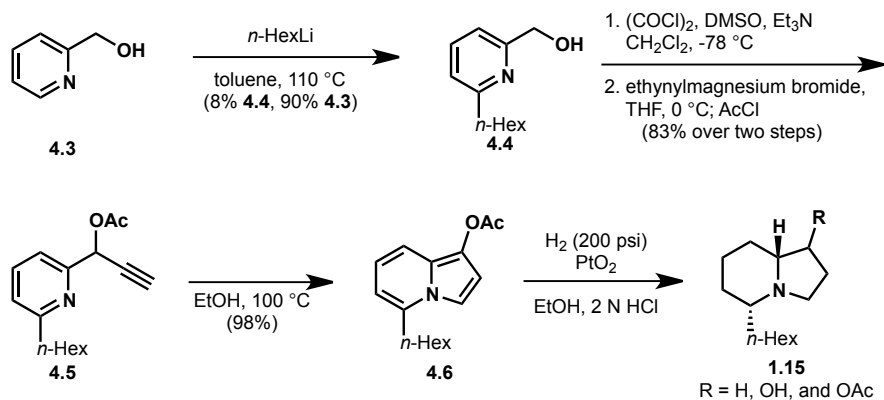
### Toward indolizidine 209D

The first task in the synthesis of **1.15** was installation of an alkyl substituent on the pyridine ring. On the basis of precedent from our synthesis of tricyclic marine alkaloids (see Chapter 7), we envisioned incorporating the *n*-hexyl chain in a Chichibabin-type reaction of 2-pyridinemethanol (**4.3**) with *n*-hexyllithium (Scheme 4.2.1). Despite our success with this reaction on a similar substrate, significant quantities of starting material were recovered from the crude reaction mixture. Efforts to increase the yield of the desired product (**4.4**) above 8% by increasing the number of equivalents of *n*-hexyllithium, increasing the reaction temperature, or extending the reaction time were unsuccessful. While alternative methods for introducing the hexyl-chain were under investigation, we proceeded with the synthesis.

Swern oxidation of alcohol **4.4** gave an intermediate aldehyde that was subsequently treated with ethynylmagnesium bromide. The resulting magnesium alkoxide

was intercepted with acetyl chloride to deliver propargylic ester **4.5** as the sole product. Heating **4.5** in ethanol at 100 °C gave indolizine **4.6**. From indolizine **4.6**, only a global reduction was necessary to arrive at the natural product. We opted to use platinum(IV) oxide in acid media to carry out this hydrogenation with the objective of achieving a hydrogenolysis of the C-O bond at C-1. After four days, indolizidine 209D (**1.15**) was isolated from the reaction as a mixture with the corresponding C1-hydroxy and C1-acetoxy compounds.

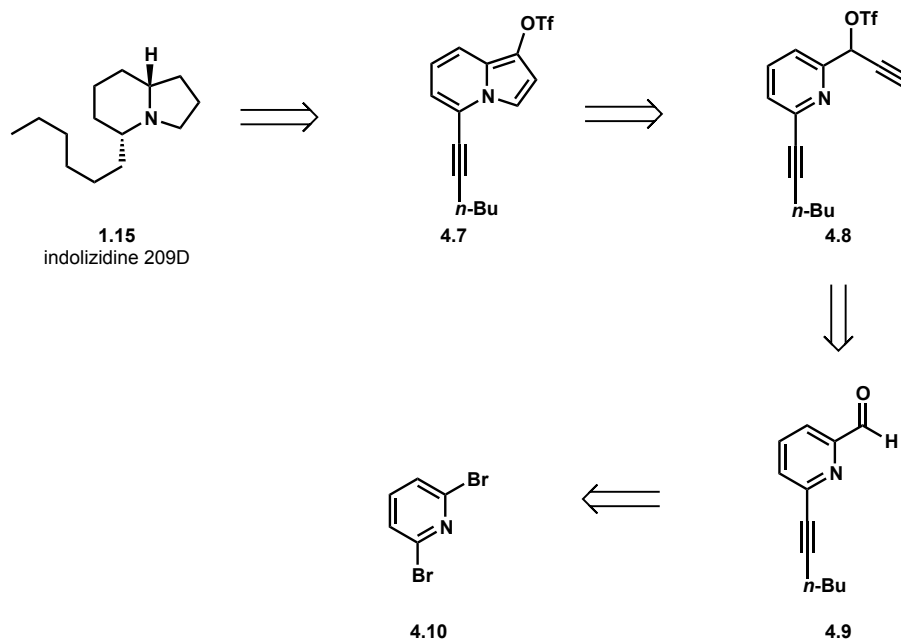
**Scheme 4.2.1.** First-generation synthesis of indolizidine 209D.



According to the route outlined in Scheme 4.2.1, we were able to access indolizidine 209D in five synthetic steps; however, this first-generation synthesis had several weaknesses. The installation of the hexyl chain in the first step provided an unacceptably low yield of **4.4**. Additionally, the purification of the tertiary amine natural product from the mixture of products obtained in the hydrogenation step was challenging and prohibited us from obtaining pure **1.15**. In an effort to remedy these shortcomings, we devised a second-generation approach toward indolizidine 209D.



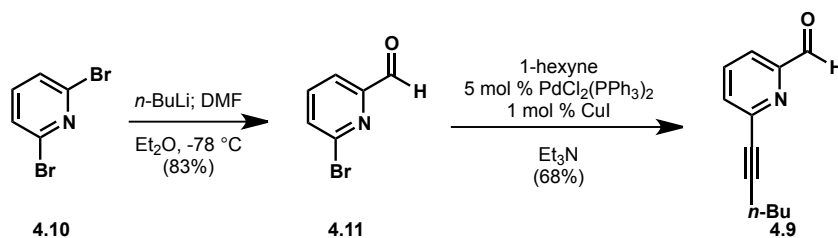
**Figure 4.2.2.** Revised retrosynthesis for indolizidine 209D.



In our revised approach, we envisioned indolizidine 209D arising from reduction of indolizidine **4.7** (Figure 4.2.2). It was anticipated that the hydrogenolysis of the triflate moiety in indolizidine **4.7** would be more facile than hydrogenolysis of the acetoxy group in the first-generation synthesis. Access to indolizidine **4.7** was planned via cyclization of pyridine **4.8**. In turn, **4.8** could be built from aldehyde **4.9**, which would ultimately arise from 2,6-dibromopyridine (**4.10**) via formylation and subsequent Sonogashira coupling.

To date, we have developed a high-yielding route to aldehyde **4.9** (Scheme 4.2.2). From 2,6-dibromopyridine (**4.10**), lithium-halogen exchange at  $-78\text{ }^{\circ}\text{C}$  followed by addition of the 2-lithiopyridine intermediate to DMF provides an excellent yield of aldehyde **4.11**. Next, the six-carbon chain was installed via Sonogashira coupling with 1-hexyne under standard conditions to deliver **4.9**. The nearly quantitative Sonogashira method is superior to the Chichibabin-type approach in introducing the six-carbon chain present in the natural product.

**Scheme 4.2.2.** Second generation synthesis of indolizidine 209D.



Efforts to convert aldehyde **4.9** to indolizidine 209D according to the synthetic plan outlined in Scheme 4.2.2 are on going. Once a high-yielding five-step synthesis of indolizidine 209D has been accomplished, the route will be applied to the synthesis of related natural and non-natural indolizidine alkaloids.

### 4.3 Securinine

#### *Isolation, Biological Activity and Structure*

Securinine (**1.26**) is an indolizidine alkaloid that was first isolated from the leaves of *Securinega suffruticosa* in 1956 by Muraveva and Bankovskii.<sup>6</sup> They took special note of securinine because it demonstrated strychnine-like activity in their assays. The biological activity of this molecule continued to be investigated over the next several decades, which established a range of physiological responses to securinine in tissue samples as well as in small mammals. Early studies indicated that securinine was a powerful central nervous system stimulant for cats (0.1-0.2 mg/kg) and at higher doses (5-30 mg/kg) was shown to induce convulsions.<sup>7</sup> Further investigations probed the mechanism of biological action of securinine and related securinega alkaloids. Although strychnine is known to be a potent glycine receptor antagonist, work by Enna and coworkers suggested that securinine is instead a  $\gamma$ -aminobutyric acid (GABA) receptor antagonist.<sup>8</sup> These findings have been supported by others and have led to the use of securinine and related alkaloids to assess the pharmacological properties of GABA receptors.<sup>9</sup>

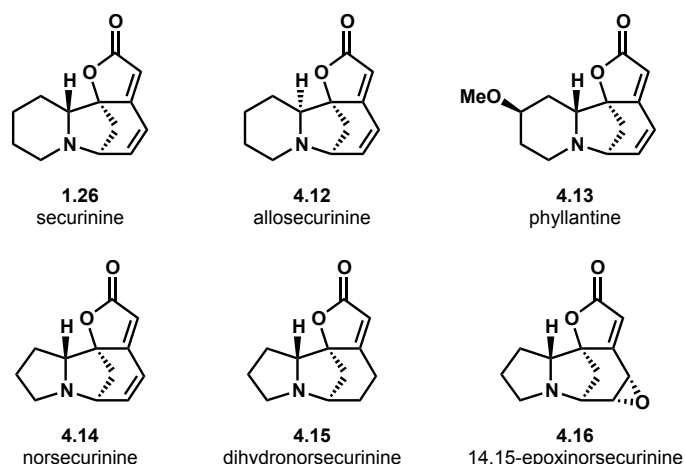
In addition to its use for the study of GABA receptors, securinine has been implicated in the treatment of a variety of diseases. Securinine can selectively induce apoptosis in human leukemia HL-60 cells in a time and concentration dependent manner, validating this alkaloid as a potential cancer drug.<sup>10</sup> Xu and Zhang conducted preliminary research that highlights securinine as a potential therapy for Alzheimer's disease.<sup>11</sup> Their 2004 study examined the effect of securinine on the cognitive deficit experienced by rats after being injected with  $\beta$ -amyloid protein. After being dosed with  $\beta$ -amyloid protein, the rats displayed signs of impaired memory, which were reversed by subsequent treatment with securinine.

Investigation of the biological activity of securinine had been underway for seven years before the structure of this alkaloid was ultimately established. Muraveva and Bankovskii initially reported that securinine was a basic tertiary amine of the molecular formula  $C_{13}H_{15}NO_2$ , and that securinine contained a lactone moiety in conjugation with an unsaturated system.<sup>6</sup> Saito and Horii first reported the structure of securinine in 1963.<sup>12</sup> Coupling the information from the  $^1H$  NMR, infrared, and ultraviolet spectra of securinine with degradation studies, they proposed the correct structure of securinine, which has been confirmed through synthetic efforts over the last fifty years. Shortly after the relative structure of securinine was reported, Saito and Horii established the absolute configuration of this alkaloid.<sup>13,14</sup>

Securinine was the most abundant of the alkaloids isolated from *Securinega suffruticosa*, and was isolated along with several structurally related molecules, which are collectively known as the *Securinega* alkaloids. The [3.2.1]azabicyclo core as well as a fused five-membered lactone is conserved throughout this family of natural products. The two major distinctions between *Securinega* alkaloids are (1) the size of the *N*-fused ring and (2)

the stereochemistry at the ring-fusion. These differences are illustrated by securinine (**1.26**) and norsecurinine (**4.14**), which possess six- and five-membered A rings, respectively (Figure 4.3.1). Securinine is also closely related to allosecurinine (**4.12**), which differs only in the stereochemistry of the hydrogen atom at the 6,5-ring fusion. Other members of this family have additional functionalization such as phyllantine (**4.13**) and 14,15-epoxinorsecurinine (**4.16**).

**Figure 4.3.1.** *Securinega* alkaloids.

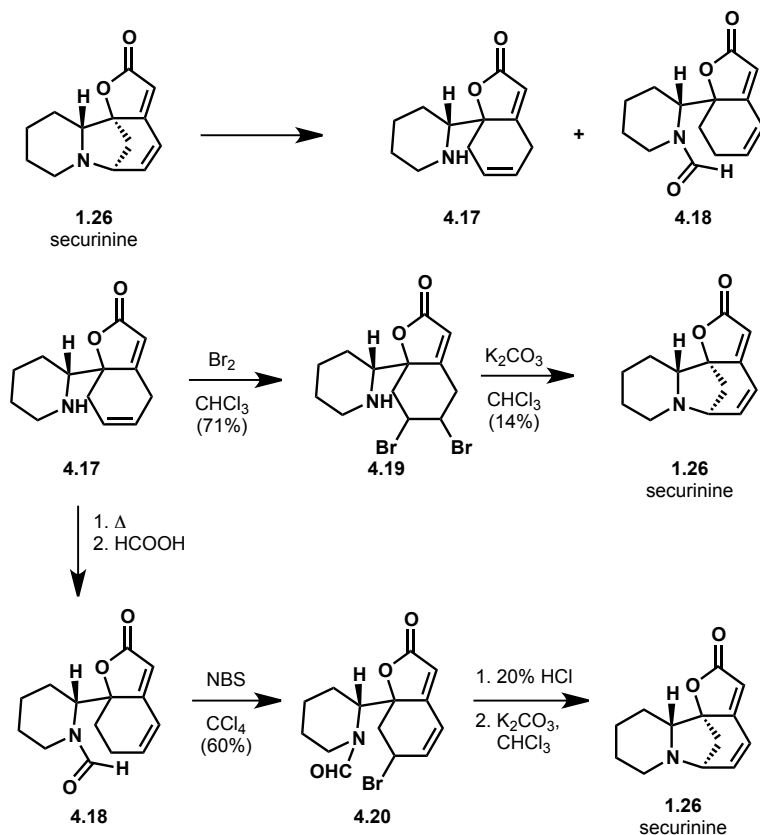


### Previous Synthetic Work

The biological activity and interesting tetracyclic skeleton of the *Securinega* alkaloids have attracted the attention of the synthetic chemistry community, leading to several approaches toward these molecules. Securinine, specifically, has been built through partial syntheses thrice and has served as the target of six total synthetic efforts and one formal synthesis to date. With the exception of the two most recent approaches to securinine, all of the successful synthetic strategies have constructed the [3.2.1]azabicycle in the final step via formation of the N-C7 bond.

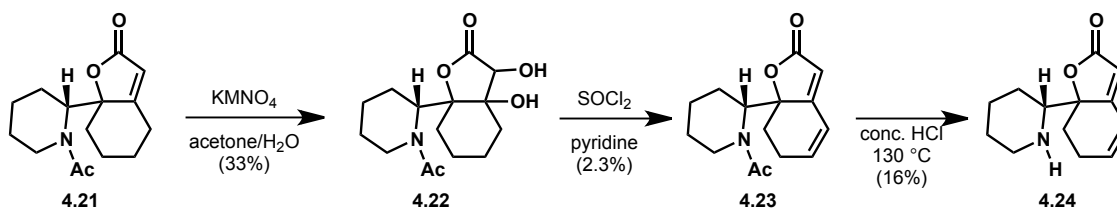
Saito and Horii reported several partial syntheses of securinine by reconstituting the natural product from its degradation products. They recognized that the N-C7 bond of securinine was readily cleaved under a variety of conditions to yield 6,5-fused bicycles possessing an appended piperidine ring (e.g., **4.17** and **4.18**, Scheme 4.3.1, and **4.21**, Scheme 4.3.2). Working from these degradation products, Saito and Horii established a protocol for constructing the [3.2.1]azabicycle that was adopted by the majority of groups that have since taken on the total synthesis of securinine (Scheme 4.3.1).<sup>15</sup> Their first reported partial synthesis commenced with the bromination of **4.17** in chloroform to provide dibromide **4.19** in 71% yield. Dibromide **4.19** was next transformed to securinine by a base promoted cyclization/elimination cascade. In a similar approach, degradation product **4.17** could be converted to **4.18**, itself also a degradation product, by heating in formic acid. Bromination of **4.18** with *N*-bromosuccinimide gave allylic bromide **4.20**, which could be treated with acid to unveil the secondary amine. Finally, exposure of the amine to potassium carbonate effected the cyclization to the natural product.<sup>15</sup>

**Scheme 4.3.1.** Saito and Horii's first and second partial syntheses.



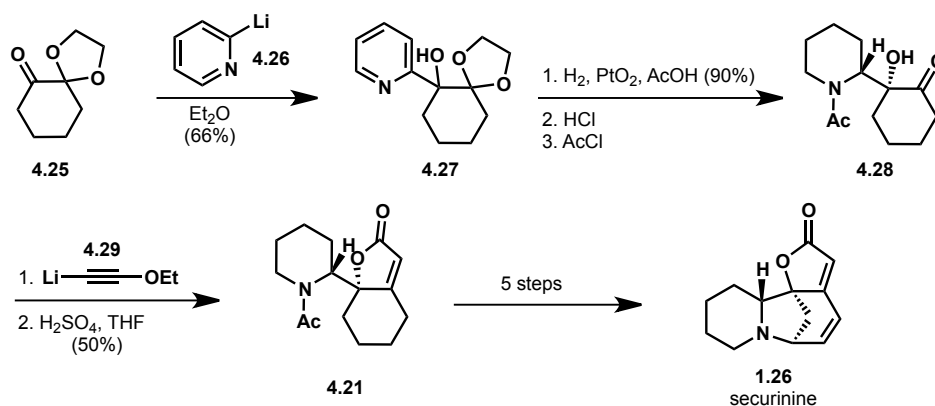
Three years later (1966), Saito and Horii reported a third partial synthesis of securinine from a degradation product lacking a unit of unsaturation in the six-membered ring.<sup>16</sup> From lactone **4.21**, treatment with potassium permanganate in aqueous acetone for three days gave diol **4.22** (Scheme 4.3.2). The conjugated  $\pi$ -system in the natural product could be directly installed via dehydration with thionyl chloride to provide small amounts of **4.23**. Next, the acetate was removed to yield secondary amine **4.24**, which was elaborated to the natural product via the bromination/cyclization sequence outlined in Scheme 4.3.1.

**Scheme 4.3.2.** Saito and Horii's third partial synthesis.



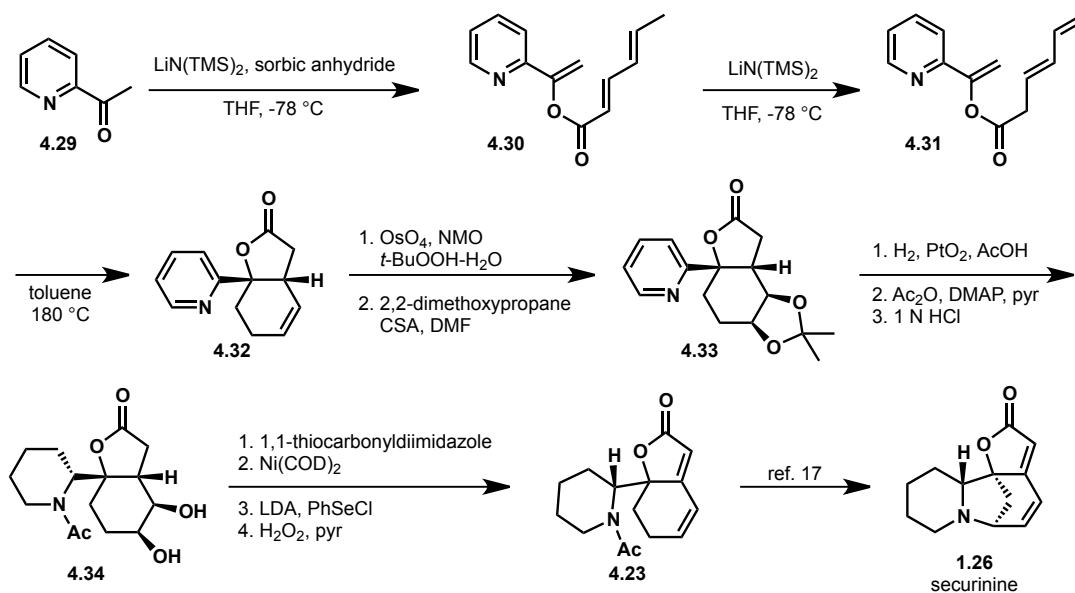
Armed with the knowledge gained from their partial syntheses, Saito and Horii completed the first total synthesis of securinine in 1967.<sup>17</sup> From 1,4-dioxaspiro[4,5]decan-6-one (**4.25**), the piperidine ring was introduced in the form of a pyridine via addition of 2-lithiopyridine (**4.26**) in ether to provide alcohol **4.27** (Scheme 4.3.3). Next, the pyridine ring was hydrogenated to the corresponding piperidine to give a diastereomeric mixture of products. The ketal moiety was removed to unveil the ketone and the piperidine nitrogen was then acetylated to yield  $\alpha$ -ketol **4.28**. The butenolide present in the natural product was constructed by addition of lithium ethoxyacetylide (**4.29**) to the ketone, followed by rearrangement of the propargylic alcohol product in acid to form butenolide **4.21**. From butenolide **4.21**, the total synthesis was completed in five steps as previously developed in the context of a partial synthesis (Scheme 4.3.2).

**Scheme 4.3.3.** The first total synthesis of securinine.



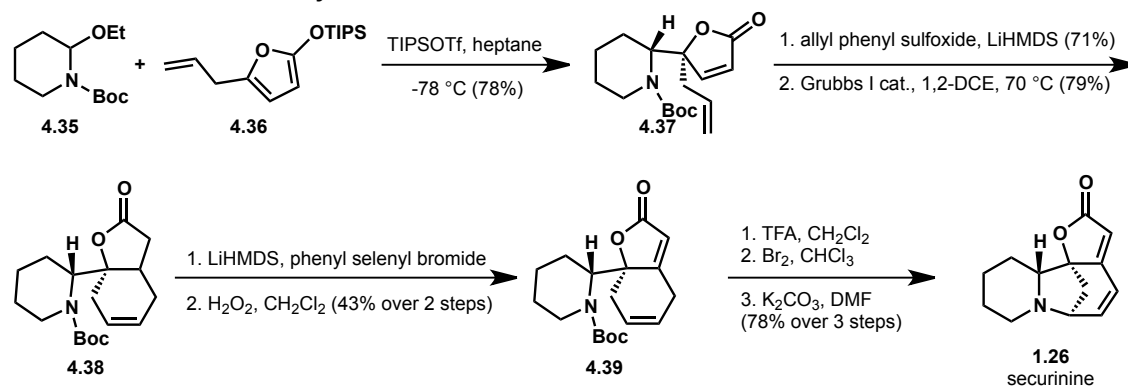
The second total synthesis of securinine was not reported until 2000, when Honda disclosed an intramolecular Diels-Alder strategy for the construction of the 6,5-fused lactone-containing bicycle.<sup>18,19</sup> Honda was able to build the Diels-Alder substrate in two steps from 2-acetylpyridine **4.29** (see **4.29** to **4.31**, Scheme 4.3.4). From ester **4.31** the [4+2] cycloaddition proceeded at 180 °C in toluene to provide *exo* product **4.32** in 70% yield, which was accompanied by a minor diastereomeric product in 8% yield. Before reducing the pyridine moiety to the corresponding piperidine, the double bond in the six-membered ring was dihydroxylated and protected as the acetonide (**4.33**). With the double bond now suitably masked, the pyridine was reduced using platinum(IV) oxide as a catalyst. The reduction was followed by a nitrogen protection and a deprotection of the diol to give **4.34**. To reach a common intermediate utilized in Saito and Horii's route, Honda installed the unsaturation in conjugation with the lactone in four steps. The diol was transformed to the alkene in a Corey-Winter reaction via formation of the thiocarbonate followed by nickel-mediated reductive elimination, and the final double bond was introduced by  $\alpha$ -selenation of the lactone and subsequent oxidative elimination to provide **4.23**. The  $\alpha,\beta,\gamma,\delta$ -unsaturated lactone was converted to securinine using the same conditions developed by Saito and Horii.<sup>17</sup>

**Scheme 4.3.4.** Honda's intramolecular Diels-Alder strategy for the total synthesis of securinine.



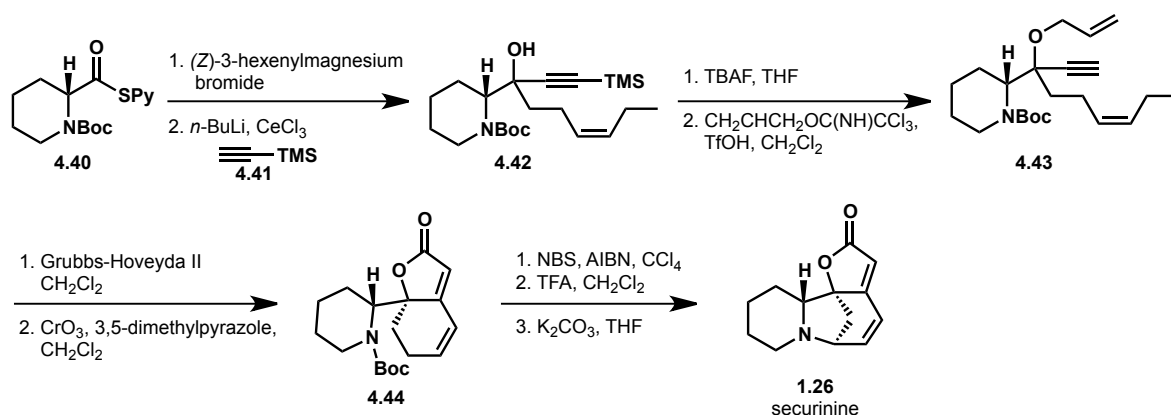
Honda's synthesis was the first in a new wave of synthetic work toward securinine, which was quickly followed by a nine-step synthesis from Lira.<sup>20</sup> The streamlined synthesis from Lira and coworkers features the addition of a silyloxyfuran (**4.36**) to an iminium ion as well as a ring-closing metathesis as key steps (Scheme 4.3.5). More specifically, treatment of **4.35** with TIPSOTf gave rise to an iminium ion, which was intercepted by silyloxyfuran **4.36** to provide adduct **4.37** in 78% yield. Next, the six-membered ring was constructed in two steps, starting with the conjugate addition of lithiated allylphenyl sulfoxide to the lactone followed by ring-closing metathesis with Grubbs I catalyst to obtain the 6,5-fused ring system (**4.38**) in good yield. Lira and coworkers' next challenge was installation of the proper unsaturation pattern. To this end,  $\alpha$ -selenation of the lactone followed by oxidative elimination provided butenolide **4.39**. Removal of the Boc group and subsequent bromination gave dibromide **4.19** (see Scheme 4.3.1). This dibromide (**4.19**) was converted to the natural product as previously established by Saito and Horii.

**Scheme 4.3.5.** Liras total synthesis of securinine.



Honda devised a second approach to securinine starting from the chiral pool, thus achieving the first asymmetric synthesis of this alkaloid.<sup>21</sup> From (+)-pipercolinic acid derivative **4.40**, Grignard addition to the thioester and subsequent cerium acetylide addition to the resulting ketone gave propargylic alcohol **4.42**. Next, removal of the trimethylsilyl group from the alkyne and allylation of the tertiary hydroxyl group provided the metathesis cascade substrate **4.43**. Dienyne **4.43** smoothly underwent ring-closing metathesis mediated by the Grubbs-Hoveyda II catalyst to form the 6,5-fused ring system. The intermediate dihydrofuran was converted to the butenolide **4.44** via chromium trioxide-mediated oxidation. Elaboration of butenolide **4.44** to the natural product was conducted in a manner analogous to the original work of Saito and Horii (Scheme 4.3.1).

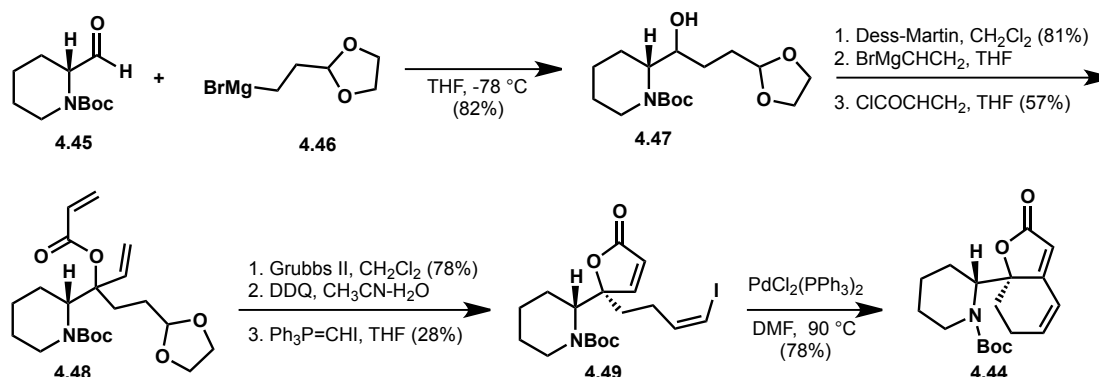
**Scheme 4.3.6.** Honda's asymmetric synthesis of securinine.



An approach toward securinine mirroring several features of the Honda metathesis route, was reported six months later by the Font group.<sup>22</sup> While Honda carried out a metathesis cascade to simultaneously constructed both rings of the 6,5-bicycle, Font employed metathesis to form the butenolide and demonstrated that the six-membered ring could be closed with a Heck reaction (Scheme 4.3.7). From (-)-pipercolinic acid, aldehyde **4.45** was obtained in three steps. Next, ester **4.48** was assembled by addition of Grignard reagent **4.46**, oxidation with Dess-Martin periodinane, a second Grignard addition and

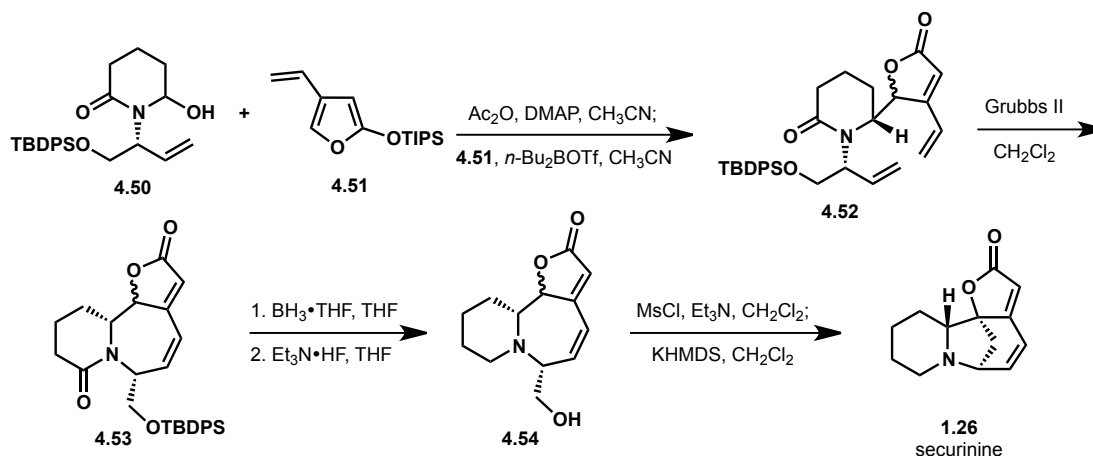
functionalization of the tertiary alcohol with acryloyl chloride. Grubbs II catalyst successfully transformed the ester **4.48** to the corresponding butenolide (**4.49**) in 78% yield. Deprotection then provided an aldehyde that was converted to vinyl iodide **4.49** via a Wittig olefination. The six-membered ring was closed using a Heck reaction to provide **4.44**, an intermediate common to Honda's synthesis in 78% yield (Scheme 4.3.6).<sup>21</sup>

**Scheme 4.3.7.** Total synthesis of securinine by Font and coworkers.



Font developed a second-generation approach to the *Securinega* alkaloids and validated this strategy through the total synthesis of securinine and norsecurinine (**4.14**) (Scheme 4.3.8).<sup>23</sup> This synthesis of securinine is a major departure from all of the previous synthetic work in that the N-C7 bond is not formed in the final step in the synthesis. Instead, Font completed securinine from 6,7,5-tricycle **4.54**. The chiral piperidine fragment **4.50**, which was constructed through a palladium-catalyzed enantioselective allylation, served as a precursor to an iminium ion that was intercepted by silyloxyfuran **4.51**, in a manner reminiscent of Lira's synthesis.<sup>20</sup> Ring-closing metathesis of **4.52** was employed to form seven-membered ring **4.53**. After reduction of the amide to the corresponding secondary amine and deprotection of the primary alcohol, an intermediate mesylate was formed. Under basic conditions, the extended enolate of the butenolide displaced the mesylate to form the one-carbon bridge of the [3.2.1]bicycle and complete the synthesis of securinine.

**Scheme 4.3.8.** Font's second-generation approach to securinine.



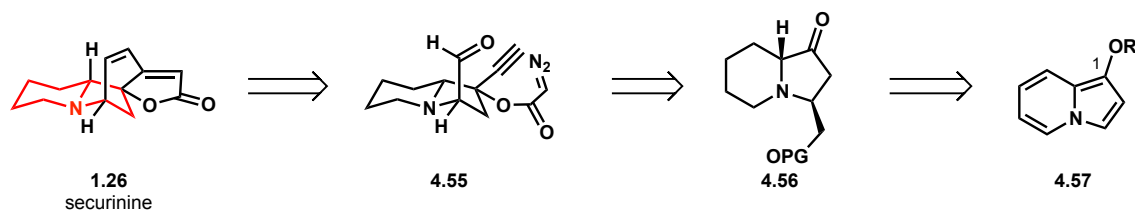


### Our Retrosynthetic Analysis

Font's synthesis of securinine demonstrated that the *Securinga* alkaloids could be assembled through a strategy that does not rely on the late-stage N-C7 bond formation tactic common to all other approaches. We also envisioned building securinine through a strategy that departs from the classic disconnections first explored by Saito and Horii. We anticipated accessing securinine in a rhodium-mediated cascade of a properly functionalized indolizidine such as **4.55** (Figure 4.3.2). The  $\alpha$ -diazoketone **4.55** could be prepared by elaboration of simplified indolizidine **4.56**, which could in turn arise from the reduction of an indolizine precursor such as **4.57**.

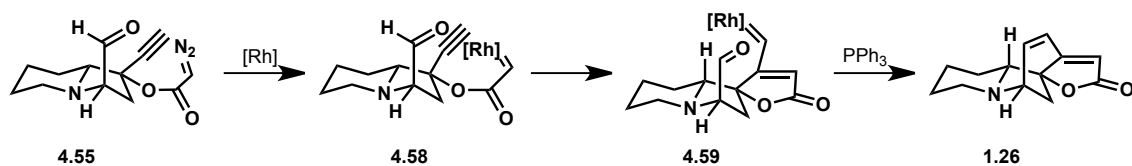
Our interest in the synthesis of securinine from indolizidine **4.57** stemmed from our desire to explore the chemistry of indolizines and their application in the synthesis of indolizidine alkaloids. Specifically, in the context of the synthesis of securinine, we anticipated that the reduction of the indolizine to the indolizidine while retaining the oxygenation at C-1 could prove to be challenging.

**Figure 4.3.2.** Strategy for building securinine from indolizine **4.57**.



Additionally, we were interested in exploring a potential cascade sequence that would assemble the C and D rings of securinine in a single step with the A and B rings already in place. We were inspired by work from Padwa on the generation of rhodium carbenoids via the rhodium-catalyzed decomposition of  $\alpha$ -diazo ketones bearing tethered alkynes (**4.55** to **4.59**, Scheme 4.3.9).<sup>24</sup> In our system, we planned to engage the rhodium-stabilized carbenoid (e.g., **4.59**) with triphenylphosphine and use the generated ylide to carry out an intramolecular Wittig olefination (see **4.59** to **1.26**), to complete the synthesis of securinine.

**Scheme 4.3.9.** Proposed rhodium-mediated cascade to form securinine.

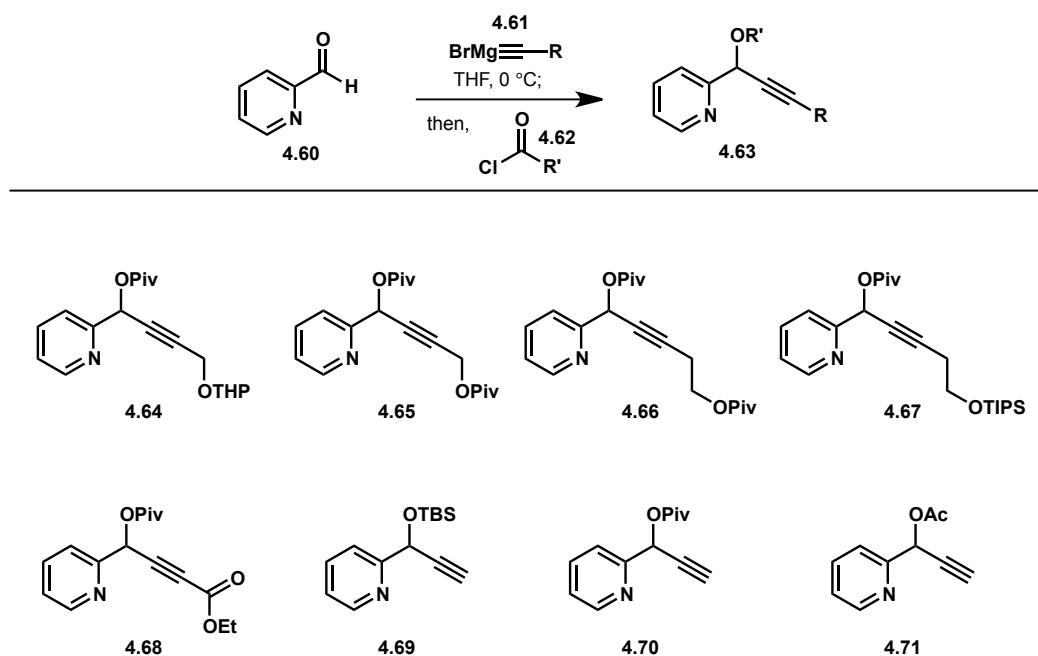


### Toward Securinine

The first objective in our synthesis was to construct a 1,3-disubstituted indolizine bearing oxygenation at the C1-position and a group at C1 that could be converted to the aldehyde moiety present in cascade substrate **4.55**. Toward this end, we synthesized a variety of cyclization substrates of which a subset is illustrated in Figure 4.3.3. Ideally, we

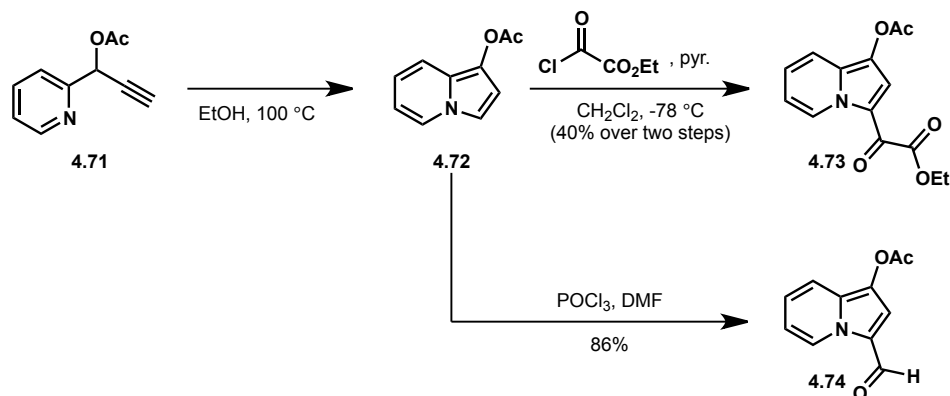
sought to build a propargylic alcohol derivative with a substituent on the alkyne that could ultimately be converted to the C3-aldehyde. First, THP-ether **4.64** was prepared from pyridine-2-carboxaldehyde in a single step and subjected to the metal-free cyclization conditions. Upon heating **4.64** in ethanol at 100 °C, we observed formation of the indolizine product accompanied by several byproducts that did not contain the THP protecting group. Next, the utility of bispivaloylate **4.65** was explored. A single indolizine product was obtained in excellent yield upon heating **4.65** in ethanol; however, the expected C3 ester group had been replaced with a molecule of the solvent to provide an ethyl ether moiety at the C3-position of the indolizine product.

**Figure 4.3.3.** Potential cyclization substrate for the synthesis of securinine.



Seeking a functional handle that could easily be converted to the C3-aldehyde, we considered placing an ester at the alkyne terminus (e.g., **4.68**) or inserting an additional methylene unit before the protected hydroxyl group (see **4.66** and **4.67**, Figure 4.3.3). Even though all three of these substrates cleanly cyclized to the corresponding indolizine upon heating in ethanol, we opted instead to focus our efforts on terminal alkyne cyclization substrates such as **4.69**, **4.70**, and **4.71**. The terminal alkyne substrates each provided a quantitative yield of the mono-substituted indolizine product. More importantly, the mono-substituted indolizines provided the opportunity to install a variety of groups at C3 in a divergent manner. For example, 1-acetoxy indolizine (**4.72**, Scheme 4.3.10) could be functionalized at the C3-position via electrophilic acylation to introduce a  $\alpha$ -ketoester at C3 (see **4.73**) or alternatively, via a standard Vilsmeier-Haack formylation protocol to deliver the desired aldehyde **4.74**.

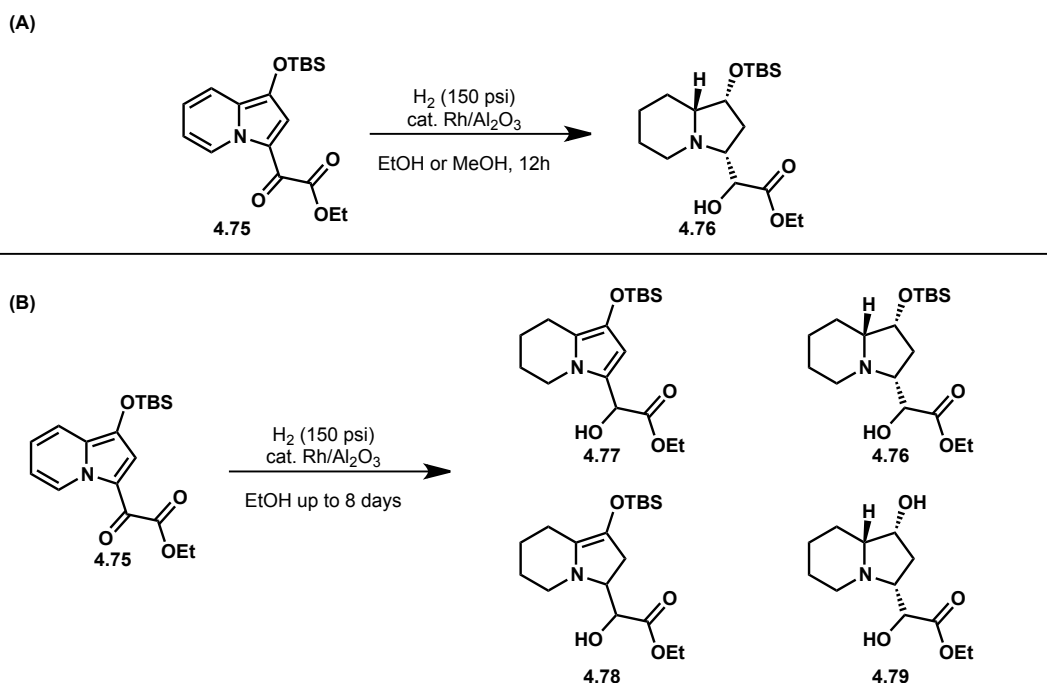
**Scheme 4.3.10.** Cyclization and functionalization to access 1,3-disubstituted indolizines



With functional handles attached to both the 1- and 3-positions, the next task was to reduce the indolizine to the fully saturated indolizidine. The complete reduction of indolizines has been accomplished by both the Gevorgyan<sup>25</sup> and Frontier<sup>26</sup> groups. The Gevorgyan example employed platinum(IV) oxide under acidic conditions to reduce an indolizine possessing only alkyl substituents. Our indolizines (**4.73** and **4.74**) proved to be extremely acid sensitive, undergoing rapid decomposition in CDCl<sub>3</sub>. Under acidic conditions, platinum(IV) oxide is known to effect hydrogenolysis of the C3-O bond of pyrroles as well as the C-O bond of vinylogous amide substrates, which further discouraged us from employing the Gevorgyan conditions. For these reasons, we initially focused on the Frontier hydrogenation conditions, which required rhodium supported on alumina as a catalyst and modest pressures of hydrogen ranging from 1-5 atm (Figure 4.3.4A). Although the Frontier work was focused on the reduction of pyrroles, they reported the diastereoselective reduction of indolizine **4.76**, a compound that nicely mapped onto our indolizines with C1-oxygenation and an electron withdrawing substituent at the 3-position. Unfortunately, attempts to reproduce the Frontier result with an identical substrate (**4.76**) resulted in the formation of pyrrole products (e.g., **4.77**) as well as decomposition products, and only trace amounts of the desired indolizidine.

More extensive efforts to obtain indolizidine **4.76** via the rhodium on alumina-catalyzed hydrogenation of indolizine **4.75** included: (1) surveying solvents, (2) varying the catalyst loading of rhodium, (3) exploring the effect of hydrogen pressures ranging from 1 atm to 1000 psi, (4) using different sources of rhodium on alumina, and (5) monitoring the reaction over extended reaction times. To summarize these attempts, only significant amounts of pyrrole **4.77** were obtained as mixtures with trace amounts of further reduced products such as **4.76**, **4.78**, and **4.79**.

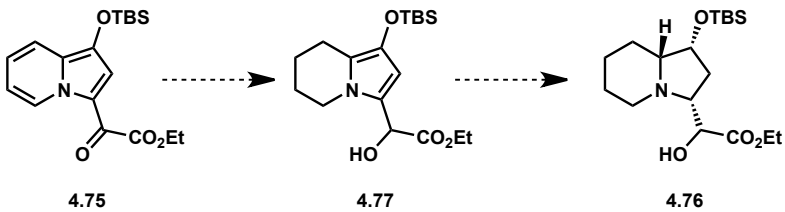
**Figure 4.3.4.** (A) Frontier's indolizine reduction; (B) Our hydrogenation attempts.



Unable to obtain significant quantities of indolizidine **4.76** using rhodium on alumina, other catalysts were explored for this transformation (Table 4.3.1). The Gevorgyan conditions, platinum(IV) oxide with HBr, led to complete decomposition of the starting material. Excluding HBr from these conditions returned only starting material, as did reactions employing either palladium or rhodium on carbon. Raney nickel under an atmosphere of hydrogen (150 psi) cleanly gave the pyrrole **4.77**. However, only rhodium on alumina led to mixtures of the pyrrole with traces of further reduced products.

Since the hydrogenation of indolizine **4.75** to indolizidine **4.76** proved to be more challenging than anticipated, we began to consider a two-step reduction to arrive at the desired indolizidine product. The reduction of indolizine **4.75** to pyrrole **4.77** could be achieved cleanly with Raney nickel, which led us to consider a variety of methods for reducing pyrroles to pyrrolidines. However, perusal of the literature highlighted some challenges associated with the reduction of 3-hydroxypyrroles.<sup>27</sup> 3-Hydroxypyrroles (**4.82**) are tautomeric with their vinylogous amide form (**4.83**); thus, hydride reduction can be thought of as 1,2-addition to the vinylogous amide followed by elimination of water to give the deoxygenated pyrrole (**4.84**) (Figure 4.3.5). This precedent discouraged us from employing a hydride reduction strategy. There are a small number of hydrogenation conditions known for the reduction of 3-hydroxypyrroles, which were not fruitful in our hands (see Table 4.3.1). The other known method for the reduction of 3-hydroxypyrroles, the Birch reduction, requires an electron-withdrawing substituent on the pyrrole ring and therefore necessitated a redesign of our substrate.

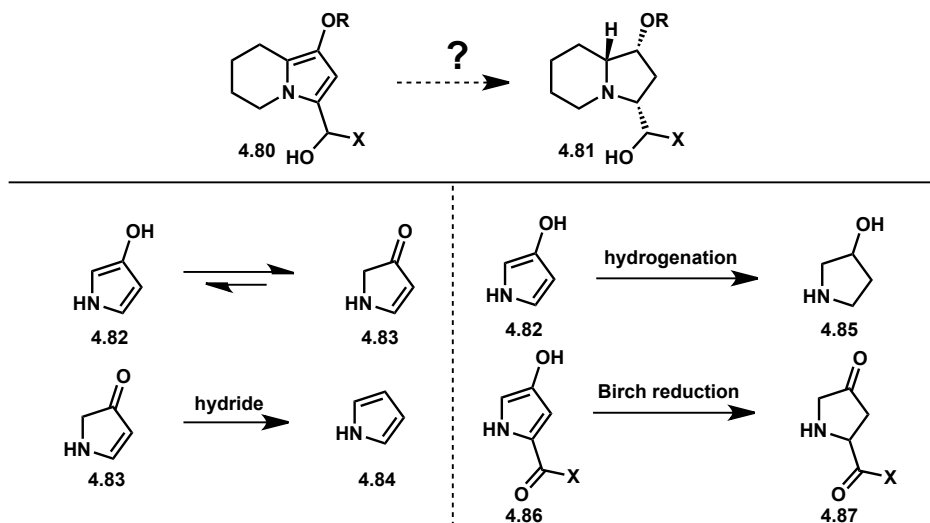
**Table 4.3.1.** A summary of various hydrogenation attempts.



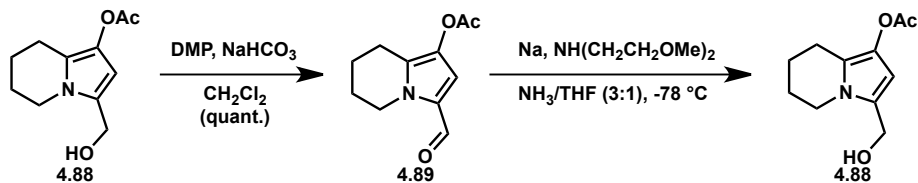
| Conditions  | Result                      |
|---|-----------------------------|
| PtO <sub>2</sub> , HBr, MeOH, H <sub>2</sub>                                    | decomposition               |
| PtO <sub>2</sub> , H <sub>2</sub> , MeOH or EtOH                                | 4.75                        |
| Pd/C, H <sub>2</sub> , EtOH or MeOH   | 4.75                        |
| Rh/C, H <sub>2</sub> (150 psi), EtOH  | 4.75                        |
| Rh/Al <sub>2</sub> O <sub>3</sub> , H <sub>2</sub> (150-1000 psi), EtOH, 8 days | 4.77 + 4.76 (ratio varies)  |
| Rh/Al <sub>2</sub> O <sub>3</sub> , H <sub>2</sub> (150 psi), MeOH, 12 h        | 4.77 + 4.76 + decomposition |
| Raney Ni, H <sub>2</sub> (150-1000 psi) EtOH, 12 h                              | 4.77                        |

To access a suitable substrate for the Birch reduction, indolizine **4.74** was reduced to pyrrole **4.88** with Raney nickel, which was followed by oxidation to the corresponding aldehyde (**4.89**) with Dess-Martin periodinane (Scheme 4.3.11). Donahoe's conditions for pyrrole reduction were employed,<sup>28</sup> but only resulted in the reduction of the aldehyde to return primary alcohol **4.88**, leaving the pyrrole moiety untouched.

**Figure 4.3.5.** Methods for the reduction of 3-hydroxypyrroles.



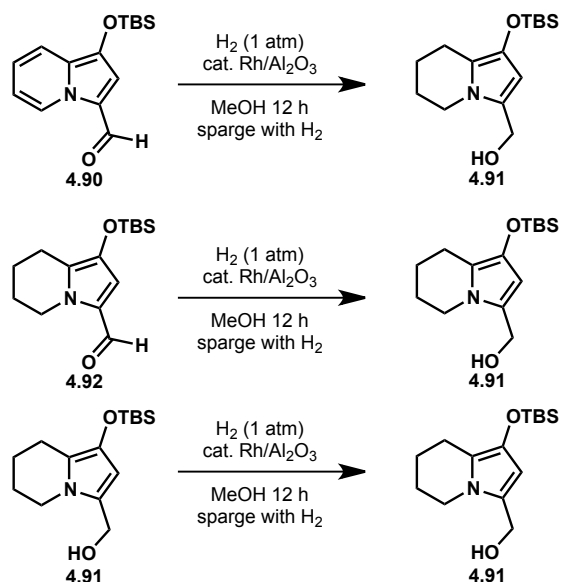
**Scheme 4.3.11.** Attempted Birch reduction of pyrrole **4.89**.



With limited success using catalysts other than rhodium on alumina for the hydrogenation or alternative strategies for pyrrole reduction, we contacted Prof. Frontier seeking insight on any experimental details that could be important to the success of this hydrogenation. Prof. Frontier promptly responded with a submitted *Organic Synthesis* manuscript. This manuscript described experimental details not included in the initial communication, including specific instructions to sparge the reaction mixture with hydrogen for 30 minutes. Performing the sparge with our indolizine **4.75** led to a 73% yield of the desired indolizidine product (**4.76**). Although it was initially surprising that sparging with hydrogen could have such a dramatic effect on the outcome of the reaction, we hypothesize that sparging removes other gases from the reaction mixture, which could acidify the reaction medium over the course of the reaction (e.g., carbon dioxide could be converted to carbonic acid), leading to decomposition of the starting material as well as intermediates.

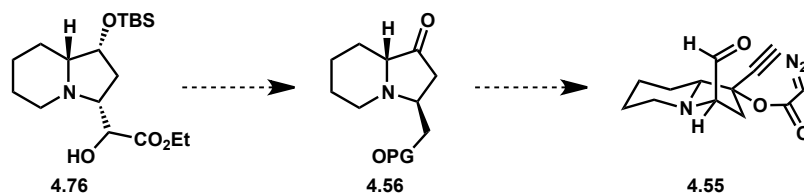
Unfortunately, subjecting other indolizine substrates to the optimized hydrogenation conditions led exclusively to pyrrole products (Scheme 4.3.12). The only difference between the indolizine that can be completely reduced to the indolizidine (i.e., **4.75**) and those that stop at the pyrrole oxidation level is the lack of an  $\alpha$ -keto ester group at C3. Under the hydrogenation conditions, the  $\alpha$ -keto ester of **4.75** is reduced to the  $\alpha$ -hydroxy ester before the pyrrole is reduced, implying that the strictly electron withdrawing nature of the  $\alpha$ -keto ester substituent does not account for the positive effect of this group on the hydrogenation. Furthermore, a methylene hydroxy group at C3 is not sufficient for hydrogenation (e.g., **4.91**).

**Scheme 4.3.12.** Scope of rhodium hydrogenation.



With access to indolizidine **4.76**, the next goal of the synthesis was conversion of **4.76** to the substrate for the rhodium-mediated cascade to form securinine (Scheme 4.3.13). We anticipated accessing  $\alpha$ -diazo ester **4.55** from a ketone such as **4.56**. To arrive at ketone **4.56** from indolizidine **4.76**, it was necessary to (1) remove the silyl protecting group, and oxidize this secondary hydroxyl group to a carbonyl and (2) cleave the C-C bond between the ester and the  $\alpha$ -hydroxy group. We first set out to tackle the latter task.

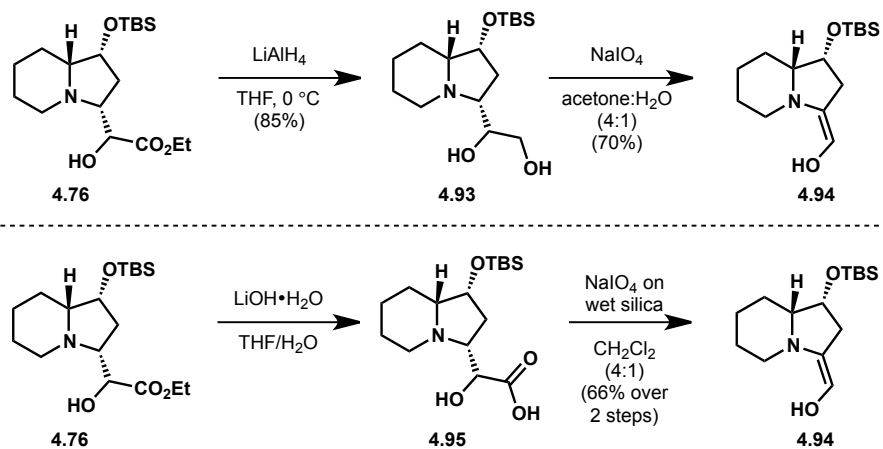
**Scheme 4.3.13.** Next steps toward cascade substrate **4.55**.



The carbon-carbon bond cleavage could be accomplished through a number of two-step protocols. The two highest yielding routes are illustrated in Scheme 4.3.14. First the  $\alpha$ -hydroxy ester can be reduced to the diol (**4.93**), and in a second step, the 1,2-diol can be cleaved to provide the desired product. The oxidative carbon-carbon bond cleavage can be carried out with either lead tetraacetate or sodium periodate; however, the latter results in cleaner formation of product. Although the product of the C-C bond cleavage reaction possessed the mass of the desired product, the  $^1H$  NMR spectrum did not contain a diagnostic aldehyde peak. Further analysis of a series of NMR spectra revealed that the product preferred the enol tautomer (**4.94**) in a number of NMR solvents. We hypothesize that a hydrogen bonding interaction between the  $-OH$  enol proton and the tertiary nitrogen

could favor this tautomeric form. Enol **4.94** can also be obtained by saponification of ester **4.76**, followed by oxidative C-C bond cleavage by sodium periodate on wet silica gel.

**Scheme 4.3.14.** Carbon-carbon bond cleavage.

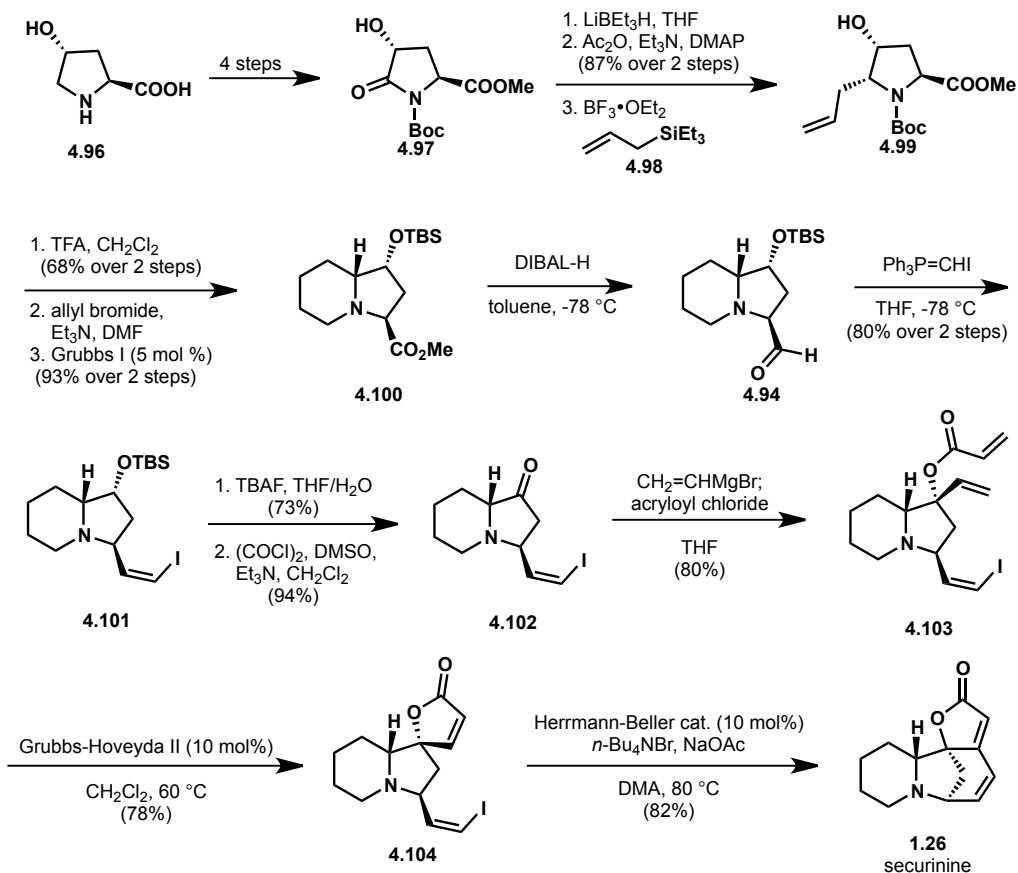


With enol **4.94** in hand, we were poised to press forward toward securinine. However, at this time, a synthesis of securinine was reported by Thadani and coworkers with several features that commanded our attention (Scheme 4.3.15).<sup>29</sup> Thadani's synthesis focused on constructing securinine from an indolizidine. Further, their synthesis built indolizidine **4.94** in 11 steps and carried this intermediate forward to the natural product using a ring-closing metathesis and subsequent Heck reaction to arrive at the natural product, in a manner analogous to Font's first synthesis.<sup>22</sup>

Our enol **4.94** intersects with Thadani's synthesis, providing a proof of concept that our indolizines can serve as useful building blocks in the synthesis of natural products. Although Thadani depicts **4.94** as an aldehyde, they describe this intermediate as unstable and immediately subject the compound to olefination conditions. In our hands, **4.94** persists as a stable compound; however, its physical data suggest the predominance of the enol form. In the context of securinine, the racemic synthesis of enol **4.94** was accomplished in five steps from commercially available materials to meet Thadani's synthesis at the eleventh step and complete a formal synthesis of securinine (**1.26**).



### Scheme 4.3.15. Thadani's total synthesis of securinine.



### 4.4 Conclusions and Future Directions

We have demonstrated the potential of indolizines in the synthesis of natural products through the total synthesis of indolizidine 209D as well as the eleven-step formal synthesis of securinine. Our ability to rapidly access highly functionalized indolizines via our metal-free cyclization represents a promising approach to the synthesis of naturally occurring indolizidine alkaloids and their derivatives.

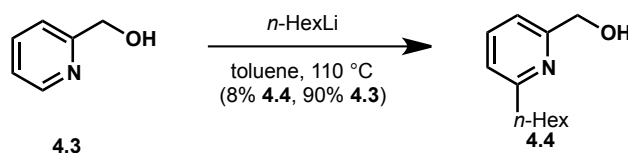
Future work toward type I indolizidine alkaloids will focus on (1) an improved route to indolizidine 209D, (2) the execution of a total synthesis of securinine via the proposed rhodium-cascade, and (3) the synthesis and biological testing of derivatives of these indolizidine natural products.

### 4.5 Experimental Contributions

Alison Hardin Narayan carried out the research detailed in Chapter 4.

## 4.6 Experimental Methods

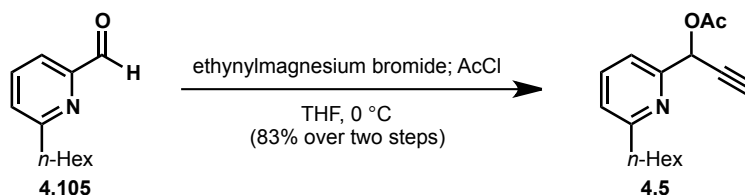
Unless otherwise stated, reactions were performed in flame-dried glassware fitted with rubber septa under a nitrogen atmosphere and were stirred with Teflon-coated magnetic stirring bars. Liquid reagents and solvents were transferred via syringe using standard Schlenk techniques. Tetrahydrofuran (THF), diethyl ether, benzene, toluene, and triethylamine were dried over alumina under a nitrogen atmosphere in a GlassContour solvent system. Dichloromethane (DCM) was distilled over calcium hydride. All other solvents and reagents were used as received unless otherwise noted. Reaction temperatures above 23 °C refer to oil or sand bath temperatures, which were controlled by an OptiCHEM temperature modulator. Thin layer chromatography was performed using SiliCycle silica gel 60 F-254 precoated plates (0.25 mm) and visualized by UV irradiation and anisaldehyde or potassium permanganate stain. SiliCycle Silica-P silica gel (particle size 40-63  $\mu\text{m}$ ) was used for flash chromatography.  $^1\text{H}$  and  $^{13}\text{C}$  NMR spectra were recorded on Bruker AVB-400, DRX-500, AV-500 and AV-600 MHz spectrometers with  $^{13}\text{C}$  operating frequencies of 100, 125, 125, and 150 MHz, respectively. Chemical shifts ( $\delta$ ) are reported in ppm relative to the residual solvent signal ( $\text{CDCl}_3$ ;  $\delta = 7.26$  for  $^1\text{H}$  NMR and  $\delta = 77.0$  for  $^{13}\text{C}$  NMR;  $\text{C}_6\text{D}_6$ ;  $\delta = 7.15$  for  $^1\text{H}$  NMR and  $\delta = 128.39$  for  $^{13}\text{C}$  NMR). Data for  $^1\text{H}$  NMR spectra are reported as follows: chemical shift (multiplicity, coupling constants, number of hydrogens). Abbreviations are as follows: s (singlet), d (doublet), t (triplet), dd (doublet of doublets), m (multiplet), br (broad). IR spectra were recorded on a Nicolet MAGNA-IR 850 spectrometer and are reported in frequency of absorption ( $\text{cm}^{-1}$ ). Only selected IR absorbencies are reported. High resolution mass spectral data were obtained from the Mass Spectral Facility at the University of California, Berkeley.



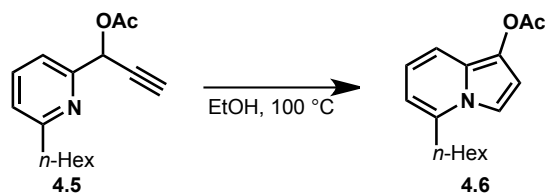
**Pyridine 4.4:** *n*-Hexyllithium (2.05 mmol in 2.49 mL *n*-hexanes) was added dropwise over 10 min to 2-pyridinethanol (4.3) (289  $\mu\text{L}$ , 3.00 mmol). Over the course of the addition, the color of the solution changed from clear green to clear colorless and then deep red. The reaction mixture was sealed in a Schleck flask and heated to 110 °C. After 12 h, the reaction mixture was cooled to room temperature. Methanol (5.00 mL) was added slowly followed by saturated aq.  $\text{NH}_4\text{Cl}$  solution (15.0 mL). The aqueous layer was extracted with EtOAc (3 x 15 mL). The combined organic layers were washed with brine, dried over  $\text{MgSO}_4$  and concentrated under reduced pressure. The crude brown oil obtained was purified via flash chromatography (gradient of 4:1 hexanes/EtOAc to 1:1 hexanes/EtOAc) to afford 4.4 in 8% yield (46.4 mg, 0.240 mmol).  $^1\text{H}$  NMR (600 MHz,  $\text{CDCl}_3$ )  $\delta$  7.56 (t,  $J = 7.6$  Hz, 1H), 7.02 (dd,  $J = 7.2, 3.8$  Hz, 2H), 4.71 (s, 2H), 4.40 (br, 1H), 2.76 (t,  $J = 7.8$  Hz, 2H), 1.69 (dd,  $J = 15.1, 7.6$  Hz, 2H), 1.44 – 1.17 (m, 6H), 0.87 (t,  $J = 6.1$  Hz, 3H);  $^{13}\text{C}$  NMR (151 MHz,  $\text{CDCl}_3$ )  $\delta$  161.4, 158.0, 136.8, 121.1, 117.5, 63.8, 38.0, 31.6, 29.6, 29.0, 22.5, 14.0; IR (film)  $\nu_{\text{max}}$  3250, 2927, 2801, 1459  $\text{cm}^{-1}$ .



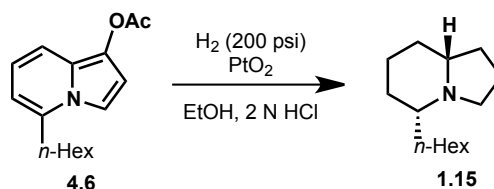
**Aldehyde 4.105:** Oxalyl chloride (32.0  $\mu\text{L}$ , 0.372 mmol) was added dropwise to DMSO (53.0  $\mu\text{L}$ , 0.744 mmol) in 1.30 mL  $\text{CH}_2\text{Cl}_2$  at  $-78\text{ }^\circ\text{C}$ . The reaction mixture was stirred at this temperature for 15 min, then, alcohol **4.4** (36.0 mg, 0.186 mmol) in 500  $\mu\text{L}$   $\text{CH}_2\text{Cl}_2$  was added dropwise. The reaction mixture was stirred at  $-78\text{ }^\circ\text{C}$  for 30 min, then  $\text{Et}_3\text{N}$  (207  $\mu\text{L}$ , 1.49 mmol) was added dropwise. The reaction mixture was stirred for 3 h as the cold bath was allowed to gradually expire. The reaction mixture was poured onto 20 mL water. The aqueous layer was extracted with  $\text{CH}_2\text{Cl}_2$  (3 x 10 mL). The combined organic layer was washed with brine (15 mL), dried over  $\text{MgSO}_4$ , and concentrated under reduced pressure. The crude brown oil was taken on without further purification.  $^1\text{H NMR}$  (500 MHz,  $\text{CDCl}_3$ )  $\delta$  10.02 (s, 1H), 7.76 – 7.71 (m, 2H), 7.37 – 7.33 (m, 1H), 3.08 (q,  $J = 7.3$  Hz, 2H), 2.87 – 2.82 (m, 2H), 1.72 (dd,  $J = 15.4, 7.7$  Hz, 2H), 1.37 (t,  $J = 7.3$  Hz, 6H), 0.84 (t,  $J = 6.9$  Hz, 3H);  $^{13}\text{C NMR}$  (126 MHz,  $\text{CDCl}_3$ )  $\delta$  193.8, 163.3, 152.2, 137.0, 127.0, 119.0, 38.0, 31.5, 29.6, 28.9, 22.4, 13.9.



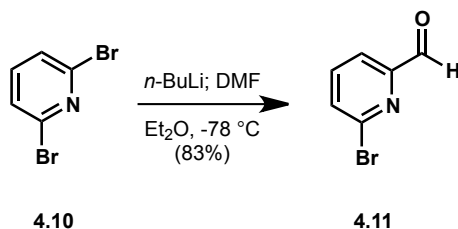
**Propargylic ester 4.5:** Ethynylmagnesium bromide (304  $\mu\text{L}$ , 0.152 mmol, 0.5 M in hexanes) was added dropwise to aldehyde **4.105** (22.4 mg, 0.117 mmol) in 1.0 mL THF at  $0\text{ }^\circ\text{C}$ . The reaction mixture was stirred at this temperature for 30 min, then acetyl chloride (12.0  $\mu\text{L}$ , 0.176 mmol) was added dropwise. After being stirred for an additional 25 min, the reaction was quenched with a saturated aq.  $\text{NH}_4\text{Cl}$  solution (1.0 mL). The aqueous layer was extracted with  $\text{EtOAc}$  (3 x 1.0 mL). The combined organic layer was washed with brine, dried over  $\text{MgSO}_4$ , and concentrated under reduced pressure to provide **4.5** as a brown oil in 83% yield over two steps (40.0 mg, 0.154 mmol).  $^1\text{H NMR}$  (500 MHz,  $\text{CDCl}_3$ )  $\delta$  7.65 (t,  $J = 7.7$  Hz, 1H), 7.41 (d,  $J = 7.6$  Hz, 1H), 7.14 (d,  $J = 7.6$  Hz, 1H), 6.43 (s, 1H), 2.84 – 2.77 (m, 2H), 2.64 (s, 1H), 2.15 (s, 3H), 2.10 (d,  $J = 5.5$  Hz, 2H), 1.74 – 1.66 (m, 2H), 1.30 (dd,  $J = 7.2, 3.4$  Hz, 4H), 0.88 (dd,  $J = 9.6, 4.4$  Hz, 3H).



**Indolizine 4.6:** A solution of **4.5** (20.0 mg, 0.0771 mmol) in EtOH (500  $\mu$ L) was sparged with  $N_2$  for 3 min. The solution was then heated to 100  $^\circ$ C in a 4 mL vial equipped with a green Teflon-lined cap and Teflon tape. After 1.5 h, the reaction mixture was cooled to room temperature and the solvent was removed under reduced pressure to provide a quantitative yield of indolizine **4.6** (19.8 mg, .0763 mmol) as a deep green oil.  $^1H$  NMR (600 MHz,  $C_6D_6$ )  $\delta$  7.18 (d,  $J$  = 2.9 Hz, 1H), 7.10 (d,  $J$  = 9.0 Hz, 1H), 6.67 (d,  $J$  = 2.9 Hz, 1H), 6.61 (dd,  $J$  = 8.8, 6.8 Hz, 1H), 6.33 (d,  $J$  = 6.6 Hz, 1H), 2.79 (t,  $J$  = 7.6 Hz, 2H), 2.27 (s, 3H), 1.80 – 1.70 (m, 2H), 1.43 (s, 2H), 1.33 (d,  $J$  = 3.4 Hz, 4H), 0.88 (t,  $J$  = 6.7 Hz, 3H);  $^{13}C$  NMR (151 MHz,  $C_6D_6$ )  $\delta$  173.86, 140.1, 130.4, 126.8, 120.2, 116.8, 111.8, 109.6, 109.5, 35.2, 34.7, 32.6, 29.0, 26.1, 23.0, 16.8; IR (film)  $\nu_{max}$  3354, 2927, 1790, 1603, 1180  $cm^{-1}$ .

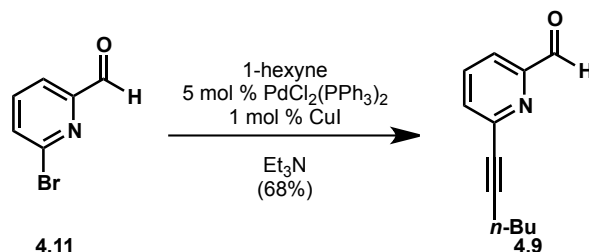


**Indolizidine 209D (1.15):** Indolizine **4.6** (1.00 mg, 0.00384 mmol) and platinum(IV) oxide (1.00 mg) were combined in EtOH (200  $\mu$ L) and 2 N  $HCl_{(aq)}$ . The reaction mixture was stirred in a Parr bomb under 200 psi  $H_2$  for 2 d. The reaction mixture was diluted with MeOH (2.0 mL), filtered through a plug of celite and concentrated. The residue was dissolved in  $CH_2Cl_2$  (1.0 mL) and washed with 1 N  $NaOH_{(aq)}$ . The organic layer was concentrated to give a mixture of indolizidine 209D (**1.15**) and other tertiary amine products.

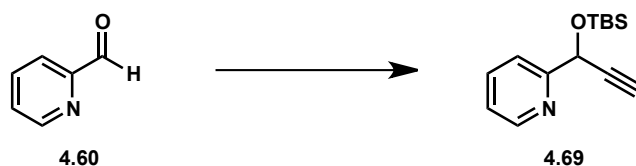


**2-Bromo-6-carboxaldehyde (4.11):** A solution of 2,6-dibromopyridine (**4.10**, 355 mg, 1.50 mmol) in 15 mL  $Et_2O$  was cooled to  $-78$   $^\circ$ C.  $n-BuLi$  (600  $\mu$ L, 1.50 mmol, 2.5 M in hexanes) was added dropwise over 5 min at  $-78$   $^\circ$ C. The reaction mixture was stirred at this temperature for 1 h. DMF (174  $\mu$ L, 2.25 mmol) was added dropwise over 3 min, and the reaction mixture was stirred for 1 h while the cold bath was allowed to gradually expire. The reaction was quenched with MeOH (1.0 mL), then a saturated  $NH_4Cl$  solution (2.0 mL) was added. The aqueous layer was extracted with  $EtOAc$  (3 x 2.0 mL). The combined

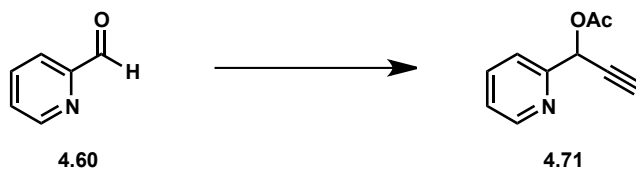
organic layer was washed with brine, dried over  $\text{MgSO}_4$  and concentrated under reduced pressure to provide aldehyde **4.11** in 83% yield (232 mg, 1.25 mmol).  $^1\text{H NMR}$  (500 MHz,  $\text{CDCl}_3$ )  $\delta$  10.01 (s, 1H), 8.38 (dd,  $J = 4.7, 1.7$  Hz, 1H), 7.93 (dd,  $J = 7.0, 1.4$  Hz, 1H), 7.78 – 7.71 (dd, 1H).



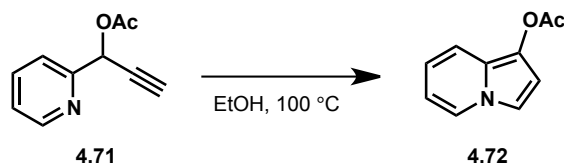
**Alkyne 4.9:** Aldehyde **4.11** (116 mg, 0.624 mmol), 1-hexyne (143  $\mu\text{L}$ , 1.25 mmol),  $\text{PdCl}_2(\text{PPh}_3)_2$  (22.0 mg, 0.0321 mmol) and copper(I) iodide (2.00 mg, 0.00624 mmol) were combined in  $\text{Et}_3\text{N}$  (3.0 mL). The mixture was sparged with  $\text{N}_2$  for 10 min. The 20 mL vial was capped and stirred for 3 d at room temperature. The reaction mixture was concentrated and diluted with water. The aqueous layer was extracted with  $\text{CH}_2\text{Cl}_2$  (3 x 2.0 mL). The combined organic layer was dried over  $\text{MgSO}_4$  and concentrated to afford alkyne **4.9** in 68% yield.



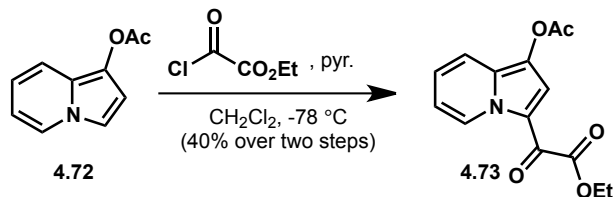
**Silyl ether 4.69:** Ethynylmagnesium bromide (35.2 mL, 17.6 mmol, 0.5 M in THF) was added dropwise to 2-pyridinecarboxaldehyde (**4.60**, 1.52 mL, 16.0 mmol) in THF (100 mL) at 0  $^\circ\text{C}$ . The reaction mixture was stirred as the cold bath gradually expired. After 1 h, the reaction was quenched with a saturate  $\text{NH}_4\text{Cl}_{(\text{aq})}$  solution (40 mL). The aqueous layer was extracted with  $\text{EtOAc}$  (3 x 30 mL). The combined organic layer was washed with brine, dried over  $\text{MgSO}_4$  and concentrated under reduced pressure. The yellow oil was dissolved in DMF (50 mL). Imidazole (4.30 g, 64.0 mmol) and *tert*-butyldimethylsilyl chloride (4.80 g, 32.0 mmol) were added to the solution, and the reaction mixture was stirred at room temperature for 12 h. The reaction mixture was diluted with  $\text{Et}_2\text{O}$  (200 mL). The organic layer was washed with water (3 x 100 mL), brine (100 mL), dried over  $\text{MgSO}_4$  and concentrated to afford **4.69** as a yellow oil in 47% yield over two steps (1.86 g, 7.52 mmol).  $^1\text{H NMR}$  (500 MHz,  $\text{CDCl}_3$ )  $\delta$  8.56 (dd,  $J = 4.8, 0.7$  Hz, 1H), 7.74 (td,  $J = 7.7, 1.8$  Hz, 1H), 7.63 (d,  $J = 7.9$  Hz, 1H), 7.22 (ddd,  $J = 7.4, 4.8, 0.9$  Hz, 1H), 5.56 (d,  $J = 2.2$  Hz, 1H), 2.54 (d,  $J = 2.3$  Hz, 1H), 0.97 – 0.93 (m, 10H), 0.21 (d,  $J = 5.7$  Hz, 4H), 0.14 (d,  $J = 5.9$  Hz, 3H).



**Propargylic ester 4.71:** Ethynylmagnesium bromide (42.0 mL, 21.0 mmol, 0.5 M in THF) was added dropwise to 2-pyridinecarboxaldehyde (**4.60**, 1.90 mL, 20.0 mmol) in THF (60 mL) at 0 °C. The reaction mixture was stirred this temperature for 30 min; then, acetyl chloride (1.66 mL, 22.0 mmol) was added. The reaction mixture was stirred as the cold bath was allowed to gradually expire. After 1 h, the reaction was quenched with a saturated  $\text{NH}_4\text{Cl}_{(\text{aq})}$  solution (30 mL). The aqueous layer was extracted with EtOAc (3 x 30 mL). The combined organic layer was washed with brine, dried over  $\text{MgSO}_4$  and concentrated under reduced pressure to provide **4.71** as a yellow oil in 82% yield (2.89 g, 16.5 mmol).  $^1\text{H NMR}$  (500 MHz,  $\text{C}_6\text{D}_6$ )  $\delta$  8.36 (d,  $J = 4.1$  Hz, 1H), 7.32 (d,  $J = 7.9$  Hz, 1H), 6.97 (td,  $J = 7.7, 1.8$  Hz, 1H), 6.85 (d,  $J = 2.3$  Hz, 1H), 6.51 (ddd,  $J = 7.5, 4.8, 0.9$  Hz, 1H), 2.13 – 2.09 (m, 1H), 1.59 (s, 3H).

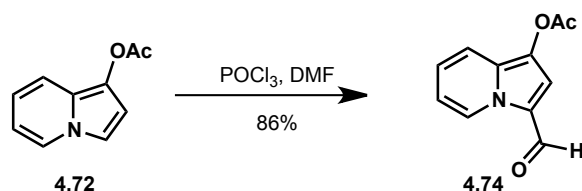


**Indolizine 4.72:** A solution of propargylic ester **4.71** (2.89 g, 16.5 mmol) in EtOH (120 mL) was sparged with  $\text{N}_2$  for 20 min. The reaction flask was equipped with a condenser and heated to 100 °C for 3 h. The reaction mixture was cooled to room temperature and concentrated to afford indolizine **4.72** (2.80 g, 99% yield).  $^1\text{H NMR}$  (500 MHz,  $\text{C}_6\text{D}_6$ )  $\delta$  7.20 (d,  $J = 9.1$  Hz, 1H), 6.93 – 6.90 (m, 2H), 6.59 (d,  $J = 2.9$  Hz, 1H), 6.25 (ddd,  $J = 9.1, 6.4, 0.8$  Hz, 1H), 5.92 – 5.87 (m, 1H), 1.80 (s, 3H).

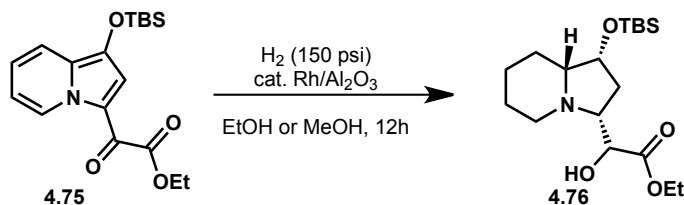


**$\alpha$ -Ketoester 4.73:** Pyridine (78.0  $\mu\text{L}$ , 0.959 mmol) was added dropwise to the acid chloride (91.0  $\mu\text{L}$ , 0.822 mmol) in  $\text{CH}_2\text{Cl}_2$  (5.0 mL) at -78 °C. Next, indolizine **4.72** (120 mg, 0.685 mmol) in  $\text{CH}_2\text{Cl}_2$  (1.8 mL) was added dropwise at -78 °C. Upon addition of the indolizine, the reaction mixture took on an emerald green color that persisted over the course of the reaction. The reaction mixture was stirred as the cold bath was allowed to gradually

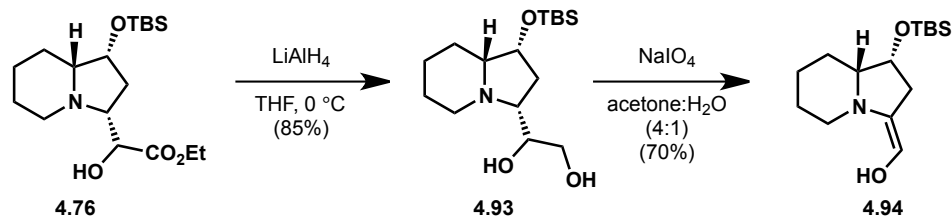
expired. After 4 h, the reaction mixture was diluted with CH<sub>2</sub>Cl<sub>2</sub> (30 mL), washed with 1% HCl<sub>(aq)</sub>, water, brine, dried over MgSO<sub>4</sub> and concentrated under reduced pressure to provide a dark green oil. The crude product was purified via flash chromatography (4:1 hexanes/EtOAc) to afford **4.73** as a green oil in 40% yield (75.4 mg, 0.274 mmol). <sup>1</sup>H NMR (500 MHz, CDCl<sub>3</sub>) δ 9.92 (d, *J* = 7.1 Hz, 1H), 7.88 (s, 1H), 7.53 (d, *J* = 8.8 Hz, 1H), 7.33 (dd, *J* = 11.3, 4.3 Hz, 1H), 7.08 – 7.03 (m, 1H), 4.42 (d, *J* = 7.1 Hz, 2H), 2.38 (s, 3H), 1.43 (t, *J* = 7.1 Hz, 3H); HRMS (ESI+) calcd for [C<sub>14</sub>H<sub>13</sub>O<sub>5</sub>NNa]<sup>+</sup> (M-Na)<sup>+</sup>: *m/z* 298.0686, found 298.0689.



**Aldehyde 4.74:** POCl<sub>3</sub> (963 μL, 10.5 mmol) was added to DMF (75.0 mL) at 0 °C, the mixture was stirred at this temperature for 30 min. Indolizine **4.72** (1.67 g, 9.53 mmol) in DMF (20.0 mL) was added dropwise to the reaction mixture at 0 °C. The reaction mixture was stirred as the cold bath gradually expired. After 10 h, the reaction was quenched with by addition of a saturated NaHCO<sub>3(aq)</sub> solution (30 mL). The aqueous layer was extracted with CHCl<sub>3</sub> (3 x 30 mL). The combined organic layer was washed with water (3 x 20 mL), brine, dried over MgSO<sub>4</sub> and concentrated under reduced pressure to provide aldehyde **4.74** as a brown oil in 86% yield (1.66 g, 8.20 mmol). <sup>1</sup>H NMR (400 MHz, ) δ 9.61 (s, 1H), 8.02 (s, 1H), 7.48 (d, *J* = 8.9 Hz, 1H), 7.39 (s, 1H), 7.21 (ddd, *J* = 8.9, 6.8, 1.0 Hz, 1H), 6.94 (dd, *J* = 7.0, 1.1 Hz, 1H), 2.38 (s, 3H).



**Indolizidine 4.76:** A mixture of indolizine **4.76** (1.00 g, 2.88 mmol) and rhodium on alumina (1.0 g) in MeOH (6.0 mL) was sparged with H<sub>2</sub> for 30 min. The reaction mixture was stirred at ambient temperature under an atmosphere of H<sub>2</sub> (balloon). After 24 h, an additional 500 mg rhodium on alumina was added and the reaction mixture was sparged with H<sub>2</sub> for 1 h. The reaction mixture was stirred under H<sub>2</sub> for an additional 24 h before it was filtered through a pad of celite and concentrated to provide indolizidine **4.76** in a 73% yield (75.2 mg, 2.10 mmol). The <sup>1</sup>H NMR data is consistent with that reported for **4.76** in the literature. HRMS (ESI+) calcd for [C<sub>18</sub>H<sub>36</sub>NO<sub>4</sub>Si]<sup>+</sup> (M-H)<sup>+</sup>: *m/z* 358.2408, found 358.2408.



**Enol 4.94:** Lithium aluminum hydride (3.7 mg, 0.098 mmol) was added to **4.76** (11.2 mg, 0.0489 mmol) in THF (500  $\mu$ L) at 0 °C. The reaction mixture was stirred as the cold bath gradually expired. After 2 h, the sequential addition of water (10  $\mu$ L), 10% NaOH<sub>(aq)</sub> (10  $\mu$ L) and water (30  $\mu$ L) induced the formation of a white precipitate. The white solid was removed by filtration through a plug of celite. The filtrate was concentrated under reduced pressure to provide diol **4.93**. NaIO<sub>4</sub> supported on silica gel<sup>30</sup> (30 mg) was added to diol **4.93** in CH<sub>2</sub>Cl<sub>2</sub> (300  $\mu$ L), the mixture was stirred vigorously at room temperature. After 3 h, the mixture was diluted with 9:1 CH<sub>2</sub>Cl<sub>2</sub>/MeOH (2.0 mL), filtered and concentrated under reduced pressure to afford enol **4.94** which intersects Thadani's route toward securinine.<sup>29</sup>

#### 4.7 References and Notes

- (1) Daly, J. W.; Spande, T. F.; Garraffo, H. M. *J. Nat. Prod.* **2005**, *68*, 1556.
- (2) Daly, J. W.; Nishizawa, Y.; Padgett, W. L.; Tokuyama, T.; Smith, A. L.; Holmes, A. B.; Kibayashi, C.; Aronstam, R. S. *Neurochem. Res.* **1991**, *16*, 1213.
- (3) Changeux, J. P.; Devillersthiery, A.; Chemouilli, P. *Science* **1984**, *225*, 1335.
- (4) Juge, M.; Grimaud, N.; Biard, J. F.; Sauviat, M. P.; Nabil, M.; Verbist, J. F.; Petit, J. Y. *Toxicon* **2001**, *39*, 1231.
- (5) Sauviat, M. P.; Vercauteren, J.; Grimaud, N.; Juge, M.; Nabil, M.; Petit, J. Y.; Biard, J. F. *J. Nat. Prod.* **2006**, *69*, 558.
- (6) Muraveva, V. I.; Bankovskii, A. I. *Med. Prom. S.S.S.R.* **1956**, *10*, 27.
- (7) Friess, S. L.; Reber, L. J.; Durant, R. C.; Thommesen, W. C.; Whitcomb, E. R. *Toxicol. Appl. Pharmacol.* **1961**, *3*, 347.
- (8) Beutler, J. A.; Karbon, E. W.; Brubaker, A. N.; Malik, R.; Curtis, D. R.; Enna, S. J. *Brain Res.* **1985**, *330*, 135.
- (9) Lubick, K.; Radke, M.; Jutila, M. *J. Leukocyte Biol.* **2007**, *82*, 1062.
- (10) Dong, N. Z.; Gu, Z. L.; Chou, W. H.; Kwok, C. Y. *Acta Pharmacol. Sin.* **1999**, *20*, 267.

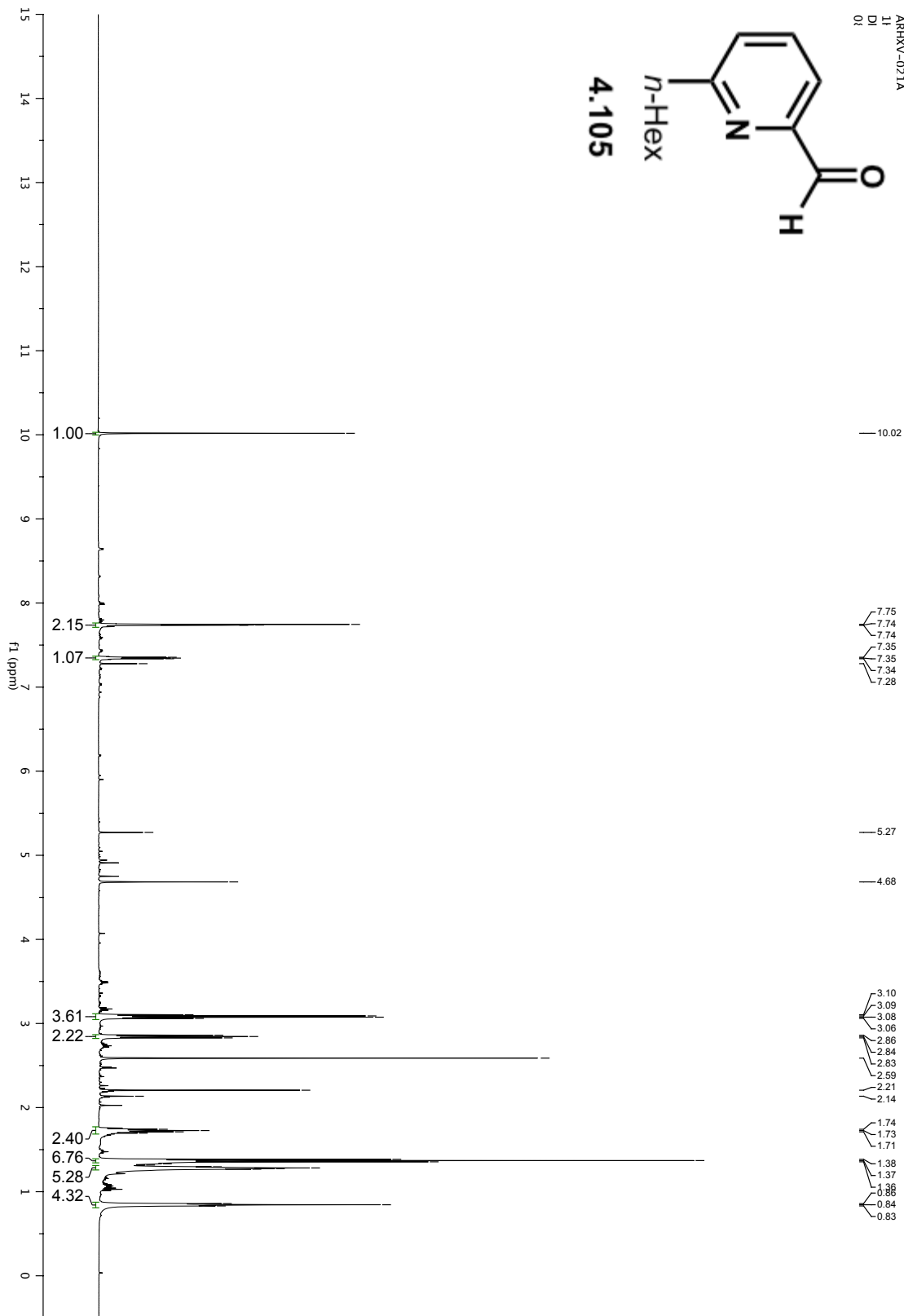
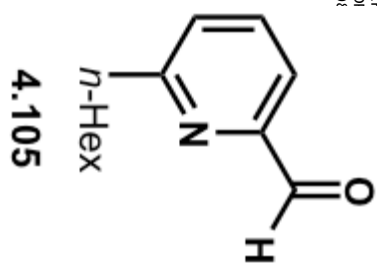


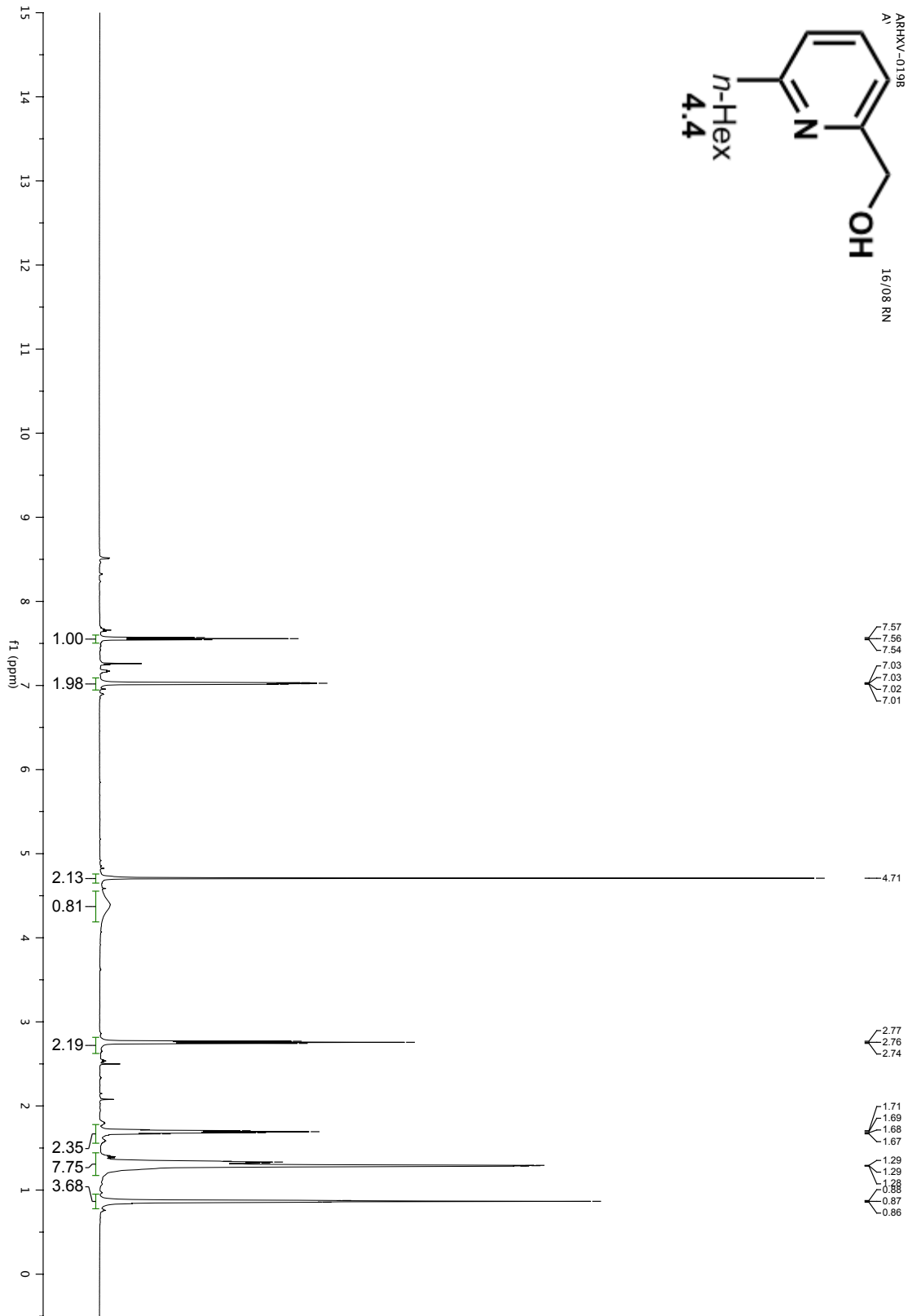
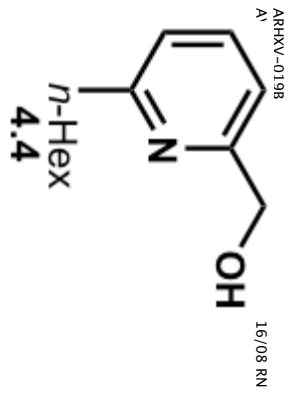
- (11) Xu, L.; Zhang, J. T. *Neurol. Res.* **2004**, *26*, 792.
- (12) Saito, S.; Yamawaki, Y.; Kotera, K.; Ide, A.; Shigematsu, N.; Horii, Z.; Hanaoka, M.; Sugimoto, N.; Tamura, Y. *Tetrahedron* **1963**, *19*, 2085.
- (13) Horii, Z.; Kodera, K.; Ikeda, M.; Saito, S.; Tamura, Y.; Yamawaki, Y. *Chem. Pharm. Bull.* **1963**, *11*, 817.
- (14) Horii, Z.; Yamawaki, Y.; Saito, S.; Tamura, Y.; Kodera, K.; Ikeda, M. *Tetrahedron* **1963**, *19*, 2101.
- (15) Saito, S.; Yoshikawa, H.; Shigematsu, N.; Tamura, Y.; Horii, Z. *Chem. Pharm. Bull.* **1963**, *11*, 1219.
- (16) Saito, S.; Yoshikawa, H.; Sato, Y.; Nakai, H.; Sugimoto, N.; Horii, Z. I.; Hanaoka, M.; Tamura, Y. *Chem. Pharm. Bull.* **1966**, *14*, 313.
- (17) Horii, Z.; Hanaoka, M.; Yamawaki, Y.; Tamura, Y.; Saito, S.; Shigematsu, N.; Kotera, K.; Yoshikawa, H.; Sato, Y.; Nakai, H.; Sugimoto, N. *Tetrahedron* **1967**, *23*, 1165.
- (18) Honda, T.; Namiki, H.; Kudoh, M.; Watanabe, N.; Nagase, H.; Mizutani, H. *Tetrahedron Lett.* **2000**, *41*, 5927.
- (19) Honda, T.; Namiki, H.; Kudoh, M.; Nagase, H.; Mizutani, H. *Heterocycles* **2003**, *59*, 169.
- (20) Liras, S.; Davoren, J. E.; Bordner, J. *Org. Lett.* **2001**, *3*, 703.
- (21) Honda, T.; Namiki, H.; Kaneda, K.; Mizutani, H. *Org. Lett.* **2004**, *6*, 87.
- (22) Alibes, R.; Ballbe, M.; Busque, F.; de March, P.; Elias, L.; Figueredo, M.; Font, J. *Org. Lett.* **2004**, *6*, 1813.
- (23) Gonzalez-Galvez, D.; Garcia-Garcia, E.; Alibes, R.; Bayon, P.; de March, P.; Figueredo, M.; Font, J. *J. Org. Chem.* **2009**, *74*, 6199.
- (24) Padwa, A. *Molecules* **2001**, *6*, 1.
- (25) Kell'in, A. V.; Sromek, A. W.; Gevorgyan, V. *J. Am. Chem. Soc.* **2001**, *123*, 2074.
- (26) Jiang, C.; Frontier, A. J. *Org. Lett.* **2007**, *9*, 4939.
- (27) Jones, R. A.; Bean, G. P. *The chemistry of pyrroles*; Academic Press: London, **1977**; Vol. 34.
- (28) Donohoe, T. J.; Thomas, R. E. *Nat. Protoc.* **2007**, *2*, 1888.

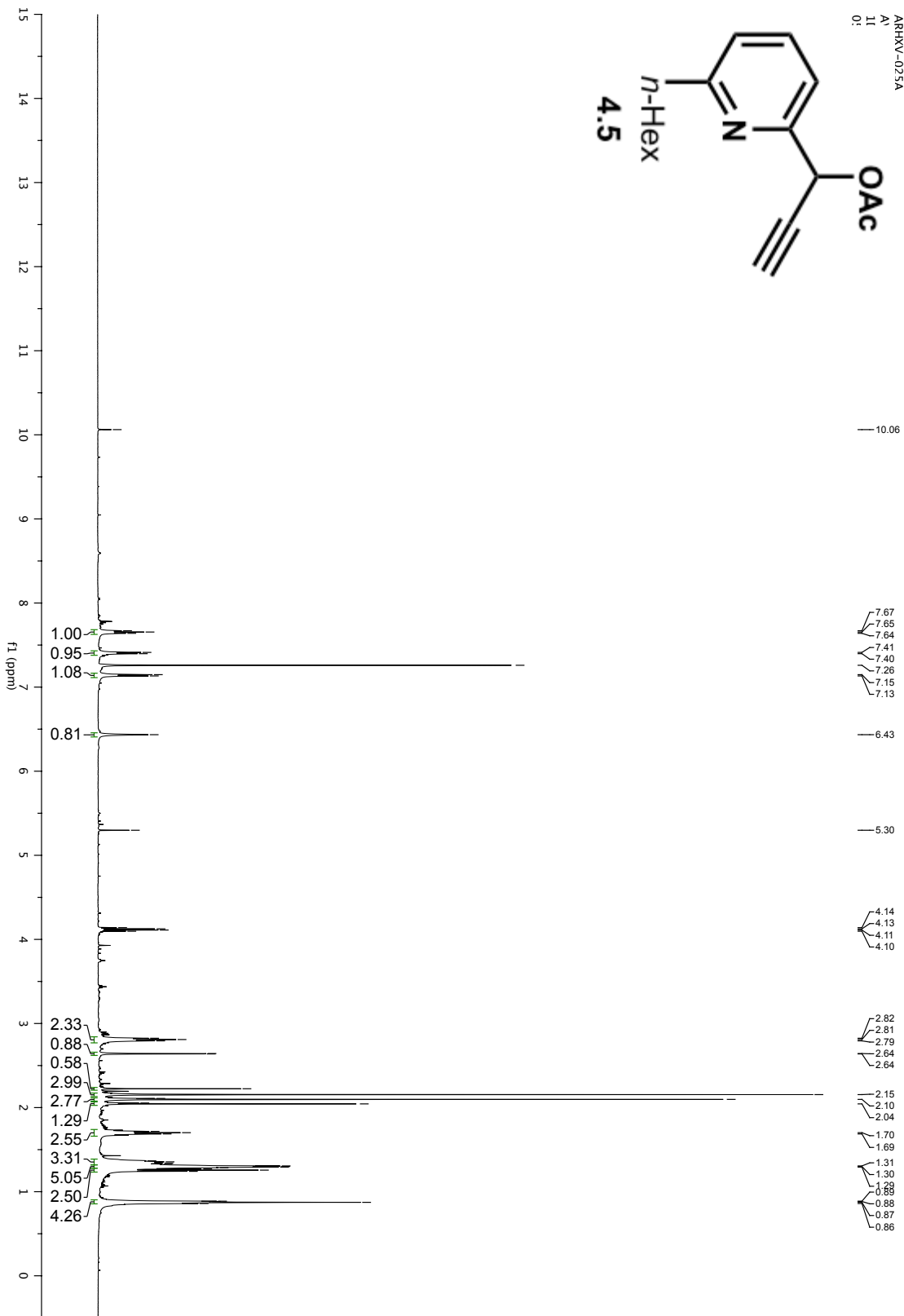
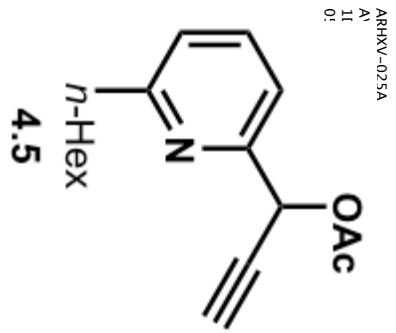
- (29) Dhudshia, B.; Cooper, B. F. T.; Macdonald, C. L. B.; Thadani, A. N. *Chem. Commun.* **2009**, 463.
- (30) Zhong, Y. L.; Shing, T. K. M. *J. Org. Chem.* **1997**, *62*, 2622.

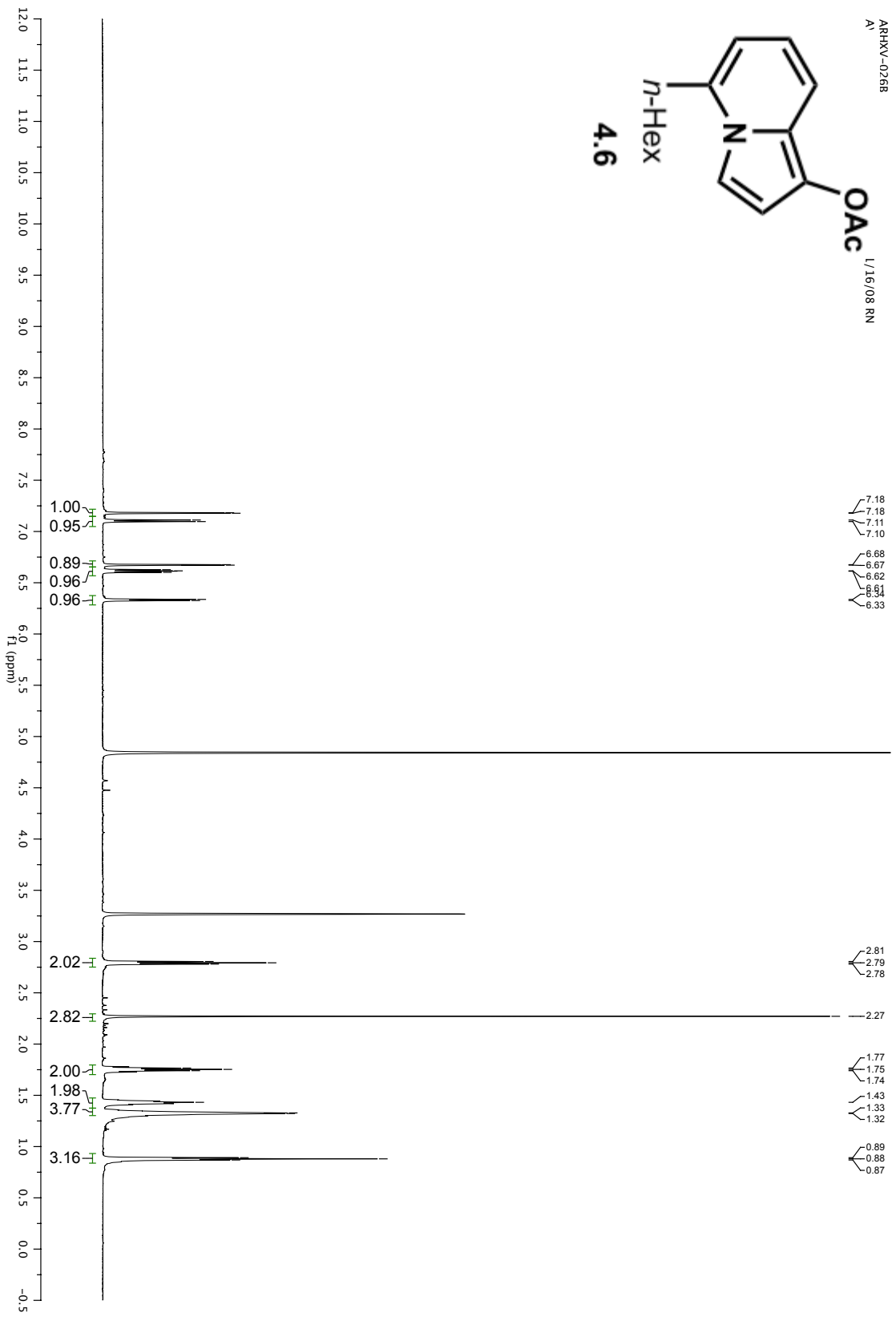
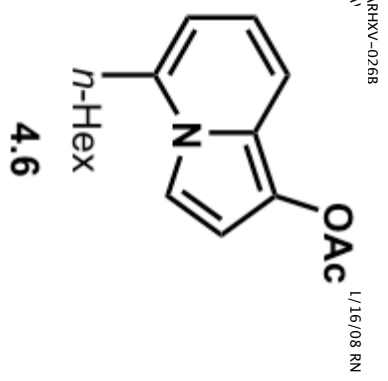
*Appendix Three:  
Spectra Relevant to Chapter Four*

ARRXV-021A  
11  
DI  
01

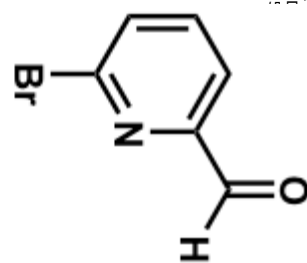




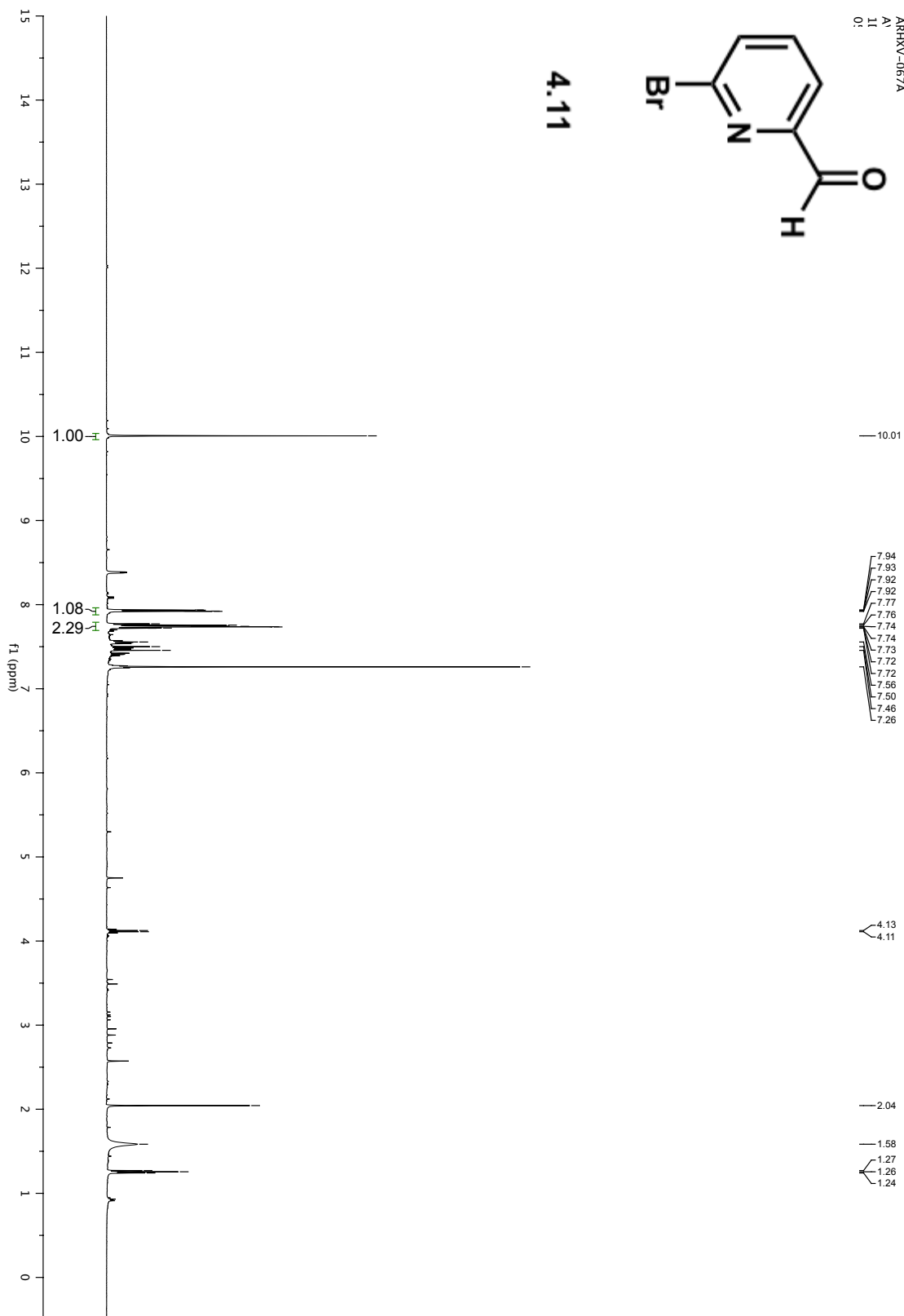




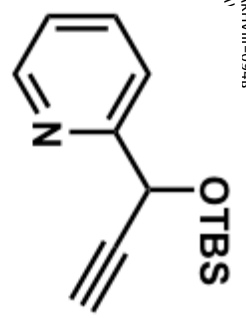
ARHXV-067A  
A1  
11  
0:



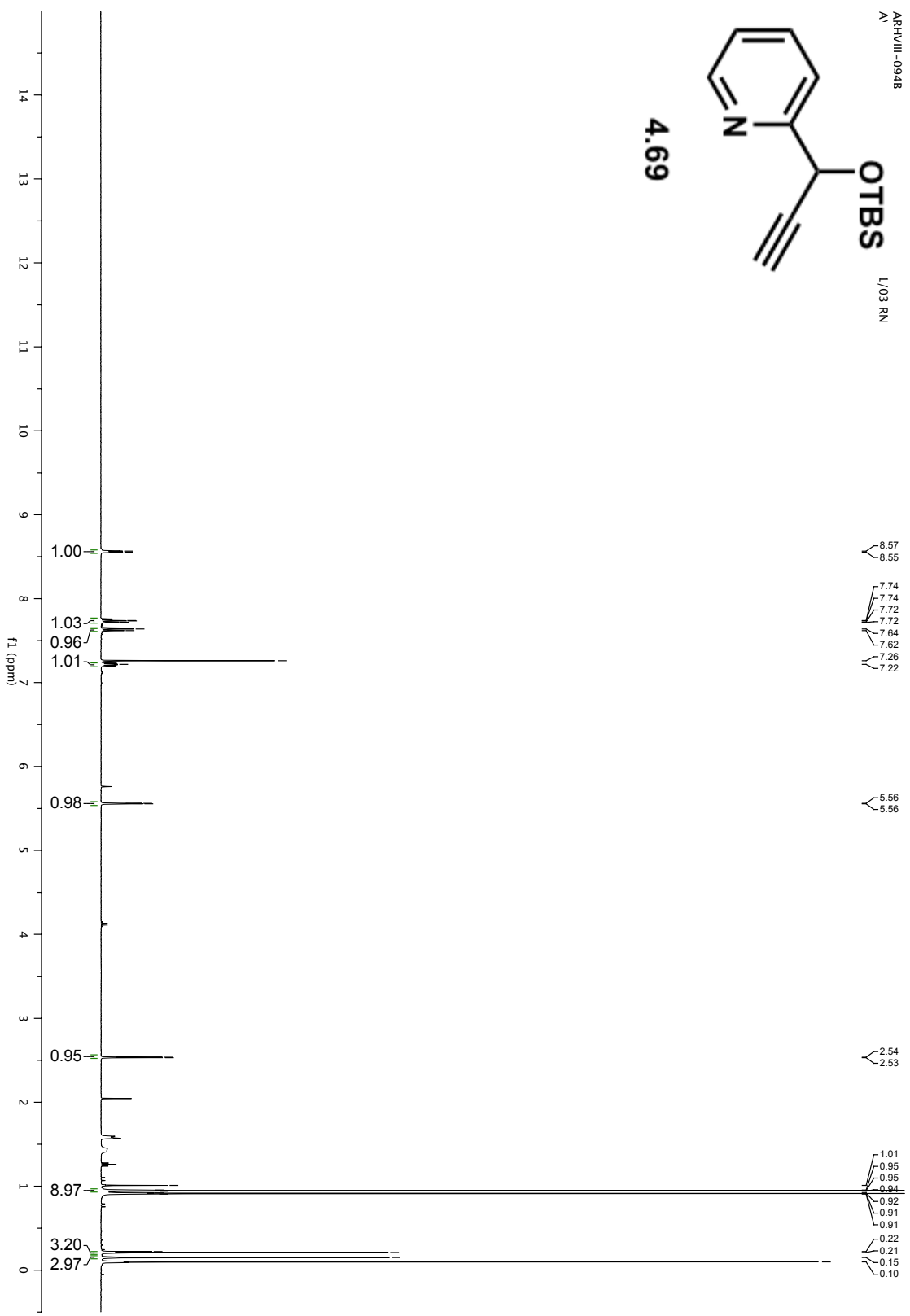
4.11



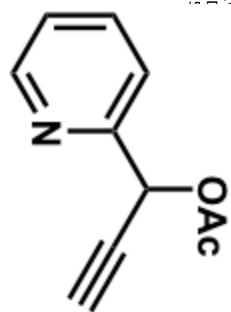




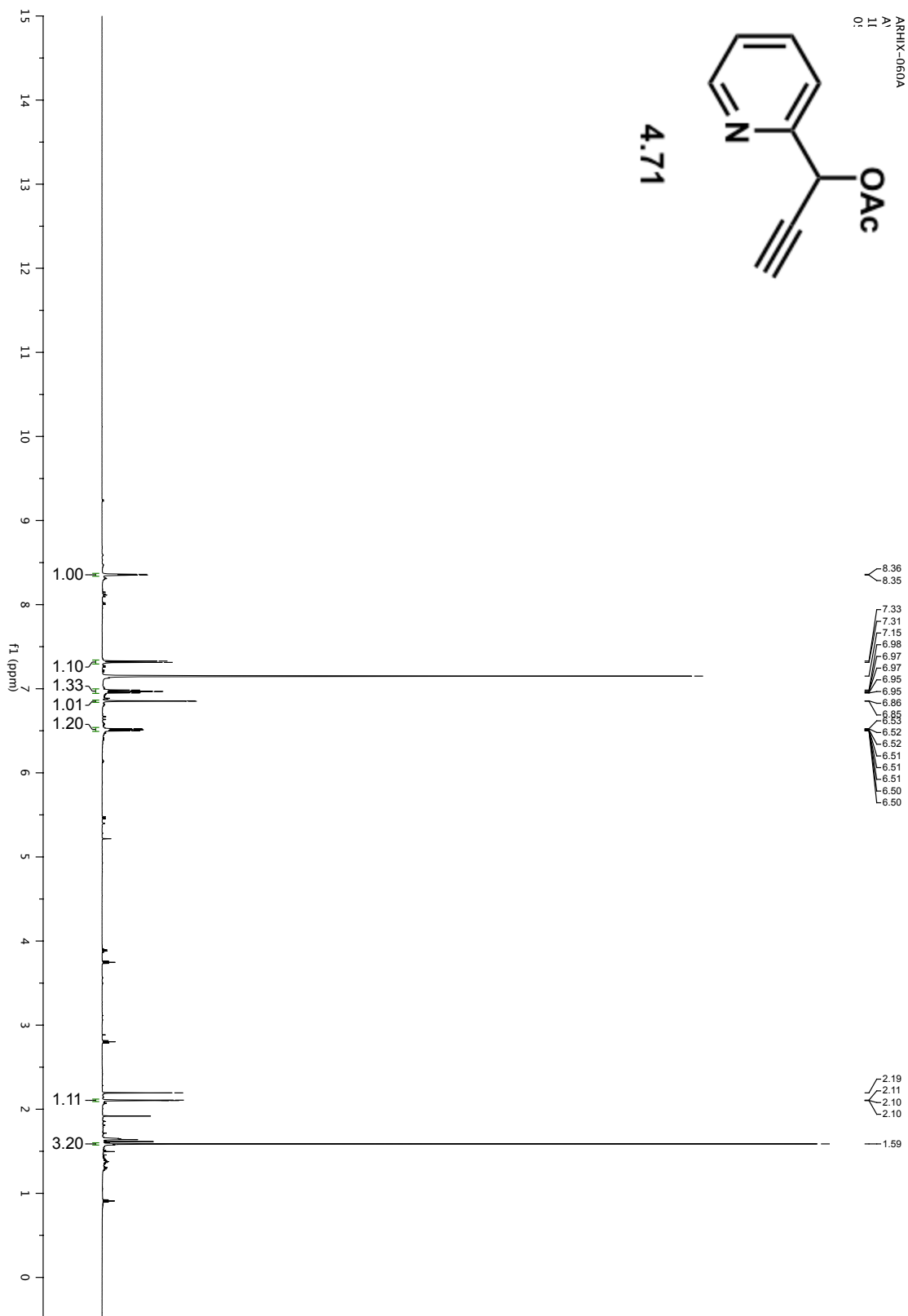
4.69



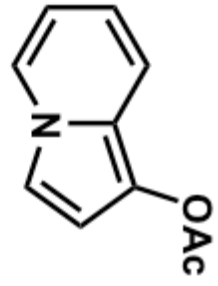
ARHX-060A  
A:  
1:  
0:



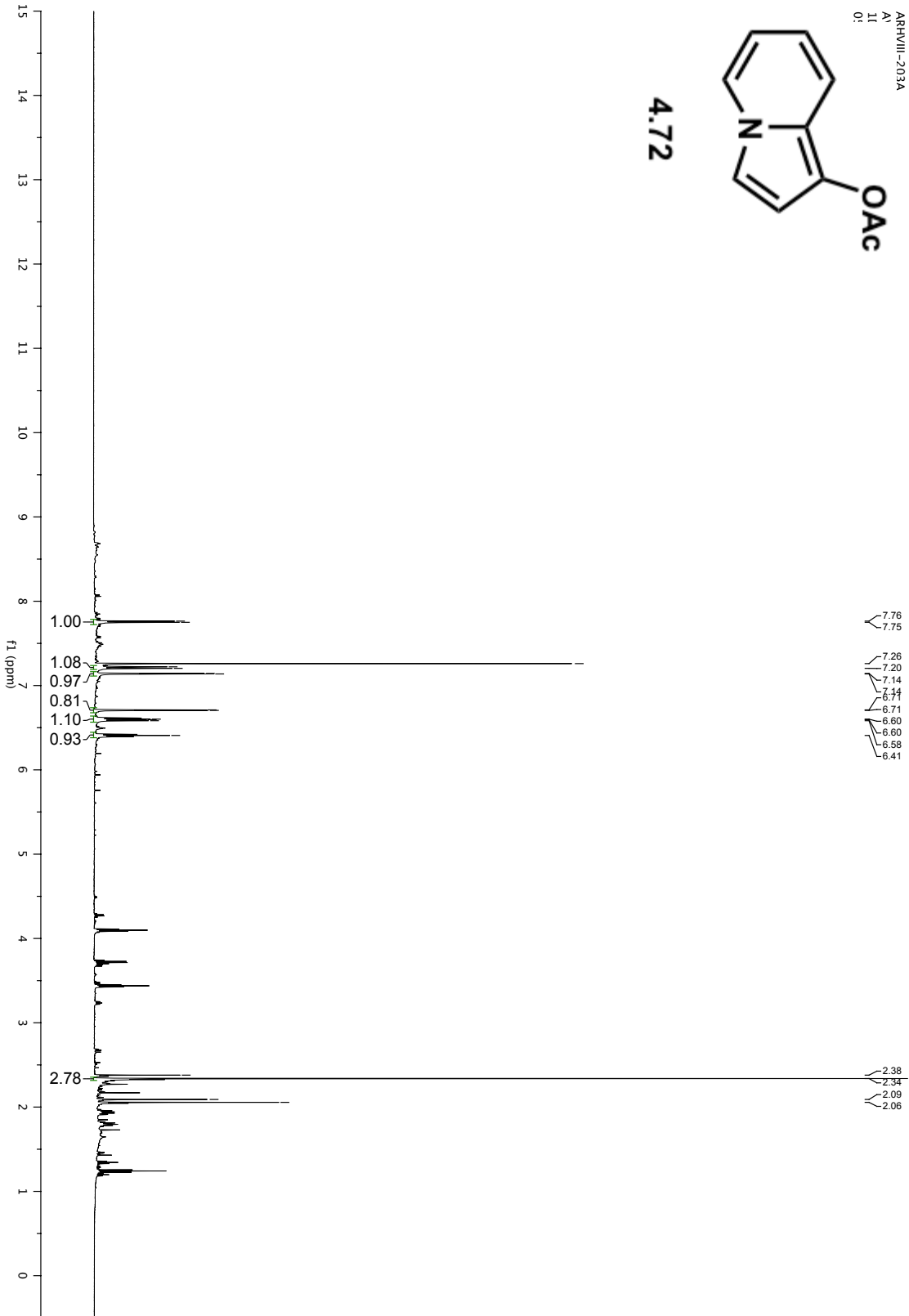
4.71

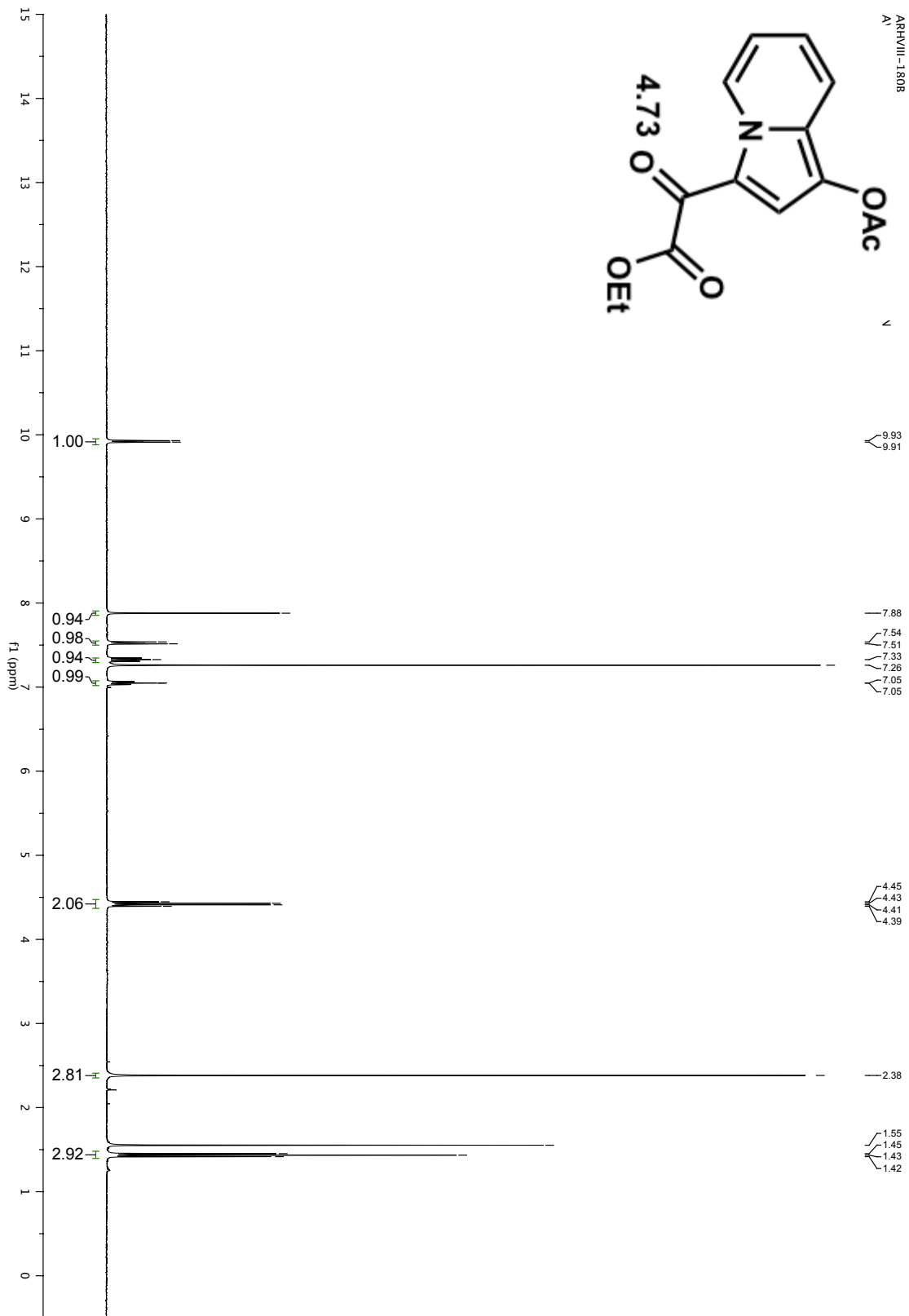


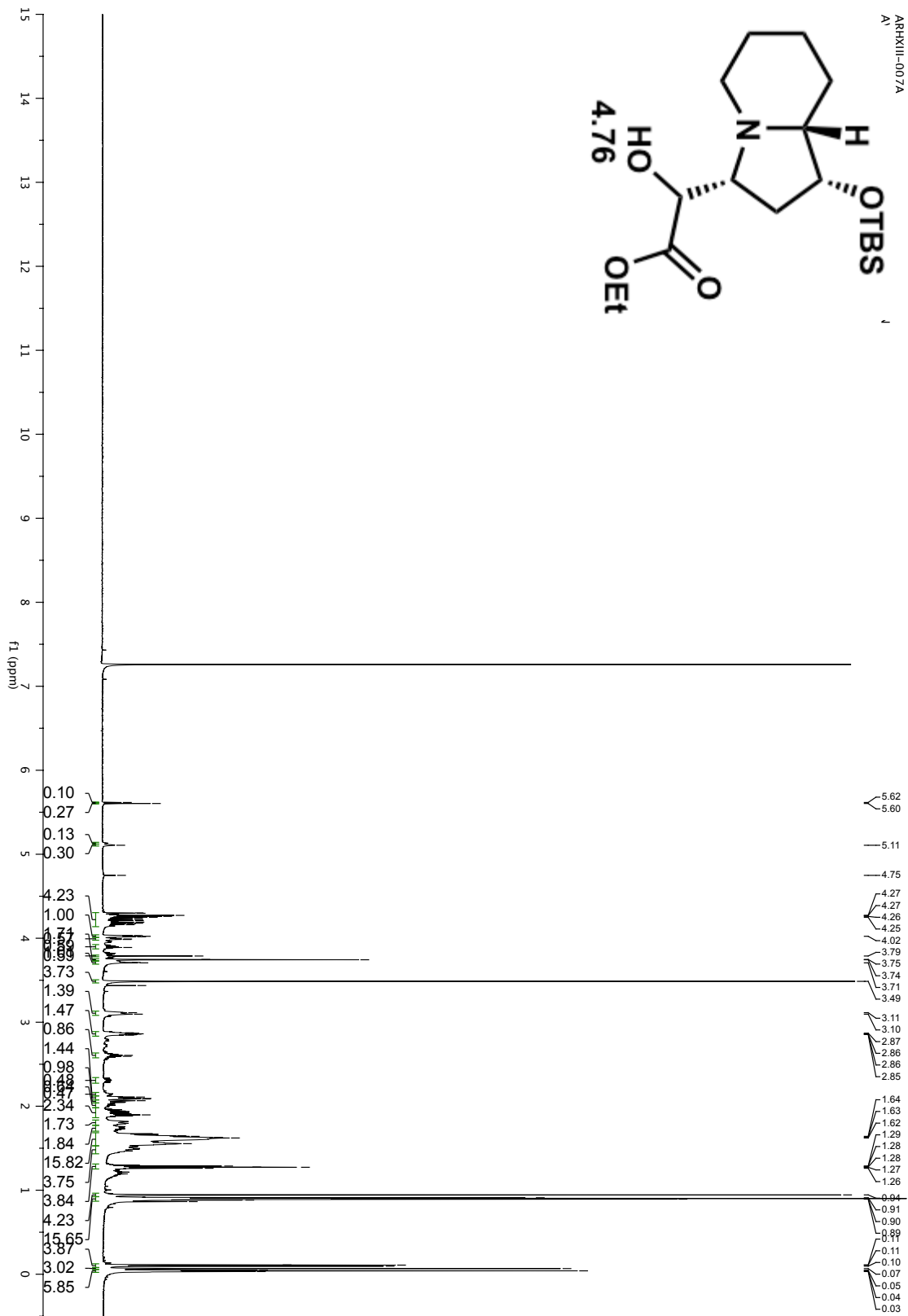
ARRHIII-203A  
A:  
I:  
O:

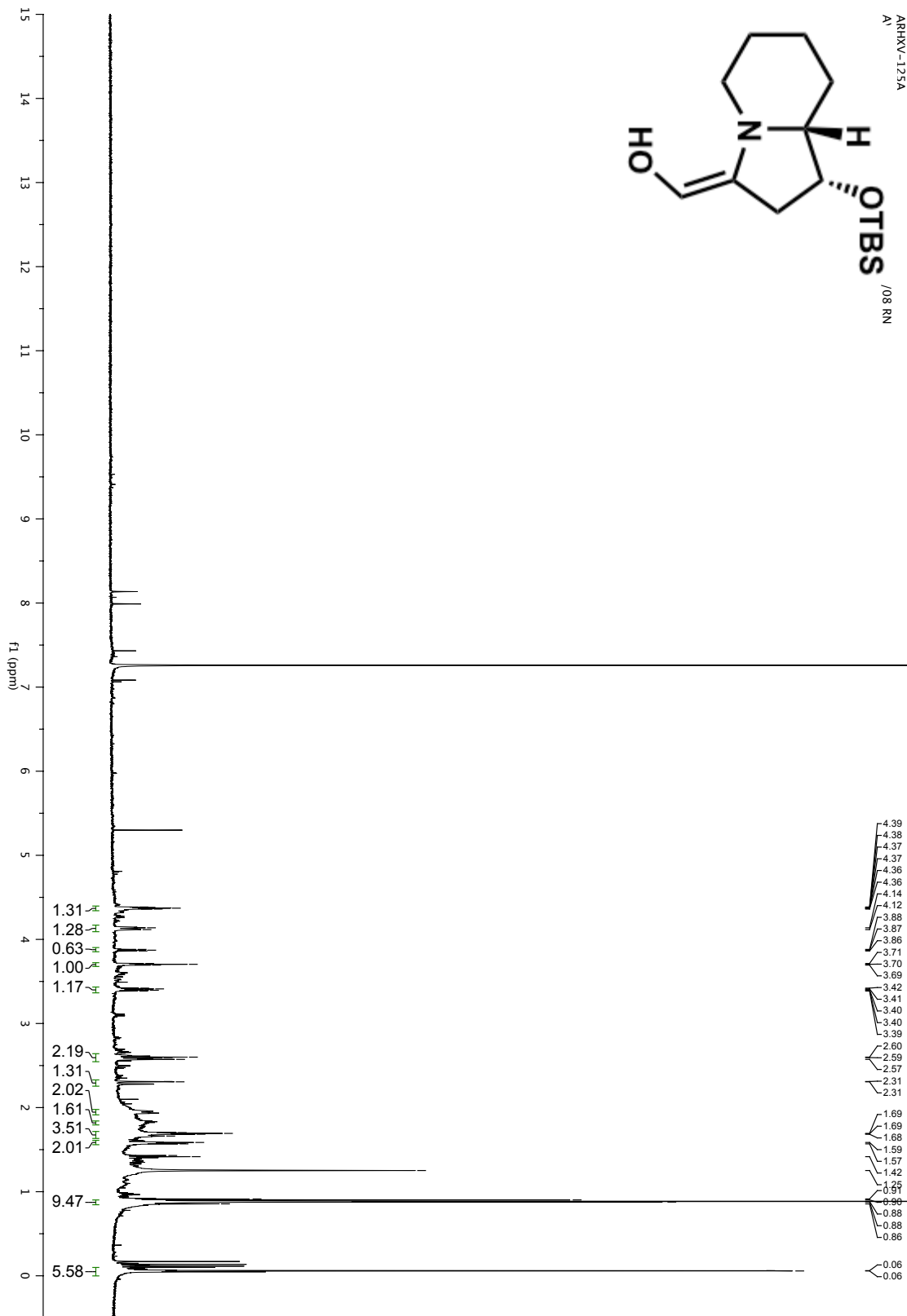
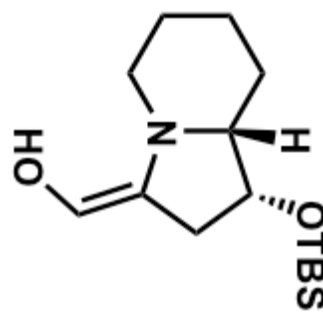


4.72







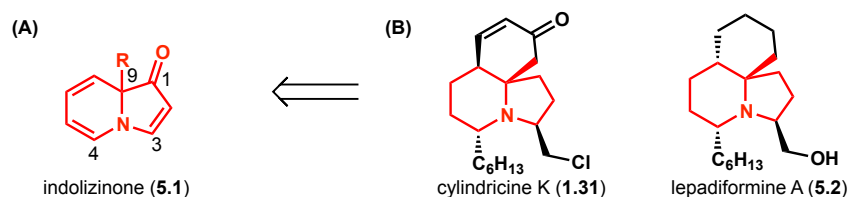


## Chapter 5. The Chemistry of Indolizinones

### 5.1 Introduction

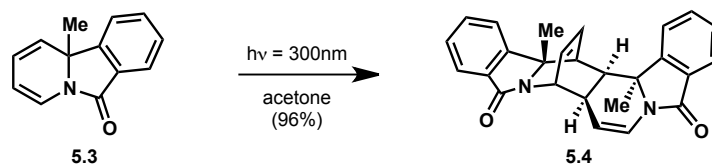
During the development of a metal-free cyclization of propargylic alcohols to indolizinones (see Chapter 3), we became interested in utilizing these bicycles as strategic intermediates in the synthesis of indolizidine natural products. Specifically, we envisioned accessing a subset of indolizidine alkaloids that possess a substituent at C-9 (Figure 5.1.1A). We theorized that indolizinones would provide rapid access to molecules such as the cylindricines<sup>1</sup> and lepadiformines.<sup>2</sup> Strategically, the ring-fusion substituent of the indolizinone would be retained in the natural product and also dictate regio- and facial-selectivity in the reactions of the indolizinone (Figure 5.1.1).

**Figure 5.1.1.** (A) indolizinone core; (B) potential natural product targets.



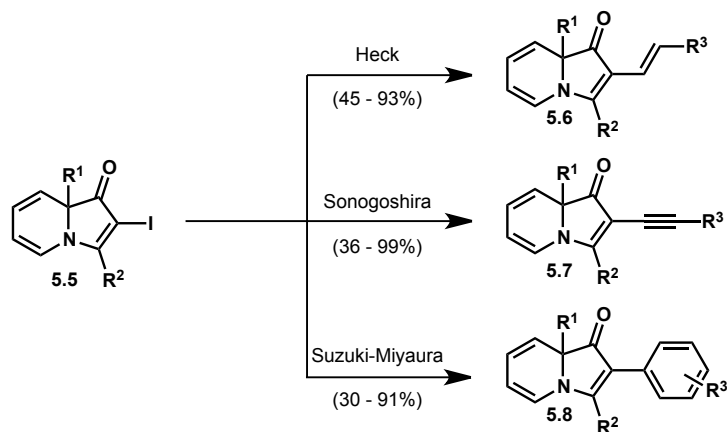
However, we quickly realized that although the utility of indolizines as building blocks has been developed and employed in the synthesis of molecules with a range of applications, the exploration of indolizinone chemistry has been much less explored. Over the last five years, several methods for the construction of indolizinones have been developed (see Chapter 3);<sup>3-6</sup> however, the innate reactivity of these *N*-heterocycles has remained a mystery with the exception of two recent isolated reports.<sup>7,8</sup> In 2008 Paquette and co-workers described the dimerization of benzannulated indolizinones (see 5.3) via a light promoted [4+2] cyclization between the diene contained within the six-membered ring of one indolizinone molecule and a double bond that makes up half of the diene in another molecule of the indolizinone (Scheme 5.1.1).<sup>7</sup>

**Scheme 5.1.1.** Paquette's photodimerization of pyrido[2,1- $\alpha$ ]isoindol-6(4*H*)-one (5.3).



The second disclosure of indolizinone chemistry came in 2010 from Kim and Kim on the palladium-catalyzed cross-coupling of 2-iodoindolizinones (Scheme 5.1.2).<sup>8</sup> Kim and coworkers demonstrated the competence of 2-iodoindolizinones as the halide component in Heck, Sonogoshira, and Suzuki-Miyaura reactions. They were able to rapidly assemble a library of differentially substituted indolizinones using this chemistry with the intent of studying the biological properties of these molecules in their medicinal research program.

**Scheme 5.1.2.** Palladium-catalyzed cross couplings of 2-iodoindolizinone (**5.5**).



In order to devise a synthetic strategy toward the cylindricines and other indolizinone natural products, it was first necessary to explore the innate reactivity of these bicycles. Toward this end, our initial investigations of indolizinone chemistry focused on reactions that we anticipated could be useful in the synthesis of the cylindricine core (see Figure 5.1.1B).

### 5.2 Indolizinone Reactive Sites

The reactive sites of the indolizinone core can be separated into two moieties: the dienamine and the vinylogous amide (Figure 5.2.1). At the onset of this work, we anticipated that the dienamine would behave as a nucleophile and the vinylogous amide would exhibit reactivity as an electrophile. This hypothesis arises from the independent analysis of these two functional groups where a dienamine is expected to be relatively electron-rich and a vinylogous amide is electron deficient. These relative electron densities are reflected in the calculated HOMO and LUMO of methylindolizinone (**5.11**, Figure 5.2.2). However, this picture does not account for the interaction of these two moieties as they exist in conjugation with each other and can be thought of as a continuous  $\pi$ -system. Modeling of simple methyl indolizinone (**5.11**) suggests the complete conjugation of the diene with the vinylogous amide through a  $sp^2$ -hybridized nitrogen atom at the ring-fusion. This creates a flat bicycle as opposed to a book-like, cupped bicycle which would suggest the separation of these two  $\pi$ -systems (Figure 5.2.3).

**Figure 5.2.1.** Reactive sites of the indolizinone core.





**Figure 5.2.2.** Calculated HOMO and LUMO of methylindolizinone (**5.11**).

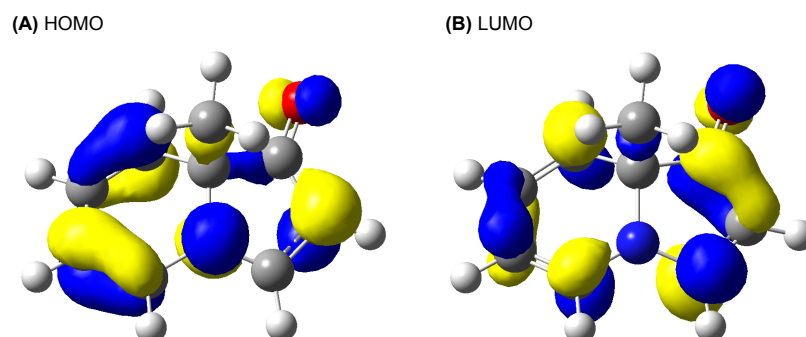
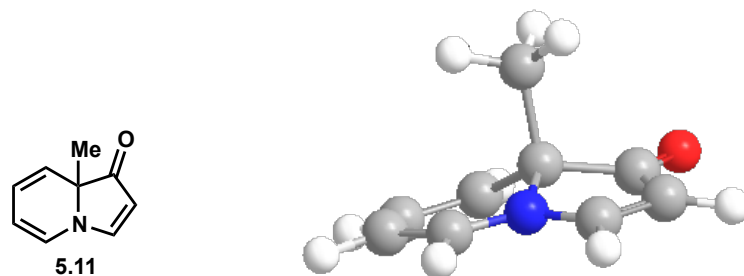


**Figure 5.2.3.** Predicted conformation of methylindolizinone (**5.11**).



Given the conjugation of the dienamine and vinylogous amide through the shared ring-fusion nitrogen atom, there is uncertainty associated with the predicted reactivity of the indolizinone core. This has spurred our investigation into the innate reactivity of this N-fused bicycle. Methyl indolizinone (**5.11**) was used as a model substrate in our investigations of indolizinone chemistry. The generality of the chemistry discovered was tested with a variety of indolizinone substrates to provide further information on the basic reactivity of these bicycles and gain access to intermediates that could be employed in the synthesis of the frameworks of several indolizidine natural products.

### 5.3 Bromination

The regioselective incorporation of a halogen atom on the indolizinone core would provide a powerful functional handle for further elaboration of the bicycle. For example, a vinyl halide could be employed in a variety of cross-couplings to form carbon-carbon or carbon-heteroatom bonds. Alternatively, this functional group could serve as an initiation point for radical chemistry. With the potential to access compounds with high synthetic utility, we became interested in the prospect of a halogenation of indolizinones; however, it was unclear if any regioselectivity would be observed in this transformation, or if mono-halogenation would be possible.

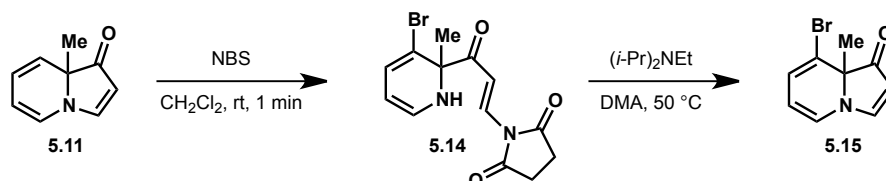
It was possible that the dienamine could react with an electrophilic halogen source at either the 6- or 8-position of the indolizinone (Figure 5.3.1). We hypothesized that halogenation at C-8 could be disfavored by an unfavorable steric interaction between the ring-fusion substituent (R) and the halogen source.

**Figure 5.3.1.** Potential sites of halogenation.



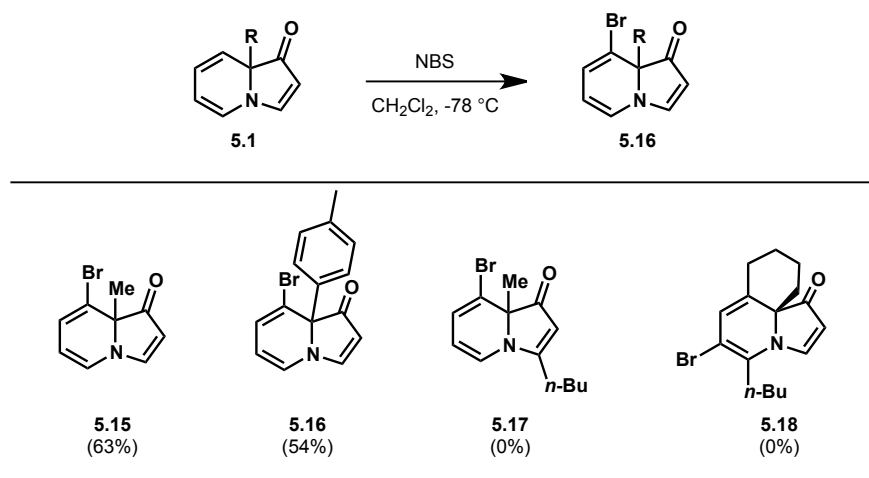
When methyl indolizinone (**5.11**) was treated with *N*-bromosuccinimide (NBS) in dichloromethane at ambient temperature, a single brominated product was obtained in less than a minute. However, the product was not simply the 6- or 8-bromoindolizinone. Instead, the succinimide was also incorporated to provide an extremely polar product. <sup>1</sup>H NMR and <sup>13</sup>C NMR were consistent with secondary amine **5.14** (Scheme 5.3.1). The duality of the reactivity of the indolizinone is illustrated in this transformation: (1) the nucleophilicity of the dienamine in its ability to attack the electrophilic bromine atom of NBS, and (2) the electrophilicity of the vinylogous amide as evidenced by the facile conjugate addition of the succinimide, which leads to the opening of the five-membered ring. The desired mono-halogenated product (**5.15**) can be accessed from secondary amine **5.14** through a base mediated ring closure.

**Scheme 5.3.1.** Synthesis of 8-bromomethylindolizinone (**5.15**).



Ideally, 8-bromoindolizinone **5.15** would be obtained in a single operation. Therefore, we explored the parameters of the reaction starting with alternative brominating reagents such as 1,3-dibromo-5,5-dimethylhydantoin and pyridinium perbromide. Unfortunately, regioselective bromination was not achieved with these reagents. Next, the reaction temperature was lowered to 0 °C, which resulted in addition of the succinimide followed by ring-opening. Gratifyingly, lowering the temperature to -78 °C provided the 8-bromoindolizinone product in good yield. Given this result, the low temperature conditions were applied to a variety of indolizinone substrates to study the generality of this transformation (see Figure 5.3.2).

**Figure 5.3.2.** Bromination of indolizinones.

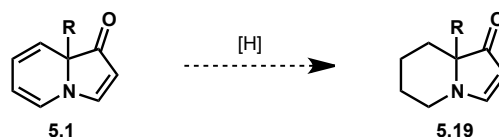


The regioselective bromination was tested on a range of indolizinone substrates (Figure 5.3.2). Both alkyl and aryl substituents at the ring fusion were tolerated. However, further substitution on the indolizinone altered the outcome of the reaction, returning only starting material (see **5.17** and **5.18**).

#### 5.4 Hydrogenation

In parallel with the studies on the nucleophilicity of the dienamine fragment of the indolizinone, we were interested in removing this reactive moiety from the bicycle through hydrogenation to arrive at a saturated six-membered ring (Scheme 5.4.1). We anticipated that the electron-rich diene would be selectively reduced in the presence of the relatively electron poor vinylogous amide double bond. Initial experimentation revealed a range of conditions sufficient for providing the reduced product, including heterogeneous catalysts such as palladium on carbon and Raney nickel in conjunction with pressures of hydrogen ranging from 1 to 15 atm.

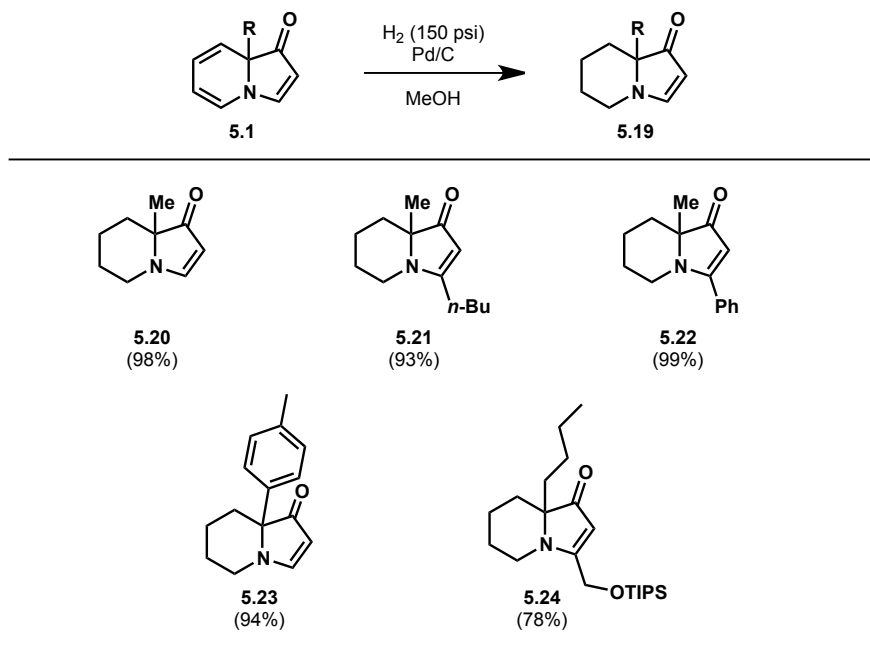
**Scheme 5.4.1.** Selective reduction of the diene.



The standard conditions adopted for this transformation were 150 psi of hydrogen gas in the presence of palladium on carbon in methanol for 12 hours. Shorter reaction times and lower pressures of hydrogen led to incomplete reduction of the starting material in some cases. Ethyl acetate and ethanol are also competent solvents for this transformation; however, the use of these solvents led to incomplete conversion of starting material in some cases. The standard conditions were applied to a variety of indolizinone substrates (Figure 5.4.1). The hydrogenation proceeded

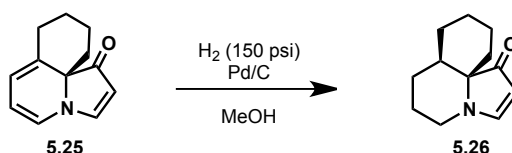
without event on indolizinones with a range of substituents at the ring fusion, including methyl and *p*-tol. It is noteworthy that the double bond of the homoallyl group is hydrogenated under these conditions in addition to the desired reduction (see 5.24). Substitution on the five-membered ring is also tolerated and does not qualitatively affect the course of the reaction (see 5.21 and 5.22).

**Figure 5.4.1.** Hydrogenation of the diene.



The hydrogenation of a more substituted diene provides insight into the facial selectivity of the transformation. We anticipated that the hydrogen would be delivered from the less sterically hindered face of the bicycle, opposite the ring-fusion substituent. Tricyclic indolizinones **5.25** and **5.27** provided the opportunity to test this hypothesis. Exposure of the 6,6,5-tricycle **5.25** to palladium on carbon under 150 psi of hydrogen cleanly yielded a single diastereomer of a tricycle that had gained two molecules of H<sub>2</sub>. The identity of the reduced product was assigned as **5.26**, a tricycle with a *cis*-ring fusion between the two six-membered rings (Scheme 5.4.2).

**Scheme 5.4.2.** Hydrogenation of tricyclic indolizinone **5.25**.

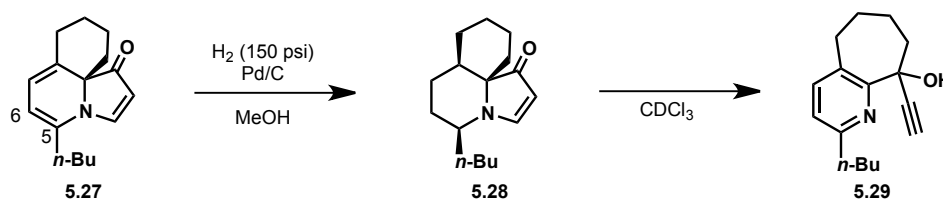


The stereochemical outcome of the hydrogenation of indolizinone **5.25** is significant in the context of natural product synthesis. The *cis*-ring fused product (**5.26**) obtained in the

hydrogenation of indolizinone **5.25** maps onto members of the cylindricine family of marine natural products (see **1.31**, Figure 5.1.1B). An alternative outcome would lead to the *trans*-ring fusion of the six-membered rings, this stereochemical relationship is present in another group of molecules, the lepadiformines (see, **5.2**, Figure 5.1.1B).

Further substituting the diene makes it possible to probe the facial selectivity of the hydrogenation of the double bond most proximal to the nitrogen between C-5 and C-6. To this end, a tricyclic indolizinone possessing an *n*-butyl group at C-5 (**5.27**) was synthesized (see Chapter 6.4 for a detailed synthesis of **5.27**) and exposed to the standard hydrogenation conditions. After 12 hours, TLC analysis suggested the complete conversion of the starting material (**5.27**) to a single product. However, the crude <sup>1</sup>H NMR indicated the presence of two products in approximately a 1:1 ratio. Attempts to separate the two products via column chromatography were successful, only to be met with conversion of the less polar product to the more polar product in CDCl<sub>3</sub>. The more polar compound was identified as pyridine **5.29**, a precursor to indolizinone **5.27**. The less polar compound lacks the unsaturation of the diene as evidenced by the loss of intense yellow color indicative of indolizinone **5.27** but maintains the five-membered ring at the vinylogous amide oxidation level. We hypothesize that the hydrogenation of both double bonds of the diene takes place from the less hindered face of indolizinone **5.27** to give tricycle **5.28** in which the *n*-butyl substituent has a *syn* relationship to the *cis*-fused six-membered ring. Constructing models of **5.28** both with Chem3D and Dreiding-type models illustrates the steric clash between the *cis*-fused six-membered ring and the butyl group *syn* to this ring. We believe that it is this unfavorable steric interaction that leads to the instability of tricycle **5.28**, and its propensity to revert to pyridine **5.29**.

**Scheme 5.4.3.** Hydrogenation of tricyclic indolizinone **5.27**.



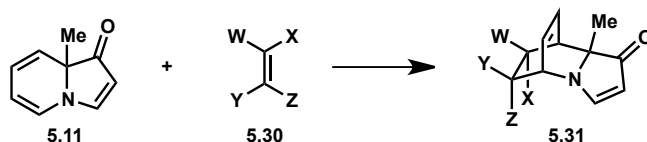
### 5.5 Diels-Alder Cycloaddition

The ability of the indolizinone dienamine to act as a nucleophile was demonstrated in its facile bromination with *N*-bromosuccinimide; this innate reactivity is evidence of the electron-rich nature of the dienamine portion of the indolizinone. As an electron-rich diene, we anticipated that the indolizinone diene would be well suited for Diels-Alder cycloaddition reactions. This chemical intuition was bolstered by the report from Paquette and co-workers of the photo-dimerization of an indolizinone, which involved a formal [4+2] cycloaddition between the diene of one indolizinone and the vinylogous amide double bond of another molecule of the indolizinone (see Scheme 5.1.2).<sup>7</sup>

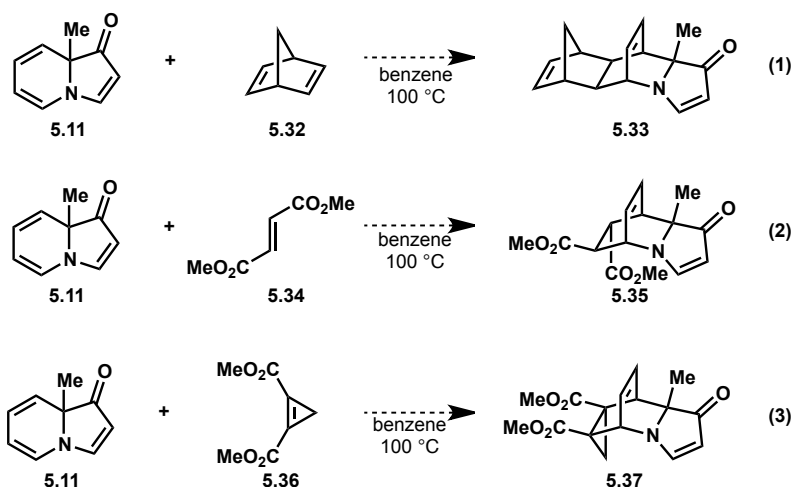
At the onset of this work, we were cognizant of the possibility for dimerization of the indolizinone starting material with itself as observed by Paquette and co-workers under photo-conditions. However, we envisioned avoiding this undesired pathway by utilizing more reactive

dienophiles and further discouraging the dimerization by using multiple equivalents of the dienophile. This strategy was ultimately fruitful.

**Scheme 5.5.1.** Diel-Alder cycloaddition to generate [2.2.2]azabicycles (**5.31**).



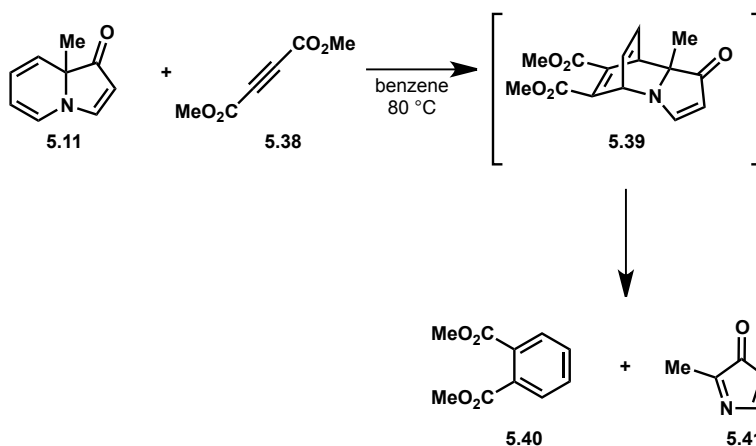
Using methylindolizinone **5.11** as a model substrate, the competency of several dienophiles was evaluated in the Diels-Alder cycloaddition. Norbornadiene (**5.32**), dimethyl fumarate (**5.34**), and cyclopropene **5.36** were each heated with methylindolizinone (**5.11**) in benzene at temperatures ranging from 80 to 100 °C (Eq 1, 2, and 3, respectively). Each of these reactions resulted in a mixture of indolizinone starting material along with multiple products.



Continuing the search for an ideal dienophile for the Diels-Alder cycloaddition with methylindolizinone (**5.11**), dimethylacetylenedicarboxylate (DMAD, **5.38**) was combined with **5.11** and heated to 80 °C in benzene for 12 hours. The sole product recovered from this reaction was a highly symmetrical aromatic compound with three peaks present in the <sup>1</sup>H NMR. The product was identified as dimethyl phthalate (**5.40**) which could arise from the retro-Diels-Alder of the anticipated product, [2.2.2]azabicycle **5.39**. Additional attempts to isolate Diels-Alder adduct **5.39** were not fruitful, but dimethyl phthalate (**5.40**) was consistently isolated as the major product.

The generation of dimethyl phthalate (**5.40**) via a retro [4+2] of **5.39** would also produce azacyclopentadienone **5.41**. Anticipating that **5.41** would be extremely reactive, we attempted to trap **5.41** with either dienes or dienophiles but were ultimately not successful in isolating any compounds derived from **5.41**.

**Scheme 5.5.2.** Diels-Alder attempt with dimethyl acetylenedicarboxylate (**5.38**).



The retro-Diels-Alder from [2.2.2]azabicycle **5.39** cautioned us against the use of alkynes as dienophiles, so we returned to alkene dienophiles that are commonly employed in the Diels-Alder reaction. Maleic anhydride rose to the top of our list of potential dienophiles as it is ideally suited electronically (low-lying LUMO) and sterically (*cis*-carbonyls tied back as an anhydride) for Diels-Alder chemistry. Heating methylindolizinone (**5.11**) with a slight excess of maleic anhydride in benzene at 80 °C for 4 hours provided [2.2.2]azabicycle **5.44** in quantitative yield (Figure 5.5.1). The Diels-Alder reaction between indolizinones and maleic anhydride proved to be a robust reaction with a variety of indolizinone starting materials. High yields of [2.2.2] azabicyclic products were obtained with crude products only contaminated with traces of maleic anhydride and maleic acid. The maleic anhydride contaminant can be minimized by using precisely one equivalent of the reagent, and the maleic acid can be removed by performing a basic wash in the work up of these reactions. In addition to tolerating a variety of substituents at the ring fusion of the indolizinone, alkyl and aryl groups on the five-membered ring do not qualitatively affect the smooth conversion of the indolizinone to the Diels-Alder adduct (Table Figure 5.5.1). Tricyclic indolizinone **5.27** provided an extra challenge in the Diels-Alder reaction, where a productive cycloaddition would join the indolizinone with the anhydride through two carbon-carbon bonds and generate two quaternary centers. In practice, this Diels-Alder proceeded without event to give pentacycle **5.49** in 88% yield.

It is noteworthy that in all cases, the Diels-Alder reaction between an indolizinone and maleic anhydride provided a single diastereomer of the [2.2.2]azabicyclic product. While subsequent studies (see Chapter 6.3) have confirmed the *syn* relationship between the two-carbon unsaturated bridge and the ring fusion substituent, the orientation of the cyclic anhydride remains unknown. An *endo*-transition state would lead to products of the stereochemistry depicted in Figure 5.5.1; whereas, an *exo*-transition state would yield [2.2.2]bicycles with the unsaturated two-carbon bridge and cyclic anhydride in an *anti* relationship (**5.50**, Figure 5.5.2).

**Figure 5.5.1.** Diels-Alder cycloadditions with maleic anhydride.

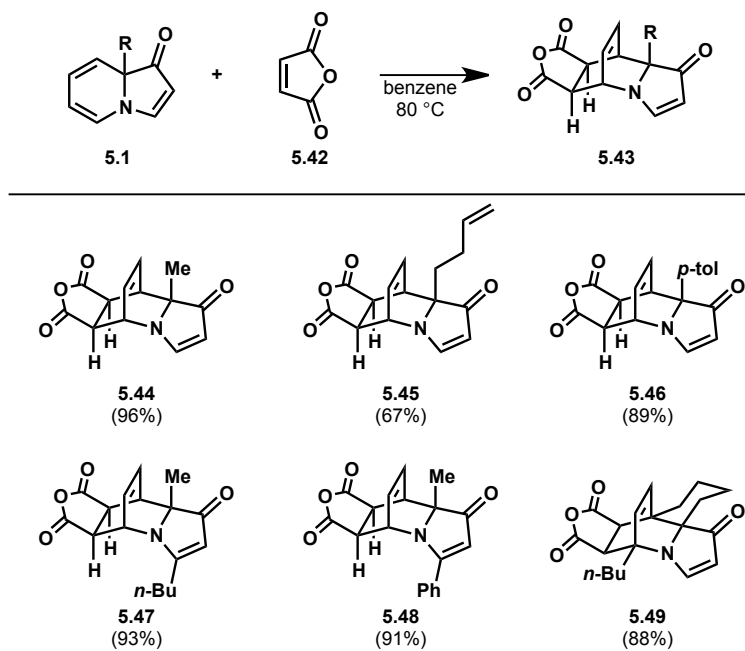
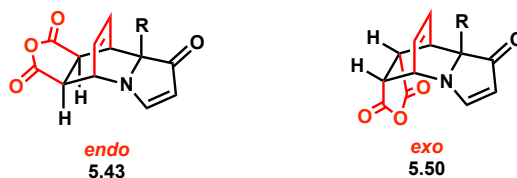


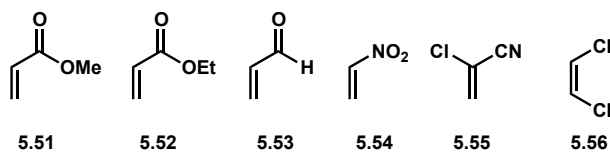
**Figure 5.5.2.** Potential diastereomers from the Diels-Alder with maleic anhydride.



It is also possible that instead of a traditional concerted Diels-Alder transition state, this [2.2.2]bicyclic could arise by a stepwise process which commences with the nucleophilic attack of the indolizinone dienamine on maleic anhydride followed by formation of the second carbon-carbon bond through attack of the generated enolate into the iminium ion to provide the observed product.

In addition to maleic anhydride, several other dienophiles were successful partners with indolizinones in the thermal Diels-Alder cycloadditions, including methyl acrylate, ethyl acrylate, acrolein, nitroethylene, 2-chloroacrylonitrile, and *cis*-1,2-dichloroethylene.

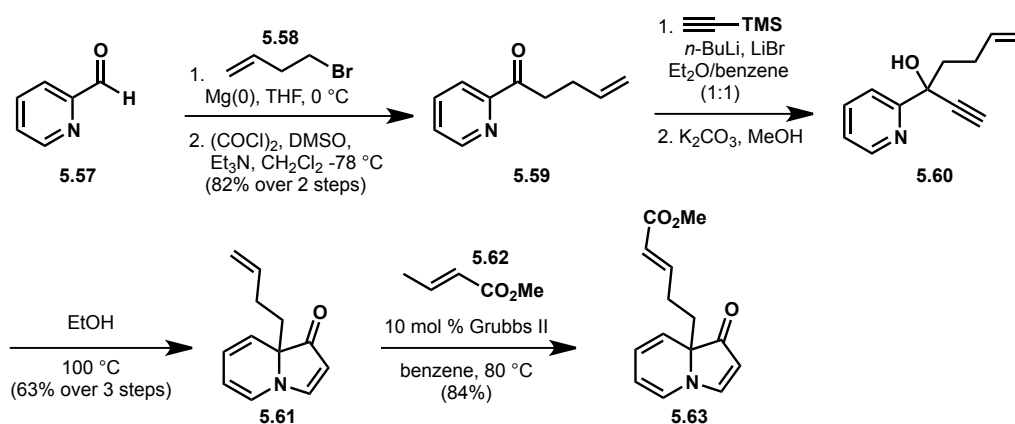
**Figure 5.5.3.** Dienophiles.





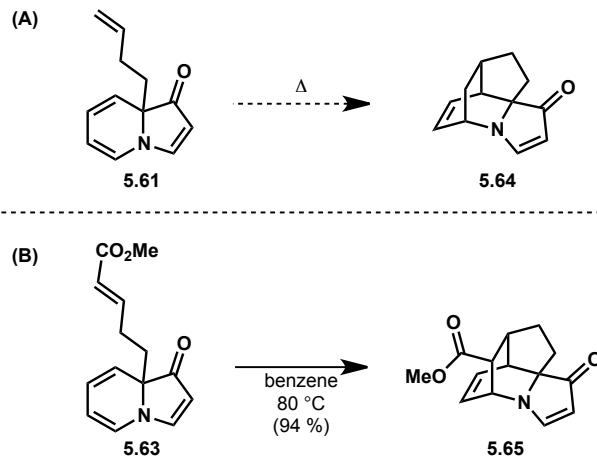
Intrigued by the ability to rapidly build complexity from indolizinone building blocks through Diels-Alder cycloadditions, we envisioned employing an intramolecular [4+2] cycloaddition to assemble a highly caged skeleton. To this end, we devised two indolizinone substrates which possessed an internal dienophile: homoallylindolizinone **5.61** and ester **5.63**. Homoallylindolizinone **5.61** was synthesized in five steps, from 2-pyridinecarboxaldehyde (**5.57**), which are outlined in Scheme 5.5.3. Heating **5.61** in benzene at 80 °C or in toluene at temperatures up to 120 °C resulted only in recovery of the starting material (Scheme 5.5.4). Presumably, the [4+2] cycloaddition does not occur because **5.61** is not equipped with a double bond electronically suited for the Diels-Alder reaction. To access a substrate with an electron deficient dienophile, homoallylindolizinone **5.61** was converted to  $\alpha,\beta$ -unsaturated ester **5.63** via cross metathesis with methyl crotonate mediated by the Grubbs II catalyst. Prior to attempting the cross metathesis with methyl crotonate, methyl and ethyl acrylate were used but proved to be unsuccessful for this cross metathesis. They returned the unmodified starting material with only trace amounts of the desired cross metathesis product (**5.63**). This result is consistent with literature reports of sluggish metathesis reactions with  $\beta$ -unsubstituted acrylates.<sup>9</sup>

**Scheme 5.5.3.** Synthesis of intramolecular Diels-Alder substrates.



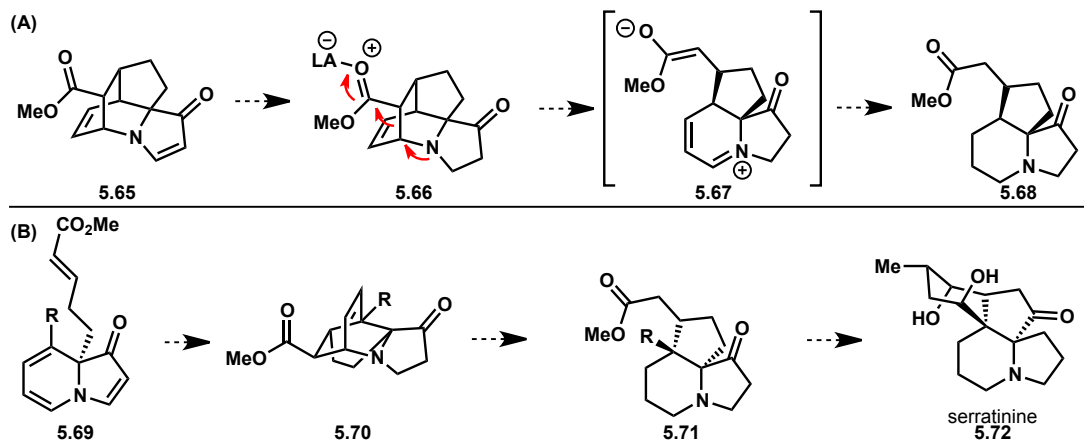
With  $\alpha,\beta$ -unsaturated ester **5.63** in hand, we possessed a compound with both an electron-rich diene and an electron-poor dienophile, which should be ideal for an intramolecular Diels-Alder reaction. We anticipated that the intramolecular Diels-Alder could be challenging as the desired product contains a [2.2.2]bicycle with two additional fused five-membered rings. Despite the strain inherent in the desired product, heating **5.63** in benzene at 80 °C for 12 hours led to the desired [2.2.2]bicycle **5.65**, which was isolated in 84% yield by simply concentrating the reaction mixture (Scheme 5.5.4). The intramolecular Diels-Alder led to a product with a different stereochemical relationship between the C-9 ring-fusion substituent and the unsaturated two-carbon bridge as compared to the intermolecular reaction. The tethered dienophile can only approach the diene from the same face of the molecule, resulting in an *anti* relationship between the unsaturated two-carbon bridge and the ring-fusion substituent.

**Scheme 5.5.4.** Intramolecular Diels-Alder cycloadditions.



The highly caged skeleton (see **5.65**) generated in the intramolecular Diels-Alder reaction is unprecedented in both known natural products and the greater chemical literature; however, this polycycle may provide rapid access to indolizidine alkaloids such as serratinine (Scheme 5.5.5, **5.72**) via rupture of a carbon-carbon bond. For example, from the Diels-Alder product **5.65**, reduction of the vinylogous amide double bond would give the tertiary amine **5.66**. With the nitrogen lone-pair free from conjugation with the carbonyl, activation of the ester with a Lewis acid could induce iminium ion formation and concomitant carbon-carbon cleavage (see **5.66**  $\rightarrow$  **5.67**). Reduction of iminium ion **5.67** would give tricycle **5.68**, which possesses a *cis*-fused five-membered ring. This 5,6,5-tricycle (**5.68**) contains three of the four rings of serratinine (**5.72**). In order to arrive at the natural product, a more substituted Diels-Alder substrate is required. To this end, an indolizinone substituted at C-8 (**5.69**), with a functional handle that could be employed in the formation of the final six-membered ring, would serve as the Diels-Alder substrate. From indolizinone **5.69**, Diels-Alder cycloaddition followed by reduction and carbon-carbon bond cleavage would provide tricycle **5.71**, a precursor to the Lycopodium alkaloid, serratinine (**5.72**)

**Scheme 5.5.5.** (A) Proposed fragmentation of [2.2.2]bicycle; (B) Proposed application of intramolecular Diels-Alder cycloaddition to the synthesis of serratinine (**5.72**).



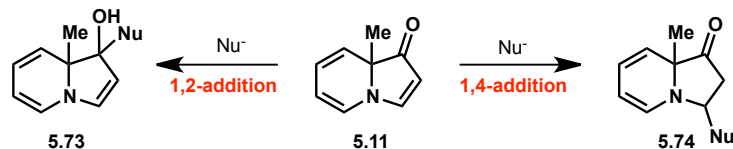
## 5.6 Chemistry of the Vinylogous Amide

Our initial exploration of the reactivity of indolizinones unveiled chemistry of the diene moiety including its nucleophilic nature as well as its competence in Diels-Alder reactions; however, the vinylogous amide was left untouched under the vast majority of the reaction conditions. We, therefore, were interested in learning (1) which nucleophiles would add to this moiety, (2) the conditions necessary for successful additions to the vinylogous amide, and (3) to which position nucleophiles would add. To answer these questions, we first focused our efforts on two classes of nucleophiles: Grignard reagents and hydride sources, which are both discussed, herein.

Methylindolizinone (**5.11**) was chosen as a model substrate for the investigation of the vinylogous amide reactivity due to its accessibility and lack of extraneous functional groups. A series of experiments wherein methylindolizinone (**5.11**) was treated with Grignard reagents in THF or diethyl ether at temperatures ranging from -78 to -42 °C resulted in the recovery of the indolizinone starting material. At temperatures above -42 °C, only complex mixtures of extremely polar products were obtained. Treatment of methylindolizinone (**5.11**) with a variety of hydride sources including sodium borohydride, diisobutylaluminum hydride, and triethylsilane were not effective in accomplishing clean reduction and led only to recovery of starting material or the isolation of an unidentifiable mixture of products.

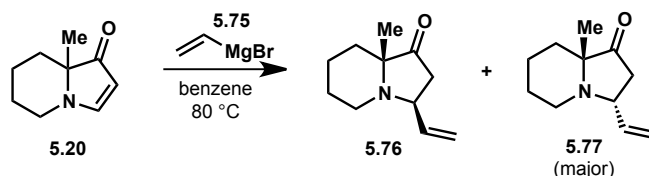
These unfruitful attempts to add nucleophiles to the indolizinone vinylogous amide led us to think more critically about the potential outcomes of nucleophilic addition. In one scenario, the nucleophile could add in a 1,2-fashion to the vinylogous amide to generate an allylic alcohol such as **5.73** (Scheme 5.6.1). Contemplating the stability of this product raised several red flags. The product of 1,2-addition is a trienamine, which we hypothesized could be highly reactive. The alternative reaction pathway, 1,4-addition to the vinylogous amide, would result in dienamine **5.74**. Although we anticipated dienamine **5.74** could be slightly more stable than trienamine **5.73**, similar undesired reactions would be possible from this product as well.

**Scheme 5.6.1.** Potential products of nucleophilic addition to the vinylogous amide.



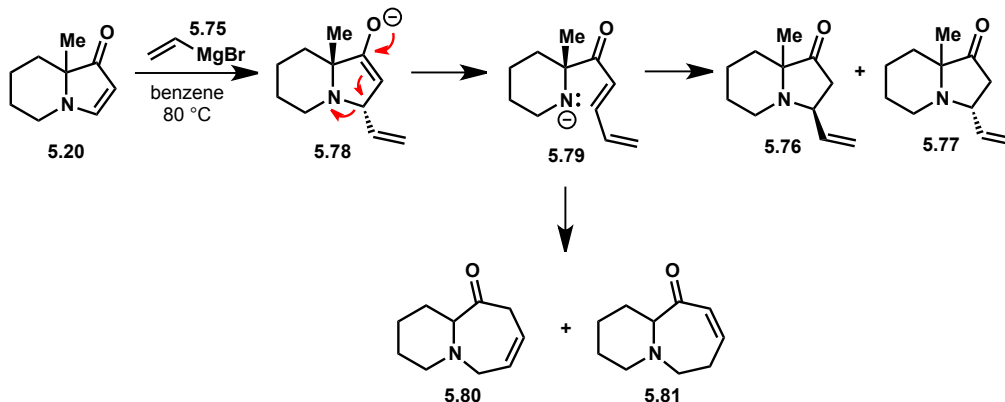
With some understanding of the challenges associated with nucleophilic additions to indolizinones, we sought to isolate the vinylogous amide in order to study its chemistry. Methylindolizinone (**5.11**) was hydrogenated to provide vinylogous amide **5.20**. Upon treatment of **5.20** with vinylmagnesium bromide at temperatures ranging from  $-78\text{ }^{\circ}\text{C}$  to ambient temperature, the starting material was recovered. However, when several equivalents of Grignard reagent were employed in conjunction with increased reaction temperatures, the 1,4-addition product was obtained as a mixture of diastereomers (**5.76** and **5.77**, Scheme 5.6.2). The major diastereomer was established to possess a *trans* relationship between the ring-fusion methyl group and the newly added vinyl substituent through nOe experiments (see **5.77**).

**Scheme 5.6.2.** Grignard addition to vinylogous amide **5.20**.



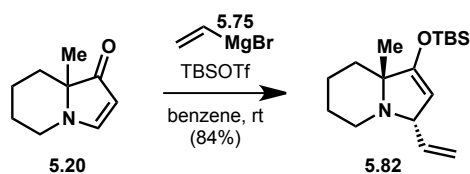
Addition from the more sterically accessible face of the vinylogous amide, opposite the methyl group at C-9 was expected, which would provide a single diastereomer. However, the mixture of diastereomers indicated that one of the two following scenarios was occurring: (1) the vinylmagnesium bromide was adding from both faces of the five-membered ring or (2) the enolate formed as a direct result of 1,4-addition could collapse to eliminate the amine (Scheme 5.6.3, see **5.78**  $\rightarrow$  **5.79**). In addition to isolating a mixture of diastereomers of the ketone product (**5.76** and **5.77**), a trace amount of product was obtained that did not possess a terminal vinyl group, yet contained two more carbon atoms than vinylogous amide **5.20**.  $^1\text{H}$  NMR data for this minor product suggests a mixture of similar products, which were assigned as 6,7-bicycles **5.80** and **5.81** that differ only in the position of the double bond contained within the seven-membered ring. Mechanistically, the seven-membered ring could form from the ring-opened intermediate **5.79** by 1,6-addition of the amide to form the seven-membered ring.

**Scheme 5.6.3.** Potential mechanism for erosion of diastereoselectivity in conjugate addition.



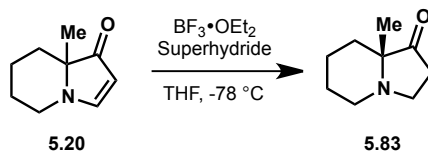
In order to understand the root of the poor diastereoselectivity observed in the addition to the vinylogous amide, we sought to trap the enolate (**5.78**). In the event the enolate was leading to fragmentation of the five-membered ring, trapping the enolate could avoid racemization of the stereocenter created upon nucleophilic addition. If instead the lack of diastereoselectivity stemmed from a lack of facial selectivity in the addition, the same mixture of diastereomers should be obtained when the enolate is trapped. In practice, the addition of TBSOTf to the reaction mixture successfully intercepted the enolate and led to a single diastereomer of silyl enol ether **5.82** (Scheme 5.6.4). The TBSOTf had two effects on this transformation: (1) a single diastereomer of the product could be obtained and (2) the activation of the vinylogous amide by the TBSOTf made it possible for the nucleophile to add at lower temperatures.

**Scheme 5.6.4.** Activation and trapping with TBSOTf.



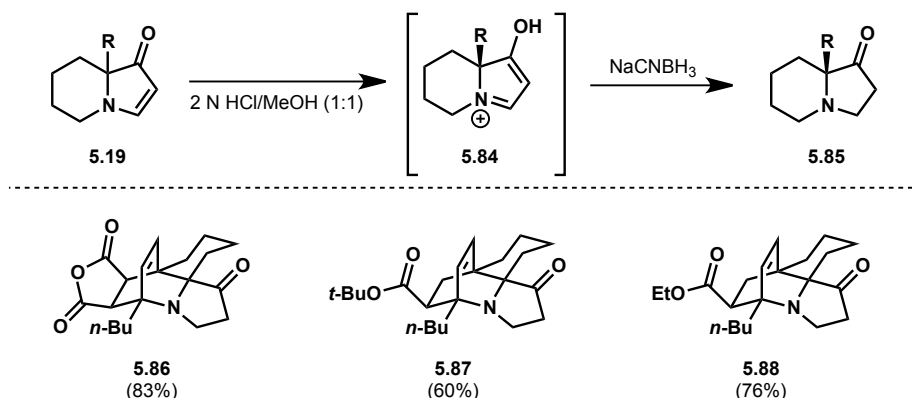
Similar to the addition of carbon nucleophiles, hydrides also add in a conjugate fashion to the vinylogous amide. To achieve synthetically useful yields of reduced product, it was necessary to first activate the vinylogous amide to increase its electrophilicity. A variety of Lewis acids were screened for this purpose. In addition to silylating reagents such as TBSOTf and TMSOTf that provide silyl enol ether products, boron trifluoride diethyl etherate was also sufficient for amide activation. In parallel with the Lewis acid screen, a variety of hydride sources were evaluated for the conjugate reduction of the vinylogous amide. DIBAL-H, Superhydride, and L-Selectride were competent in this reduction in the presence of an exogenous Lewis acid. Superhydride provided the highest and most reproducible yields.

**Scheme 5.6.5.** Conjugate reduction of the vinylogous amide.



Further experimentation, within the context of the synthesis of lepadiformine C (Chapter 6.4), unveiled conditions for the selective reduction of the vinylogous amide in the presence of esters, anhydrides, and ketones. Under strongly acidic conditions, the vinylogous amide was reduced by  $\text{NaCNBH}_3$  (Scheme 5.6.6). This reagent, famous for its ability to reduce iminium ions formed in reductive aminations over the carbonyls contained within the starting materials, can competently deliver a hydride to the iminium ion (**5.84**) formed upon treatment of the vinylogous amide with 2 N HCl.

**Scheme 5.6.6.** Reduction of the vinylogous amide with sodium cyanoborohydride.



## 5.7 Conclusions

Exploration of the innate reactivity of indolizinones has uncovered several regio- and stereoselective reactions. We have just begun to uncover the types of reactions that indolizinones readily undergo. Specifically, the indolizinone diene can be brominated, hydrogenated, or engaged in a Diels-Alder cycloaddition. The vinylogous amide has proven to be significantly less reactive, requiring activation for the addition of nucleophiles to proceed.

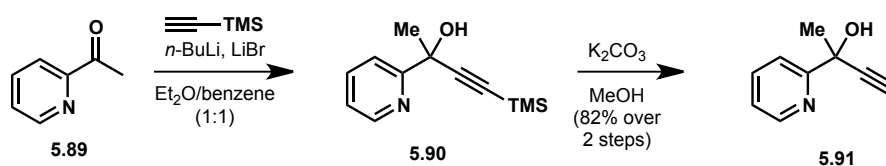
Beyond teaching us about the reactivity of indolizinones, we anticipate that the reactions discussed herein, will set the stage for the synthesis of complex molecules from indolizinone building blocks. We will specifically apply this knowledge to the synthesis of indolizidine alkaloids, but these unique molecules hold promise across a broad range of fields from materials to medicine.

## 5.8 Experimental Contributions

Alison Hardin Narayan carried out the research detailed in Chapter 5.

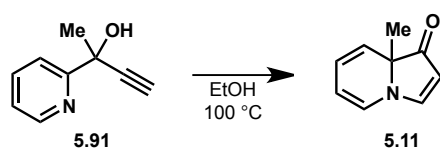
## 5.9 Experimental Methods

Unless otherwise stated, reactions were performed in flame-dried glassware fitted with rubber septa under a nitrogen atmosphere and were stirred with Teflon-coated magnetic stirring bars. Liquid reagents and solvents were transferred via syringe using standard Schlenk techniques. Tetrahydrofuran (THF), diethyl ether, benzene, toluene, and triethylamine were dried over alumina under a nitrogen atmosphere in a GlassContour solvent system. Dichloromethane (DCM) was distilled over calcium hydride. All other solvents and reagents were used as received unless otherwise noted. Reaction temperatures above 23 °C refer to oil or sand bath temperatures, which were controlled by an OptiCHEM temperature modulator. Thin layer chromatography was performed using SiliCycle silica gel 60 F-254 precoated plates (0.25 mm) and visualized by UV irradiation and anisaldehyde or potassium permanganate stain. SiliCycle Silica-P silica gel (particle size 40-63  $\mu\text{m}$ ) was used for flash chromatography.  $^1\text{H}$  and  $^{13}\text{C}$  NMR spectra were recorded on Bruker AVB-400, DRX-500, AV-500 and AV-600 MHz spectrometers with  $^{13}\text{C}$  operating frequencies of 100, 125, 125, and 150 MHz, respectively. Chemical shifts ( $\delta$ ) are reported in ppm relative to the residual solvent signal ( $\text{CDCl}_3$ ;  $\delta = 7.26$  for  $^1\text{H}$  NMR and  $\delta = 77.0$  for  $^{13}\text{C}$  NMR;  $\text{C}_6\text{D}_6$ ;  $\delta = 7.15$  for  $^1\text{H}$  NMR and  $\delta = 128.39$  for  $^{13}\text{C}$  NMR). Data for  $^1\text{H}$  NMR spectra are reported as follows: chemical shift (multiplicity, coupling constants, number of hydrogens). Abbreviations are as follows: s (singlet), d (doublet), t (triplet), dd (doublet of doublets), m (multiplet), br (broad). IR spectra were recorded on a Nicolet MAGNA-IR 850 spectrometer and are reported in frequency of absorption ( $\text{cm}^{-1}$ ). Only selected IR absorbencies are reported. High resolution mass spectral data were obtained from the Mass Spectral Facility at the University of California, Berkeley.

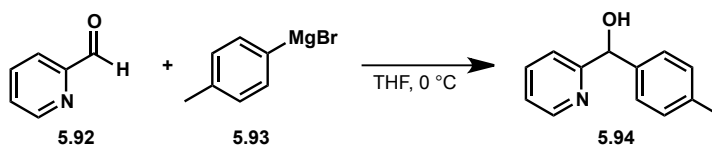


**Tertiary alcohol 5.91:** *n*-Butyllithium (5.60 mL, 14.0 mmol, 2.5 M in hexanes) was added dropwise to trimethylsilylacetylene (2.14 mL, 15.0 mmol) in Et<sub>2</sub>O (10.0 mL) at 0 °C, and the resulting mixture was stirred for 30 min at this temperature. The lithium acetylide solution was added dropwise to a vigorously stirred mixture of 2-acetylpyridine (**5.89**) (1.12 mL, 10.0 mmol) and lithium bromide (2.60 g, 30.0 mmol) in a 1:1 mixture of Et<sub>2</sub>O and benzene (total volume = 60.0 mL). The reaction mixture was stirred at ambient temperature for 12 h at which point a saturated  $\text{NH}_4\text{Cl}_{(\text{aq})}$  solution (30 mL) was added to quench the reaction. The aqueous layer was extracted with EtOAc (3 x 40 mL). The organic layers were combined, washed with brine, dried over  $\text{MgSO}_4$  and concentrated under reduced pressure to afford the trimethylsilyl alkyne, which

was used without further purification.  $^1\text{H NMR}$  (400 MHz,  $\text{CDCl}_3$ )  $\delta$  8.50 (s, 1H), 7.74 (s, 1H), 7.61 (d,  $J = 7.9$  Hz, 1H), 7.26 (s, 1H), 5.49 (s, 1H), 1.75 (s, 3H), 0.16 (s, 9H). Potassium carbonate (3.00 g, 21.7 mmol) was added to the crude trimethylsilyl alkyne in MeOH (100 mL), and the mixture was stirred at room temperature for 2 h. The reaction mixture was concentrated and the residue was taken up in water (30 mL) and EtOAc (30 mL). The aqueous layer was extracted with EtOAc (3 x 30 mL). The organic layers were combined, washed with brine, dried over  $\text{MgSO}_4$  and concentrated under reduced pressure to afford tertiary alcohol **5.91** in 82% yield over 2 steps (1.21 g, 8.23 mmol).  $^1\text{H NMR}$  (400 MHz,  $\text{CDCl}_3$ )  $\delta$  8.50 – 8.40 (m, 1H), 7.69 (td,  $J = 7.8, 1.7$  Hz, 1H), 7.57 (d,  $J = 8.0$  Hz, 1H), 7.24 – 7.15 (m, 1H), 5.53 (s, 1H), 2.51 (s, 1H), 1.73 (s, 3H);  $^{13}\text{C NMR}$  (101 MHz,  $\text{CDCl}_3$ )  $\delta$  161.2, 147.3, 137.3, 122.7, 119.7, 86.9, 71.8, 68.3, 31.7; **HRMS** (EI+) calcd for  $[\text{C}_9\text{H}_9\text{NO}]$ :  $m/z$  147.0684, found 147.0684.

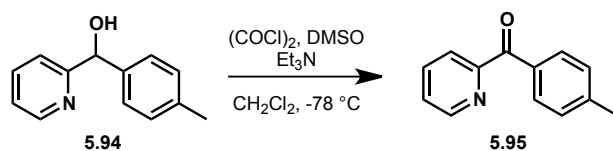


**Methyl indolizinone 5.11:** A solution of the tertiary alcohol (77.0 mg, 0.523 mmol) in EtOH (500  $\mu\text{L}$ ) was sparged with  $\text{N}_2$  for 5 min. The reaction vessel, a 4 mL vial, was equipped with a green Teflon-lined cap and Teflon tape and heated at 100  $^\circ\text{C}$  for 4 h. The reaction mixture was cooled to room temperature and concentrated to provide indolizinone **5.11** in 97% yield (75.0 mg, 0.507 mmol).  $^1\text{H NMR}$  (600 MHz,  $\text{CDCl}_3$ )  $\delta$  7.75 (d,  $J = 3.6$  Hz, 1H), 6.36 (d,  $J = 7.0$  Hz, 1H), 5.86 (dt,  $J = 23.6, 7.3$  Hz, 2H), 5.40 (t,  $J = 6.2$  Hz, 1H), 5.05 (d,  $J = 3.6$  Hz, 1H), 1.31 (s, 3H);  $^{13}\text{C NMR}$  (151 MHz,  $\text{CDCl}_3$ )  $\delta$  204.5, 159.3, 124.5, 123.0, 122.0, 108.2, 97.6, 66.8, 24.3; **HRMS** (ESI+) calcd for  $[\text{C}_9\text{H}_{10}\text{ON}]^+$  (M-H) $^+$ :  $m/z$  148.0757, found 148.0757.

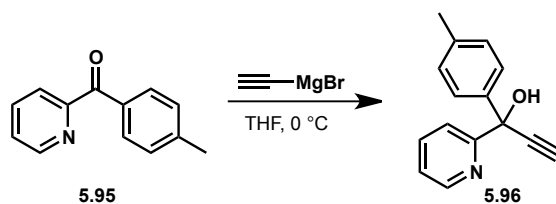


**Secondary alcohol 5.94:** *p*-tolylmagnesium bromide (5.50 mL, 5.50 mmol, 1.0 M) was added to pyridine-2-carboxaldehyde (478  $\mu\text{L}$ , 5.00 mmol) in THF (50 mL) at 0  $^\circ\text{C}$ . After 1 h, the reaction was quenched by the addition of a saturated  $\text{NH}_4\text{Cl}_{(\text{aq})}$  solution (30 mL). The aqueous layer was extracted with EtOAc (3 x 30 mL). The organic layers were combined, washed with brine, dried over  $\text{MgSO}_4$  and concentrated under reduced pressure to afford secondary alcohol **5.94** in 86% yield (862 mg, 4.33 mmol).  $^1\text{H NMR}$  (500 MHz,  $\text{CDCl}_3$ )  $\delta$  10.09 (d,  $J = 0.7$  Hz, 1H), 8.56 (d,  $J = 4.9$  Hz, 1H), 7.62 (td,  $J = 7.7, 1.5$  Hz, 1H), 7.29 – 7.24 (m, 2H), 7.19 (dd,  $J = 7.2, 5.1$  Hz, 1H), 7.15 (t,  $J = 7.8$  Hz, 3H), 5.74 (s, 1H), 2.32 (s, 3H); **HRMS** (ESI+) calcd for  $[\text{C}_{13}\text{H}_{14}\text{ON}]^+$  (M-H) $^+$ :  $m/z$  200.1070, found 200.1068.

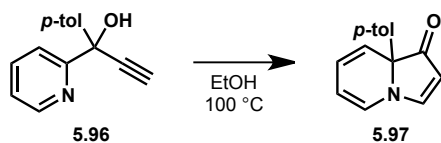




**Ketone 5.95:** DMSO (1.23 mL, 17.3 mmol) was added dropwise to oxalyl chloride (755  $\mu$ L, 8.66 mmol) in  $\text{CH}_2\text{Cl}_2$  (25 mL) at  $-78\text{ }^\circ\text{C}$ . After 30 min, alcohol **5.94** (862 mg, 4.33 mmol) in  $\text{CH}_2\text{Cl}_2$  (5.0 mL) was added dropwise at  $-78\text{ }^\circ\text{C}$ . The reaction mixture was stirred for 30 min at this temperature.  $\text{Et}_3\text{N}$  (4.80 mL, 34.6 mmol) was added at  $-78\text{ }^\circ\text{C}$ . The cold bath was allowed to gradually expire as the reaction mixture was stirred for 4 h. The reaction was quenched with water (30 mL). The aqueous layer was extracted with  $\text{CH}_2\text{Cl}_2$  (2 x 30 mL). The combined organic layer was washed with water, dried over  $\text{MgSO}_4$  and concentrated to afford a brown oil. The crude oil was purified via flash chromatography (4:1 hexanes/ $\text{EtOAc}$ ) to provide **5.95** as a yellow oil in 58% yield (493 mg, 2.49 mmol).  $^1\text{H NMR}$  (400 MHz,  $\text{CDCl}_3$ )  $\delta$  8.70 (d,  $J = 4.7$  Hz, 1H), 7.98 (dd,  $J = 13.7, 8.0$  Hz, 3H), 7.88 (dd,  $J = 7.7, 1.7$  Hz, 1H), 7.48 – 7.43 (m, 1H), 7.26 (t,  $J = 6.1$  Hz, 2H), 2.41 (s, 3H);  $^{13}\text{C NMR}$  (101 MHz,  $\text{CDCl}_3$ )  $\delta$  193.5, 155.4, 148.4, 143.8, 137.0, 133.6, 131.2, 128.8, 125.9, 124.5, 21.7; **HRMS** (ESI+) calcd for  $[\text{C}_{13}\text{H}_{12}\text{ON}]^+$  (M-H) $^+$ :  $m/z$  198.0913, found 198.0913.

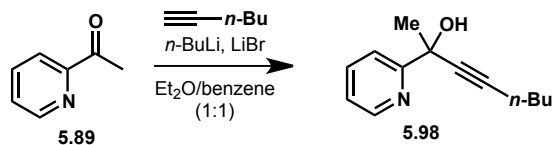


**Tertiary alcohol 5.96:** Ethynylmagnesium bromide (5.20 mL, 2.62 mmol, 2.5 M in THF) was added dropwise to ketone **5.95** (470 mg, 2.38 mmol) in THF (20.0 mL) at  $0\text{ }^\circ\text{C}$ . The reaction mixture was stirred for 1.5 h at which point the reaction was quenched by the addition of a saturated  $\text{NH}_4\text{Cl}_{(\text{aq})}$  solution (30 mL). The aqueous layer was extracted with  $\text{EtOAc}$  (3 x 30 mL). The organic layers were combined, washed with brine, dried over  $\text{MgSO}_4$  and concentrated under reduced pressure to afford tertiary alcohol **5.96** in 94% yield (498 mg, 2.23 mmol). **HRMS** (ESI+) calcd for  $[\text{C}_{15}\text{H}_{14}\text{ON}]^+$  (M-H) $^+$ :  $m/z$  224.1070, found 224.1068.

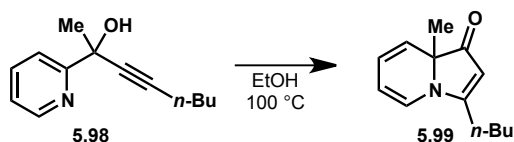


***p*-tolyl indolizinone 5.97:** A solution of the tertiary alcohol (75.5 mg, 0.339 mmol) in  $\text{EtOH}$  (500  $\mu$ L) was sparged with  $\text{N}_2$  for 5 min. The reaction vessel, a 4 mL vial, was equipped with a green Teflon-lined cap and Teflon tape and heated at  $100\text{ }^\circ\text{C}$  for 4 h. The reaction mixture was cooled to room temperature and concentrated to provide indolizinone **5.97** in 98% yield (74.0 mg, 0.332 mmol).  $^1\text{H NMR}$  (400 MHz,  $\text{CDCl}_3$ )  $\delta$  7.99 (d,  $J = 3.7$  Hz, 1H), 7.29 (d,  $J = 8.2$  Hz,

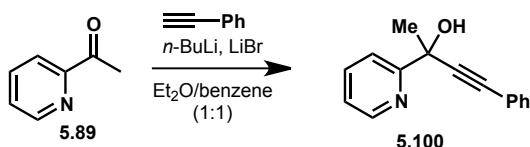
2H), 7.13 (d,  $J = 8.2$  Hz, 2H), 6.51 (d,  $J = 7.0$  Hz, 1H), 6.24 (d,  $J = 9.3$  Hz, 1H), 6.00 (dd,  $J = 9.3, 5.5$  Hz, 1H), 5.40 (s, 1H), 5.07 (d,  $J = 3.7$  Hz, 1H), 2.30 (s, 3H);  $^{13}\text{C}$  NMR (101 MHz,  $\text{CDCl}_3$ )  $\delta$  202.6, 161.1, 137.7, 136.5, 129.3, 125.6, 124.3, 122.9, 122.2, 109.2, 98.3, 70.4, 21.0; HRMS (ESI+) calcd for  $[\text{C}_{15}\text{H}_{14}\text{ON}]^+$  (M-H) $^+$ :  $m/z$  224.1070, found 224.1070.



**Internal alkyne 5.98:** *n*-Butyllithium (5.60 mL, 14.0 mmol, 2.5 M in hexanes) was added dropwise to 1-hexyne (1.12 mL, 15.0 mmol) in  $\text{Et}_2\text{O}$  (10.0 mL) at 0 °C, and the resulting mixture was stirred for 30 min at this temperature. The lithium acetylide solution was added dropwise to a vigorously stirred mixture of 2-acetylpyridine (**5.89**) (1.12 mL, 10.0 mmol) and lithium bromide (2.60 g, 30.0 mmol) in a 1:1 mixture of  $\text{Et}_2\text{O}$  and benzene (total volume = 60.0 mL). The reaction mixture was stirred at ambient temperature for 12 h at which point a saturated  $\text{NH}_4\text{Cl}_{(\text{aq})}$  solution (30 mL) was added to quench the reaction. The aqueous layer was extracted with  $\text{EtOAc}$  (3 x 40 mL). The organic layers were combined, washed with brine, dried over  $\text{MgSO}_4$  and concentrated under reduced pressure to afford alkyne **5.98** in 83% yield (1.68 g, 8.28 mmol), which was used without further purification.

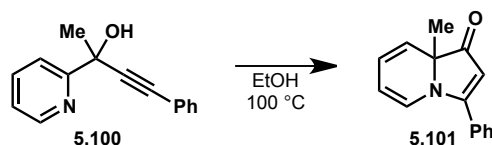


***n*-Butyl indolizinone 5.99:** A solution of the tertiary alcohol (200 mg, 0.984 mmol) in  $\text{EtOH}$  (9.0 mL) was sparged with  $\text{N}_2$  for 5 min. The reaction vessel, a 20 mL vial, was equipped with a green Teflon-lined cap and Teflon tape and heated at 100 °C for 4 h. The reaction mixture was cooled to room temperature and concentrated to provide indolizinone **5.99** in 98% yield (196 mg, 0.964 mmol).  $^1\text{H}$  NMR (600 MHz,  $\text{CDCl}_3$ )  $\delta$  6.43 (d,  $J = 7.1$  Hz, 1H), 5.89 (d,  $J = 4.2$  Hz, 2H), 5.45 (s, 1H), 4.93 (s, 1H), 2.50 – 2.45 (m, 2H), 1.64 (s, 2H), 1.43 (d,  $J = 7.5$  Hz, 2H), 1.30 (s, 3H), 0.96 (t,  $J = 7.4$  Hz, 3H); HRMS (EI+) calcd for  $[\text{C}_{13}\text{H}_{17}\text{NO}]$ :  $m/z$  203.1310, found 203.1310.



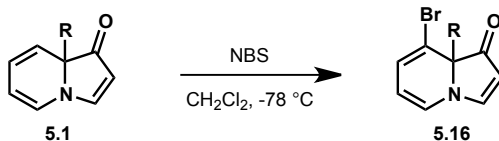
**Tertiary alcohol 5.100:** *n*-Butyllithium (5.60 mL, 14.0 mmol, 2.5 M in hexanes) was added dropwise to phenylacetylene (1.65 mL, 15.0 mmol) in  $\text{Et}_2\text{O}$  (10.0 mL) at 0 °C, and the resulting mixture was stirred for 30 min at this temperature. The lithium acetylide solution was added

dropwise to a vigorously stirred mixture of 2-acetylpyridine (**5.89**) (1.12 mL, 10.0 mmol) and lithium bromide (2.60 g, 30.0 mmol) in a 1:1 mixture of Et<sub>2</sub>O and benzene (total volume = 60.0 mL). The reaction mixture was stirred at ambient temperature for 12 h at which point a saturated NH<sub>4</sub>Cl<sub>(aq)</sub> solution (30 mL) was added to quench the reaction. The aqueous layer was extracted with EtOAc (3 x 40 mL). The organic layers were combined, washed with brine, dried over MgSO<sub>4</sub> and concentrated under reduced pressure to afford alkyne **5.100** in 98% yield (2.20 g, 9.82 mmol), which was used without further purification.

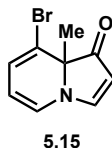


**Phenyl indolizinone 5.101:** A solution of the tertiary alcohol (200 mg, 0.896 mmol) in EtOH (9.0 mL) was sparged with N<sub>2</sub> for 5 min. The reaction vessel, a 20 mL vial, was equipped with a green Teflon-lined cap and Teflon tape and heated at 100 °C for 4 h. The reaction mixture was cooled to room temperature and concentrated to provide indolizinone **5.101** in 98% yield (196 mg, 0.878 mmol). <sup>1</sup>H NMR (500 MHz, CDCl<sub>3</sub>) δ 7.51 (s, 6H), 6.53 (d, *J* = 7.3 Hz, 1H), 5.97 – 5.89 (m, 2H), 5.38 (s, 1H), 5.18 (s, 1H), 1.45 (s, 3H); HRMS (ESI+) calcd for [C<sub>15</sub>H<sub>14</sub>ON]<sup>+</sup> (M-H)<sup>+</sup>: *m/z* 224.1070, found 224.1070.

#### Representative procedure for the bromination of indolizinones:

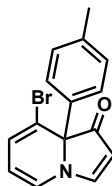


A solution of the indolizinone (**5.11**) (10.0 mg, 0.0679 mmol) in CH<sub>2</sub>Cl<sub>2</sub> (600 μL) was cooled to -78 °C in a dry ice/acetone bath. *N*-bromosuccinimide (14.5 mg, 0.0815 mmol) was added in one portion to the cooled solution. The reaction mixture was stirred at -78 °C for five minutes; then, a saturated solution of Na<sub>2</sub>SO<sub>3(aq)</sub> was added (1 mL). The biphasic mixture was removed from the cold bath and allowed to warm to ambient temperature. The reaction mixture was extracted with CH<sub>2</sub>Cl<sub>2</sub> (3 x 1 mL). The organic layers were combined, washed with brine, dried over MgSO<sub>4</sub> and concentrated to give an intensely yellow oil. Flash chromatography afforded 8-bromo-9-methylindolizinone (**5.15**, 9.7 mg, 0.0429 mmol) in 63% yield.



**Bromoindolizinone 5.15:** Bromination under the standard conditions afforded **5.15** in 63% yield <sup>1</sup>H NMR (600 MHz, CDCl<sub>3</sub>) δ 8.35 – 8.22 (m, 1H), 6.44 (ddd, *J* = 9.5, 6.3, 2.8 Hz, 1H),

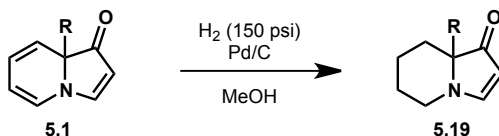
6.14 (dt,  $J = 9.3, 2.7$  Hz, 1H), 5.83 (ddd,  $J = 9.8, 4.7, 2.9$  Hz, 1H), 5.29 (d,  $J = 4.4$  Hz, 1H), 1.46 (s, 3H).



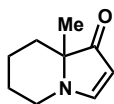
5.16

**Bromoindolizinone 5.16:** Bromination under the standard conditions afforded **5.16** in 54% yield.  $^1\text{H NMR}$  (500 MHz,  $\text{CDCl}_3$ )  $\delta$  8.68 (s, 1H), 7.08 (d,  $J = 7.8$  Hz, 2H), 7.00 (s, 2H), 6.36 – 6.31 (m, 1H), 6.07 (s, 1H), 5.91 (d,  $J = 9.9$  Hz, 1H), 5.41 (d,  $J = 6.2$  Hz, 1H), 2.30 (s, 3H).

#### Representative procedure for the partial hydrogenation of indolizinones:

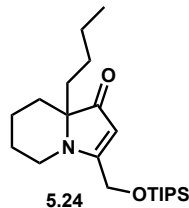


Palladium (10 wt %) on activated carbon was added to a solution on methylindolizinone **5.11** (10.0 mg, 0.0679 mmol) in methanol (600  $\mu\text{L}$ ). The mixture was stirred vigorously under an atmosphere of hydrogen (200 psi) in a Parr bomb for 12 h. The reaction mixture was filtered through a plug of celite and concentrated to provide **5.19** as a light yellow oil in 98% yield (10.1 mg, 0.0668 mmol).  $^1\text{H NMR}$  (600 MHz,  $\text{CDCl}_3$ )  $\delta$  7.71 (d,  $J = 3.0$  Hz, 1H), 5.04 (d,  $J = 3.1$  Hz, 1H), 3.55 (dd,  $J = 13.4, 5.0$  Hz, 1H), 3.37 (td,  $J = 13.2, 3.2$  Hz, 1H), 1.82 (d,  $J = 13.6$  Hz, 1H), 1.79 – 1.71 (m, 3H), 1.65 (dd,  $J = 13.4, 3.2$  Hz, 2H), 1.40 – 1.29 (m, 3H), 1.26 (s, 3H).  $^{13}\text{C NMR}$  (151 MHz,  $\text{CDCl}_3$ )  $\delta$  207.44, 161.65, 94.60, 65.43, 46.47, 32.64, 27.95, 19.81, 17.15.

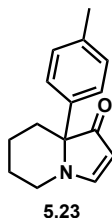


5.20

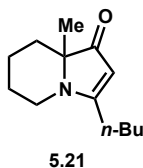
**Vinylogous amide 5.20:** The standard hydrogenation protocol afforded **5.20** in 98% yield.  $^1\text{H NMR}$  (600 MHz,  $\text{CDCl}_3$ )  $\delta$  7.71 (d,  $J = 3.0$  Hz, 1H), 5.04 (d,  $J = 3.1$  Hz, 1H), 3.55 (dd,  $J = 13.4, 5.0$  Hz, 1H), 3.37 (td,  $J = 13.2, 3.2$  Hz, 1H), 1.82 (d,  $J = 13.6$  Hz, 1H), 1.79 – 1.71 (m, 3H), 1.65 (dd,  $J = 13.4, 3.2$  Hz, 2H), 1.40 – 1.29 (m, 3H), 1.26 (s, 3H).  $^{13}\text{C NMR}$  (151 MHz,  $\text{CDCl}_3$ )  $\delta$  207.44, 161.65, 94.60, 65.43, 46.47, 32.64, 27.95, 19.81, 17.15.



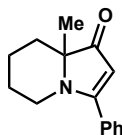
**Vinyllogous amide 5.24:** The standard hydrogenation protocol afforded **5.24** in 78% yield.  $^1\text{H}$  NMR (600 MHz,  $\text{CDCl}_3$ )  $\delta$  5.14 (s, 1H), 4.56 (s, 2H), 3.89 (s, 1H), 3.79 (d,  $J = 12.0$  Hz, 1H), 3.46 (s, 2H), 3.07 (s, 1H), 1.91 – 1.76 (m, 4H), 1.76 – 1.59 (m, 6H), 1.38 (d,  $J = 4.1$  Hz, 4H), 1.22 (dd,  $J = 15.7, 7.7$  Hz, 3H), 1.13 (dd,  $J = 14.3, 7.1$  Hz, 3H), 1.10 – 0.99 (m, 18H), 0.90 (d,  $J = 6.5$  Hz, 2H), 0.81 (t,  $J = 7.0$  Hz, 3H);  $^{13}\text{C}$  NMR (151 MHz,  $\text{CDCl}_3$ )  $\delta$  205.5, 174.7, 96.2, 70.5, 59.0, 42.0, 33.3, 31.0, 27.8, 24.8, 22.8, 19.8, 17.8, 13.9, 11.8.



**Vinyllogous amide 5.23:** The standard hydrogenation protocol afforded **5.23** in 94% yield.  $^1\text{H}$  NMR (600 MHz,  $\text{CDCl}_3$ )  $\delta$  7.96 (d,  $J = 3.2$  Hz, 1H), 7.18 (d,  $J = 8.1$  Hz, 2H), 7.15 (d,  $J = 8.3$  Hz, 2H), 5.01 (d,  $J = 3.2$  Hz, 1H), 3.64 (dd,  $J = 13.4, 4.9$  Hz, 1H), 3.40 – 3.34 (m, 1H), 2.66 (d,  $J = 14.2$  Hz, 1H), 2.32 (s, 3H), 1.71 (t,  $J = 15.0$  Hz, 3H), 1.62 – 1.56 (m, 1H), 1.49 (s, 1H), 1.46 – 1.39 (m, 1H).  $^{13}\text{C}$  NMR (151 MHz,  $\text{CDCl}_3$ )  $\delta$  204.9, 163.4, 137.2, 131.8, 129.8, 125.9, 94.0, 71.4, 47.0, 32.5, 28.1, 21.0, 20.3; HRMS (ESI+) calcd for  $[\text{C}_{15}\text{H}_{18}\text{ON}]^+$  (M-H) $^+$ :  $m/z$  228.1383, found 228.1383.

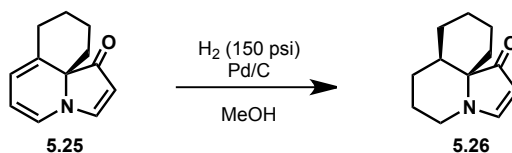


**Vinyllogous amide 5.21:** The standard hydrogenation protocol afforded **5.21** in 93% yield.  $^1\text{H}$  NMR (500 MHz,  $\text{CDCl}_3$ )  $\delta$  4.95 (s, 1H), 3.74 (dd,  $J = 13.8, 4.4$  Hz, 1H), 3.14 (d,  $J = 2.9$  Hz, 1H), 2.39 (td,  $J = 7.5, 2.8$  Hz, 2H), 1.83 (d,  $J = 13.6$  Hz, 1H), 1.78 – 1.68 (m, 2H), 1.66 (d,  $J = 13.3$  Hz, 1H), 1.56 (dd,  $J = 15.1, 7.2$  Hz, 2H), 1.40 (dd,  $J = 14.9, 7.4$  Hz, 2H), 1.36 – 1.29 (m, 2H), 1.25 (s, 3H), 0.94 (t,  $J = 7.3$  Hz, 3H).



5.22

**Vinyllogous amide 5.22:** The standard hydrogenation protocol afforded **5.22** in 99% yield.  $^1\text{H}$  NMR (500 MHz,  $\text{CDCl}_3$ )  $\delta$  7.48 (d,  $J = 4.0$  Hz, 3H), 7.41 (d,  $J = 3.9$  Hz, 2H), 5.17 (s, 1H), 3.84 (dd,  $J = 13.6, 4.1$  Hz, 1H), 3.22 (d,  $J = 2.8$  Hz, 1H), 1.93 (d,  $J = 13.4$  Hz, 1H), 1.72 (dd,  $J = 20.4, 7.5$  Hz, 2H), 1.64 (d,  $J = 14.3$  Hz, 1H), 1.52 (dd,  $J = 13.0, 4.3$  Hz, 1H), 1.39 (s, 4H), 1.24 (dt,  $J = 9.7, 4.4$  Hz, 1H).

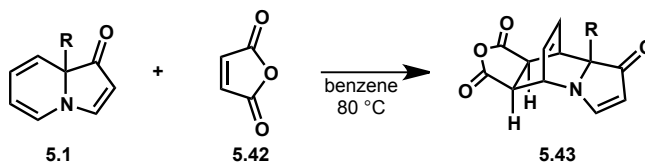


5.25

5.26

**Tricycle 5.26:** Palladium (4.0 mg, 10 wt %) on activated carbon was added to a solution of indolizininone **5.25** (4.7 mg, 0.0251 mmol) in methanol (400  $\mu\text{L}$ ). The mixture was stirred vigorously under an atmosphere of hydrogen (200 psi) in a Parr bomb for 12 h. The reaction mixture was filtered through a plug of celite and concentrated to provide **5.26** as a light yellow oil in 94% yield (4.5 mg, 0.0235 mmol).  $^1\text{H}$  NMR (600 MHz,  $\text{CDCl}_3$ )  $\delta$  7.66 (d,  $J = 3.2$  Hz, 1H), 4.98 (d,  $J = 3.1$  Hz, 1H), 3.46 (d,  $J = 4.9$  Hz, 1H), 3.29 – 3.24 (m, 1H), 2.50 (s, 2H), 2.35 (d,  $J = 13.4$  Hz, 1H), 1.87 (ddd,  $J = 17.5, 13.2, 3.8$  Hz, 1H), 1.75 (d,  $J = 12.9$  Hz, 1H), 1.65 (d,  $J = 13.0$  Hz, 1H), 1.62 – 1.51 (m, 2H), 1.48 – 1.42 (m, 2H), 1.38 (ddd,  $J = 18.6, 10.5, 6.3$  Hz, 3H);  $^{13}\text{C}$  NMR (151 MHz,  $\text{CDCl}_3$ )  $\delta$  207.7, 161.3, 95.1, 66.7, 46.0, 36.3, 27.0, 26.0, 25.5, 24.5, 19.6, 19.4; HRMS (ESI+) calcd for  $[\text{C}_{12}\text{H}_{18}\text{ON}]^+$  (M-H) $^+$ :  $m/z$  192.1383, found 192.138

**Representative procedure for the Diels-Alder cycloaddition of indolizininones with maleic anhydride:**

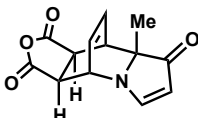


5.1

5.42

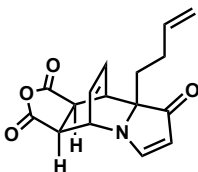
5.43

A solution of methylindolizininone **5.11** (5.0 mg, 0.0340 mmol) and maleic anhydride (4.0 mg, 0.0408 mmol) in benzene (400  $\mu\text{L}$ ) was heated to 80  $^\circ\text{C}$  for 12 h in a 4 mL vial equipped with a green Teflon-lined cap and Teflon tape. The reaction mixture was cooled and concentrated to provide a light yellow oil.



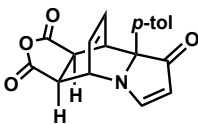
5.44

**[2.2.2]bicycle 5.44:** The standard Diels-Alder protocol afforded **5.44** in 96% yield.  $^1\text{H NMR}$  (600 MHz,  $\text{C}_6\text{D}_6$ )  $\delta$  7.71 (d,  $J = 3.5$  Hz, 1H), 6.46 (dd,  $J = 5.0, 2.5$  Hz, 2H), 5.56 (d,  $J = 3.6$  Hz, 1H), 4.70 (d,  $J = 2.2$  Hz, 1H), 3.46 (d,  $J = 2.5$  Hz, 1H), 3.19 (dd,  $J = 8.6, 4.4$  Hz, 1H), 3.02 – 2.98 (m, 1H), 1.06 (s, 3H);  $^{13}\text{C NMR}$  (151 MHz,  $\text{C}_6\text{D}_6$ )  $\delta$  206.6, 170.2, 169.8, 133.6, 130.2, 128.3, 112.3, 68.9, 52.9, 44.4, 39.6, 38.6 22.9.



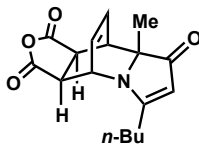
5.45

**[2.2.2]bicycle 5.45:** The standard Diels-Alder protocol afforded **5.45** in 67% yield.  $^1\text{H NMR}$  (500 MHz,  $\text{CDCl}_3$ )  $\delta$  7.89 (d,  $J = 3.5$  Hz, 1H), 6.55 (dd,  $J = 4.8, 2.5$  Hz, 2H), 5.71 (d,  $J = 3.6$  Hz, 1H), 5.63 (d,  $J = 6.7$  Hz, 1H), 4.92 (dd,  $J = 20.9, 5.3$  Hz, 2H), 4.80 (d,  $J = 2.4$  Hz, 1H), 3.60 – 3.55 (m, 1H), 3.31 (dd,  $J = 8.6, 4.4$  Hz, 1H), 3.10 (dd,  $J = 8.6, 3.1$  Hz, 1H), 1.95 – 1.86 (m, 1H), 1.73 (d,  $J = 8.3$  Hz, 2H), 1.58 (td,  $J = 12.8, 4.3$  Hz, 1H).



5.46

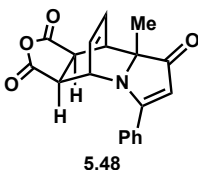
**[2.2.2]bicycle 5.46:** The standard Diels-Alder protocol afforded **5.46** in 89% yield.  $^1\text{H NMR}$  (600 MHz,  $\text{CDCl}_3$ )  $\delta$  7.98 (d,  $J = 3.5$  Hz, 1H), 7.33 (d,  $J = 8.1$  Hz, 2H), 7.09 (d,  $J = 8.1$  Hz, 2H), 6.45 (d,  $J = 7.5$  Hz, 1H), 6.16 (t,  $J = 7.1$  Hz, 1H), 5.56 (d,  $J = 3.6$  Hz, 1H), 4.95 (t,  $J = 5.2$  Hz, 1H), 4.13 (d,  $J = 3.6$  Hz, 1H), 3.47 (dd,  $J = 8.6, 4.4$  Hz, 1H), 3.33 (dd,  $J = 8.6, 2.9$  Hz, 1H), 2.29 (s, 3H);  $^{13}\text{C NMR}$  (151 MHz,  $\text{CDCl}_3$ )  $\delta$  203.8, 167.4, 164.1, 136.5, 133.4, 129.8, 129.3, 128.3, 125.6, 111.9, 72.4, 52.7, 45.2, 41.4, 38.6, 21.0.



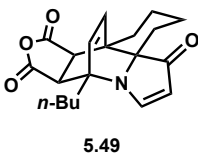
5.47

**[2.2.2]bicycle 5.47:** The standard Diels-Alder protocol afforded **5.47** in 93% yield.  $^1\text{H NMR}$  (600 MHz,  $\text{CDCl}_3$ )  $\delta$  6.57 (d,  $J = 6.8$  Hz, 1H), 6.53 (d,  $J = 6.3$  Hz, 1H), 5.50 (s, 1H), 4.86 – 4.82

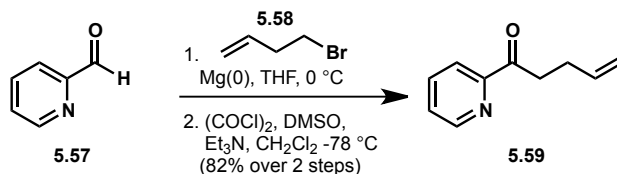
(m, 1H), 3.53 – 3.49 (m, 1H), 3.14 (dd,  $J = 16.8, 3.5$  Hz, 2H), 2.52 (d,  $J = 7.9$  Hz, 1H), 2.46 (d,  $J = 7.8$  Hz, 1H), 1.69 – 1.62 (m, 2H), 1.44 (dd,  $J = 7.4, 3.2$  Hz, 2H), 1.13 (s, 3H), 0.97 (t,  $J = 7.3$  Hz, 3H);  $^{13}\text{C}$  NMR (151 MHz,  $\text{CDCl}_3$ )  $\delta$  205.7, 170.4, 170.0, 134.1, 129.7, 128.3, 111.2, 69.8, 50.6, 42.8, 38.8, 38.7, 29.5, 29.2, 23.5, 22.4, 13.7.



**[2.2.2]bicyclic 5.48:** The standard Diels-Alder protocol afforded **5.48** in 91% yield.  $^1\text{H}$  NMR (600 MHz,  $\text{CDCl}_3$ )  $\delta$  7.66 – 7.62 (m, 2H), 7.61 (d,  $J = 7.3$  Hz, 1H), 7.56 (t,  $J = 7.4$  Hz, 2H), 6.61 (d,  $J = 6.8$  Hz, 1H), 6.56 (d,  $J = 6.3$  Hz, 1H), 5.85 (s, 1H), 4.86 – 4.82 (m, 1H), 3.62 – 3.58 (m, 1H), 3.26 (dd,  $J = 8.6, 3.1$  Hz, 1H), 3.11 (dd,  $J = 8.6, 4.2$  Hz, 1H), 1.27 (s, 3H);  $^{13}\text{C}$  NMR (151 MHz,  $\text{CDCl}_3$ )  $\delta$  205.6, 170.4, 169.9, 133.9, 132.6, 130.2, 130.2, 129.6, 128.3, 127.9, 111.3, 70.5, 52.1, 42.2, 39.2, 38.6, 23.8.



**[2.2.2]bicyclic 5.49:** The standard Diels-Alder protocol afforded **5.49** in 88% yield.  $^1\text{H}$  NMR (600 MHz,  $\text{CDCl}_3$ )  $\delta$  7.80 (d,  $J = 3.7$  Hz, 1H), 6.26 (t,  $J = 5.9$  Hz, 2H), 5.53 (d,  $J = 3.7$  Hz, 1H), 3.01 – 2.96 (m, 2H), 2.64 (dd,  $J = 13.6, 4.1$  Hz, 1H), 2.47 – 2.39 (m, 1H), 2.19 (d,  $J = 13.7$  Hz, 1H), 2.13 – 2.05 (m, 1H), 2.05 – 1.97 (m, 2H), 1.85 (d,  $J = 13.2$  Hz, 1H), 1.59 (ddd,  $J = 13.2, 10.6, 3.9$  Hz, 2H), 1.54 – 1.41 (m, 5H), 1.39 (d,  $J = 15.0$  Hz, 1H), 0.99 (t,  $J = 7.1$  Hz, 3H);  $^{13}\text{C}$  NMR (151 MHz,  $\text{CDCl}_3$ )  $\delta$  207.2, 169.7, 168.8, 162.5, 137.2, 132.0, 111.9, 70.9, 61.3, 51.7, 45.2, 45.0, 30.7, 30.7, 25.6, 25.1, 22.9, 21.2, 17.2, 14.0.

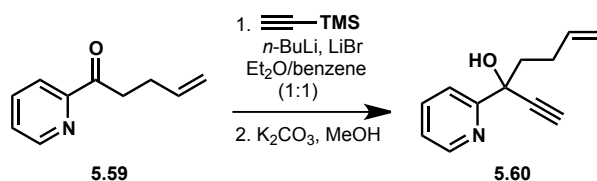


**Homoallyl alcohol:** 1-Bromo-4-butene (**5.58**, 7.61 mL, 75.0 mmol) was added dropwise to  $\text{Mg}(0)$  in THF (10 mL). Following initiation of the Grignard formation, which was marked by vigorous bubbling, an additional 10 mL of THF was added. The round bottom flask was equipped with a reflux condenser and heated to reflux (oil bath temperature =  $70^\circ\text{C}$ ) for 1 h. The Grignard solution was removed from the oil bath and cooled to room temperature, then further cooled to  $0^\circ\text{C}$  in an ice bath. The Grignard solution was diluted with THF (80 mL) and pyridine-



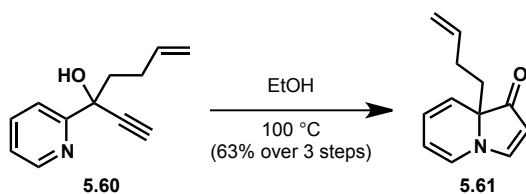
2-carboxaldehyde (**5.57**, 4.76 mL, 50 mmol) in THF (20 mL) was added dropwise over 10 min. The reaction mixture was stirred while the ice bath expired. The reaction was quenched with by addition of a saturated solution of ammonium chloride (30 mL). The mixture was extracted with EtOAc (3 x 50 mL). the organic layers were combined, washed with brine (100 mL), dried over MgSO<sub>4</sub>, and concentrated to give a brown oil. Flash chromatography (1:1 hexanes/EtOAc) provided the alcohol in 97% yield. <sup>1</sup>H NMR (400 MHz, CDCl<sub>3</sub>) δ 8.50 (d, *J* = 3.4 Hz, 2H), 7.66 (td, *J* = 7.7, 1.4 Hz, 1H), 7.28 – 7.24 (m, 2H), 7.17 (dd, *J* = 7.2, 5.1 Hz, 2H), 5.82 (ddt, *J* = 16.9, 10.2, 6.6 Hz, 1H), 5.01 (dt, *J* = 8.8, 4.4 Hz, 1H), 4.94 (dd, *J* = 10.2, 0.9 Hz, 1H), 4.77 – 4.72 (m, 2H), 2.23 – 2.12 (m, 2H), 1.90 (dddd, *J* = 13.5, 9.2, 6.9, 4.3 Hz, 1H), 1.81 – 1.71 (m, 1H); <sup>13</sup>C NMR (101 MHz, CDCl<sub>3</sub>) δ 162.1, 148.1, 136.6, 122.2, 120.3, 114.8, 72.2, 64.2, 37.6, 29.5; HRMS (ESI+) calcd for [C<sub>10</sub>H<sub>14</sub>ON]<sup>+</sup> (M-H)<sup>+</sup>: *m/z* 164.1070, found 164.1069.

**Ketone 5.59:** DMSO (6.10 mL, 85.6 mmol) was added dropwise to oxalyl chloride in CH<sub>2</sub>Cl<sub>2</sub> (80 mL) at -78 °C. After 30 min, the homoallyl alcohol (3.50 g, 21.4 mmol) in CH<sub>2</sub>Cl<sub>2</sub> (20 mL) was added dropwise at -78 °C. The reaction mixture was stirred for 30 min at this temperature. Et<sub>3</sub>N (24.0 mL, 171 mmol) was added at -78 °C. The cold bath was allowed to gradually expire as the reaction mixture was stirred for 4 h. The reaction was quenched with water (100 mL). The aqueous layer was extracted with CH<sub>2</sub>Cl<sub>2</sub> (2 x 100 mL). The combined organic layer was washed with water, dried over MgSO<sub>4</sub> and concentrated to afford **5.59** as a brown oil in 98% yield (3.39 g, 21.0 mmol) that was used without further purification. <sup>1</sup>H NMR (500 MHz, CDCl<sub>3</sub>) δ 8.68 (d, *J* = 4.7 Hz, 1H), 8.03 (d, *J* = 7.9 Hz, 1H), 7.83 (d, *J* = 1.6 Hz, 1H), 7.49 – 7.44 (m, 1H), 5.91 (d, *J* = 6.6 Hz, 1H), 5.09 (dd, *J* = 17.1, 1.6 Hz, 1H), 4.99 (dd, *J* = 10.2, 1.2 Hz, 1H), 3.33 (t, *J* = 7.4 Hz, 2H), 2.50 (d, *J* = 7.2 Hz, 2H); <sup>13</sup>C NMR (151 MHz, CDCl<sub>3</sub>) δ 200.8, 153.0, 148.6, 137.2, 136.8, 126.9, 121.5, 114.8, 36.6, 27.7; HRMS (ESI+) calcd for [C<sub>10</sub>H<sub>12</sub>ON]<sup>+</sup> (M-H)<sup>+</sup>: *m/z* 162.0913, found 162.1310.

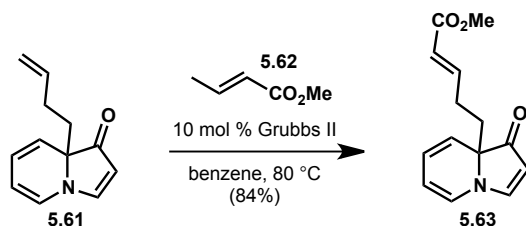


**Propargylic alcohol 5.60:** *n*-Butyllithium (6.95 mL, 17.4 mmol, 2.5 M in hexanes) was added dropwise to trimethylsilylacetylene (2.82 mL, 19.8 mmol) in Et<sub>2</sub>O (20 mL) at 0 °C. After 30 min, the lithium acetylide solution was added dropwise to a mixture of ketone **5.59** (2.00 g, 12.4 mmol) and lithium bromide (3.20 g, 37.2 mmol) in a 1:1 mixture of Et<sub>2</sub>O and benzene (total volume = 120 mL) at ambient temperature. The reaction mixture was stirred vigorously for 18 h. The reaction was quenched with the addition of a saturated NH<sub>4</sub>Cl<sub>(aq)</sub> solution (60 mL). The aqueous phase was extracted with EtOAc (3 x 80 mL). The combined organic layer was washed with brine, dried over MgSO<sub>4</sub>, and concentrated under reduced pressure to provide the trimethylsilyl alkyne as a brown oil in 80% yield (2.00 g, 4.69 mmol). <sup>1</sup>H NMR (500 MHz, CDCl<sub>3</sub>) δ 8.51 (d, *J* = 4.9 Hz, 1H), 7.74 (dd, *J* = 7.7, 1.6 Hz, 1H), 7.60 (d, *J* = 7.9 Hz, 1H), 7.26 (q, *J* = 4.7 Hz, 1H), 5.80 (d, *J* = 6.6 Hz, 1H), 5.47 (s, 1H), 4.98 (dd, *J* = 17.1, 1.6 Hz, 1H), 4.91 (d, *J* = 10.3 Hz, 1H), 2.33 – 2.25 (m, 1H), 2.17 – 2.10 (m, 1H), 2.10 – 2.03 (m, 1H), 1.94 – 1.87 (m, 1H), 0.20 – 0.15 (m, 9H); <sup>13</sup>C NMR (101 MHz, CDCl<sub>3</sub>) δ 160.8, 147.2, 138.1, 137.2, 122.8,

120.6, 114.5, 107.2, 89.3, 71.6, 44.2, 28.5, -0.2; **HRMS** (ESI+) calcd for  $[C_{15}H_{22}ONSi]^+$  (M-H)<sup>+</sup>:  $m/z$  260.1465, found 260.1464. Potassium carbonate (2.02 g, 14.6 mmol) was added to the trimethylsilyl alkyne (1.90 g, 7.32 mmol) in MeOH (70 mL). The reaction mixture was stirred for 2 h at ambient temperature. The reaction mixture was concentrated under reduced pressure. The residue was taken up in water (100 mL) and extracted with CH<sub>2</sub>Cl<sub>2</sub> (3 x 50 mL). The combined organic layer was washed with brine, dried over MgSO<sub>4</sub> and concentrated under reduced pressure to provide **5.60** as a brown oil in 97% yield (1.33 g, 7.10 mmol). **<sup>1</sup>H NMR** (400 MHz, CDCl<sub>3</sub>) δ 8.51 (d,  $J$  = 4.9 Hz, 1H), 7.74 (td,  $J$  = 7.7, 1.7 Hz, 1H), 7.60 (d,  $J$  = 8.0 Hz, 1H), 7.28 – 7.22 (m, 1H), 5.77 (d,  $J$  = 6.4 Hz, 1H), 5.48 (s, 1H), 4.97 (dd,  $J$  = 17.1, 1.5 Hz, 1H), 4.90 (d,  $J$  = 10.2 Hz, 1H), 2.56 (s, 1H), 2.29 (s, 1H), 2.17 – 2.09 (m, 2H), 1.93 (dd,  $J$  = 11.7, 8.4 Hz, 1H); **<sup>13</sup>C NMR** (151 MHz, CDCl<sub>3</sub>) δ 160.4, 147.3, 137.8, 137.3, 122.9, 120.4, 114.6, 85.9, 72.7, 71.2, 43.6, 28.2; **HRMS** (ESI+) calcd for  $[C_{12}H_{14}ON]^+$  (M-H)<sup>+</sup>:  $m/z$  188.1070, found 188.1069.

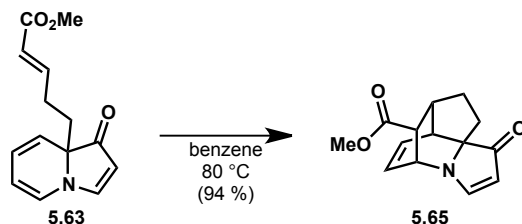


**Homoallyl indolizinone 5.61:** A solution of the tertiary alcohol (600 mg, 3.20 mmol) in EtOH (6.0 mL) was sparged with N<sub>2</sub> for 5 min. The reaction vessel, a 20 mL vial, was equipped with a green Teflon-lined cap and Telfon tape and heated at 100 °C for 4 h. The reaction mixture was cooled to room temperature and concentrated to provide indolizinone **5.61** in 99% yield (594 mg, 3.17 mmol). **<sup>1</sup>H NMR** (400 MHz, CDCl<sub>3</sub>) δ 7.79 (d,  $J$  = 3.7 Hz, 1H), 6.36 (d,  $J$  = 7.0 Hz, 1H), 5.89 (d,  $J$  = 5.5 Hz, 1H), 5.76 (d,  $J$  = 9.3 Hz, 1H), 5.67 (ddt,  $J$  = 16.8, 10.2, 6.5 Hz, 1H), 5.37 (s, 1H), 5.07 (d,  $J$  = 3.7 Hz, 1H), 4.94 (dd,  $J$  = 17.1, 1.6 Hz, 1H), 4.89 (dd,  $J$  = 10.2, 1.2 Hz, 1H), 2.06 (s, 1H), 1.98 (s, 1H), 1.86 – 1.68 (m, 2H); **<sup>13</sup>C NMR** (101 MHz, CDCl<sub>3</sub>) δ 204.0, 160.9, 137.4, 125.2, 122.5, 122.4, 114.9, 108.8, 99.0, 69.6, 37.6, 26.2; **HRMS** (ESI+) calcd for  $[C_{12}H_{14}ON]^+$  (M-H)<sup>+</sup>:  $m/z$  188.1070, found 188.1069.

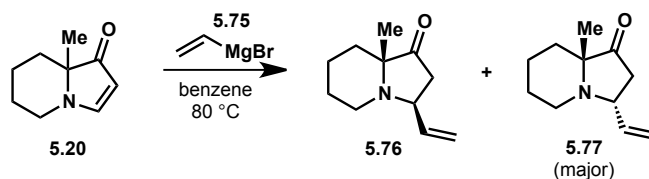


**Ester 5.63:** A solution of indolizinone **5.61** (100 mg, 0.534 mmol), methyl crotonate (**5.62**, 283 μL, 2.67 mmol) and Grubbs 2<sup>nd</sup> generation catalyst (45.0 mg, 0.0534 mmol) in CH<sub>2</sub>Cl<sub>2</sub> (5.0 mL) was stirred at room temperature for 20 h. The reaction mixture was concentrated under reduced pressure and purified via flash chromatography to afford ester **5.63** in 84% yield (69.4 mg, 0.283 mmol). **<sup>1</sup>H NMR** (600 MHz, CDCl<sub>3</sub>) δ 7.81 (d,  $J$  = 3.7 Hz, 1H), 6.85 (d,  $J$  = 15.6 Hz, 1H), 6.37 (d,  $J$  = 7.0 Hz, 1H), 5.95 (dd,  $J$  = 9.3, 5.5 Hz, 1H), 5.80 – 5.74 (m, 2H), 5.41 (dd,  $J$  = 9.2, 3.3 Hz, 1H), 5.11

(d,  $J = 3.7$  Hz, 1H), 3.70 (s, 3H), 2.30 – 2.23 (m, 1H), 2.21 – 2.13 (m, 1H), 1.89 (ddd,  $J = 13.5$ , 11.1, 5.3 Hz, 1H), 1.79 (ddd,  $J = 13.5$ , 11.2, 5.1 Hz, 1H).

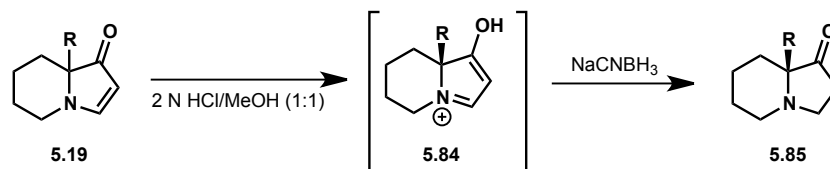


**Caged polycycle 5.65:** A solution of indolizinone **5.63** (25.3 mg, 0.103 mmol) in xylenes (1.0 mL) was heated to 150 °C for 20 h. The reaction mixture was cooled to room temperature and concentrated under reduced pressure to afford polycycle **5.65** in a 99% yield (25.0 mg, 0.102 mmol).  $^1\text{H NMR}$  (600 MHz,  $\text{CDCl}_3$ )  $\delta$  7.65 (d,  $J = 3.5$  Hz, 1H), 6.14 – 6.10 (m, 1H), 6.07 – 6.02 (m, 1H), 5.49 (d,  $J = 3.5$  Hz, 1H), 4.43 – 4.39 (m, 1H), 3.67 (s, 3H), 2.98 – 2.93 (m, 1H), 2.81 – 2.77 (m, 1H), 2.63 (s, 1H), 2.24 (dd,  $J = 13.5$ , 3.4 Hz, 1H), 2.16 – 2.08 (m, 1H), 1.89 – 1.83 (m, 1H), 1.74 – 1.68 (m, 1H).



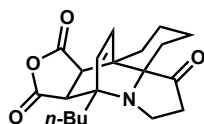
**Tertiary amines 5.76 and 5.77:** Vinylmagnesium bromide (142  $\mu\text{L}$ , 0.0992 mmol, 0.7 M in hexanes) was added dropwise to **5.20** (10.0 mg, 0.0661 mmol) in benzene (600  $\mu\text{L}$ ). The reaction mixture was heated to 80 °C for 2 h. The mixture was cooled to room temperature and quenched by the addition of water (1.0 mL). The product was extracted with  $\text{CH}_2\text{Cl}_2$  (3 x 2.0 mL) from 1 M  $\text{NaOH}_{(\text{aq})}$ . The organic layers were combined, dried over  $\text{MgSO}_4$  and concentrated under reduced pressure to afford a 3:1 mixture of **5.77** to **5.76** in 64% yield.  $^1\text{H NMR}$  (500 MHz,  $\text{CDCl}_3$ )  $\delta$  5.68 – 5.59 (m, 1H), 5.31 – 5.23 (m, 1H), 5.21 (dd,  $J = 10.0$ , 1.5 Hz, 1H), 3.83 (d,  $J = 6.4$  Hz, 1H), 3.04 – 2.97 (m, 1H), 2.88 (d,  $J = 2.2$  Hz, 1H), 2.61 (dd,  $J = 18.5$ , 6.4 Hz, 1H), 2.19 (dd,  $J = 18.5$ , 9.7 Hz, 1H), 1.72 – 1.56 (m, 4H), 1.29 (s, 3H), 1.23 – 1.12 (m, 2H).

**Representative procedure for the reduction of vinylogous amides with sodium cyanoborohydride:**



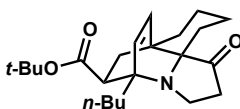
2 N  $\text{HCl}_{(\text{aq})}$  (300  $\mu\text{L}$ ) was added dropwise to vinylogous amide **5.19** (0.150 mmol) in MeOH (700  $\mu\text{L}$ ).  $\text{NaCNBH}_3$  (0.375 mmol, 2.50 equiv) was added slowly to the reaction mixture. After 6 h, a

saturated  $\text{NaHCO}_3(\text{aq})$  (1.0 mL) was added dropwise. The reaction mixture was extracted with  $\text{CH}_2\text{Cl}_2$  (3 x 2.0 mL). The combined organic layers were concentrated under reduced pressure to afford a tertiary amine (**5.85**).



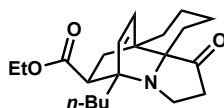
**5.86**

**Tertiary amine 5.86:** The standard reduction protocol afforded **5.86** in 83% yield.  $^1\text{H}$  NMR (500 MHz,  $\text{CDCl}_3$ )  $\delta$  5.71 (d,  $J = 10.0$  Hz, 1H), 5.58 (d,  $J = 10.4$  Hz, 1H), 4.70 (s, 1H), 3.66 (s, 1H), 3.63 – 3.59 (m, 1H), 3.35 (s, 1H), 3.23 (s, 1H), 3.17 (m, 1H), 2.76 (d,  $J = 7.4$  Hz, 1H), 2.71 (d,  $J = 7.8$  Hz, 2H), 2.63 (d,  $J = 7.2$  Hz, 2H), 2.50 (m, 4H), 2.41 (d,  $J = 8.7$  Hz, 2H), 2.36 (s, 3H), 1.41 (m, 1H), 0.97 – 0.91 (t, 3H).



**5.87**

**Tertiary amine 5.87:** The standard reduction protocol afforded **5.87** in 60% yield.  $^1\text{H}$  NMR (500 MHz,  $\text{CDCl}_3$ )  $\delta$  5.71 (d,  $J = 10.0$  Hz, 1H), 5.58 (d,  $J = 10.4$  Hz, 1H), 4.70 (s, 1H), 3.66 (s, 2H), 3.63 – 3.59 (m, 1H), 3.35 (s, 1H), 3.23 (s, 2H), 3.17 (s, 2H), 2.76 (d,  $J = 7.4$  Hz, 2H), 2.71 (d,  $J = 7.8$  Hz, 2H), 2.63 (d,  $J = 7.2$  Hz, 2H), 2.41 (d,  $J = 8.7$  Hz, 2H), 2.36 (m, 4H), 1.41 (m, 3H), 1.25 (t, 3H), 0.97 – 0.91 (s, 9H).



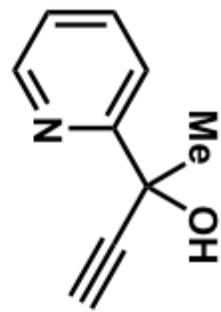
**5.88**

**Tertiary amine 5.88:** The standard reduction protocol afforded **5.88** in 76% yield.  $^1\text{H}$  NMR (500 MHz,  $\text{CDCl}_3$ )  $\delta$  6.11 (d,  $J = 8.2$  Hz, 1H), 6.07 (d,  $J = 8.2$  Hz, 1H), 4.10 – 4.01 (m, 2H), 3.18 (t,  $J = 8.2$  Hz, 2H), 2.74 (dd,  $J = 9.1, 5.8$  Hz, 2H), 2.51 (dd,  $J = 16.2, 8.1$  Hz, 2H), 2.14 (d,  $J = 3.9$  Hz, 1H), 1.74 – 1.59 (m, 6H), 1.56 – 1.49 (m, 3H), 1.49 – 1.41 (m, 7H), 1.33 (dt,  $J = 11.5, 10.2$  Hz, 8H), 1.24 (dt,  $J = 14.3, 5.1$  Hz, 9H), 0.92 (dd,  $J = 9.2, 4.8$  Hz, 6H).

### 5.10 References and Notes

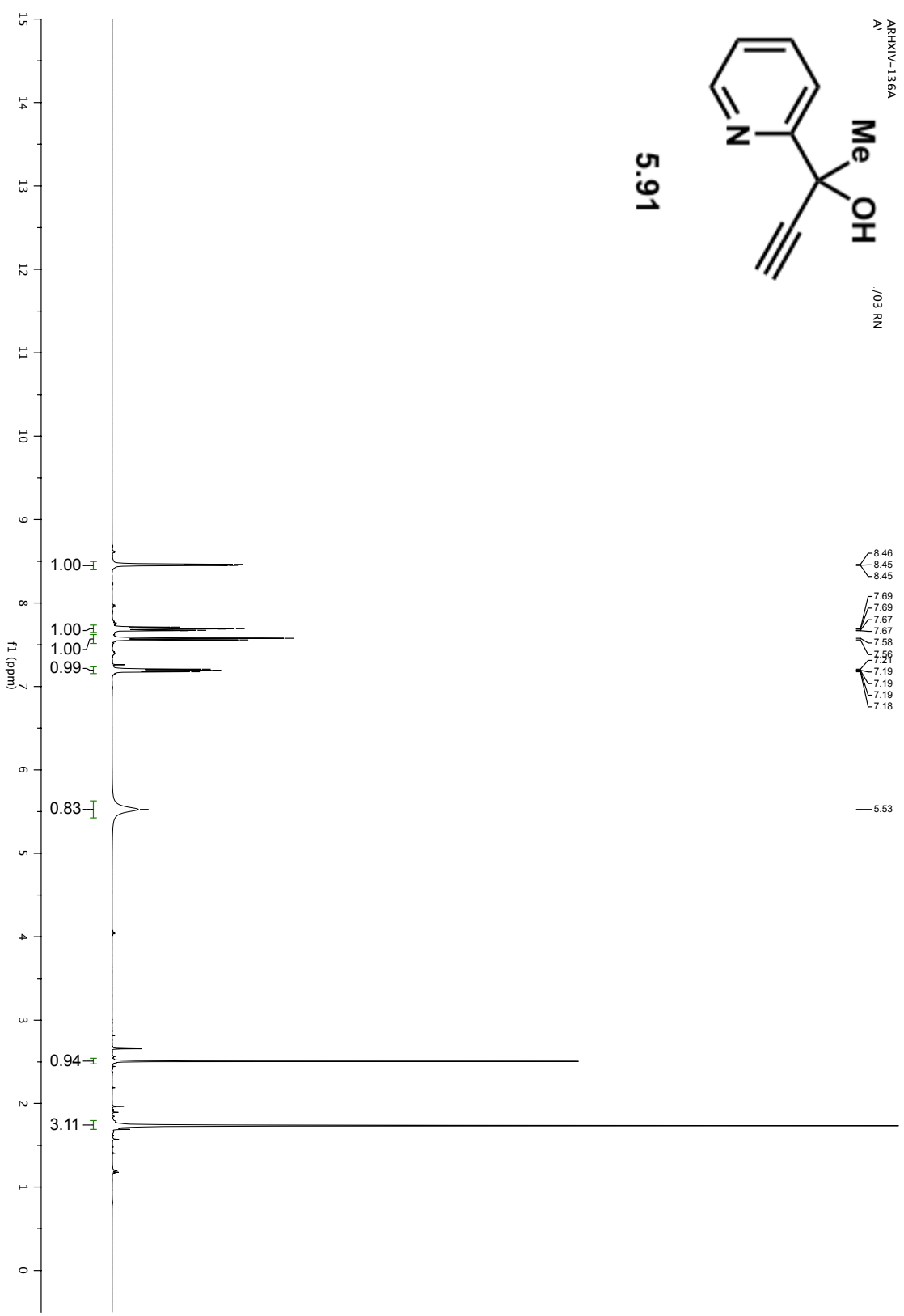
- (1) Blackman, A. J.; Li, C. P.; Hockless, D. C. R.; Skelton, B. W.; White, A. H. *Tetrahedron* **1993**, *49*, 8645.
- (2) Biard, J. F.; Guyot, S.; Roussakis, C.; Verbist, J. F.; Vercauteren, J.; Weber, J. F.; Boukef, K. *Tetrahedron Lett.* **1994**, *35*, 2691.
- (3) Smith, C. R.; Bunnelle, E. M.; Rhodes, A. J.; Sarpong, R. *Org. Lett.* **2007**, *9*, 1169.
- (4) Yan, B.; Zhou, Y. B.; Zhang, H.; Chen, J. J.; Liu, Y. H. *J. Org. Chem.* **2007**, *72*, 7783.
- (5) Choi, J.; Lee, G. H.; Kim, I. *Synlett* **2008**, 1243.
- (6) Kim, I.; Choi, J.; Lee, S.; Lee, G. H. *Synlett* **2008**, 2334.
- (7) Paquette, L. A.; Dura, R. D.; Gallucci, J. C. *Heterocycles* **2008**, *76*, 129.
- (8) Kim, K.; Kim, I. *J. Comb. Chem.* **2010**, *12*, 379.
- (9) Morrill, C.; Grubbs, R. H. *J. Org. Chem.* **2003**, *68*, 6031.

*Appendix Four:  
Spectra Relevant to Chapter Five*

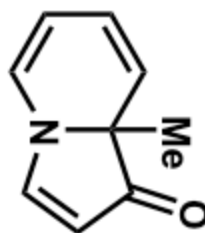


5.91

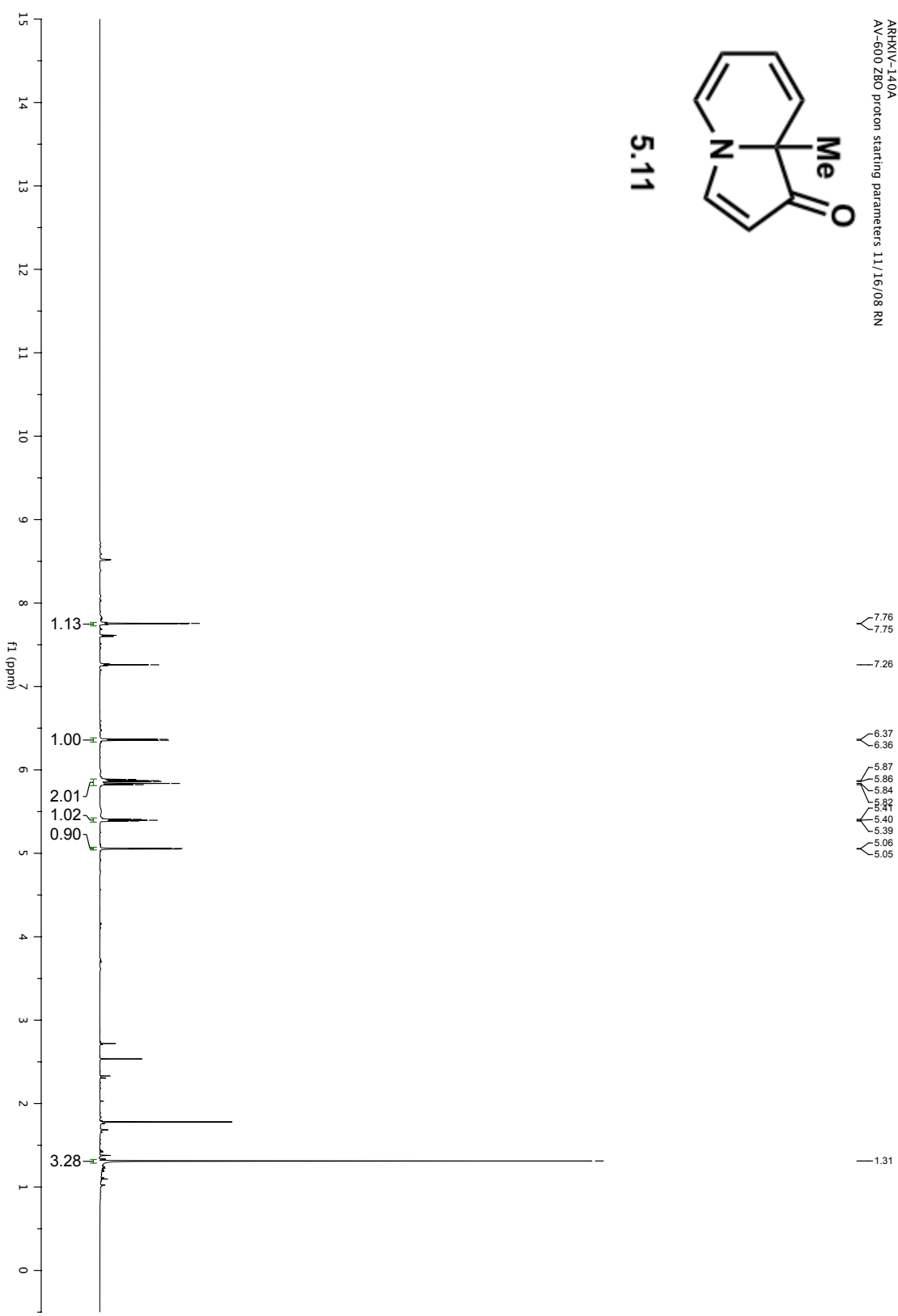
ARRXIV-136A  
A1 /03 RN



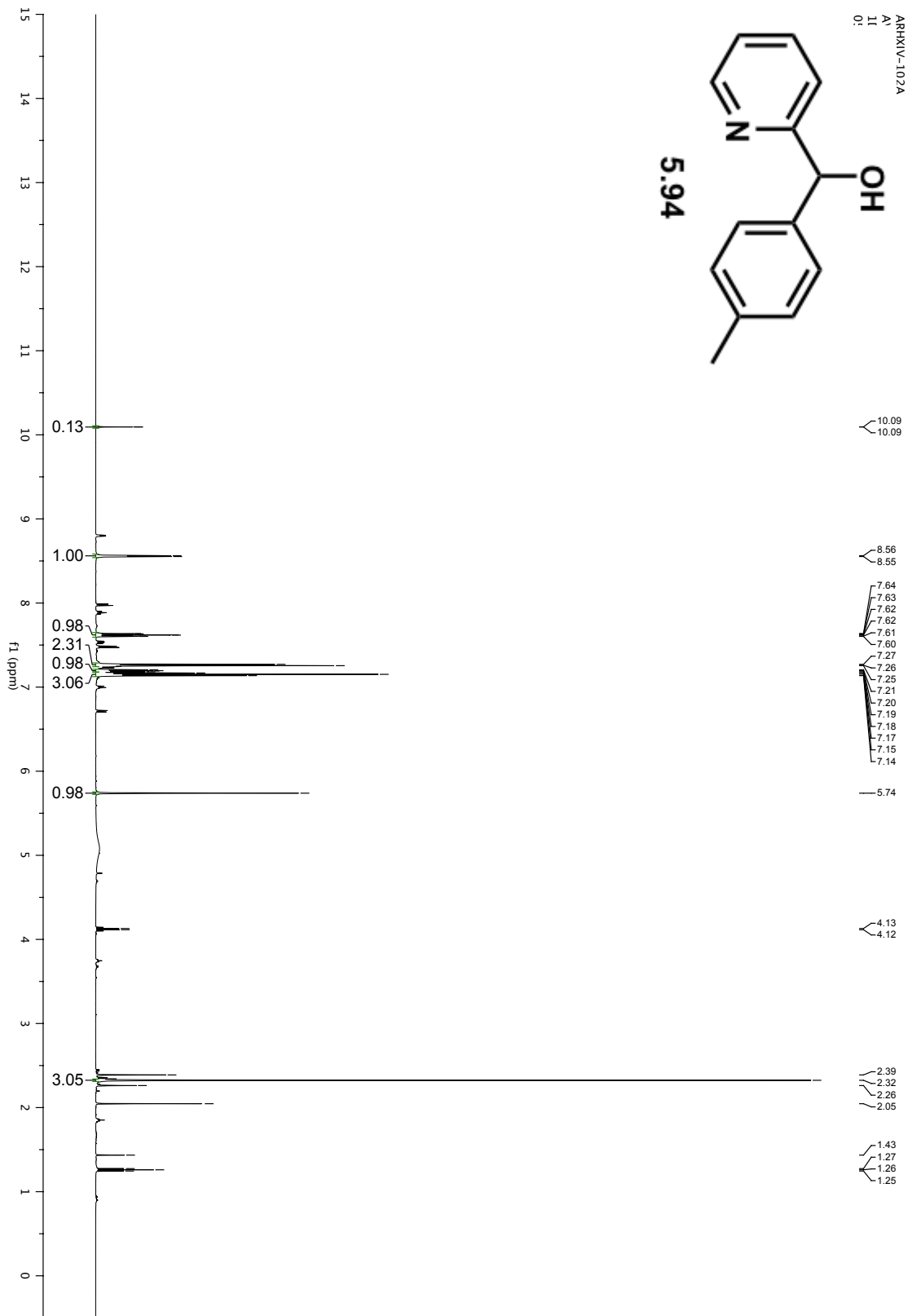
ARRXIV-140A  
AV-600 Z80 proton starting parameters 11/16/08 RN



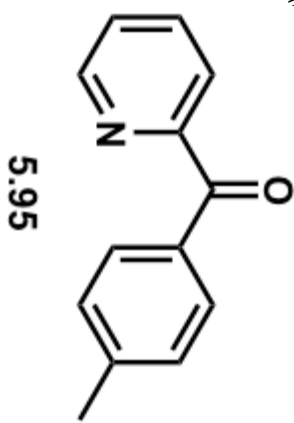
5.11



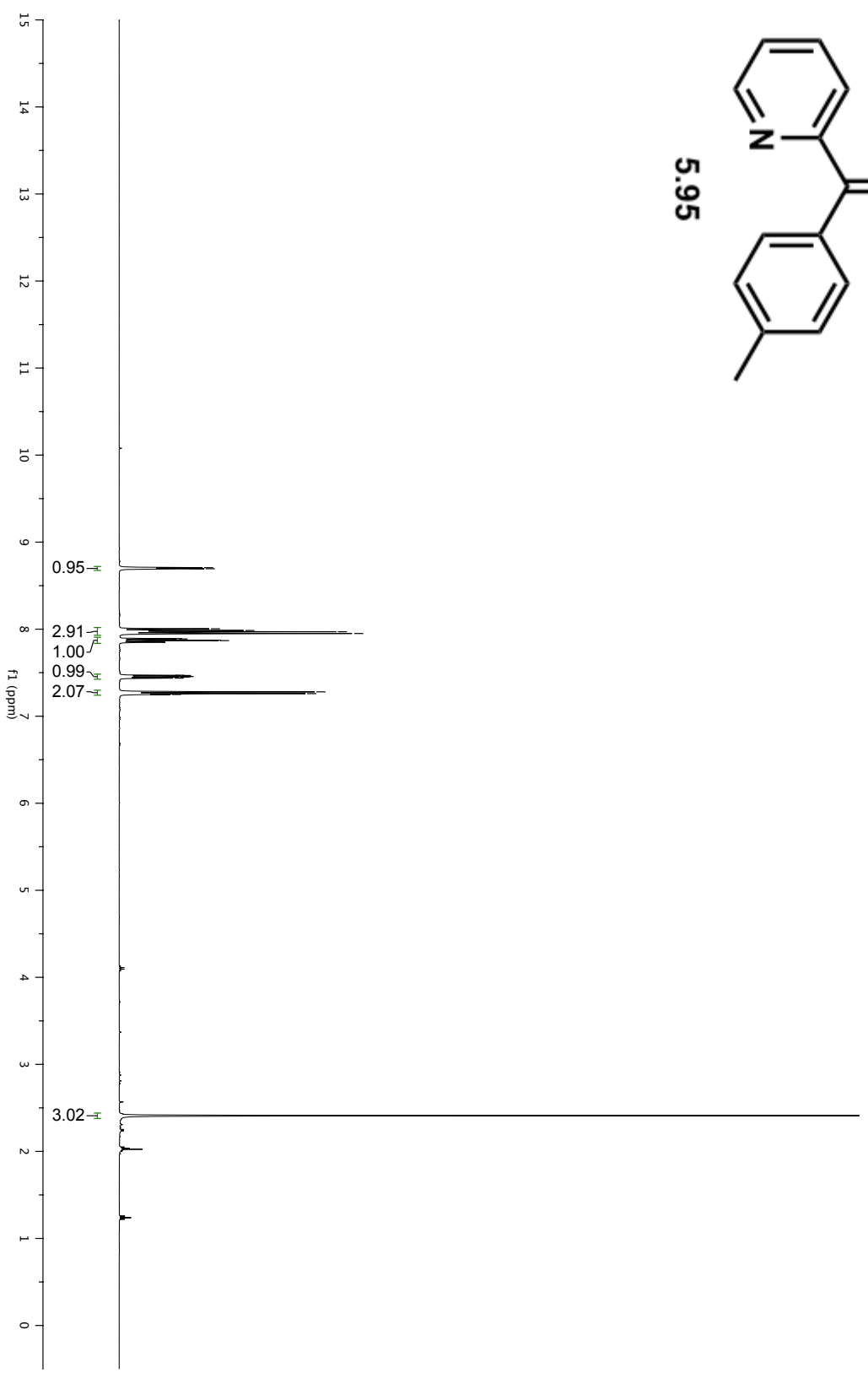




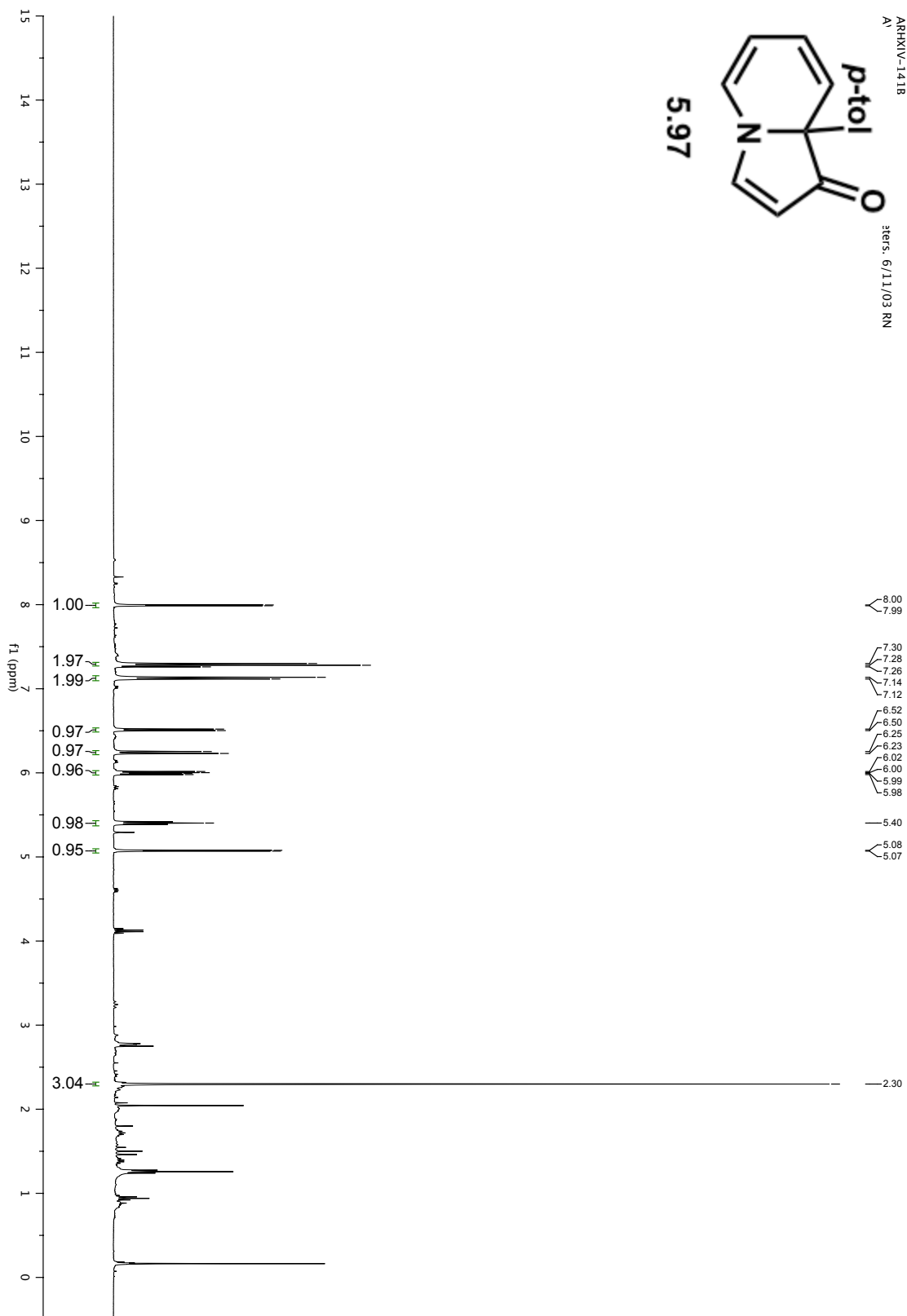
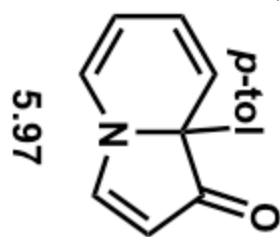
ARXIV-1298  
A'

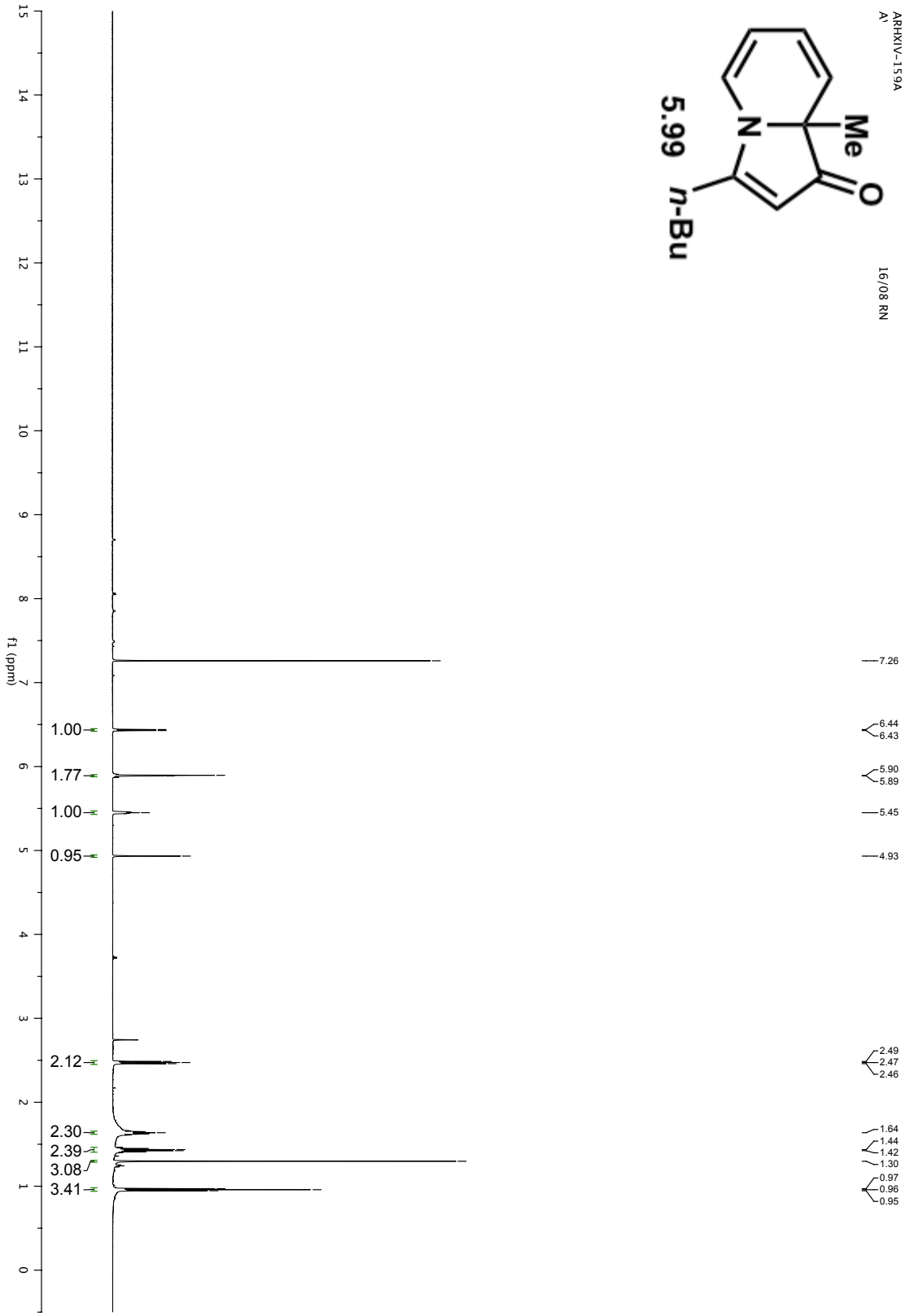
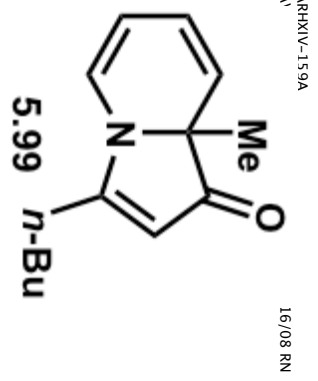


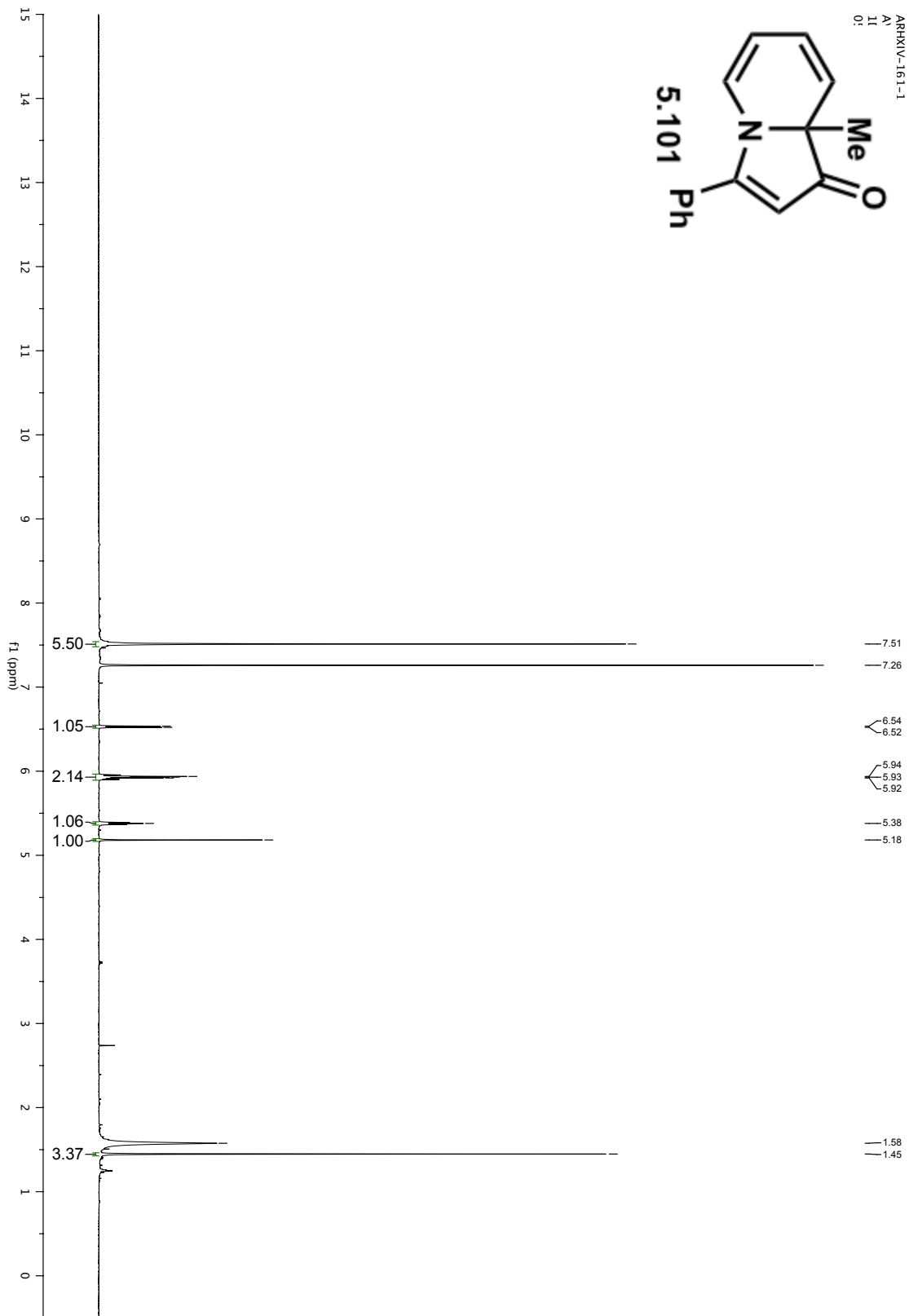
8.71  
8.69  
8.00  
7.98  
7.97  
7.95  
7.87  
7.87  
7.47  
7.46  
7.46  
7.45  
7.45  
7.44  
7.28  
7.26  
7.25



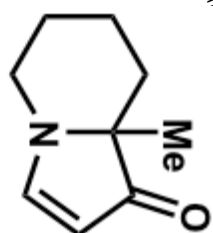
ARRXIV-1418  
A)  
3eters: 6/11/03 RN



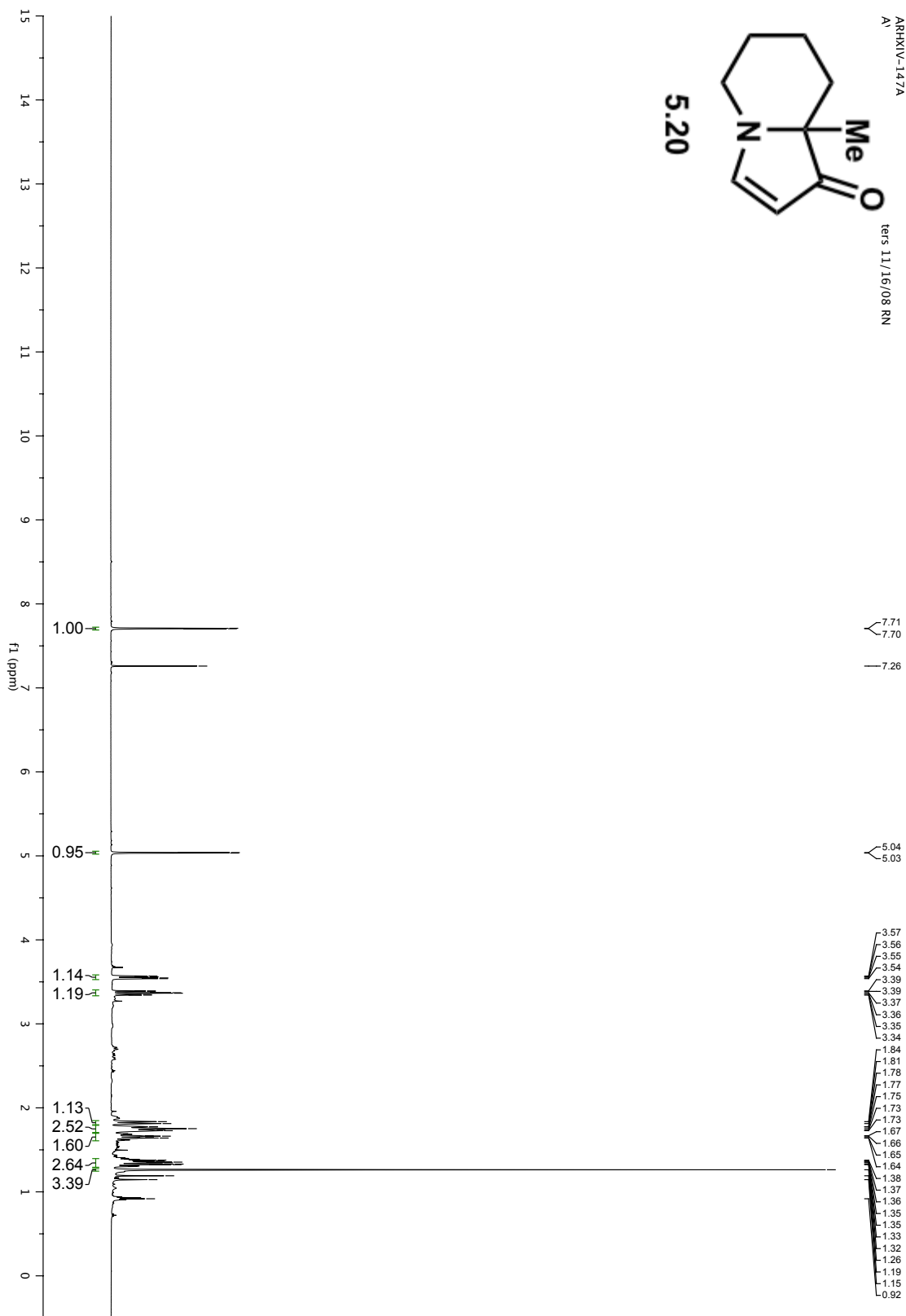




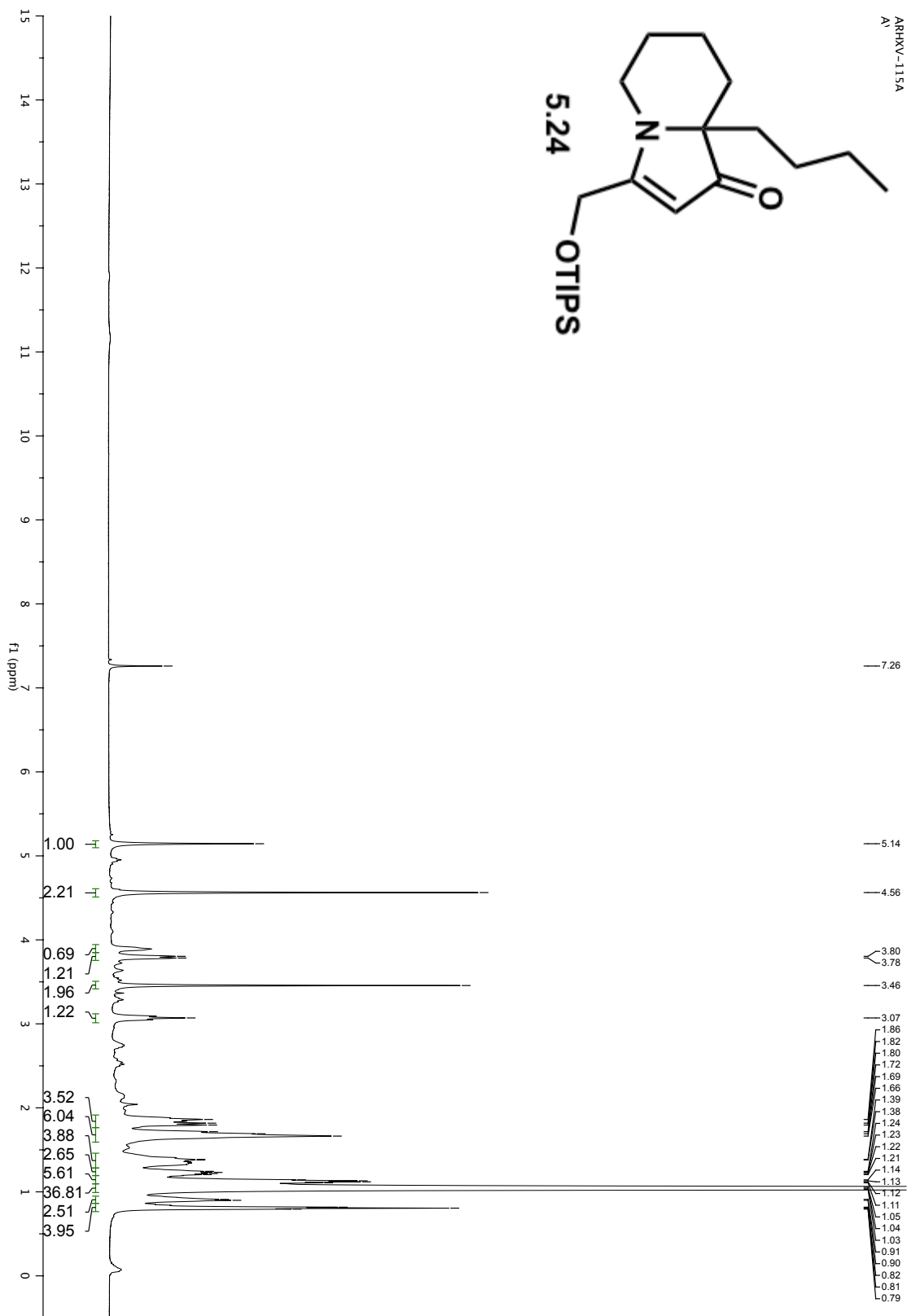
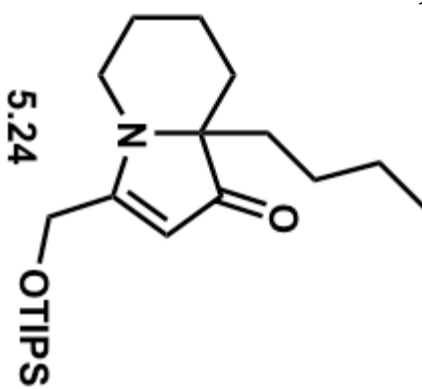
ARRXIV-147A  
A1  
vers 11/16/08 RN

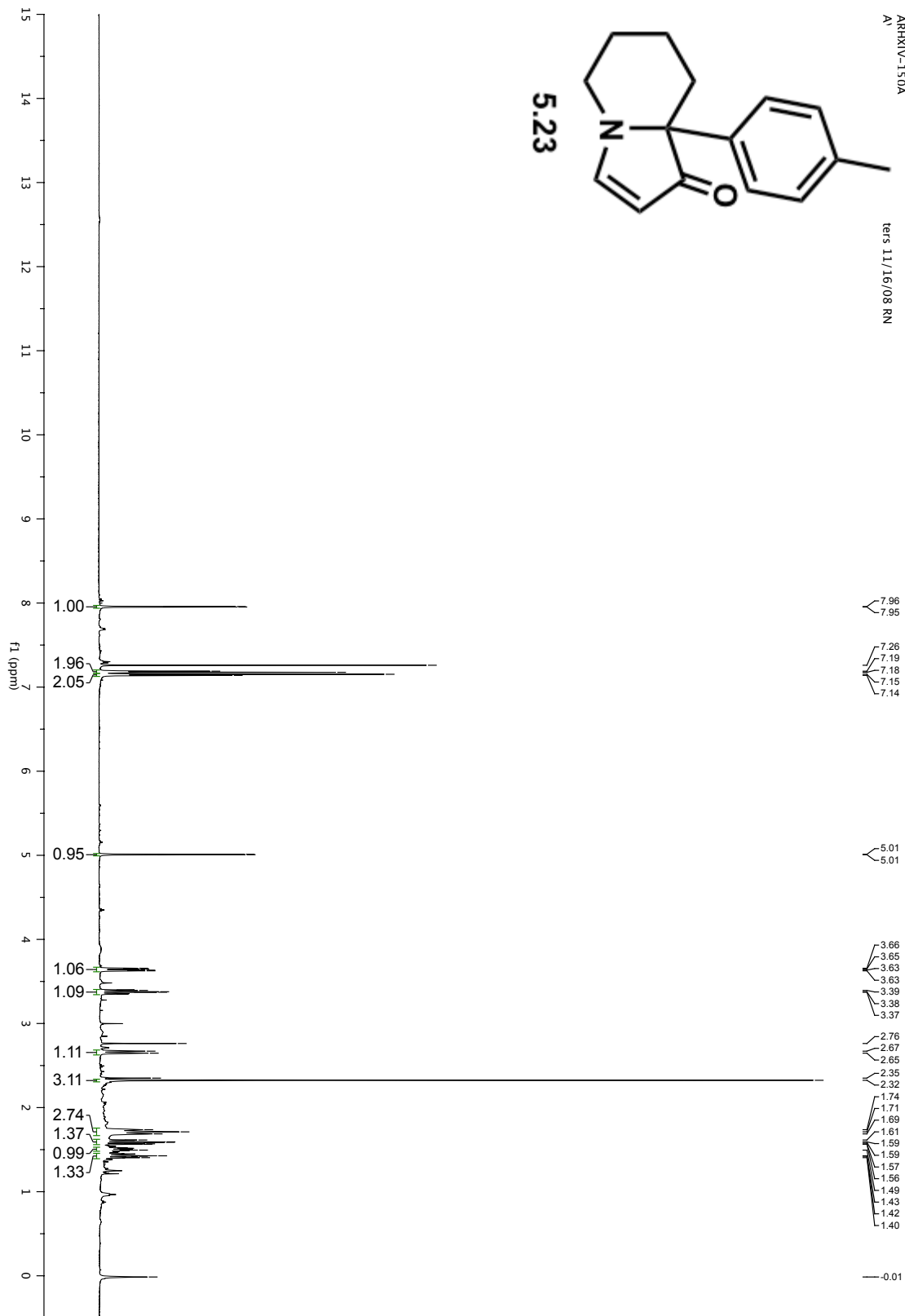
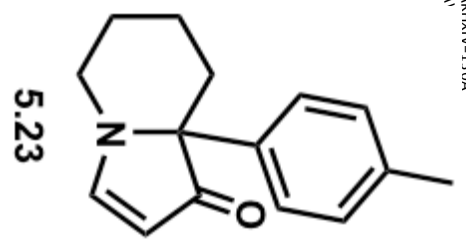


5.20



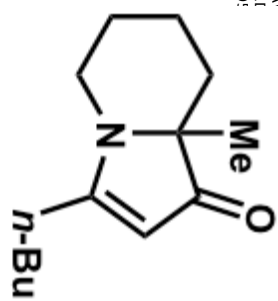
ARRXV-115A  
A'



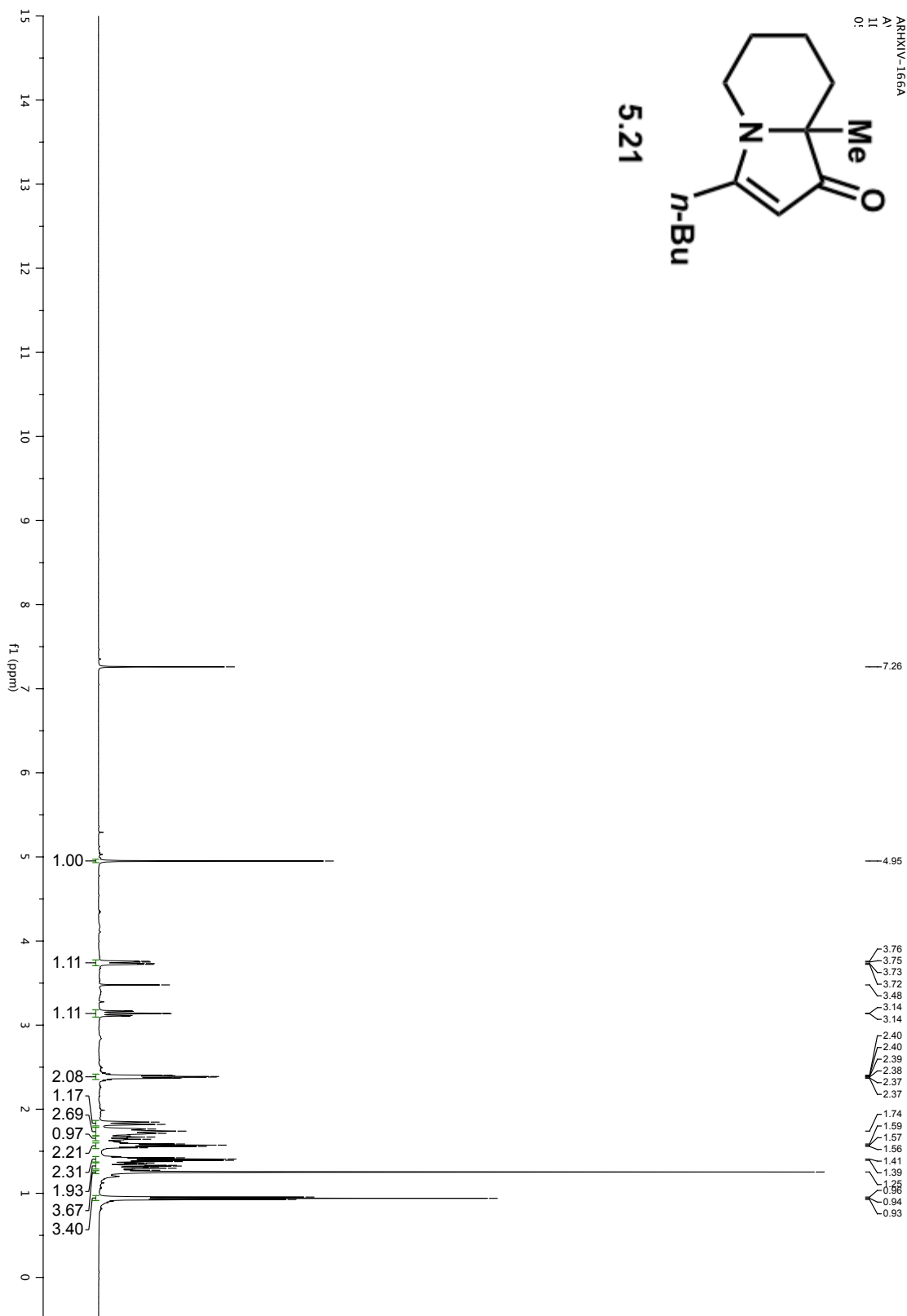




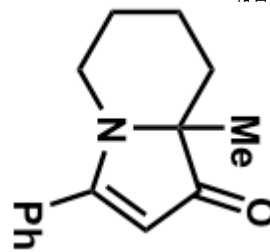
ARHXIV-166A  
A:  
1:  
0:



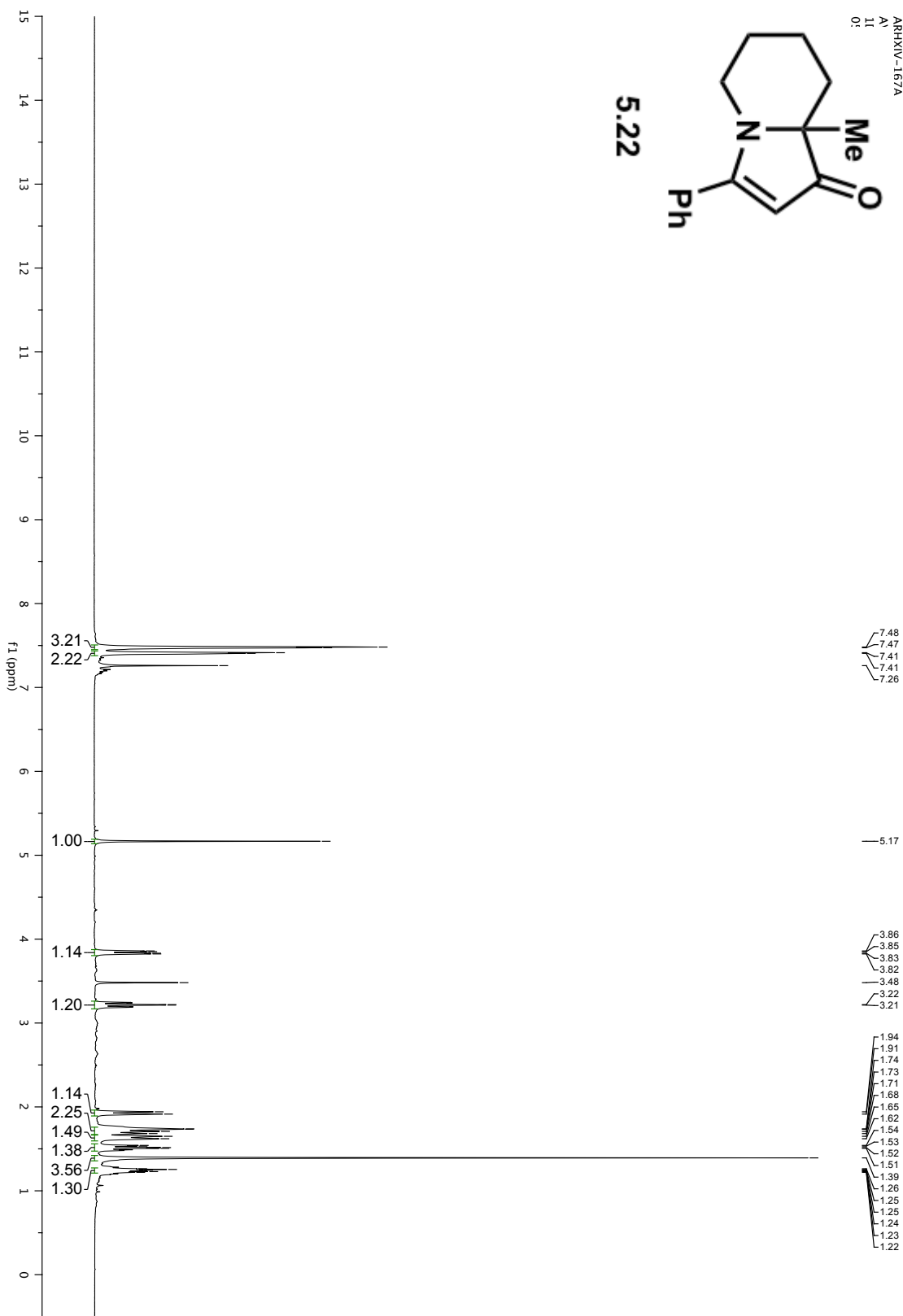
5.21

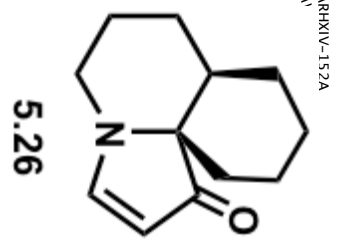


ARHXV-167A  
A)  
11  
0:

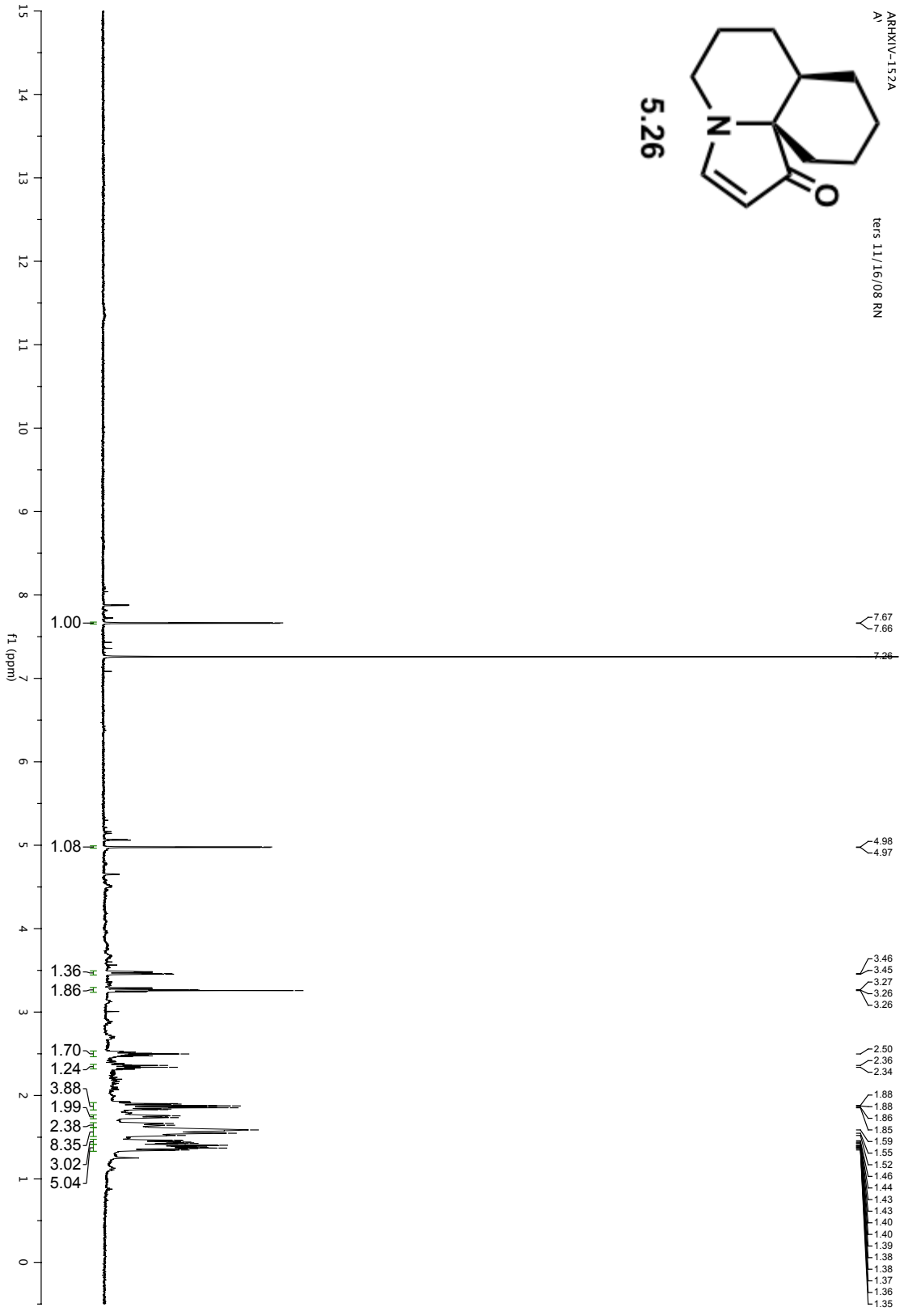


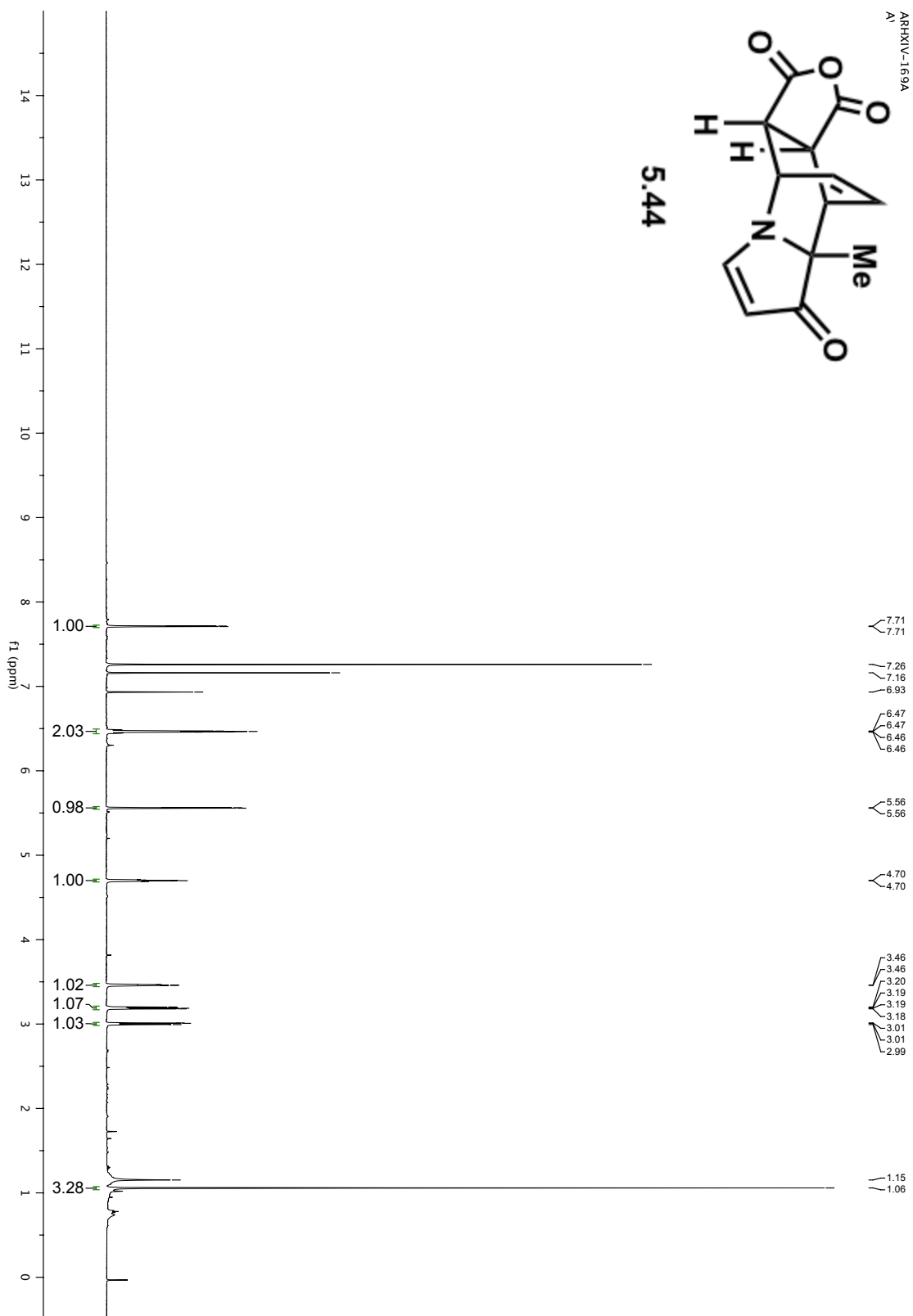
5.22



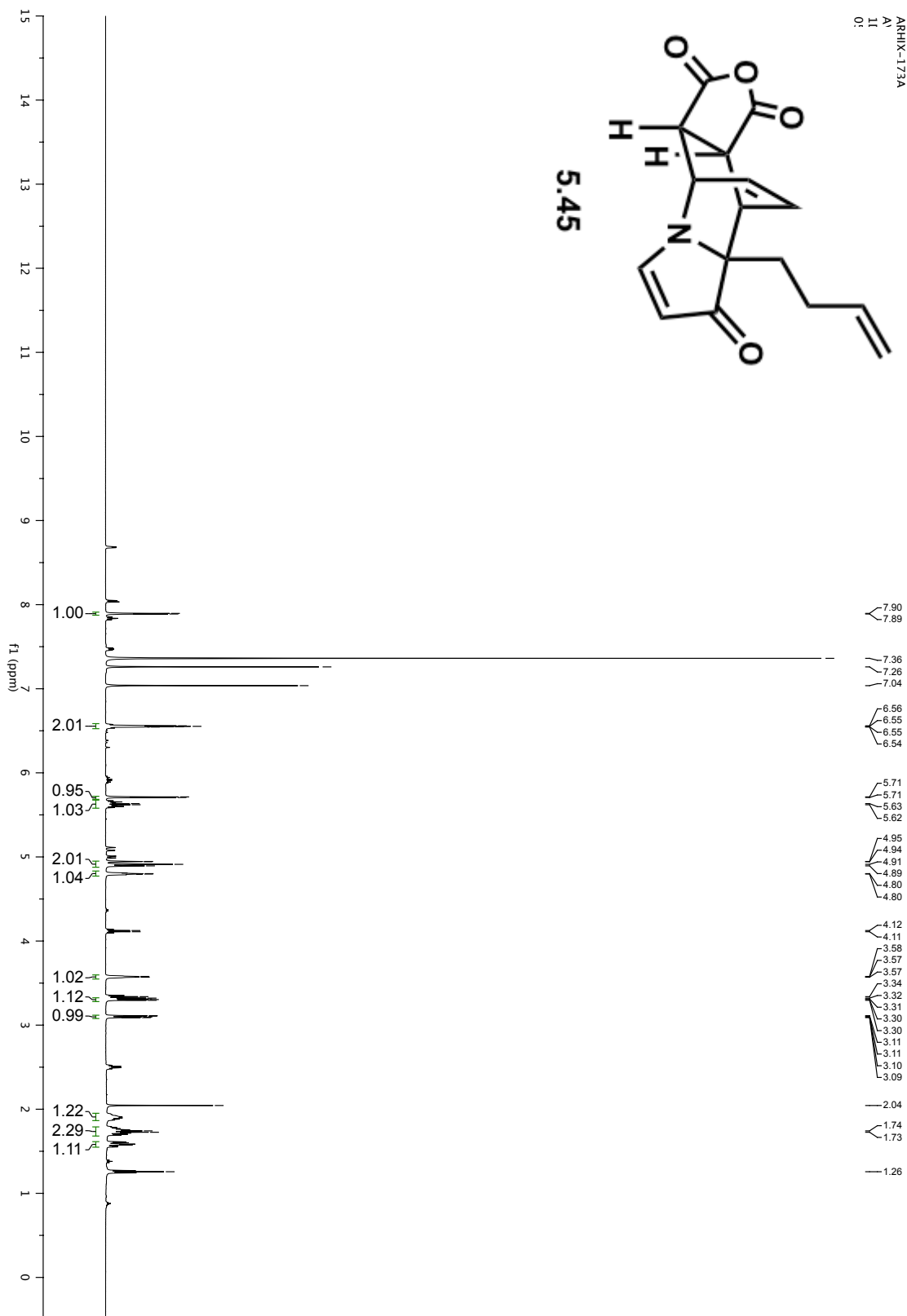
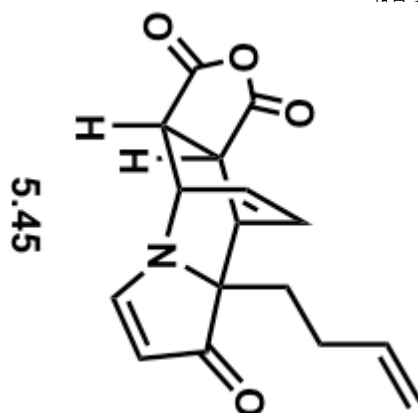


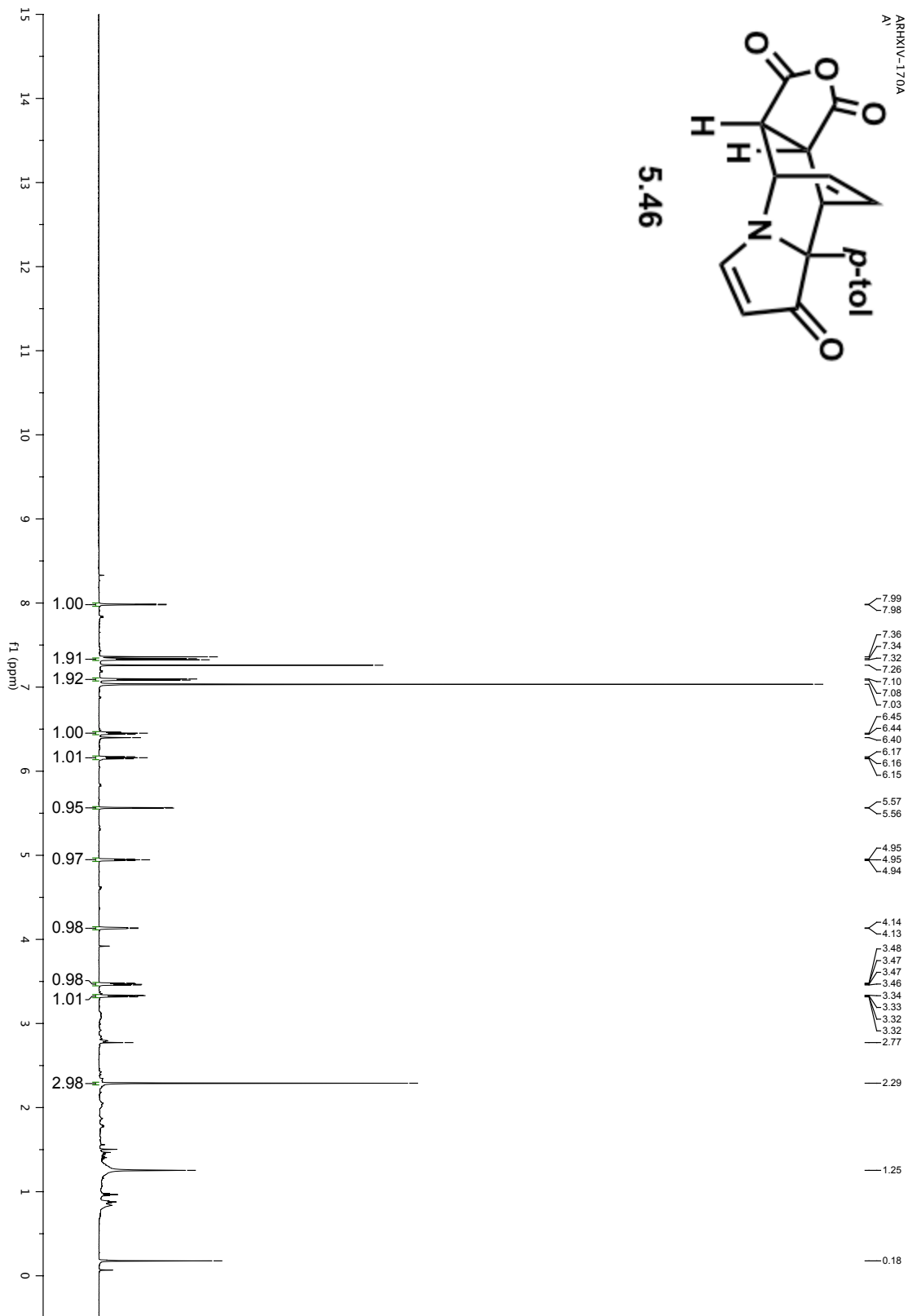
vers 11/16/08 RN

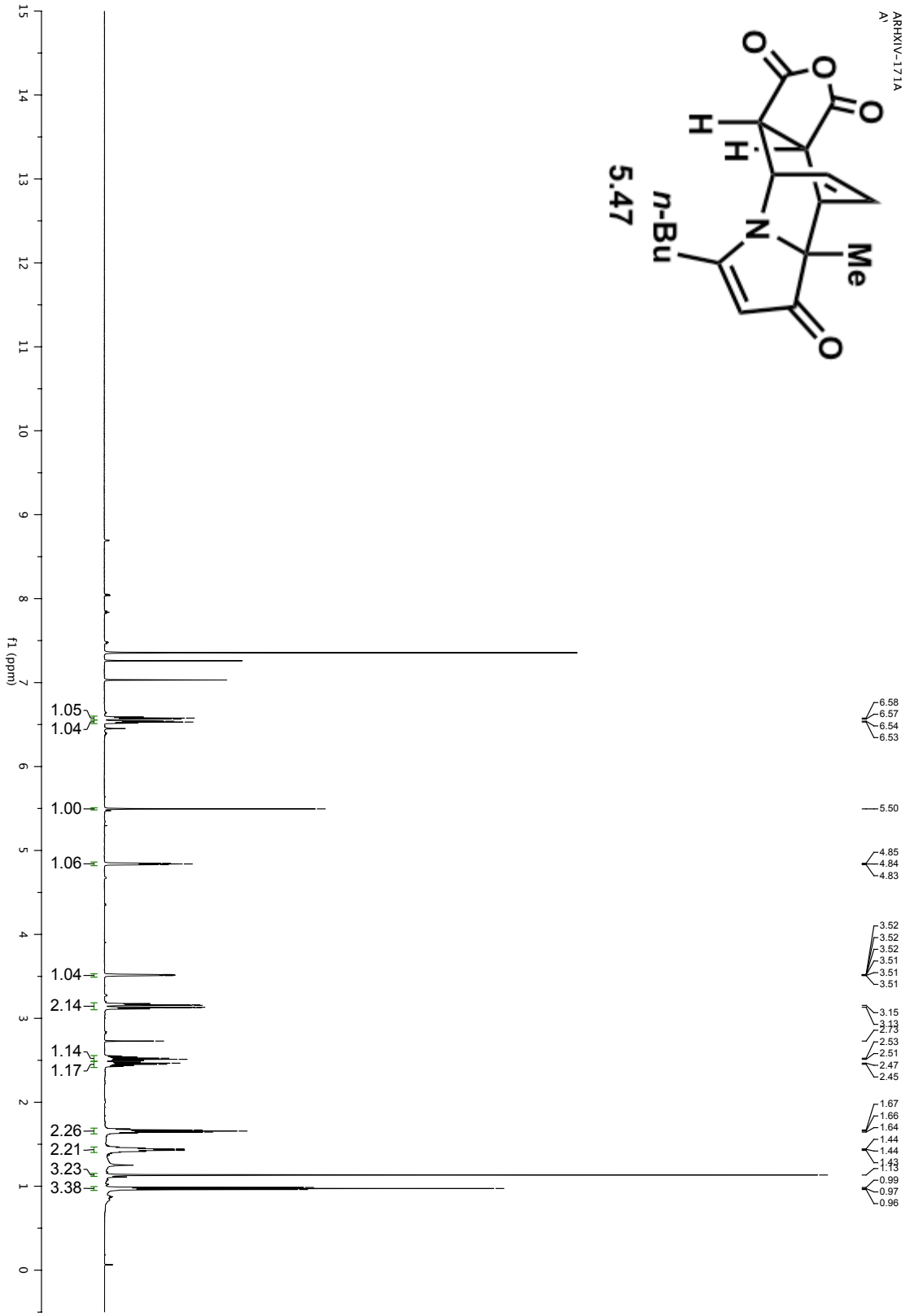
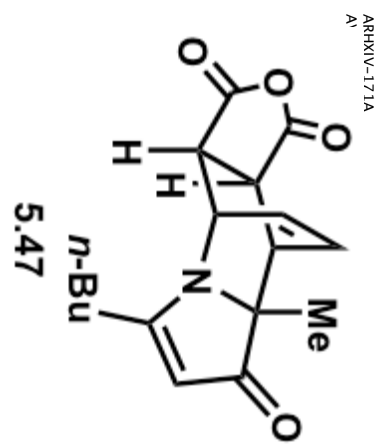


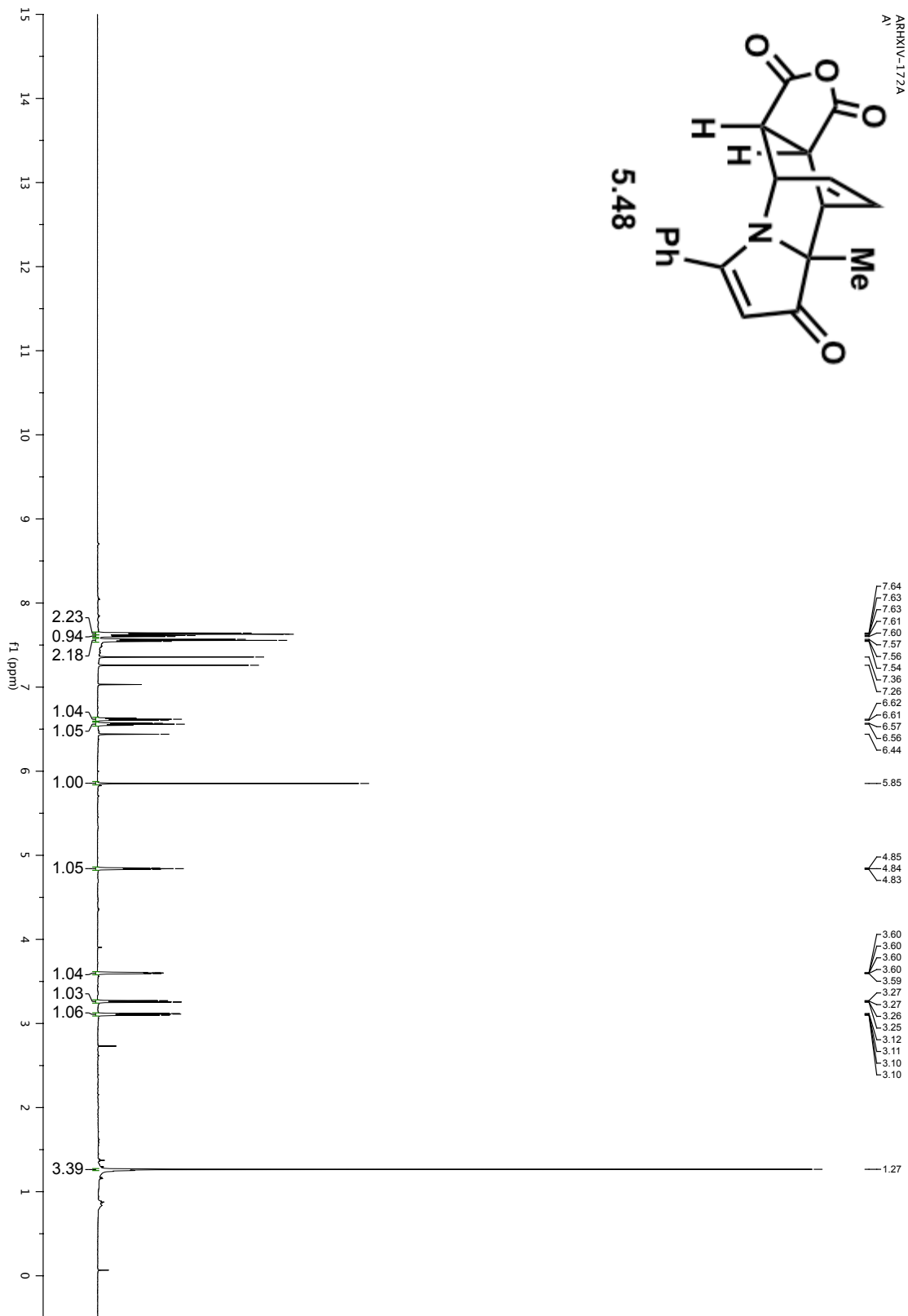


ARRHX-173A  
A:  
1:  
0:

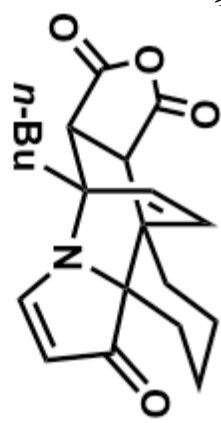




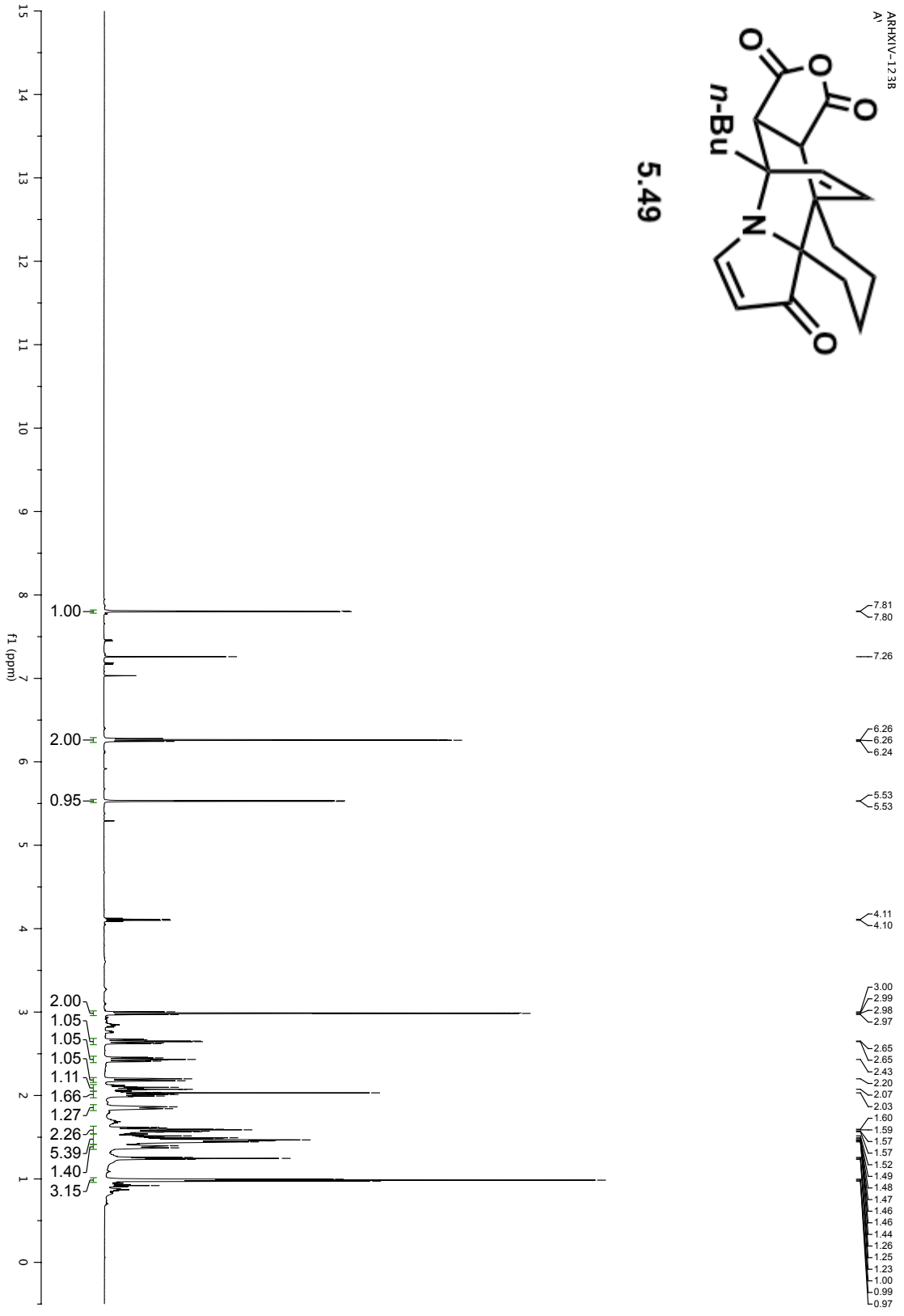


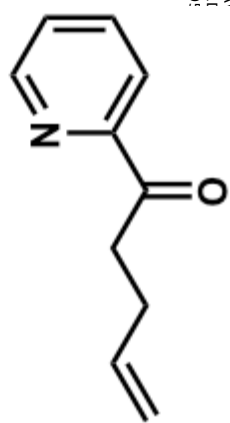




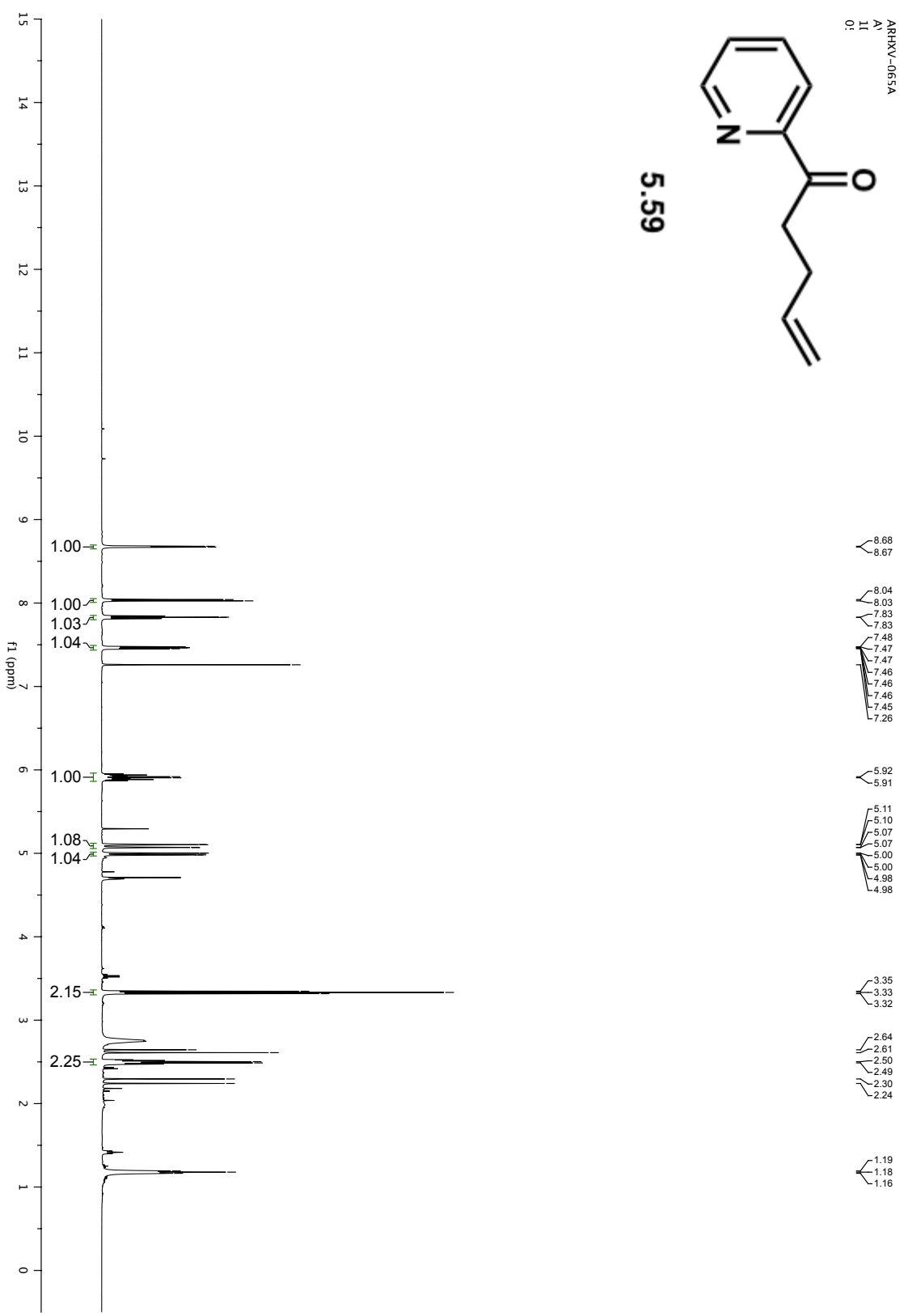


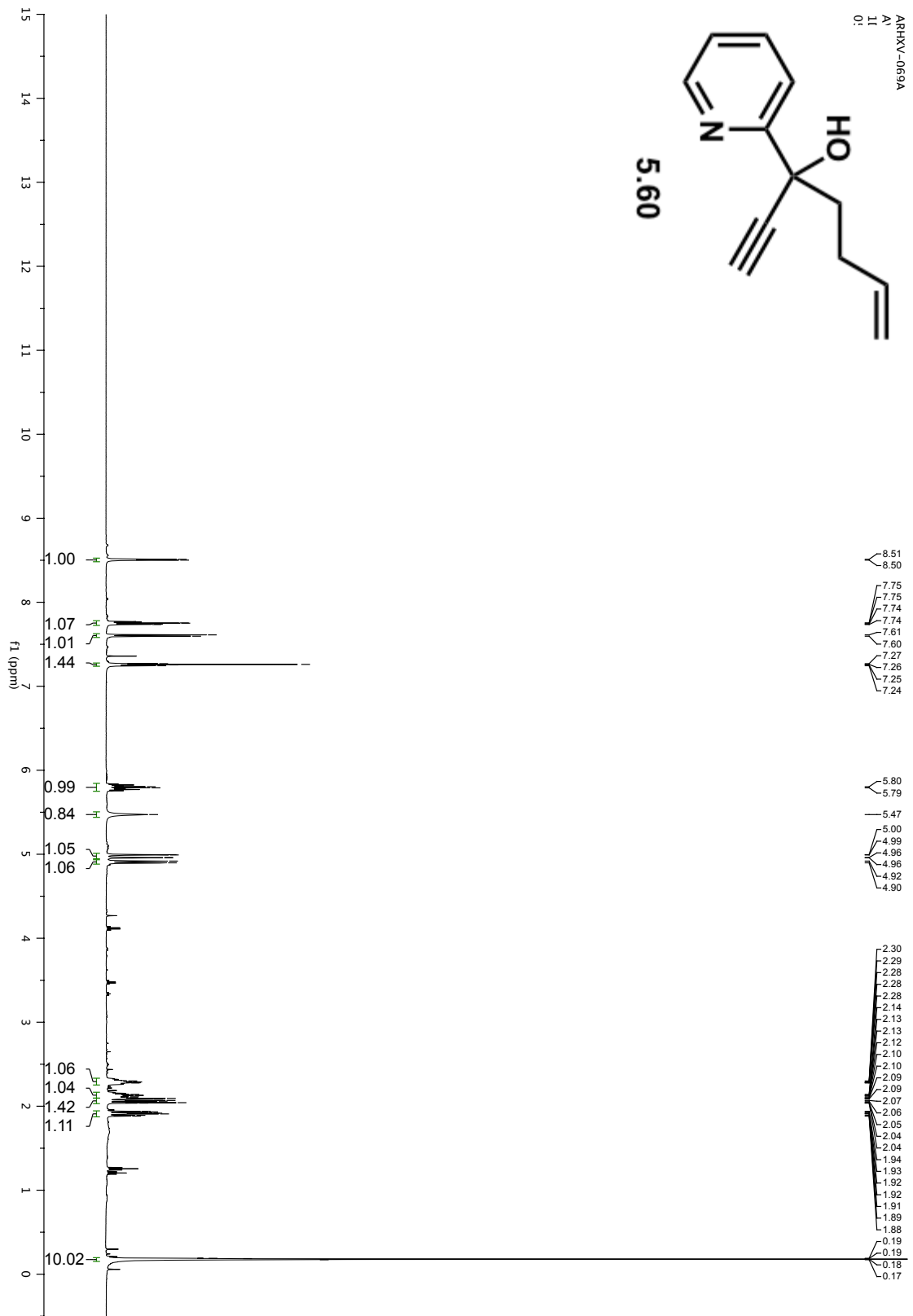
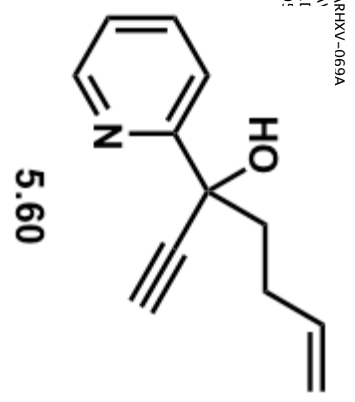
5.49

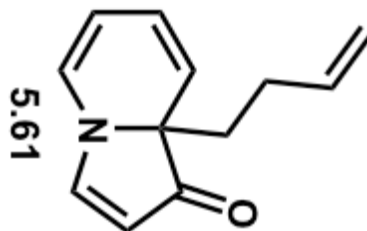




5.59

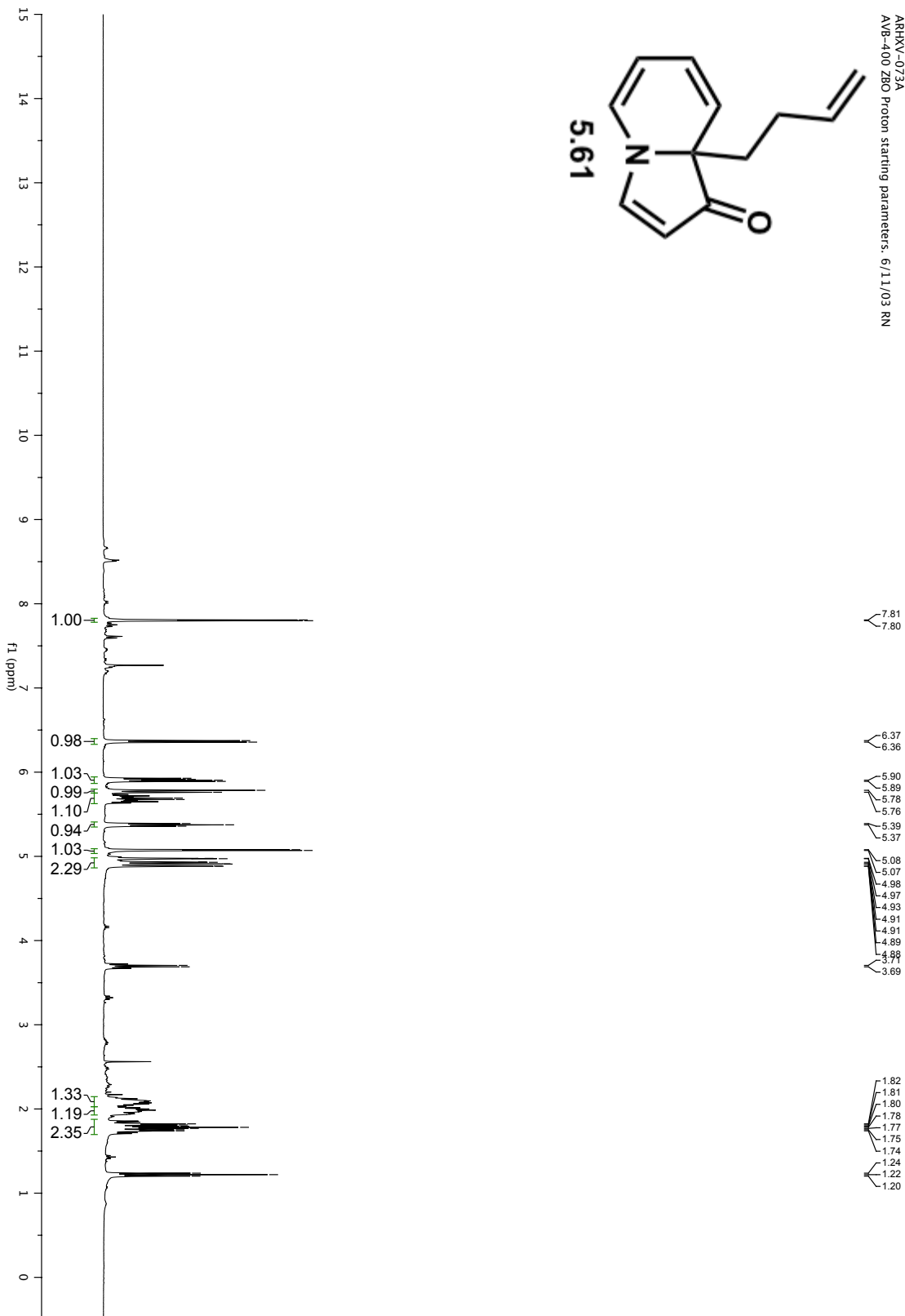


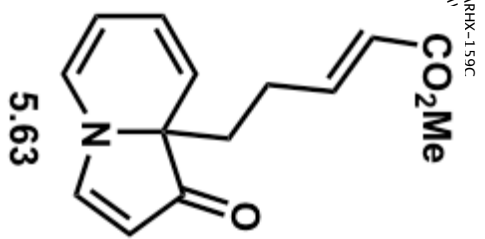




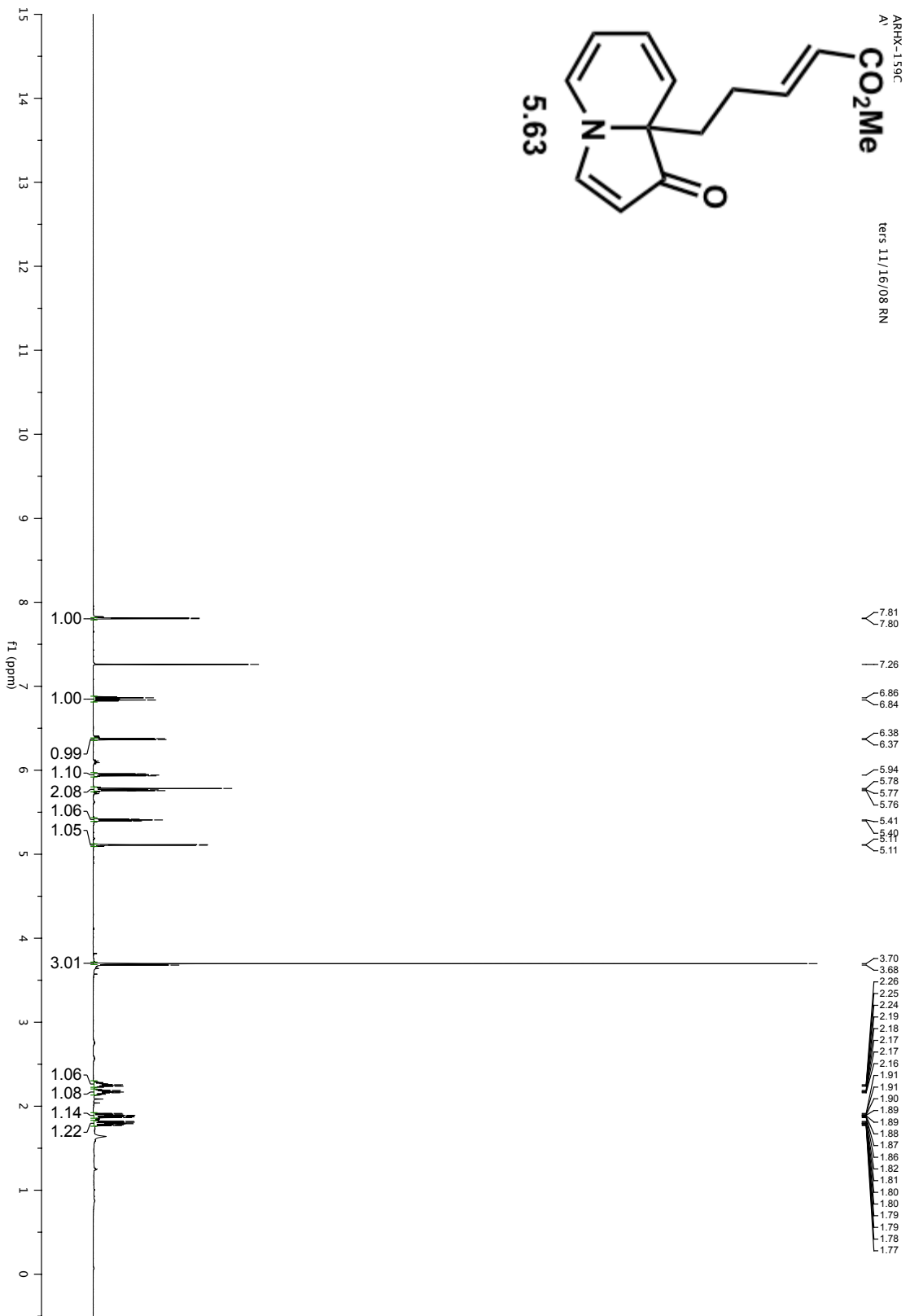
5.61

ARRXV-073A  
AVB-4.00 Z80 Proton starting parameters: 6/11/03 RN

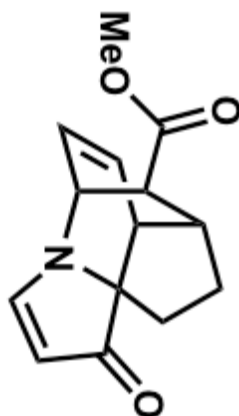




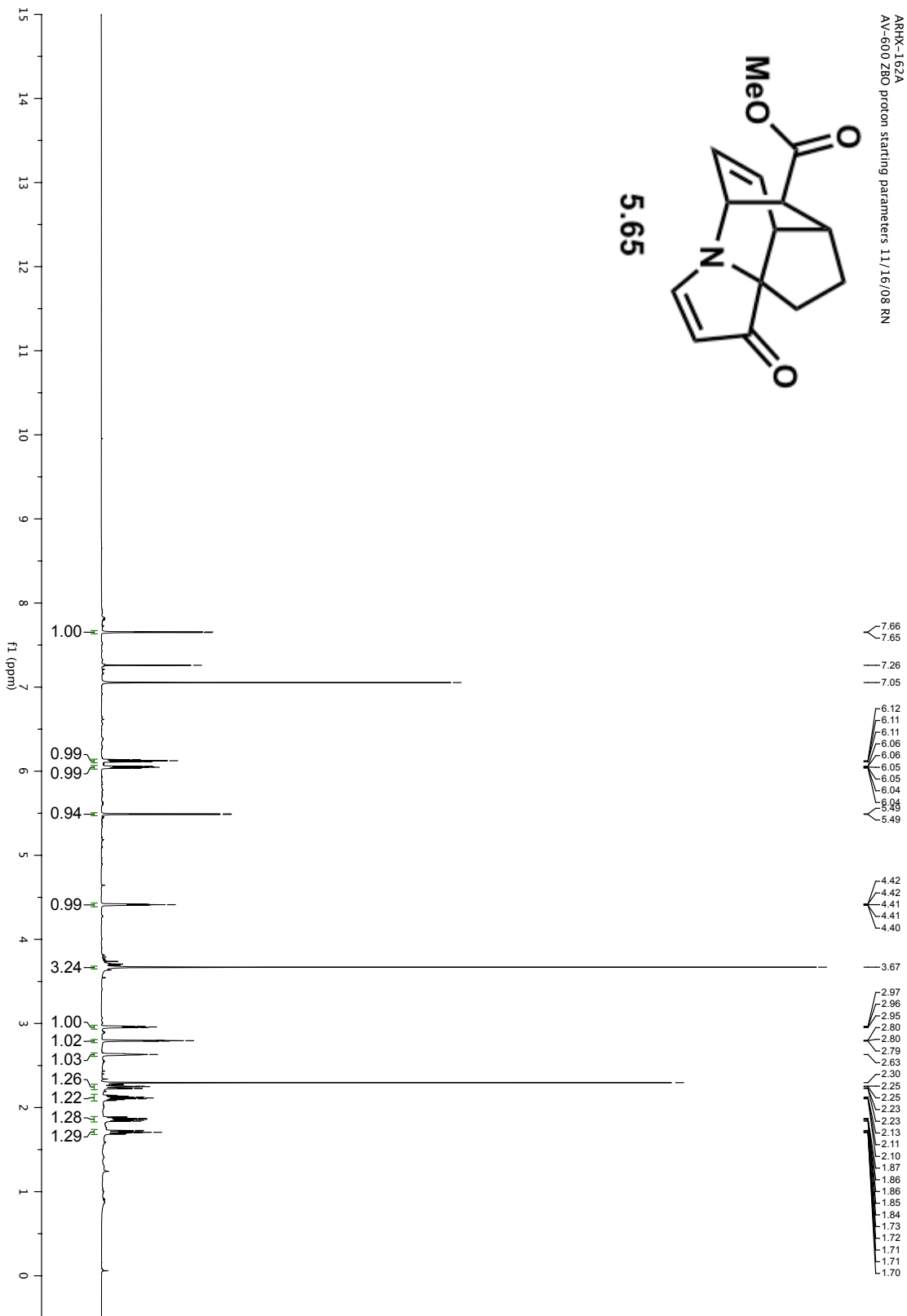
vers 11/16/08 RN

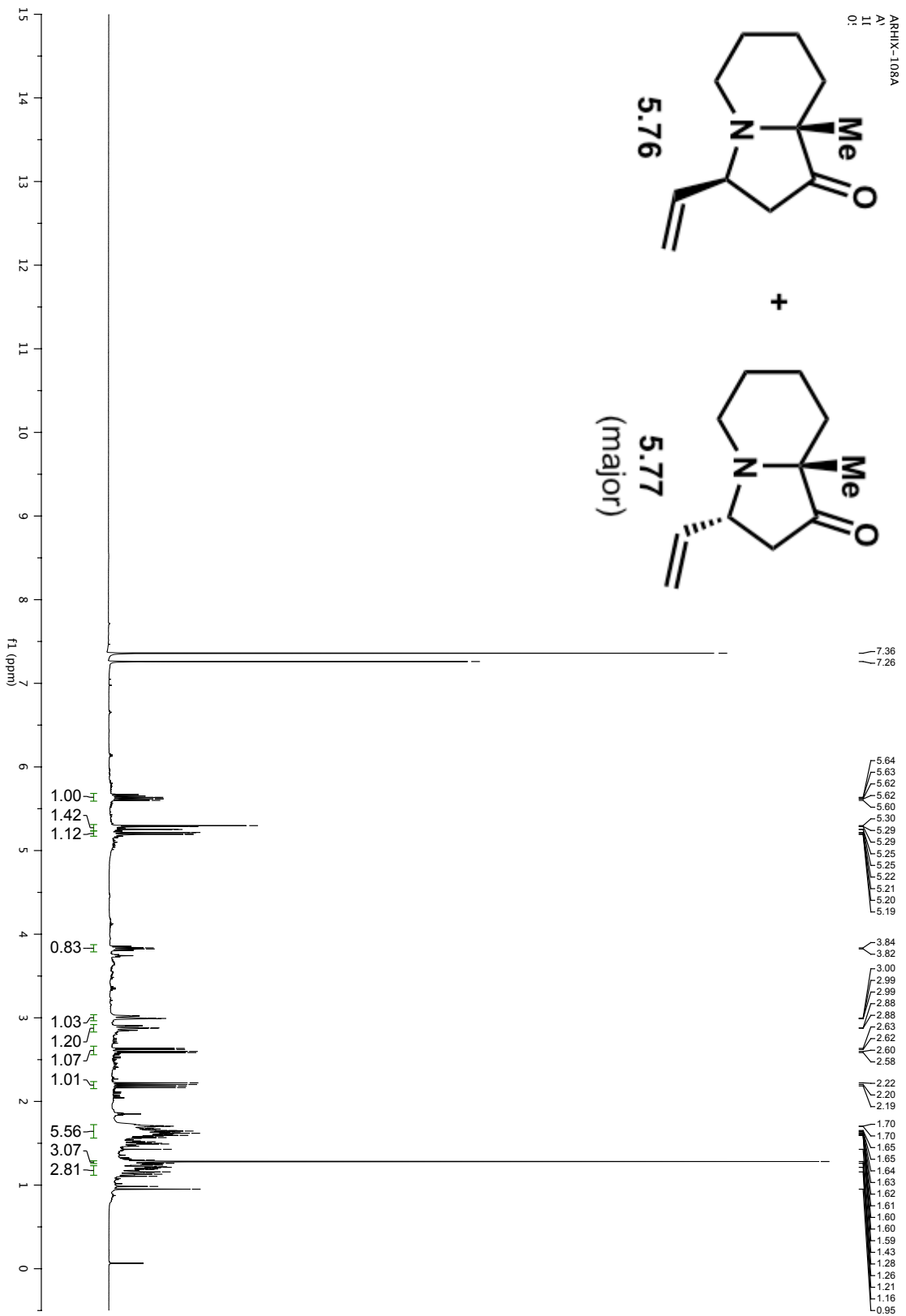


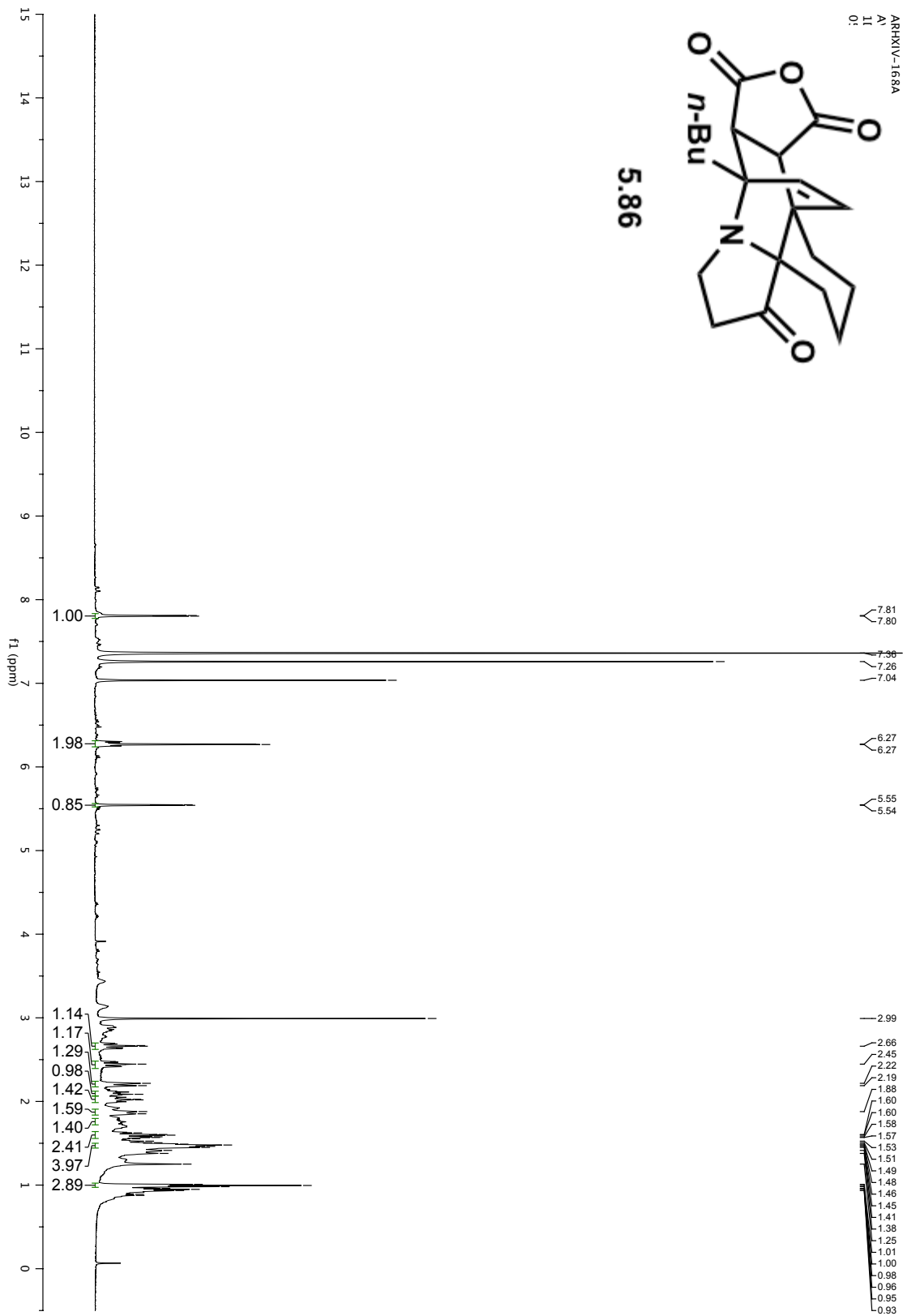
ARHX-162A  
AV-600 Z80 proton starting parameters 11/16/08 RN



5.65

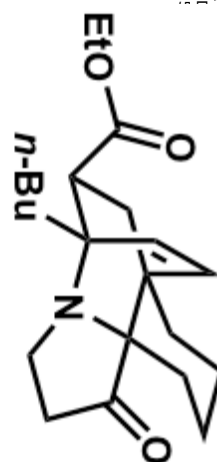




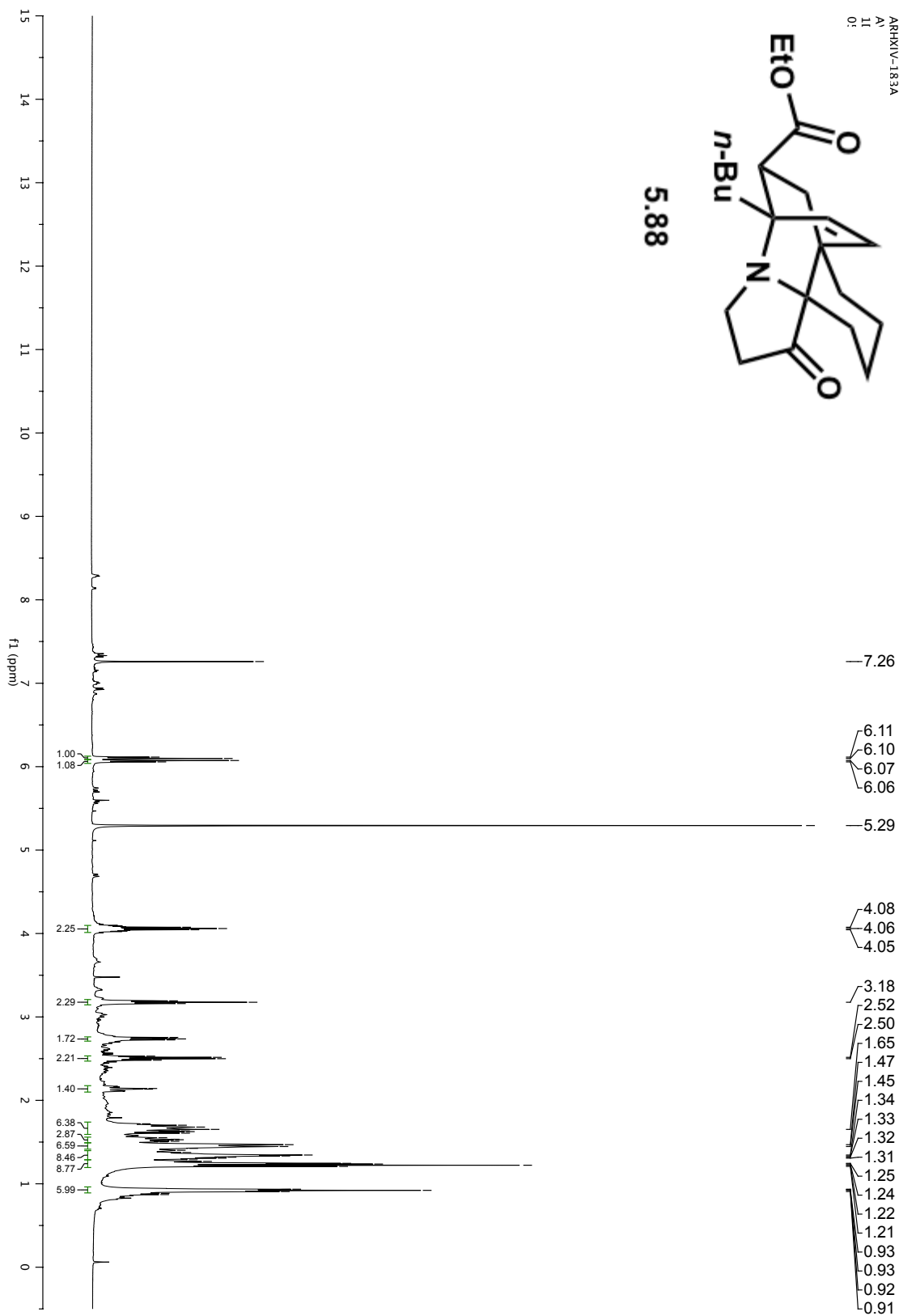




ARRXIV-183A  
A:  
1:  
0:



5.88



## Chapter 6. Synthetic Studies Toward Type II Indolizidine Alkaloids

### 6.1 Selection of Type II Indolizidine Targets

Our considerations for selecting type II indolizidine natural product targets were primarily based on structure. We envisioned accessing type II indolizidine alkaloids from indolizinone precursors, taking advantage of the quaternary carbon present at the ring-fusion in these bicycles (see Chapter 1). Further, we prioritized a target molecule that would capitalize on the innate indolizinone reactivity we discovered through our initial studies on these compounds (see Chapter 5).

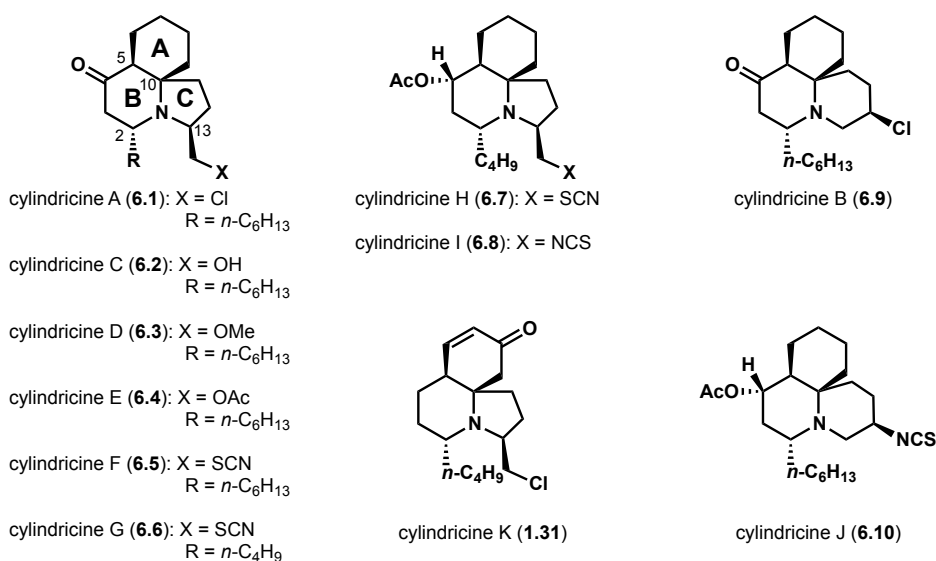
Ultimately, our goal for the synthesis of type II indolizidine alkaloids was to demonstrate the utility of indolizinones as building blocks and showcase the feasibility of relaying the stereochemistry at the ring-fusion carbon to the formation of subsequent stereocenters. To this end, we chose to target tricyclic marine alkaloids of the cylindricine and lepadiformine families (see Figures 6.2.1 and 6.2.3). These alkaloids contain up to five stereocenters about their indolizidine core, providing an ideal landscape to test the relay of stereochemical information from the ring-fusion to the other stereocenters in the bicycle.

### 6.2 Tricyclic Marine Alkaloids: The Cylindricines and Lepadiformines

#### Isolation and Biological Activity

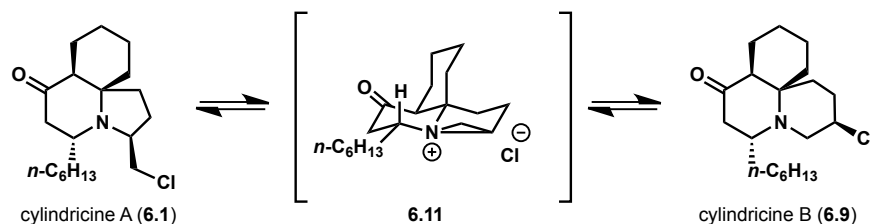
The first two members of the cylindricine family, cylindricines A (6.1) and B (6.9), were isolated in 1993 by Blackman and Li.<sup>1</sup> Cylindricines A and B were the most abundant alkaloids in extracts from the sea ascidian *Clavelina cylindrica* that was collected off the coast of Tasmania. The structures of these tricyclic marine alkaloids were confirmed through X-ray crystallography to possess a *cis*-ring fusion between the two six-membered rings (Figure 6.2.1).

Figure 6.2.1. Cylindricine alkaloids.



Cylindricines A and B were isolated as a mixture, and once purified were shown to independently revert to the same 3:2 ratio of cylindricine A:B.<sup>1</sup> Blackman and Li hypothesized that these natural products interconvert through an aziridinium intermediate such as **6.11** (Figure 6.2.2). This inter-conversion provides some insight into their biological mode of action as proposed DNA-alkylating agents. Aziridinium intermediate **6.11** is reminiscent of a famous class of compounds capable of alkylating DNA, the sulfur mustards.<sup>2</sup>

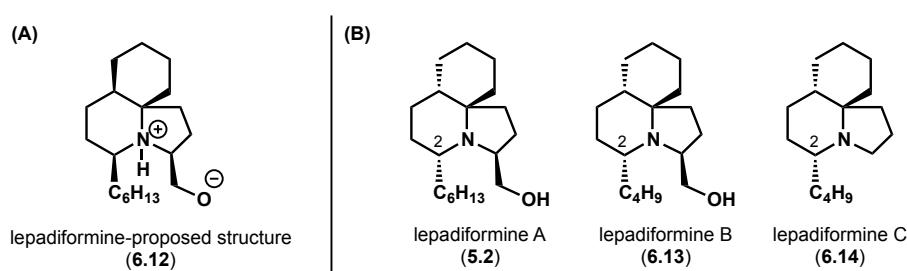
**Figure 6.2.2.** Conversion between cylindricines A and B.



Subsequent to the discovery of cylindricines A and B, nine additional cylindricines were isolated from the same ascidian species.<sup>3,4</sup> The major structural distinctions among these congeners are the size of the C-ring, the identity of the nucleofuge appended to the C-ring, the length of the B-ring alkyl chain, and the oxidation level of the A and B rings (Figure 6.2.1). Cylindricines B (**6.9**) and J (**6.10**) are the only cylindricines that have been isolated in the 6,6,6-tricyclic form. However, other cylindricines are anticipated to undergo the 6,6,5- to 6,6,6-tricyclic rearrangement. One target of our studies is to be able to observe and study this equilibrium through synthetic access to these natural products.

Following the isolation of the cylindricines, a similar tricyclic marine alkaloid was extracted first from *Clavelina lepadiformis* off the coast of Tunisia and shortly thereafter from *Clavelina moluccensis* found in the waters near Djibouti.<sup>5</sup> This alkaloid, given the name lepadiformine, was originally proposed to exist as zwitterion **6.12** (Figure 6.2.3A). However, pioneering synthetic work by Weinreb toward lepadiformine revealed that synthetic **6.12** did not match the physical data of the isolated natural product.<sup>6</sup>

**Figure 6.2.3.** Lepadiformine alkaloids (A) initially proposed structure and (B) structures confirmed through synthetic efforts.



Synthetic chemists played an integral role in determining the lepadiformine structure. As previously mentioned, Weinreb and coworkers identified that natural lepadiformine was not a zwitterion.<sup>7</sup> Pearson made several diastereomers of the proposed lepadiformine structure (**6.12**),

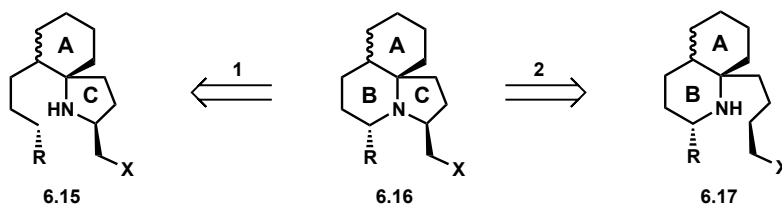
and by process of elimination was able to identify the correct configuration of naturally isolated lepadiformine.<sup>8</sup> The natural product is in fact a 6,6,5-tricycle with substituents at the 2- and 13-positions, like the cylindricines. However, the 6,6-ring fusion of the lepadiformines is *trans* (see **5.2**, Figure 6.2.3B). Lepadiformine (**5.2**), also referred to as lepadiformine A, was the first of three known alkaloids that share a common tricyclic skeleton. The alkyl chain at C2 is two carbons shorter in lepadiformine B (**6.13**) and C (**6.14**). Additionally, lepadiformine C (**6.14**) lacks the hydroxymethylene group present on the five-membered ring of other lepadiformines and the cylindricines.

Beyond having potential activity as DNA-alkylating agents, the lepadiformines have displayed moderate cytotoxic activity on KB cells and non-small-cell lung carcinoma (NSCLC-N6).<sup>5</sup> More recently, the lepadiformines were shown to moderate the inward rectifying potassium ion outward current ( $I_{K1}$ ) in cardiac muscle tissue by binding to a receptor inside the ion channel pore.<sup>9</sup> The binding affinity was dependent on both the length of the alkyl chain at C2 as well as the presence of the hydroxymethylene group at C13. This is an interesting result, considering that there are not many molecules known to block  $I_{K1}$ .

### Previous Synthetic Approaches

Following the isolation of the first cylindricines in 1993, several synthetic chemists have developed and executed routes to these alkaloids. The first total synthesis of a cylindricine alkaloid was achieved by Weinreb and coworkers in 1999, when they disclosed their nitronolefin dipolar cycloaddition approach toward these tricyclic alkaloids and completed the synthesis of cylindricine C (**6.2**).<sup>7</sup> The excitement over these molecules has not faded over the last decade as multiple approaches toward these molecules continue to appear annually, with six strategies disclosed in 2010 alone.<sup>10-15</sup> The work toward these alkaloids through 2006 has been documented in reviews by Weinreb<sup>16</sup> and Renaud.<sup>17</sup> Despite the great number of publications describing total syntheses and progress toward these tricyclic marine alkaloids, there are two common retrosynthetic disconnections shared throughout the reported work. The 6,6,5-core (**6.16**) is most often constructed from a 6,5-spirocyclic precursor, such as **6.15** (Figure 6.2.4). Alternatively, the tricyclic core has also been assembled from decahydroquinolines such as **6.17**.

**Figure 6.2.4.** The two most common retrosynthetic disconnections toward 6,6,5-tricyclic marine alkaloids.



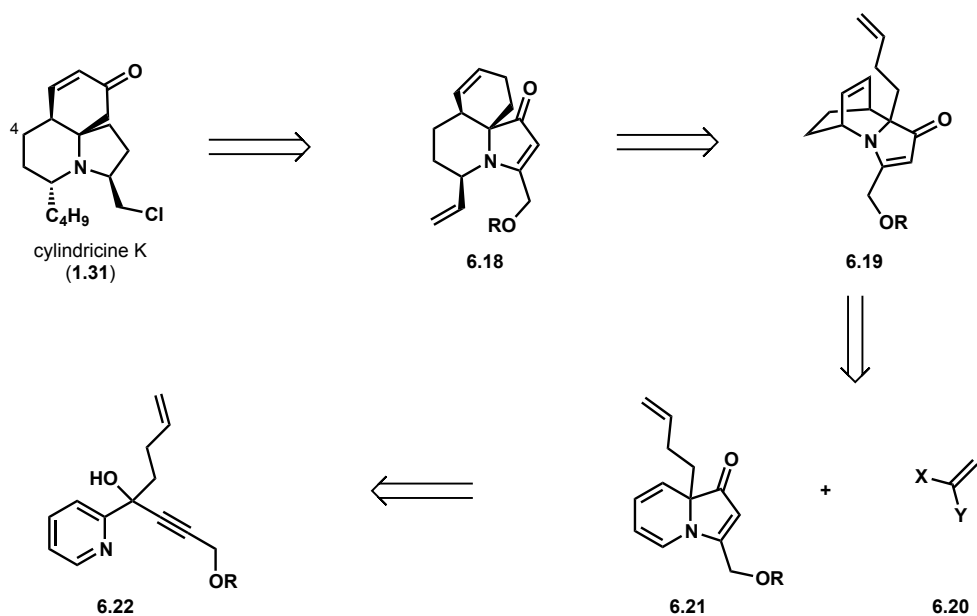
We envisioned accessing these tricyclic marine alkaloids from an indolizinone precursor that would become the B and C-rings of the natural product and appending the A-ring at a later stage. Toward this goal, we have developed a synthesis of the cylindricine K framework outlined in section 6.3 as well as a divergent approach that holds potential for accessing both the cylindricines and the lepadiformines from a common indolizinone intermediate (see Section 6.4).

### 6.3 Toward *Cylindricine K*

In our preliminary efforts toward the cylindricine family of natural products, we chose to focus on the synthesis of cylindricine K (**1.31**). This alkaloid is unique as a cylindricine in several respects. First, it lacks oxygenation at C-4 in the B-ring, which is present in all other known cylindricines. Instead of B-ring oxygenation, cylindricine K possess a higher oxidation level in the A-ring in the form of an enone. Finally, cylindricine K is in the minority of cylindricines having a four-carbon chain at C2 as opposed to the more common six-carbon chain. These structural differences make cylindricine K an uncommon synthetic target and to date no approaches toward this molecule have been reported.

Although cylindricine K is a structural outcast in this family, it was these features that provided a fit with our retrosynthetic analysis. We envisioned accessing cylindricine K (**1.31**) from the 6,6,5-tricycle **6.18** (Figure 6.3.1). This advanced intermediate (**6.18**) contains a double bond within the A-ring that could be elaborated to the enone of the natural product via allylic oxidation. We anticipated arriving at the 6,6,5-tricycle from a ring-opening/ring-closing metathesis of [2.2.2]azabicyclo **6.19**. The metathesis reaction would construct the *cis*-fused A-ring in a single step from the homoallyl group and the unsaturated two-carbon bridge of **6.19**. The [2.2.2]azabicyclo could be accessed through a Diels-Alder cycloaddition of a dienophile (**6.20**) and homoallyl indolizinone (**6.21**). We planned to obtain homoallyl indolizinone (**6.21**) in a metal-free cyclization of a tertiary propargylic alcohol such as **6.22**.

**Figure 6.3.1.** Antithetical analysis of cylindricine K.

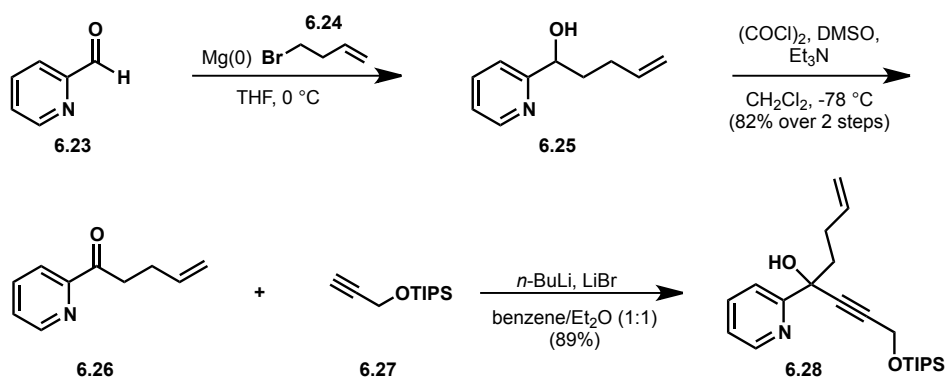


The synthetic work toward cylindricine K began with the preparation of the tertiary alcohol cyclization substrate (**6.28**, Scheme 6.3.1). We envisioned building this cyclization substrate from pyridine-2-carboxaldehyde (**6.23**) by sequentially introducing the homoallyl and propargyl substituents. In the forward direction, a homoallyl Grignard species was generated by refluxing 1-bromo-3-butene (**6.24**) with magnesium turnings in THF. Subsequent addition of this

Grignard to pyridine-2-carboxaldehyde at 0 °C provided secondary alcohol **6.25**. The crude alcohol (**6.25**) was next oxidized under standard Swern conditions to provide pyridyl ketone **6.26**. Although the Swern oxidation is a relatively inexpensive method, the pungent by-products and multi-step procedure inspired us to consider alternative oxidation protocols. However, other oxidation conditions were not successful, including the closely related Parikh-Doering conditions. We hypothesized that the pyridine moiety of **6.25** could be impairing the reaction through coordination to the oxidizing agents such as SO<sub>3</sub> (in the case of the Parikh-Doering). Despite its requirement of low temperatures and pungent odor of by-products, the Swern was adopted as the standard oxidation for this sequence, which delivered ketone **6.26** in 82% yield over two steps.

With the homoallyl group installed, only addition of an acetylide was necessary to reach the desired cyclization substrate (**6.28**). Initial attempts to add lithium or magnesium acetylide species to **6.26** in THF at 0 °C led to low yields of alcohol **6.28** (10-30%), with the mass balance of the material accounted for by ketone **6.26**. Accordingly, optimization of this 1,2-addition was then carried out using trimethylsilylacetylene as a model acetylide nucleophile. Quenching these reactions with deuterated methanol led to deuterium incorporation  $\alpha$  to the carbonyl group, confirming our suspicions that deprotonation was the predominant reaction pathway. To favor 1,2-addition over  $\alpha$ -deprotonation, the cerium acetylide species was generated and reacted with ketone **6.26**. The shift to a cerium acetylide nucleophile led to increased yields of alcohol product (e.g., 63%). However, significant amounts of starting material still remained. The literature suggested 2-acetylpyridines were particularly problematic substrates for 1,2-addition, but that the addition of a lithium salt such as lithium bromide as well as the addition of a less polar co-solvent, like benzene, could improve yields of the 1,2-addition product. The addition of three equivalents of lithium bromide to the reaction mixture and switching from THF to a 1:1 diethyl ether/benzene mixture provided an 89% yield of the 1,2-addition product. Gratifyingly, these modified conditions have delivered high yields of 1,2-addition product for several pyridyl ketones. These conditions translated to an excellent yield of **6.28** when *O*-silylpropargyl alcohol was employed. However, it is worth noting that the use of other *O*-silylpropargyl alcohols with smaller silyl groups led to low yields of 1,2-addition product.

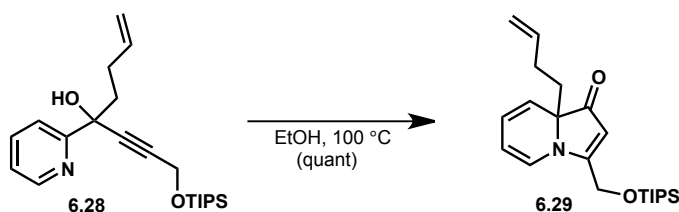
**Scheme 6.3.1.** Synthesis of tertiary alcohol **6.28**.



With access to gram-quantities of tertiary alcohol **6.28**, the synthesis continued with the metal-free cyclization of **6.28** to provide quantitative yields of homoallyl indolizinone **6.29** after

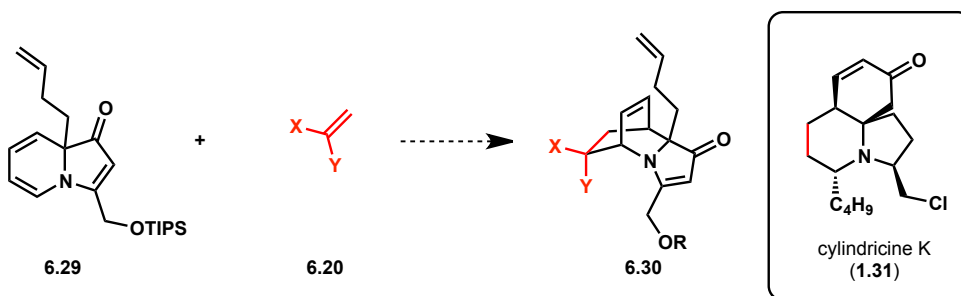
heating in ethanol at 100 °C for approximately two hours. Following cyclization in ethanol, the indolizinone was recovered in pure form by evaporation of the solvent. Indolizinone **6.29** was used directly in subsequent reactions.

**Scheme 6.3.2.** Cyclization of tertiary alcohol **6.28** to indolizinone **6.29**.



At this juncture, we considered several potential dienophiles to employ in a Diels-Alder cycloaddition with indolizinone **6.29**. The two carbons incorporated from the dienophile will ultimately become the two methylene units contained within the B-ring of the natural product (see atoms shown in red, Scheme 6.3.3). Thus, the use of ethylene as the dienophile would be ideal for our synthetic strategy. However, Diels-Alder reactions with ethylene are known to require extreme temperatures and pressures (175 °C, 6000 psi)<sup>18</sup> that we anticipated could be procedurally difficult to attain for gram-scale reactions in an academic laboratory setting. To this end, we considered a variety of dienophiles that would serve as ethylene or ketene equivalents.<sup>19</sup>

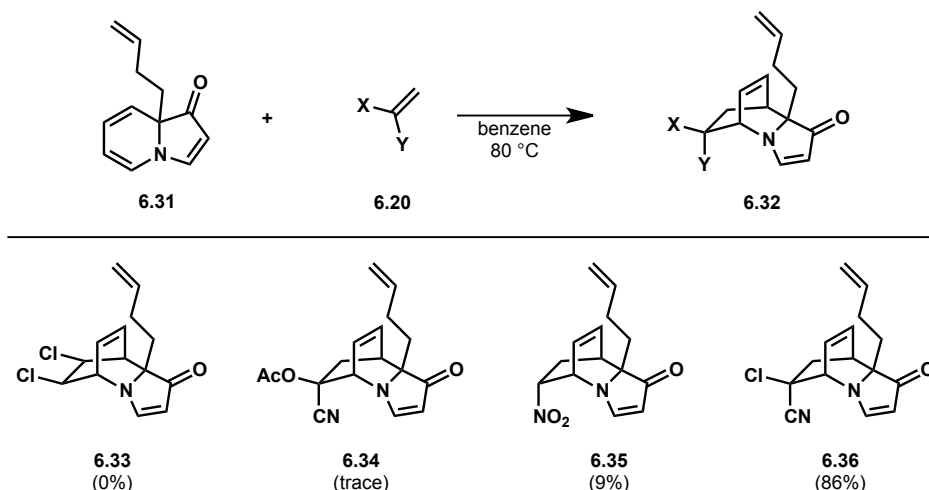
**Scheme 6.3.3.** Illustration of the fate of the dienophile carbons in the natural product.



Evaluation of potential dienophiles was carried out on a homoallyl indolizinone lacking the methylene-OTIPS substituent on the five-membered ring (**6.31**, Figure 6.3.2, see Experimental Methods for details on the synthesis of this compound). The use of *cis*-1,2-dichloroethylene did not provide detectable amounts of Diels-Alder adduct **6.33** under the conditions shown in Figure 6.3.2; however, further experimentation in related systems revealed that higher temperatures (e.g., 120 °C) does lead to a productive Diels-Alder reaction between indolizinones and *cis*-1,2-dichloroethylene. Similarly, 2-acetoxyacrylonitrile gave only trace amounts of [2.2.2]azabicyclic **6.34**. However, heating indolizinone **6.31** with nitroethylene, which was generated *in situ*, led to the isolation of [2.2.2]bicyclic **6.35** in a meager 9% yield. Attempts to improve upon this yield were met with minor success, but included: (1) the addition of catechol, (2) freshly distilling nitroethylene, and (3) a screen of a range of reaction temperatures.

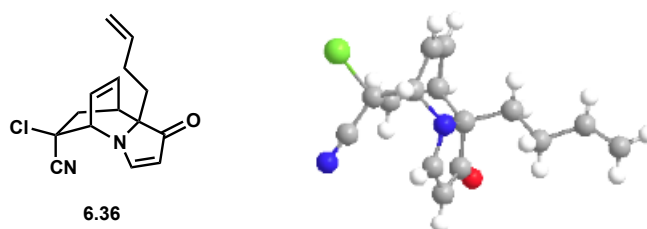
Finally, when 2-chloroacrylonitrile was used as the dienophile, we were rewarded with an 86% yield of the desired Diels-Alder adduct (**6.36**).

**Figure 6.3.2.** Screen of potential dienophiles.



All of the Diels-Alder products were obtained as a single diastereomer. We initially hypothesized that the dienophile would approach from the face of the indolizinone opposite the ring-fusion substituent, and this hypothesis was ultimately confirmed through X-ray crystallographic analysis of a Diels-Alder adduct. The crystal structure of chloronitrile **6.36** (Figure 6.3.3) indicated that the homoallyl substituent and unsaturated bridge reside on the same face of the bicycle. The stereochemistry of the chloride and nitrile groups were also ascertained from the crystal structure, indicating the chloride *syn* to the unsaturated bridge.

**Figures 6.3.3.** X-ray crystal structure of Diels-Alder product **6.36**.

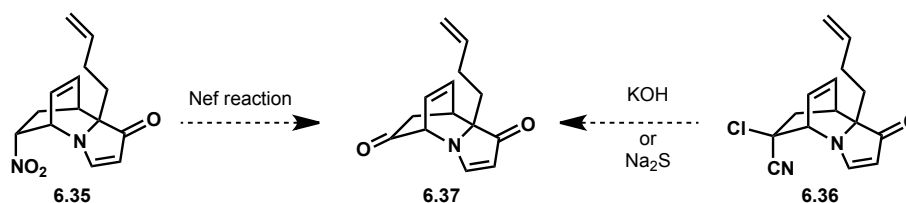


Using the nitro- and chloronitrile [2.2.2]bicycles (**6.35** and **6.36**, respectively), we investigated the conversion of these molecules to ketone **6.37** (Scheme 6.3.4). The conversion of a nitro group to a carbonyl, the Nef reaction, is well preceded.<sup>20</sup> The classic Nef conditions require initial formation of a nitronate salt under basic conditions followed by hydrolysis in a strong acid to afford the carbonyl-containing product. Unfortunately, exposure of **6.35** to a variety of strong bases led to decomposition of the starting material. We postulate that decomposition pathways could be initiated by addition of hydroxide to the vinylogous amide to form a vinylogous acid. Alternatively, potential fragmentation of the [2.2.2]bicycle could occur



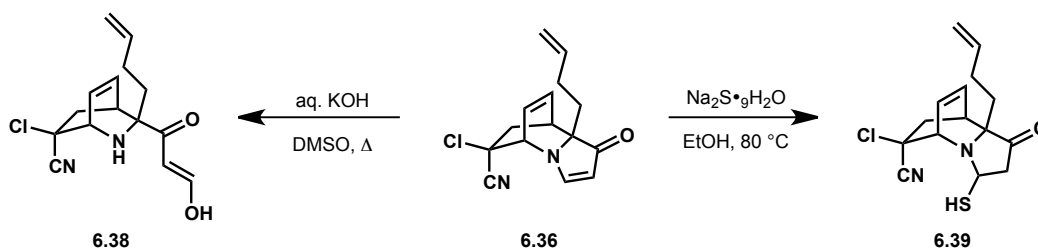
from the anion generated  $\alpha$  to the nitro group of **6.35**. In addition to the classic Nef conditions, both reductive and oxidative protocols for effecting this transformation were attempted; however, neither starting material nor the desired product were recovered from these reaction mixtures. At this stage, low yields for the Diels-Alder cycloaddition with nitroethylene, coupled with the initial difficulties in transforming **6.35** to ketone **6.37** led us to focus on the chloronitrile **6.36**.

**Scheme 6.3.4.** Proposed conversion of Diels-Alder adducts to ketone **6.37**.



As with a nitro group, the conversion of chloronitriles to carbonyls has been known for several decades and tested in the context of complex molecule synthesis.<sup>19</sup> The method with the most precedent for this transformation is treatment of a chloronitrile with aqueous potassium hydroxide in hot DMSO. Applying these conditions to **6.36** led to the exclusive formation of vinylogous acid **6.38** (Scheme 6.3.5). Alternative conditions for effecting this transformation include heating the chloronitrile substrate in ethanol with sodium sulfide. Similarly to hydroxide, the sulfide nucleophile interacts preferentially with the vinylogous amide moiety of **6.36** over the chloronitrile group; however, 1,4-addition of the sulfur to the vinylogous amide did not lead to opening of the five-membered ring, and thioaminal **6.39** was isolated as the product. To avoid the undesired 1,4-addition of nucleophiles to the vinylogous amide, we attempted to reduce the vinylogous amide of **6.36**. However, a range of reducing agents (including, but not limited to: lithium aluminum hydride, sodium borohydride, and diisobutylaluminum hydride) led to complex mixtures of products that showed some preference for reduction of the nitrile over the vinylogous amide.

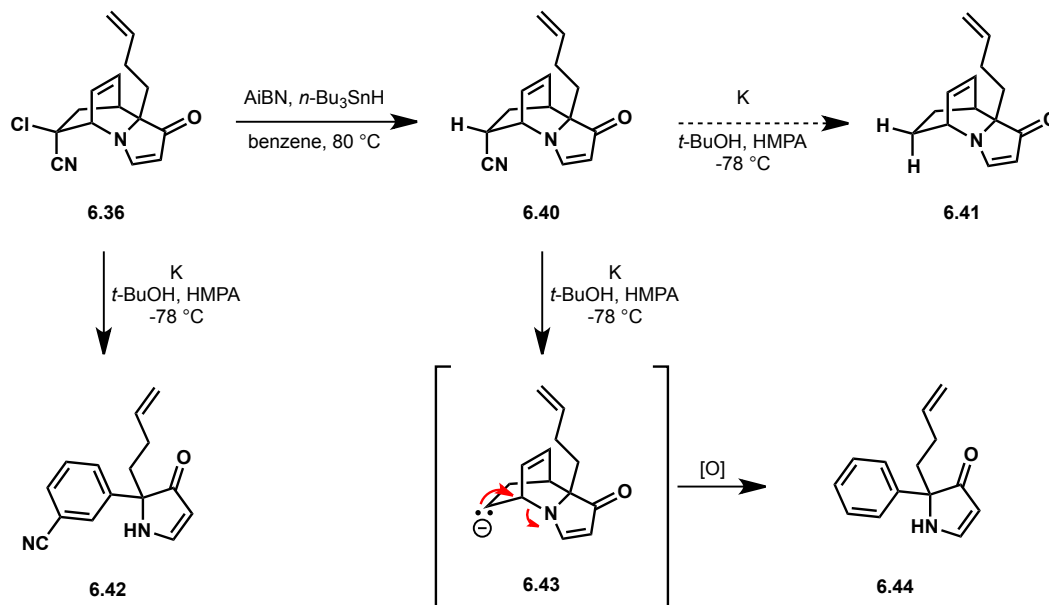
**Scheme 6.3.5.** Attempts to convert chloronitrile **6.36** to ketone **6.37**.



Although conventional methods for transforming a chloronitrile to carbonyl group were not fruitful in our system, we envisioned a variety of alternative routes for obtaining desired ketone **6.37** or methylene compound **6.41** from chloronitrile **6.36**. One two-step plan toward **6.41** required a radical dechlorination of **6.36** followed by reductive cleavage of the nitrile group. The first half of this approach could be cleanly accomplished by the treatment of **6.36** with AIBN and

tributyltin hydride in refluxing benzene (see **6.36** to **6.40**, Scheme 6.3.6). With dechlorinated compound **6.40** in hand, the next task was reductive cleavage of the nitrile group from the [2.2.2]bicycle under dissolving metal conditions. A single product was obtained from this reaction in good yield; however, the product did not resemble desired [2.2.2]bicycloproduct **6.41**. Instead, a monosubstituted aromatic compound was obtained, and  $^1\text{H}$  NMR and mass spectral data confirmed the identity of the product as **6.44**. Although this was not the expected product, upon closer examination of the intermediates generated, the formation of arene **6.44** is not surprising. Reductive C-C bond cleavage presumably generates anion **6.43**, which we had initially anticipated would be protonated to give the desired product. Instead, it appears that the anionic intermediate **6.43** undergoes fragmentation to cleave the C-N bond of the [2.2.2]bicycle (see arrows, **6.43**) and form a cyclohexadiene, which, following oxidation in air, provides arene **6.44**. Employing toluene as the solvent in this reaction, varying the temperature, or the addition of 18-crown-6 all still resulted in formation of arene **6.44** as the sole product. Additionally, subjecting the chloronitrile **6.36** to the same dissolving metal conditions gave benzonitrile **6.42** as the major product. Although fragmentation of the [2.2.2]azabicyclo was not desirable in the context of our progress toward cylindricine K, one can imagine transforming products such as **6.42** and **6.44** into biologically relevant classes of molecules, such as protease inhibitors.<sup>21</sup>

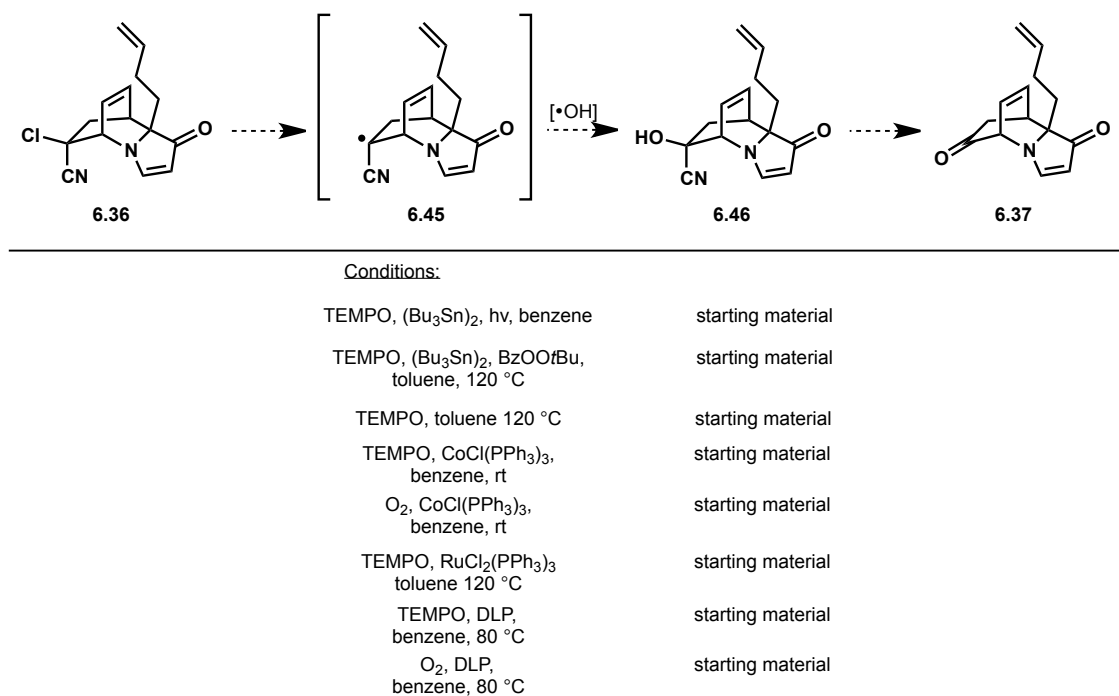
**Scheme 6.3.6.** Two-step strategy to convert **6.36** to **6.41**.



Our next approach involved intercepting the radical generated under radical dechlorination conditions (**6.45**) with oxygen to form a cyanohydrin (**6.46**), which could collapse to provide ketone **6.37** (Figure 6.3.4). We tested the competence of several radical initiators in conjunction with various sources of oxygen radicals. Specifically, we investigated the use of hexabutylditin as a radical source by either thermal or photochemically-induced homolysis of the tin-tin bond, but observed only starting material in these reactions. Next we explored the potential for radical dechlorination with metal complexes such as  $\text{CoCl}(\text{PPh}_3)_3$  and  $\text{RuCl}_2(\text{PPh}_3)_2$  without success. Finally, lauroyl peroxide was employed under thermal conditions was

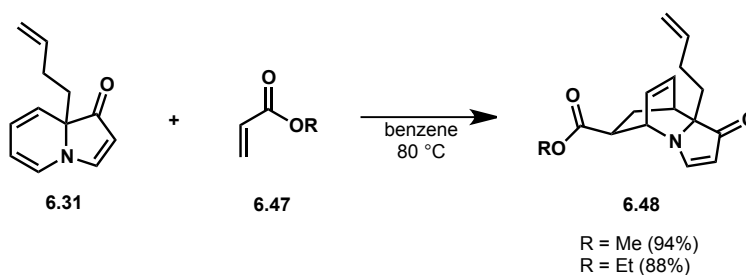
employed with both TEMPO and molecular oxygen as radical sources. These reactions resulted only in the recovery of starting material, indicating that the radical dechlorination did not occur under any of these conditions.

**Figure 6.3.4.** Attempted cyanohydrin (**6.46**) formation.



Without success in transforming the chloronitrile (**6.36**) to either ketone **6.37** or methylene **6.41**, we began to consider alternative dienophiles to 2-chloroacrylonitrile. Specifically, we sought to investigate potential dienophiles beyond ethylene or ketene equivalents, opting instead for acrylates. Upon heating either methyl or ethyl acrylate (**6.47**) with homoallyl indolizinone (**6.31**) in boiling benzene, the corresponding [2.2.2]azabicycle (**6.48**) was obtained in good yield (Scheme 6.3.7).

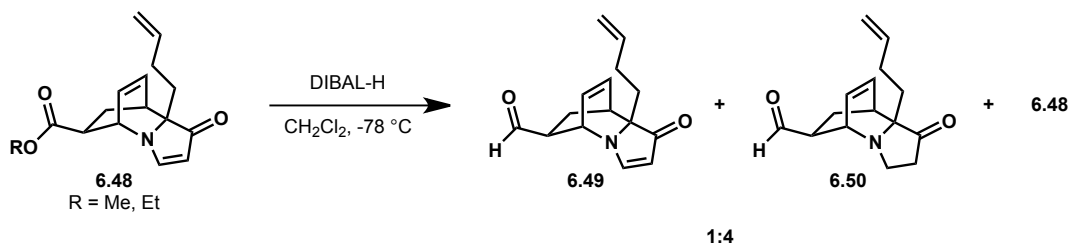
**Scheme 6.3.7.** Diels-Alder cycloaddition with acrylates.



We envisioned two potential methods for cleavage of the carbon-carbon bond adjoining the ester group and the bicycle. Our first strategy involved saponification to the corresponding

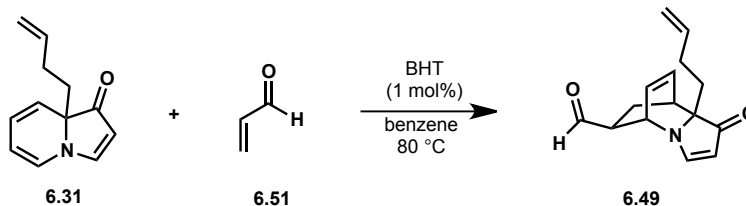
carboxylic acid followed by Barton decarboxylation to deliver bicycle **6.41**. Under a variety of saponification conditions, both the methyl and ethyl esters (**6.48**) remained intact; however, the vinylogous amide moiety was readily converted to the vinylogous acid. The second strategy was to reduce the ester to an aldehyde and perform a decarbonylation in a second step. Treatment of ester **6.48** with one equivalent of diisobutylaluminum hydride in dichloromethane at  $-78\text{ }^{\circ}\text{C}$  led to reduction of the ester group to an aldehyde (Scheme 6.3.8). Although the desired aldehyde **6.49** was obtained, a greater amount of a second aldehyde product was formed in which the vinylogous amide had also been reduced (**6.50**). The mass balance of the reaction was accounted for by ester **6.48** with the vinylogous amide intact. This suggests that reduction of the vinylogous amide occurs only after the ester is reduced, and that the reduction of the vinylogous amide of **6.49** is faster than the reduction of the ester group in the starting material. This result could be repeated; however, attempts to convert all starting material to the doubly reduced product (**6.50**) by increasing the equivalents of diisobutylaluminum hydride led to further reduction of the aldehyde to a primary hydroxyl group.

**Scheme 6.3.8.** Treatment of ester **6.48** with diisobutylaluminum hydride.



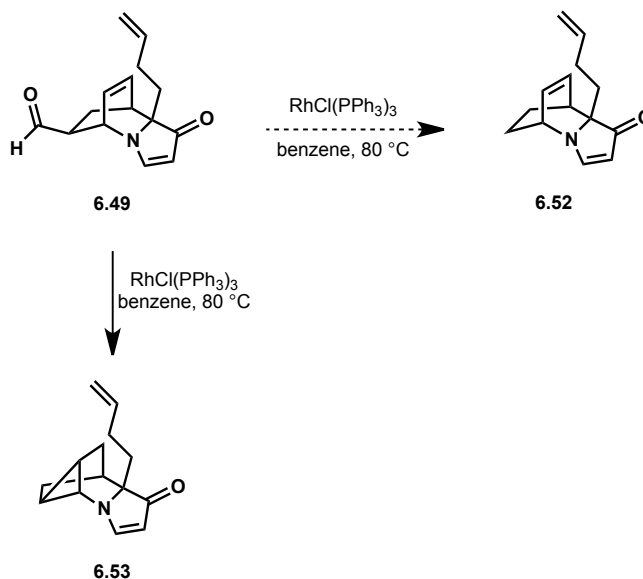
Because only small amounts of aldehyde **6.49** could be obtained from reduction of ester **6.48**, we devised a more direct route to aldehyde **6.49**. Opposed to converting the ester appended to the [2.2.2]bicycle to an aldehyde, we anticipated accessing aldehyde **6.49** in a single step from homoallyl indolizone **6.31** by employing acrolein (**6.51**) as the dienophile. Despite concerns of acrolein polymerizing under the Diels-Alder conditions, there are a plethora of examples of acrolein participating in thermal and Lewis acid-catalyzed [4+2] cycloadditions.<sup>22</sup> Freshly distilled acrolein was combined with homoallyl indolizone **6.31** and heated to reflux in benzene. Modest yields of the desired aldehyde were obtained; however, the addition of butylated hydroxytoluene (BHT), a radical scavenger, improved yields of **6.49** to 73% (Scheme 6.3.9). Alternatively, this transformation could be accomplished with 5 mol%  $\text{BF}_3 \cdot \text{OEt}_2$  in dichloromethane at ambient temperature to provide a comparable yield of aldehyde **6.49**.

**Schemem 6.3.9.** Diels-Alder cycloaddition with acrolein.



With rapid access to aldehyde **6.49**, we focused our efforts on the decarbonylation of this intermediate. Classically, decarbonylation reactions are performed with stoichiometric amounts of Wilkinson's catalyst because the rhodium carbonyl complex generated upon reductive elimination does not re-enter the catalytic cycle. Although there have been significant developments in achieving catalytic methods for this transformation, these catalytic systems are often limited to primary aldehydes.<sup>23</sup> Thus, the stoichiometric reaction is routinely employed in decarbonylations of more complex systems. With these considerations in mind, our first attempt at decarbonylation of **6.49** employed one equivalent of Wilkinson's catalyst (Scheme 6.3.10). The mass spectral data for the product obtained after two days corresponded to the loss of CO from the parent molecule; however, the <sup>1</sup>H and <sup>13</sup>C NMR data did not support the formation of the expected decarbonylation product (**6.52**). Notably, the product did not contain an unsaturated two-carbon bridge. Ultimately, the physical data was consistent with the cyclopropane-containing product, **6.53**.

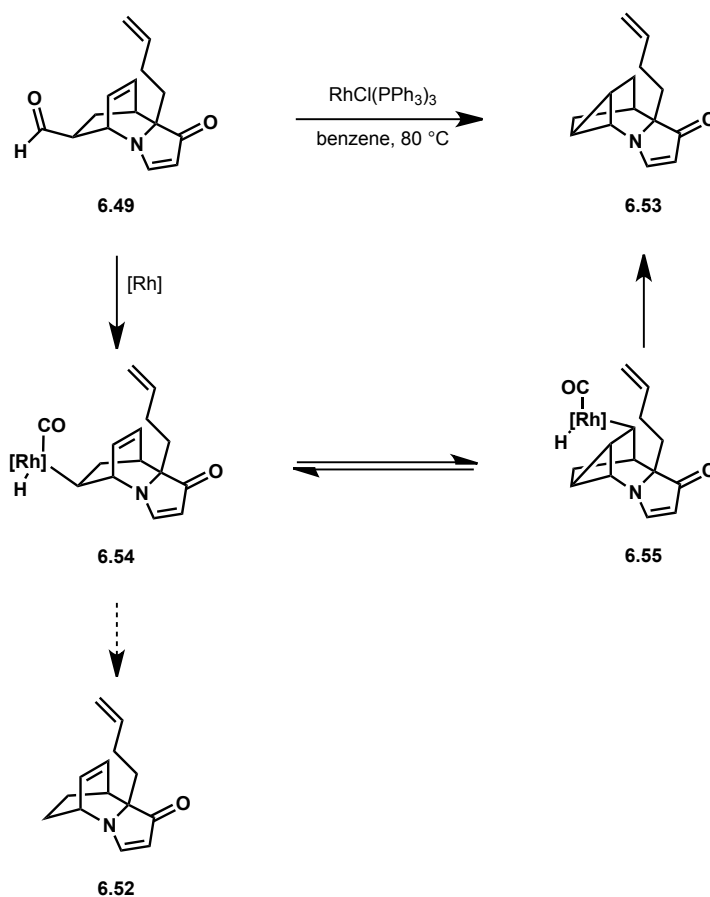
**Scheme 6.3.10.** Attempted decarbonylation of aldehyde **6.49**.



Our proposed mechanistic rationale for the formation of cyclopropane **6.53** instead of the anticipated decarbonylation product **6.52** relies on the relative rates of reductive elimination from intermediates **6.54** and **6.55** (Scheme 6.3.11). Oxidative addition of the C-H bond of the aldehyde to the initial rhodium complex, followed by CO deinsertion would provide rhodium

intermediate **6.54**. Reductive elimination from this intermediate would provide desired decarbonylated product **6.52**. However, we hypothesize that rhodium intermediate **6.54** could be stabilized through an interaction with the proximal  $\pi$ -system of the bicycle, disfavoring reductive elimination from this intermediate. An alternative pathway available to intermediate **6.54** would be insertion of the unsaturated two-carbon bridge into the rhodium-carbon bond to provide a cyclopropane-containing rhodium intermediate, which upon reductive elimination would deliver the observed product (**6.53**). It is worth noting that a similar result was obtained by Horton and coworkers in the context of a norbornene system.<sup>24</sup>

**Scheme 6.3.11.** Proposed mechanism of cyclopropane formation.

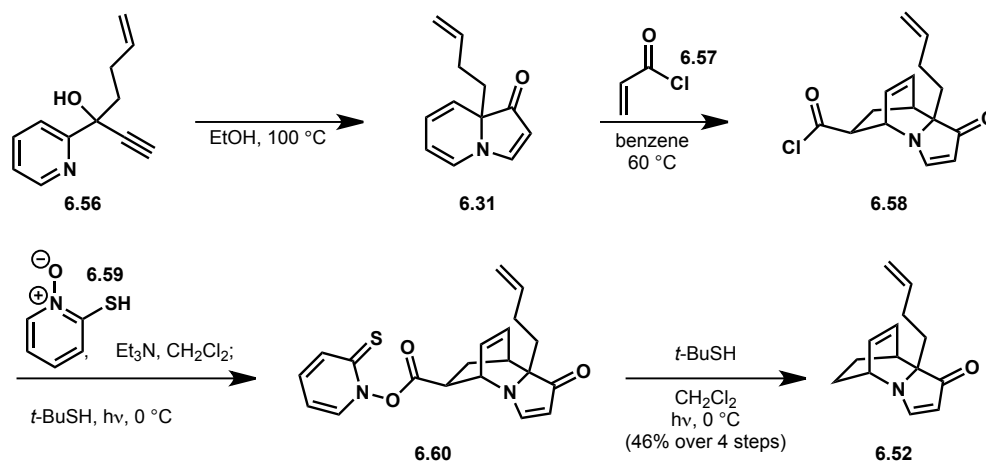


Efforts to obtain **6.52** as a major product via decarbonylation were not fruitful. However, other substrates that possessed a methyl or ethyl group in place of the homoallyl substituent led to mixtures of decarbonylated and cyclopropane-containing products. This implicates the homoallyl group in causing an effect that does not exist in related systems. Alternatively, aldehyde **6.49** was also exploited as a carboxylic acid precursor, by employing standard Pinnick oxidation conditions. Unfortunately, attempts to directly form the Barton ester from the carboxylic acid (en route to a decarboxylation reaction) were unsuccessful.

Ultimately, the sought after [2.2.2]azabicycle was obtained in a four-step sequence from tertiary alcohol **6.56** (Scheme 6.3.12). Freshly made indolizinone **6.31** was reacted with acryloyl

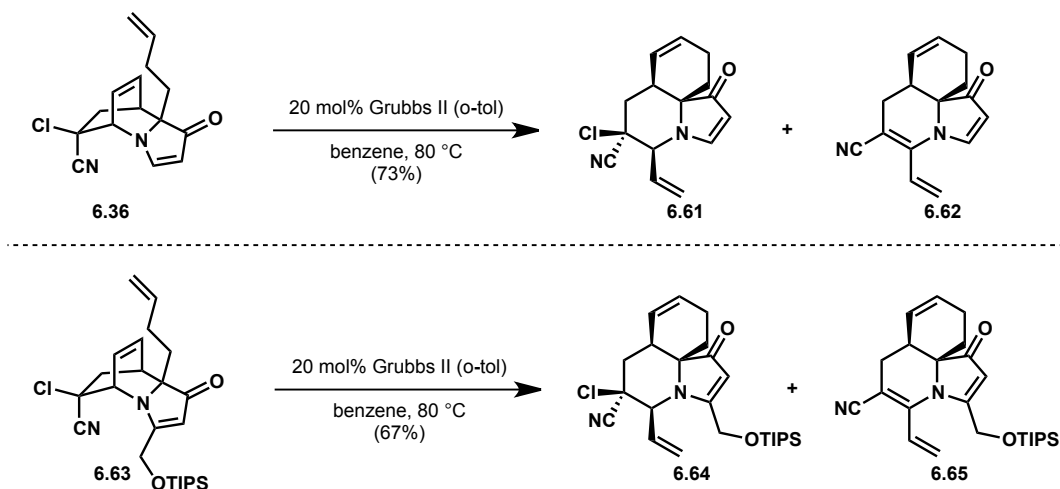
chloride at 60 °C in benzene to provide Diels-Alder adduct **6.58**. The crude acid chloride (**6.58**) was next converted to the Barton ester. Optimal yields of the Barton ester required the acid chloride and 2-mercaptopyridine *N*-oxide to stir together in complete darkness for 24 hours. Decarboxylation of the Barton ester (**6.60**) was accomplished by treatment with *tert*-butylthiol at 0 °C, immediately followed by irradiation with a Tungsten lamp for two hours. This protocol provided bicyclic **6.52** in 46% yield over four steps.

**Scheme 6.3.12.** Barton decarboxylation to obtain [2.2.2]azabicyclic **6.52**.



From the [2.2.2]azabicyclic, the next significant step toward cylindricine K was the ring-opening-ring-closing metathesis to access the 6,6,5-tricyclic cylindricine core. Although [2.2.2]azabicyclic **6.52** was our desired substrate for this transformation in our initial analysis, we first attempted this key step from chloronitrile **6.36**, which we were able to access first. Standard ruthenium-based metathesis catalysts were screened including Grubbs I, Grubbs II, Grubbs-Hoveyda II, and the *o*-tol version of the Grubbs II catalyst. The desired product was obtained with all these catalyst except Grubbs I. The highest, most reproducible, yields were provided with the *o*-tol catalyst. Presumably, the increased steric bulk of the mesityl group of the Grubbs II catalyst is not ideal for the densely functionalize bicycle (**6.36**). Additionally, saturating the reaction mixture with ethylene was advantageous for the formation of product. It is noteworthy that sparging the reaction mixture for 5-10 minutes was optimal, but running the reaction under an atmosphere of ethylene resulted in lower yields of the desired product.

**Scheme 6.3.13.** Optimized conditions for the RORC metathesis of chloronitriles **6.36** and **6.63**.

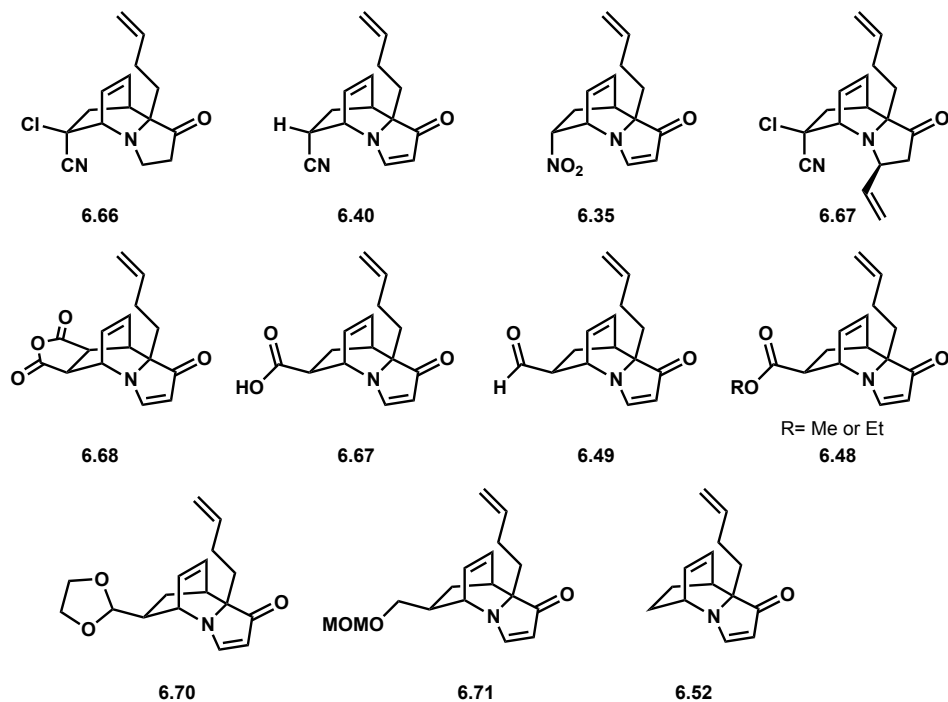


Running the ring-opening metathesis on a larger scale led to the isolation of a by-product. The by-product was identified as **6.62**, resulting from the elimination of HCl from metathesis product **6.61**. A control experiment revealed that simply heating **6.61** in benzene did not lead to the formation of **6.62**, but that **6.62** was formed in the presence of the ruthenium catalyst.

En route to the targeted [2.2.2]bicycle (**6.52**), dozens of unique [2.2.2]azabicycles were synthesized and subjected to optimized metathesis conditions. However under the conditions optimized for **6.36** and **6.63**, ring-opening/ring-closing metathesis products were not obtained for any of the bicycles listed in Figure 6.3.5. It is remarkable that none of the [2.2.2]bicycle substrates led to the metathesis product. There are several explanations that can be offered for individual substrates. For example, tertiary amines **6.66** and **6.67** could be too basic, leading to an unproductive interaction between the basic nitrogen and the catalyst. The dechlorinated bicycle **6.40** did not react, which led us to hypothesize that two substituents were necessary at this position. This theory was supported by recovery of starting material from reactions with nitro-bicycle **6.35**, anhydride **6.68**, acetal **6.70**, and MOM-protected alcohol **6.71**. Several substrates underwent decomposition including carboxylic acid **6.69**, aldehyde **6.49**, and ester **6.48**. We hypothesized that these substrates decomposed via pathways that commence with deprotonation  $\alpha$  to the carbonyl group.



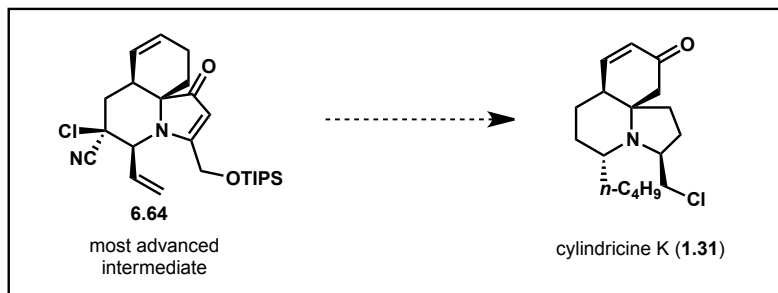
**Figure 6.3.5.** Substrates that did not participate in the ring-opening/ring-closing metathesis under conditions optimized for **6.36** and **6.63**.



Alas, the long-sought-after methylene bicycle **6.52** did not participate in the ring-opening/ring-closing metathesis with Grubbs II or Grubbs II (*o*-tol) catalysts. Although this is disadvantageous in the context of the synthesis of cylindricine K, it provides further intrigue regarding the factors governing the ring-opening/ring-closing metathesis of the [2.2.2]azabicyclic system. Our results suggest that higher substitution about the bicycle is beneficial; thus, it is plausible that the substituents could contribute to the strain of the [2.2.2]bicyclic system, creating a more reactive substrate.

Exploration of the ring-opening/ring-closing metathesis revealed the ideal compound was not in fact the methylene compound **6.52**, but rather the chloronitrile **6.63**. However, to elaborate tricyclic **6.64** to cylindricine K, several synthetic challenges remained (Figure 6.3.6): (1) the chloronitrile moiety still needed to be converted to the methylene; (2) oxidation of the A-ring double bond to the enone was necessary; and (3) the C-2 vinyl group should be extended by two carbons, reduced, and the stereochemistry inverted. Finally, (4) the vinylogous amide required complete reduction to the pyrrolidine.

**Figure 6.3.6.** Most advanced intermediate en route to cylindricine K.

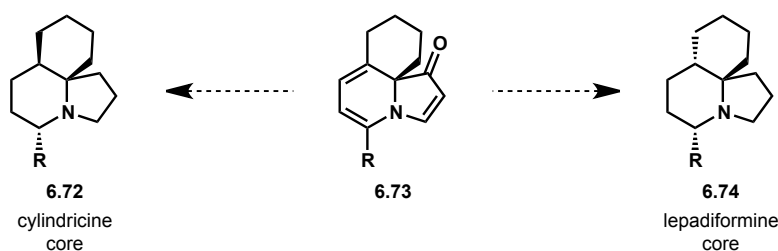


Even though the metathesis product **6.64** does not provide immediate access to the natural product, this 6,6,5-tricycle constitutes the tricyclic core common to several marine alkaloids with the requisite *cis*-6,6-ring fusion of the cylindricine family. Toward our greater goal of understanding the reactivity of indolizinones, **6.64** represents the most complex and highly-functionalized molecule built from an indolizinone to date.

#### **6.4 A Consolidated Approach Toward the Lepadiformines and Cylindricines via a Ring-Contractive Cyclization**

During the development of our first generation route toward cylindricine K, we became interested in devising a divergent approach that would grant access to the cylindricine and lepadiformine alkaloids. The fundamental difference between these alkaloid families is the configuration of the 6,6-ring fusion that is *cis* in the cylindricines and *trans* in the lepadiformines (Figure 6.4.1). We envisioned arriving at either the *trans*- or the *cis*-ring fusion from an indolizinone intermediate such as **6.73**. The key to this approach lies in our ability to harness the stereochemistry at the indolizinone ring-fusion to control the diastereoselectivity of subsequent transformations.

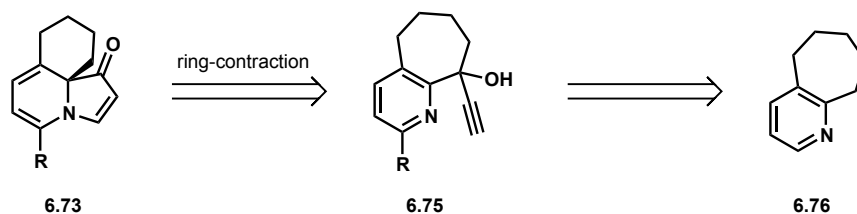
**Figure 6.4.1.** Access to the cylindricine and lepadiformine alkaloids from a common intermediate.



Toward this goal, we sought to build key indolizinone intermediate **6.73** using the metal-free cyclization of a tertiary alcohol such as **6.75** (Figure 6.4.2). This tertiary alcohol could ultimately be accessed from commercially available 2,3-cycloheptenopyridine (**6.76**). In the forward sense, indolizinone formation from **6.75** would require a ring-contraction, which had not previously been explored in the context of an indolizinone-forming cyclization. Accordingly,

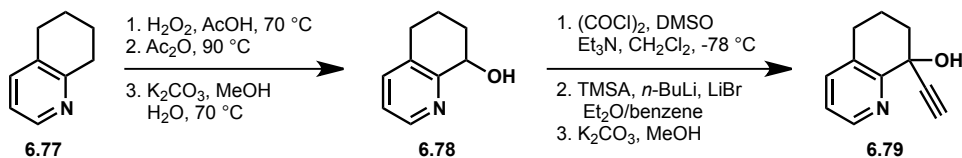
prior to building seven-membered ring substrate **6.75**, we were interested in exploring the feasibility of a ring-contractive cyclization of a more accessible six-membered ring substrate (**6.79**, Scheme 6.4.1).

**Figure 6.4.2.** Synthetic plan for accessing common intermediate **6.73**.



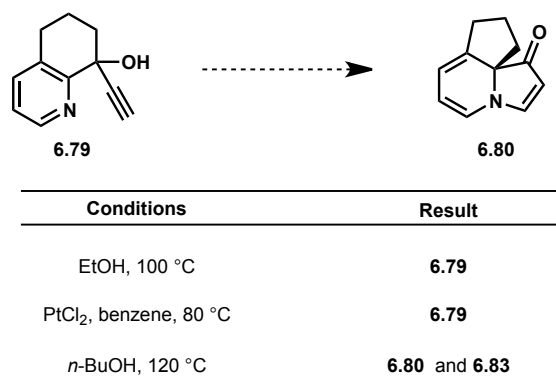
The model six-membered ring substrate (**6.79**, Scheme 6.4.1) was built in six steps from tetrahydroquinoline **6.77**. First, a hydroxyl group was regioselectively installed through a three-step Boekelheide sequence to provide alcohol **6.78**. Alcohol **6.78** was elaborated to the cyclization substrate (**6.79**) through a Swern oxidation, followed by addition of the lithium acetylide of trimethylsilylacetylene. Finally, removal of the silyl group from the alkyne terminus with potassium carbonate in methanol unveiled terminal alkyne **6.79**.

**Scheme 6.4.1.** Synthesis of ring-contraction model system.



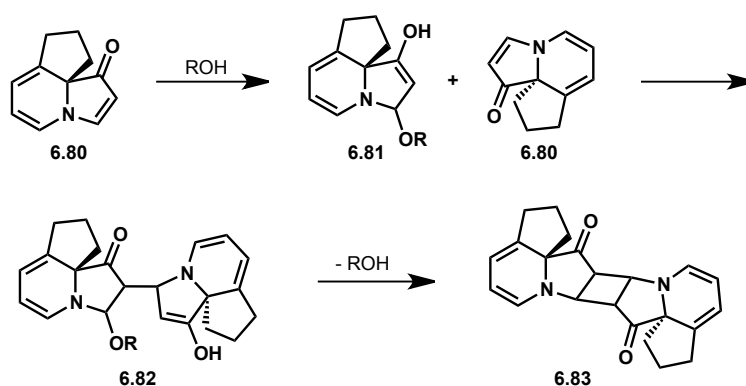
With cyclization substrate **6.79** in hand, we were eager to explore the potential for a ring-contractive cyclization under metal-free conditions. Using the standard metal-free cyclization conditions (ethanol at 100 °C) **6.79** was not converted to the indolizinone product **6.80**. Even after heating for several days, the starting material was recovered unchanged. In an effort to compare the scope of the metal-free conditions to the platinum-catalyzed reaction, platinum(II) chloride was heated with **6.79** at 80 °C in benzene. Again, no indolizinone product was formed. We hypothesized that higher temperatures could be necessary to accomplish the six-to-five membered ring contraction and found that heating propargylic alcohol **6.79** in *n*-butanol at 120 °C did indeed lead to a ring-contractive cyclization. Yet despite complete conversion of the starting material, only small amounts of the desired indolizinone were isolated. The mass balance of the reaction was accounted for by a second product that appeared to form from indolizinone **6.80**.

**Figure 6.4.3.** Ring-contractive indolizinone formation.



<sup>1</sup>H NMR analysis indicated that the major product contained peaks characteristic of the indolizinone diene moiety; however, the vinylogous amide peaks were notably absent from the spectrum. Closer examination of the data suggested that the major product was a dimer of the indolizinone **6.80**. We envisioned the dimerization occurring through a solvent mediated Baylis-Hilman type process. At high temperatures in butanol, the alcohol could add in a conjugate fashion to the vinylogous amide moiety of indolizinone **6.80** (Figure 6.4.2). The resulting enol could then add in a similar manner to a second molecule of indolizinone **6.80**, generating an intermediate such as **6.82**. Finally, elimination of a molecule of the solvent from **6.82** would lead to an iminium ion that could be intercepted by the enol, providing the observed dimer **6.83**. Efforts to obtain a crystal structure of **6.83** were thwarted by facile conversion of the dimer to an unidentified product.

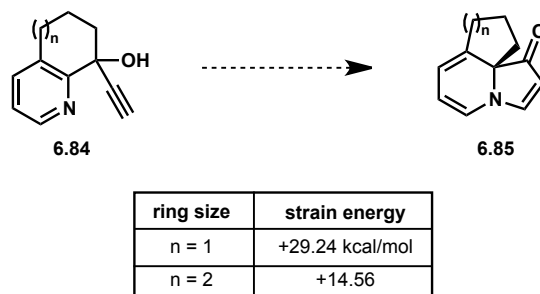
**Scheme 6.4.2.** Potential mechanism of dimer formation.



The ring-contraction product (**6.80**) exhibited reactivity unique from indolizinones made previously in our laboratory. The crucial structural difference between **6.80** and other indolizinones is the additional fused five-membered ring. Using simple molecular modeling, the strain of the newly formed aza triquinane is evident. Indolizinone models suggest that they are fairly flat molecules with the exception of the ring-fusion substituent, which juts up at a nearly 90° angle. Low level calculations performed using Chem3D to approximate the strain of **6.80**

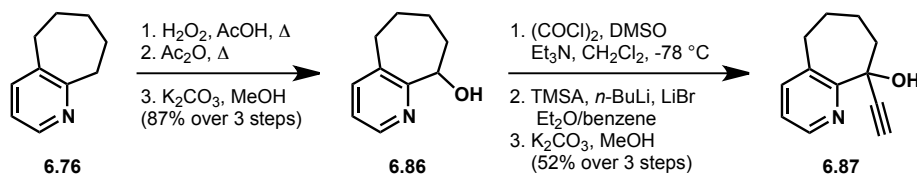
indicated that the ring strain built into the ring-contraction product in relation of the propargylic alcohol starting material (**6.79**) is +29.2 kcal/mol (Figure 6.4.4). We were interested in how the magnitude of increased strain energy would compare to our ultimate substrate of interest, the seven-to-six ring contraction product. Carrying out the same calculation on the seven-to-six membered ring contraction provides a significantly lower number, +14.6 kcal/mol. We were optimistic that the less strained indolizinone (**6.88**) would be sufficiently stable to avoid the dimerization observed with the six-to-five membered ring contraction product.

**Figure 6.4.4.** Strain energy associated with ring-contraction cyclization.



The seven-membered ring substrate **6.87** was synthesized in a manner analogous to the six-membered ring derivative (**6.79**). 2,3-Cycloheptenopyridine (**6.76**) was first derivatized to the *N*-oxide. The Boekelheide reaction was used to regioselectively install the requisite hydroxyl group and provide alcohol **6.86** in 87% yield over three steps (Scheme 6.4.3). Next, Swern conditions were sufficient for oxidation to the ketone. Finally, 1,2-addition of the lithium acetylide of trimethylsilylacetylene and removal of the silyl group provided cyclization substrate **6.87** in 52% over three steps.

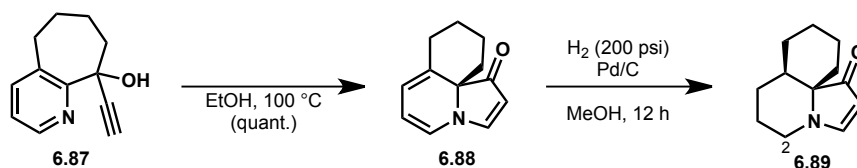
**Scheme 6.4.3.** Synthesis of seven-membered ring substrate.



Unlike the six-to-five ring-contraction, the cyclization of seven-membered ring substrate **6.87** proceeded in quantitative yield upon heating in ethanol at 100 °C (Scheme 6.4.4). More importantly, indolizinone **6.88** did not display the same propensity for dimerization as 5,6,5-indolizinone **6.80**. From indolizinone **6.88**, we seized the opportunity to access the *cis*-6,6-ring fusion common to the cylindricine alkaloids. Hydrogenation of indolizinone **6.88** in the presence of palladium on carbon in methanol provided **6.89** as a single diastereomer. Much like the Diels-Alder cycloadditions utilized in our first approach toward cylindricine K (Section 6.3), hydrogen is delivered on the more sterically accessible face of the indolizinone, opposite the ring-fusion substituent.

Our ability to access the cylindricine core (**6.89**) from indolizinoone **6.88** represents an important proof-of-concept for our divergent approach toward the cylindricines and lepadiformines. The *cis*-6,6-cylindricine ring-fusion can be set in a single step from the intermediate common to both families of alkaloids. Having accomplished the synthesis of the tricyclic cylindricine core in eight steps from commercially available pyridine **6.76**, our next goals were (1) installation of the C-2 alkyl chain and (2) achieving access to the lepadiformine core.

**Scheme 6.4.4.** Cyclization to form common intermediate **6.88** and hydrogenation to the cylindricine core.



To introduce an alkyl chain at C2 (cylindricine numbering), we considered a variety of methods for pyridine functionalization. Alkylation of pyridine **6.76** as well as alcohol **6.86** was examined (Figure 6.4.5). Ideally, we sought to introduce the C2 alkyl chain after the installation of the hydroxyl group because we feared that the Boekelheide reaction would not be selective for the seven-membered ring over the C2 alkyl chain. Gratifyingly, the alkylation under a variety of conditions proceeded with superior regioselectivity and yields for alcohol **6.86** as compared to pyridine **6.76**. Specifically, we explored the addition of lithium reagents and Grignard reagents to the pyridine moiety of **6.86**. Treatment of **6.86** with two equivalents of R-Li or R-MgBr (where R = *n*-Bu, *n*-Hex, or Et) in THF at temperatures ranging from 0 to 60 °C returned only the starting material. Alternatively, formation of the pyridine *N*-oxide of **6.86** followed by exposure to ethylmagnesium bromide led to a 1:2.5 mixture of product **6.91** and recovered starting material. Conducting this reaction at higher temperatures did not yield a greater ratio of product to starting material. Additionally, increasing the equivalents of the Grignard led to dialkylated product. Further exploration of this reaction revealed that lithium reagents do add to pyridine **6.86** at significantly higher temperatures to provide a single isomer of the monoalkylated product **6.91**. When hydroxy pyridine **6.86** was reacted with two equivalents of *n*-BuLi in refluxing toluene, a 91% yield of **6.91** was obtained.

Applying the conditions optimal for alkylation of hydroxylated compound **6.86** to the pyridine substrate lacking the hydroxyl group (**6.76**), significantly lower yields of regioisomeric products were obtained. We suspect that the superior reactivity and selectivity observed for the hydroxylated pyridine **6.86** results from activation of the pyridine by the proximal lithium alkoxide group (Figure 6.4.6B). Upon deprotonation of the hydroxyl group of **6.86** with the first equivalent of alkyl lithium, a lithium alkoxide such as **6.93** is formed. Models of this intermediate (**6.93**) indicated that the lithium bound to the alkoxide is held in close proximity to the pyridine nitrogen (Figure 6.4.6B). We theorize that the interaction between the pyridine-nitrogen and lithium cation provides substantial activation of the pyridine, lowering the energy barrier for the Chichibabin-type reaction. This mode of activation is analogous to the activation provided by formation of the pyridine *N*-oxide (Figure 6.4.6A); however, in the case of

alkylation of **6.86**, *N*-oxide formation provides an inferior alkylation substrate to that achieved with lithium alkoxide **6.93**.

**Figure 6.4.5.** Strategies for pyridine alkylation.

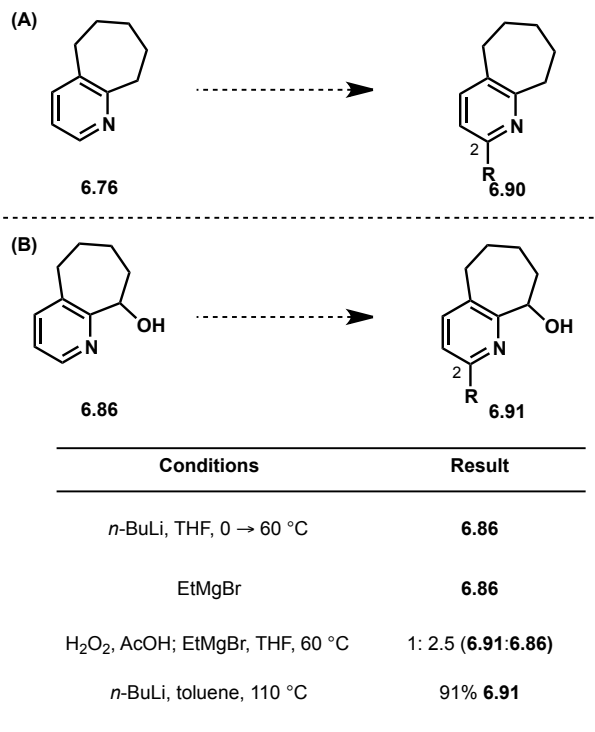
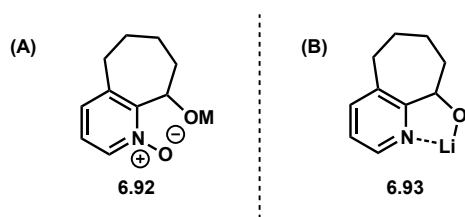
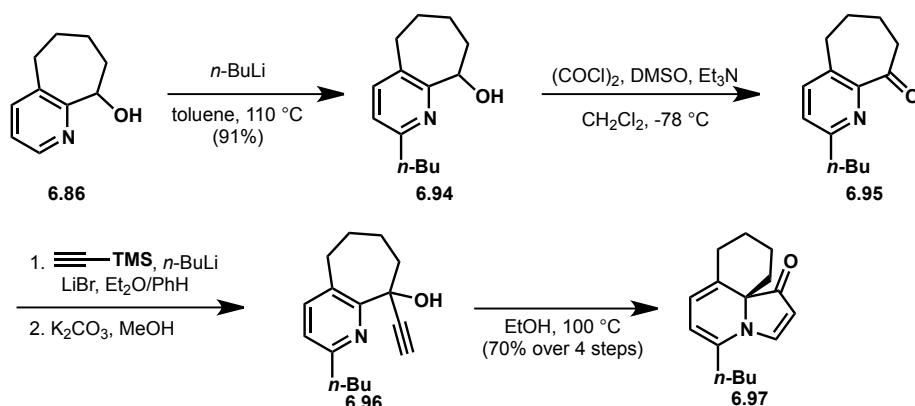


**Figure 6.4.6.** Activated alkylation substrate



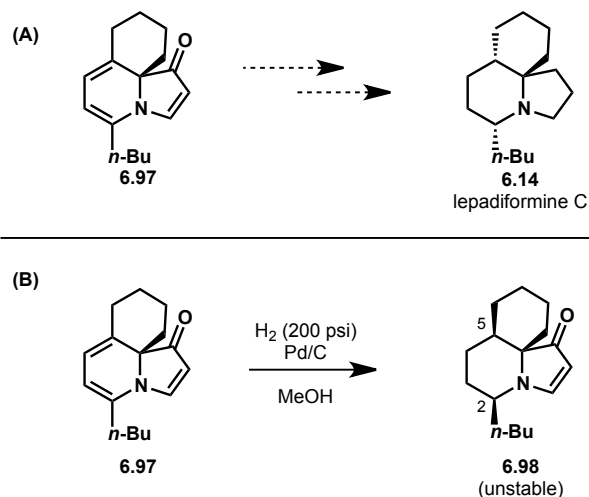
With optimized alkylation conditions, 6-butylpyridine **6.94** can be obtained in 91% yield from **6.86** (Scheme 6.4.5). Alcohol **6.94** can be elaborated to the cyclization substrate (**6.96**) in three steps according to the previously described protocol (see Scheme 6.4.3). Cyclization of propargyl alcohol **6.96** under the metal-free conditions provided the ring-contracted product **6.97** in 70% yield over four steps. Using this route, gram quantities of indolizinone **6.97** were obtained in eight steps from commercially available 2,3-cycloheptenopyridine (**6.76**).

**Scheme 6.4.5.** Synthesis of alkylated common intermediate.



At this juncture, we were interested exploring the potential for conversion of the common indolizinone intermediate (**6.97**) into the *trans*-6,6-fused lepadiformine core. Specifically, we sought to advance indolizinone **6.97** to lepadiformine C (Figure 6.4.7A). Although lepadiformine C requires only an exhaustive reduction of indolizinone **6.97** to the indolizidine, the diastereoselectivity of a hydrogenation of the indolizinone (**6.97**) diene proceeds from the less sterically encumbered face of the molecule to set both the C-2 and C-5 stereocenters with the configuration opposite to that required for the natural product (Figure 6.4.7B). Since a simple hydrogenation was not a fruitful option for converting indolizinone **6.97** to lepadiformine C, we devised several strategies for controlling the stereochemistry at C-2 and C-5. Two of these approaches are described, herein.

**Figure 6.4.7.** (A) First natural product target, lepadiformine C; (B) Selectivity of hydrogenation.

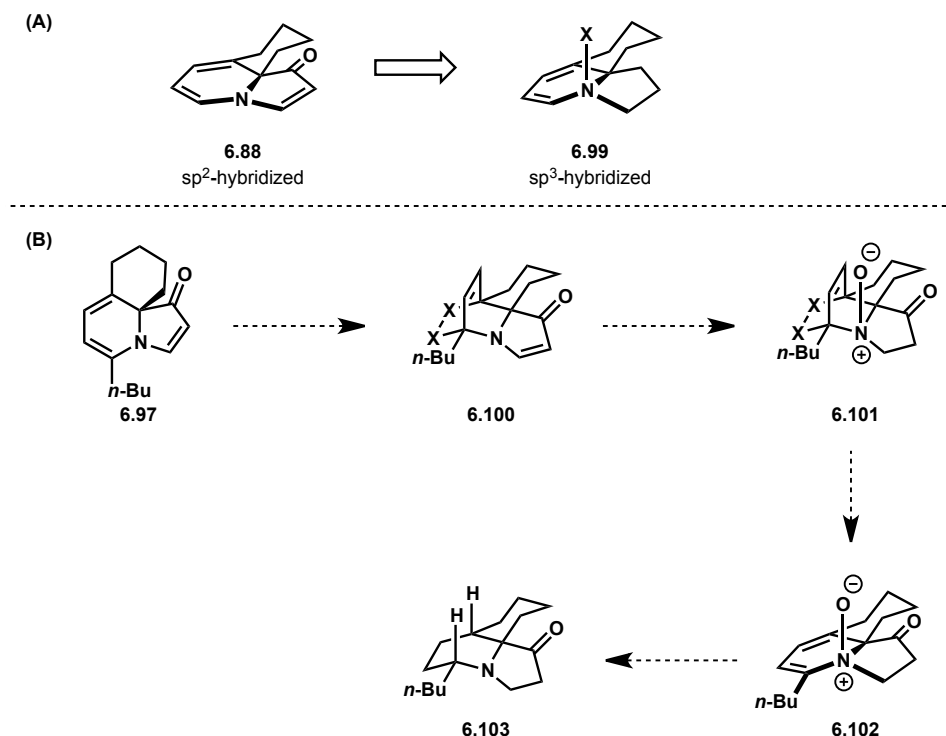


Our first approach to convert indolizinone **6.97** to lepadiformine C focused on transforming the  $\text{sp}^2$ -hybridized indolizinone nitrogen **6.88** into a pyramidalized nitrogen (see **6.99**) to access a cupped molecule (Figure 6.4.8A). Our experience with indolizinones taught us that chemistry on the vinylogous amide is only fruitful once the diene has been removed;



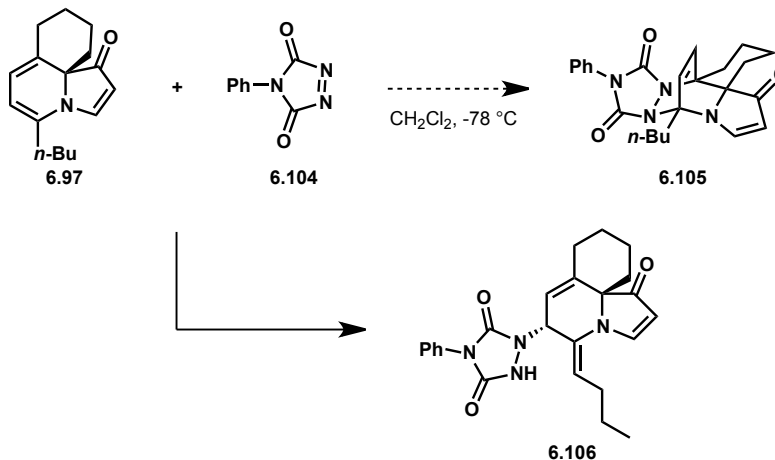
therefore, we planned to protect the diene through a reversible Diels-Alder cycloaddition (see **6.97** to **6.100**, Figure 6.4.8B). With the diene protected, the vinylogous amide would be reduced to the tertiary amine, which could be pyramidalized through formation of the *N*-oxide (**6.101**). From the *N*-oxide, a retro-Diels-Alder reaction would regenerate the diene to provide a cup-shaped molecule such as **6.102**.

**Figure 6.4.8.** (A) 3D illustration of indolizinone **6.88**, (B) Strategy towards lepadiformine C.



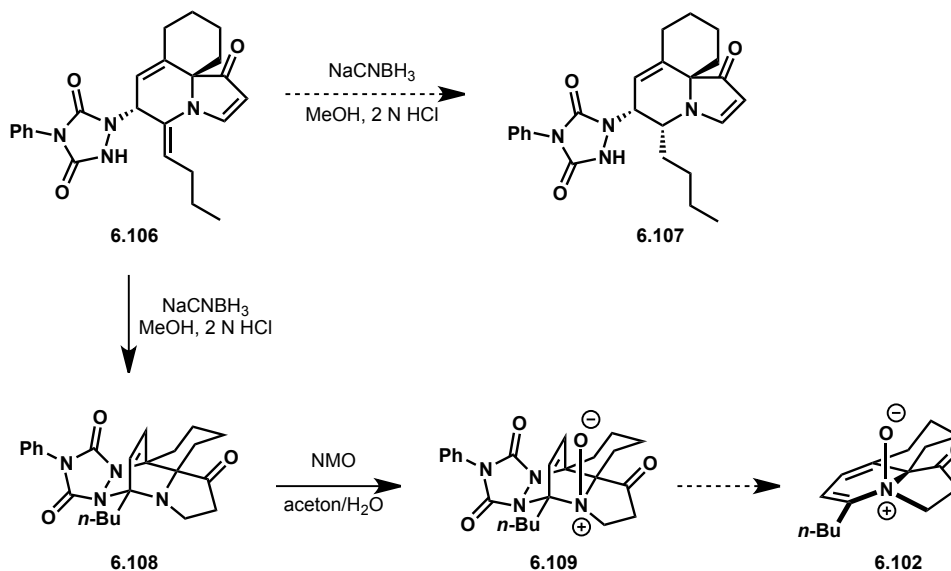
We considered a variety of dienophiles that could lead to a reversible Diels-Alder reaction and decided to employ PTAD in our first attempt to protect the diene. We chose PTAD (**6.104**) based on its reactivity under mild conditions as well as the literature precedent for converting PTAD-Diels-Alder adducts back to dienes. When PTAD was added to indolizinone **6.97** at  $-78\text{ }^{\circ}\text{C}$  in dichloromethane, a single diastereomer of a single adduct was obtained in quantitative yield (Scheme 6.4.6). However, the product was not the anticipated [2.2.2]bicycle **6.105**. The  $^1\text{H}$  and  $^{13}\text{C}$  NMR data were not consistent with the formation of the [4+2] cycloaddition product, but instead with ene product **6.106**.

**Scheme 6.4.6.** Chemistry of indolizine **6.97** and PTAD.



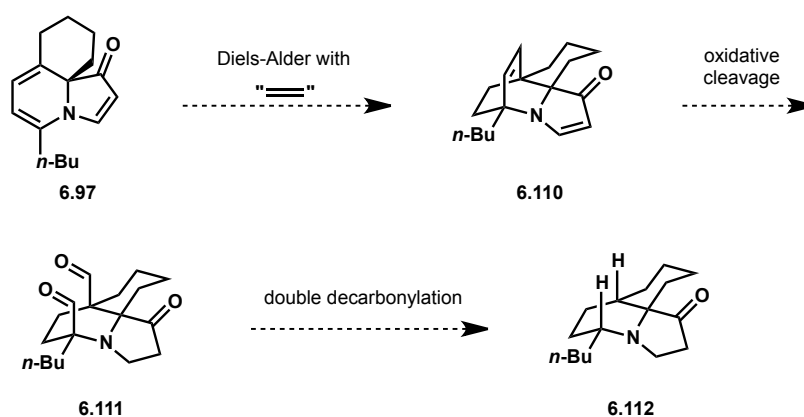
Although we initially envisioned protecting the diene via Diels-Alder cycloaddition, the ene product **6.106** held promise toward lepadiformine C. The triazole moiety is most likely *anti* to the ring-fusion substituent, blocking the bottom face of the molecule. We were interested in reducing the enamine formed in the ene reaction. Treatment of **6.106** with sodium cyanoborohydride under acidic conditions did not provide the anticipated product (**6.107**, Scheme 6.4.7). Instead [2.2.2]bicycle **6.108** was obtained in which the vinylogous amide had been reduced. We hypothesize that the vinylogous amide moiety of **6.106** was first reduced, followed by rearrangement to the [2.2.2]bicycle **6.108**. This serendipitous result provided an intermediate from our original plan (see Figure 6.4.8B). The tertiary amine of **6.108** could be converted to the *N*-oxide (**6.109**) by treatment with NMO in a mixture of acetone and water. Next a variety of conditions were explored for the retro-Diels-Alder of **6.109** to **6.102**, and although the starting material was consumed in several cases, a stable product was never obtained.

**Scheme 6.4.7.** Chemistry of the ene product **6.106**.



The second plan for introducing hydrogen atoms at C2 and C5 *syn* to the ring-fusion substituent, exploited the diastereoselectivity previously observed in the Diels-Alder cycloaddition of indolizinones. We envisioned carrying out a Diels-Alder reaction between indolizinone **6.97** and an ethylene equivalent to obtain a [2.2.2]azabicyclic system such as **6.110** (Scheme 6.4.8). From **6.110** we planned to effect an oxidative cleavage of the unsaturated two-carbon bridge to access dialdehyde **6.111**. The key element of this strategy was contingent on the feasibility of a stereoretentive double decarbonylation of dialdehyde **6.111**. Even though decarbonylations often require stoichiometric amounts of a metal complex and high temperatures, the precedent for these transformations to proceed exclusively with retention of configuration was enticing.

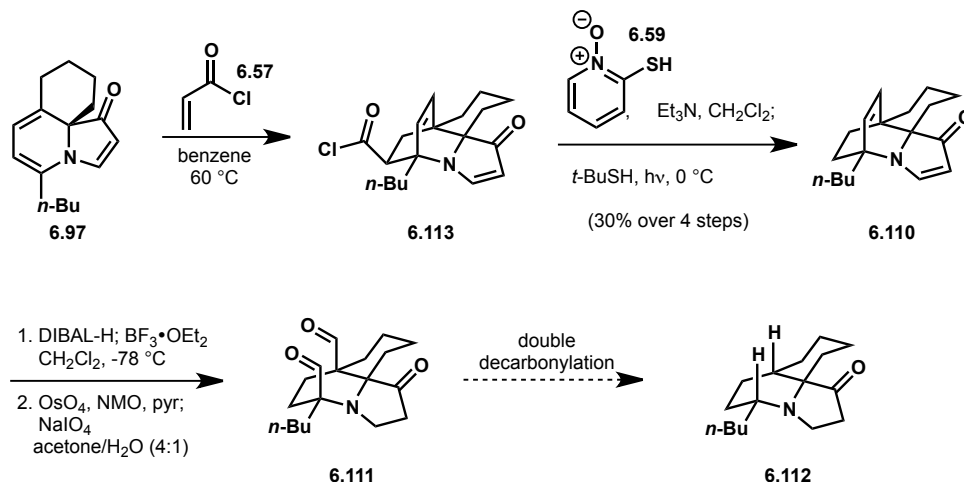
**Scheme 6.4.8.** Decarbonylation strategy.



To date, significant progress has been made in the execution of the decarbonylation strategy. The first hurdle was a Diels-Alder reaction with an ethylene equivalent. On the basis of knowledge gained in our first generation approach toward cylindricine K, a [4+2] cycloaddition with acryloyl chloride was employed. Heating indolizinone **6.97** with acryloyl chloride at 60 °C in benzene for one hour provided the Diels-Alder adduct **6.113** (Scheme 6.3.9). This is the first example of a tetra-substituted indolizinone diene undergoing a Diels-Alder reaction to set two quaternary centers. From acid chloride **6.113**, the Barton ester was formed and decarboxylation was effected in the same pot according to the protocol described in Section 6.3. Overall, this sequence provided [2.2.2]bicyclic system **6.110** in 30% yield over four steps from tertiary alcohol **6.96**, an average of 75% per step. Prior to oxidative cleavage of the bridging double bond, the vinylogous amide was reduced with DIBAL-H in the presence of  $\text{BF}_3 \cdot \text{OEt}_2$  to the tertiary amine in good yield. Attempted osmium tetroxide dihydroxylation prior to reduction of the vinylogous amide double bond resulted in oxidation of the vinylogous amide over the unsaturated two-carbon bridge. However, from the tertiary amine, dihydroxylation with catalytic osmium tetroxide and NMO in the presence of pyridine provided a 1,2-diol, which was oxidatively cleaved to the dialdehyde in the same pot with sodium periodate. The dialdehyde (**6.111**) exists as a mixture of the dialdehyde along with its hydrate form. It is noteworthy that the exclusion of pyridine from the dihydroxylation led to *N*-oxide formation at the expense of the dihydroxylated product. Preliminary results indicated that the double decarbonylation proceeds with two

equivalents of Wilkinson's catalyst at 200 °C. Efforts are currently focused on optimizing this transformation and advancing the decarbonylated product (**6.112**) to lepadiformine C.

**Scheme 6.4.9.** Progress toward lepadiformine C.



## 6.5 Conclusions and Future Directions

Indolizinones have been enlisted as building blocks for the synthesis of tricyclic marine alkaloids. A first generation approach toward these molecules targeted cylindricine K and hinged on building the *cis*-6,6-ring fusion through a ring-opening/ring-closing metathesis of a [2.2.2]azabicyclo. The cylindricine core was obtained using this route.

A second approach toward the cylindricine alkaloids has also been described which diverges from an intermediate that also permits access to the lepadiformine family of molecules. This route toward these tricyclic marine alkaloids employs a ring-contractive indolizone formation that proceeds under metal-free conditions. Using this divergent approach, the tricyclic cylindricine core was obtained in eight steps. Efforts to complete the total synthesis of lepadiformine C are currently ongoing.

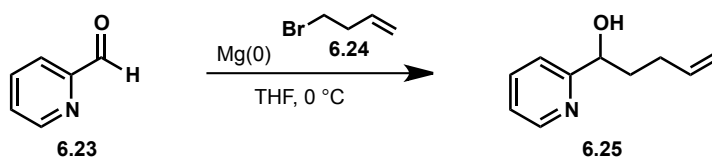
## 6.6 Experimental Contributions

Alison Hardin Narayan carried out the research detailed in Chapter 6.

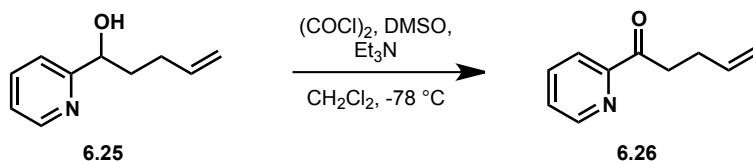
## 6.7 Experimental Methods

Unless otherwise stated, reactions were performed in flame-dried glassware fitted with rubber septa under a nitrogen atmosphere and were stirred with Teflon-coated magnetic stirring bars. Liquid reagents and solvents were transferred via syringe using standard Schlenk techniques. Tetrahydrofuran (THF), diethyl ether, benzene, toluene, and triethylamine were dried over alumina under a nitrogen atmosphere in a GlassContour solvent system. Dichloromethane (DCM) was distilled over calcium hydride. All other solvents and reagents were used as received.

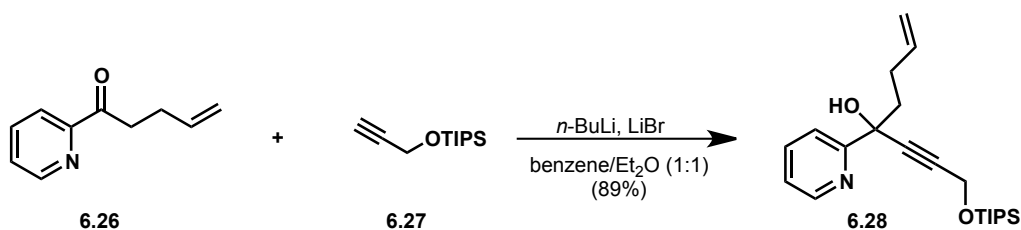
unless otherwise noted. Reaction temperatures above 23 °C refer to oil or sand bath temperatures, which were controlled by an OptiCHEM temperature modulator. Thin layer chromatography was performed using SiliCycle silica gel 60 F-254 precoated plates (0.25 mm) and visualized by UV irradiation and anisaldehyde or potassium permanganate stain. SiliCycle Silica-P silica gel (particle size 40-63  $\mu\text{m}$ ) was used for flash chromatography.  $^1\text{H}$  and  $^{13}\text{C}$  NMR spectra were recorded on Bruker AVB-400, DRX-500, AV-500 and AV-600 MHz spectrometers with  $^{13}\text{C}$  operating frequencies of 100, 125, 125, and 150 MHz, respectively. Chemical shifts ( $\delta$ ) are reported in ppm relative to the residual solvent signal ( $\text{CDCl}_3$ ;  $\delta = 7.26$  for  $^1\text{H}$  NMR and  $\delta = 77.0$  for  $^{13}\text{C}$  NMR;  $\text{C}_6\text{D}_6$ ;  $\delta = 7.15$  for  $^1\text{H}$  NMR and  $\delta = 128.39$  for  $^{13}\text{C}$  NMR). Data for  $^1\text{H}$  NMR spectra are reported as follows: chemical shift (multiplicity, coupling constants, number of hydrogens). Abbreviations are as follows: s (singlet), d (doublet), t (triplet), dd (doublet of doublets), m (multiplet), br (broad). IR spectra were recorded on a Nicolet MAGNA-IR 850 spectrometer and are reported in frequency of absorption ( $\text{cm}^{-1}$ ). Only selected IR absorbencies are reported. High resolution mass spectral data were obtained from the Mass Spectral Facility at the University of California, Berkeley.



**Alcohol 6.25:** 1-Bromo-4-butene (**6.24**, 7.61 mL, 75.0 mmol) was added dropwise to Mg(0) in THF (10 mL). Following initiation of the Grignard formation, which was marked by vigorous bubbling, an additional 10 mL of THF was added. The round bottom flask was equipped with a reflux condenser and heated to reflux (oil bath temperature = 70 °C) for 1 h. The Grignard solution was removed from the oil bath and cooled to room temperature, then further cooled to 0 °C in an ice bath. The Grignard solution was diluted with THF (80 mL) and pyridine-2-carboxaldehyde (**6.23**, 4.76 mL, 50 mmol) in THF (20 mL) was added dropwise over 10 min. The reaction mixture was stirred while the ice bath expired. The reaction was quenched with by addition of a saturated solution of ammonium chloride (30 mL). The mixture was extracted with EtOAc (3 x 50 mL). the organic layers were combined, washed with brine (100 mL), dried over  $\text{MgSO}_4$ , and concentrated to give a brown oil. Flash chromatography (1:1 hexanes/EtOAc) provided the alcohol **6.25** in 97% yield.  $^1\text{H}$  NMR (400 MHz,  $\text{CDCl}_3$ )  $\delta$  8.50 (d,  $J = 3.4$  Hz, 2H), 7.66 (td,  $J = 7.7, 1.4$  Hz, 1H), 7.28 – 7.24 (m, 2H), 7.17 (dd,  $J = 7.2, 5.1$  Hz, 2H), 5.82 (ddt,  $J = 16.9, 10.2, 6.6$  Hz, 1H), 5.01 (dt,  $J = 8.8, 4.4$  Hz, 1H), 4.94 (dd,  $J = 10.2, 0.9$  Hz, 1H), 4.77 – 4.72 (m, 2H), 2.23 – 2.12 (m, 2H), 1.90 (dddd,  $J = 13.5, 9.2, 6.9, 4.3$  Hz, 1H), 1.81 – 1.71 (m, 1H);  $^{13}\text{C}$  NMR (101 MHz,  $\text{CDCl}_3$ )  $\delta$  162.1, 148.1, 136.6, 122.2, 120.3, 114.8, 72.2, 64.2, 37.6, 29.5; IR (film)  $\nu_{\text{max}}$  3363, 3080, 2918, 1641, 1595, 1071  $\text{cm}^{-1}$ ; HRMS (ESI+) calcd for  $[\text{C}_{10}\text{H}_{14}\text{ON}]^+$  (M-H) $^+$ :  $m/z$  164.1070, found 164.1069.

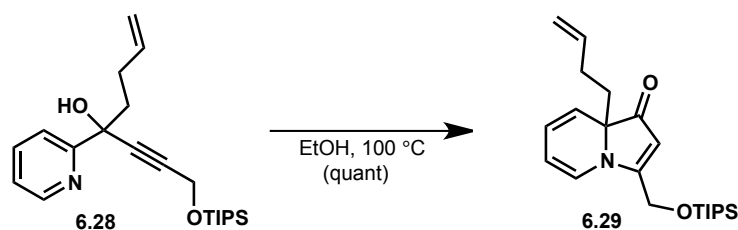


**Ketone 6.26:** DMSO (6.10 mL, 85.6 mmol) was added dropwise to oxalyl chloride in  $\text{CH}_2\text{Cl}_2$  (80 mL) at  $-78\text{ }^\circ\text{C}$ . After 30 min, alcohol **6.25** (3.50 g, 21.4 mmol) in  $\text{CH}_2\text{Cl}_2$  (20 mL) was added dropwise at  $-78\text{ }^\circ\text{C}$ . The reaction mixture was stirred for 30 min at this temperature.  $\text{Et}_3\text{N}$  (24.0 mL, 171 mmol) was added at  $-78\text{ }^\circ\text{C}$ . The cold bath was allowed to gradually expire as the reaction mixture was stirred for 4 h. The reaction was quenched with water (100 mL). The aqueous layer was extracted with  $\text{CH}_2\text{Cl}_2$  (2 x 100 mL). The combined organic layer was washed with water, dried over  $\text{MgSO}_4$  and concentrated to afford **6.26** as a brown oil in 98% yield (3.39 g, 21.0 mmol) that was used without further purification.  $^1\text{H NMR}$  (500 MHz,  $\text{CDCl}_3$ )  $\delta$  8.68 (d,  $J = 4.7$  Hz, 1H), 8.03 (d,  $J = 7.9$  Hz, 1H), 7.83 (d,  $J = 1.6$  Hz, 1H), 7.49 – 7.44 (m, 1H), 5.91 (d,  $J = 6.6$  Hz, 1H), 5.09 (dd,  $J = 17.1, 1.6$  Hz, 1H), 4.99 (dd,  $J = 10.2, 1.2$  Hz, 1H), 3.33 (t,  $J = 7.4$  Hz, 2H), 2.50 (d,  $J = 7.2$  Hz, 2H);  $^{13}\text{C NMR}$  (151 MHz,  $\text{CDCl}_3$ )  $\delta$  200.8, 153.0, 148.6, 137.2, 136.8, 126.9, 121.5, 114.8, 36.6, 27.7; **IR** (film)  $\nu_{\text{max}}$  3381, 3077, 2979, 2600, 1698, 1437, 995  $\text{cm}^{-1}$ ; **HRMS** (ESI+) calcd for  $[\text{C}_{10}\text{H}_{12}\text{ON}]^+$  (M-H) $^+$ :  $m/z$  162.0913, found 162.1310.

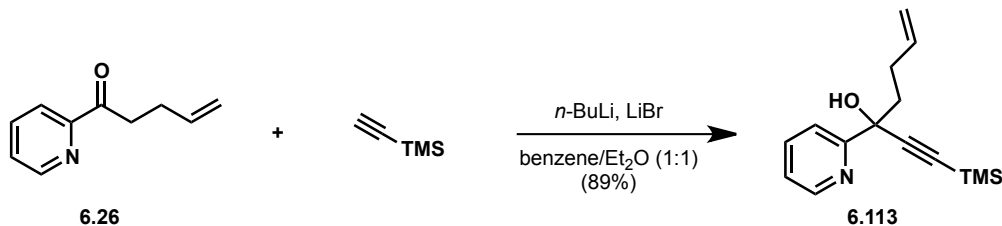


**Propargyl alcohol 6.28:** *n*-Butyllithium (3.47 mL, 8.68 mmol, 2.5 M in hexanes) was added dropwise to **6.27** (1.98 g, 9.30 mmol) in  $\text{Et}_2\text{O}$  (10 mL) at  $0\text{ }^\circ\text{C}$ . After 30 min, the lithium acetylide solution was added dropwise to a mixture of ketone **6.26** (1.00 g, 6.20 mmol) and lithium bromide (1.62 g, 18.6 mmol) in a 1:1 mixture of  $\text{Et}_2\text{O}$  and benzene (total volume = 60 mL) at ambient temperature. The reaction mixture was stirred vigorously for 18 h. The reaction was quenched with the addition of a saturated  $\text{NH}_4\text{Cl}_{(\text{aq})}$  solution (30 mL). The aqueous phase was extracted with  $\text{EtOAc}$  (3 x 40 mL). The combined organic layer was washed with brine, dried over  $\text{MgSO}_4$ , and concentrated under reduced pressure to provide **6.28** as a brown oil in 80% yield (1.85 g, 4.69 mmol).  $^1\text{H NMR}$  (500 MHz,  $\text{CDCl}_3$ )  $\delta$  8.51 (d,  $J = 4.8$  Hz, 1H), 7.74 (d,  $J = 1.5$  Hz, 1H), 7.60 (d,  $J = 7.9$  Hz, 1H), 7.26 – 7.23 (m, 1H), 5.83 – 5.73 (m, 1H), 5.49 (s, 1H), 5.01 – 4.94 (m, 1H), 4.90 (d,  $J = 10.3$  Hz, 1H), 4.44 (d,  $J = 4.1$  Hz, 2H), 4.38 (d,  $J = 2.3$  Hz, 2H), 2.39 (t,  $J = 2.3$  Hz, 1H), 2.31 (dt,  $J = 16.2, 7.9$  Hz, 1H), 2.14 – 2.09 (m, 2H), 1.93 (dd,  $J = 11.8, 8.6$  Hz, 1H), 1.14 – 1.10 (m, 3H), 1.10 – 1.02 (m, 18H);  $^{13}\text{C NMR}$  (151 MHz,  $\text{CDCl}_3$ )  $\delta$  160.9, 147.2, 138.1, 137.2, 122.8, 120.7, 114.5, 97.7, 86.4, 83.5, 71.3, 52.1, 43.7, 37.6, 28.4, 26.4, 17.9,

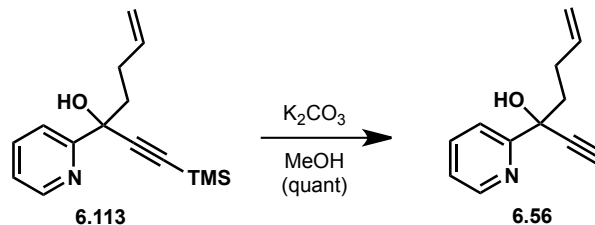
12.0; **IR** (film)  $\nu_{\max}$  3312, 2943, 2866, 1464, 1101  $\text{cm}^{-1}$ ; **HRMS** (ESI+) calcd for  $[\text{C}_{22}\text{H}_{36}\text{O}_2\text{NSi}]^+$  (M-H) $^+$ :  $m/z$  374.2510, found 374.2520.



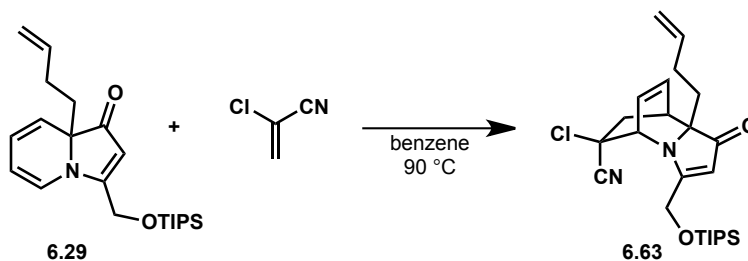
**Indolizinone 6.29:** A solution of tertiary alcohol **6.28** (300 mg, 0.803 mmol) in EtOH (5.0 mL) was sparged with  $\text{N}_2$  for 5 min. The reaction vessel, a 20 mL vial, was equipped with a green Teflon-lined cap and Telfon tape and heated at 100 °C for 4 h. The reaction mixture was cooled to room temperature and concentrated to provide indolizinone **6.29** in 99% yield (298 mg, 0.800 mmol).  $^1\text{H NMR}$  (400 MHz,  $\text{CDCl}_3$ )  $\delta$  6.48 (d,  $J = 7.2$  Hz, 1H), 5.87 (dd,  $J = 17.9, 7.3$  Hz, 2H), 5.69 (ddt,  $J = 16.8, 10.2, 6.5$  Hz, 1H), 5.40 (s, 1H), 5.14 (s, 1H), 4.95 (dd,  $J = 17.1, 1.7$  Hz, 1H), 4.90 (dd,  $J = 10.2, 1.6$  Hz, 1H), 4.65 (d,  $J = 0.5$  Hz, 2H), 2.04 (m, 4H), 1.80 (d,  $J = 5.7$  Hz, 2H), 1.15 (dd,  $J = 14.3, 6.7$  Hz, 3H), 1.08 (d,  $J = 6.2$  Hz, 18H);  $^{13}\text{C NMR}$  (101 MHz,  $\text{CDCl}_3$ )  $\delta$  202.7, 137.7, 124.0, 123.0, 122.2, 114.8, 109.5, 97.7, 71.0, 58.6, 37.6, 26.5, 17.9, 11.9; **IR** (film)  $\nu_{\max}$  2943, 2866, 1677, 1572, 1457, 1131  $\text{cm}^{-1}$ ; **HRMS** (ESI+) calcd for  $[\text{C}_{22}\text{H}_{36}\text{O}_2\text{NSi}]^+$  (M-H) $^+$ :  $m/z$  374.2510, found 374.2520.



**Propargylic alcohol 6.113:** *n*-Butyllithium (6.95 mL, 17.4 mmol, 2.5 M in hexanes) was added dropwise to trimethylsilylacetylene (2.82 mL, 19.8 mmol) in  $\text{Et}_2\text{O}$  (20 mL) at 0 °C. After 30 min, the lithium acetylide solution was added dropwise to a mixture of ketone **6.26** (2.00 g, 12.4 mmol) and lithium bromide (3.20 g, 37.2 mmol) in a 1:1 mixture of  $\text{Et}_2\text{O}$  and benzene (total volume = 120 mL) at ambient temperature. The reaction mixture was stirred vigorously for 18 h. The reaction was quenched with the addition of a saturated  $\text{NH}_4\text{Cl}_{(\text{aq})}$  solution (60 mL). The aqueous phase was extracted with EtOAc (3 x 80 mL). The combined organic layer was washed with brine, dried over  $\text{MgSO}_4$ , and concentrated under reduced pressure to provide propargylic alcohol **6.113** as a brown oil in 80% yield (2.00 g, 4.69 mmol).  $^1\text{H NMR}$  (500 MHz,  $\text{CDCl}_3$ )  $\delta$  8.51 (d,  $J = 4.9$  Hz, 1H), 7.74 (dd,  $J = 7.7, 1.6$  Hz, 1H), 7.60 (d,  $J = 7.9$  Hz, 1H), 7.26 (q,  $J = 4.7$  Hz, 1H), 5.80 (d,  $J = 6.6$  Hz, 1H), 5.47 (s, 1H), 4.98 (dd,  $J = 17.1, 1.6$  Hz, 1H), 4.91 (d,  $J = 10.3$  Hz, 1H), 2.33 – 2.25 (m, 1H), 2.17 – 2.10 (m, 1H), 2.10 – 2.03 (m, 1H), 1.94 – 1.87 (m, 1H), 0.20 – 0.15 (m, 9H);  $^{13}\text{C NMR}$  (101 MHz,  $\text{CDCl}_3$ )  $\delta$  160.8, 147.2, 138.1, 137.2, 122.8, 120.6, 114.5, 107.2, 89.3, 71.6, 44.2, 28.5, -0.2; **IR** (film)  $\nu_{\max}$  3363, 3077, 2959, 2078, 1593, 844  $\text{cm}^{-1}$ ; **HRMS** (ESI+) calcd for  $[\text{C}_{15}\text{H}_{22}\text{ONSi}]^+$  (M-H) $^+$ :  $m/z$  260.1465, found 260.1464.

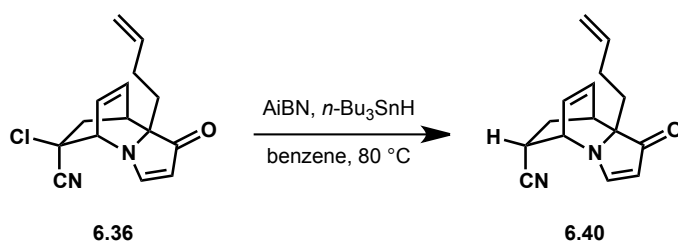


**Propargylic alcohol 6.56:** Potassium carbonate (2.02 g, 14.6 mmol) was added to the trimethylsilyl alkyne (1.90 g, 7.32 mmol) in MeOH (70 mL). The reaction mixture was stirred for 2 h at ambient temperature. The reaction mixture was concentrated under reduced pressure. The residue was taken up in water (100 mL) and extracted with CH<sub>2</sub>Cl<sub>2</sub> (3 x 50 mL). The combined organic layer was washed with brine, dried over MgSO<sub>4</sub> and concentrated under reduced pressure to provide **6.56** as a brown oil in 97% yield (1.33 g, 7.10 mmol). <sup>1</sup>H NMR (400 MHz, CDCl<sub>3</sub>) δ 8.51 (d, *J* = 4.9 Hz, 1H), 7.74 (td, *J* = 7.7, 1.7 Hz, 1H), 7.60 (d, *J* = 8.0 Hz, 1H), 7.28 – 7.22 (m, 1H), 5.77 (d, *J* = 6.4 Hz, 1H), 5.48 (s, 1H), 4.97 (dd, *J* = 17.1, 1.5 Hz, 1H), 4.90 (d, *J* = 10.2 Hz, 1H), 2.56 (s, 1H), 2.29 (s, 1H), 2.17 – 2.09 (m, 2H), 1.93 (dd, *J* = 11.7, 8.4 Hz, 1H); <sup>13</sup>C NMR (151 MHz, CDCl<sub>3</sub>) δ 160.4, 147.3, 137.8, 137.3, 122.9, 120.4, 114.6, 85.9, 72.7, 71.2, 43.6, 28.2; IR (film) ν<sub>max</sub> 3299, 3150, 1641, 1593, 1435, 1079 cm<sup>-1</sup>; HRMS (ESI<sup>+</sup>) calcd for [C<sub>12</sub>H<sub>14</sub>ON]<sup>+</sup> (M-H)<sup>+</sup>: *m/z* 188.1070, found 188.1069.

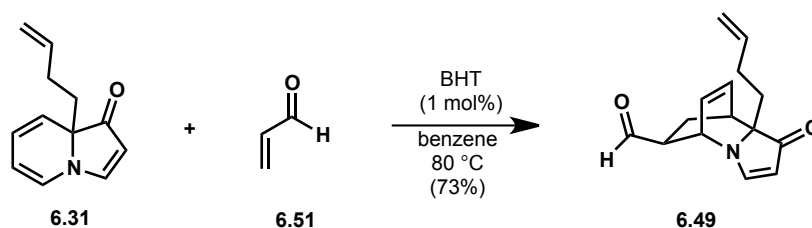


**[2.2.2]azabicyclic 6.63:** A solution of indolizinone **6.29** (200 mg, 0.535 mmol) and 2-chloroacrylonitrile were heated in benzene (5.0 mL) at 90 °C for 24 h. The reaction mixture was cooled to room temperature and concentrated to afford a brown oil. The crude product was purified via flash chromatography (gradient 4:1 hexanes/EtOAc, then 2:1 hexanes/EtOAc). <sup>1</sup>H NMR (500 MHz, CDCl<sub>3</sub>) δ 6.60 (t, *J* = 7.3 Hz, 1H), 6.44 – 6.40 (m, 1H), 5.71 (s, 1H), 5.67 – 5.58 (m, 1H), 5.08 (d, *J* = 6.2 Hz, 1H), 5.01 (d, *J* = 16.2 Hz, 1H), 4.91 (ddd, *J* = 19.3, 10.0, 8.4 Hz, 3H), 3.17 – 3.13 (m, 1H), 2.44 (dd, *J* = 15.5, 1.7 Hz, 1H), 2.12 (dd, *J* = 15.5, 3.9 Hz, 1H), 1.97 – 1.89 (m, 1H), 1.84 – 1.75 (m, 1H), 1.65 (dq, *J* = 13.0, 8.0 Hz, 3H), 1.17 (d, *J* = 7.7 Hz, 3H), 1.12 – 1.07 (m, 18H); <sup>13</sup>C NMR (151 MHz, CDCl<sub>3</sub>) δ 205.2, 182.9, 137.6, 134.4, 128.2, 119.2, 114.9, 112.1, 73.8, 61.1, 57.1, 53.4, 37.8, 36.8, 36.3, 26.6, 17.9, 11.8; IR (film) ν<sub>max</sub> 2943, 2866, 1681, 1568, 1119 cm<sup>-1</sup>; HRMS (ESI<sup>+</sup>) calcd for [C<sub>25</sub>H<sub>38</sub>ClN<sub>2</sub>O<sub>2</sub>Si]<sup>+</sup> (M-H)<sup>+</sup>: *m/z* 461.2386, found 461.2395.

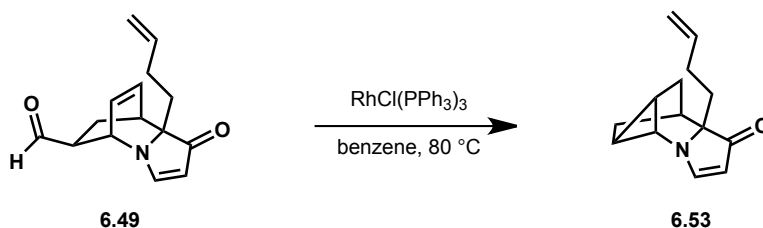




**[2.2.2]azabicyclic 6.40:** *n*-Bu<sub>3</sub>SnH (6.0 μL, 0.22 mmol) was added to [2.2.2]bicyclic **6.36** (2.0 mg, 0.0073 mmol) and AIBN (0.20 mg, 0.0015 mmol) in benzene (200 μL). The reaction mixture was heated to 80 °C for 6 h. The reaction mixture was cooled to room temperature and concentrated under reduced pressure. The crude oil was purified via flash chromatography to afford **6.40** in 92% yield (1.6 mg, 0.0067 mmol). <sup>1</sup>H NMR (500 MHz, CDCl<sub>3</sub>) δ 7.94 (d, *J* = 3.5 Hz, 1H), 6.53 (t, *J* = 7.3 Hz, 1H), 6.39 – 6.34 (m, 1H), 5.69 – 5.57 (m, 2H), 4.94 – 4.85 (m, 2H), 4.69 – 4.64 (m, 1H), 3.12 (s, 1H), 3.04 (s, 1H), 2.87 (d, *J* = 9.4 Hz, 1H), 1.86 (ddd, *J* = 18.2, 12.5, 5.1 Hz, 2H), 1.76 (dd, *J* = 10.7, 6.8 Hz, 2H), 1.72 – 1.55 (m, 5H), 1.28 – 1.22 (m, 2H).

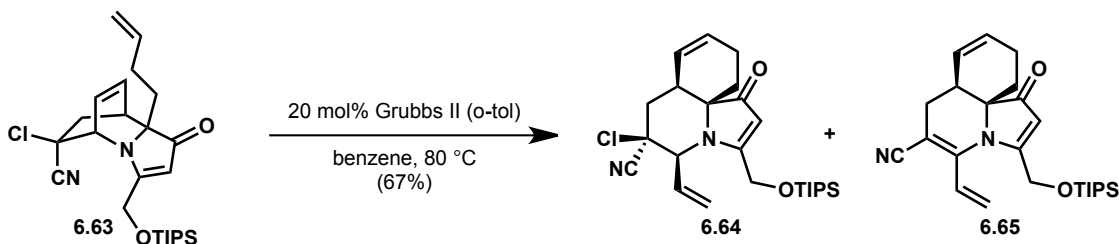


**Aldehyde 6.49:** A solution of indolizinone **6.31** (100 mg, 0.534 mmol), BHT (1.0 mg) and freshly distilled acrolein (214 μL, 3.20 mmol) in benzene (5.0 mL) was heated to 80 °C. After 12 h, the reaction mixture was cooled to room temperature and concentrated under reduced pressure to afford aldehyde **6.49** as a brown oil in 73% yield (94.7 mg, 0.390 mmol). <sup>1</sup>H NMR (500 MHz, CDCl<sub>3</sub>) δ 9.35 (d, *J* = 0.8 Hz, 1H), 7.92 (d, *J* = 3.5 Hz, 1H), 6.54 – 6.48 (m, 1H), 6.37 – 6.28 (m, 1H), 5.63 (dd, *J* = 9.5, 6.9 Hz, 2H), 4.93 – 4.84 (m, 2H), 4.65 (dd, *J* = 5.7, 3.8 Hz, 1H), 3.09 (d, *J* = 2.4 Hz, 1H), 2.83 – 2.76 (m, 1H), 1.94 – 1.79 (m, 2H), 1.79 – 1.63 (m, 5H), 1.60 (dd, *J* = 12.3, 4.2 Hz, 2H).

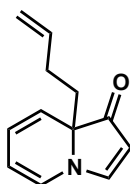


**Cyclopropane 6.53:** A mixture of aldehyde **6.49** (1.5 mg, 0.0062 mmol) and RhCl(PPh<sub>3</sub>)<sub>3</sub> (6.8 mg, 0.0074 mmol) in benzene (500 μL) was heated to 80 °C. After 2 d, the reaction mixture was filtered through a plug of celite and concentrated under reduced pressure. The crude residue was purified via flash chromatography to provide cyclopropane **6.53** in 83% yield (1.1 mg, 0.0051

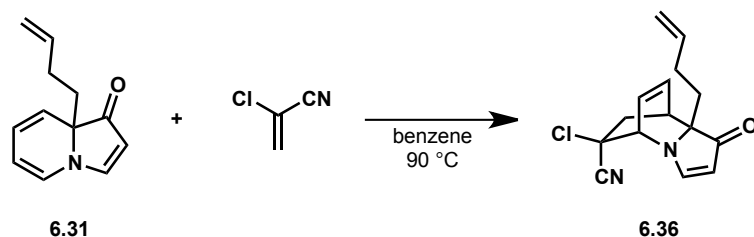
mmol).  $^1\text{H NMR}$  (500 MHz,  $\text{CDCl}_3$ )  $\delta$  8.01 (d,  $J = 3.4$  Hz, 1H), 5.72 (d,  $J = 6.7$  Hz, 1H), 5.44 (d,  $J = 3.4$  Hz, 1H), 4.97 (dd,  $J = 17.1, 1.8$  Hz, 1H), 4.90 (dd,  $J = 10.1, 1.8$  Hz, 1H), 2.84 – 2.78 (m, 1H), 2.31 – 2.23 (m, 3H), 1.87 (d,  $J = 6.4$  Hz, 2H), 1.78 – 1.69 (m, 3H), 1.66 – 1.61 (m, 1H), 1.46 (dd,  $J = 7.8, 4.5$  Hz, 2H). LRMS = 215.



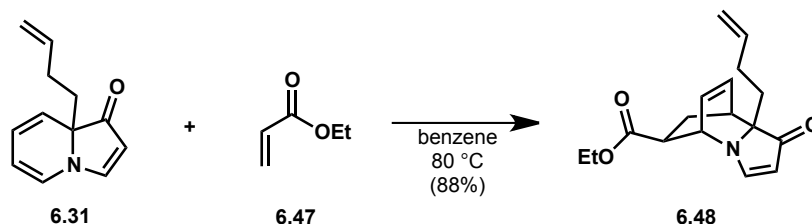
**Tricycle 6.65:** A solution of **6.63** (6.0 mg, 0.013 mmol) and Grubbs II (*o*-tol) catalyst (2.2 mg, 0.0026 mmol) in benzene (2.5 mL) was sparged with ethylene for 5 min. The 4 mL vial was equipped with a Teflon cap and heated to 85 °C. After 12 h, the reaction mixture was cooled to room temperature and concentrated under reduced pressure to give a brown oil. The crude oil was purified via flash chromatography to afford **6.64** and **6.65**. Relative amounts of these products varied depending on the scale of the reaction. In this case, **6.65** was obtained in 67% yield.  $^1\text{H NMR}$  (500 MHz,  $\text{CDCl}_3$ )  $\delta$  6.54 (d,  $J = 4.8$  Hz, 1H), 6.18 – 6.11 (m, 2H), 5.90 (s, 1H), 5.78 – 5.69 (m, 1H), 5.06 (s, 1H), 5.01 – 4.95 (m, 1H), 4.93 (d,  $J = 10.3$  Hz, 1H), 4.80 (d,  $J = 16.2$  Hz, 1H), 4.74 (d,  $J = 16.1$  Hz, 1H), 2.84 (d,  $J = 3.8$  Hz, 1H), 2.40 (dd,  $J = 9.7, 1.9$  Hz, 1H), 2.34 (dd,  $J = 10.0, 1.7$  Hz, 1H), 1.96 (t,  $J = 11.6$  Hz, 1H), 1.84 (td,  $J = 11.8, 7.2$  Hz, 3H), 1.19 (dd,  $J = 8.4, 6.8$  Hz, 3H), 1.09 (dd,  $J = 7.1, 1.4$  Hz, 18H); **HRMS** (ESI+) calcd for  $[\text{C}_{25}\text{H}_{38}\text{ClO}_2\text{N}_2\text{Si}]^+$  (M-H) $^+$ :  $m/z$  461.2386, found 461.2398.



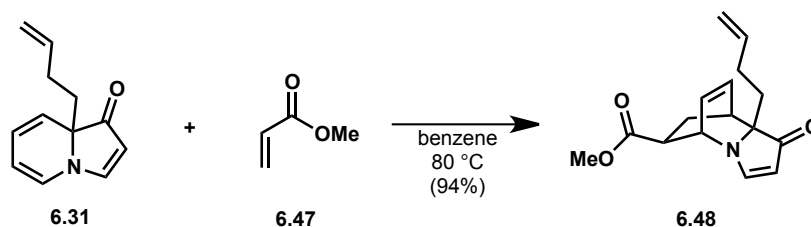
**Homoallyl indolizinone 6.31:** A solution of the tertiary alcohol (600 mg, 3.20 mmol) in EtOH (6.0 mL) was sparged with  $\text{N}_2$  for 5 min. The reaction vessel, a 20 mL vial, was equipped with a green Teflon-lined cap and Teflon tape and heated at 100 °C for 4 h. The reaction mixture was cooled to room temperature and concentrated to provide indolizinone **6.31** in 99% yield (594 mg, 3.17 mmol).  $^1\text{H NMR}$  (400 MHz,  $\text{CDCl}_3$ )  $\delta$  7.79 (d,  $J = 3.7$  Hz, 1H), 6.36 (d,  $J = 7.0$  Hz, 1H), 5.89 (d,  $J = 5.5$  Hz, 1H), 5.76 (d,  $J = 9.3$  Hz, 1H), 5.67 (ddt,  $J = 16.8, 10.2, 6.5$  Hz, 1H), 5.37 (s, 1H), 5.07 (d,  $J = 3.7$  Hz, 1H), 4.94 (dd,  $J = 17.1, 1.6$  Hz, 1H), 4.89 (dd,  $J = 10.2, 1.2$  Hz, 1H), 2.06 (s, 1H), 1.98 (s, 1H), 1.86 – 1.68 (m, 2H);  $^{13}\text{C NMR}$  (101 MHz,  $\text{CDCl}_3$ )  $\delta$  204.0, 160.9, 137.4, 125.2, 122.5, 122.4, 114.9, 108.8, 99.0, 69.6, 37.6, 26.2; **IR** (film)  $\nu_{\text{max}}$  3255, 3076, 2870, 1674, 1522, 1426, 995  $\text{cm}^{-1}$ ; **HRMS** (ESI+) calcd for  $[\text{C}_{12}\text{H}_{14}\text{ON}]^+$  (M-H) $^+$ :  $m/z$  188.1070, found 188.1069.



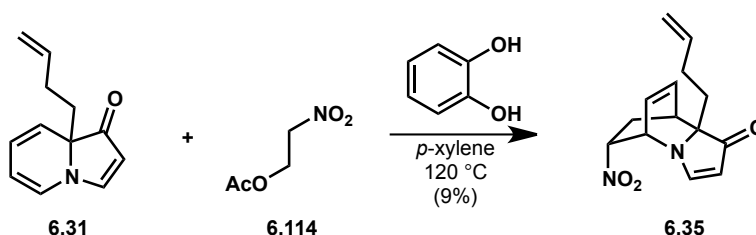
**[2.2.2]azabicyclic 6.36:** A solution of indolizinone **6.31** (250 mg, 1.34 mmol) and 2-chloroacrylonitrile were heated in benzene (6.0 mL) at 80 °C for 24 h. The reaction mixture was cooled to room temperature and concentrated to afford a brown oil. The crude product was purified via flash chromatography (gradient 4:1 hexanes/EtOAc, then 2:1 hexanes/EtOAc) to afford **6.36** as a yellow oil in 55% yield (201 mg, 0.731 mmol).  $^1\text{H NMR}$  (500 MHz,  $\text{CDCl}_3$ )  $\delta$  9.35 (d,  $J = 0.8$  Hz, 1H), 7.92 (d,  $J = 3.4$  Hz, 1H), 6.51 (t,  $J = 7.3$  Hz, 1H), 6.35 – 6.30 (m, 1H), 5.69 – 5.59 (m, 2H), 4.91 (dd,  $J = 17.2, 1.7$  Hz, 1H), 4.87 (dd,  $J = 10.2, 1.7$  Hz, 1H), 4.65 (dd,  $J = 5.7, 3.8$  Hz, 1H), 3.09 (dd,  $J = 5.5, 2.4$  Hz, 1H), 2.82 – 2.76 (m, 1H), 1.92 – 1.81 (m, 2H), 1.78 – 1.54 (m, 8H).



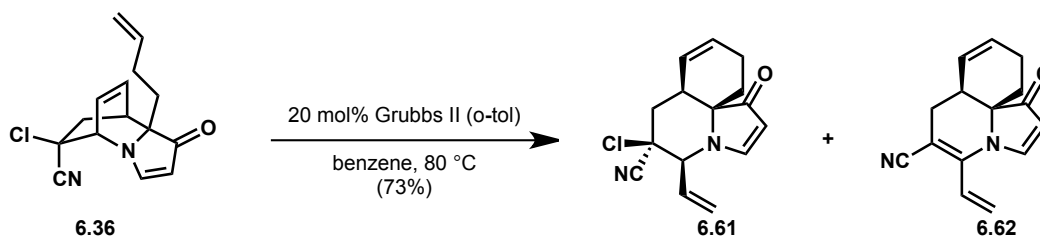
**Ethyl ester 6.48:** A solution of indolizine **6.31** (30.0 mg, 0.160 mmol) in ethyl acrylate (**6.47**, 300  $\mu\text{L}$ ) was heated to 90 °C. After 24 h, the reaction mixture was cooled to room temperature and concentrated under reduced pressure. The crude oil was purified via flash chromatography (4:1 hexanes/EtOAc) to provide [2.2.2]azabicyclic **6.48** in 88% yield (40.1 mg, 0.141 mmol).  $^1\text{H NMR}$  (600 MHz,  $\text{CDCl}_3$ )  $\delta$  7.92 (s, 1H), 6.48 (t,  $J = 7.0$  Hz, 1H), 6.28 (t,  $J = 6.6$  Hz, 1H), 5.60 (d,  $J = 17.0$  Hz, 2H), 4.86 (dd,  $J = 27.8, 13.6$  Hz, 2H), 4.63 (s, 1H), 4.14 – 4.00 (m, 2H), 3.00 (s, 1H), 2.84 – 2.72 (m, 1H), 1.91 – 1.49 (m, 7H), 1.21 (dd,  $J = 14.6, 7.6$  Hz, 4H).



**Methyl ester 6.48:** A solution of indolizinone **6.31** (30.0 mg, 0.160 mmol) in methyl acrylate (300  $\mu$ L) was heated to 80  $^{\circ}$ C. After 18 h, the reaction mixture was cooled to room temperature and concentrated under reduced pressure to afford [2.2.2]azabicyclic **6.48** in 94% yield (41.1 mg, 0.150 mmol).  $^1\text{H NMR}$  (500 MHz,  $\text{CDCl}_3$ )  $\delta$  7.92 (d,  $J = 3.3$  Hz, 1H), 6.51 (t,  $J = 7.3$  Hz, 1H), 6.30 (ddd,  $J = 7.8, 6.0, 1.4$  Hz, 1H), 5.63 (dd,  $J = 15.8, 5.1$  Hz, 2H), 4.94 – 4.84 (m, 2H), 4.64 (dd,  $J = 5.5, 4.0$  Hz, 1H), 3.65 (s, 3H), 3.03 (s, 1H), 2.85 – 2.79 (m, 1H), 1.90 – 1.81 (m, 1H), 1.78 (dd,  $J = 10.7, 7.0$  Hz, 1H), 1.69 (s, 1H), 1.68 – 1.57 (m, 4H).

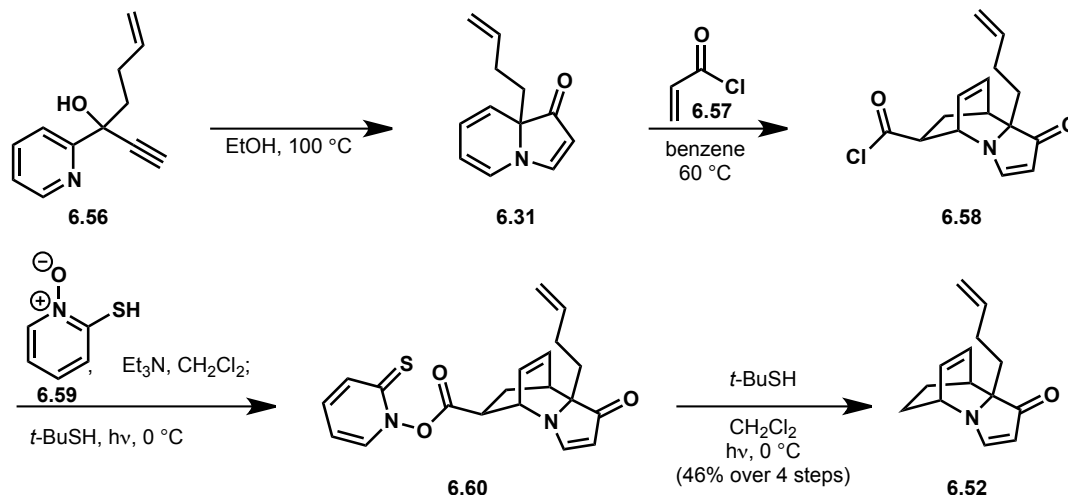


**Nitro [2.2.2]azabicyclic 6.35:** A solution of indolizinone **6.31** (5.00 mg, 0.0175 mmol), **6.114** (4.70 mg, 0.0351 mmol) and catechol (1.0 mg) in *p*-xylenes (300  $\mu$ L) was heated at 120  $^{\circ}$ C. After 15 h, the reaction mixture was cooled to room temperature and concentrated under reduced pressure. The crude oil was purified via flash chromatography to afford the nitro [2.2.2]bicyclic in 9% yield (0.40 mg, 0.0016 mmol).  $^1\text{H NMR}$  (500 MHz,  $\text{CDCl}_3$ )  $\delta$  7.99 (d,  $J = 3.5$  Hz, 1H), 6.64 (t,  $J = 7.3$  Hz, 1H), 6.31 – 6.24 (m, 1H), 5.69 – 5.58 (m, 2H), 5.01 – 4.95 (m, 1H), 4.95 – 4.86 (m, 2H), 4.57 (ddd,  $J = 8.8, 4.1, 2.7$  Hz, 1H), 3.20 – 3.14 (m, 1H), 2.29 – 2.24 (m, 1H), 1.83 (ddd,  $J = 15.2, 8.8, 1.6$  Hz, 2H), 1.71 (ddd,  $J = 16.9, 10.5, 5.8$  Hz, 2H), 1.62 – 1.58 (m, 1H).

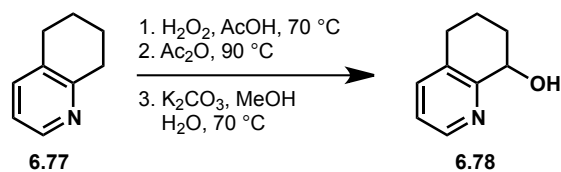


**Tricyclic 6.61:** A solution of **6.36** (10 mg, 0.036 mmol) and Grubbs II (*o*-tol) catalyst (3.1 mg, 0.0036 mmol) in benzene (3.6 mL) was sparged with ethylene for 5 min. The 20 mL vial was equipped with a Teflon cap and heated to 80  $^{\circ}$ C. After 12 h, the reaction mixture was cooled to room temperature and concentrated under reduced pressure to give a brown oil. The crude oil was purified via flash chromatography to afford **6.61** and **6.62**. Relative amounts of these products varied depending on the scale of the reaction. In this case, **6.61** was obtained in 73% yield.  $^1\text{H NMR}$  (500 MHz,  $\text{CDCl}_3$ )  $\delta$  7.85 (d,  $J = 3.6$  Hz, 1H), 6.23 – 6.12 (m, 1H), 5.94 (dd,  $J =$

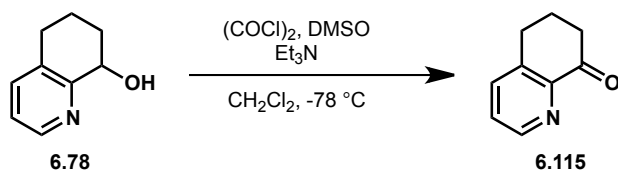
9.9, 5.1 Hz, 1H), 5.57 – 5.50 (m, 3H), 5.19 (d,  $J = 3.6$  Hz, 1H), 4.53 (dd,  $J = 7.1, 1.4$  Hz, 1H), 2.77 (d,  $J = 2.4$  Hz, 1H), 2.60 (d,  $J = 12.9$  Hz, 1H), 2.47 (ddd,  $J = 14.1, 4.0, 1.6$  Hz, 1H), 2.11 (ddd,  $J = 19.3, 15.9, 9.2$  Hz, 2H), 2.02 – 1.96 (m, 1H), 1.61 (dd,  $J = 13.7, 5.6$  Hz, 1H).



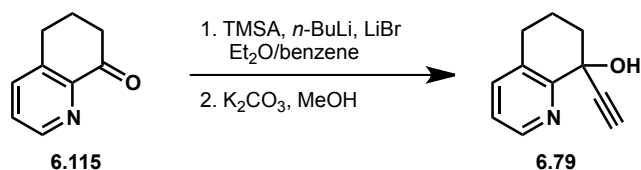
**[2.2.2]azabicyclo 6.52:** A solution of tertiary alcohol **6.56** (30.0 mg, 0.160 mmol) in EtOH (300  $\mu$ L) was sparged with  $N_2$  for 3 min, then heated at 100  $^\circ$ C. After 2 h, the reaction mixture was cooled to room temperature and concentrated to afford **6.31**, which was taken on without purification. A solution of indolizinone **6.31** (entire crude) and acryloyl chloride (130  $\mu$ L, 1.60 mmol) in benzene (1.50 mL) was heated to 60  $^\circ$ C for 1 h. The reaction mixture was cooled to room temperature, concentrated under reduced pressure and dried under high vac for 2 h. Next, the acid chloride (**6.58**) was dissolved in  $CH_2Cl_2$  (1.0 mL) and a solution of 2-mercaptopyridine *N*-oxide (**6.59**, 32.6 mg, 0.256 mmol) and  $Et_3N$  (45.0  $\mu$ L, 0.320 mmol) in  $CH_2Cl_2$  (600  $\mu$ L) was added dropwise over 1 h in the dark. The reaction mixture was stirred for 12 h at ambient temperature. The reaction mixture was cooled to 0  $^\circ$ C and *tert*-butylthiol (180  $\mu$ L, 1.60 mmol) was added dropwise over 1 min. The mixture was irradiated with a tungsten lamp for 2.5 h, while the temperature was maintained at 0  $^\circ$ C. The reaction mixture was diluted with water (2.0 mL). The aqueous layer was extracted with  $CH_2Cl_2$  (3 x 2.0 mL). The combined organic layer was washed with brine, dried over  $MgSO_4$  and concentrated under reduced pressure to afford a brown oil. The crude product was purified via flash chromatography (4:1 hexanes/EtOAc) to provide [2.2.2]azabicyclo **6.52** in 46% yield over 4 steps (15.7 mg, 0.0729 mmol).  $^1H$  NMR (600 MHz,  $CDCl_3$ )  $\delta$  7.89 (d,  $J = 3.3$  Hz, 1H), 6.41 (dd,  $J = 7.5, 4.1$  Hz, 2H), 5.69 – 5.61 (m, 1H), 5.53 (d,  $J = 3.4$  Hz, 1H), 4.90 (d,  $J = 17.1$  Hz, 1H), 4.85 (d,  $J = 10.2$  Hz, 1H), 4.25 (d,  $J = 4.0$  Hz, 1H), 2.95 (d,  $J = 1.9$  Hz, 1H), 1.83 (s, 1H), 1.77 – 1.70 (m, 1H), 1.66 – 1.62 (m, 2H), 1.47 (s, 1H), 1.26 (dd,  $J = 12.1, 4.8$  Hz, 1H), 1.23 – 1.19 (m, 1H);  $^{13}C$  NMR (151 MHz,  $CDCl_3$ )  $\delta$  209.4, 171.2, 138.3, 133.9, 130.4, 114.4, 111.2, 74.8, 53.4, 38.9, 35.9, 28.4, 26.6, 17.9.



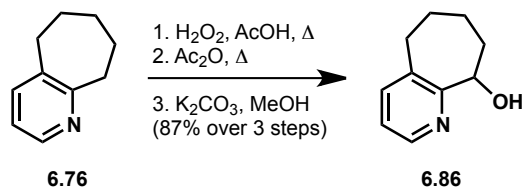
**Alcohol 6.78:** H<sub>2</sub>O<sub>2</sub> (2.26 mL, 30% in H<sub>2</sub>O) was added dropwise to pyridine **6.77** (1.50 g, 11.3 mmol) in AcOH (6.0 mL). The reaction mixture was heated to 70 °C for 12 h before it was cooled and concentrated under reduced pressure. The residue was dissolved in CHCl<sub>3</sub> (9.0 mL) and sodium carbonate (6.0 g) was added slowly in portions. The mixture was stirred for 2 h at room temperature. The solids were removed via filtration, and the organic layer was concentrated under reduced pressure to afford the *N*-oxide. The *N*-oxide was taken up in Ac<sub>2</sub>O (12.0 mL). The mixture was stirred at 90 °C for 36 h before being cooled to room temperature and concentrated under reduced pressure. The residue was dissolved in water (30 mL) and potassium carbonate (3.0 g) was added in portions over 10 min. Next, MeOH (5.0 mL) was added and the reaction mixture was stirred at 70 °C. After 24 h, the reaction mixture was cooled to room temperature and extracted with CH<sub>2</sub>Cl<sub>2</sub> (3 x 50 mL). The combined organic layer was concentrated to provide alcohol **6.78** (1.01 g, 6.78 mmol), which was used without further purification. <sup>1</sup>H NMR (400 MHz, CDCl<sub>3</sub>) δ 8.40 (d, *J* = 4.7 Hz, 1H), 7.44 (d, *J* = 7.0 Hz, 1H), 7.15 (dd, *J* = 7.8, 4.8 Hz, 1H), 4.74 (s, 1H), 2.87 – 2.75 (m, 3H), 2.31 – 2.22 (m, 1H), 2.11 (s, 1H), 2.10 (s, 1H), 2.05 – 1.97 (m, 1H), 1.88 – 1.76 (m, 3H).



**Ketone 6.115:** Oxalyl chloride (351 μL, 4.02 mmol) was added dropwise to DMSO (573 μL, 8.04 mmol) in CH<sub>2</sub>Cl<sub>2</sub> (30 mL) at -78 °C. The mixture was stirred at this temperature for 15 min, then, alcohol **6.78** (500 mg, 3.35 mmol) in CH<sub>2</sub>Cl<sub>2</sub> (2.0 mL) was added dropwise. The reaction mixture was stirred for 30 min at -78 °C. Et<sub>3</sub>N (2.24 mL, 16.1 mmol) was added at -78 °C, and the reaction mixture was stirred as the cold bath was allowed to gradually expire. The reaction was quenched with water (30 mL). The aqueous phase was extracted with CH<sub>2</sub>Cl<sub>2</sub> (3 x 30 mL). The combined organic layer was washed with brine (50 mL), dried over MgSO<sub>4</sub> and concentrated under reduced pressure to afford ketone **6.115** in quantitative yield. The crude ketone was used without further purification. <sup>1</sup>H NMR (500 MHz, CDCl<sub>3</sub>) δ 8.70 (d, *J* = 4.0 Hz, 1H), 7.66 (d, *J* = 7.8 Hz, 1H), 7.38 (dd, *J* = 7.8, 4.5 Hz, 1H), 5.12 (s, 1H), 3.14 – 3.06 (m, 2H), 3.03 (t, *J* = 6.1 Hz, 2H), 2.84 – 2.77 (m, 2H), 2.26 – 2.16 (m, 3H), 2.10 (s, 1H), 1.41 (t, *J* = 7.3 Hz, 3H).

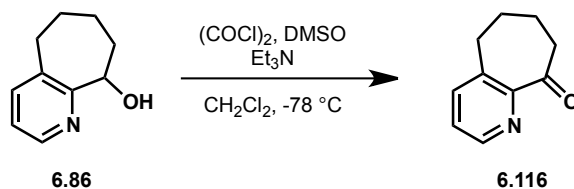


**Propargylic alcohol 6.79:** *n*-Butyllithium (1.89 mL, 4.73 mmol, 2.5 M in hexanes) was added dropwise to trimethylsilylacetylene (829  $\mu$ L, 5.83 mmol) in Et<sub>2</sub>O (5.0 mL) at 0 °C and stirred at this temperature for 30 min. The lithium acetylide solution was added dropwise to a vigorously stirred mixture of ketone **6.115** (536 mg, 3.64 mmol) and lithium bromide (948 mg, 10.9 mmol) in a 1:1 mixture of benzene and Et<sub>2</sub>O (total volume = 30 mL). The mixture was stirred for 36 h and ambient temperature. The reaction was quenched with a saturated NH<sub>4</sub>Cl<sub>(aq)</sub> solution (20 mL). The aqueous layer was extracted with EtOAc (3 x 20 mL). The combined organic layer was washed with brine (40 mL), dried over MgSO<sub>4</sub> and concentrated under reduced pressure to provide the tertiary alcohol in 75% yield (667 mg, 2.72 mmol). <sup>1</sup>H NMR (500 MHz, CDCl<sub>3</sub>)  $\delta$  8.44 (d, *J* = 4.6 Hz, 1H), 7.46 (d, *J* = 7.8 Hz, 1H), 7.18 (dd, *J* = 7.6, 4.8 Hz, 1H), 4.71 (s, 1H), 2.86 (s, 2H), 2.47 – 2.40 (m, 1H), 2.18 – 2.07 (m, 1H), 2.03 – 1.93 (m, 2H), 1.74 (s, 1H), 0.12 (s, 9H). The trimethylsilyl alkyne (667 mg, 2.72 mmol) was taken up in MeOH (27 mL) and potassium carbonate (751 mg, 5.44 mmol) was added. The reaction mixture was stirred at room temperature for 2 h. The reaction mixture was concentrated and diluted with water (30 mL). The aqueous phase was extracted with EtOAc (3 x 30 mL). The combined organic layer was washed with brine, dried over MgSO<sub>4</sub> and concentrated under reduced pressure to afford propargylic alcohol **6.79** in 87% yield (409 mg, 2.37 mmol). <sup>1</sup>H NMR (500 MHz, CDCl<sub>3</sub>)  $\delta$  8.46 (d, *J* = 4.6 Hz, 1H), 7.46 (d, *J* = 7.7 Hz, 1H), 7.19 (dd, *J* = 7.7, 4.7 Hz, 1H), 4.60 (s, 1H), 2.85 (dd, *J* = 9.3, 5.6 Hz, 2H), 2.57 (d, *J* = 1.0 Hz, 1H), 2.50 – 2.41 (m, 1H), 2.11 (s, 1H), 2.07 – 1.99 (m, 2H).

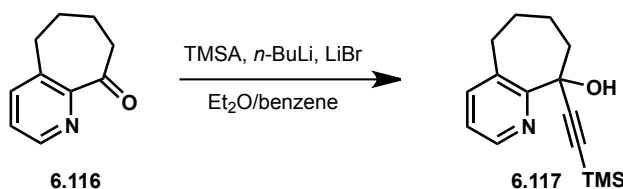


**Alcohol 6.86:** H<sub>2</sub>O<sub>2</sub> (959  $\mu$ L, 30% in H<sub>2</sub>O) was added dropwise to pyridine **6.76** (700 mg, 4.75 mmol) in AcOH (2.66 mL). The reaction mixture was heated to 70 °C for 12 h before it was cooled and concentrated under reduced pressure. The residue was dissolved in CHCl<sub>3</sub> (4.5 mL) and sodium carbonate (2.8 g) was added slowly in portions. The mixture was stirred for 2 h at room temperature. The solids were removed via filtration, and the organic layer was concentrated under reduced pressure to afford the *N*-oxide. The *N*-oxide was taken up in Ac<sub>2</sub>O (5.0 mL). The mixture was stirred at 90 °C for 36 h before being cooled to room temperature and concentrated under reduced pressure. The residue was dissolved in water (13 mL) and potassium carbonate (1.33 g) was added in portions over 10 min. Next, MeOH (3.0 mL) was added and the reaction mixture was stirred at 70 °C. After 24 h, the reaction mixture was cooled to room temperature and extracted with CH<sub>2</sub>Cl<sub>2</sub> (3 x 20 mL). The combined organic layer was concentrated to provide alcohol **6.86** in 87% yield over 3 steps (675 mg, 4.13 mmol), which was used without further purification. <sup>1</sup>H NMR (500 MHz, CDCl<sub>3</sub>)  $\delta$  8.36 (dd, *J* = 4.9, 1.1 Hz, 1H),

7.44 (d,  $J = 7.3$  Hz, 1H), 7.12 (dd,  $J = 7.4, 4.9$  Hz, 1H), 4.76 (dd,  $J = 11.2, 2.0$  Hz, 1H), 2.82 (s, 1H), 2.77 – 2.69 (m, 2H), 2.51 (d,  $J = 4.8$  Hz, 1H), 2.26 – 2.20 (m, 1H), 2.07 (dd,  $J = 10.8, 7.7$  Hz, 1H), 2.02 – 1.94 (m, 2H), 1.91 – 1.78 (m, 2H), 1.76 – 1.65 (m, 1H), 1.47 – 1.35 (m, 1H), 1.22 (dd,  $J = 13.1, 2.4$  Hz, 1H).



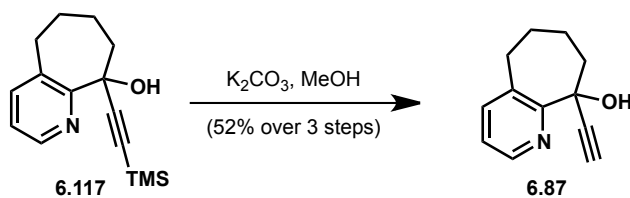
**Ketone 6.116:** Oxalyl chloride (217  $\mu\text{L}$ , 2.48 mmol) was added dropwise to DMSO (354  $\mu\text{L}$ , 4.97 mmol) in  $\text{CH}_2\text{Cl}_2$  (18 mL) at  $-78$   $^\circ\text{C}$ . The mixture was stirred at this temperature for 15 min, then, alcohol **6.86** (338 mg, 2.07 mmol) in  $\text{CH}_2\text{Cl}_2$  (2.0 mL) was added dropwise. The reaction mixture was stirred for 30 min at  $-78$   $^\circ\text{C}$ .  $\text{Et}_3\text{N}$  (1.38 mL, 9.94 mmol) was added at  $-78$   $^\circ\text{C}$ , and the reaction mixture was stirred as the cold bath was allowed to gradually expire. The reaction was quenched with water (20 mL). The aqueous phase was extracted with  $\text{CH}_2\text{Cl}_2$  (3 x 20 mL). The combined organic layer was washed with brine (30 mL), dried over  $\text{MgSO}_4$  and concentrated under reduced pressure to afford ketone **6.116** in quantitative yield. The crude ketone was used without further purification.  $^1\text{H NMR}$  (500 MHz,  $\text{CDCl}_3$ )  $\delta$  8.64 (d,  $J = 4.7$  Hz, 1H), 7.58 (d,  $J = 7.7$  Hz, 1H), 7.34 (d,  $J = 4.7$  Hz, 1H), 3.10 (dd,  $J = 7.3, 4.9$  Hz, 2H), 2.94 – 2.89 (m, 2H), 2.83 – 2.78 (m, 2H), 1.95 – 1.86 (m, 2H).



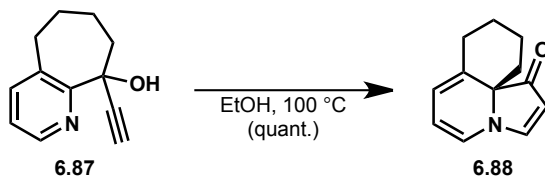
**Propargylic alcohol 6.117:** *n*-Butyllithium (1.27 mL, 3.18 mmol, 2.5 M in hexanes) was added dropwise to trimethylsilylacetylene (604  $\mu\text{L}$ , 4.24 mmol) in  $\text{Et}_2\text{O}$  (3.0 mL) at  $0$   $^\circ\text{C}$  and stirred at this temperature for 30 min. The lithium acetylide solution was added dropwise to a vigorously stirred mixture of ketone **6.116** (342 mg, 2.12 mmol) and lithium bromide (552 mg, 6.36 mmol) in a 1:1 mixture of benzene and  $\text{Et}_2\text{O}$  (total volume = 20 mL). The mixture was stirred for 36 h and ambient temperature. The reaction was quenched with a saturated  $\text{NH}_4\text{Cl}_{(\text{aq})}$  solution (20 mL). The aqueous layer was extracted with  $\text{EtOAc}$  (3 x 20 mL). The combined organic layer was washed with brine (40 mL), dried over  $\text{MgSO}_4$  and concentrated under reduced pressure to provide the tertiary alcohol in 53% yield (354 mg, 1.12 mmol), which was used without further purification.  $^1\text{H NMR}$  (600 MHz,  $\text{CDCl}_3$ )  $\delta$  8.32 (d,  $J = 4.8$  Hz, 1H), 7.48 (d,  $J = 7.4$  Hz, 1H), 7.17 (dd,  $J = 7.4, 4.8$  Hz, 1H), 3.29 (s, 1H), 2.70 (d,  $J = 6.0$  Hz, 1H), 2.28 – 2.22 (m, 2H), 2.01 – 1.95 (m, 2H), 1.87 (s, 2H), 1.71 – 1.62 (m, 1H), 1.56 (d,  $J = 2.6$  Hz, 1H), 0.16 – 0.13 (m, 10H);  $^{13}\text{C NMR}$  (151 MHz,  $\text{CDCl}_3$ )  $\delta$  158.7, 143.8, 138.9, 136.5, 123.1, 105.9, 90.5, 71.4, 40.5, 34.2,



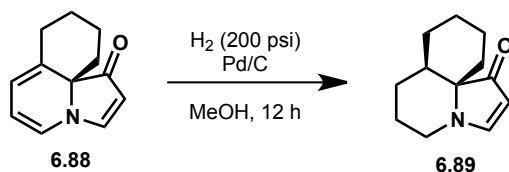
27.5, 27.5, -0.1; **IR** (film)  $\nu_{\max}$  3350, 2930, 2175, 1398, 843  $\text{cm}^{-1}$ ; **HRMS** (ESI+) calcd for  $[\text{C}_{15}\text{H}_{22}\text{ONSi}]^+$  (M-H) $^+$ :  $m/z$  260.1465, found 260.1463.



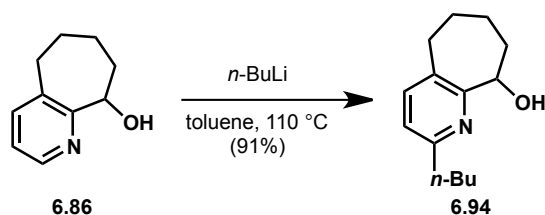
**Tertiary alcohol 6.87:** Potassium carbonate (288 mg, 2.08 mmol) was added to a solution of the trimethylsilyl alkyne (270 mg, 1.04 mmol) in MeOH (10 mL). The reaction mixture was stirred at room temperature for 2 h. The reaction mixture was concentrated and diluted with water (20 mL). The aqueous phase was extracted with EtOAc (3 x 20 mL). The combined organic layer was washed with brine, dried over  $\text{MgSO}_4$  and concentrated under reduced pressure to afford propargylic alcohol **6.87** in 80% yield (147 mg, 0.785 mmol).  $^1\text{H NMR}$  (600 MHz,  $\text{CDCl}_3$ )  $\delta$  8.34 (d,  $J = 4.9$  Hz, 1H), 7.50 (d,  $J = 7.4$  Hz, 1H), 7.19 (dd,  $J = 7.4, 4.9$  Hz, 1H), 3.30 (t,  $J = 13.7$  Hz, 1H), 2.72 (dd,  $J = 14.6, 6.1$  Hz, 1H), 2.58 (s, 1H), 2.29 (dd,  $J = 19.8, 17.0$  Hz, 2H), 2.07 – 1.98 (m, 3H), 1.62 (dd,  $J = 13.5, 2.5$  Hz, 1H), 1.31 – 1.23 (m, 1H);  $^{13}\text{C NMR}$  (151 MHz,  $\text{CDCl}_3$ )  $\delta$  146.6, 143.8, 139.0, 136.4, 123.2, 84.6, 73.7, 71.0, 40.3, 34.3, 27.3, 27.3; **IR** (film)  $\nu_{\max}$  3418, 2950, 1647, 1047  $\text{cm}^{-1}$ ; **HRMS** (ESI+) calcd for  $[\text{C}_{12}\text{H}_{14}\text{ON}]^+$  (M-H) $^+$ :  $m/z$  188.1070, found 188.1068.



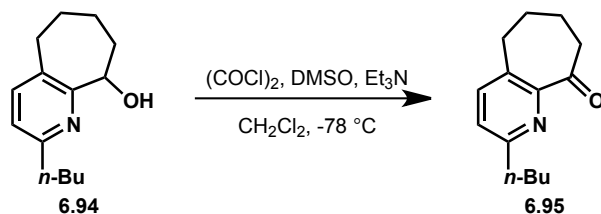
**Indolizinone 6.88:** A solution of tertiary alcohol **6.87** (73.5 mg, 0.393 mmol) in EtOH (2.0 mL) was sparged with  $\text{N}_2$  for 5 min, then heated to 100 °C. After 4 h, the reaction mixture was cooled to room temperature and concentrated to provide a crude yellow oil. The oil was purified via flash chromatography (9:1 hexanes/EtOAc) to afford indolizinone **6.88** in 95% yield (70.1 mg, 0.374 mmol).  $^1\text{H NMR}$  (600 MHz,  $\text{CDCl}_3$ )  $\delta$  7.65 (d,  $J = 3.6$  Hz, 1H), 6.18 (d,  $J = 7.1$  Hz, 1H), 5.43 (d,  $J = 5.7$  Hz, 1H), 5.14 (t,  $J = 6.5$  Hz, 1H), 4.93 (d,  $J = 3.6$  Hz, 1H), 3.24 (d,  $J = 4.2$  Hz, 1H), 2.32 (d,  $J = 13.5$  Hz, 1H), 2.23 (dd,  $J = 11.9, 3.4$  Hz, 1H), 2.08 – 1.94 (m, 3H), 1.57 (dd,  $J = 16.0, 6.9$  Hz, 2H), 1.45 (d,  $J = 12.8$  Hz, 1H);  $^{13}\text{C NMR}$  (151 MHz,  $\text{CDCl}_3$ )  $\delta$  205.1, 158.9, 140.5, 124.0, 114.1, 107.2, 95.7, 72.0, 36.8, 31.2, 30.7, 19.3; **IR** (film)  $\nu_{\max}$  3467, 2076, 1640  $\text{cm}^{-1}$ ; **HRMS** (ESI+) calcd for  $[\text{C}_{12}\text{H}_{13}\text{NO}]^+$  (M-H) $^+$ :  $m/z$  188.1070, found 188.1069.



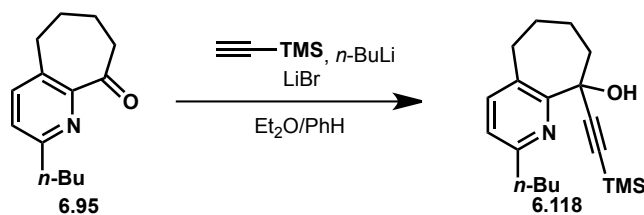
**Tricyclic 6.89:** Palladium (4.0 mg, 10 wt %) on activated carbon was added to a solution of indolizinone **6.88** (4.7 mg, 0.0251 mmol) in methanol (400  $\mu\text{L}$ ). The mixture was stirred vigorously under an atmosphere of hydrogen (200 psi) in a Parr bomb for 12 h. The reaction mixture was filtered through a plug of celite and concentrated to provide **6.89** as a light yellow oil in 94% yield (4.5 mg, 0.0235 mmol).  $^1\text{H NMR}$  (600 MHz,  $\text{CDCl}_3$ )  $\delta$  7.66 (d,  $J = 3.2$  Hz, 1H), 4.98 (d,  $J = 3.1$  Hz, 1H), 3.46 (d,  $J = 4.9$  Hz, 1H), 3.29 – 3.24 (m, 1H), 2.50 (s, 2H), 2.35 (d,  $J = 13.4$  Hz, 1H), 1.87 (ddd,  $J = 17.5, 13.2, 3.8$  Hz, 1H), 1.75 (d,  $J = 12.9$  Hz, 1H), 1.65 (d,  $J = 13.0$  Hz, 1H), 1.62 – 1.51 (m, 2H), 1.48 – 1.42 (m, 2H), 1.38 (ddd,  $J = 18.6, 10.5, 6.3$  Hz, 3H);  $^{13}\text{C NMR}$  (151 MHz,  $\text{CDCl}_3$ )  $\delta$  207.7, 161.3, 95.1, 66.7, 46.0, 36.3, 27.0, 26.0, 25.5, 24.5, 19.6, 19.4; **IR** (film)  $\nu_{\text{max}}$  2926, 2854, 1540, 1445  $\text{cm}^{-1}$ ; **HRMS** (ESI+) calcd for  $[\text{C}_{12}\text{H}_{18}\text{ON}]^+$  (M-H) $^+$ :  $m/z$  192.1383, found 192.1383.



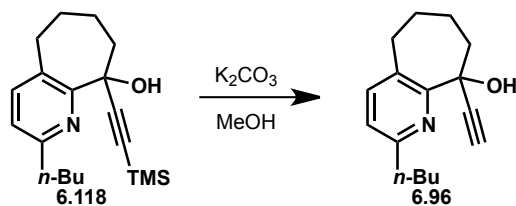
**Trisubstituted pyridine 6.94:** *n*-Butyllithium (2.51 mL, 6.27 mmol, 2.5 M in hexanes) was added dropwise to pyridine **6.86** (500 mg, 3.06 mmol) in toluene (30 mL). The Schlenk flask was sealed and heated to 110  $^\circ\text{C}$ . After 18 h, the reaction mixture was cooled to room temperature. The reaction was quenched by the addition of MeOH (2.0 mL) followed by a saturated  $\text{NH}_4\text{Cl}_{(\text{aq})}$  solution (20 mL). The aqueous layer was extracted with EtOAc (3 x 20 mL). The combined organic layer was washed with brine (30 mL), dried over  $\text{MgSO}_4$  and concentrated under reduced pressure to provide **6.94** in 91% yield (611 mg, 2.78 mmol) as a brown oil that was used without further purification.  $^1\text{H NMR}$  (400 MHz,  $\text{CDCl}_3$ )  $\delta$  7.32 (d,  $J = 7.6$  Hz, 1H), 6.93 (d,  $J = 7.6$  Hz, 1H), 6.23 (s, 1H), 4.70 (dd,  $J = 11.2, 2.2$  Hz, 1H), 2.79 – 2.71 (m, 2H), 2.69 (dd,  $J = 11.6, 8.3$  Hz, 2H), 2.25 – 2.17 (m, 1H), 2.04 (s, 1H), 1.95 (ddd,  $J = 9.7, 4.7, 1.9$  Hz, 1H), 1.82 (dt,  $J = 12.8, 2.6$  Hz, 1H), 1.74 – 1.66 (m, 2H), 1.42 – 1.32 (m, 3H), 1.27 – 1.17 (m, 1H), 0.93 (t,  $J = 7.4$  Hz, 3H);  $^{13}\text{C NMR}$  (101 MHz,  $\text{CDCl}_3$ )  $\delta$  159.9, 157.1, 137.6, 132.4, 120.7, 72.0, 37.1, 36.4, 33.9, 31.6, 29.1, 27.2, 22.4, 13.9; **IR** (film)  $\nu_{\text{max}}$  3353, 2927, 2854, 1594, 1470, 1064  $\text{cm}^{-1}$ ; **HRMS** (ESI+) calcd for  $[\text{C}_{14}\text{H}_{22}\text{ON}]^+$  (M-H) $^+$ :  $m/z$  220.1696, found 220.1695.



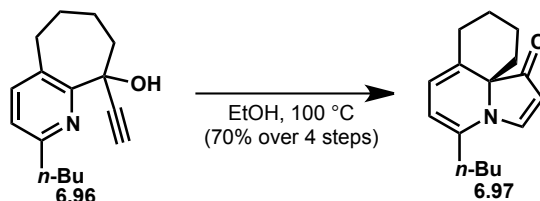
**Ketone 6.95:** Oxalyl chloride (836  $\mu\text{L}$ , 9.58 mmol) was added dropwise to DMSO (1.37 mL, 19.2 mmol) in  $\text{CH}_2\text{Cl}_2$  (40 mL) at  $-78\text{ }^\circ\text{C}$ . The mixture was stirred at this temperature for 15 min, then, alcohol **6.94** (1.05 g, 4.79 mmol) in  $\text{CH}_2\text{Cl}_2$  (5.0 mL) was added dropwise. The reaction mixture was stirred for 30 min at  $-78\text{ }^\circ\text{C}$ .  $\text{Et}_3\text{N}$  (5.30 mL, 38.3 mmol) was added at  $-78\text{ }^\circ\text{C}$ , and the reaction mixture was stirred as the cold bath was allowed to gradually expire. The reaction was quenched with water (40 mL). The aqueous phase was extracted with  $\text{CH}_2\text{Cl}_2$  (3 x 40 mL). The combined organic layer was washed with brine (50 mL), dried over  $\text{MgSO}_4$  and concentrated under reduced pressure to afford ketone **6.95**. The crude ketone was used without further purification.  $^1\text{H NMR}$  (400 MHz,  $\text{CDCl}_3$ )  $\delta$  7.45 (d,  $J = 7.8$  Hz, 1H), 7.17 (d,  $J = 7.8$  Hz, 1H), 2.84 (dd,  $J = 13.8, 5.9$  Hz, 4H), 2.79 – 2.73 (m, 2H), 1.90 – 1.82 (m, 4H), 1.68 (ddd,  $J = 12.7, 6.7, 4.0$  Hz, 2H), 1.38 (dd,  $J = 14.9, 7.4$  Hz, 2H), 0.92 (t,  $J = 7.3$  Hz, 3H);  $^{13}\text{C NMR}$  (101 MHz,  $\text{CDCl}_3$ )  $\delta$  205.4, 161.3, 154.4, 138.2, 133.1, 124.7, 40.5, 37.8, 32.1, 30.6, 25.1, 22.6, 21.5, 13.9; **IR** (film)  $\nu_{\text{max}}$  2931, 2860, 1698, 1590, 1461  $\text{cm}^{-1}$ ; **HRMS** (ESI+) calcd for  $[\text{C}_{14}\text{H}_{20}\text{ON}]^+$  (M-H) $^+$ :  $m/z$  218.1539, found 218.1538.



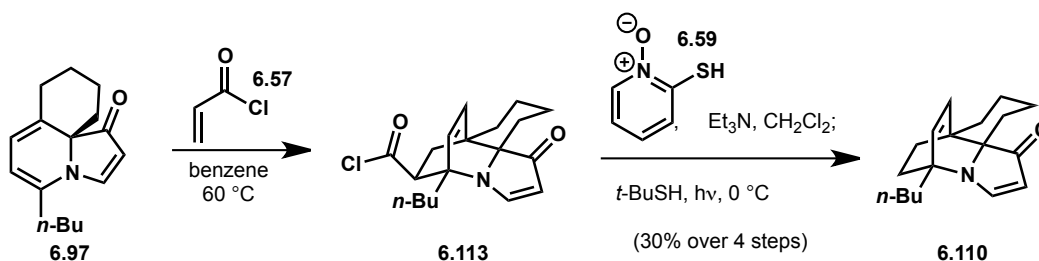
**Alkyne 6.118:** *n*-Butyllithium (948  $\mu\text{L}$ , 2.37 mmol, 2.5 M in hexanes) was added dropwise to trimethylsilylacetylene (451  $\mu\text{L}$ , 3.17 mmol) in  $\text{Et}_2\text{O}$  (3.0 mL) at  $0\text{ }^\circ\text{C}$  and stirred at this temperature for 30 min. The lithium acetylide solution was added dropwise to a vigorously stirred mixture of ketone **6.95** (344 mg, 1.58 mmol) and lithium bromide (412 mg, 4.74 mmol) in a 1:1 mixture of benzene and  $\text{Et}_2\text{O}$  (total volume = 20 mL). The mixture was stirred for 36 h and ambient temperature. The reaction was quenched with a saturated  $\text{NH}_4\text{Cl}_{(\text{aq})}$  solution (20 mL). The aqueous layer was extracted with  $\text{EtOAc}$  (3 x 20 mL). The combined organic layer was washed with brine (40 mL), dried over  $\text{MgSO}_4$  and concentrated under reduced pressure to provide the tertiary alcohol, which was used without further purification.  $^1\text{H NMR}$  (600 MHz,  $\text{CDCl}_3$ )  $\delta$  7.38 (d,  $J = 7.6$  Hz, 1H), 7.00 (d,  $J = 7.5$  Hz, 1H), 3.23 (t,  $J = 13.6$  Hz, 1H), 2.80 – 2.72 (m, 3H), 2.66 (dd,  $J = 14.7, 5.6$  Hz, 1H), 2.24 (d,  $J = 12.4$  Hz, 2H), 2.00 (s, 2H), 1.70 (dd,  $J = 15.4, 7.7$  Hz, 4H), 1.57 (d,  $J = 13.3$  Hz, 3H), 1.38 (dd,  $J = 14.9, 7.4$  Hz, 3H), 0.94 (d,  $J = 7.4$  Hz, 3H), 0.16 (s, 9H); **IR** (film)  $\nu_{\text{max}}$  3423, 2929, 2857, 2156, 1387, 843  $\text{cm}^{-1}$ ; **HRMS** (ESI+) calcd for  $[\text{C}_{19}\text{H}_{30}\text{ONSi}]^+$  (M-H) $^+$ :  $m/z$  316.2091, found 316.2088.



**Tertiary alcohol 6.96:** Potassium carbonate (281 mg, 2.03 mmol) was added to a solution of the trimethylsilyl alkyne (320 mg, 1.02 mmol) in MeOH (10 mL). The reaction mixture was stirred at room temperature for 2 h. The reaction mixture was concentrated and diluted with water (20 mL). The aqueous phase was extracted with EtOAc (3 x 20 mL). The combined organic layer was washed with brine, dried over MgSO<sub>4</sub> and concentrated under reduced pressure to afford propargylic alcohol **6.96**, which was used without further purification. <sup>1</sup>H NMR (600 MHz, CDCl<sub>3</sub>) δ 7.39 (d, *J* = 7.6 Hz, 1H), 7.01 (d, *J* = 7.6 Hz, 1H), 3.23 (s, 1H), 2.75 (dd, *J* = 13.8, 5.9 Hz, 3H), 2.28 (s, 2H), 2.04 – 1.97 (m, 2H), 1.70 (dd, *J* = 15.3, 7.8 Hz, 2H), 1.59 (d, *J* = 2.1 Hz, 1H), 1.37 (dd, *J* = 14.9, 7.4 Hz, 2H), 1.26 (d, *J* = 12.9 Hz, 2H), 0.93 (t, *J* = 7.4 Hz, 3H); <sup>13</sup>C NMR (151 MHz, CDCl<sub>3</sub>) δ 157.2, 156.8, 139.5, 133.2, 122.0, 84.9, 73.5, 70.8, 40.4, 36.9, 33.8, 31.4, 27.5, 27.4, 22.4, 13.9; IR (film) ν<sub>max</sub> 3286, 2929, 2857, 1595, 1468, 1054 cm<sup>-1</sup>; HRMS (ESI<sup>+</sup>) calcd for [C<sub>16</sub>H<sub>22</sub>ON]<sup>+</sup> (M-H)<sup>+</sup>: *m/z* 244.1696, found 244.1693.

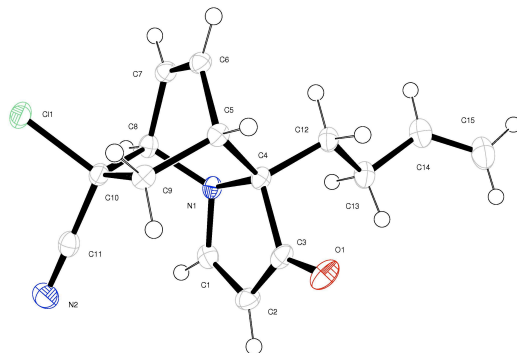


**Indolizinone 6.97:** A solution of tertiary alcohol **6.96** (53.0 mg, 0.218 mmol) in EtOH (1.0 mL) was sparged with N<sub>2</sub> for 5 min, then heated to 100 °C. After 4 h, the reaction mixture was cooled to room temperature and concentrated to provide a crude yellow oil. The oil was purified via flash chromatography (9:1 hexanes/EtOAc) to afford indolizinone **6.97** in 70% yield over 4 steps (from alcohol **6.94**). <sup>1</sup>H NMR (400 MHz, CDCl<sub>3</sub>) δ 7.88 (d, *J* = 3.7 Hz, 1H), 5.41 (d, *J* = 5.9 Hz, 1H), 5.04 (d, *J* = 5.9 Hz, 1H), 4.95 (d, *J* = 3.7 Hz, 1H), 3.71 (d, *J* = 7.0 Hz, 1H), 3.28 (d, *J* = 4.5 Hz, 1H), 3.03 – 2.97 (m, 1H), 2.70 (s, 1H), 2.34 (d, *J* = 8.8 Hz, 2H), 2.21 (s, 1H), 2.16 – 2.10 (m, 1H), 2.08 (d, *J* = 3.6 Hz, 1H), 2.01 (s, 3H), 1.89 – 1.82 (m, 1H), 1.71 – 1.60 (m, 2H), 1.54 (dd, *J* = 15.5, 5.8 Hz, 3H), 1.47 (s, 3H), 1.39 (d, *J* = 12.5 Hz, 4H), 0.93 (dd, *J* = 9.2, 5.2 Hz, 3H); <sup>13</sup>C NMR (101 MHz, CDCl<sub>3</sub>) δ 205.1, 155.9, 139.1, 134.6, 114.5, 106.0, 95.7, 72.9, 36.5, 31.3, 30.3, 29.9, 28.7, 22.1, 19.3, 13.8; HRMS (ESI<sup>+</sup>) calcd for [C<sub>16</sub>H<sub>22</sub>ON]<sup>+</sup> (M-H)<sup>+</sup>: *m/z* 244.1696, found 244.1693.



**[2.2.2]azabicyclohexane 6.110:** A solution of tertiary alcohol **6.96** (155 mg, 0.637 mmol) in EtOH (5.0 mL) was sparged with N<sub>2</sub> for 3 min, then heated at 100 °C. After 2 h, the reaction mixture was cooled to room temperature and concentrated to afford **6.97**, which was taken on without purification. A solution of indolizone **6.97** (entire crude) and acryloyl chloride (518 μL, 6.37 mmol) in benzene (5.0 mL) was heated to 60 °C for 2 h. The reaction mixture was cooled to room temperature, concentrated under reduced pressure and dried under high vac for 2 h. Next, the acid chloride (**6.113**) was dissolved in CH<sub>2</sub>Cl<sub>2</sub> (5.0 mL) and a solution of 2-mercaptopyridine *N*-oxide (**6.59**, 122 mg, 0.956 mmol) and Et<sub>3</sub>N (178 μL, 1.27 mmol) in CH<sub>2</sub>Cl<sub>2</sub> (1.0 mL) was added dropwise over 1 h in the dark. The reaction mixture was stirred for 12 h at ambient temperature. The reaction mixture was cooled to 0 °C and *tert*-butylthiol (718 μL, 6.37 mmol) was added dropwise over 1 min. The mixture was irradiated with a tungsten lamp for 2.5 h, while the temperature was maintained at 0 °C. The reaction mixture was diluted with water (5.0 mL). The aqueous layer was extracted with CH<sub>2</sub>Cl<sub>2</sub> (3 x 5.0 mL). The combined organic layer was washed with brine, dried over MgSO<sub>4</sub> and concentrated under reduced pressure to afford a brown oil. The crude product was purified via flash chromatography (9:1 hexanes/EtOAc) to provide [2.2.2]azabicyclohexane **6.110** in 30% yield over 4 steps (51.0 mg, 0.188 mmol). <sup>1</sup>H NMR (600 MHz, CDCl<sub>3</sub>) δ 7.79 (d, *J* = 3.5 Hz, 1H), 6.16 (d, *J* = 8.0 Hz, 2H), 5.38 (d, *J* = 3.5 Hz, 1H), 2.44 (d, *J* = 4.2 Hz, 1H), 2.14 (d, *J* = 14.2 Hz, 1H), 1.87 – 1.80 (m, 1H), 1.72 (s, 1H), 1.68 – 1.63 (m, 2H), 1.63 – 1.57 (m, 4H), 1.53 – 1.48 (m, 3H), 1.45 – 1.39 (m, 5H), 1.36 – 1.30 (m, 4H), 1.27 (ddd, *J* = 11.4, 8.5, 4.6 Hz, 2H), 1.12 – 1.08 (m, 1H), 0.96 (t, *J* = 7.1 Hz, 4H), 0.88 (t, *J* = 7.2 Hz, 1H); <sup>13</sup>C NMR (151 MHz, CDCl<sub>3</sub>) δ 210.0, 164.2, 138.2, 131.8, 109.4, 73.7, 61.0, 43.3, 35.6, 33.6, 30.9, 28.7, 28.2, 26.2, 23.2, 21.6, 17.5, 14.0.

## X-Ray Structure of 6.36:



**X-Ray Experimental Details:** A colorless plate 0.12 x 0.10 x 0.06 mm in size was mounted on a Cryoloop with Paratone oil. Data were collected in a nitrogen gas stream at 100(2) K using phi and omega scans. Crystal-to-detector distance was 60 mm and exposure time was 5 seconds per frame using a scan width of 1.0°. Data collection was 99.8% complete to 67.00° in  $\theta$ . A total of 14245 reflections were collected covering the indices,  $-10 \leq h \leq 10$ ,  $-7 \leq k \leq 8$ ,  $-26 \leq l \leq 26$ . 2476 reflections were found to be symmetry independent, with an  $R_{\text{int}}$  of 0.0123. Indexing and unit cell refinement indicated a primitive, monoclinic lattice. The space group was found to be P2(1)/n (No. 14). The data were integrated using the Bruker SAINT software program and scaled using the SADABS software program. Solution by direct methods (SIR-2004) produced a complete heavy-atom phasing model consistent with the proposed structure. All non-hydrogen atoms were refined anisotropically by full-matrix least-squares (SHELXL-97). All hydrogen atoms were placed using a riding model. Their positions were constrained relative to their parent atom using the appropriate HFIX command in SHELXL-97.

## X-Ray Data:

|                        |                           |                   |
|------------------------|---------------------------|-------------------|
| Empirical formula      | C15 H15 Cl N2 O           |                   |
| Formula weight         | 274.74                    |                   |
| Temperature            | 100(2) K                  |                   |
| Wavelength             | 1.54178 Å                 |                   |
| Crystal system         | Monoclinic                |                   |
| Space group            | P2(1)/n                   |                   |
| Unit cell dimensions   | a = 8.4660(3) Å           | a = 90°.          |
|                        | b = 7.2644(2) Å           | b = 95.0810(10)°. |
|                        | c = 22.2712(7) Å          | g = 90°.          |
| Volume                 | 1364.31(7) Å <sup>3</sup> |                   |
| Z                      | 4                         |                   |
| Density (calculated)   | 1.338 Mg/m <sup>3</sup>   |                   |
| Absorption coefficient | 2.418 mm <sup>-1</sup>    |                   |

|                                   |   |
|-----------------------------------|---|
| F(000)                            | 576   |
| Crystal size                      | 0.12 x 0.10 x 0.06 mm <sup>3</sup>          |
| Crystal color/habit               | colorless plate                             |
| Theta range for data collection   | 3.99 to 68.08°.                             |
| Index ranges                      | -10<=h<=10, -7<=k<=8, -26<=l<=26            |
| Reflections collected             | 14245                                       |
| Independent reflections           | 2476 [R(int) = 0.0123]                      |
| Completeness to theta = 67.00°    | 99.8 %                                      |
| Absorption correction             | Semi-empirical from equivalents             |
| Max. and min. transmission        | 0.8685 and 0.7601                           |
| Refinement method                 | Full-matrix least-squares on F <sup>2</sup> |
| Data / restraints / parameters    | 2476 / 0 / 172                              |
| Goodness-of-fit on F <sup>2</sup> | 1.057                                       |
| Final R indices [I>2sigma(I)]     | R1 = 0.0353, wR2 = 0.0949                   |
| R indices (all data)              | R1 = 0.0361, wR2 = 0.0956                   |
| Largest diff. peak and hole       | 0.357 and -0.326 e.Å <sup>-3</sup>          |

## 6.8 References and Notes

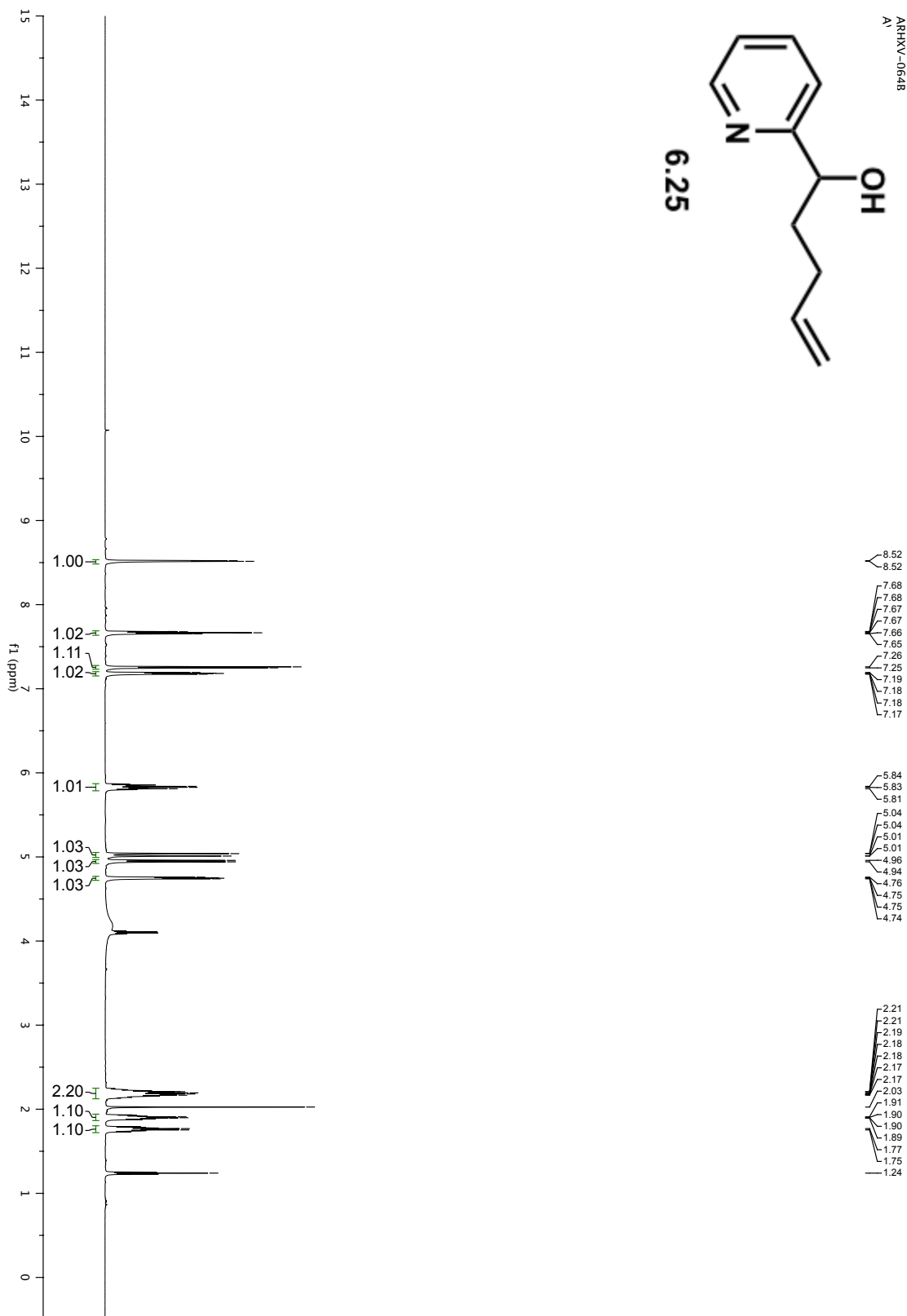
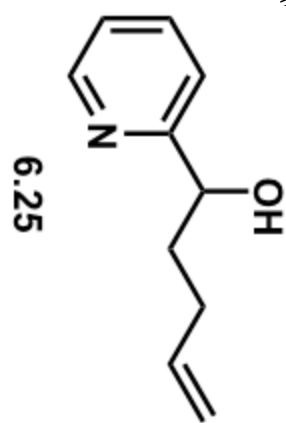
- (1) Blackman, A. J.; Li, C. P.; Hockless, D. C. R.; Skelton, B. W.; White, A. H. *Tetrahedron* **1993**, *49*, 8645.
- (2) Bignold, L. P. *Anticancer Res.* **2006**, *26*, 1327.
- (3) Li, C. P.; Blackman, A. J. *Aust. J. Chem.* **1994**, *47*, 1355.
- (4) Li, C. P.; Blackman, A. J. *Aust. J. Chem.* **1995**, *48*, 955.
- (5) Biard, J. F.; Guyot, S.; Roussakis, C.; Verbist, J. F.; Vercauteren, J.; Weber, J. F.; Boukef, K. *Tetrahedron Lett.* **1994**, *35*, 2691.
- (6) Weinreb, S. M. *Acc. Chem. Res.* **2003**, *36*, 59.
- (7) Werner, K. M.; de los Santos, J. M.; Weinreb, S. M.; Shang, M. Y. *J. Org. Chem.* **1999**, *64*, 4865.
- (8) Pearson, W. H.; Barta, N. S.; Kampf, J. W. *Tetrahedron Lett.* **1997**, *38*, 3369.
- (9) Juge, M.; Grimaud, N.; Biard, J. F.; Sauviat, M. P.; Nabil, M.; Verbist, J. F.; Petit, J. Y. *Toxicon* **2001**, *39*, 1231.
- (10) Donohoe, T. J.; Brian, P. M.; Hargaden, G. C.; O'Riordan, T. J. C. *Tetrahedron* **2010**, *66*, 6411.
- (11) Flick, A. C.; Caballero, M. J. A.; Padwa, A. *Tetrahedron* **2010**, *66*, 3643.
- (12) Fujitani, M.; Tsuchiya, M.; Okano, K.; Takasu, K.; Ihara, M.; Tokuyama, H. *Synlett* **2010**, 822.
- (13) Mei, S. L.; Zhao, G. *Eur. J. Org. Chem.* **2010**, 1660.
- (14) Meyer, A. M.; Katz, C. E.; Li, S. W.; Velde, D. V.; Aube, J. *Org. Lett.* **2010**, *12*, 1244.
- (15) Zou, J. W.; Cho, D. W.; Mariano, P. S. *Tetrahedron* **2010**, *66*, 5955.
- (16) Weinreb, S. M. *Chem. Rev.* **2006**, *106*, 2531.
- (17) Schar, P.; Cren, S.; Renaud, P. *Chimia* **2006**, *60*, 131.
- (18) Bartlett, P. D.; Schuelle, K. *J. Am. Chem. Soc.* **1968**, *90*, 6071.

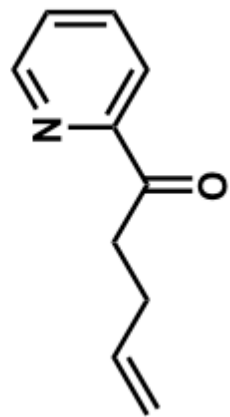


- (19) Aggarwal, V. K.; Ali, A.; Coogan, M. P. *Tetrahedron* **1999**, *55*, 293.
- (20) Ballini, R.; Petrini, M. *Tetrahedron* **2004**, *60*, 1017.
- (21) Peukert, S.; Sun, Y. C.; Zhang, R.; Hurley, B.; Sabio, M.; Shen, X. Y.; Gray, C.; Dzink-Fox, J.; Tao, J. S.; Cebula, R.; Wattanasin, S. *Bioorg. Med. Chem. Lett.* **2008**, *18*, 1840.
- (22) Liu, H. F.; Yin, D. H.; Yin, D. L.; Fu, Z. H.; Li, Q. H.; Lu, G. X. *J. Mol. Cat. Chem.* **2004**, *209*, 171.
- (23) Oconnor, J. M.; Ma, J. *J. Org. Chem.* **1992**, *57*, 5075.
- (24) Horton, D.; Usui, T. *Carbohydr. Res.* **1991**, *216*, 33.

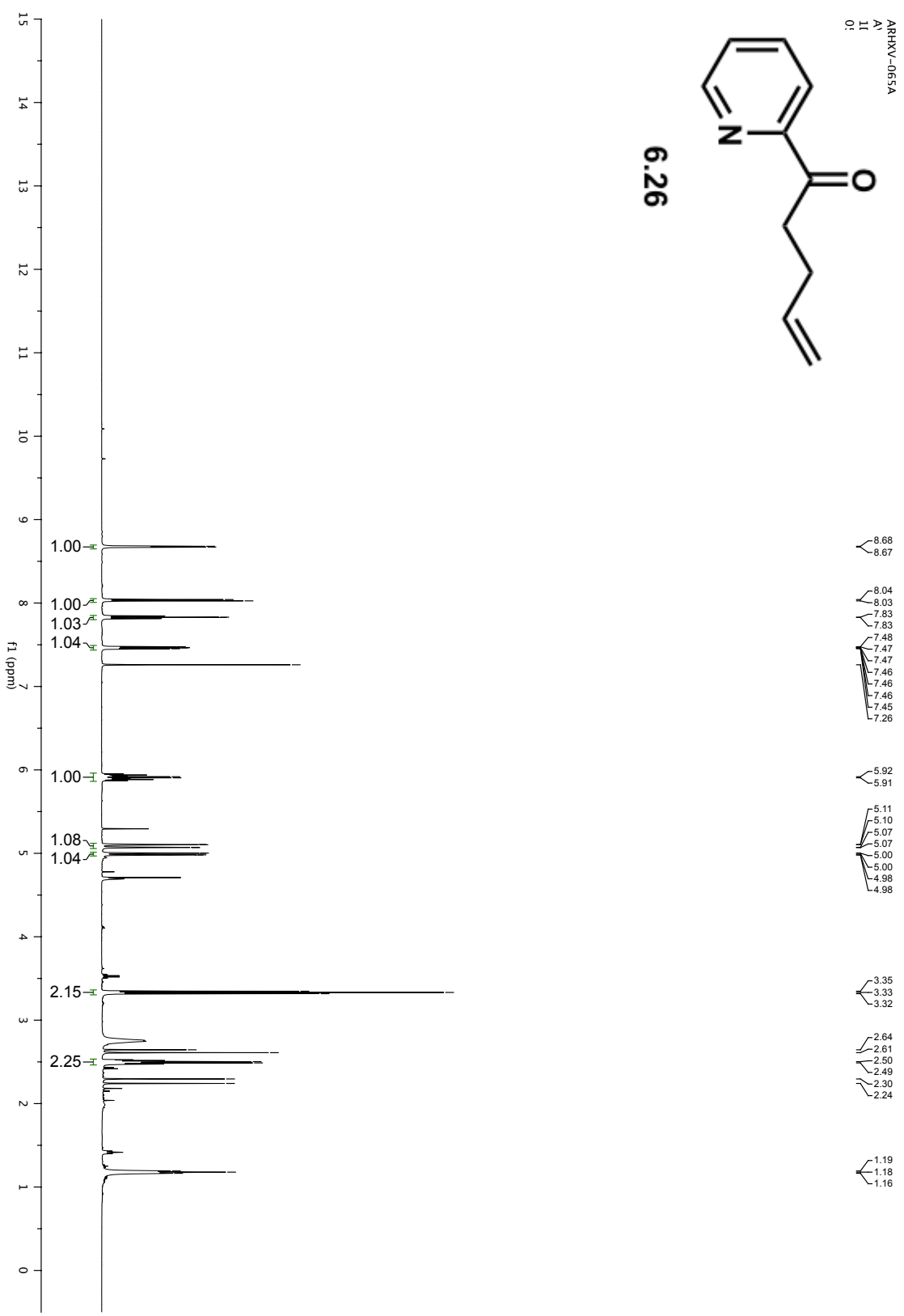
*Appendix Five:  
Spectra Relevant to Chapter Six*

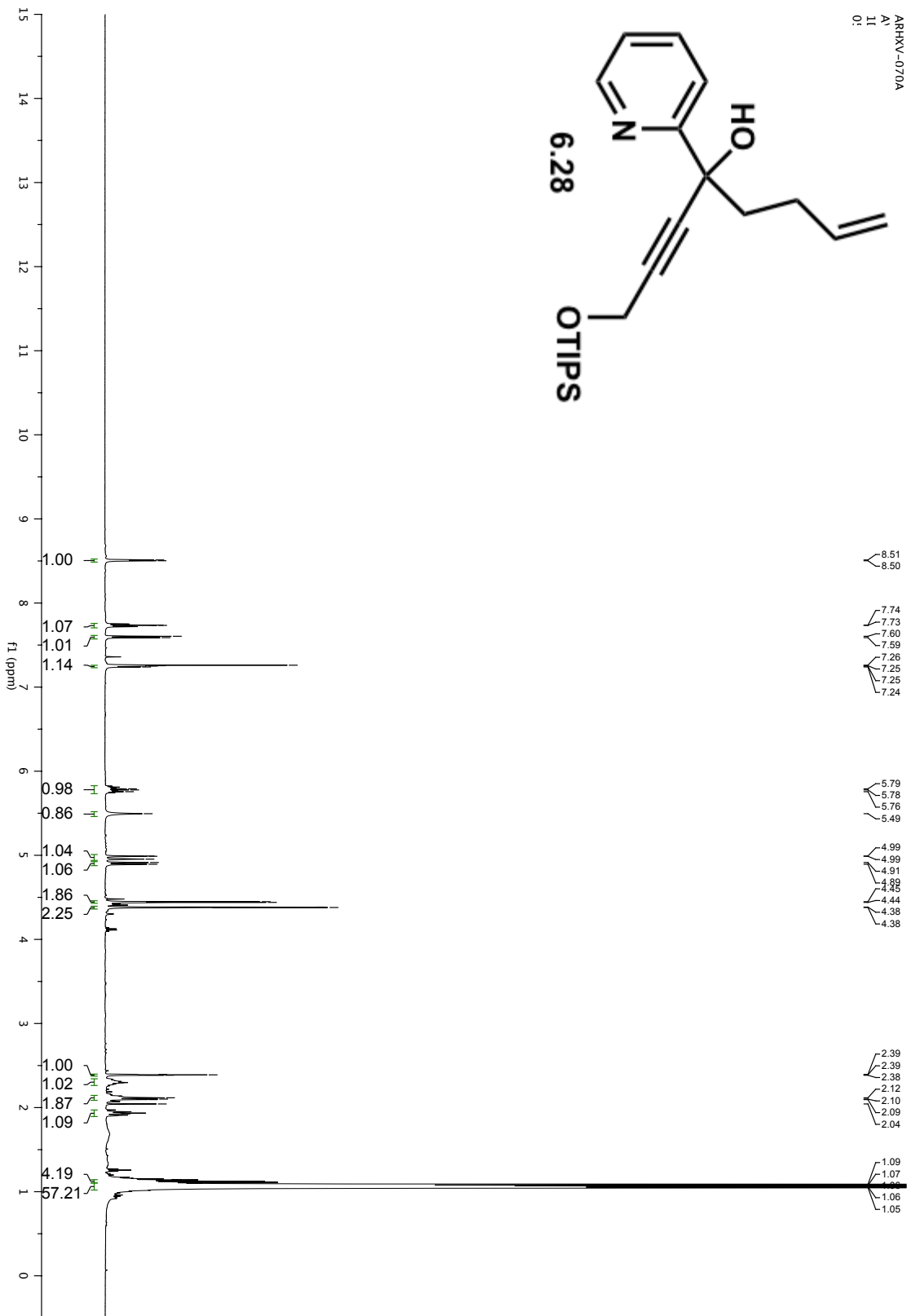
ARRXV-0648  
A'

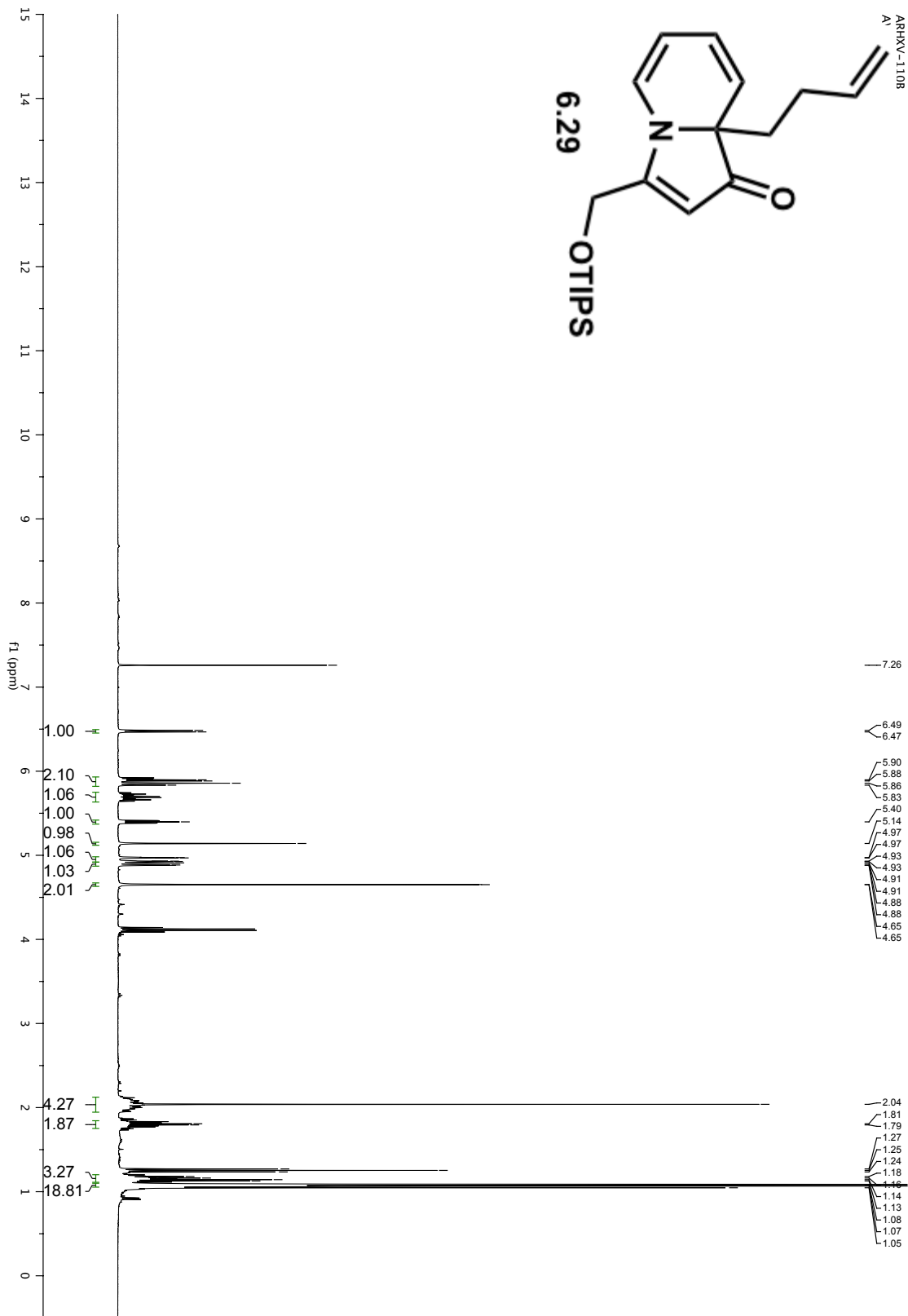


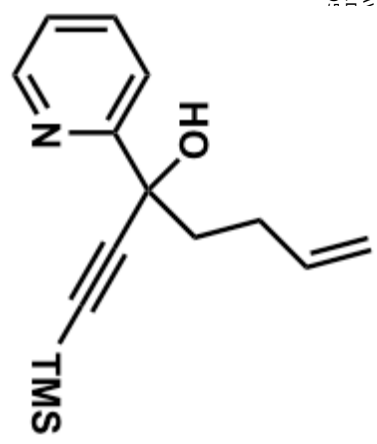


6.26

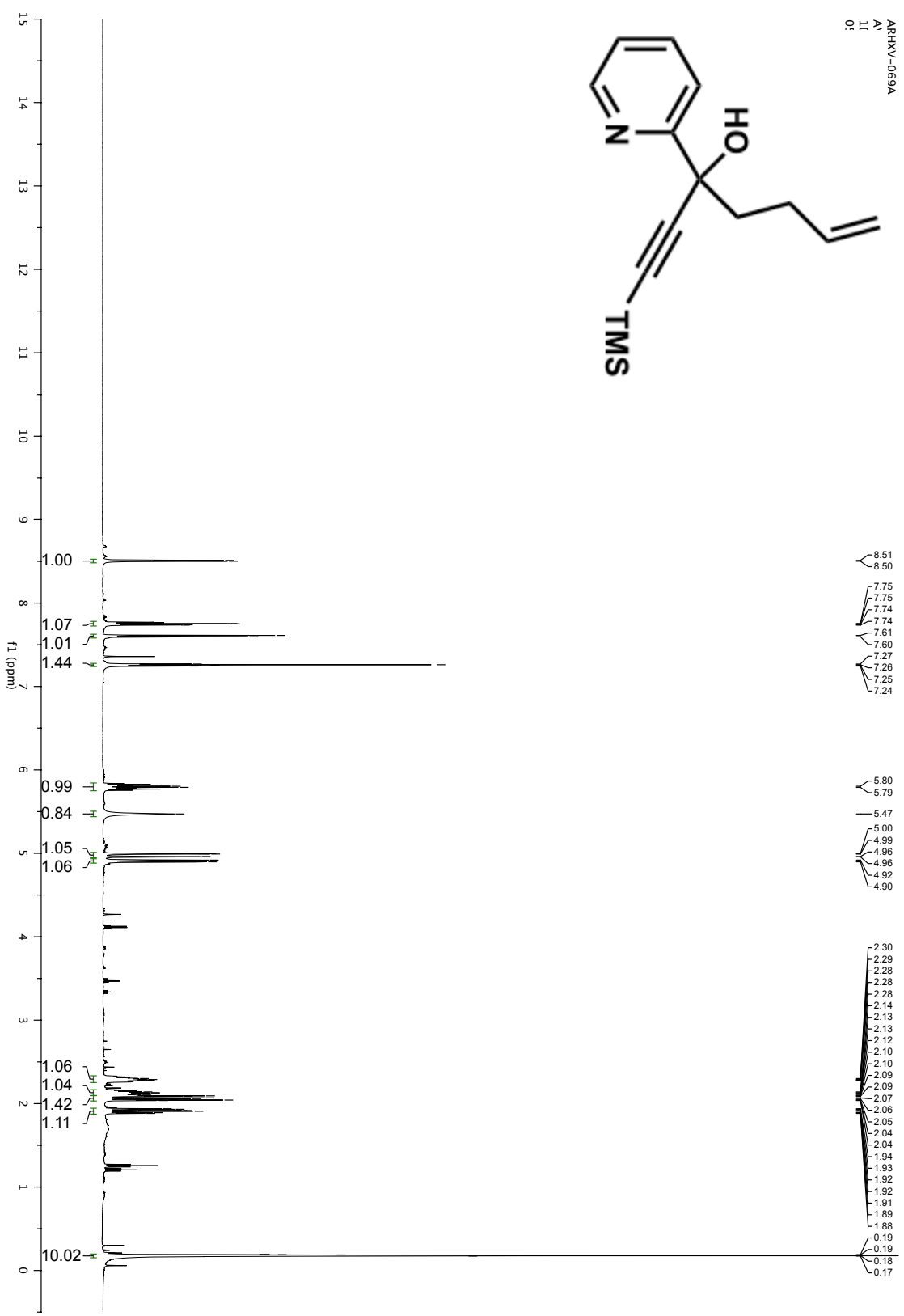


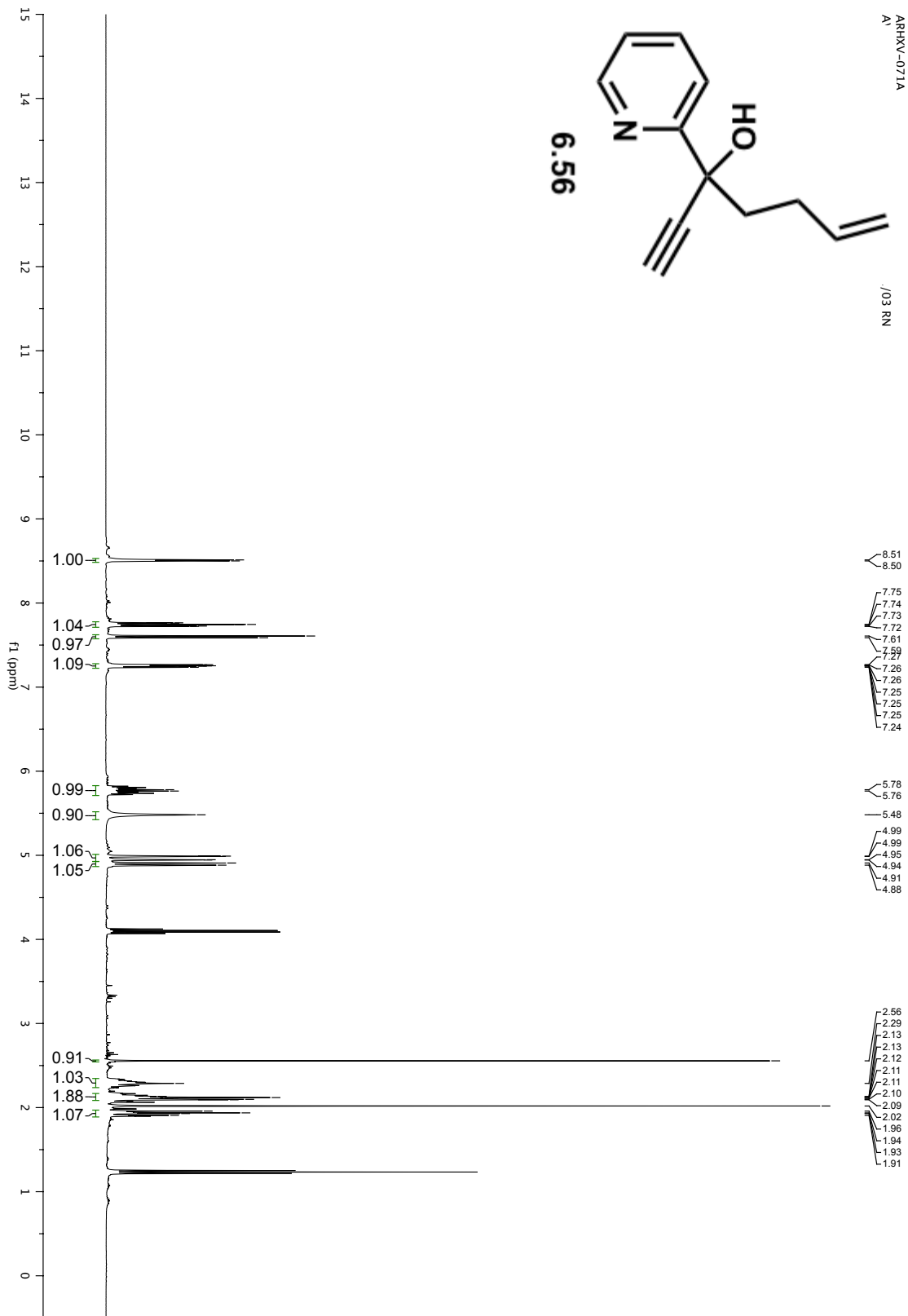
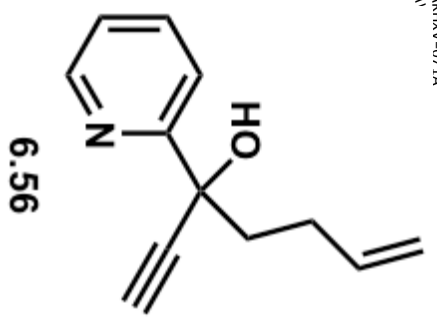






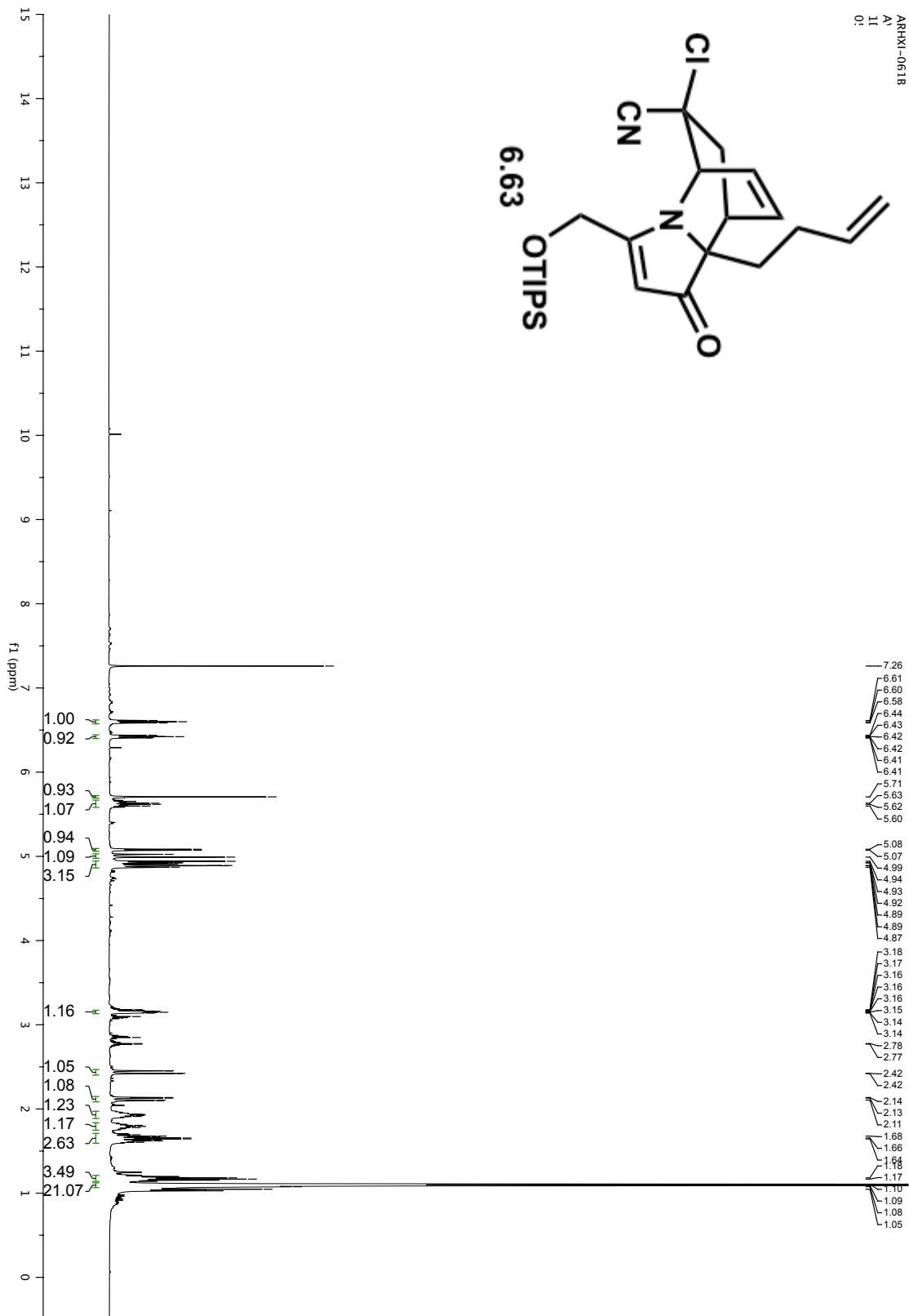
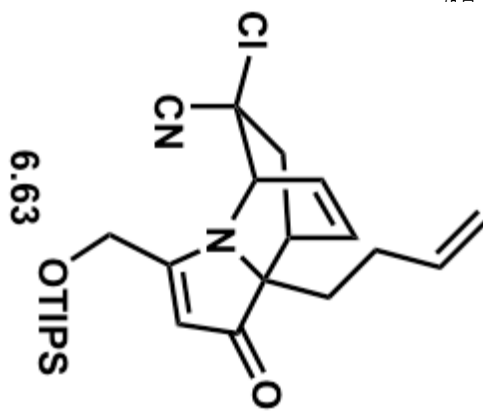
ARRHXV-069A  
A1  
11  
0:

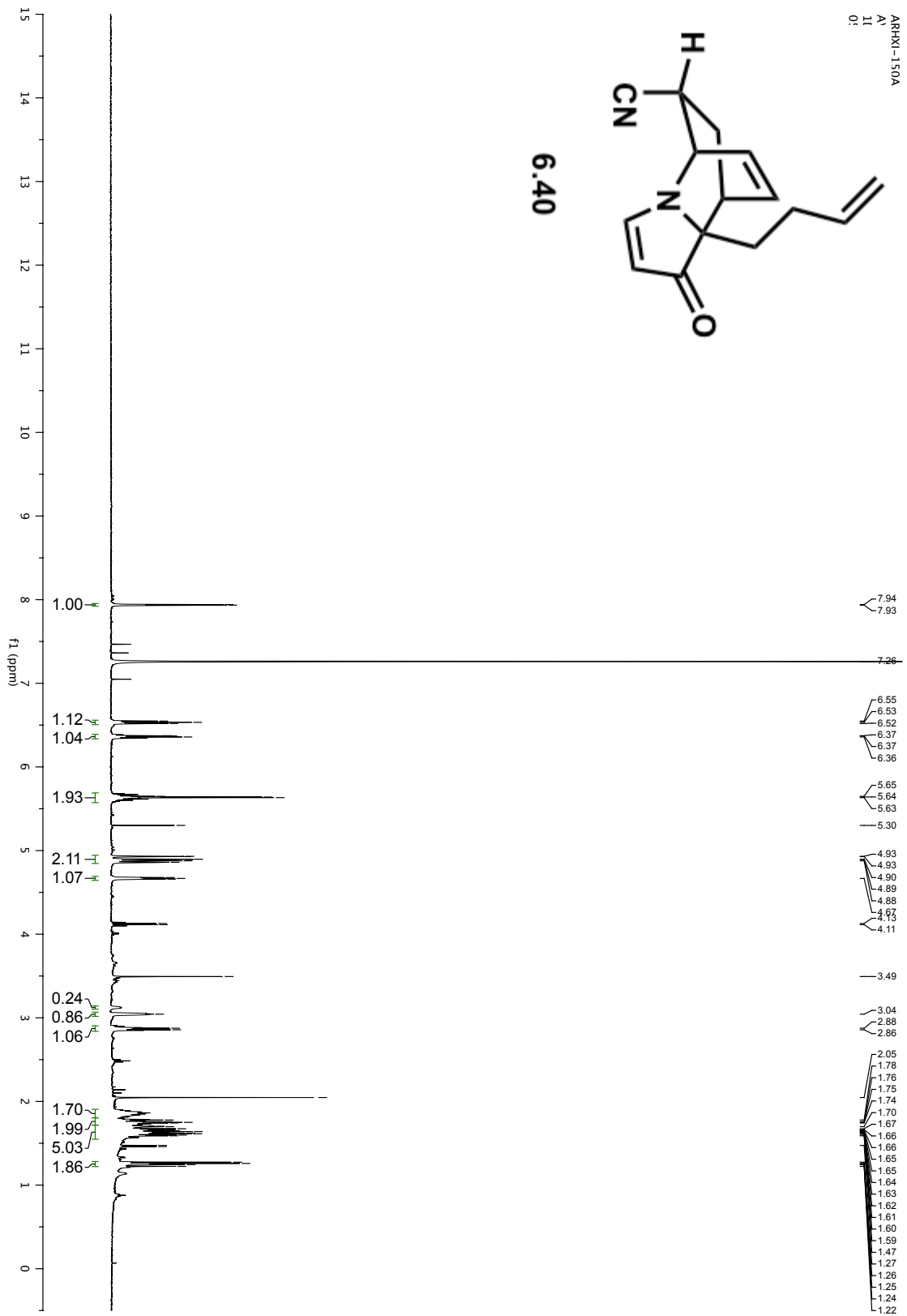




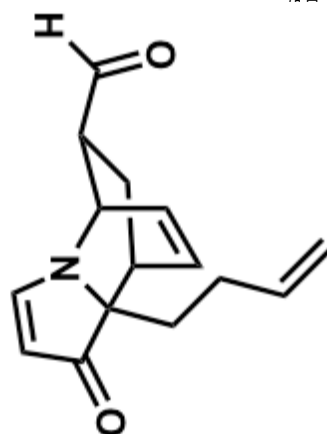


ARRHX-0618  
A:  
1:  
0:

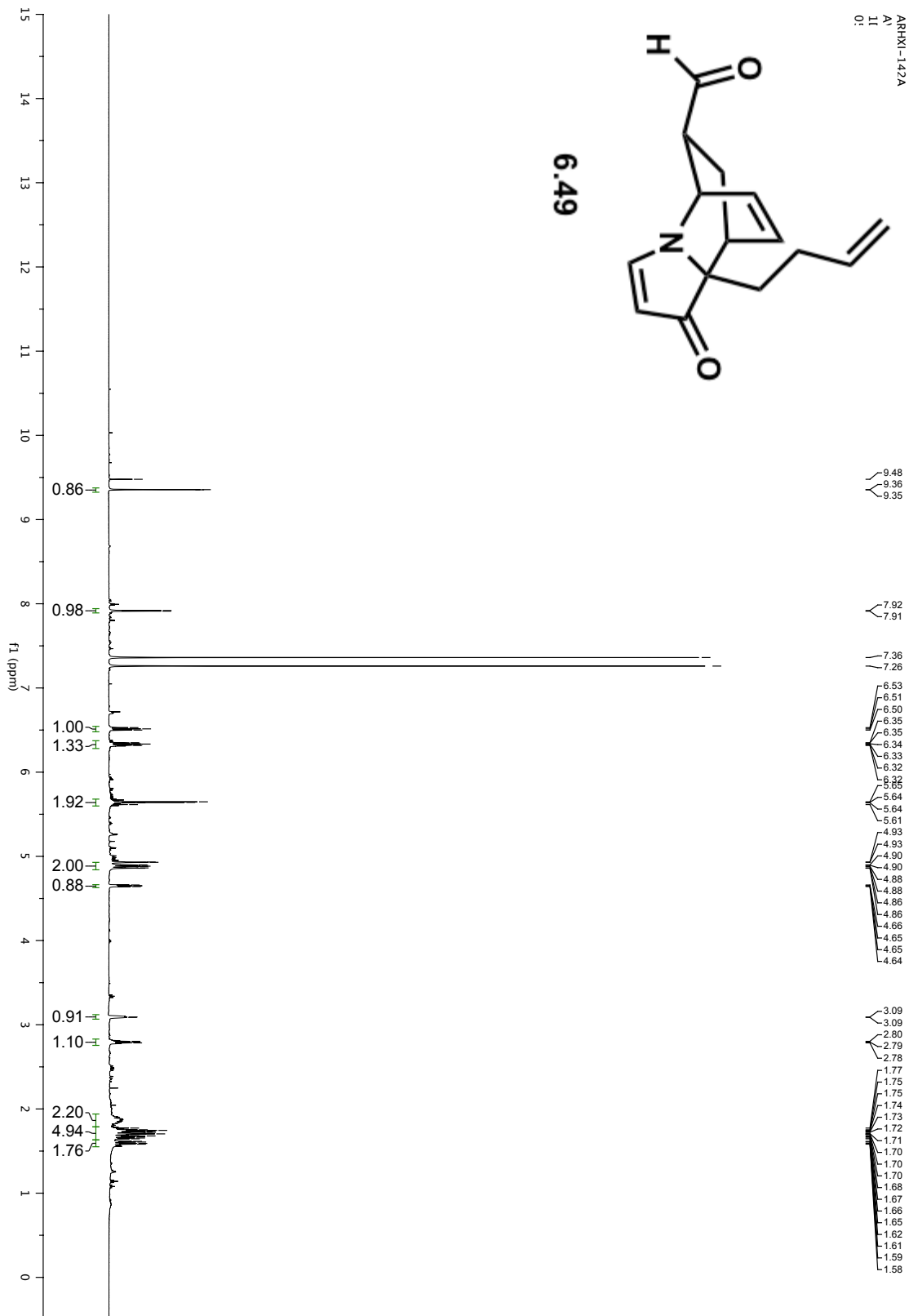


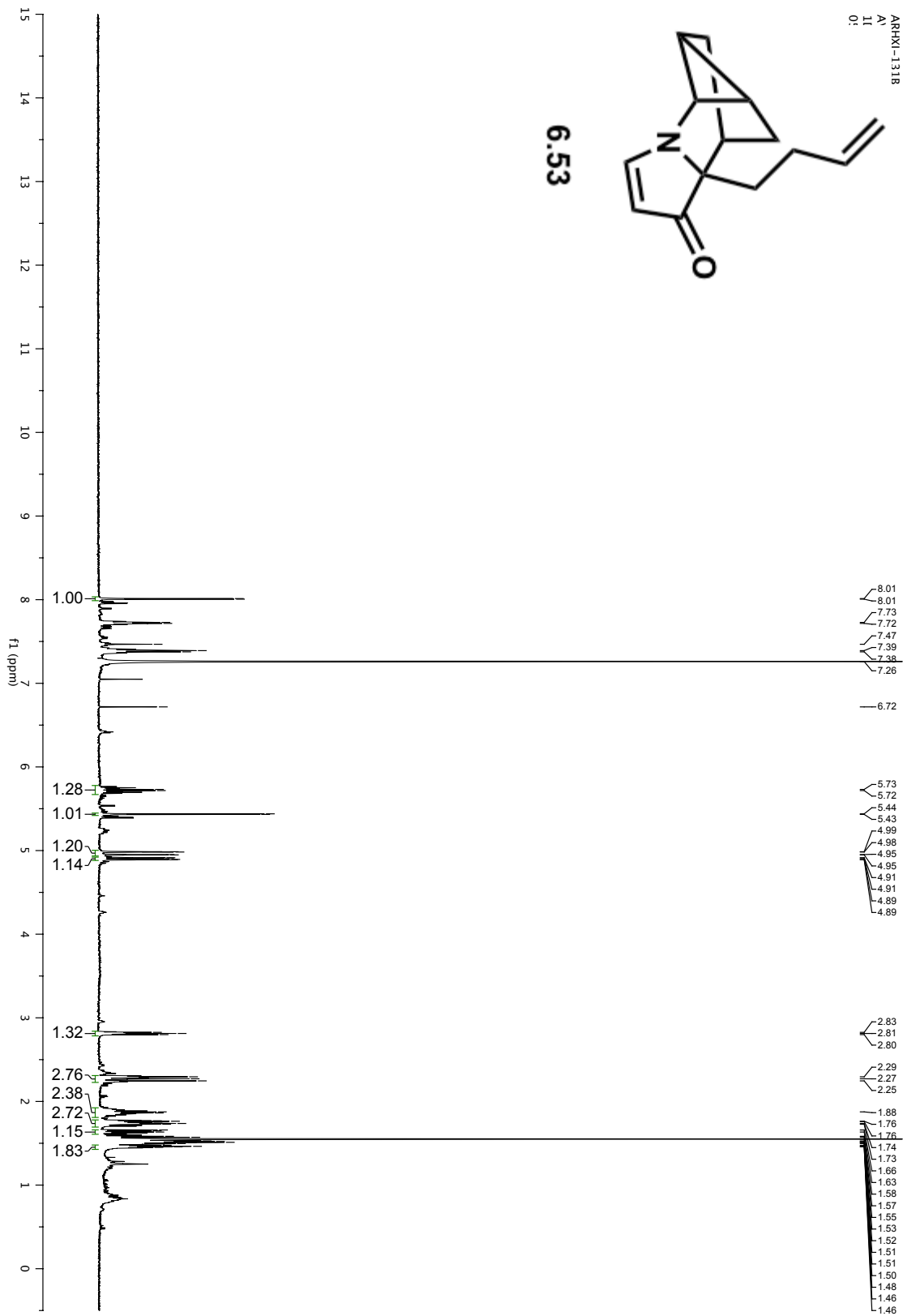


ARRHX-142A  
A:  
11:  
0:

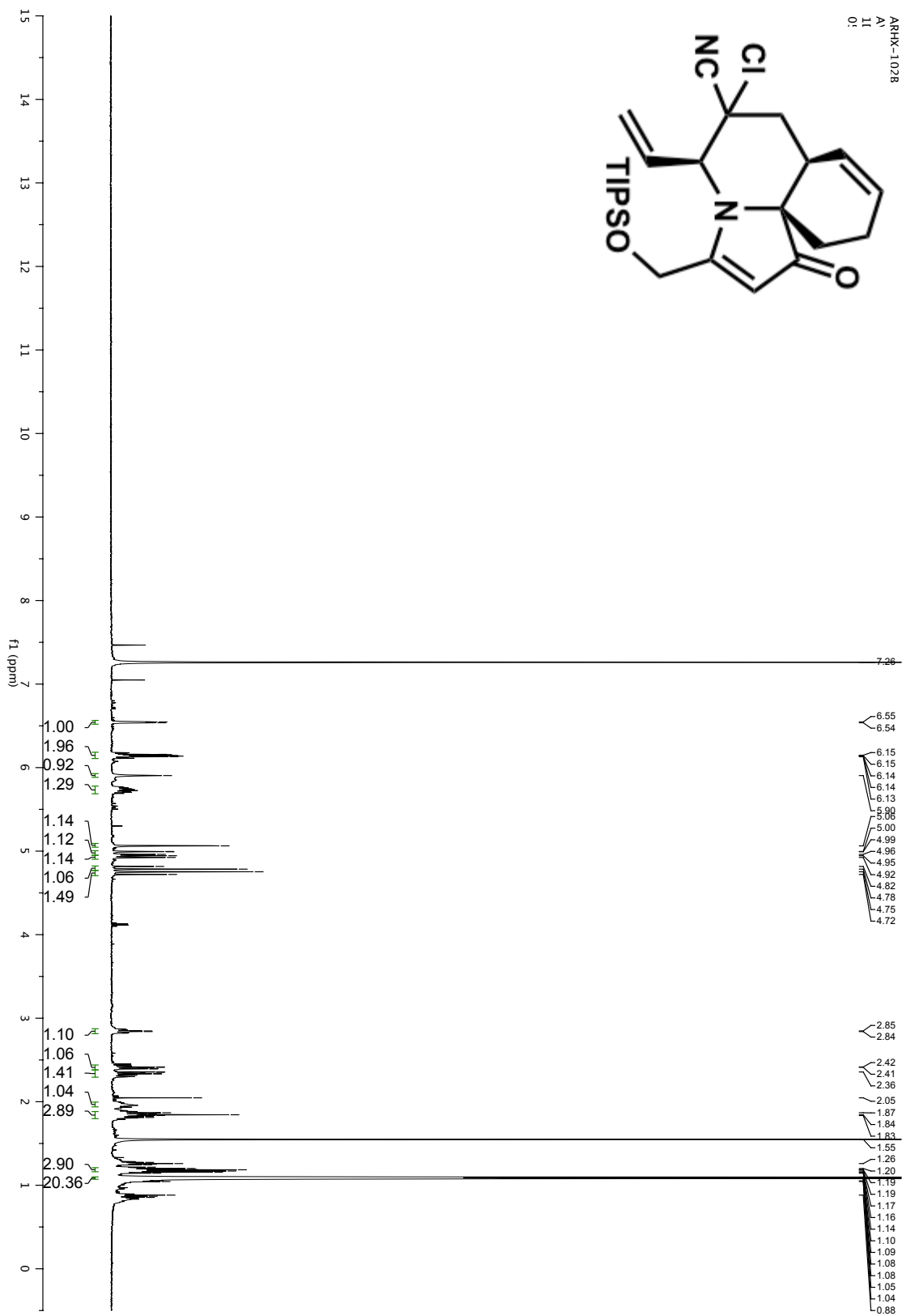
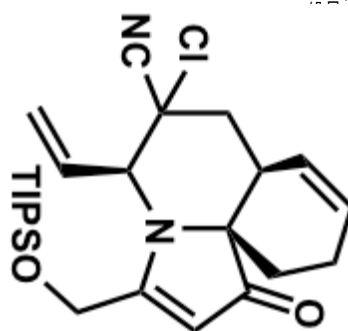


6.49

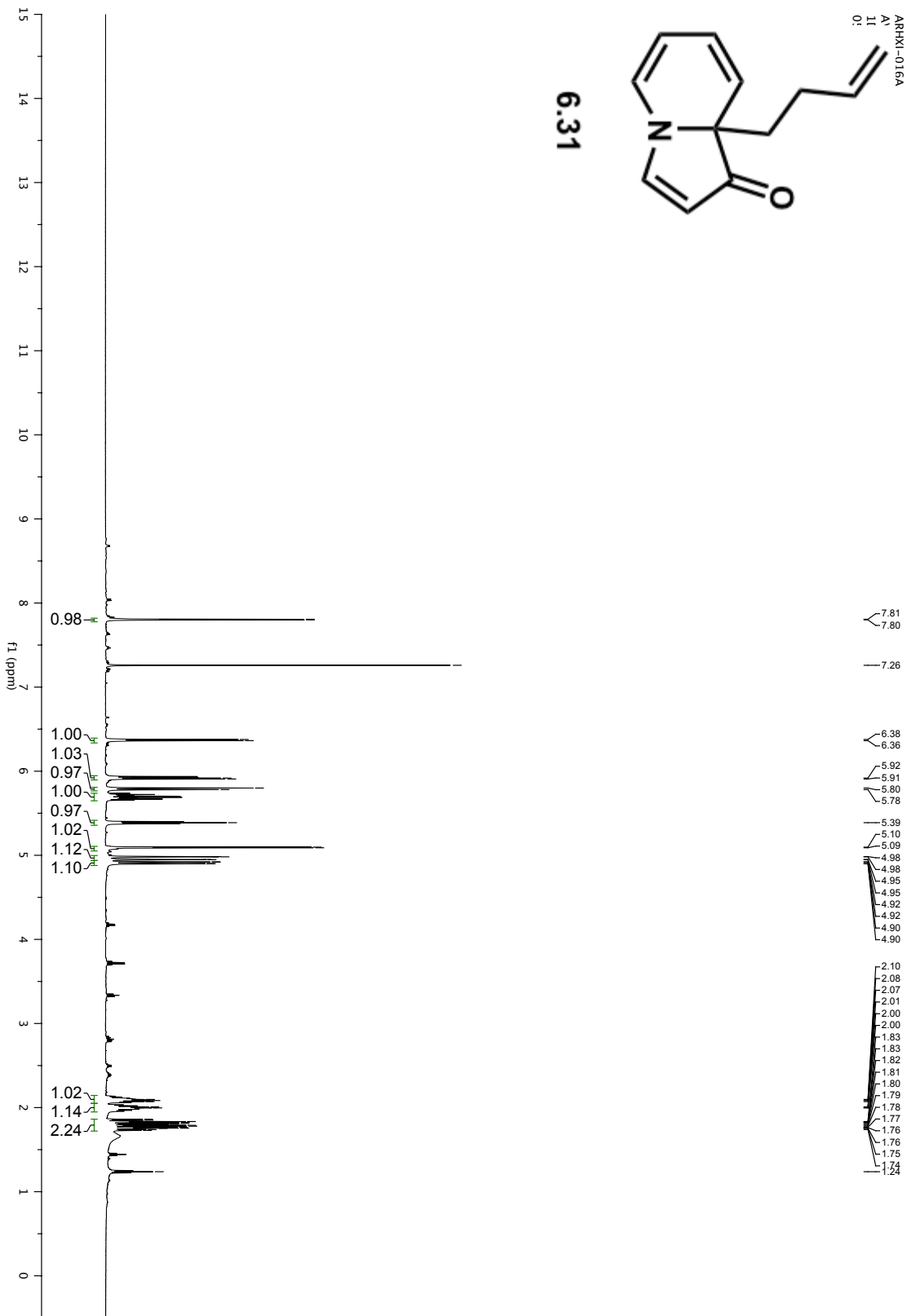
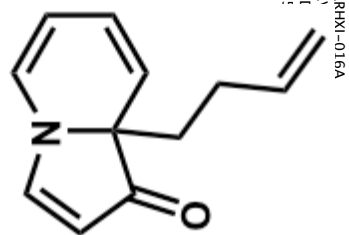




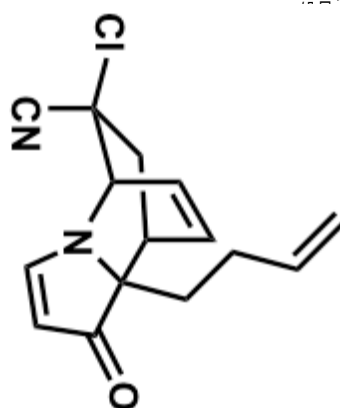
ARRX-1028  
A:  
1:  
0:



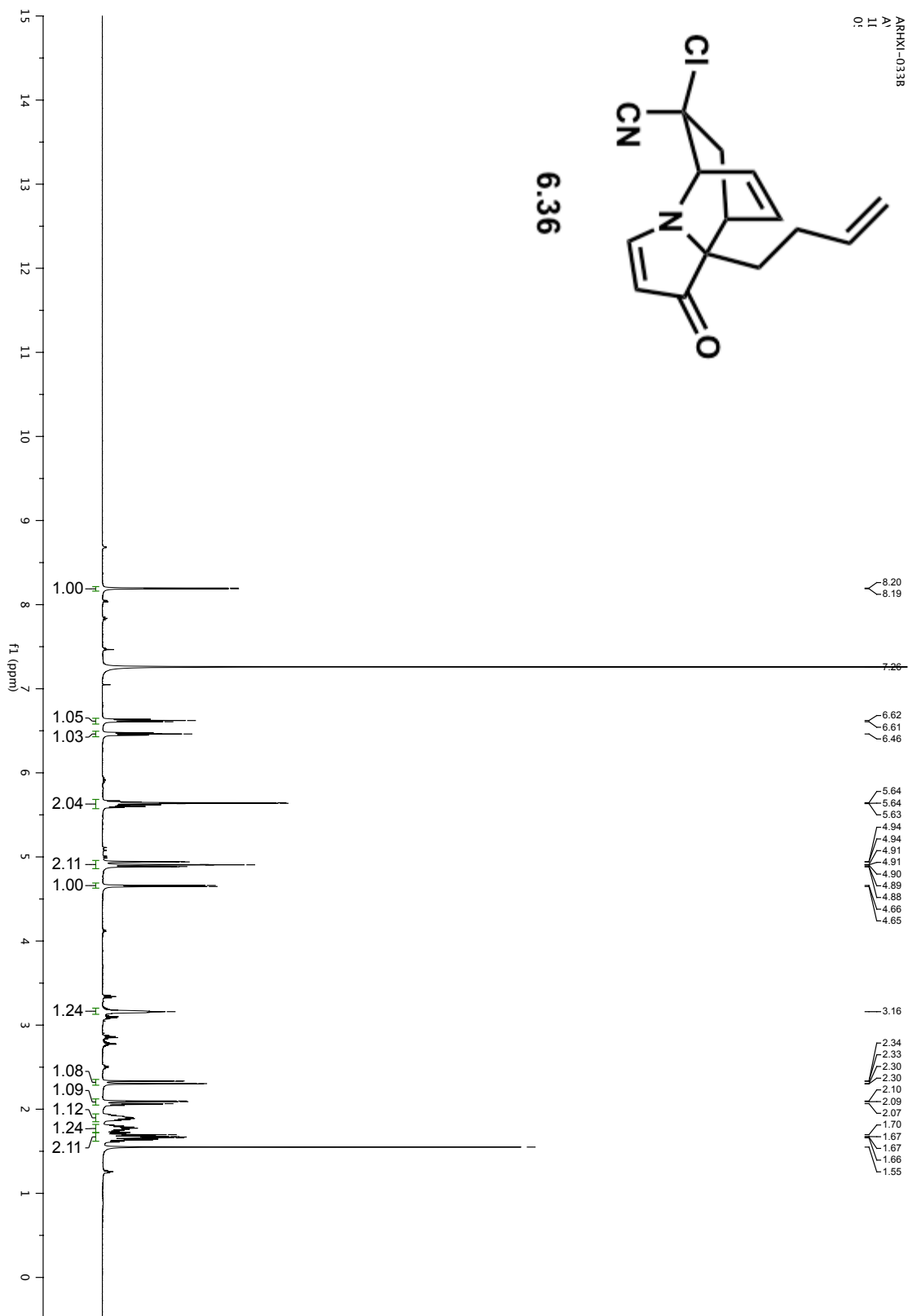
6.31



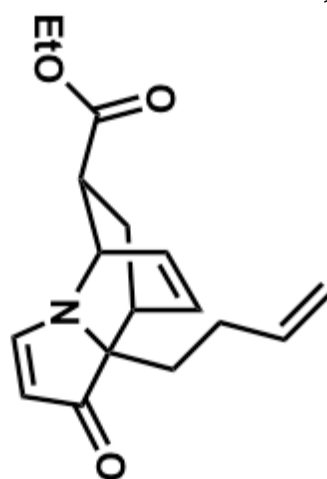
ARHX1-0338  
A:  
11  
0:



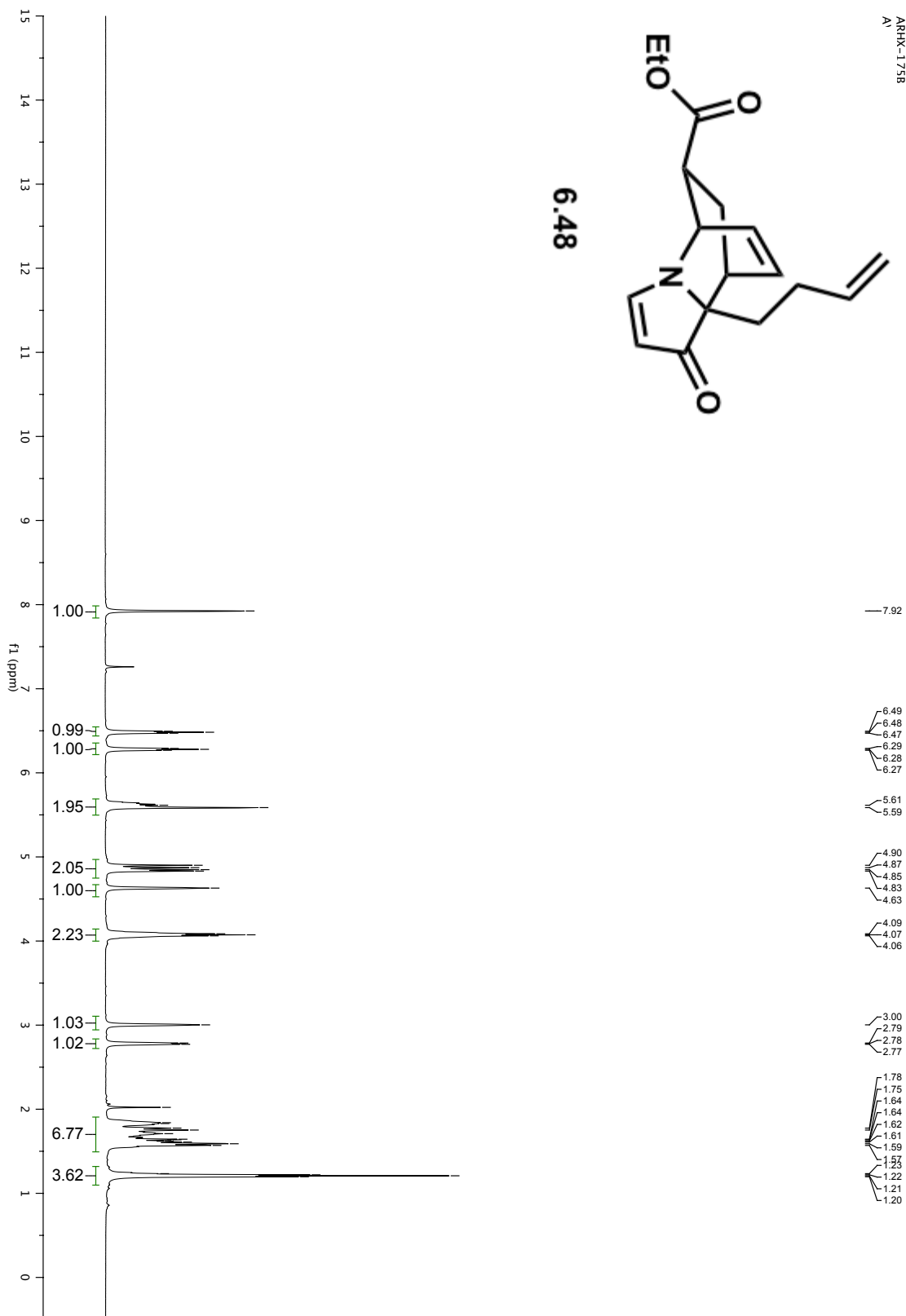
6.36



ARRX-1758  
A'

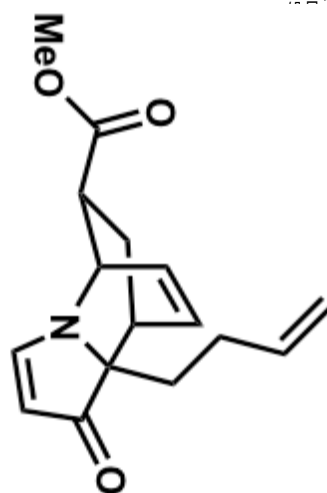


6.48

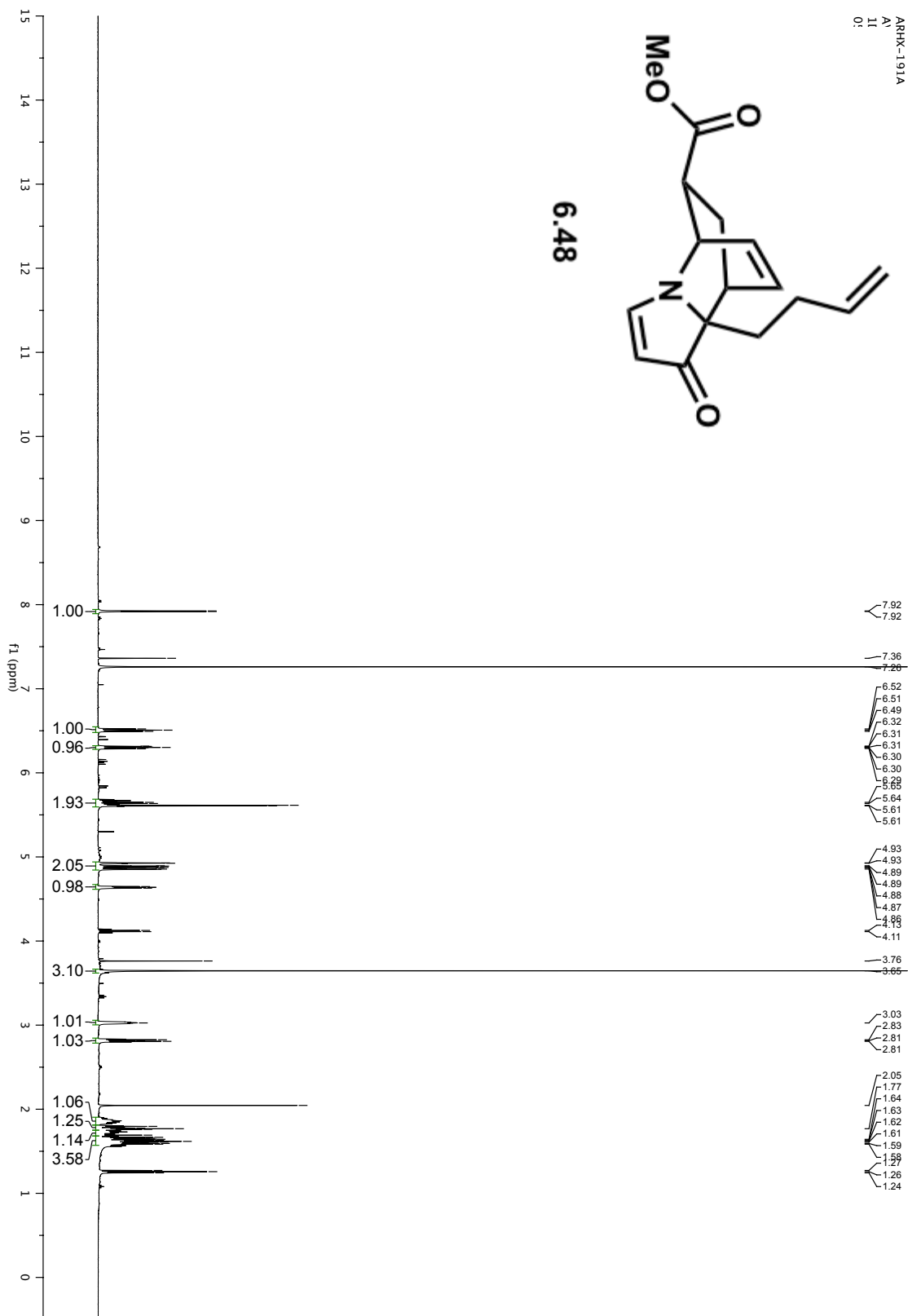




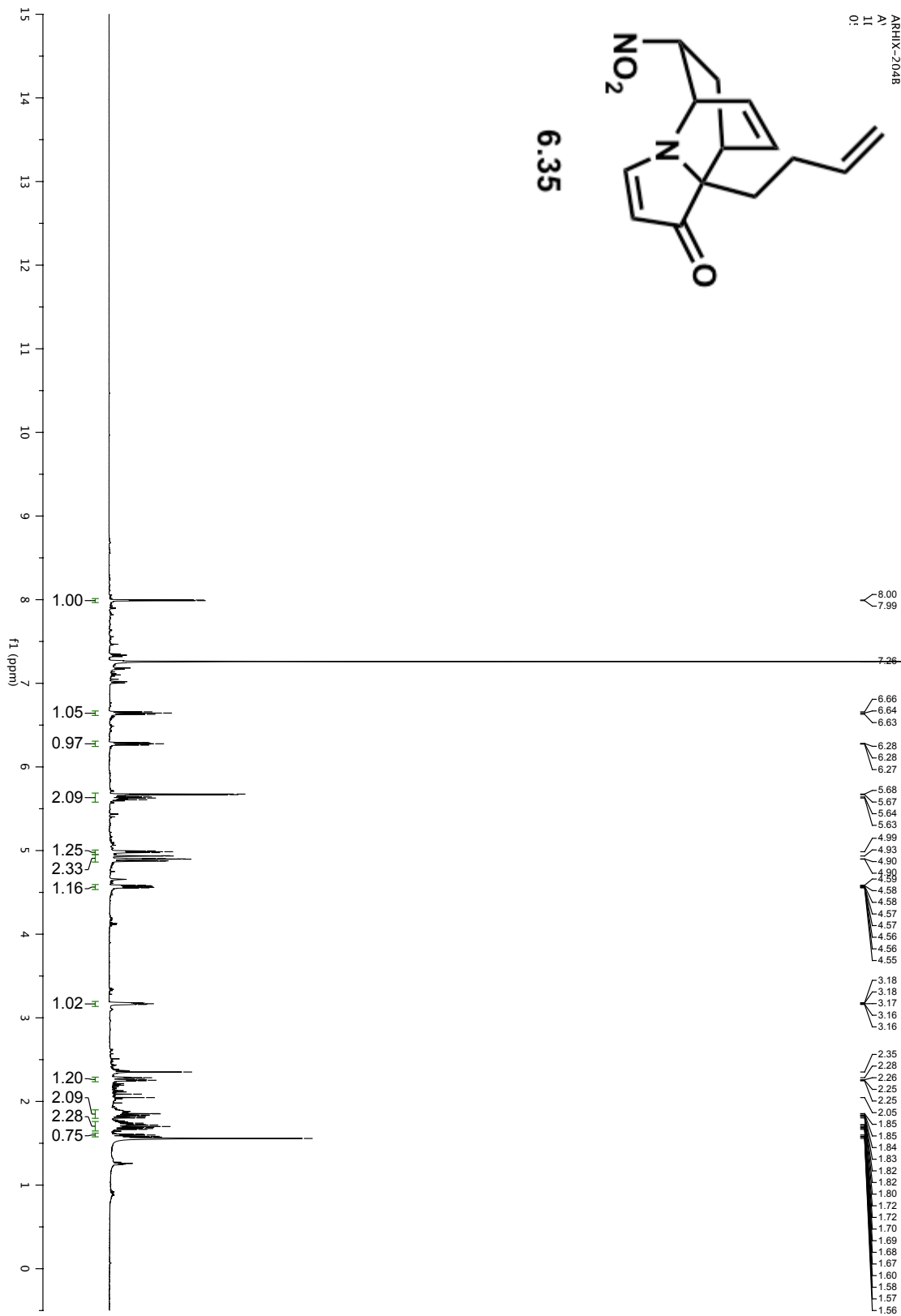
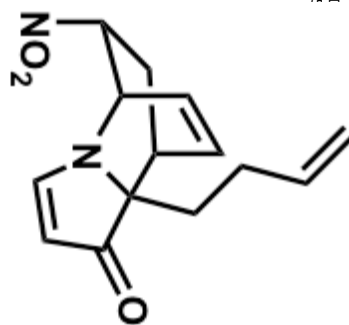
ARRX-191A  
A:  
11  
0:

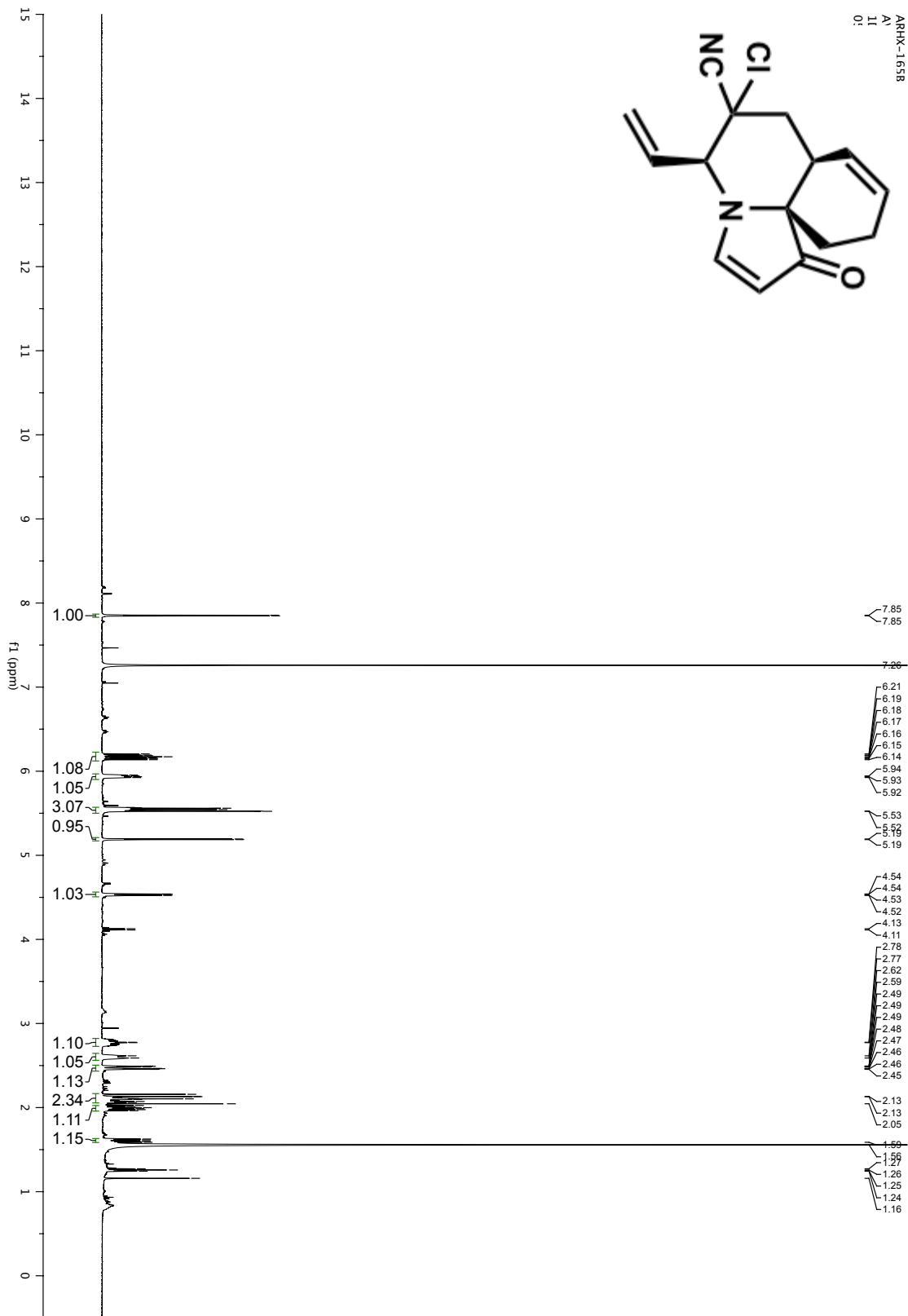


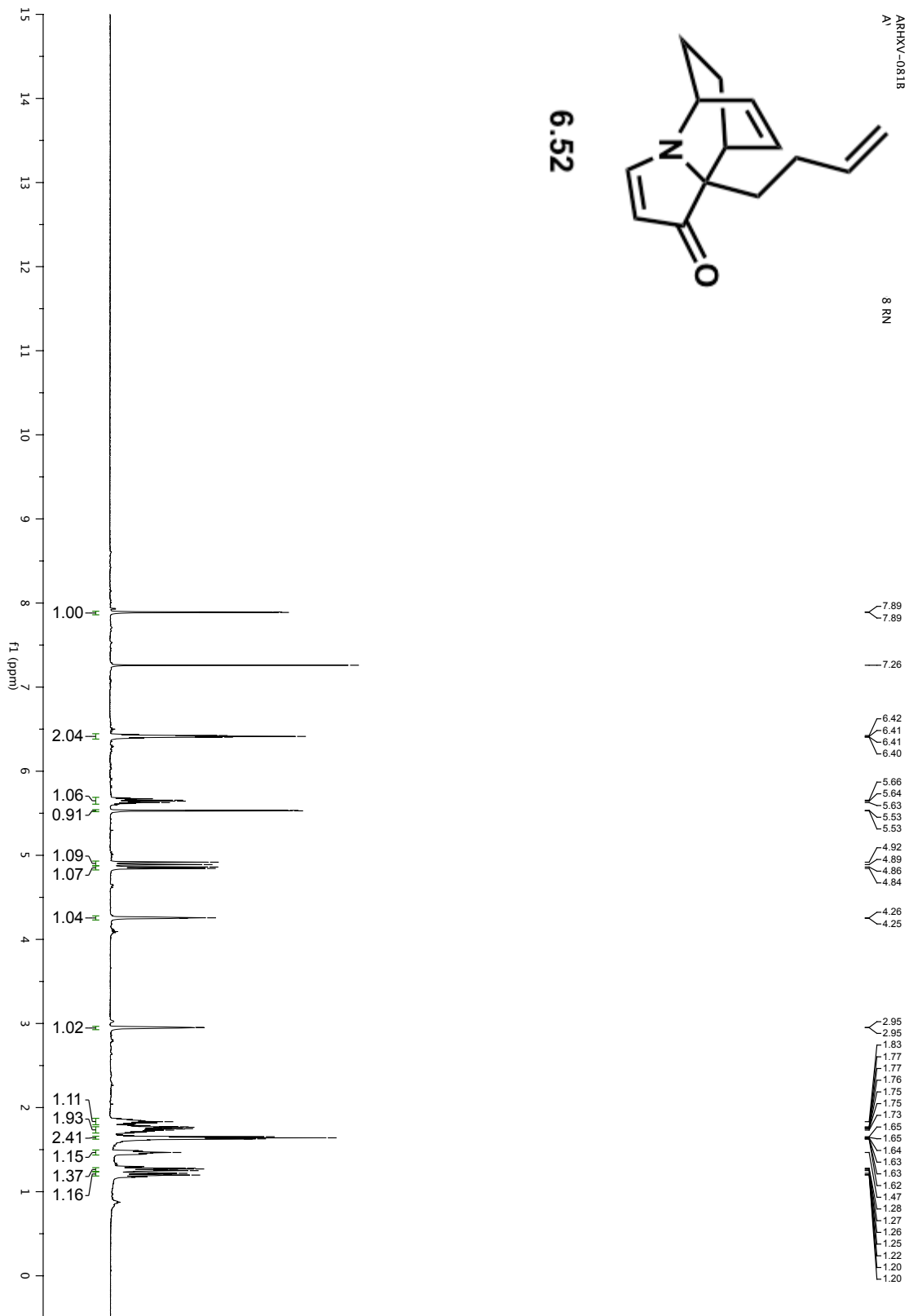
6.48

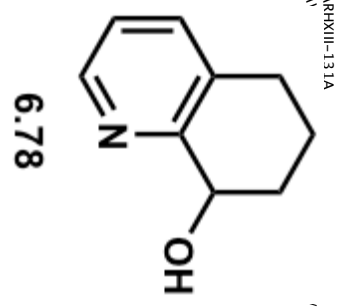


ARRHX-2048  
A:  
11:  
0:

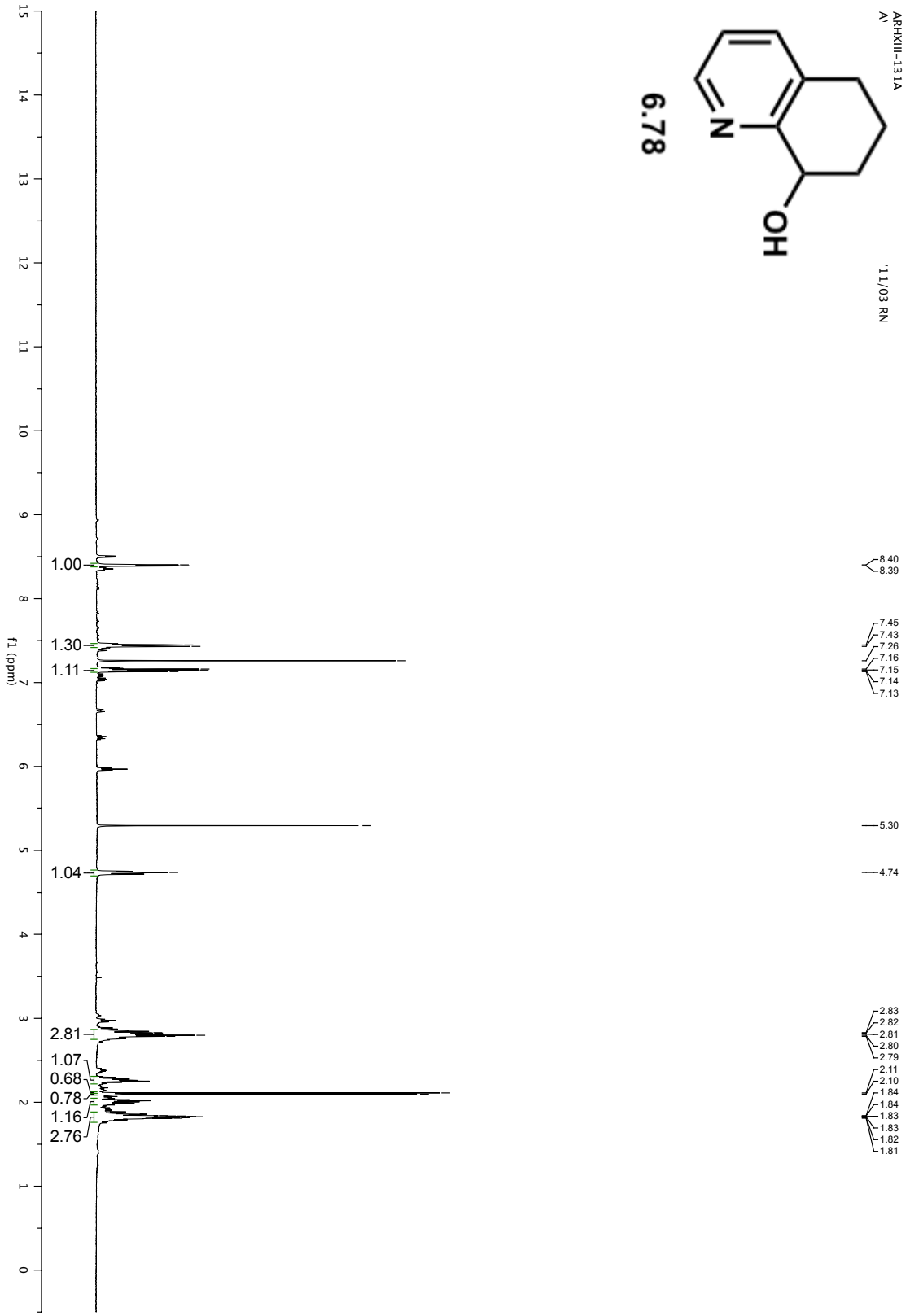


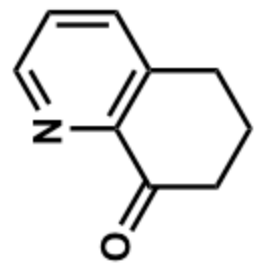




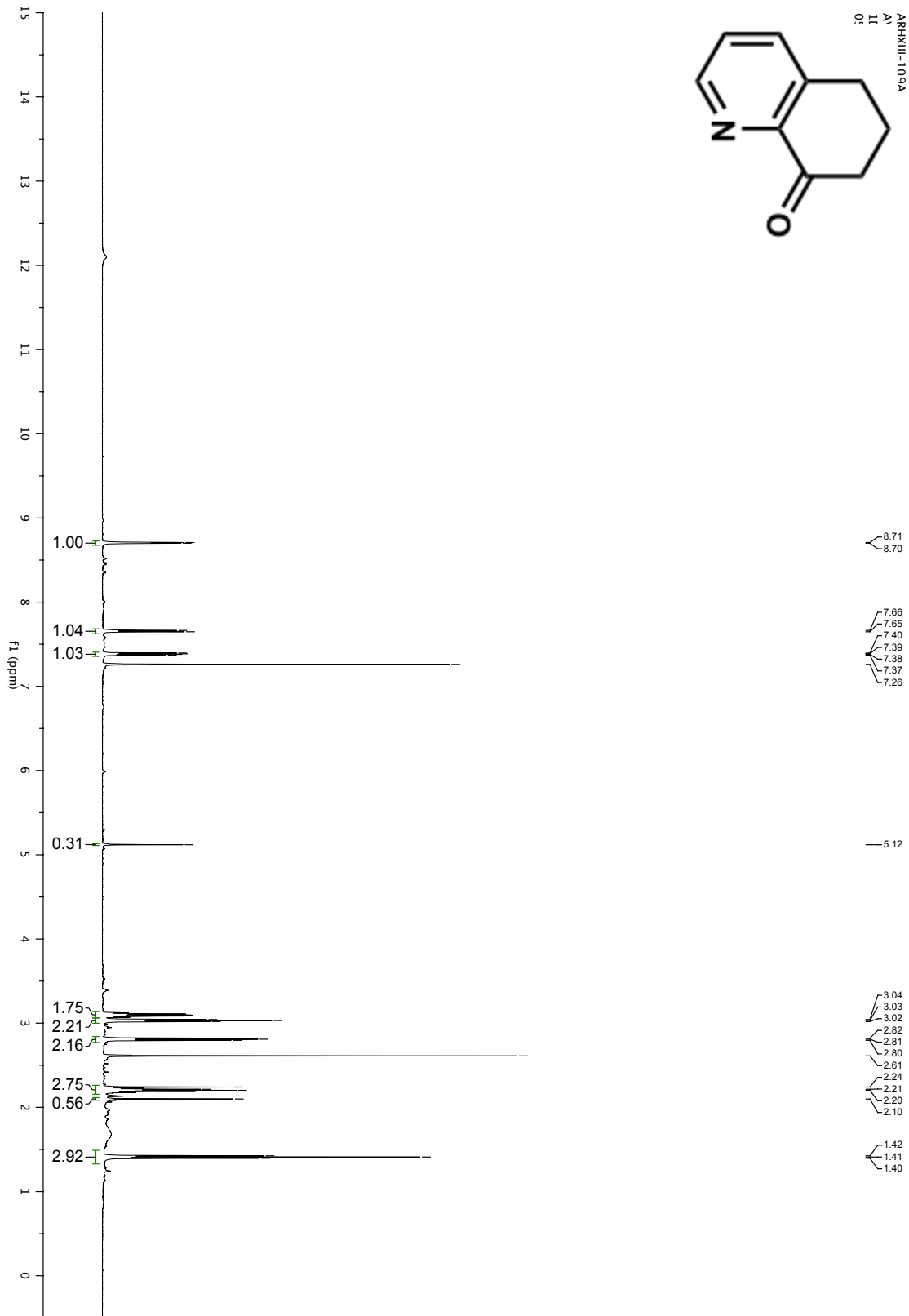


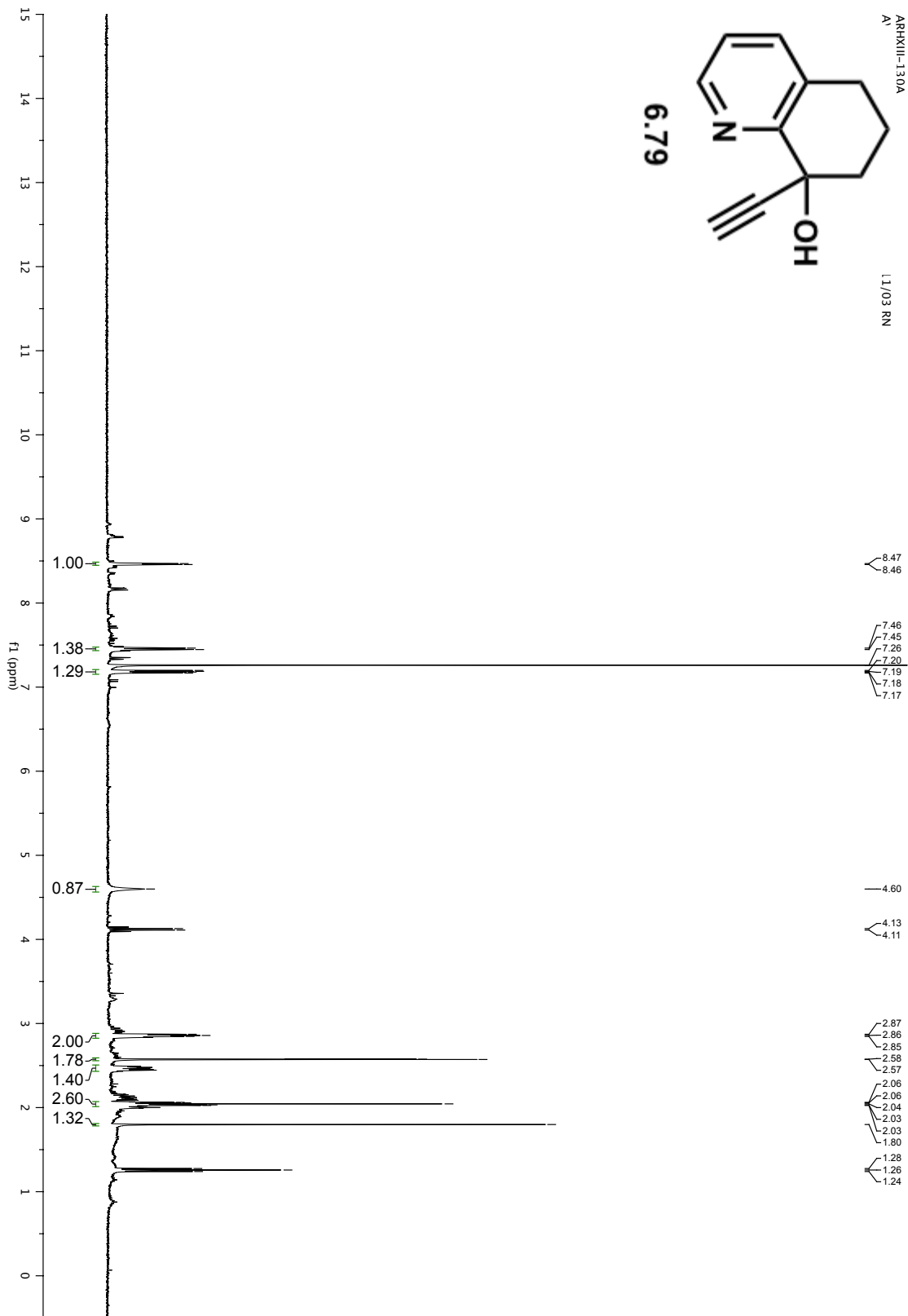
11/03 RN

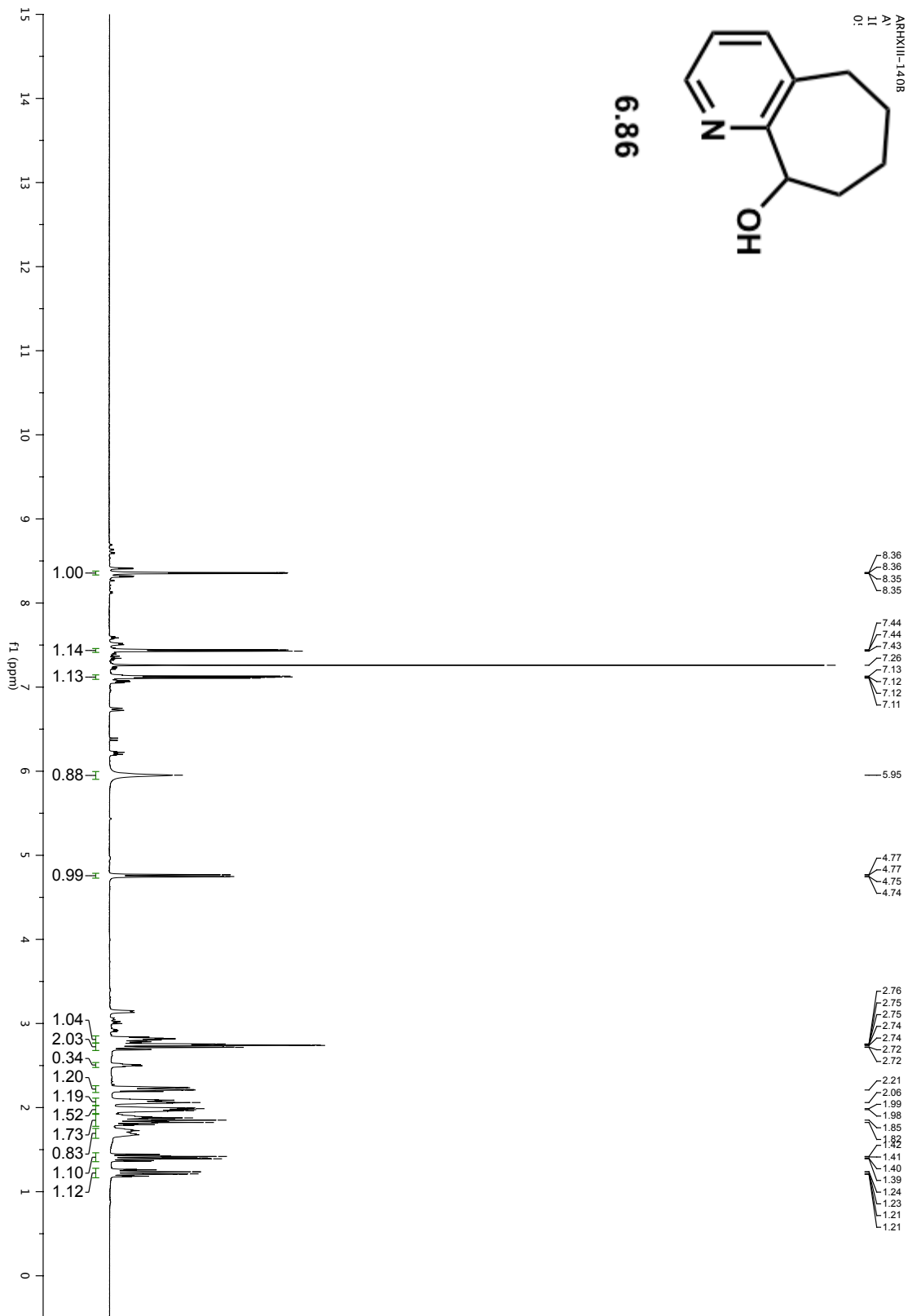




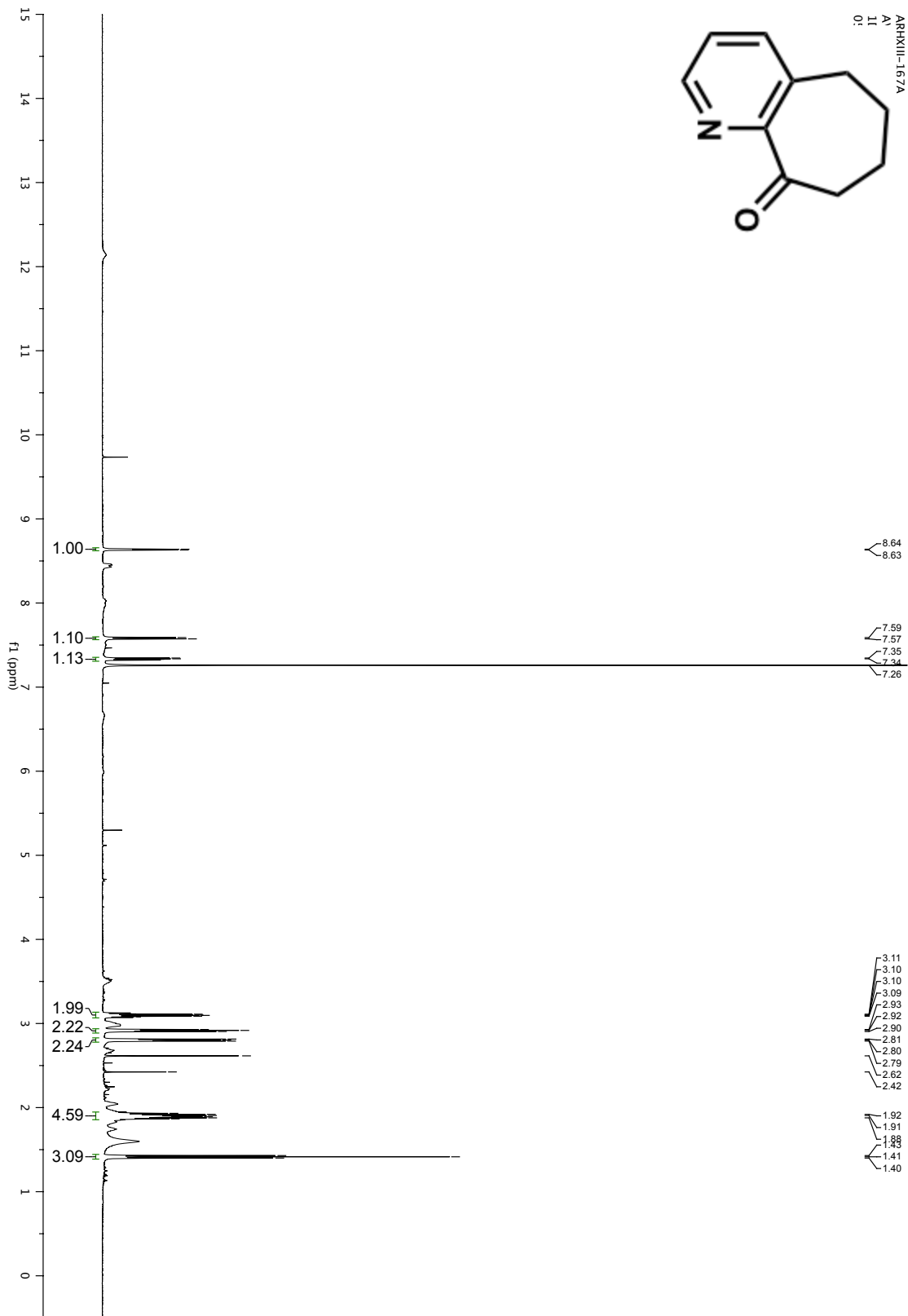
ARRHXIII-109A  
A:  
11  
0:

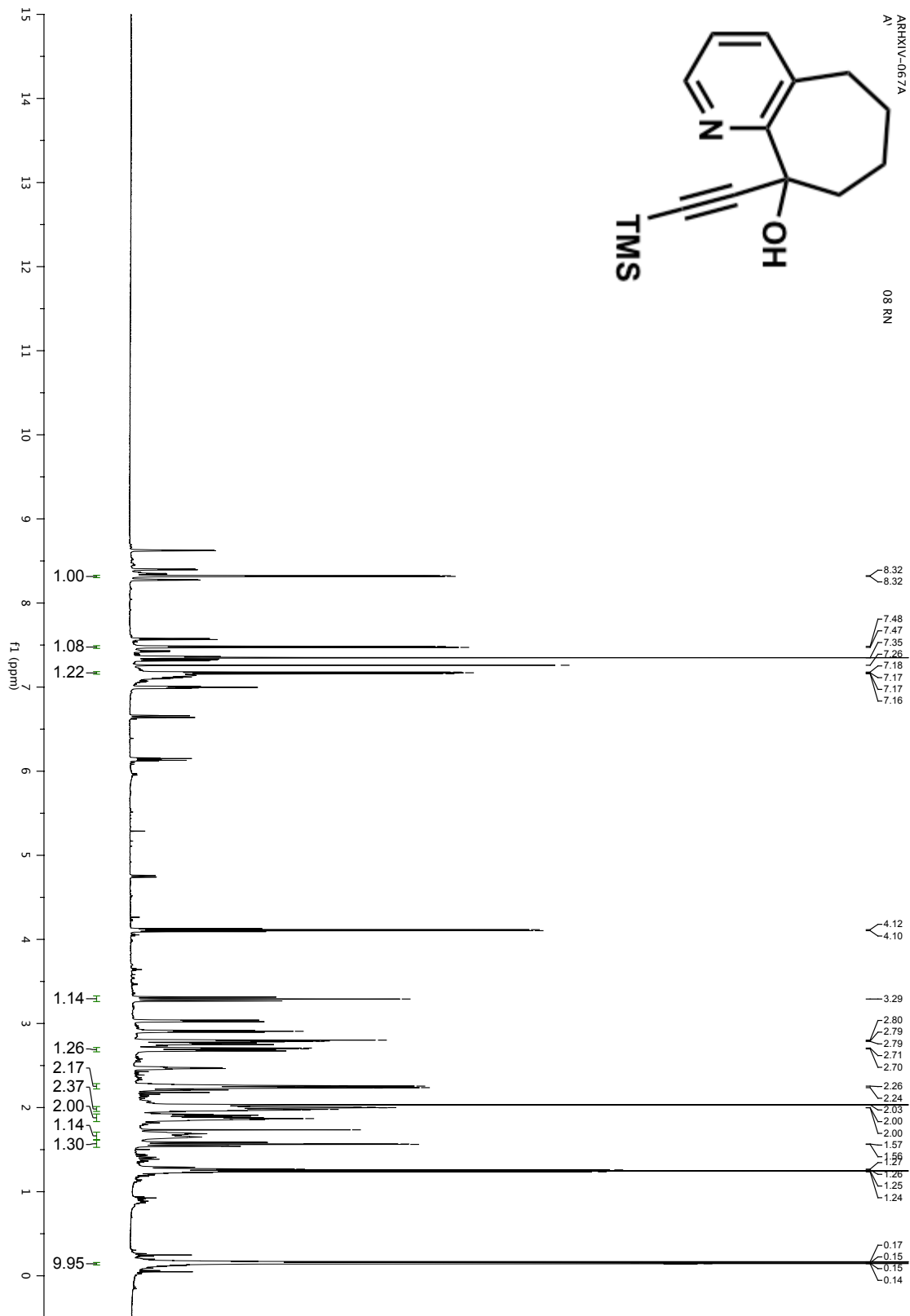


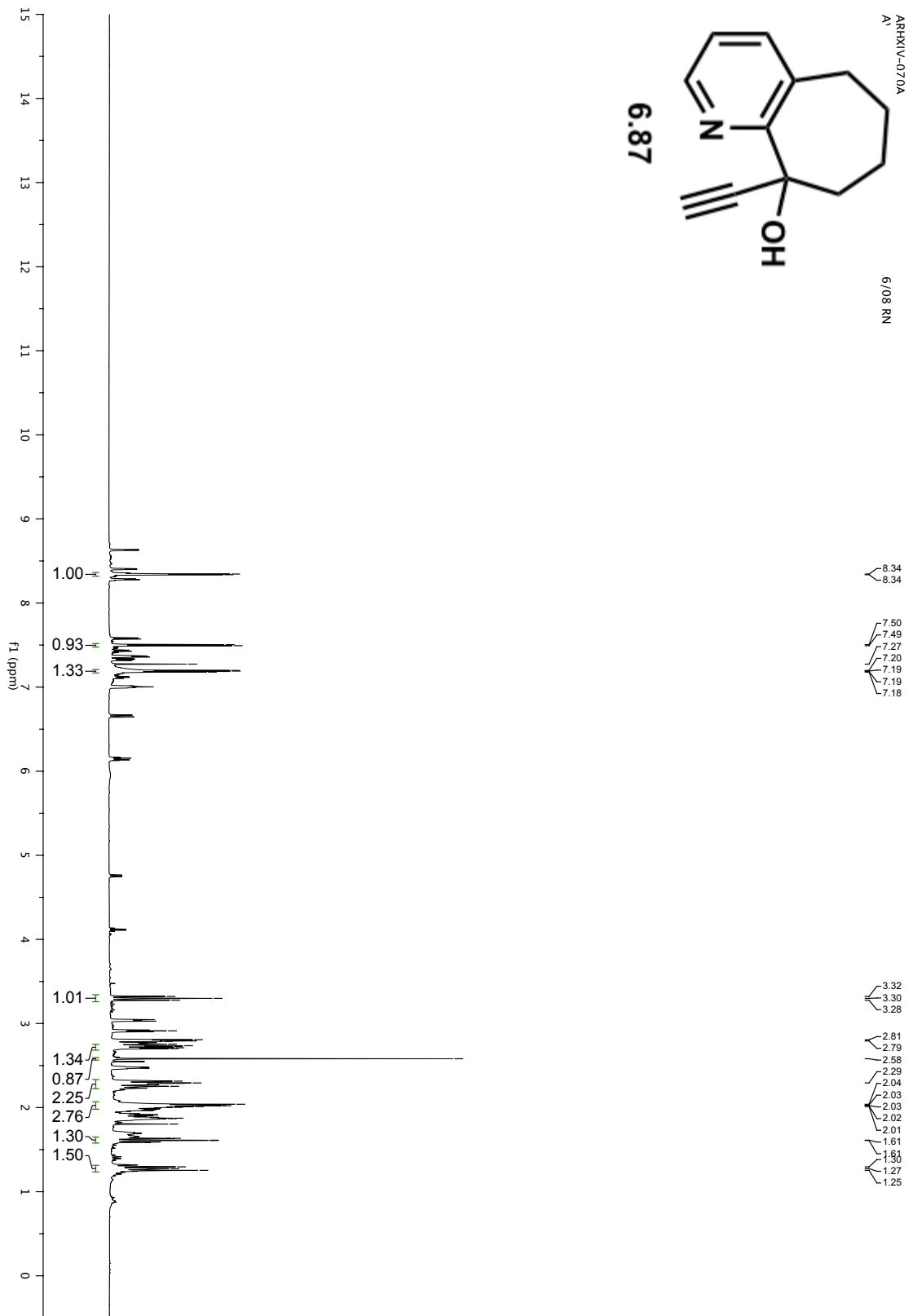
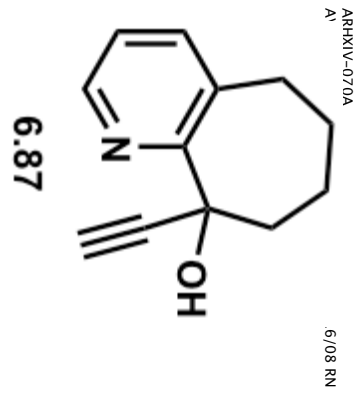


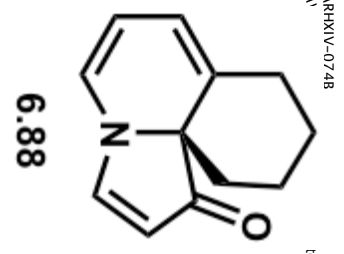




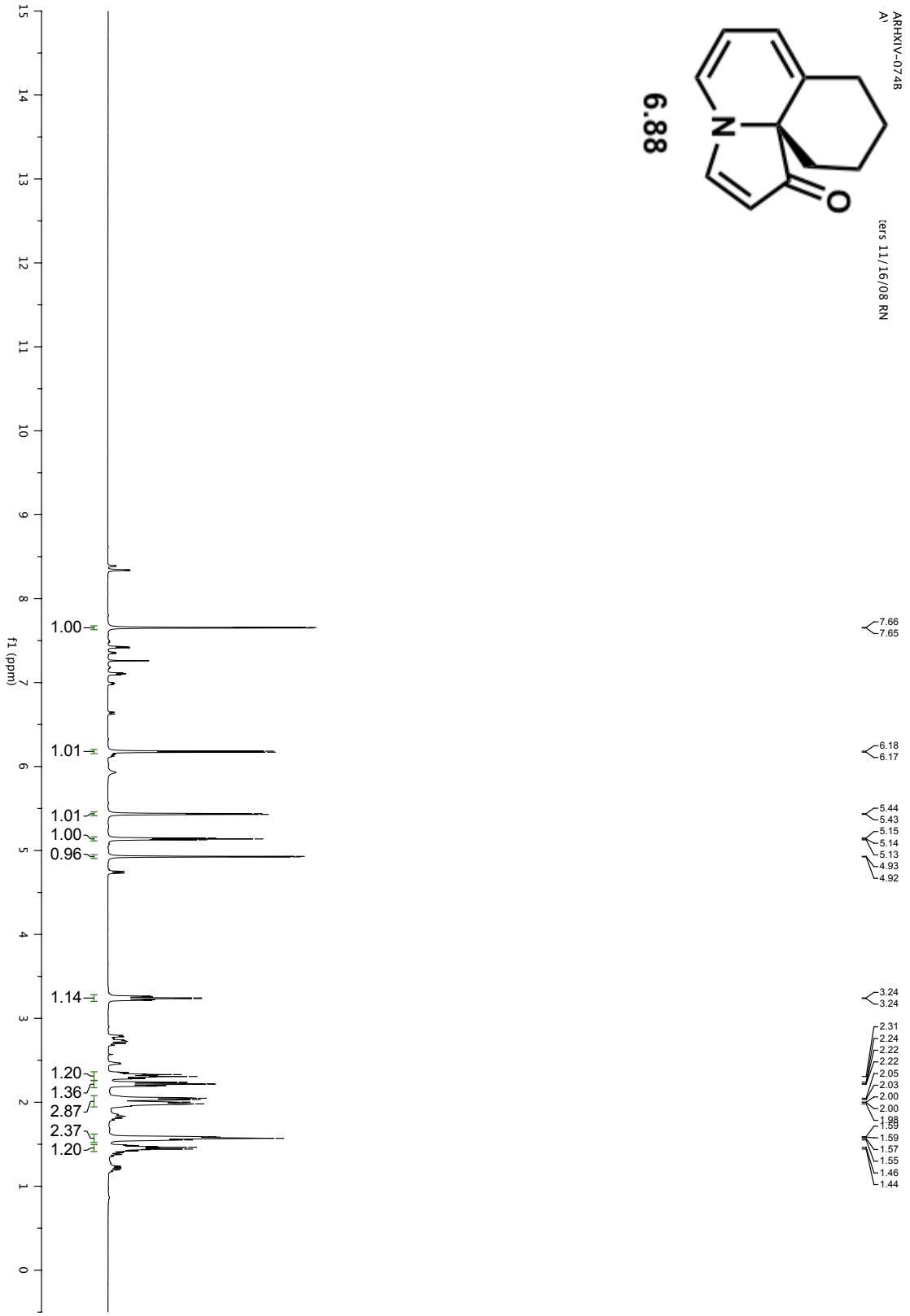


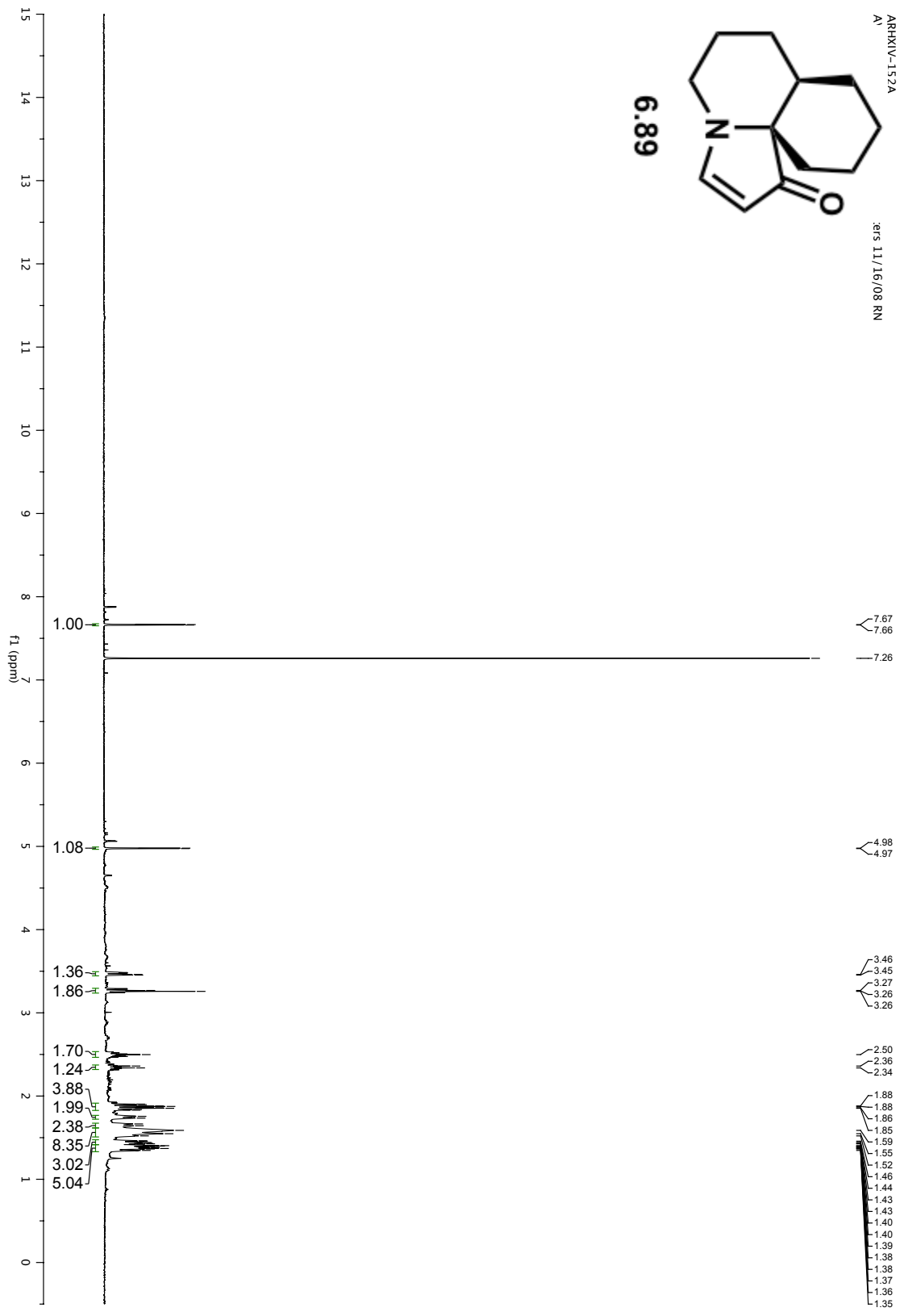
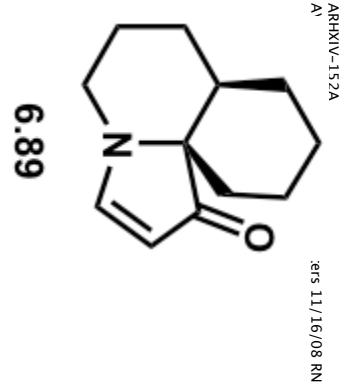


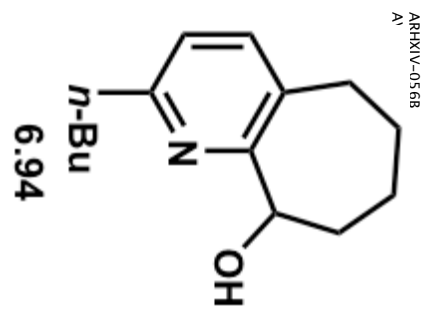




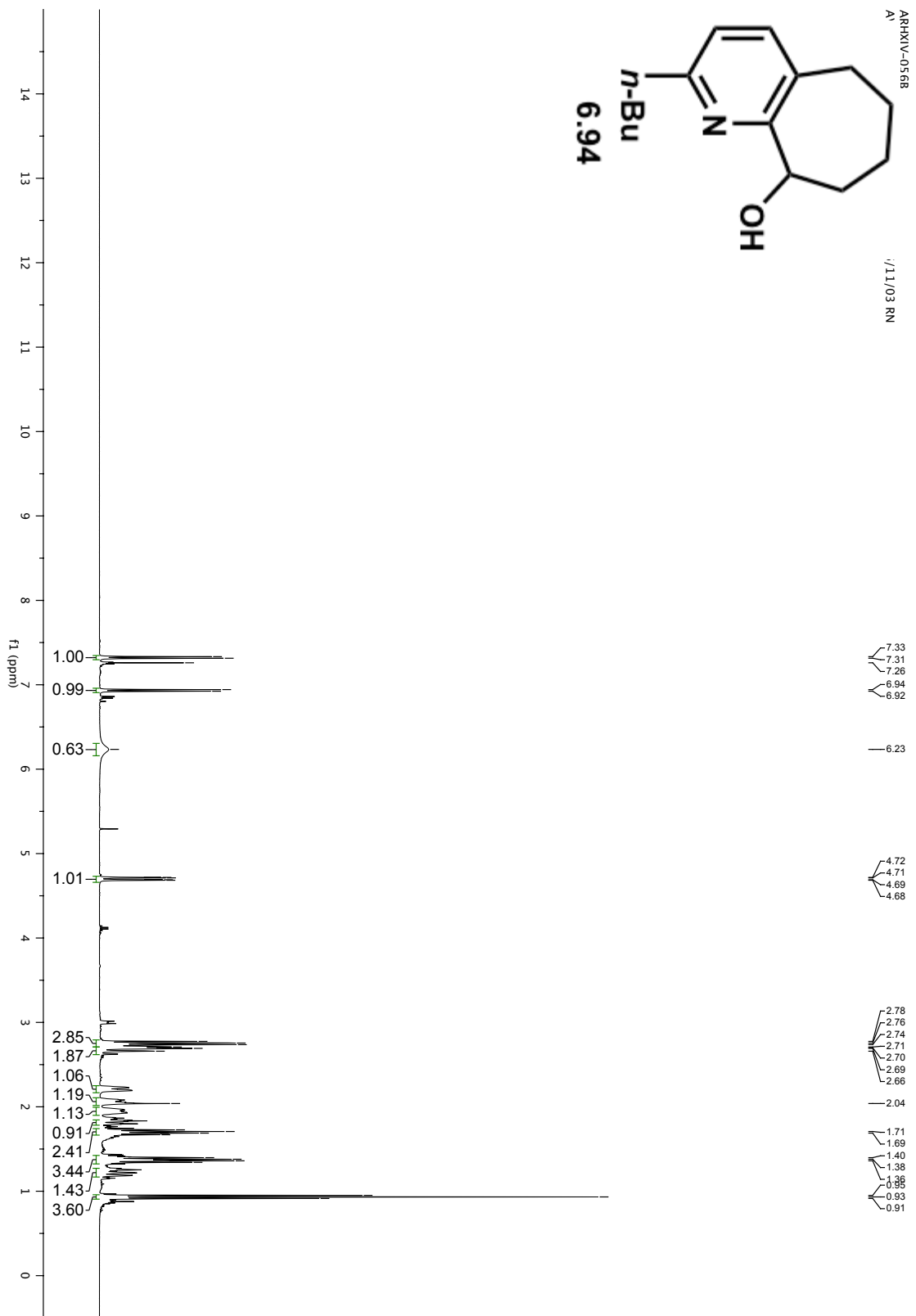
16/11/2016 08:11

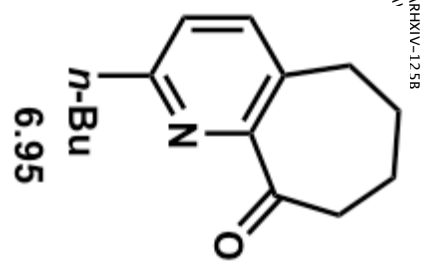




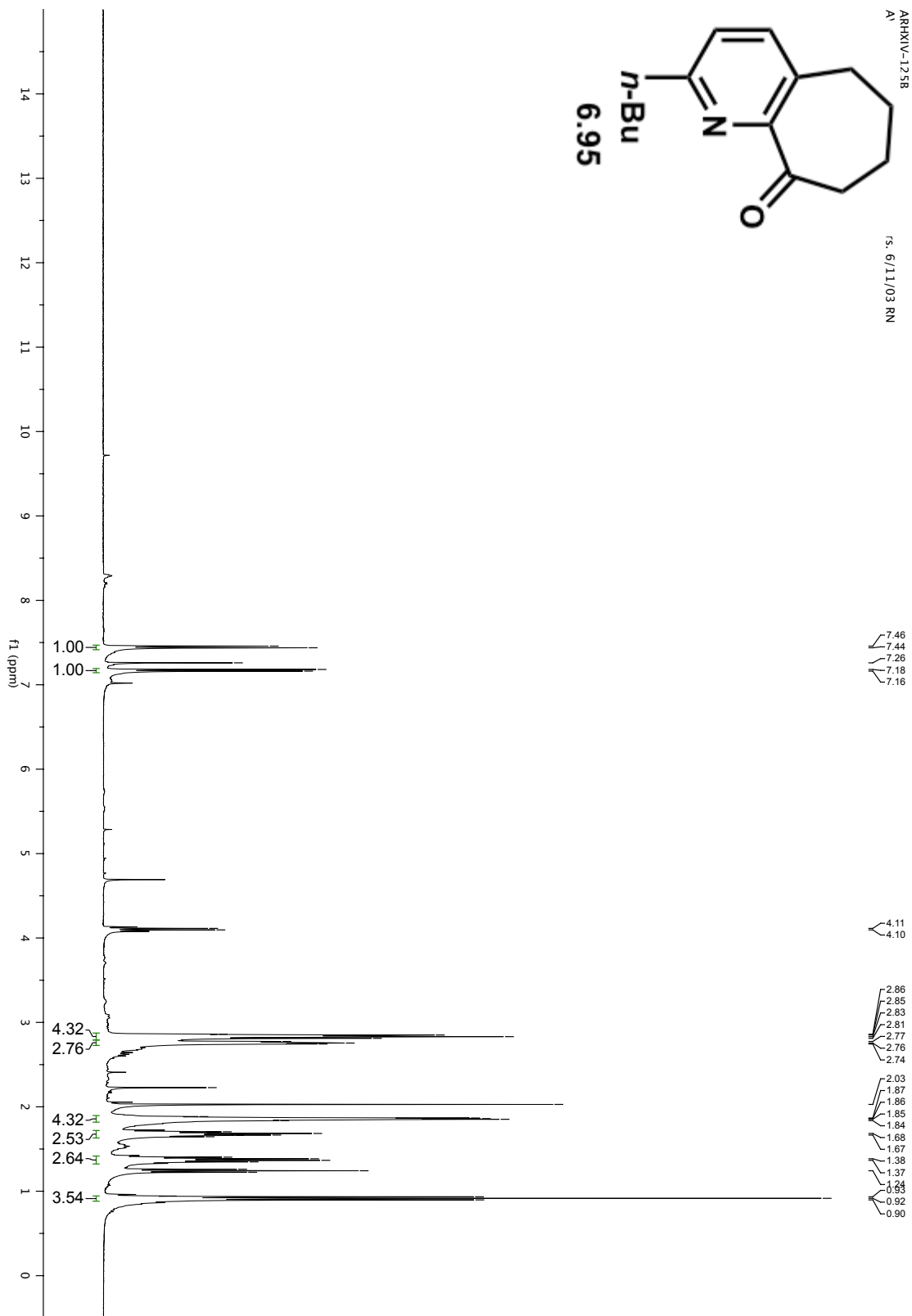


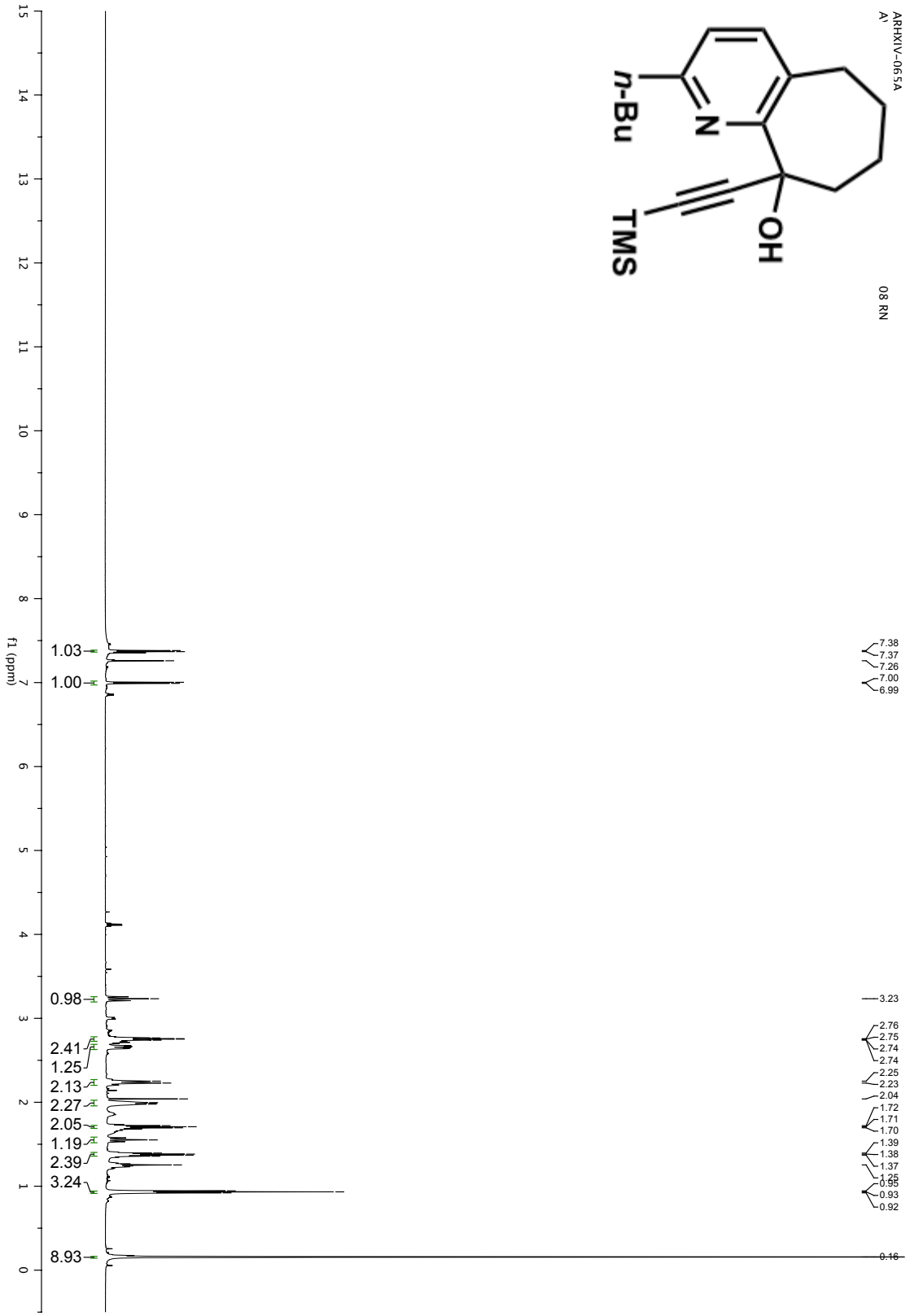
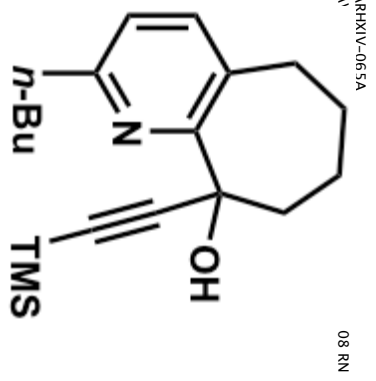
/11/03 RN



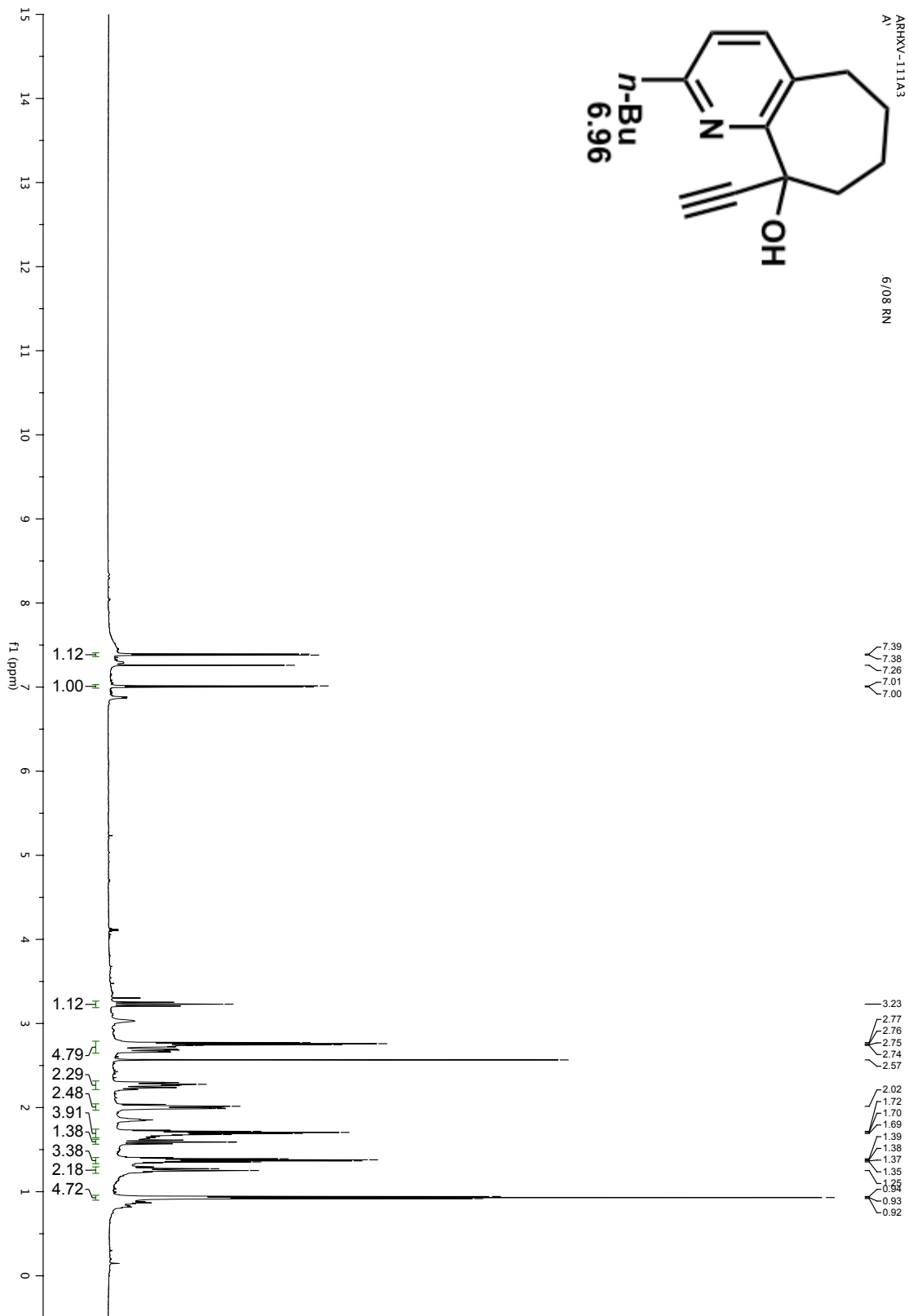
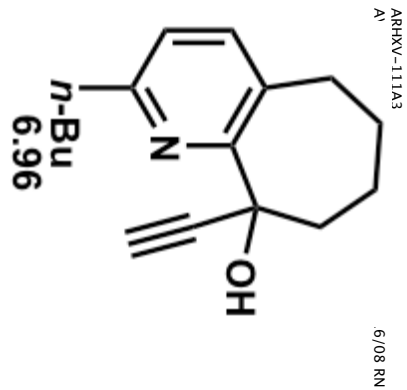


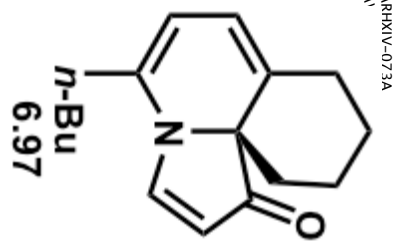
rs: 6/11/03 RN



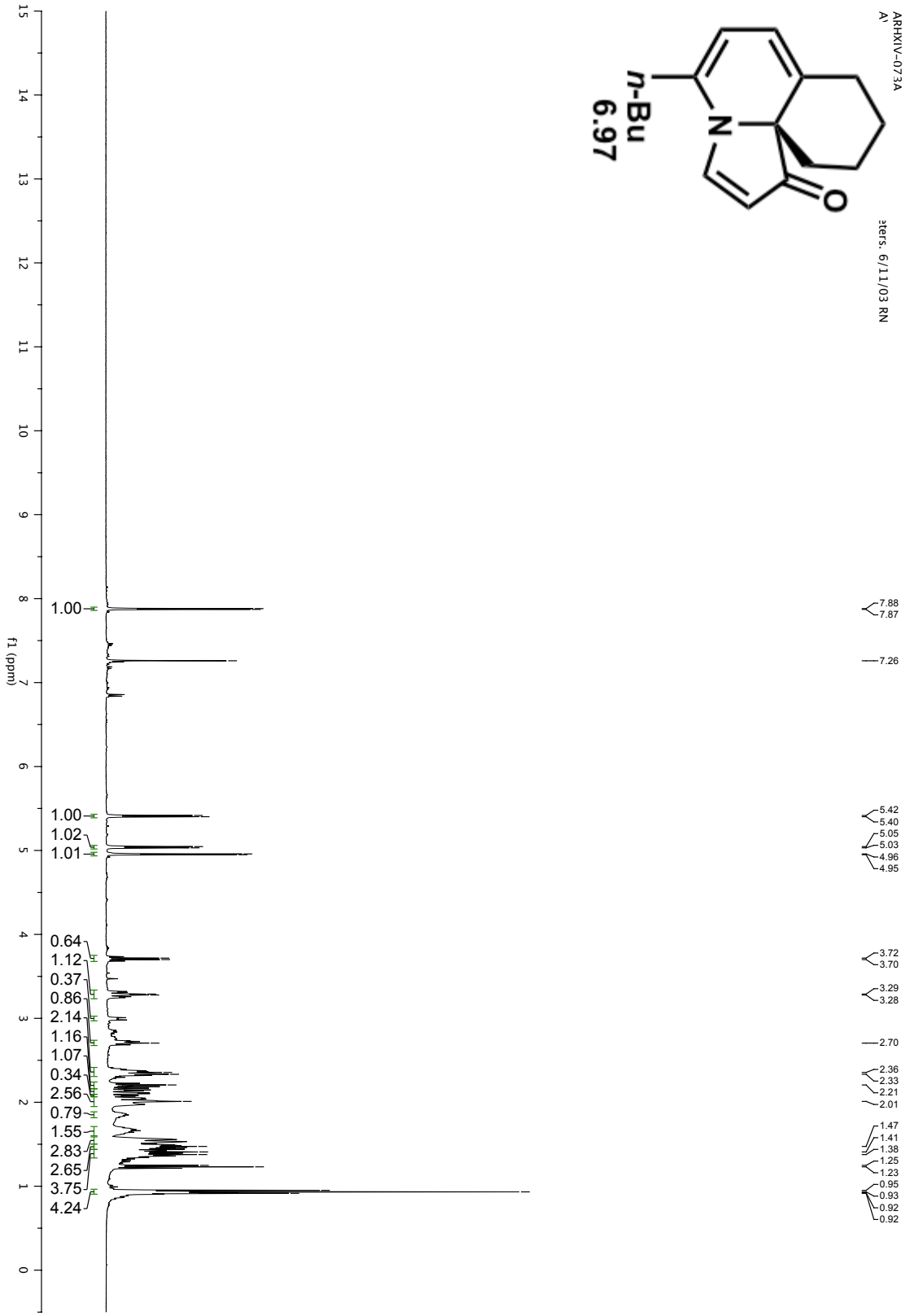




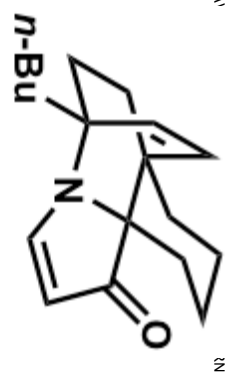




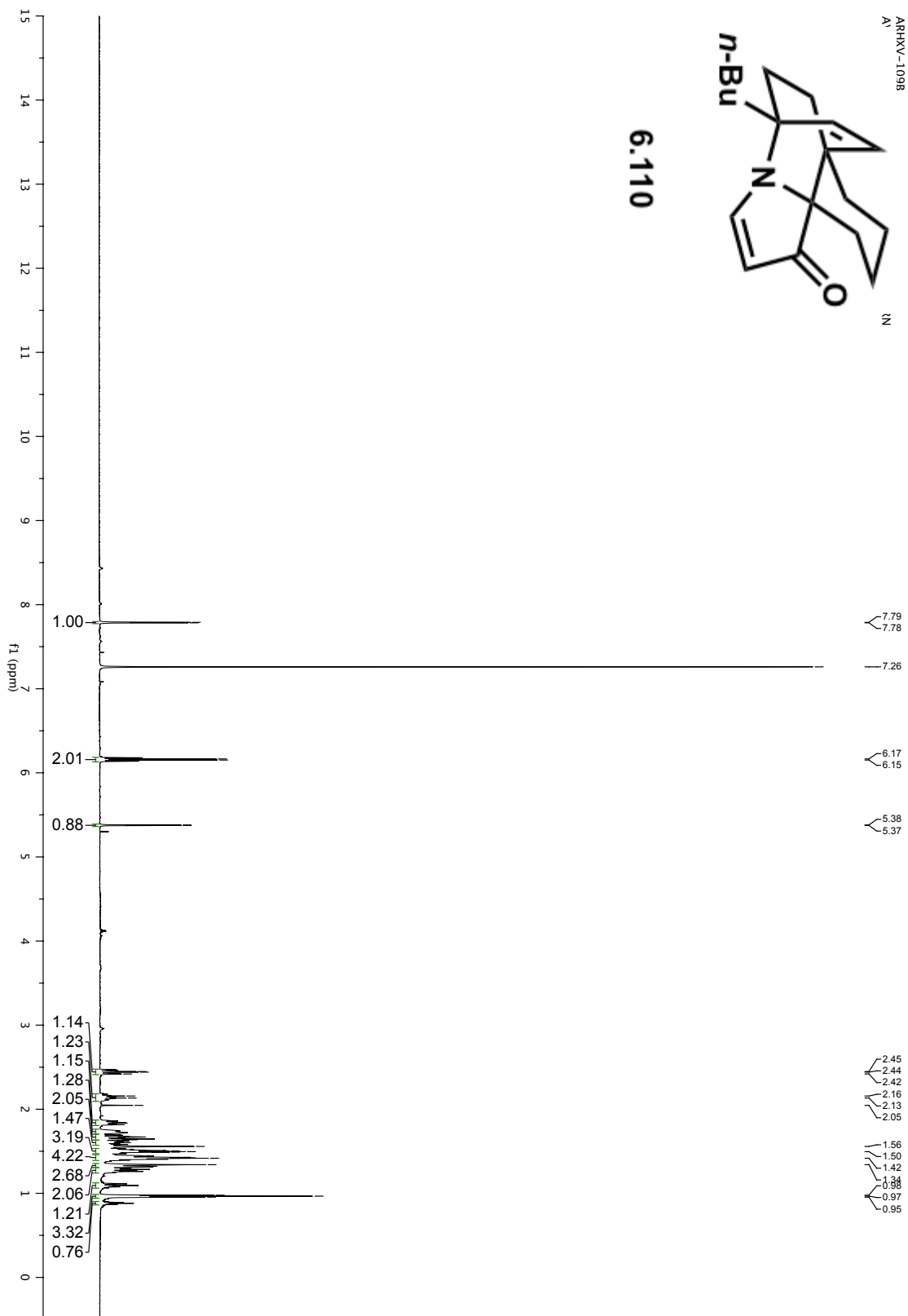
3exrs: 6/11/03 RN



ARRXV-1098  
A'



6.110



## Chapter 7. Synthetic Endeavors Toward *Pallavicinia subciliata* Diterpenes

### 7.1 Introduction to the *Pallavicinia subciliata* Diterpenes

Liverworts, or *Marchantiophyta*, are a subclass of bryophytes, which are non-vascular plants. These plants are found in almost all ecosystems with the exception of aquatic environments. Traditionally, liverworts have been used to treat a variety of ailments, including liver disease; thus, these plants were given the name liverworts, which literally translates to “liver plant.”<sup>1</sup> The medicinal properties of these plants that have been enjoyed for centuries are only now beginning to be understood at the molecular level. Isolation chemists have found that liverworts produce a diverse structural array of secondary metabolites, including: sesquiterpenes, sterols, fatty acids, triglycerides and diterpenes.

*Pallavicinia subciliata*, a liverwort species common to Japan and Taiwan, produces several structurally complex diterpenes (Figure 7.1.1).<sup>2</sup> The first of these diterpenes, pallavicinin (7.1), was originally identified from extracts of *P. subciliata* collected near Taipei city. Wu and coworkers elucidated the structure of pallavicinin on the basis of NMR and mass spectral data and were able to confirm their assignments through X-ray analysis.<sup>3</sup> Pallavicinin’s tetracyclic core is composed of a [3.2.1]bicycle as well as fused tetrahydrofuran and lactone rings. A related diterpene, neopallavicinin (7.2), differs only in the stereochemistry at the fusion of the tetrahydrofuran and lactone rings (see 7.2, C-11 and C-12).<sup>4</sup> In addition to pallavicinin and neopallavicinin, the [3.2.1]bicycle is conserved throughout other *P. subciliata* diterpenes, 7.4, 7.5, and isopallavicinin (7.6). However, not all diterpenes isolated from this liverwort share the same skeleton, several secondary metabolites of *P. subciliata* possess a rearranged 6,6,5,5-core (see 7.3).

Figure 7.1.1. Diterpenes isolated from *Pallavicinia subciliata*.

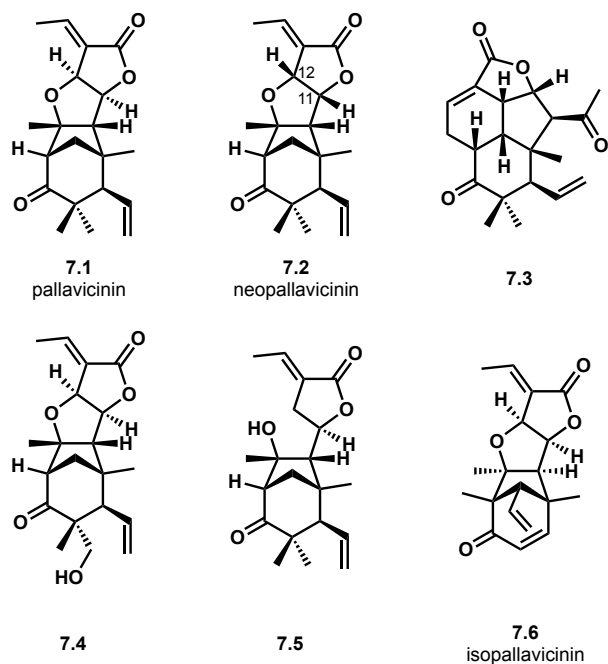
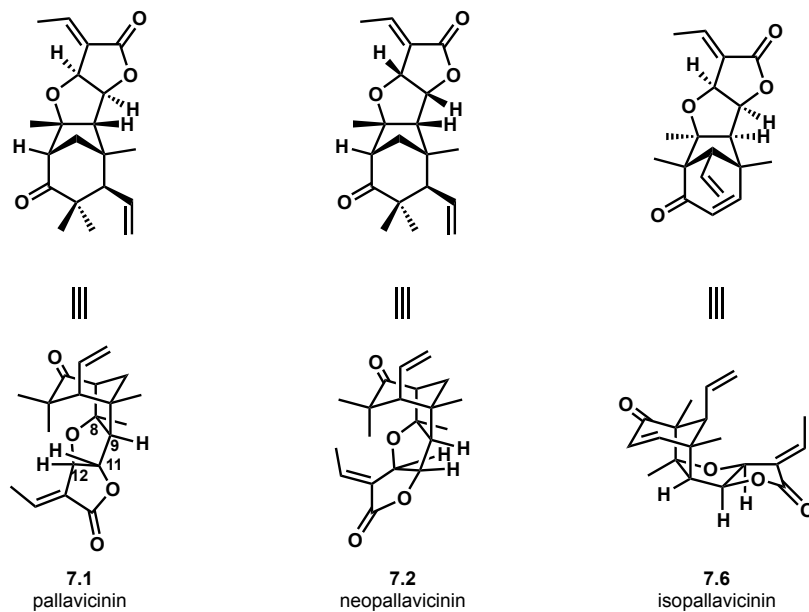


**Figure 7.1.2.** Three dimensional representation of pallavicinin and neopallavicinin.

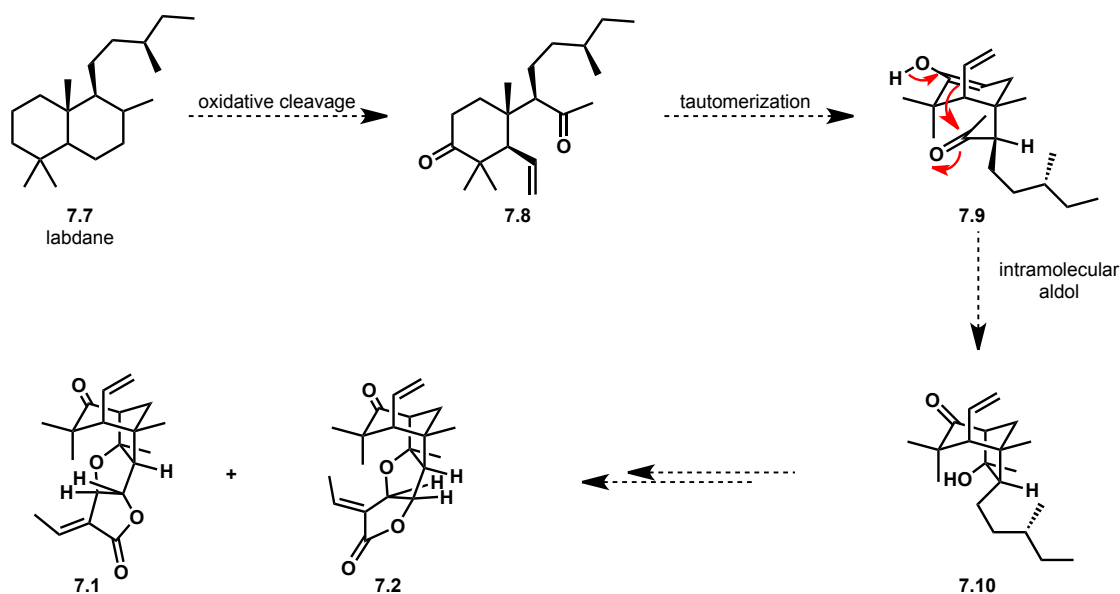


Analysis of a three-dimensional depiction of pallavicinin and neopallavicinin illustrates the effect of the ring-fusion stereochemistry on the overall shape of these molecules (Figure 7.1.2). The tetrahydrofuran ring is joined to the concave face of the [3.2.1]bicycle in both pallavicinin and neopallavicinin. However, isopallavicinin (**7.6**) possesses the opposite stereochemistry at C-8 and C-9, creating a very different architecture. The stereochemistry at C-11 and C-12 is conserved in pallavicinin and isopallavicinin, but is epimeric in neopallavicinin.

The proposed biosynthesis of these diterpenes from labdane (**7.7**) accounts for these stereochemical differences (Scheme 7.1.1).<sup>2</sup> Pallavicinin and structurally similar diterpenes are thought to arise from the oxidative cleavage of the labdane decalin system to provide a diketone such as **7.8**. From **7.8**, the [3.2.1]bicycle could be constructed by an intramolecular aldol reaction (see **7.9** to **7.10**), which sets the stereochemistry of the future tetrahydrofuran ring. Finally a series of oxidations and cyclization would provide the completed natural products. This biosynthetic pathway is supported by the isolation of compounds similar to **7.8** and **7.10** from *P. subciliata*.

Our interest in pallavicinin and related diterpenes as targets for total synthesis stems from their unique skeleton, which we anticipated would constitute a significant synthetic challenge, and also their potential biological activity. For example, pallavicinin has shown potential bioactivity as an antipyretic and also induces muscle regeneration.<sup>2,5</sup>

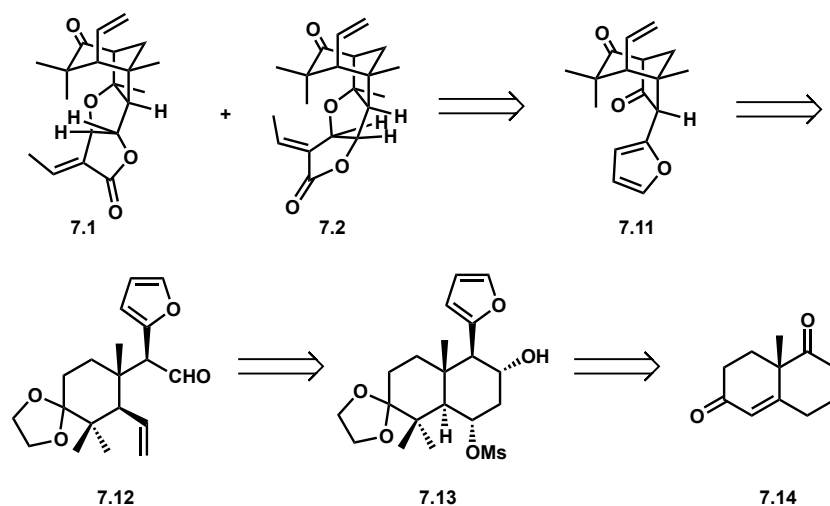
### Scheme 7.1.1. Proposed biosynthesis of pallavicinin.



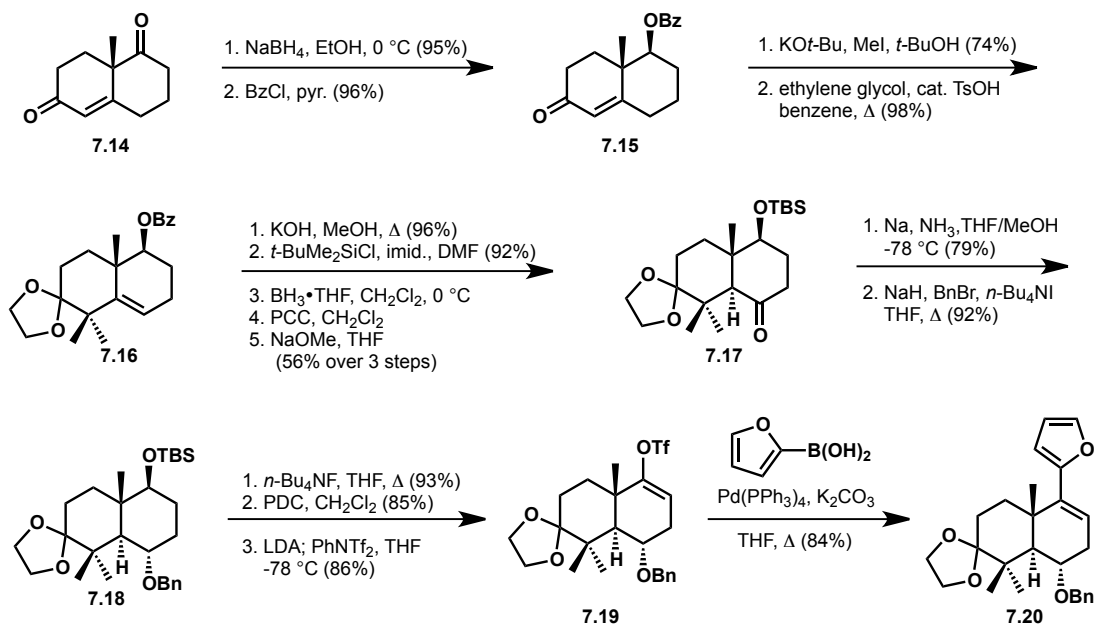
### 7.2 Previous Synthetic Work Toward Pallavicinin and Neopallavicinin

The first and only approach and synthesis of pallavicinin and neopallavicinin was disclosed by Wong and coworkers in 2006.<sup>5</sup> They drew inspiration for their total synthesis from the proposed biosynthetic route to these diterpenes, constructing the [3.2.1]bicycle of pallavicinin and neopallavicinin through an intramolecular aldol reaction. Wong's retrosynthetic reasoning simplifies pallavicinin and neopallavicinin to a common [3.2.1]bicycle (**7.11**, Scheme 7.2.1). The bicycle (**7.11**) could be formed via intramolecular aldol reaction of **7.12**, which could arise from a Grob fragmentation of a functionalized decalin such as **7.13**. The decorated decalin (**7.13**) could ultimately be derived from the Wieland-Miescher ketone (**7.14**).

### Scheme 7.2.1. Wong's bio-inspired retrosynthetic analysis of pallavicinin and neopallavicinin

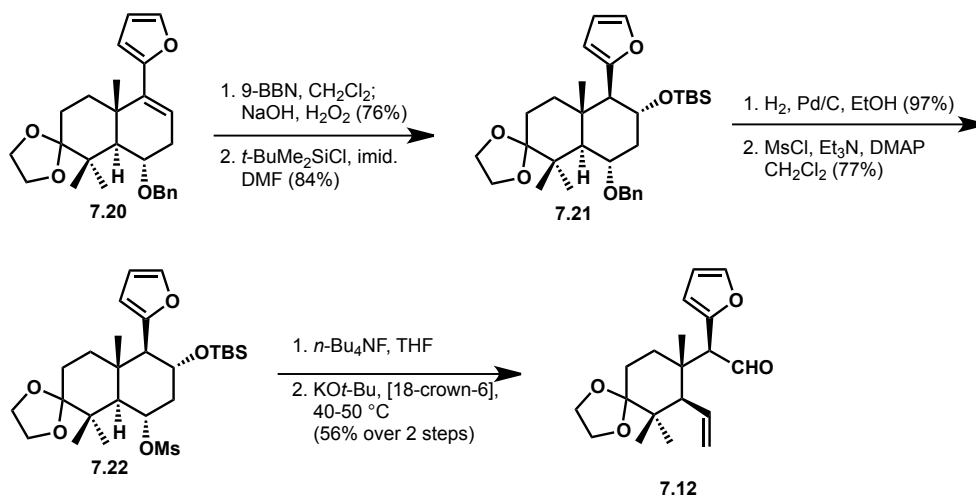


**Scheme 7.2.2.** Synthesis of Wong's Grob fragmentation substrate.



In the forward sense, Wong's total synthesis of pallavicinin and neopallavicinin began with the reduction of the Wieland-Miescher ketone (**7.14**), followed by protection of the secondary alcohol to yield benzoate **7.15** (Scheme 7.2.2). Next, dimethylation of the extended potassium enolate of **7.15** provided the desired gem-dimethylated product in 74% yield. The number of equivalents of base and iodomethane were crucial to the outcome of this transformation. Using greater than three equivalents of base or alkylating agent led to over alkylated products. Protection of the ketone with ethylene glycol proceeded smoothly to give ketal **7.16**. To obtain the desired Grob fragmentation substrate (**7.22**), a series of functional group manipulations were necessary. First, the benzoate was converted to a silyl ether in two high yielding steps. This protecting group switch was followed by hydroboration, which afforded the undesired *cis*-fusion between the two six-membered rings. The stereochemistry could be corrected through a three-step sequence that involved oxidation to the ketone, a base-mediated epimerization to the *trans*-ring fusion, and Birch reduction to regenerate the alcohol with the hydroxyl group in the required equatorial position. The equatorial hydroxyl group was subsequently protected as the benzyl ether (**7.18**). The next task was incorporation of the furan via cross coupling. The required vinyl triflate (**7.19**) was accessed from **7.18** by removal of the *tert*-butyldimethylsilyl group, oxidation of the alcohol to the ketone, and finally, vinyl triflate formation. A Suzuki cross-coupling was carried out between the triflate (**7.19**) and 2-furylboronic acid to provide the desired product in 84% yield. The functionalized decalin (**7.20**) was constructed in fifteen steps from Wieland-Miescher ketone.

**Scheme 7.2.3.** Wong's Grob fragmentation en route to pallavicinin and neopallavicinin.



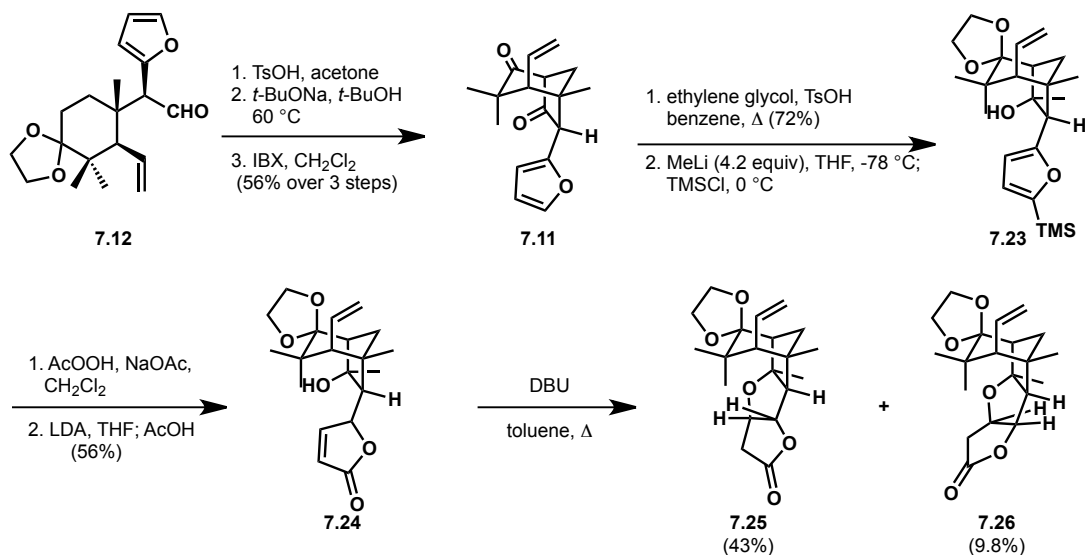
With functionalized bicycle **7.20** in hand, Wong and coworkers were only five steps away from the Grob fragmentation substrate (**7.22**). From **7.20**, hydroboration followed by protection provided silyl ether **7.21** (Scheme 7.2.2). In preparation for the fragmentation, the benzyl ether (**7.21**) was converted to mesylate **7.22** in two steps. Removal of the silyl group of **7.22** with TBAF and subsequent treatment of the free alcohol with potassium *tert*-butoxide led to Grob fragmentation, providing aldehyde **7.12** in 56% yield over two steps.

The Grob fragmentation product possessed three of the methyl groups and the lone vinyl group present on the bicycle in the natural products. The functionalized [3.2.1]bicycle (see **7.11**) was formed upon deprotection of the ketone and treatment with base to effect the intramolecular aldol reaction. IBX oxidation of the aldol product provided diketone **7.11** in 56% yield over three steps. Selective ketalization was possible on the carbonyl located on the carbon-bridge. Next, 1,2-addition of methyllithium and simultaneous deprotonation of the furan, followed by treatment with trimethylsilylchloride led to the formation of **7.23**. The 2-silylfuran was transformed to butenolide **7.24** by the action of peracetic acid, which was followed by double bond isomerization to afford butenolide **7.24**. The tetrahydrofuran ring was formed by conjugate addition of the tertiary alcohol into the butenolide moiety to provide a mixture of diastereomer products (**7.25** and **7.26**, which were isolated in 43% and 9.8%, respectively).

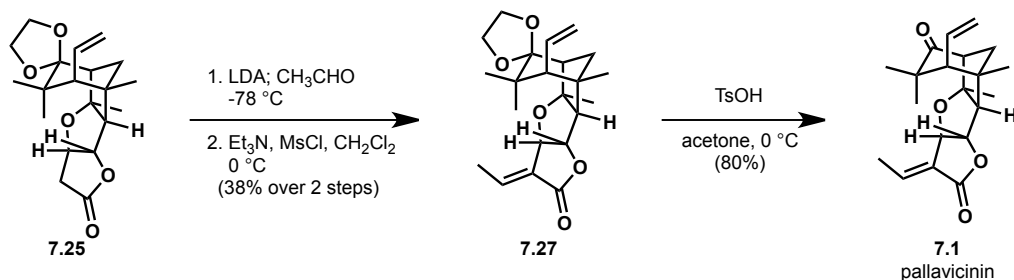
The major diastereomer (**7.25**) was elaborated to pallavicinin to complete the first total synthesis of this natural product (Scheme 7.2.5). An aldol reaction between **7.25** and acetaldehyde followed by mesylation and elimination provided **7.27** in 38% over two steps. Finally, removal of the ketal group from **7.27** yielded pallavicinin in 80% yield. An analogous three-step sequence was conducted on the minor diastereomer (**7.26**), to provide neopallavicinin in 10% over three steps.



### Scheme 7.2.4.



### Scheme 7.2.5. Completion of the total synthesis of pallavicinin.



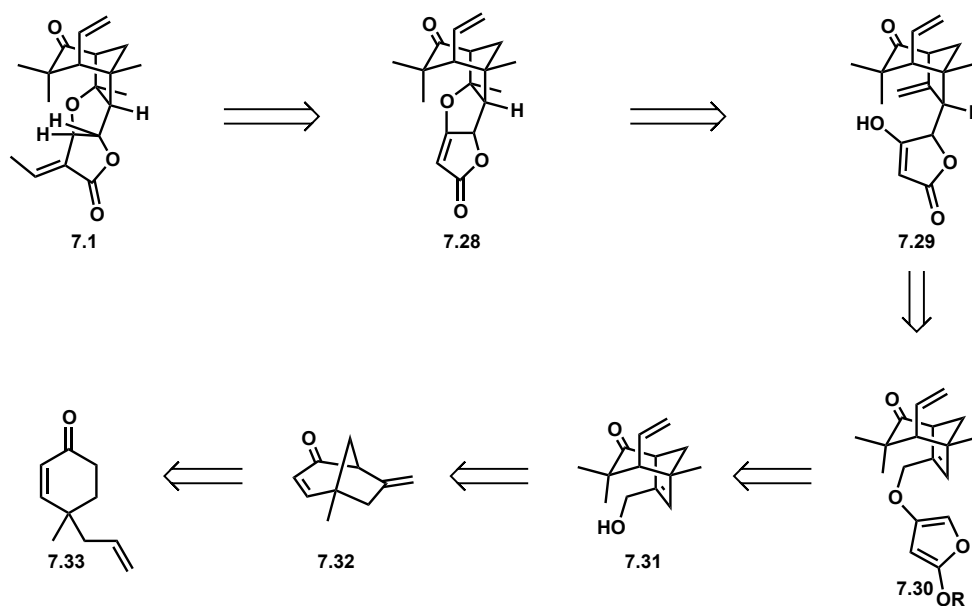
Wong and coworkers completed the synthesis of pallavicinin and neopallavicinin in 32 steps from Wieland-Miescher ketone. Their biomimetic approach illustrates the feasibility of an intramolecular aldol reaction to construct the [3.2.1]bicycle conserved throughout many of the *P. subciliata* diterpenes.

### 7.3 First-Generation Approach Toward Pallavicinin

Although Wong and coworkers had accomplished the first total syntheses of pallavicinin and neopallavicinin, we were intrigued by the possibility of devising a rapid and more efficient route to the [3.2.1]bicyclic motif conserved throughout many of these diterpenes. We believed that access to this bicycle would enable the synthesis of not only pallavicinin and neopallavicinin, but also **7.4**, **7.5**, and **7.6**. More specifically, we envisioned accessing these diterpenes from a simplified tetracycle such as **7.28** (Scheme 7.3.1). This tetracycle (**7.28**) could be obtained via intramolecular etherification of tetronic acid **7.29**. A key step in this synthetic

endeavor would involve the Claisen rearrangement of **7.30** to form the C-9 to C-11 carbon-carbon bond. Claisen substrate **7.30** could be derived from allylic alcohol **7.31**, which we anticipated would be readily accessible from bicycle **7.32**. We envisioned constructing the bicycle (**7.32**) in a cyclization of a properly functionalized cyclohexenone such as **7.33**.

**Scheme 7.3.1.** Retrosynthetic analysis of pallavicinin.

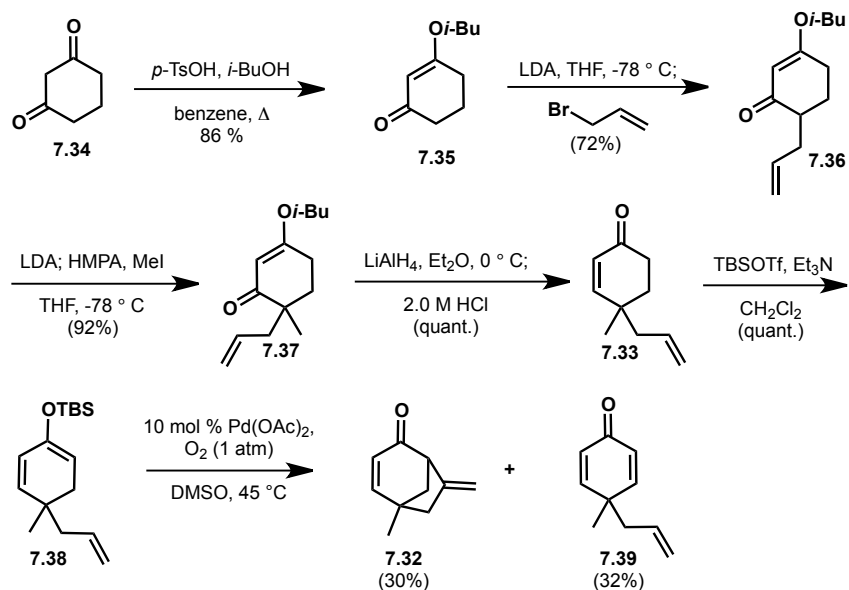


Our efforts toward pallavicinin commenced with the synthesis of [3.2.1]bicycle **7.32** from 1,3-cyclohexanedione (**7.34**, Scheme 7.3.2). In the forward sense, a Stork-Danheiser sequence was employed to access enone **7.33** in four steps. First, vinylogous ester **7.35** was obtained in 86% yield by refluxing 1,3-cyclohexanedione (**7.34**) with isobutyl alcohol and a catalytic amount of *p*-toluenesulfonic acid under Dean-Stark conditions. Next, the installation of the allyl group was accomplished by formation of the lithium enolate of **7.35** followed by treatment with allyl bromide to provide **7.36** in 72% yield accompanied by trace amounts of over alkylated product. The methylation of **7.36** proceeded in low yields when iodomethane was added to the lithium enolate of **7.36** in THF. To obtain **7.37** in yields greater than 20%, one equivalent of hexamethylphosphoramide (HMPA) was added to the reaction mixture prior to introduction of the methylating agent. HMPA may have been effective as an additive by breaking up lithium enolate aggregates, thus, facilitating the alkylation reaction. With HMPA, dialkylated vinylogous ester **7.37** was obtained in 92% yield. The vinylogous ester (**7.37**) was next converted to enone **7.33** in a two-step, one-vessel procedure. From enone **7.33**, the cyclization substrate **7.38** was obtained by silyl enol ether formation under soft conditions.

With silyl enol ether **7.38** in hand, we were eager to employ a palladium-catalyzed oxidative cyclization to obtain [3.2.1]bicycle **7.32**. This palladium-catalyzed cyclization was developed and previously utilized to construct similar bicyclic products by Kende and coworkers.<sup>6</sup> Exposing **7.38** to 10 mol % palladium acetate under an atmosphere of oxygen in warm DMSO, a 1:1 mixture of products was obtained (Scheme 7.3.2). Although the desired

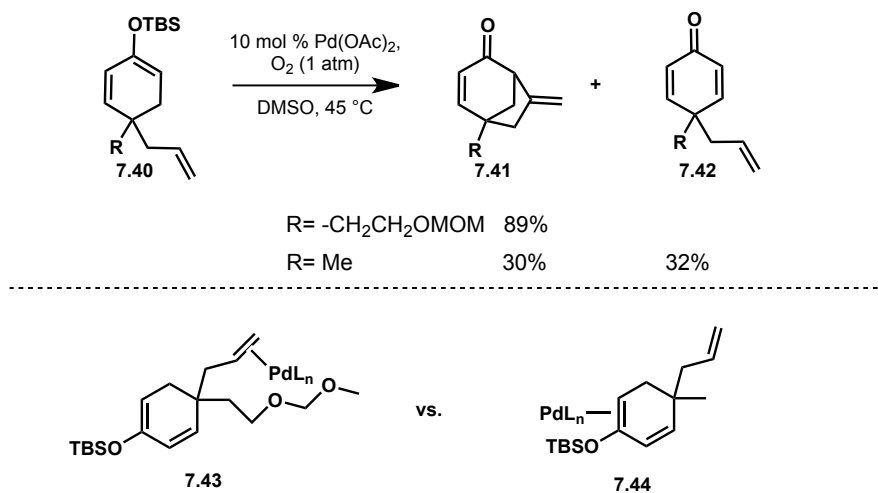
bicycle **7.32** was obtained in a 30% yield, it was accompanied by an equal amount of dieneone **7.39**.

**Scheme 7.3.2.** First-generation approach toward [3.2.1]bicycle **7.32**.



The Saegusa-Ito product (**7.39**) arises from  $\beta$ -hydride elimination from a palladium-enolate such as **7.44**, whereas, productive cyclization requires that the palladium-enolate engage the allyl group (see **7.43**, Figure 7.3.1). Toyota et al. were able to achieve higher yields of cyclized product for a similar substrate that possessed a tethered methyl methoxy ether (see **7.40**). We hypothesize that the methyl methoxy ether binds the metal center and mitigates  $\beta$ -hydride elimination, favoring cyclization over formation of the dienone (**7.42**). Efforts to obtain increased yields of bicycle **7.32** by altering the reaction conditions were ultimately not fruitful. This oxidative palladium-catalyzed cyclization provided small amounts of bicycle **7.32** to explore further chemistry; however, we were not satisfied with this low-yielding route.

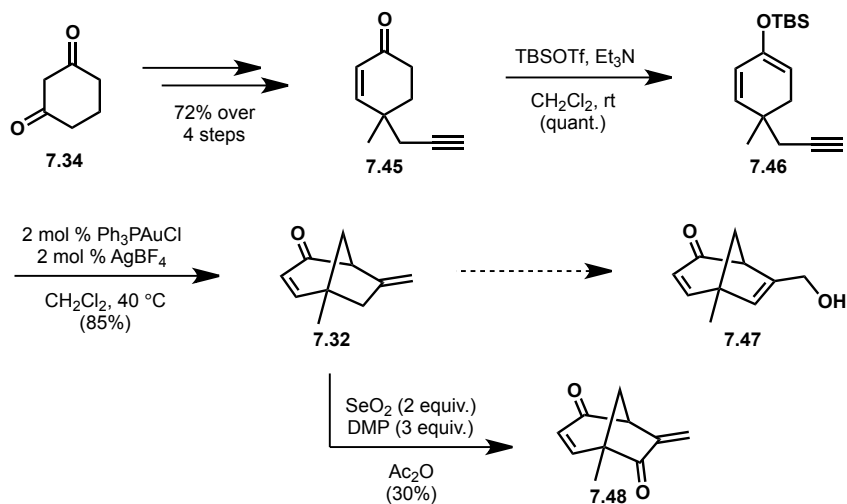
**Figure 7.3.1.** Effect of R group.



We revised our synthetic strategy toward bicycle **7.32**, replacing the palladium cyclization with a gold-catalyzed cyclization onto an alkyne developed by Toste and coworkers.<sup>7</sup> Enone **7.45** was synthesized in four steps from 1,3-cyclohexanedione utilizing a similar Stork-Danheiser sequence to that employed in the synthesis of enone **7.33** (Scheme 7.3.3). Under soft enolization conditions, silyl enol ether **7.46** was formed in quantitative yield. Adopting the conditions developed by Toste et al. provided the desired bicycle (**7.32**) in 85% yield, with the mass balance of the reaction accounted for by enone **7.45**.

With access to gram-quantities of [3.2.1]bicycle **7.32**, our next targeted intermediate was allylic alcohol **7.47** (Scheme 7.3.3). To arrive at allylic alcohol **7.47** from **7.32**, formally only a double bond isomerization and allylic oxidation were required. However, efforts to isomerize the exocyclic double bond into the bicycle were not fruitful. Simple calculations as well as evidence from the literature, suggest that this isomerization is unfavorable by 1.5 kcal/mol.<sup>6,8</sup> Alternatively, attempts to oxidize the exocyclic methylene group of **7.32** resulted in no reaction or fragmentation of the [3.2.1]bicycle. Upon exposure of **7.32** to selenium dioxide, we observed the allylic oxidation of bicycle **7.32** to install a second enone motif. Efforts to differentiate between these enones were not successful.

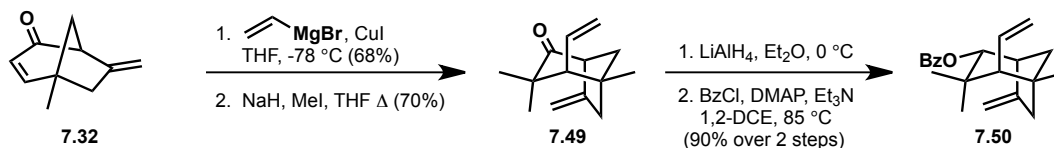
**Scheme 7.3.3.** Alternative route to [3.2.1]bicycle **7.32**.



Given the propensity of bicycle **7.32** to fragment, we hypothesized that it was highly strained. We anticipated that replacing sp<sup>2</sup>-hybridized carbon atoms within the bicycle with sp<sup>3</sup>-carbons could alleviate a portion of the ring strain and enable productive reactions. To this end, we installed the groups present along the western-edge of the natural product at this stage. The conjugate addition of the vinyl group proceeded to provide a single diastereomer of the desired product in 68% yield (Scheme 7.3.4). The stereochemistry of the vinyl group with respect to the bicycle was determined to be that required for pallavicinin based on nOe studies. This stereochemical assignment was later confirmed through an X-ray crystal structure of an advanced intermediate. The conjugate addition product was further elaborated by exhaustive methylation with sodium hydride and methyl iodide to give **7.49** in 70% yield. Further chemistry was explored from ketone **7.49**, which now contained two less sp<sup>2</sup>-carbon atoms. This ketone

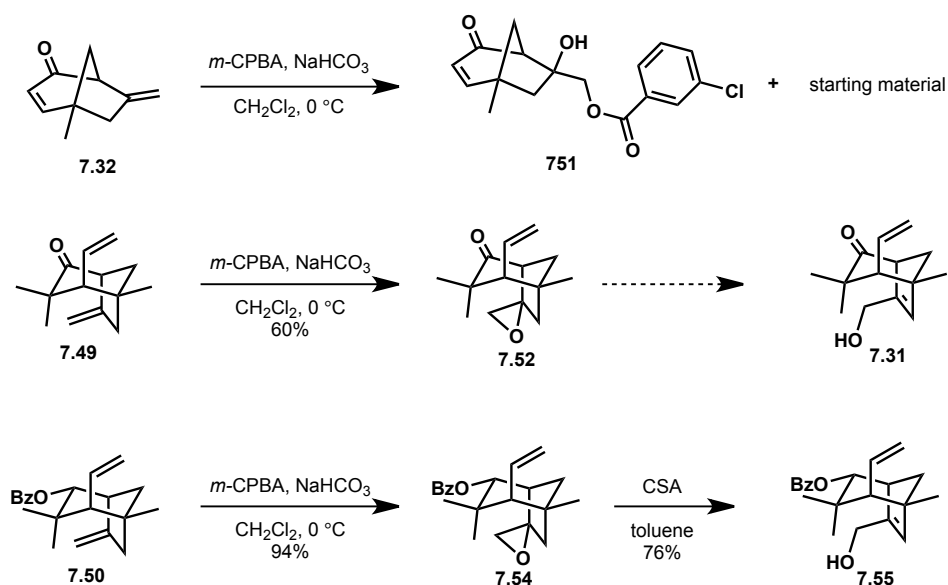
(7.49) was also reduced and protected as the benzoate (7.50) to remove a third  $sp^2$ -center from the bicycle.

**Scheme 7.3.4.** Elaboration of [3.2.1]bicycle.



A comparison of the reactivity of the [3.2.1]bicycles containing differing numbers of  $sp^2$ -centers revealed a clear trend (Scheme 7.3.5). Attempts to epoxidize the original bicycle (7.32) led to an unstable epoxide that was readily opened under the reaction conditions to yield tertiary alcohol 7.51. Under the same conditions, the ketone-containing bicycle (7.49) underwent epoxidation without event to provide a stable epoxide (7.52) in 60% yield. It is worth noting that the vinyl group of 7.49 was not epoxidized when *m*-chloroperbenzoic acid was used. Although we were initially hesitant to install this vinyl group early in the synthesis, the unreactive nature of this substituent was observed throughout this work. We hypothesized that the inert nature of the vinyl group is a result of the steric demands of the adjacent methyl groups, which act as a cage around the vinyl group. Despite the ability to epoxidize 7.49, the epoxide (7.52) was not converted to the allylic alcohol (7.53) under a broad screen of both basic and acidic conditions. However, the further reduced bicycle (7.50) could be transformed to the epoxide (7.54) in a much higher 94% yield. Toward our ultimate goal, epoxide 7.54 was opened in the presence of a catalytic amount of camphorsulfonic acid to provide the desired allylic alcohol (7.55) in 76% yield.

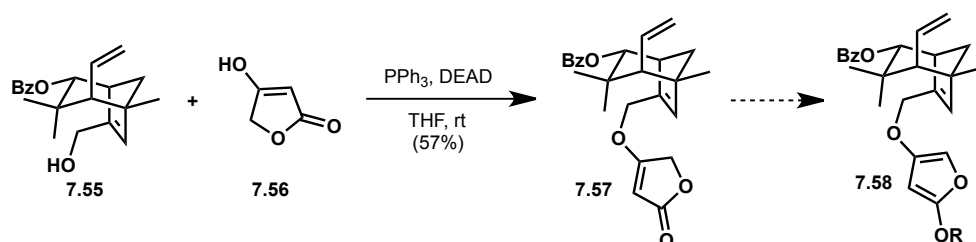
**Scheme 7.3.5.** Relative reactivities of [3.2.1]bicycles.



Removing the unsaturation on the western-edge of the [3.2.1]bicycle enabled the conversion of the *exo*-cyclic methylene of **7.55** to an allylic alcohol. Although the oxidation level of the natural product at C-3 is at the ketone and not the alcohol level, the additional redox steps were necessary to continue with the synthesis as planned.

With a robust route to allylic alcohol **7.55** developed, we focused on the synthesis of the Claisen substrate (**7.58**, Scheme 7.3.6). Allylic alcohol **7.55** underwent Mitsunobu reaction with tetronic acid (**7.56**) to provide a modest 57% yield of tetronic ester **7.57**. From **7.57**, we envisioned accessing the Claisen substrate by transforming the tetronic ester moiety into a silyloxy furan such as **7.58** (R = SiR<sub>3</sub>). Although this transformation was accomplished on a model system, we were not able to prepare the requisite silyloxy furan for the Claisen rearrangement.

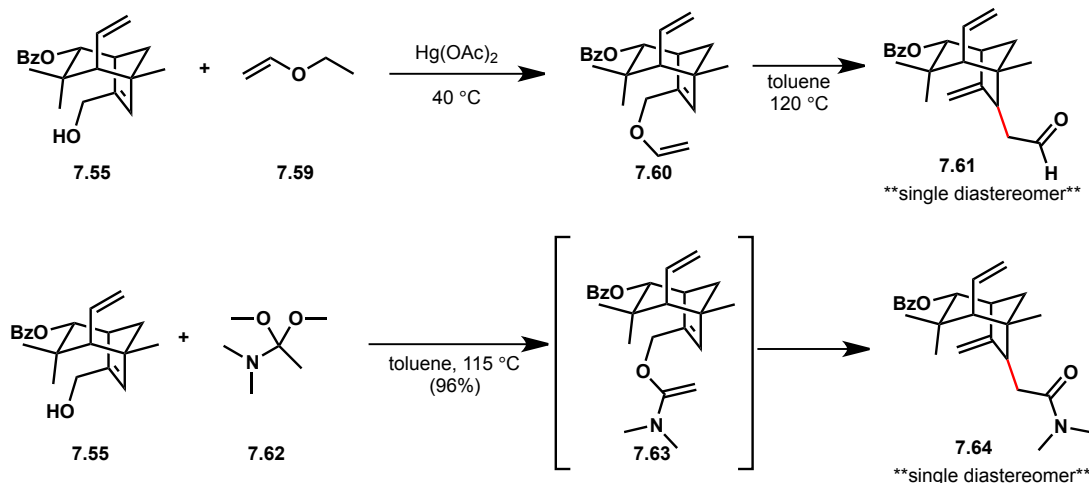
**Scheme 7.3.6.** Synthesis of the Claisen rearrangement substrate.



In addition to attempting to isolate silyloxy furan **7.58**, efforts to enolize the tetronic ester to the furan *in situ* and effect the Claisen rearrangement were unfruitful. Unable to reach our desired Claisen rearrangement substrate (**7.58**), our focus shifted to constructing a simplified Claisen substrate. With a simplified substrate, we sought to test the viability of employing a Claisen rearrangement on the [3.2.1]bicycle and also gain insight into the diastereoselectivity of this transformation.

Classic derivations of the Claisen rearrangement were explored from allylic alcohol **7.55**. Etherification of allylic alcohol **7.55** with ethylvinyl ether in the presence of a catalytic amount of mercuric acetate provided allylvinyl ether **7.60** (Scheme 7.3.7). Allylvinyl ether **7.60** readily hydrolyzed to return the allylic alcohol (**7.55**). To avoid hydrolysis, the allylvinyl ether (**7.60**) was not isolated; instead, toluene was added to the allylvinyl ether (**7.60**) and the solution was heated to 120 °C. These conditions effected the Claisen rearrangement to provide variable amounts of aldehyde **7.61** as a single diastereomer that was accompanied by allylic alcohol **7.55**. Efforts to purify aldehyde **7.61** via silica gel chromatography led to decomposition of the aldehyde. However, the aldehyde (**7.61**) could be reduced to a stable primary alcohol. This alcohol was derivatized as the *p*-nitrobenzoate in an attempt to obtain X-ray quality crystals, which would unambiguously determine the stereochemistry of the Claisen product.

### Scheme 7.3.7. Alternative Claisen substrates.

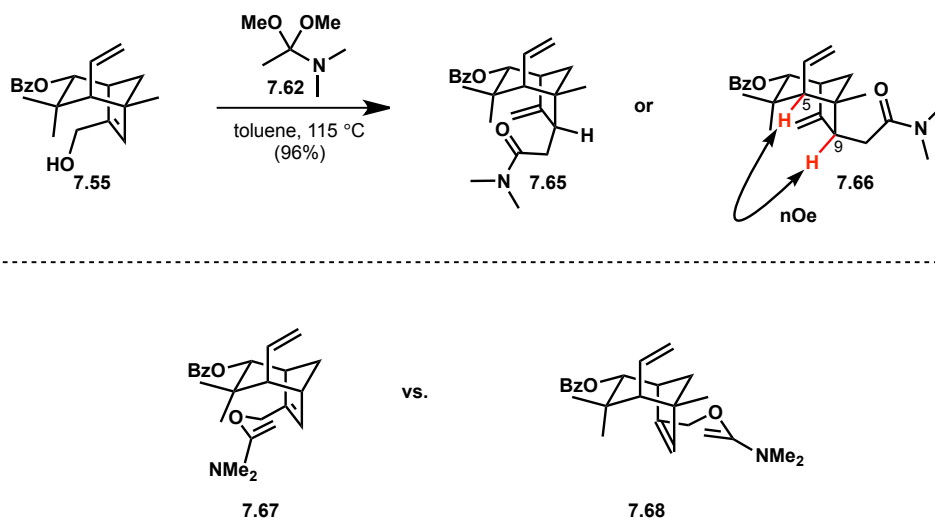


At the same time, the viability of other variants of the Claisen rearrangement was tested. Johnson-orthoester Claisen conditions led only to the recovery of allylic alcohol **7.55**. At this point, we attempted an Eschenmoser-Claisen rearrangement. The Eschenmoser variant of the Claisen rearrangement is known to occur at lower temperatures compared to other Claisen rearrangements.<sup>9</sup> Heating allylic alcohol **7.55** neat in *N,N*-dimethylacetamide dimethyl acetal (DMA-DMA, **7.62**) at  $120\text{ }^\circ\text{C}$  led to the formation of dimethyl amide **7.64** as a single diastereomer. Further experimentation indicated that the Eschenmoser-Claisen proceeded with as few as five equivalents of DMA-DMA (**7.62**) in toluene at  $115\text{ }^\circ\text{C}$  to provide dimethyl amide **7.64** in 96% yield on gram scale.

The Eschenmoser-Claisen offered several advantages over the rearrangement of allylvinyl ether **7.60**. The Eschenmoser-Claisen could be carried out in a single step from allylic alcohol **7.55**, whereas, the etherification of alcohol **7.55** and the thermal rearrangement required a solvent switch. Additionally, the hydrolysis of allylvinyl ether **7.60** was in competition with the desired rearrangement leading to lowered yields of the Claisen product (**7.61**) that was contaminated with allylic alcohol **7.55**. In addition to higher yields and a simple reaction protocol, the Eschenmoser-Claisen provided a stable product that could be chromatographed and stored for long periods of time. The stability of amide **7.64** was a significant advantage over aldehyde **7.61**, which could not be purified or stored for any period of time without degrading.

The Eschenmoser-Claisen rearrangement of allylic alcohol **7.55** proceeded with exquisite diastereoselectivity; however, the stereochemistry of the amide product (**7.64**) was not known. To determine the orientation of the dimethyl amide with respect to the bicycle, NMR studies of **7.64** were carried out. First, COSY data was used to assign the identity of each  $^1\text{H}$  NMR peak. This set the stage for distinguishing between the desired product (**7.65**) and the undesired diastereomer (**7.66**, Scheme 7.3.8). An nOe was observed between the hydrogen atoms appended to the bicycle at C-5 and C-9, this confirmed that the undesired diastereomer (**7.66**) was formed in the Claisen rearrangement.

**Scheme 7.3.8.** Determination of the Eschenmoser-Claisen product stereochemistry.



The formation of the undesired diastereomer, amide **7.66**, could be rationalized by modeling the two potential Claisen transition states. The transition state leading to the unobserved product contains unfavorable steric interactions between the geminal-methyl groups at C-4 and the requisite six-membered ring transition state (see **7.67**, Scheme 7.3.8). The alternative transition state avoids these steric interactions.

At this juncture, we considered two options: (1) correct the stereochemistry at C-9 or (2) employ an alternative strategy for the formation of the pallavicinin C-9-C-11 bond. Both of these options were pursued. Selected strategies toward these goals are discussed in Sections 7.4 and 7.5.

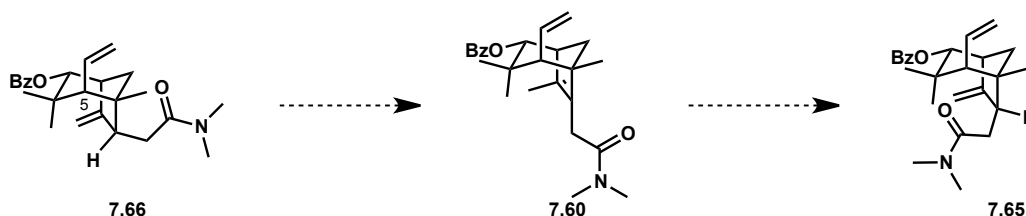
#### **7.4 Forward from Amide 7.66: Correcting the Stereochemistry at C-9**

With a robust route to amide **7.66**, we sought to correct the stereochemistry at C-9 to resemble the natural product, pallavicinin. Toward this goal, we devised several strategies to invert the C-9 stereochemistry that involved utilizing either the *exo*-methylene or dimethyl amide moieties as functional handles.

We envisioned obliterating the C-9 stereochemistry by isomerizing the exocyclic double bond into the bicycle (see, **7.66** to **7.69**, Figure 7.4.1). From the tetrasubstituted alkene (**7.69**), further double bond isomerization could permit access to **7.65**. Alternatively, we envisioned iodolactonization of tetrasubstituted alkene **7.69** could yield a lactone with the corrected stereochemistry at C-9. Toward this end, amide **7.66** was treated with a variety of metals and/or acids in a host of solvents in an attempt to isomerized the exocyclic double bond (Figure 7.4.1). We were pleased that the vinyl group at C-5 did not undergo isomerization to the trisubstituted double bond under any of the conditions screened. However, the exocyclic double bond was also resistant to isomerization.



**Figure 7.4.1.** Double bond isomerization.



|  |
|--|
| <b>Metals:</b> Pd(OAc), Pd(TFA) <sub>2</sub> , PdCl <sub>2</sub> and FeCl <sub>3</sub> , PdCl <sub>2</sub> (PhCN) <sub>2</sub> , RhCl <sub>3</sub> , RhCl(PPh <sub>3</sub> ) <sub>3</sub> , Crabtree's catalyst, Grubbs II |
| <b>Solvents:</b> EtOH, MeOH, BuOH, H <sub>2</sub> O, AcOH, DMSO, EtOAc, CH <sub>2</sub> Cl <sub>2</sub> , toluene, benzene, xylenes, DCE, acetone  |
| <b>Acids:</b> benzoic acid, H <sub>2</sub> SO <sub>4</sub> , formic acid   |

**Conditions:**

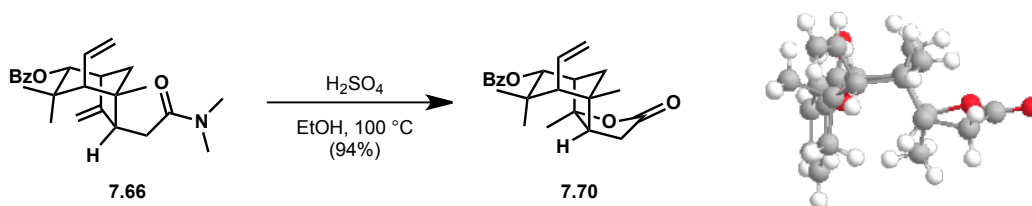
RhCl<sub>3</sub>, EtOH 80 °C, 24 h → 1:1 (**7.66:7.69**)

RhCl<sub>3</sub>, EtOH 80 °C, 3 d → 1:1:1 (**7.66:7.69:7.70**)

H<sub>2</sub>SO<sub>4</sub>, EtOH/H<sub>2</sub>O (10:1) 100 °C → **7.70** (63%)

The exocyclic methylene (**7.66**) was recovered unchanged from all conditions screened, except those that employed rhodium(III) chloride or sulfuric acid. When **7.66** was refluxed in ethanol with rhodium(III) chloride for 24 h, a mixture of the *exo* and *endo* alkenes was obtained (see **7.66** and **7.69**). These products could be separated using column chromatography. Efforts to carry out an iodolactonization from *endo*-product **7.69** were unsuccessful. When **7.66** was reacted with rhodium(III) for periods greater than one day, a third compound was observed in the crude reaction mixture. This product was not the epimerized product (**7.65**), but instead, the lactonized product (**7.70**, Scheme 7.4.1) derived from **7.66**. Under strongly acidic conditions, lactone **7.70** could be formed quantitatively from **7.66**. The identity of lactone **7.70** and its stereochemistry were confirmed by X-ray crystallography. The ring-fusion between the lactone and bicycle of **7.70** is epimeric at both C-9 and C-8 compared to pallavicinin. Although lactone **7.70** could not be advanced to pallavicinin, downstream chemistry was explored on this compound (see Section 7.6).

**Scheme 7.4.1.** Lactone formation and structure.

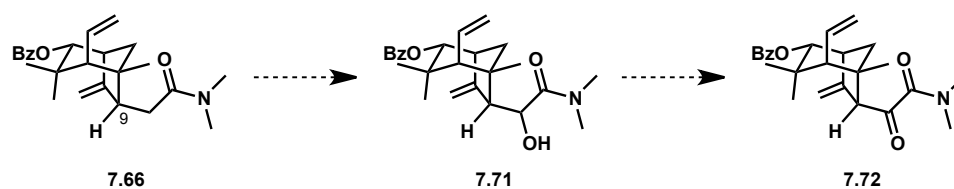


A second approach toward correcting the C-9 stereochemistry of Claisen product **7.66** involved  $\alpha$ -oxygenation of the amide followed by oxidation to the  $\alpha$ -ketoamide to provide the opportunity to epimerize at C-9 (Figure 7.4.2).  $\alpha$ -Oxygenation of amide **7.66** proved to be a

challenge. Surveying bases as well as oxygen sources indicated that deprotonation with LDA followed by sparging with oxygen and a reductive work-up led to incomplete conversion to the desired product (**7.71**). Interestingly, a 3:1 ratio of recovered starting material (**7.66**) to  $\alpha$ -hydroxylated product (**7.71**) was routinely obtained when several reaction parameters were altered. For example, increasing the number of equivalents of LDA, altering the deprotonation time, or sparging with oxygen for various amounts of time all resulted in a 3:1 mixture of **7.66** to **7.71**.

The  $\alpha$ -hydroxylated amide could be oxidized to the  $\alpha$ -ketoamide (**7.72**); however, attempts to epimerize at C-9 were not fruitful. Epimerization attempts under both basic and acidic conditions returned the starting material (**7.72**) unchanged. We hypothesize that epimerization at C-9 leads to significant steric clash between the amide moiety and the geminal-methyls at C-4.

**Figure 7.4.2.**  $\alpha$ -Oxygenation of amide **7.66**.

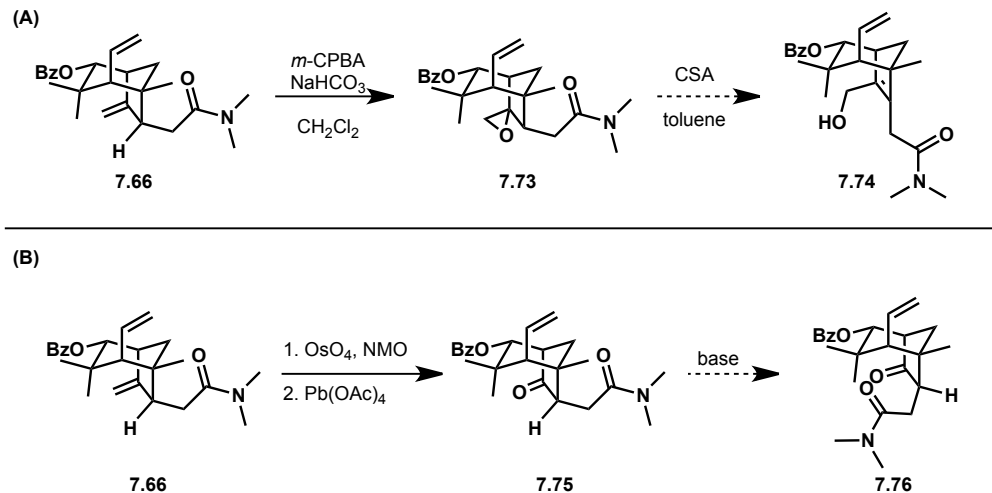


| Conditions                 | Result                            |
|----------------------------|-----------------------------------|
| LDA, Davis oxaziradine     | <b>7.66</b>                       |
| LDA, O <sub>2</sub>        | 3:1 ( <b>7.66</b> : <b>7.71</b> ) |
| LDA, O <sub>2</sub> , HMPA | 3:1 ( <b>7.66</b> : <b>7.71</b> ) |
| LDA, MoOPh                 | <b>7.66</b>                       |

Other efforts to correct the C-9 stereochemistry focused on oxidation of the exocyclic methylene of **7.66**. We envisioned obliterating the C-9 stereochemistry by epoxidizing the exocyclic methylene of **7.66** and opening the epoxide to allylic alcohol **7.74** (Scheme 7.4.2A). The first half of this plan was executed by epoxidation of **7.66** with *m*-chloroperbenzoic acid, providing a single diastereomer of **7.73**. However, attempts to open epoxide **7.73** under the previously successful acidic conditions led to a complex mixture of products. It is possible that the amide moiety could be engaged in the epoxide opening, leading to a plethora of reaction pathways. Subjection of epoxide **7.73** to basic conditions resulted in recovery of the starting material.

In addition to attempting to epimerize at C-9 from  $\alpha$ -ketoamide **7.72**, we installed a ketone at C-8 in anticipation that epimerization would occur more readily from this compound (see Scheme 7.4.2B). The exocyclic double bond of **7.66** was transformed to a carbonyl in two steps, by first dihydroxylating with osmium tetroxide and subsequently cleaving the 1,2-diol to the ketone (**7.75**) with lead(IV) acetate. Lead(IV) acetate was enlisted to cleave the 1,2-diol after attempts to effect this oxidative cleavage with sodium periodate returned 1,2-diol. From ketone **7.75**, epimerization at C-9 under strongly basic conditions was not observed.

### Scheme 7.4.2. Other inversion strategies.

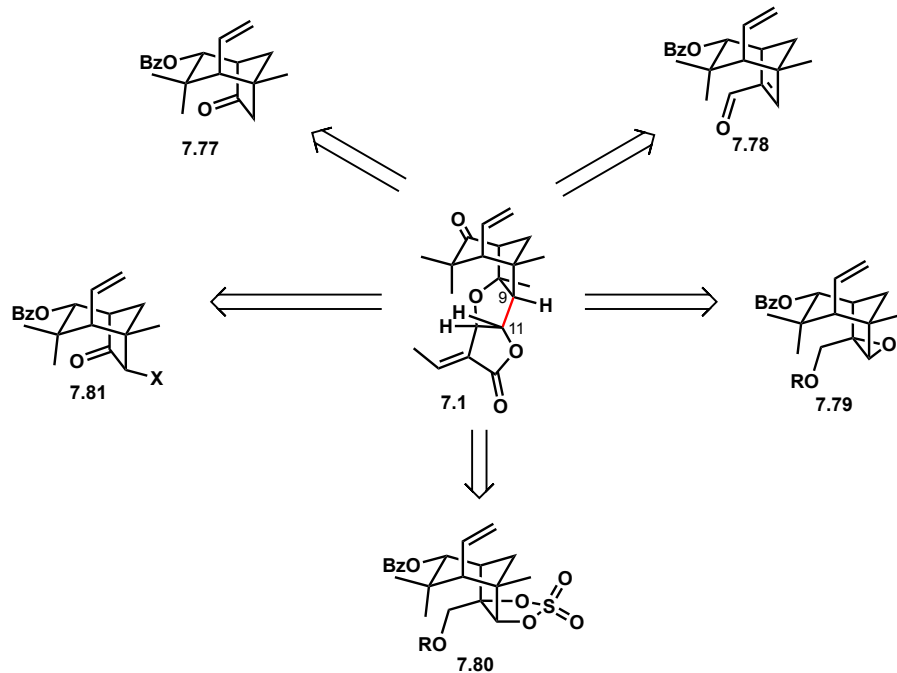


### 7.5 Alternative Approaches Toward Pallavicinin

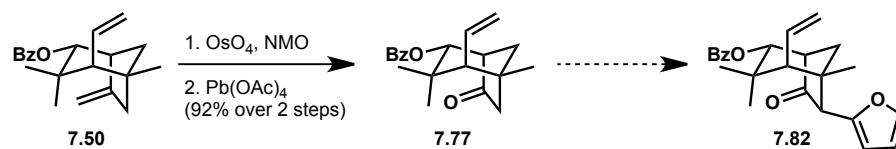
Thus far, the work toward pallavicinin has involved forming the C-9-C-11 bond through a Claisen rearrangement. Concurrent with our efforts to arrive at Claisen product **7.66** and correct its stereochemistry at C-9, we also explored alternative strategies for constructing the C-9-C-11 bond. We envisioned forming this key carbon-carbon bond from strategically functionalized [3.2.1]bicycles (Figure 7.5.1), several of which are described herein.

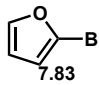
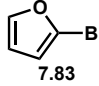
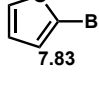
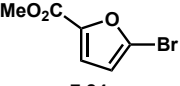
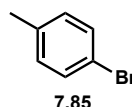
Several possibilities for formation of the C-9-C-11 bond from ketone **7.77** or derivatives of this compound have been explored. From the gold-cyclization product (**7.50**), ketone **7.77** was obtained via dihydroxylation of the exocyclic double bond and subsequent oxidative cleavage with lead(IV) acetate. Ketone **7.77** was subjected to several variants of the standard  $\alpha$ -arylation conditions (Figure 7.5.2).<sup>10</sup> Reactions with either 2-bromofuran (**7.83**) or a more electron-deficient bromofuran **7.84** did not lead to arylation of ketone **7.77** under a variety of conditions. Although, literature precedent exists for the  $\alpha$ -arylation of ketones with 2-bromofurans, these often proceeded in low yields. As a control reaction, the reactivity of bromotoluene **7.85** with our [3.2.1]bicycle **7.77** was tested. No arylated product was observed in this reaction, suggesting that the aryl component of the reaction was not the problem. We hypothesized that the inability of ketone **7.77** to participate in the  $\alpha$ -arylation reaction could be attributed to the steric bulk surrounding the carbonyl or poor orbital-overlap resulting in an unexpectedly high pKa at the  $\alpha$ -position. Further exploration of the reactivity of ketone **7.77** points to the former explanation, as the latter is discredited by our ability to form the silyl enol ether of the ketone.

**Figure 7.5.1.** Alternative carbon-carbon bond forming strategies.



**Figure 7.5.2.** Arylation attempts.



| conditions  | coupling partner  | result |
|---|---|--------|
| 5 mol % Pd <sub>2</sub> (dba) <sub>3</sub> , 20 mol % Johnphos<br>NaOt-Bu, toluene, 70 °C                       | <br>7.83 | SM     |
| 5 mol % Pd <sub>2</sub> (dba) <sub>3</sub> , 20 mol % Johnphos<br>NaOt-Bu, toluene, 100 °C                      | <br>7.83 | SM     |
| 5 mol % Pd <sub>2</sub> (dba) <sub>3</sub> , 20 mol % P( <i>t</i> -Bu) <sub>3</sub><br>NaOt-Bu, toluene, 120 °C | <br>7.83 | SM     |
| 5 mol % Pd <sub>2</sub> (dba) <sub>3</sub> , 20 mol % P( <i>t</i> -Bu) <sub>3</sub><br>NaOt-Bu, toluene, 120 °C | <br>7.84 | SM     |
| 5 mol % Pd <sub>2</sub> (dba) <sub>3</sub> , 20 mol % P( <i>t</i> -Bu) <sub>3</sub><br>NaOt-Bu, toluene, 120 °C | <br>7.85 | SM     |

Although direct arylation of ketone **7.77** was not fruitful, the ketone could be converted to silyl enol ether **7.91** under soft enolization conditions (Scheme 7.5.1). From silyl enol ether **7.91**, we envisioned forming the C-9-C-11 bond from an intermediate palladium-enolate. After a survey of reaction conditions, the best result was obtained when silyl enol ether **7.91** was treated with palladium(II) acetate and furan. These conditions provided **7.82** in up to a 20% yield. We were encouraged by the ability to form the desired carbon-carbon bond with this method; however, efforts to increase the yield of this transformation were not fruitful, but more importantly the stereochemistry at C-9 of **7.82** was epimeric to that required for pallavicinin (see **7.11**, Scheme 7.2.4).

Alternatively, we envisioned forming the C-9-C-11 bond via 1,4-addition of a furan nucleophile to the enal (see **7.78** to **7.86**, Figure 7.5.3). Toward this goal, a survey of reaction conditions evaluated both organocatalytic as well as Lewis acid activation modes and a variety of furan nucleophiles (see **7.87-7.90**). However, upon activation with Lewis acids, only 1,2-addition products were obtained. In cases where organocatalysts were employed, only starting material was recovered. This result was not surprising given the steric bulk of our system and the steric limitations of this method.

**Scheme 7.5.1.** Carbon-carbon bond formation from silyl enol ether **7.91**.

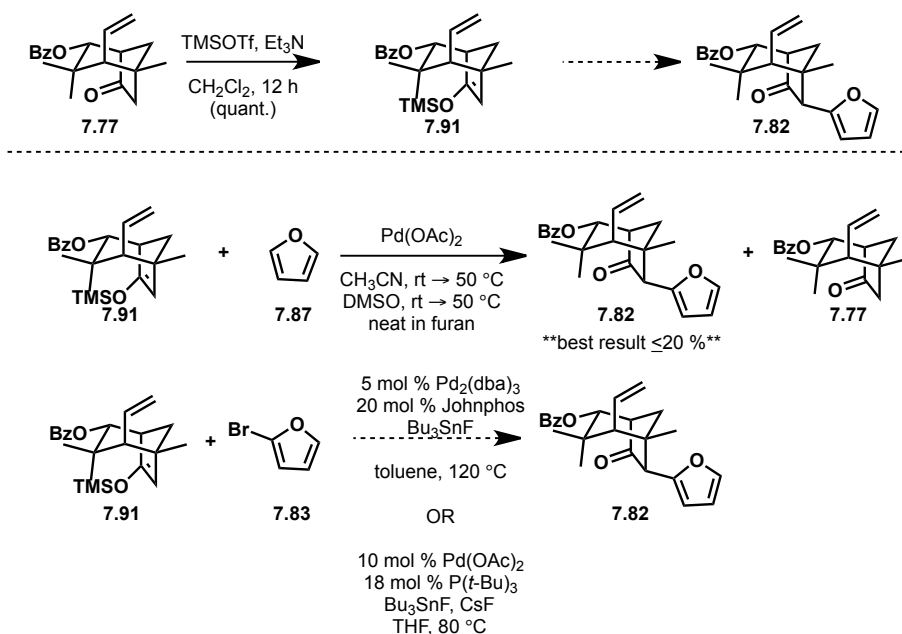
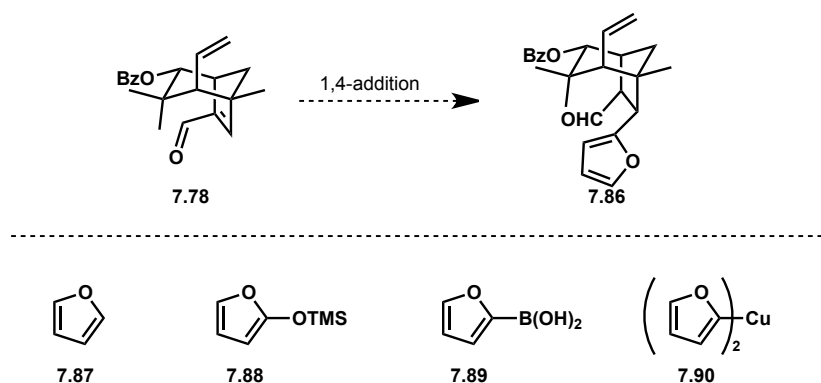
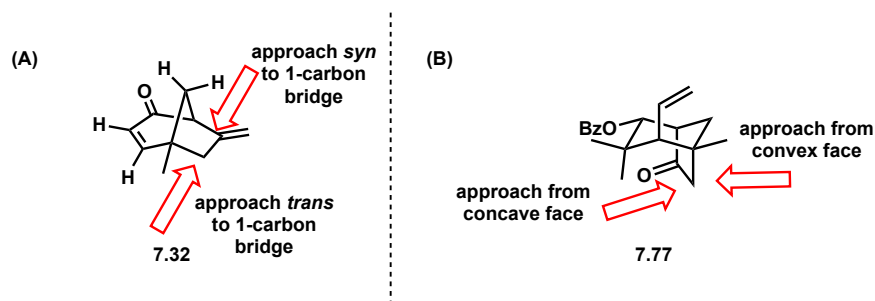


**Figure 7.5.3.** 1,4-addition to enal **7.78**.



Our initial efforts to form the C-9-C-11 bond demonstrated both the challenge in forming this bond and the added difficulty in achieving the correct stereochemistry at C-9. Although the original [3.2.1]bicycle (**7.32**) does not have a clear concave and convex face, the elaborated bicycle (**7.77**) possess a more sterically hindered concave face (Figure 7.5.4). Analysis of the two faces of the bicycle provides insight into the propensity of carbon-carbon bond formation to occur on the convex face of the bicycle (Figure 7.5.4B). To achieve the desired stereochemistry at C-9, a carbon-carbon bond must form on the concave face of the bicycle, which is extremely sterically encumbered with a C-4 methyl group blocking trajectories toward C-9. To overcome unfavorable steric interaction, we envisioned several strategies that would only permit carbon-carbon bond formation on the convex-face of the [3.2.1]bicycle.

**Figure 7.5.4.** Approach from convex and concave faces of bicycle.

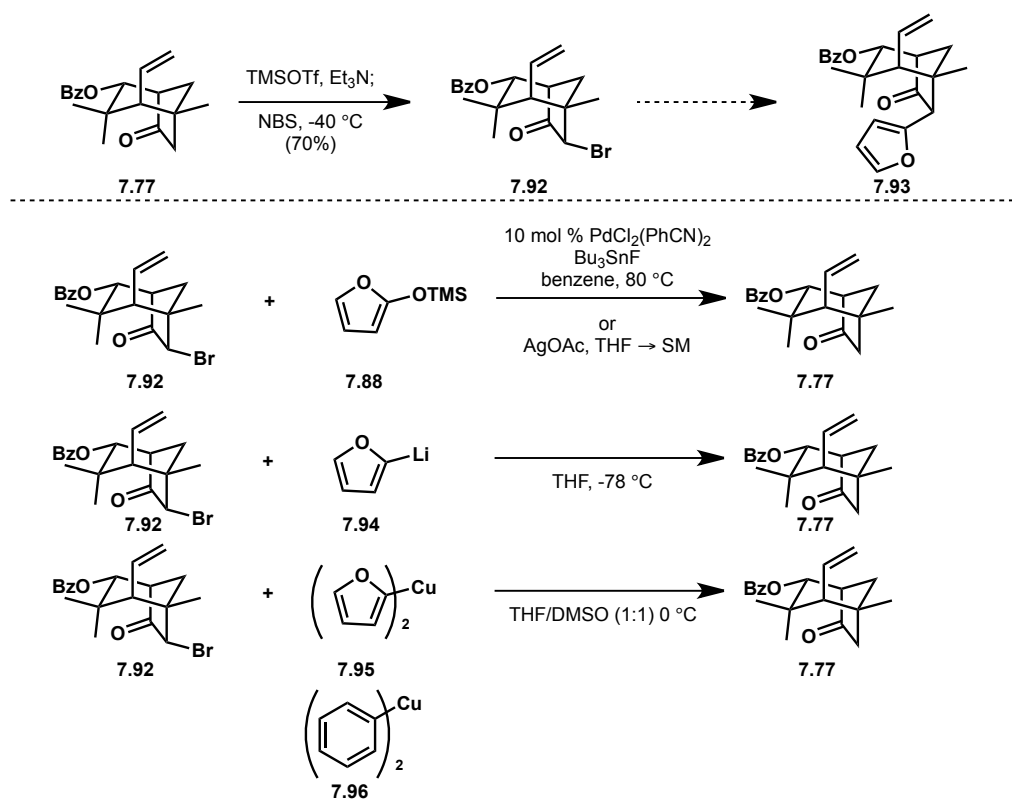


Taking advantage of the innate facial selectivity of **7.77**, a single diastereomer of  $\alpha$ -bromoketone **7.92** was synthesized from ketone **7.77** (Scheme 7.5.2). Under soft enolization conditions, the trimethylsilyl enol ether of ketone **7.77** was formed. *N*-bromosuccinimide was added to the same pot following silyl enol ether formation, affording  $\alpha$ -bromoketone **7.92** in 70% yield. The stereochemistry at C-9 was predicted to arise from bromination of the less sterically hindered face of the silyl enol ether and was subsequently confirmed by an nOe between the hydrogen atoms at C-9 and C-5. From bromide **7.92**, we envisioned stereospecific formation of the C-9-C-11 bond through an S<sub>N</sub>2-type displacement reaction.

Ideally, we sought to employ a furan nucleophile, which would ultimately become the lactone ring present in the natural product. Toward this goal, we attempted to achieve carbon-

carbon bond formation with silyloxyfuran **7.88**. Although silyloxyfuran **7.88** is known to act as a nucleophile in a variety of reactions, it was not productive for carbon-carbon bond formation with bicycle **7.92**. Reactions with the silyloxyfuran **7.88** alone returned the  $\alpha$ -bromoketone. Efforts to create a better nucleophile from **7.88** through formation of the tin or palladium-enolate, afforded des-bromoketone **7.77**. We hypothesize that nucleophile attack occurred at the bromide and not at C-9, generating an enolate that is protonated upon work-up to deliver **7.77**. Utilizing 2-metallated furan (e.g., **7.94** and **7.95**) also resulted in dehalogenation using traditional solvents such as THF as well as mixtures of THF with DMSO, which are reported to provide superior yields for this type of transformation. To eliminate the possibility that the metallated furans were incompetent in this transformation, we examined this reaction with commercially available lithium reagents as well as simple aryl cuprates. These reactions also provided the des-bromoketone **7.77**.

**Scheme 7.5.2.** Efforts to effect bromide displacement.

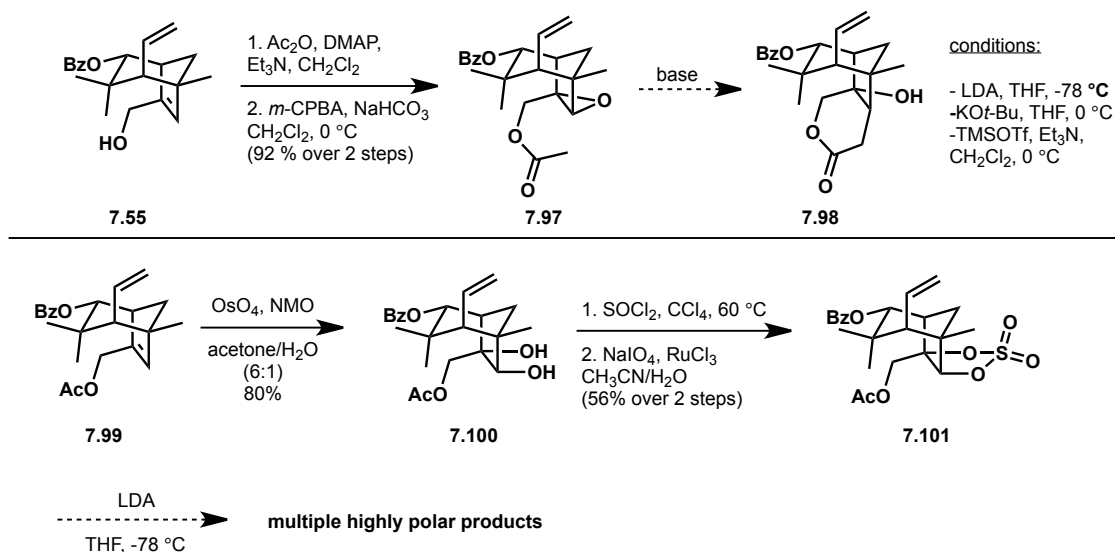


A second approach toward a stereospecific carbon-carbon bond formation was imagined from epoxide **7.97** (Scheme 7.5.3A). Allylic alcohol **7.55** could be converted to epoxide **7.97** via acylation followed by epoxidation with *m*-chloroperbenzoic acid to afford the desired compound **7.97** in 92% yield over two steps. With epoxide **7.97** in hand, we envisioned deprotonation of the acetyl group could lead to carbon-carbon bond formation and concomitant epoxide opening to give rise to lactone **7.98**. In practice, efforts to deprotonate **7.97** with strong bases such as lithium diisopropylamide or potassium *tert*-butoxide did not effect the desired carbon-carbon bond formation. Instead, the acetyl group was removed from the starting compound (**7.97**). We

anticipated that coordination of a Lewis acid could activate the epoxide of **7.97** and facilitate the desired epoxide opening. Toward this end, we treated **7.97** with trimethylsilyl trifluoromethanesulfonate and triethylamine; however, only recovered starting material was obtained from this reaction.

We considered that the epoxide opening could be unfavorable based on the orbital overlap of the epoxide and the tethered nucleophile or due to steric interactions. We devised a similar strategy that could potentially provide superior orbital-overlap between the epoxide and the internal nucleophile. More specifically, we envisioned forming a cyclic sulfate such as **7.101** that could be opened in a manner analogous to epoxide **7.97** (Scheme 7.5.3B). From acylated allylic alcohol **7.99**, dihydroxylation of the trisubstituted double bond provided diol **7.100** in 80% yield. Next, diol **7.100** was reacted with thionyl chloride in carbon tetrachloride at 60 °C to generate a cyclic sulfite. The desired compound was obtained by oxidation of the sulfite to the cyclic sulfate (**7.101**), which proceeded in 56% yield over two steps. From cyclic sulfate **7.101**, efforts to effect the desired carbon-carbon bond formation were not fruitful under basic or Lewis acidic conditions. Under basic conditions, a complex mixture of highly polar products was routinely obtained that did not resemble the desired product.

**Scheme 7.5.3.** Carbon-carbon bond formation via (A) epoxide opening or (B) cyclic sulfate opening.



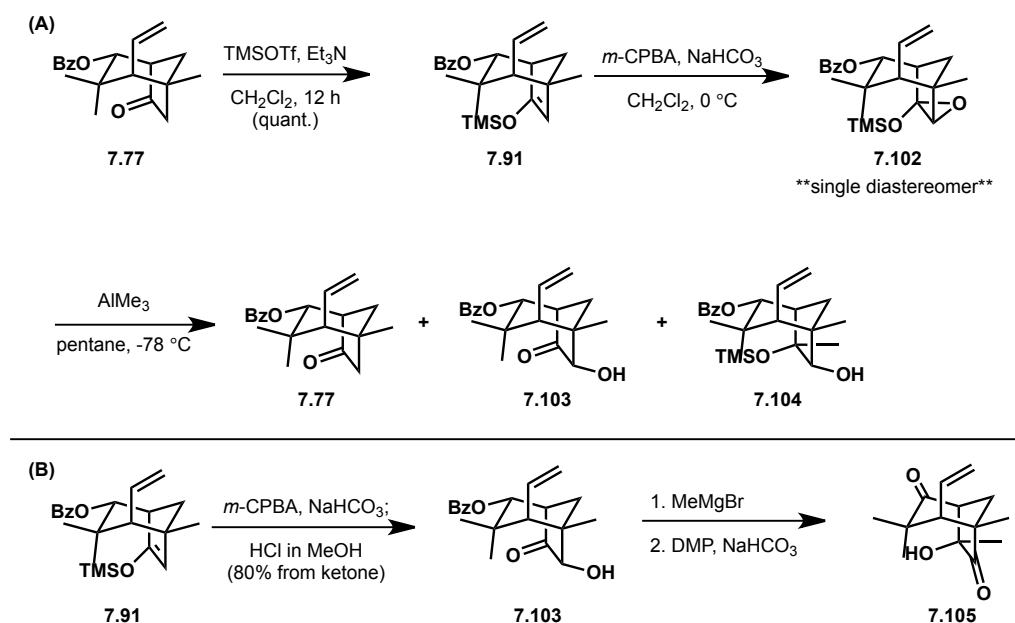
Although the first strategy for stereospecifically opening the epoxide was not successful, a report from the Myers group inspired a second epoxide opening strategy. Myers and coworkers were able to epoxidize silyl enol ethers and open the resulting epoxides with trimethylaluminum to afford *trans*-1,2-diols.<sup>11</sup> We envisioned this method could be applied to the synthesis of pallavicinin to simultaneously install the C-8 methyl group with the requisite stereochemistry and install a hydroxyl group at C-9 that could be utilized as a functional handle for downstream chemistry. In practice, ketone **7.77** was converted to the trimethylsilyl enol ether (**7.91**, Scheme 7.5.1). Although the Myers report exclusively used more robust silyl groups, the triethylsilyl and *tert*-butyldimethylsilyl enol ethers could not be formed from ketone **7.77**. From trimethylsilyl



enol ether **7.91**, epoxidation with *m*-chloroperbenzoic acid buffered with sodium bicarbonate afforded epoxide **7.102**. In the key event, epoxide **7.102** was exposed to trimethylaluminum in pentane at  $-78\text{ }^{\circ}\text{C}$ . From this reaction, a mixture of ketone **7.77**,  $\alpha$ -hydroxy ketone **7.103**, and the desired 1,2-diol (**7.104**) was obtained. The undesired products arise from hydrolysis of silyl enol ether **7.91** to regenerate ketone **7.77**, and collapse of the epoxide (**7.102**) to provide the Rubottom product **7.103**. The formation of these byproducts can be attributed to the labile nature of the trimethyl silyl group. Unable to form a more robust silyl enol ether discouraged us from continuing with this route; however, we anticipated that byproduct **7.103** could be a useful intermediate if it could be made in high yields.

From  $\alpha$ -hydroxyketone **7.103**, we envisioned a 1,2-methyl addition into the C-8 carbonyl group would proceed diastereoselectively. We were able to obtain  $\alpha$ -hydroxyketone **7.103** in 80% yield from silyl enol ether **7.91** using a Rubottom reaction (Scheme 7.5.4B).<sup>12</sup> From  $\alpha$ -hydroxyketone **7.103**, treatment with methylmagnesium bromide resulted in the desired 1,2-addition to the C-8 carbonyl as well as removal of the benzoyl group affording a triol product. The triol was both highly polar and unstable. To avoid decomposition, the triol was oxidized by treating with Dess-Martin periodinane to give a single diastereomer of diketone **7.105**. From **7.105**, attempts to distinguish between the two carbonyl groups were not fruitful and further chemistry from this compound was not explored.

**Scheme 7.5.4.** Alternative epoxide opening.

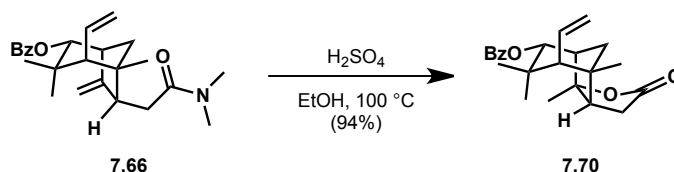


The endeavors described in this section built an appreciation of the high yielding carbon-carbon bond formation achieved in the Claisen rearrangement, but are reminders of the difficulty in achieving the correct stereochemistry at C-9.

## 7.6 Toward 8,9-*epi-epi*-Pallavicinin

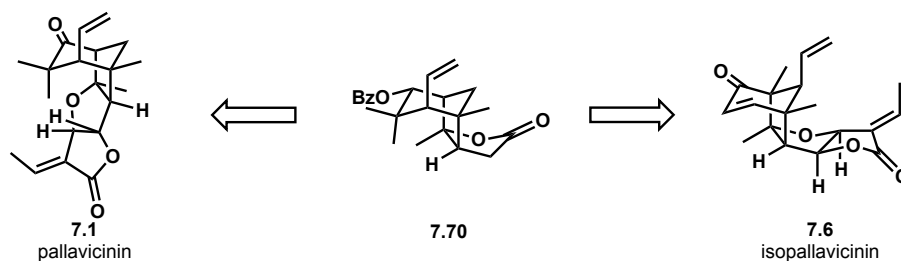
While efforts to correct the stereochemistry at C-9 were underway, we explored the reactivity of the Claisen product (**7.66**). As previously described (see Section 7.4), when treated with sulfuric acid in refluxing ethanol, **7.66** is transformed to lactone **7.70** (Scheme 7.6.1). A crystal structure of **7.70** confirmed the stereochemistry at the fusion of the bicycle and lactone. The incorrect configuration of C-8 and C-9 in **7.70** made this an unsuitable precursor to pallavicinin. However, we anticipated that the chemistry to elaborate **7.70** to 8,9-*epi-epi*-pallavicinin could be used to access pallavicinin from 9-*epi*-**7.66**.

**Scheme 7.6.1.** Lactonization of amide **7.66**.



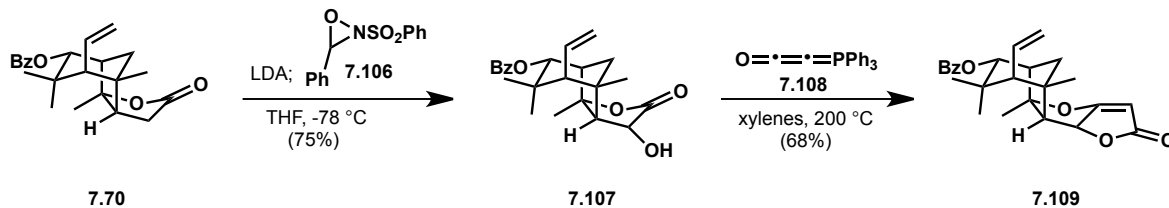
In addition to serving as a model system for late-state chemistry en route to pallavicinin, the synthesis of 8,9-*epi-epi*-pallavicinin will provide us with a compound with the same tetracyclic core as the natural product, isopallavicinin (Figure 7.6.1). We are interested not only in the chemistry that can be used to build these diterpenes, but also the biological activity of these molecules and potential structure-activity relationships that could arise from their stereochemical variants.

**Figure 7.6.1.** Potential application of lactone **7.70** in the synthesis of related diterpenes.



From lactone **7.70**, the construction of a single ring remained to reach the tetracyclic core of these diterpenes. We discovered that the final ring could be installed in two steps from lactone **7.70**. Treatment of **7.70** with lithium diisopropylamide followed by addition of Davis oxaziridine (**7.106**) provided the  $\alpha$ -hydroxylactone (**7.107**) in 75% yield (Scheme 7.6.2). Heating **7.107** with **7.108** in xylenes at 200 °C accomplished the acylation of the  $\alpha$ -hydroxy group and intramolecular Wittig reaction in the same step to afford tetronic ester **7.109** in 68% yield. Efforts to reduce the tetronic ester double bond and install the final two carbons of 8,9-*epi,epi*-pallavicinin are ongoing.

### Scheme 7.6.2. Elaboration of lactone 7.70.



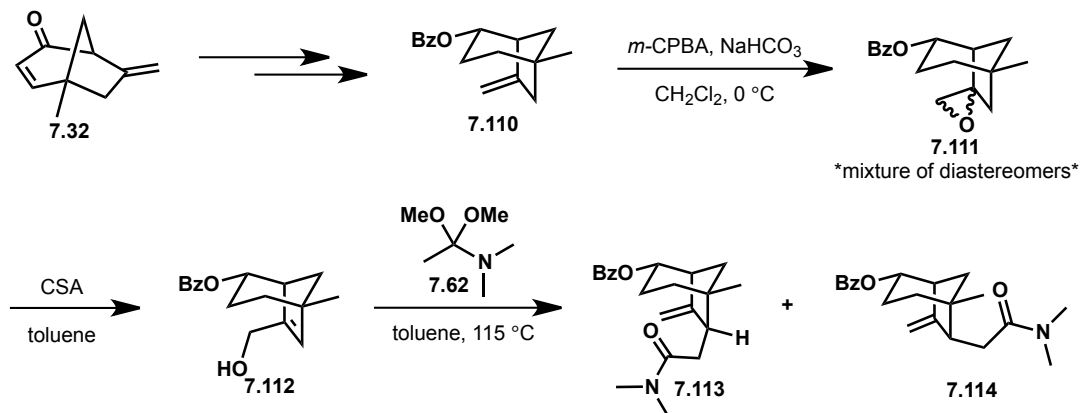
### 7.7 Conclusions and Future Directions

Efforts toward pallavicinin have taught us several lessons about the strain and innate reactivity of the key [3.2.1]bicycle. Building and elaborating bicycle **7.32** ingrained in us the correlation between the number of  $sp^2$ -centers contained within the [3.2.1]bicycle and the magnitude of the ring strain of this system. This strain manifested itself in the resistance of this bicycle to transformations that added to the strain (e.g., increase the number of  $sp^2$ -carbon atoms in the bicycle) and also in facile fragmentation pathways. Understanding the relationship between the strain and the reactivity of the bicycle enabled us to better develop productive strategies toward *P. subciliata* diterpenes.

A significant challenge that remains unsolved in the pursuit of pallavicinin is the formation of the C-9-C-11 bond with the correct configuration. Several strategies to forge this bond were not met with success (see Section 7.5), but we learned that the Eschenmoser-Claisen is a robust reaction for the formation of the key bond. Our excitement in the high-yielding Claisen rearrangement was tempered by the realization that this transformation gives rise to the undesired diastereomer of the amide product (**7.66**). In the future, efforts to correct the C-9 stereochemistry of the Claisen product will continue.

Additionally, an alternative Claisen substrate has demonstrated promise to deliver a product with the correct configuration at C-9. If the enone within bicycle **7.32** is reduced to the allylic alcohol and protected (**7.110**, Scheme 7.7.1), epoxidation of the **7.110** exocyclic methylene provides a mixture of diastereomeric epoxides (**7.111**). Exposure of the mixture of diastereomers to camphorsulfonic acid afforded allylic alcohol **7.112**. From this allylic alcohol (**7.112**), the Eschenmoser-Claisen proceeds under the previously employed conditions to provide two diastereomeric products (**7.113** and **7.114**). This result demonstrates the effect of the C-4 methyl groups on the diastereoselectivity of the Claisen rearrangement.

### Scheme 7.7.1. Des-methyl bicycle 7.112 gives rise to diastereomeric Claisen products.



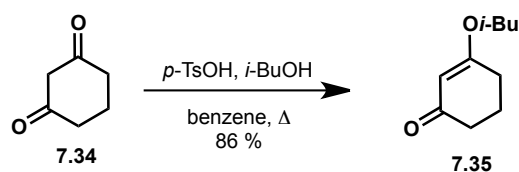
In addition to achieving the stereochemistry necessary for pallavicinin and neopallavicinin, we are also interested in exploiting Claisen product **7.66** to access 8,9-*epi,epi*-pallavicinin and the stereochemically related diterpene, isopallavicinin. With the synthesis of these molecules complete, the next phase will involve biological testing of these compounds. The biological evaluation of these compounds will provide insight into the biological relevance of these natural products and also the effect on bioactivity of the stereochemical differences between these molecules.

### 7.8 Experimental Contributions

Alison Hardin Narayan carried out the research detailed in Chapter 7.

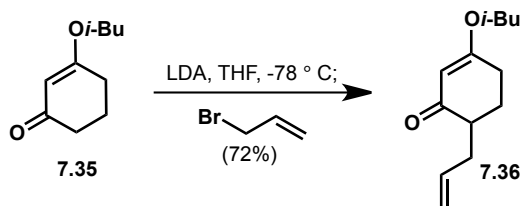
### 7.9 Experimental Methods

Unless otherwise stated, reactions were performed in flame-dried glassware fitted with rubber septa under a nitrogen atmosphere and were stirred with Teflon-coated magnetic stirring bars. Liquid reagents and solvents were transferred via syringe using standard Schlenk techniques. Tetrahydrofuran (THF), diethyl ether, benzene, toluene, and triethylamine were dried over alumina under a nitrogen atmosphere in a GlassContour solvent system. Dichloromethane (DCM) was distilled over calcium hydride. All other solvents and reagents were used as received unless otherwise noted. Reaction temperatures above 23 °C refer to oil or sand bath temperatures, which were controlled by an OptiCHEM temperature modulator. Thin layer chromatography was performed using SiliCycle silica gel 60 F-254 pre-coated plates (0.25 mm) and visualized by UV irradiation and anisaldehyde or potassium permanganate stain. SiliCycle Silica-P silica gel (particle size 40-63  $\mu\text{m}$ ) was used for flash chromatography.  $^1\text{H}$  and  $^{13}\text{C}$  NMR spectra were recorded on Bruker AVB-400, DRX-500, AV-500 and AV-600 MHz spectrometers with  $^{13}\text{C}$  operating frequencies of 100, 125, 125, and 150 MHz, respectively. Chemical shifts ( $\delta$ ) are reported in ppm relative to the residual solvent signal ( $\text{CDCl}_3$ ;  $\delta = 7.26$  for  $^1\text{H}$  NMR and  $\delta = 77.0$  for  $^{13}\text{C}$  NMR;  $\text{C}_6\text{D}_6$ ;  $\delta = 7.15$  for  $^1\text{H}$  NMR and  $\delta = 128.39$  for  $^{13}\text{C}$  NMR). Data for  $^1\text{H}$  NMR spectra are reported as follows: chemical shift (multiplicity, coupling constants, number of hydrogens). Abbreviations are as follows: s (singlet), d (doublet), t (triplet), dd (doublet of doublets), m (multiplet), br (broad). IR spectra were recorded on a Nicolet MAGNA-IR 850 spectrometer and are reported in frequency of absorption ( $\text{cm}^{-1}$ ). Only selected IR absorbencies are reported. High resolution mass spectral data were obtained from the Mass Spectral Facility at the University of California, Berkeley.

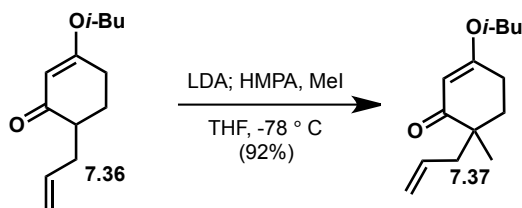


**Vinylogous ester 7.35:** 1,3-cyclohexanedione (**7.34**, 25.0 g, 223 mmol),  $p\text{-TsOH}$  (2.11 g, 11.1 mmol) and isobutanol (35.3 mL, 669 mmol) were combined in benzene (200 mL). The reaction vessel was equipped with a reflux condenser and a Dean-Stark apparatus and was heated to

reflux. After 24 h, the reaction mixture was cooled to room temperature and concentrated. The resulting oil was diluted with Et<sub>2</sub>O (200 mL) and washed with a saturated NaHCO<sub>3(aq)</sub> solution (3 x 100 mL), water (150 mL) and brine (150 mL). The organic layer was dried over MgSO<sub>4</sub> and concentrated to provide a yellow oil. The crude oil was purified via flash chromatography (2:1 hexanes/EtOAc) to afford vinylogous ester **7.35** in 86% yield (32.3 g, 192 mmol). <sup>1</sup>H NMR (400 MHz, CDCl<sub>3</sub>) δ 5.33 (d, *J* = 3.9 Hz, 1H), 3.58 (dd, *J* = 6.4, 3.4 Hz, 2H), 2.40 (td, *J* = 6.2, 3.0 Hz, 2H), 2.36 – 2.29 (m, 2H), 1.98 (dtd, *J* = 12.6, 6.4, 3.2 Hz, 3H), 0.96 (dd, *J* = 6.7, 3.6 Hz, 6H); HRMS (EI<sup>+</sup>) calcd for [C<sub>10</sub>H<sub>16</sub>O<sub>2</sub>]: *m/z* 168.1150, found 168.1151.

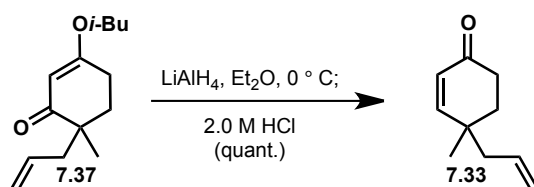


**Allylated vinylogous ester 7.36:** *n*-Butyllithium (28.6 mL, 71.4 mmol, 2.5 M in hexanes) was added dropwise to diisopropyl amine (10.8 mL, 77.4 mmol) in THF (80 mL) at 0 °C. The mixture was stirred at this temperature for 20 min and was then cooled to -78 °C. Vinylogous ester **7.35** (10.0 g, 59.5 mmol) in THF (60 mL) was added to the reaction mixture at -78 °C. After 1 h at -78 °C, allyl bromide (6.70 mL, 77.4 mmol) was added dropwise to the reaction mixture. The reaction mixture was stirred for 3 h as the cold bath gradually expired. The reaction was quenched by the addition of a saturated NH<sub>4</sub>Cl<sub>(aq)</sub> solution (30 mL). The reaction mixture was concentrated and then diluted with water. The aqueous phase was extracted with Et<sub>2</sub>O (3 x 50 mL). The combined organic layer was washed with water (80 mL), brine (80 mL), dried over MgSO<sub>4</sub> and concentrated under reduced pressure to give an orange oil. The crude oil was purified via flash chromatography (4:1 hexanes/EtOAc) to afford a yellow oil in 72% yield (8.92 g, 42.8 mmol). <sup>1</sup>H NMR (400 MHz, CDCl<sub>3</sub>) δ 5.77 (d, *J* = 7.4 Hz, 1H), 5.31 (s, 1H), 5.08 – 5.00 (m, 2H), 3.57 (d, *J* = 6.4 Hz, 2H), 2.68 – 2.59 (m, 1H), 2.44 – 2.38 (m, 2H), 2.23 (td, *J* = 9.0, 4.4 Hz, 1H), 2.17 – 2.08 (m, 1H), 2.08 – 1.97 (m, 2H), 1.75 – 1.64 (m, 1H), 0.96 (d, *J* = 6.7 Hz, 6H); HRMS (ESI<sup>+</sup>) calcd for [C<sub>13</sub>H<sub>21</sub>O<sub>2</sub>]<sup>+</sup> (M-H)<sup>+</sup>: *m/z* 209.1536, found 209.1535.

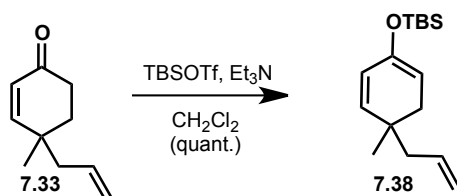


**Methylated vinylogous ester 7.37:** *n*-Butyllithium (11.5 mL, 28.8 mmol, 2.5 M in hexanes) was added dropwise to diisopropyl amine (4.37 mL, 31.2 mmol) in THF (30 mL) at 0 °C. The mixture was stirred at this temperature for 20 min and was then cooled to -78 °C. Vinylogous ester **7.36** (5.00 g, 24.0 mmol) in THF (30 mL) was added to the reaction mixture at -78 °C. After 1 h at -78 °C, HMPA (5.40 mL, 31.2 mmol) and methyl iodide (1.94 mL, 31.2 mmol) were

added dropwise to the reaction mixture. The reaction mixture was stirred for 12 h as the cold bath gradually expired. The reaction was quenched by the addition of a saturated  $\text{NH}_4\text{Cl}_{(\text{aq})}$  solution (30 mL). The reaction mixture was concentrated and then diluted with water. The aqueous phase was extracted with  $\text{Et}_2\text{O}$  (3 x 50 mL). The combined organic layer was washed with water (80 mL), brine (80 mL), dried over  $\text{MgSO}_4$  and concentrated under reduced pressure to give an orange oil. The crude oil was purified via flash chromatography (4:1 hexanes/ $\text{EtOAc}$ ) to afford **7.37** as yellow oil in 92% yield (4.91 g, 22.1 mmol).  $^1\text{H NMR}$  (500 MHz,  $\text{CDCl}_3$ )  $\delta$  5.79 – 5.69 (m, 1H), 5.25 (s, 1H), 5.07 (s, 1H), 5.04 (d,  $J = 7.3$  Hz, 1H), 3.57 (d,  $J = 6.5$  Hz, 2H), 2.42 (t,  $J = 6.4$  Hz, 2H), 2.36 (dd,  $J = 13.7, 7.2$  Hz, 1H), 2.18 (dd,  $J = 13.7, 7.7$  Hz, 1H), 2.06 – 1.98 (m, 1H), 1.92 (dt,  $J = 13.3, 6.6$  Hz, 1H), 1.73 – 1.65 (m, 2H), 1.08 (s, 3H), 0.97 (d,  $J = 6.7$  Hz, 6H); **HRMS** (ESI+) calcd for  $[\text{C}_{14}\text{H}_{23}\text{O}_2]^+$  (M-H) $^+$ :  $m/z$  223.1693, found 223.1692.

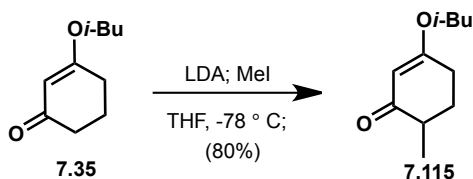


**Enone 7.33:** Lithium aluminum hydride (51.2 mg, 1.35 mmol) was added in portions to vinylogous ester **7.37** (600 mg, 2.70 mmol) in  $\text{Et}_2\text{O}$  (9.0 mL) at  $0\text{ }^\circ\text{C}$ . The reaction mixture was stirred for 30 min while slowly warming to ambient temperature. The mixture was cooled to  $0\text{ }^\circ\text{C}$  and 2 N  $\text{HCl}_{(\text{aq})}$  (9.0 mL) was slowly added over 5 min. The reaction mixture was warmed to room temperature. After 2 h, the aqueous layer was extracted with  $\text{Et}_2\text{O}$  (3 x 20 mL). The combined organic layer was washed with saturated  $\text{NaHCO}_{3(\text{aq})}$  (50 mL), brine, dried over  $\text{MgSO}_4$  and concentrated under reduced pressure to afford enone **7.33x** in 99% yield (402 mg, 2.68 mmol).  $^1\text{H NMR}$  (400 MHz,  $\text{CDCl}_3$ )  $\delta$  6.67 (d,  $J = 10.2$  Hz, 1H), 5.88 (d,  $J = 10.2$  Hz, 1H), 5.85 – 5.72 (m, 1H), 5.11 (t,  $J = 12.6$  Hz, 2H), 2.45 (dd,  $J = 7.7, 5.5$  Hz, 2H), 2.20 (d,  $J = 7.5$  Hz, 2H), 2.01 – 1.92 (m, 1H), 1.81 – 1.72 (m, 1H), 1.14 (s, 3H); **HRMS** (EI+) calcd for  $[\text{C}_{10}\text{H}_{14}\text{O}]$ :  $m/z$  150.1045, found 150.1048.

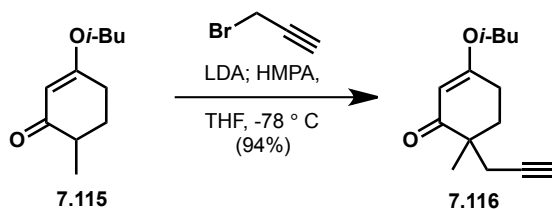


**Silyl enol ether 7.38:** *tert*-Butyldimethylsilyl trifluoromethanesulfonate (688  $\mu\text{L}$ , 3.00 mmol) was added dropwise to a mixture of enone **x.xx** (300 mg, 2.00 mmol) and  $\text{Et}_3\text{N}$  (800  $\mu\text{L}$ , 6.00 mmol) in  $\text{CH}_2\text{Cl}_2$  (4.0 mL). The reaction mixture was stirred overnight at ambient temperature. The reaction mixture was diluted with  $\text{CH}_2\text{Cl}_2$  (10 mL). The organic layer was washed with a saturated  $\text{NaHCO}_{3(\text{aq})}$  solution (2 x 10 mL), brine (10 mL), dried over  $\text{MgSO}_4$  and concentrated under reduced pressure to provide silyl enol ether **7.38** in quantitative yield (523 mg, 1.98

mmol).  $^1\text{H NMR}$  (500 MHz,  $\text{CDCl}_3$ )  $\delta$  5.77 (dd,  $J = 9.9, 2.2$  Hz, 2H), 5.46 (d,  $J = 9.9$  Hz, 1H), 5.00 (dddd,  $J = 16.9, 5.0, 2.4, 1.3$  Hz, 2H), 4.83 (td,  $J = 4.6, 2.1$  Hz, 1H), 2.18 (d,  $J = 4.6$  Hz, 1H), 2.09 – 2.04 (m, 1H), 2.00 (d,  $J = 4.7$  Hz, 2H), 1.01 – 0.96 (m, 10H), 0.15 – 0.11 (m, 6H).

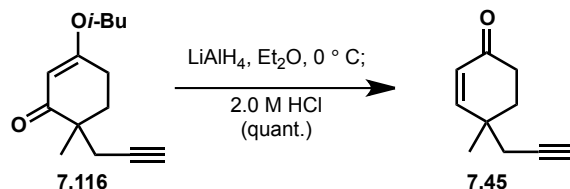


**Methylated vinyllogous ester 7.115:** *n*-Butyllithium (52.4 mL, 131 mmol, 2.5 M in hexanes) was added to diisopropyl amine (20.0 mL, 143 mmol) at  $0\text{ }^\circ\text{C}$ . The mixture was stirred at this temperature for 20 min and was then cooled to  $-78\text{ }^\circ\text{C}$ . Vinyllogous ester **7.35** (20.0 g, 119 mmol) in THF (50 mL) was added to the reaction mixture at  $-78\text{ }^\circ\text{C}$ . After 1 h at  $-78\text{ }^\circ\text{C}$ , methyl iodide (8.50 mL, 143 mmol) was added dropwise to the reaction mixture. The reaction mixture was stirred for 3 h as the cold bath gradually expired. The reaction was quenched by the addition of a saturated  $\text{NH}_4\text{Cl}_{(\text{aq})}$  solution (80 mL). The reaction mixture was concentrated and then diluted with water. The aqueous phase was extracted with  $\text{Et}_2\text{O}$  (3 x 150 mL). The combined organic layer was washed with water (150 mL), brine (150 mL), dried over  $\text{MgSO}_4$  and concentrated under reduced pressure to give yellow oil. The crude oil was purified via flash chromatography (4:1 hexanes/ $\text{EtOAc}$ ) to afford a yellow oil in 80% yield (16.9 g, 92.7 mmol).  $^1\text{H NMR}$  (500 MHz,  $\text{CDCl}_3$ )  $\delta$  5.29 (s, 1H), 3.56 (dd,  $J = 6.5, 3.8$  Hz, 2H), 2.41 (t,  $J = 4.8$  Hz, 2H), 2.27 (s, 1H), 2.02 (ddd,  $J = 13.2, 10.8, 5.8$  Hz, 2H), 1.68 (dtd,  $J = 13.2, 10.7, 5.2$  Hz, 1H), 1.13 (d,  $J = 6.9$  Hz, 3H), 0.95 (dd,  $J = 6.7, 1.0$  Hz, 6H).

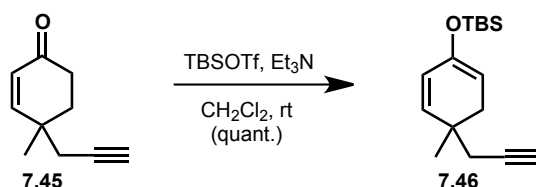


**Dialkylated vinyllogous ester 7.116:** *n*-Butyllithium (44.5 mL, 111 mmol, 2.5 M in hexanes) was added to diisopropyl amine (16.9 mL, 121 mmol) at  $0\text{ }^\circ\text{C}$ . The mixture was stirred at this temperature for 20 min and was then cooled to  $-78\text{ }^\circ\text{C}$ . Vinyllogous ester **7.115** (16.9 g, 92.7 mmol) in THF (50 mL) was added to the reaction mixture at  $-78\text{ }^\circ\text{C}$ . After 1 h at  $-78\text{ }^\circ\text{C}$ , HMPA (19.3 mL, 111 mmol) and propargyl bromide (12.0 mL, 111 mmol, 80 wt% in toluene) was added dropwise to the reaction mixture. The reaction mixture was stirred for 12 h as the cold bath gradually expired. The reaction was quenched by the addition of a saturated  $\text{NH}_4\text{Cl}_{(\text{aq})}$  solution (80 mL). The reaction mixture was concentrated and then diluted with water. The aqueous phase was extracted with  $\text{Et}_2\text{O}$  (3 x 150 mL). The combined organic layer was washed with water (150 mL), brine (150 mL), dried over  $\text{MgSO}_4$  and concentrated under reduced pressure to give yellow oil. The crude oil was purified via flash chromatography (4:1 hexanes/ $\text{EtOAc}$ ) to afford a yellow oil in 94% yield (19.3 g, 87.6 mmol).  $^1\text{H NMR}$  (500 MHz,  $\text{CDCl}_3$ )  $\delta$  5.26 (s, 1H), 3.58 (d,  $J = 6.5$  Hz, 2H), 2.54 – 2.47 (m, 1H), 2.44 (t,  $J = 3.3$  Hz, 3H),

2.11 (ddd,  $J = 14.8, 9.5, 5.5$  Hz, 1H), 2.02 (d,  $J = 24.1$  Hz, 2H), 1.90 (dt,  $J = 13.5, 5.3$  Hz, 1H), 1.17 (s, 3H), 0.97 (d,  $J = 6.7$  Hz, 6H).

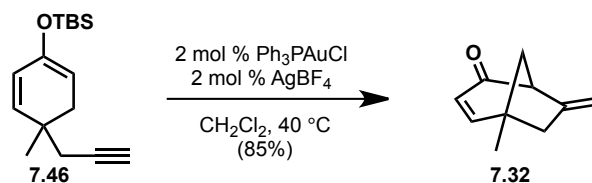


**Enone 7.45:** Lithium aluminum hydride (861 mg, 22.7 mmol) was added in portions to vinylogous ester **7.116** (10.0 g, 45.4 mmol) in Et<sub>2</sub>O (90 mL) at 0 °C. The reaction mixture was stirred for 30 min while slowly warming to ambient temperature. The mixture was cooled to 0 °C and 2 N HCl<sub>(aq)</sub> (90 mL) was slowly added over 10 min. The reaction mixture was warmed to room temperature. After 2 h, the aqueous layer was extracted with Et<sub>2</sub>O (3 x 150 mL). The combined organic layer was washed with saturated NaHCO<sub>3(aq)</sub> (150 mL), brine, dried over MgSO<sub>4</sub> and concentrated under reduced pressure to afford enone **7.45** in 99% yield (6.64 g, 44.8 mmol). <sup>1</sup>H NMR (300 MHz, CDCl<sub>3</sub>) δ 6.76 (d,  $J = 10.2$  Hz, 1H), 5.93 (d,  $J = 10.2$  Hz, 1H), 3.42 (d,  $J = 6.3$  Hz, 2H), 2.48 (t,  $J = 7.2$  Hz, 2H), 2.33 (d,  $J = 2.5$  Hz, 2H), 2.18 (d,  $J = 12.5$  Hz, 1H), 2.11 – 2.04 (m, 3H), 1.90 (d,  $J = 6.0$  Hz, 2H), 1.76 (s, 1H), 1.66 – 1.60 (m, 3H), 1.26 (s, 3H); <sup>13</sup>C NMR (151 MHz, CDCl<sub>3</sub>) δ 198.9, 156.6, 128.2, 80.2, 71.3, 35.6, 34.0, 33.6, 30.8, 24.4; IR (film)  $\nu_{\max}$  3291, 2963, 1678 cm<sup>-1</sup>.

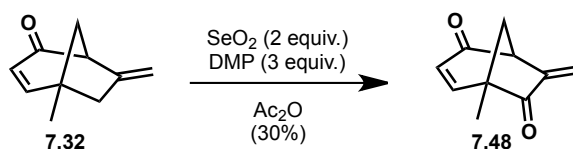


**Silyl enol ether 7.46:** *tert*-Butyldimethylsilyl trifluoromethanesulfonate (11.3 mL, 49.5 mmol) was added dropwise to a mixture of enone **7.45** (6.70 g, 45.0 mmol) and Et<sub>3</sub>N (17.9 mL, 135 mmol) in CH<sub>2</sub>Cl<sub>2</sub> (50 mL). The reaction mixture was stirred overnight at ambient temperature. The reaction mixture was diluted with CH<sub>2</sub>Cl<sub>2</sub> (100 mL). The organic layer was washed with a saturated NaHCO<sub>3(aq)</sub> solution (2 x 100 mL), brine (100 mL), dried over MgSO<sub>4</sub> and concentrated under reduced pressure to provide silyl enol ether **7.46** in 98% yield (11.6 g, 44.1 mmol). <sup>1</sup>H NMR (500 MHz, CDCl<sub>3</sub>) δ 5.74 (dd,  $J = 9.9, 2.1$  Hz, 1H), 5.54 (d,  $J = 9.9$  Hz, 1H), 4.79 (d,  $J = 1.7$  Hz, 1H), 2.30 (dd,  $J = 16.8, 4.7$  Hz, 1H), 2.09 (dd,  $J = 7.4, 2.6$  Hz, 2H), 2.01 (dd,  $J = 16.8, 4.6$  Hz, 1H), 1.76 (t,  $J = 2.7$  Hz, 1H), 1.08 (s, 3H), 0.97 – 0.95 (m, 9H), 0.11 – 0.08 (m, 6H).

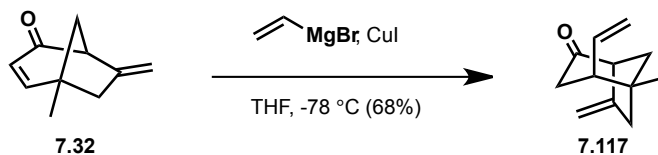




**Bicycle 7.32:** Silver tetrafluoroborate (40.0 mg, 0.190 mmol) was added to a mixture of silyl enol ether **7.46** (2.50 g, 9.52 mmol) and  $\text{AuCl}(\text{PPh}_3)$  (94.0 mg, 0.190 mmol) in a 10:1 mixture of  $\text{CH}_2\text{Cl}_2$  and water (total volume = 22 mL). The reaction vessel was sealed and heated to  $40\text{ }^\circ\text{C}$  for 12 h. The reaction mixture was cooled to room temperature and concentrated to afford a deep green oil. The crude oil was purified via flash chromatography to provide a 85% yield of bicycle **7.32** (1.20 g, 8.09 mmol).  $^1\text{H NMR}$  (500 MHz,  $\text{CDCl}_3$ )  $\delta$  6.92 (dd,  $J = 9.7, 2.0$  Hz, 1H), 5.76 (dd,  $J = 9.7, 1.5$  Hz, 1H), 5.24 (s, 1H), 5.02 (s, 1H), 3.43 (d,  $J = 4.9$  Hz, 1H), 2.41 – 2.31 (m, 2H), 2.06 (d,  $J = 11.2$  Hz, 1H), 1.78 (ddd,  $J = 11.2, 5.0, 2.0$  Hz, 1H), 1.34 (s, 3H);  $^{13}\text{C NMR}$  (126 MHz,  $\text{C}_6\text{D}_6$ )  $\delta$  198.8, 159.8, 146.1, 126.0, 112.0, 59.1, 47.0, 43.6, 42.8, 23.6; **HRMS** (EI+) calcd for  $[\text{C}_{10}\text{H}_{12}\text{O}]$ :  $m/z$  148.0888, found 148.0882.

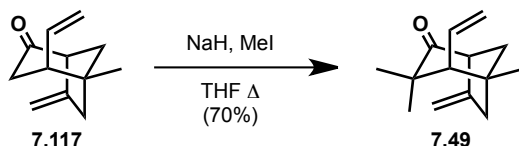


**Dienone 7.48:** Selenium dioxide (41.1 mg, 0.371 mmol) was added to a mixture of bicycle **7.32** (50.0 mg, 0.337 mmol) and Dess-Martin periodinane (314 mg, 0.714 mmol) in  $\text{Ac}_2\text{O}$  (2.0 mL). The reaction mixture was stirred at ambient temperature for 4 h. The reaction was quenched by addition of saturated  $\text{Na}_2\text{SO}_3(\text{aq})$  (2.0 mL). The aqueous phase was extracted with  $\text{Et}_2\text{O}$  (3.0 mL). The organic layer was washed with saturate  $\text{NaHCO}_3(\text{aq})$  (4 x 3.0 mL), brine (3.0 mL), dried over  $\text{MgSO}_4$  and concentrated under reduced pressure to provide a white solid. The crude product was purified via flash chromatography (4:1 hexanes/ $\text{EtOAc}$ ) to afford **7.48** in 28% yield (15.2 mg, 0.0937 mmol).  $^1\text{H NMR}$  (500 MHz,  $\text{CDCl}_3$ )  $\delta$  6.75 (dd,  $J = 9.5, 2.2$  Hz, 1H), 6.18 (s, 1H), 5.94 (dd,  $J = 9.5, 1.0$  Hz, 1H), 5.71 (s, 1H), 3.64 (d,  $J = 4.6$  Hz, 1H), 2.57 (d,  $J = 11.6$  Hz, 1H), 2.06 (ddd,  $J = 11.6, 4.7, 2.2$  Hz, 1H), 1.40 (s, 3H).

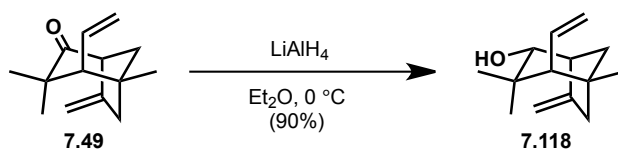


**Bicycle 7.117:** Copper(I) iodide (1.43 g, 7.50 mmol) was added to vinylmagnesium bromide (7.50 mL, 7.50 mmol, 1 M in THF) in THF (20 mL) at  $-78\text{ }^\circ\text{C}$ . After 30 min, bicycle **7.32** (1.01 g, 6.82 mmol) in THF (5.0 mL) was added dropwise at  $-78\text{ }^\circ\text{C}$ . The reaction mixture was stirred for 1 h slowly warming to room temperature. The reaction was quenched with a saturated

$\text{NH}_4\text{Cl}_{(\text{aq})}$  solution (40 mL). The aqueous phase was extracted with  $\text{Et}_2\text{O}$  (3 x 40 mL). The combined organic layer was washed with water (50 mL), brine (50 mL), dried over  $\text{MgSO}_4$  and concentrated under reduced pressure to give a yellow oil. The crude oil was purified via flash chromatography (4:1 hexanes/ $\text{EtOAc}$ ) to afford **7.117** in 68% yield (663 mg, 3.76 mmol).  $^1\text{H NMR}$  (500 MHz,  $\text{CDCl}_3$ )  $\delta$  5.91 – 5.82 (m, 1H), 5.10 (d,  $J = 10.4$  Hz, 1H), 5.03 (d,  $J = 16.1$  Hz, 2H), 4.91 (s, 1H), 3.20 (d,  $J = 5.1$  Hz, 1H), 2.82 (dd,  $J = 15.9, 8.1$  Hz, 1H), 2.58 (d,  $J = 1.6$  Hz, 1H), 2.53 – 2.44 (m, 2H), 2.15 (d,  $J = 15.9$  Hz, 1H), 1.98 (dd,  $J = 12.4, 2.0$  Hz, 1H), 1.65 (dd,  $J = 5.2, 2.2$  Hz, 1H), 1.13 (s, 3H).

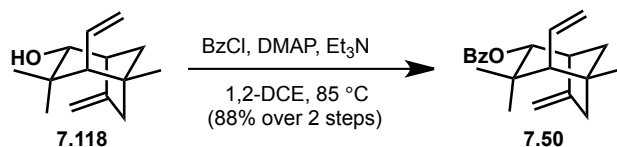


**Dimethyl bicyclic 7.49:** Sodium hydride (749 mg, 18.7 mmol, 60 wt% in mineral oil) was added in portions to bicyclic **7.117** (660 mg, 3.74 mmol) and methyl iodide (2.33 mL, 37.4 mmol) in THF (20 mL) at room temperature. The mixture was stirred, open to an atmosphere of  $\text{N}_2$  for 1 h. Then, the Schlenk flask was sealed and heated to 60 °C for 36 h. The reaction mixture was cooled to room temperature and quenched with a saturated  $\text{NH}_4\text{Cl}_{(\text{aq})}$  solution (20 mL). The aqueous phase was extracted with  $\text{Et}_2\text{O}$  (3 x 20 mL). The combined organic layer was washed with water (30 mL), brine (30 mL), dried over  $\text{MgSO}_4$  and concentrated under reduced pressure to provide a yellow oil. The crude oil was purified via flash chromatography (9:1 hexanes/ $\text{EtOAc}$ ) to afford dimethyl bicyclic **7.49** in 70% yield (534 mg, 2.62 mmol).  $^1\text{H NMR}$  (500 MHz,  $\text{CDCl}_3$ )  $\delta$  5.65 (d,  $J = 16.7$  Hz, 1H), 5.12 (s, 1H), 5.02 (dd,  $J = 10.0, 2.0$  Hz, 1H), 4.92 (dd,  $J = 16.7, 1.6$  Hz, 1H), 4.87 (s, 1H), 3.31 (d,  $J = 4.8$  Hz, 1H), 2.56 (s, 1H), 2.44 (t,  $J = 10.0$  Hz, 1H), 2.14 (dd,  $J = 10.9, 1.6$  Hz, 1H), 1.96 (d,  $J = 12.4$  Hz, 1H), 1.63 (dd,  $J = 19.6, 2.3$  Hz, 2H), 1.25 (s, 3H), 1.06 (s, 3H), 1.04 – 1.01 (m, 1H), 0.95 (s, 3H);  $^{13}\text{C NMR}$  (151 MHz,  $\text{CDCl}_3$ )  $\delta$  214.2, 148.3, 138.5, 116.1, 108.8, 62.5, 60.3, 47.1, 46.2, 42.4, 38.9, 34.2, 26.6, 26.4; **IR** (film)  $\nu_{\text{max}}$  2975, 1702, 1455, 1382  $\text{cm}^{-1}$ ; **HRMS** (EI+) calcd for  $[\text{C}_{14}\text{H}_{20}\text{O}]$ :  $m/z$  204.1514, found 204.1518.

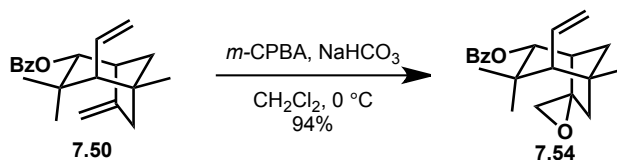


**Alcohol 7.118:** Lithium aluminum hydride (42.7 mg, 1.13 mmol) was added to ketone **7.49** (230 mg, 1.13 mmol) in  $\text{Et}_2\text{O}$  (3.0 mL) at 0 °C. The reaction mixture was stirred at 0 °C for 1 h. The reaction was quenched by the sequential addition of 50  $\mu\text{L}$  water, 50  $\mu\text{L}$  10%  $\text{NaOH}_{(\text{aq})}$  and 150  $\mu\text{L}$  water which induced the formation of a white precipitate. The mixture was filtered through a pad of celite and concentrated under reduced pressure to afford alcohol **7.118** in 90% yield (208 mg, 1.01 mmol) which was used without further purification.  $^1\text{H NMR}$  (500 MHz,  $\text{CDCl}_3$ )  $\delta$  5.73 (d,  $J = 16.8$  Hz, 1H), 5.04 (s, 1H), 4.99 (dd,  $J = 10.1, 2.3$  Hz, 1H), 4.87 (dd,  $J = 16.8, 2.2$  Hz, 1H), 4.82 (s, 1H), 3.44 (dd,  $J = 11.0, 3.5$  Hz, 1H), 2.61 (d,  $J = 4.5$  Hz, 1H), 2.46 (d,  $J = 1.7$

Hz, 1H), 2.20 (d,  $J = 17.4$  Hz, 1H), 1.92 (dd,  $J = 10.9, 1.9$  Hz, 1H), 1.75 (d,  $J = 11.0$  Hz, 1H), 1.67 (dd,  $J = 11.9, 2.7$  Hz, 1H), 1.43 – 1.36 (m, 1H), 1.06 (s, 3H), 0.96 (s, 3H), 0.86 (s, 3H);  $^{13}\text{C}$  NMR (151 MHz,  $\text{CDCl}_3$ )  $\delta$  151.94, 139.50, 115.68, 106.62, 78.21, 62.62, 51.61, 46.28, 42.85, 39.67, 37.89, 31.23, 27.13, 26.63; IR (film)  $\nu_{\text{max}}$  3457, 3071, 2948, 1431  $\text{cm}^{-1}$ ; HRMS (EI+) calcd for  $[\text{C}_{14}\text{H}_{22}\text{O}]$ :  $m/z$  206.1671, found 206.1669.

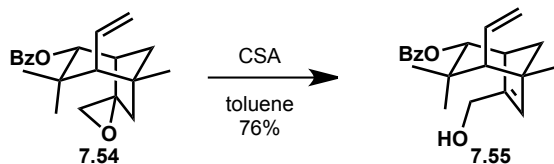


**Benzoate 7.50:** Benzoyl chloride (8.39 mL, 72.3 mmol) was added to a mixture of alcohol **7.118** (2.98 g, 14.5 mmol), DMAP (177 mg, 1.45 mmol), and  $\text{Et}_3\text{N}$  (20.2 mL, 145 mmol) in 1,2-DCE (40 mL). The reaction mixture was heated to 85  $^\circ\text{C}$  for 24 h. The reaction mixture was cooled to room temperature and diluted with  $\text{Et}_2\text{O}$  (80 mL). The organic layer was washed with saturated  $\text{NH}_4\text{Cl}_{(\text{aq})}$  (50 mL), 5%  $\text{NaOH}_{(\text{aq})}$  (50 mL), brine (50 mL), dried over  $\text{MgSO}_4$  and concentrated under reduced pressure to provide a yellow oil. The crude oil was purified via flash chromatography (9:1 hexanes/ $\text{EtOAc}$ ) to afford benzoate **7.50** in 88% yield (3.96g, 12.8 mmol).  $^1\text{H}$  NMR (500 MHz,  $\text{CDCl}_3$ )  $\delta$  8.12 – 8.07 (m, 2H), 7.56 (d,  $J = 7.4$  Hz, 1H), 7.45 (dd,  $J = 10.7, 4.8$  Hz, 2H), 5.81 (d,  $J = 16.8$  Hz, 1H), 5.04 (dd,  $J = 10.0, 2.2$  Hz, 1H), 5.00 – 4.95 (m, 2H), 4.91 (dd,  $J = 16.7, 2.1$  Hz, 1H), 4.83 (s, 1H), 2.83 – 2.79 (m, 1H), 2.58 (s, 1H), 2.26 (d,  $J = 17.3$  Hz, 1H), 2.00 (dd,  $J = 10.9, 1.7$  Hz, 1H), 1.82 (dd,  $J = 12.0, 2.7$  Hz, 1H), 1.46 – 1.39 (m, 1H), 1.36 (s, 3H), 1.02 (d,  $J = 12.8$  Hz, 3H), 0.83 (s, 3H);  $^{13}\text{C}$  NMR (126 MHz,  $\text{CDCl}_3$ )  $\delta$  166.2, 150.8, 139.2, 132.8, 130.8, 129.6, 128.4, 116.1, 107.6, 80.7, 63.0, 48.4, 46.3, 42.8, 39.6, 37.2, 31.2, 27.8, 27.2; IR (film)  $\nu_{\text{max}}$  2926, 2869, 1719, 1272  $\text{cm}^{-1}$ ; HRMS (EI+) calcd for  $[\text{C}_{21}\text{H}_{26}\text{O}_2]$ :  $m/z$  310.1933, found 310.1939.

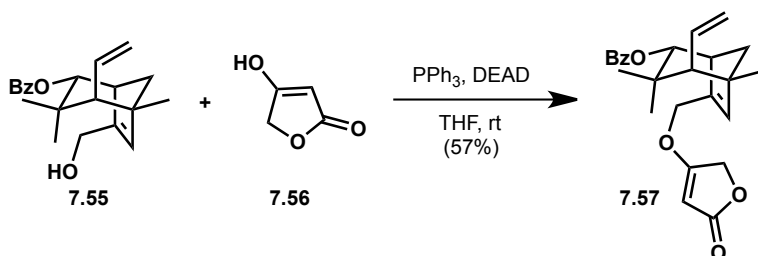


**Epoxide 7.54:** *m*-Chloroperbenzoic acid (768 mg, 3.12 mmol, 70 wt%) was added to a mixture of bicycle **7.50** (806 mg, 2.60 mmol) and sodium bicarbonate (655 mg, 7.80 mmol) in  $\text{CH}_2\text{Cl}_2$  (26 mL). The mixture was stirred at room temperature for 1 h. The reaction was quenched by the addition of a saturated  $\text{Na}_2\text{SO}_3_{(\text{aq})}$  solution (10 mL). The aqueous layer was extracted with  $\text{CH}_2\text{Cl}_2$  (3 x 20 mL). The combined organic layer was washed with  $\text{NaHCO}_3_{(\text{aq})}$  (20 mL), brine, dried over  $\text{MgSO}_4$  and concentrated under reduced pressure to give epoxide **7.54** as a colorless oil in 94% yield (798 mg, 2.44 mg). The crude epoxide was used without further purification.  $^1\text{H}$  NMR (600 MHz,  $\text{CDCl}_3$ )  $\delta$  8.02 (d,  $J = 7.8$  Hz, 2H), 7.58 (s, 1H), 7.46 (t,  $J = 7.5$  Hz, 3H), 5.81 (d,  $J = 16.8$  Hz, 1H), 5.07 (dd,  $J = 12.8, 2.6$  Hz, 2H), 4.94 (dd,  $J = 16.7, 1.8$  Hz, 1H), 3.14 (d,  $J = 4.7$  Hz, 1H), 3.01 (d,  $J = 4.7$  Hz, 1H), 2.32 (dd,  $J = 14.9, 2.0$  Hz, 1H), 2.05 (d,  $J = 3.9$  Hz, 1H), 2.01 (d,  $J = 10.8$  Hz, 1H), 1.88 (s, 4H), 1.43 (s, 3H), 1.06 (s, 3H), 0.88 (s, 4H);  $^{13}\text{C}$  NMR (151

MHz, CDCl<sub>3</sub>)  $\delta$  165.7, 138.4, 133.0, 130.2, 129.4, 129.4, 128.5, 116.7, 80.1, 64.1, 62.4, 51.3, 48.2, 46.5, 43.9, 38.8, 36.9, 31.0, 29.7, 27.2, 26.6; **IR** (film)  $\nu_{\max}$  2924, 1717, 1273, 1110 cm<sup>-1</sup>; **LRMS** (EI+) calcd for [C<sub>21</sub>H<sub>26</sub>O<sub>3</sub>]:  $m/z$  326.19, found 326.

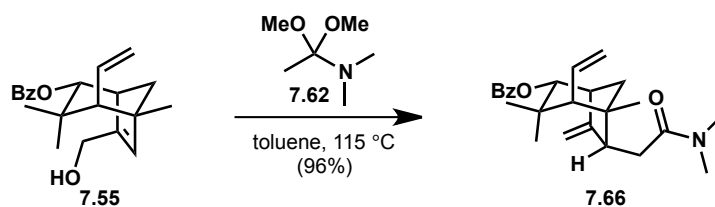


**Allylic alcohol 7.55:** Camphorsulfonic acid (128 mg, 0.551 mmol) was added to epoxide **7.54** (900 mg, 2.76 mmol) in toluene (28 mL). The reaction mixture was stirred at room temperature for 4 h before it was diluted with Et<sub>2</sub>O (40 mL). The organic layer was washed with NaHCO<sub>3(aq)</sub> (30 mL), brine (30 mL), dried over MgSO<sub>4</sub> and concentrated under reduced pressure to provide a yellow oil. The crude oil was purified via flash chromatography to afford allylic alcohol **7.55** in 76% yield (685 mg, 2.10 mmol). **<sup>1</sup>H NMR** (600 MHz, CDCl<sub>3</sub>)  $\delta$  8.03 – 8.00 (m, 2H), 7.56 (s, 1H), 7.45 (t,  $J$  = 7.8 Hz, 2H), 5.80 (d,  $J$  = 16.7 Hz, 1H), 5.66 (s, 1H), 5.14 (d,  $J$  = 3.0 Hz, 1H), 5.07 (dd,  $J$  = 10.0, 2.0 Hz, 1H), 4.94 (dd,  $J$  = 16.7, 2.0 Hz, 1H), 4.34 (dd,  $J$  = 15.0, 1.6 Hz, 1H), 4.27 (dd,  $J$  = 15.0, 1.7 Hz, 1H), 2.71 (d,  $J$  = 2.5 Hz, 1H), 1.95 (dd,  $J$  = 18.4, 10.9 Hz, 2H), 1.74 (ddd,  $J$  = 11.0, 5.6, 1.9 Hz, 1H), 1.32 (s, 3H), 1.01 (s, 3H), 0.86 (s, 3H); **<sup>13</sup>C NMR** (151 MHz, CDCl<sub>3</sub>)  $\delta$  166.0, 145.6, 138.8, 136.7, 133.0, 130.4, 129.4, 128.5, 116.9, 79.5, 62.5, 57.9, 46.9, 45.9, 44.6, 37.5, 31.0, 28.7, 24.3; **IR** (film)  $\nu_{\max}$  3451, 2966, 2871, 1716, 1274, 712 cm<sup>-1</sup>; **HRMS** (ESI+) calcd for [C<sub>21</sub>H<sub>26</sub>O<sub>3</sub>]:  $m/z$  326.1882, found 326.1938.

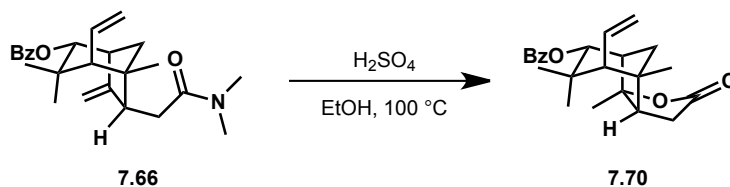


**Tetronic ester 7.57:** Diethyl azodicarboxylate (77.0  $\mu$ L, 0.490 mmol) was added to a mixture of allylic alcohol **7.55** (80.0 mg, 0.245 mmol), tetronic acid (**7.56**, 29.4 mg, 0.294 mmol) and triphenylphosphine (129 mg, 0.490 mmol) in THF (2.5 mL). The reaction mixture was stirred at room temperature for 12 h, at which point the mixture was concentrated under reduced pressure. Purification via flash chromatography (2:1 hexanes/EtOAc) afforded tetronic ester **7.57** in 57% yield (57.0 mg, 0.140 mmol). **<sup>1</sup>H NMR** (500 MHz, CDCl<sub>3</sub>)  $\delta$  8.08 (d,  $J$  = 7.2 Hz, 2H), 7.13 (d,  $J$  = 7.3 Hz, 1H), 7.08 (t,  $J$  = 7.4 Hz, 2H), 5.47 – 5.37 (m, 1H), 5.34 (s, 1H), 5.22 (d,  $J$  = 3.1 Hz, 1H), 4.95 (dd,  $J$  = 10.0, 2.2 Hz, 1H), 4.79 (dd,  $J$  = 16.7, 2.0 Hz, 1H), 4.66 (s, 1H), 4.21 – 4.11 (m, 2H), 3.77 (d,  $J$  = 15.7 Hz, 1H), 3.66 (d,  $J$  = 15.7 Hz, 1H), 2.80 (dd,  $J$  = 5.3, 3.1 Hz, 1H), 1.73 (dd,  $J$  = 10.8, 1.2 Hz, 1H), 1.59 (d,  $J$  = 11.1 Hz, 1H), 1.47 (ddd,  $J$  = 11.1, 5.5, 1.7 Hz, 1H), 1.17 (s, 3H), 0.88 (s, 3H), 0.86 (s, 3H); **<sup>13</sup>C NMR** (151 MHz, CDCl<sub>3</sub>)  $\delta$  178.9, 173.2, 165.9, 141.3, 138.8, 138.1, 133.4, 130.3, 129.3, 128.6, 128.3, 117.6, 89.3, 79.2, 71.9, 67.7, 57.5, 47.6, 45.5,

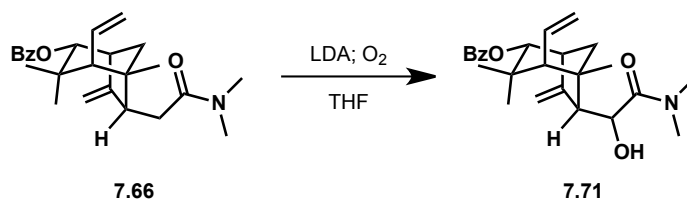
43.9, 37.4, 31.1, 28.8, 24.0; **IR** (film)  $\nu_{\text{max}}$  2967, 1775, 1451, 1315, 1272  $\text{cm}^{-1}$ ; **HRMS** (ESI+) calcd for  $[\text{C}_{25}\text{H}_{28}\text{O}_5\text{Na}]^+$  (M-Na) $^+$ :  $m/z$  431.1829, found 431.1833.



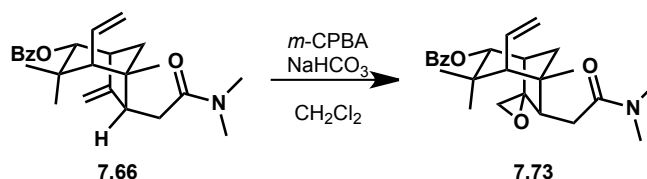
**Dimethyl amide 7.66:** A solution of allylic alcohol **7.55** (300 mg, 0.919 mmol) and *N,N*-dimethylacetamide dimethyl acetal (1.34 mL, 9.19 mmol) in toluene (9.0 mL) was heated to 115 °C for 1 h. The reaction mixture was cooled to room temperature and concentrated to give a yellow oil. The crude oil was purified via flash chromatography (2:1 hexanes/EtOAc) to provide dimethyl amide **7.66** in 96% yield (349 mg, 0.882 mmol).  $^1\text{H}$  NMR (600 MHz,  $\text{CDCl}_3$ )  $\delta$  8.11 – 8.07 (m, 2H), 7.57 (d,  $J = 7.4$  Hz, 1H), 7.46 (t,  $J = 7.7$  Hz, 2H), 5.78 (dt,  $J = 16.8, 10.5$  Hz, 1H), 5.05 – 5.00 (m, 2H), 4.97 (d,  $J = 3.1$  Hz, 1H), 4.94 – 4.88 (m, 2H), 3.45 (s, 1H), 3.02 (s, 3H), 2.98 (s, 4H), 2.79 (s, 1H), 2.53 (d,  $J = 8.9$  Hz, 1H), 2.25 (d,  $J = 5.0$  Hz, 1H), 2.17 (d,  $J = 11.0$  Hz, 1H), 1.72 (d,  $J = 12.3$  Hz, 1H), 1.49 – 1.45 (m, 1H), 1.44 (s, 3H), 0.85 – 0.81 (m, 7H);  $^{13}\text{C}$  NMR (151 MHz,  $\text{CDCl}_3$ )  $\delta$  172.4, 166.2, 156.1, 139.2, 132.8, 130.8, 129.6, 128.4, 116.2, 108.7, 80.8, 77.2, 77.0, 76.8, 63.8, 47.6, 47.2, 45.6, 37.5, 37.2, 37.2, 37.1, 35.7, 31.7, 28.2, 22.2; **HRMS** (ESI+) calcd for  $[\text{C}_{25}\text{H}_{33}\text{O}_3\text{NLi}]^+$  (M-Li) $^+$ :  $m/z$  402.2615, found 402.2616.



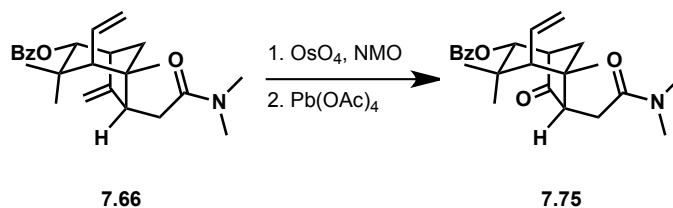
**Lactone 7.70:** A solution of dimethyl amide **7.66** (13.4 mg, 0.0339 mmol) in 1 M  $\text{H}_2\text{SO}_4$  in EtOH/ $\text{H}_2\text{O}$  (10:1, total volume 440  $\mu\text{L}$ ) was heated to 95 °C in a 20 mL vial equipped with a green Teflon-lined cap and Teflon tape. After 16 h, the reaction mixture was cooled to room temperature. The reaction mixture was diluted with a saturated  $\text{NaHCO}_3(\text{aq})$ . The aqueous layer was extracted with EtOAc (3 x 3.0 mL). The combined organic layer was dried over  $\text{MgSO}_4$  and concentrated under reduced pressure to provide lactone **7.70** in quantitative yield.  $^1\text{H}$  NMR (400 MHz,  $\text{CDCl}_3$ )  $\delta$  8.05 (dd,  $J = 5.2, 3.2$  Hz, 3H), 7.59 (d,  $J = 7.4$  Hz, 1H), 7.48 (t,  $J = 7.6$  Hz, 2H), 5.81 (d,  $J = 16.8$  Hz, 1H), 5.32 – 5.28 (m, 1H), 5.09 (dd,  $J = 10.1, 2.0$  Hz, 1H), 4.92 (dd,  $J = 16.7, 1.8$  Hz, 1H), 2.89 (d,  $J = 9.2$  Hz, 1H), 2.75 (d,  $J = 9.2$  Hz, 1H), 2.71 (s, 1H), 2.60 (d,  $J = 4.4$  Hz, 1H), 2.11 – 2.05 (m, 1H), 1.79 (s, 3H), 1.72 (s, 2H), 1.44 (s, 3H), 0.93 (s, 3H), 0.92 (s, 3H).  $^{13}\text{C}$  NMR (151 MHz,  $\text{CDCl}_3$ )  $\delta$  176.2, 165.6, 138.4, 133.2, 130.2, 129.6, 128.6, 117.2, 96.2, 79.8, 64.0, 50.5, 49.0, 44.9, 37.1, 36.7, 32.7, 31.8, 29.3, 23.1, 21.8; **HRMS** (ESI+) calcd for  $[\text{C}_{23}\text{H}_{28}\text{O}_4\text{Li}]^+$  (M-Li) $^+$ :  $m/z$  375.2142, found 375.2154.



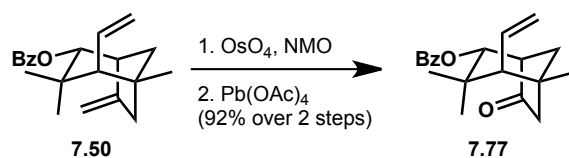
**$\alpha$ -Hydroxy amide 7.71:** Lithium diisopropylamide (100  $\mu$ L, 0.010 mmol, 0.1 M in THF) was added to *N,N*-dimethyl amide **7.66** (2.0 mg, 0.0051 mmol) in THF (200  $\mu$ L) at  $-78$   $^{\circ}$ C. The reaction mixture was stirred for 15 min at this temperature. Then,  $O_2$  was bubbled through the reaction mixture for 10 min. Note: The oxygen was dispensed from a balloon through a tube of  $P_2O_5$  and finally into the reaction mixture via metal needle. The reaction mixture was gradually warmed to room temperature over 1 h. A solution of  $SnCl_2$  in 2 N  $HCl_{(aq)}$  was added to the reaction mixture. The aqueous layer was extracted with EtOAc. The organic layer was washed with brine, dried over  $MgSO_4$  and concentrated under reduced pressure to provide an oil. The crude product was purified via flash chromatography to afford  $\alpha$ -hydroxy amide **7.71** in 38% yield (0.8 mg, 0.0019 mmol). The remainder of the material was accounted for by recovered starting material, **7.66**.  $^1H$  NMR (500 MHz,  $CDCl_3$ )  $\delta$  8.10 – 8.06 (m, 2H), 7.57 (dd,  $J = 10.5$ , 4.3 Hz, 1H), 7.45 (dd,  $J = 10.6$ , 4.7 Hz, 2H), 5.77 (d,  $J = 16.8$  Hz, 1H), 5.04 – 4.94 (m, 3H), 4.94 – 4.88 (m, 2H), 3.44 (s, 1H), 3.00 (d,  $J = 7.8$  Hz, 2H), 2.97 (d,  $J = 2.6$  Hz, 2H), 2.78 (dd,  $J = 5.3$ , 2.9 Hz, 1H), 2.52 (d,  $J = 9.0$  Hz, 1H), 2.24 (d,  $J = 5.1$  Hz, 1H), 2.19 – 2.14 (m, 1H), 1.71 (d,  $J = 12.3$  Hz, 1H), 1.49 – 1.45 (m, 1H), 1.43 (s, 3H), 0.82 (d,  $J = 6.1$  Hz, 6H).



**Epoxide 7.73:** *m*-Chloroperbenzoic acid (2.5 mg, 0.010 mmol, 70%) was added to a mixture of alkene **7.68** (2.0 mg, 0.0051 mmol) and  $NaHCO_3$  (1.7 mg, 0.020 mmol) in  $CH_2Cl_2$  (200  $\mu$ L). The reaction mixture was stirred at room temperature for 1 h. The reaction was quenched with a saturated  $Na_2SO_3_{(aq)}$  solution (1.0 mL). The aqueous layer was extracted with  $CH_2Cl_2$  (3 x 2.0 mL). The combined organic layer was washed with saturated  $NaHCO_3_{(aq)}$  solution (2.0 mL), brine, dried over  $MgSO_4$  and concentrated under reduced pressure to afford epoxide **7.73** in quantitative yield. Epoxide **7.73** was used without further purification.  $^1H$  NMR (500 MHz,  $CDCl_3$ )  $\delta$  8.02 (d,  $J = 7.2$  Hz, 2H), 7.58 (s, 1H), 7.49 – 7.46 (m, 2H), 5.79 (d,  $J = 16.8$  Hz, 1H), 5.06 (dd,  $J = 7.6$ , 2.5 Hz, 2H), 4.93 (dd,  $J = 16.7$ , 1.9 Hz, 1H), 3.25 – 3.21 (m, 1H), 3.05 – 3.02 (m, 4H), 2.99 (d,  $J = 5.2$  Hz, 1H), 2.92 (s, 3H), 2.31 (s, 1H), 2.20 – 2.13 (m, 2H), 1.95 (s, 1H), 1.74 (d,  $J = 4.8$  Hz, 2H), 1.54 (s, 4H), 0.90 (s, 3H), 0.88 (s, 3H).

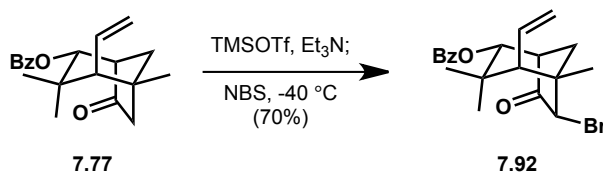


**Ketone 7.75:** OsO<sub>4</sub> (10 μL, 2.5 wt% solution) was added to a mixture of *exo*-methylene **7.66** (8.0 mg, 0.020 mmol) and NMO (4.7 mg, 0.041 mmol) in 6:1 acetone/water (total volume 230 μL). The reaction mixture was stirred at room temperature for 12 h. The mixture was diluted with EtOAc and washed with saturated Na<sub>2</sub>SO<sub>3(aq)</sub>, water, brine, dried over MgSO<sub>4</sub> and concentrated to provide the 1,2-diol. <sup>1</sup>H NMR (500 MHz, CDCl<sub>3</sub>) δ 8.06 (dd, *J* = 5.1, 3.3 Hz, 2H), 7.60 – 7.55 (m, 1H), 7.47 (t, *J* = 7.7 Hz, 2H), 5.78 (d, *J* = 16.9 Hz, 1H), 5.24 (d, *J* = 4.5 Hz, 1H), 5.02 (dd, *J* = 10.0, 2.1 Hz, 1H), 4.89 (dd, *J* = 16.7, 2.1 Hz, 1H), 4.02 (d, *J* = 7.4 Hz, 2H), 3.48 (s, 1H), 3.09 (d, *J* = 3.5 Hz, 3H), 3.05 (dd, *J* = 9.0, 5.0 Hz, 1H), 2.98 (s, 4H), 2.63 (dd, *J* = 16.0, 9.1 Hz, 1H), 2.44 – 2.36 (m, 2H), 2.20 (dd, *J* = 11.0, 1.6 Hz, 1H), 1.99 – 1.94 (m, 1H), 1.63 (d, *J* = 12.2 Hz, 2H), 1.51 (s, 3H), 0.90 (s, 3H), 0.82 (s, 3H). The diol (4.0 mg, 0.0093 mmol) was stirred with lead(IV) acetate (8.3 mg, 0.019 mmol) in benzene (200 μL) at room temperature. After 12 h, the reaction mixture was diluted with EtOAc (2.0 mL), filtered through a pad of celite, and concentrated under reduced pressure to afford ketone **7.75** as an oil in 72% over 2 steps. <sup>1</sup>H NMR (600 MHz, CDCl<sub>3</sub>) δ 8.06 – 8.02 (m, 2H), 7.56 (dd, *J* = 10.5, 4.4 Hz, 1H), 7.44 (t, *J* = 7.8 Hz, 2H), 5.86 (d, *J* = 16.8 Hz, 1H), 5.15 (d, *J* = 3.5 Hz, 1H), 5.11 (dd, *J* = 10.1, 2.0 Hz, 1H), 5.00 (dd, *J* = 16.7, 1.8 Hz, 1H), 3.40 (dt, *J* = 10.0, 3.0 Hz, 1H), 2.99 (d, *J* = 6.8 Hz, 3H), 2.97 (s, 3H), 2.63 (dd, *J* = 5.8, 3.5 Hz, 1H), 2.48 (d, *J* = 3.4 Hz, 1H), 2.43 (d, *J* = 10.0 Hz, 1H), 2.35 (dd, *J* = 9.2, 7.7 Hz, 1H), 1.99 (dd, *J* = 12.9, 2.9 Hz, 1H), 1.67 (ddd, *J* = 12.9, 5.9, 1.8 Hz, 2H), 1.39 (s, 3H), 0.92 (s, 3H), 0.90 (s, 3H).

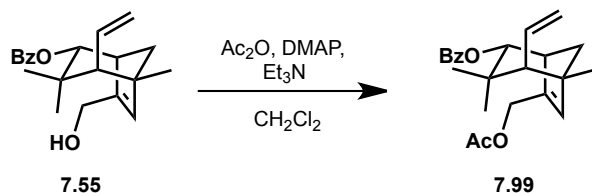


**Ketone 7.77:** OsO<sub>4</sub> (65 μL, 2.5 wt% solution) was added to a mixture of *exo*-methylene **7.50** (400 mg, 1.29 mmol) and NMO (303 mg, 2.58 mmol) in 6:1 acetone/water (total volume 3.0 mL). The reaction mixture was stirred at room temperature for 12 h. The mixture was diluted with EtOAc and washed with saturated Na<sub>2</sub>SO<sub>3(aq)</sub>, water, brine, dried over MgSO<sub>4</sub> and concentrated to provide the 1,2-diol. Lead(IV) acetate (673 mg, 1.52 mmol) was added to diol **x.xx** (475 mg, 1.38 mmol) in benzene (13.0 mL). The reaction mixture was stirred at room temperature for 12 h at which point the mixture was diluted with Et<sub>2</sub>O (20 mL) and filtered through a pad of celite. The filtrate was concentrated under reduced pressure to provide an oil that was purified via flash chromatography. Ketone **7.77** was obtained in 92% yield over 2 steps (397 mg, 1.27 mmol). <sup>1</sup>H NMR (500 MHz, CDCl<sub>3</sub>) δ 8.07 – 8.03 (m, 2H), 7.57 (t, *J* = 7.4 Hz, 1H), 7.45 (t, *J* = 7.7 Hz, 2H), 5.88 (d, *J* = 16.7 Hz, 1H), 5.14 (dd, *J* = 12.6, 2.7 Hz, 2H), 5.00 (dd, *J* = 16.7, 1.7 Hz, 1H), 2.68 – 2.62 (m, 2H), 2.15 (dd, *J* = 10.9, 1.4 Hz, 1H), 2.10 (dd, *J* = 13.3,

4.5 Hz, 2H), 1.66 (ddd,  $J = 12.6, 5.7, 1.9$  Hz, 1H), 1.30 (s, 3H), 1.12 (s, 3H), 0.90 (s, 3H);  $^{13}\text{C}$  NMR (151 MHz,  $\text{CDCl}_3$ )  $\delta$  166.1, 137.6, 133.1, 130.2, 129.8, 128.4, 128.3, 117.4, 80.5, 62.0, 53.4, 52.3, 40.8, 37.6, 37.5, 30.8, 27.8, 27.4; IR (film)  $\nu_{\text{max}}$  2972, 1745, 1717, 1246  $\text{cm}^{-1}$ ; HRMS (EI+) calcd for  $[\text{C}_{20}\text{H}_{24}\text{O}_3]$ :  $m/z$  312.1725, found 312.1730.

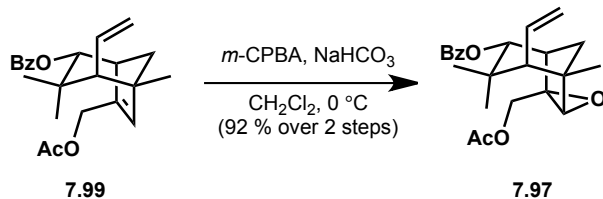


**$\alpha$ -Bromo ketone 7.92:** Trimethylsilyl trifluoromethanesulfonate (142  $\mu\text{L}$ , 0.768 mmol) was added to a solution of ketone **7.77** (80.0 mg, 0.256 mmol) and  $\text{Et}_3\text{N}$  (178  $\mu\text{L}$ , 1.28 mmol) in  $\text{CH}_2\text{Cl}_2$  (3.0 mL). After 12 h, the reaction mixture was cooled to  $-40\text{ }^\circ\text{C}$  and *N*-bromosuccinimide (54.7 mg, 0.307 mmol) was added in one portion, and the reaction mixture was stirred for 20 min. The reaction mixture was diluted with  $\text{Et}_2\text{O}$ , washed with saturated  $\text{NaHCO}_3(\text{aq})$ , brine, dried over  $\text{MgSO}_4$  and concentrated under reduced pressure to afford a yellow oil. The crude oil was purified via flash chromatography to provide  $\alpha$ -bromo ketone **7.92** in 70% yield (70.0 mg, 0.179 mmol).  $^1\text{H}$  NMR (500 MHz,  $\text{CDCl}_3$ )  $\delta$  8.05 (d,  $J = 7.6$  Hz, 2H), 7.59 (t,  $J = 7.1$  Hz, 1H), 7.46 (t,  $J = 7.2$  Hz, 2H), 5.90 (d,  $J = 16.5$  Hz, 1H), 5.17 (d,  $J = 11.4$  Hz, 2H), 5.02 (d,  $J = 16.7$  Hz, 1H), 4.67 (s, 1H), 2.78 (s, 1H), 2.26 (d,  $J = 10.8$  Hz, 1H), 2.05 (d,  $J = 5.4$  Hz, 1H), 1.98 (d,  $J = 13.0$  Hz, 1H), 1.26 (s, 6H), 0.91 (s, 3H); IR (film)  $\nu_{\text{max}}$  2976, 1754, 1716, 1271, 911, 629  $\text{cm}^{-1}$ ; HRMS (ESI+) calcd for  $[\text{C}_{20}\text{H}_{23}\text{O}_3\text{BrNa}]^+$  (M-Na) $^+$ :  $m/z$  413.0723, found 413.0725.

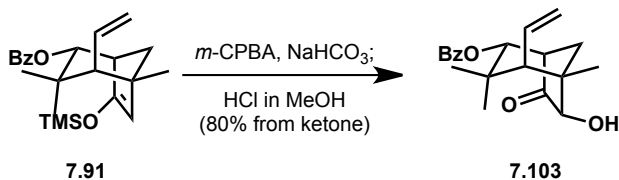


**Bicycle 7.99:** Acetic anhydride (4.6  $\mu\text{L}$ , 0.049 mmol) was added to a mixture of allylic alcohol **7.55** (8.0 mg, 0.025 mmol), DMAP (0.40 mg, 0.0025 mmol) and  $\text{Et}_3\text{N}$  (14  $\mu\text{L}$ , 0.098 mmol) in  $\text{CH}_2\text{Cl}_2$  (300  $\mu\text{L}$ ). The reaction mixture was stirred at room temperature for 3 h before it was diluted with  $\text{EtOAc}$  (3.0 mL). The organic phase was washed with water, brine, dried over  $\text{MgSO}_4$  and concentrated under reduced pressure to afford **7.99**.  $^1\text{H}$  NMR (400 MHz,  $\text{CDCl}_3$ )  $\delta$  8.03 (dt,  $J = 8.5, 1.7$  Hz, 2H), 7.57 (dd,  $J = 10.5, 4.3$  Hz, 1H), 7.45 (dd,  $J = 10.5, 4.7$  Hz, 2H), 5.80 (d,  $J = 17.0$  Hz, 1H), 5.68 (s, 1H), 5.13 (d,  $J = 3.0$  Hz, 1H), 5.09 (dd,  $J = 10.0, 2.2$  Hz, 1H), 4.95 (dd,  $J = 16.7, 2.0$  Hz, 1H), 4.76 (dd,  $J = 5.7, 1.7$  Hz, 2H), 2.79 (dd,  $J = 5.4, 3.0$  Hz, 1H), 1.98 (s, 3H), 1.93 (d,  $J = 11.0$  Hz, 2H), 1.75 (ddd,  $J = 11.1, 5.6, 2.0$  Hz, 1H), 1.29 (s, 3H), 1.02 (s, 3H), 0.87 (s, 3H).

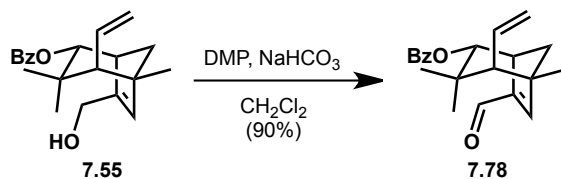




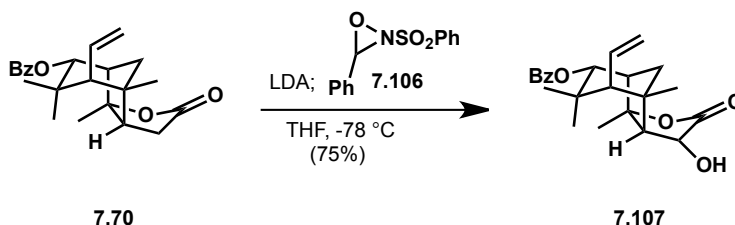
**Epoxide 7.55:** *m*-Chloroperbenzoic acid (5.0 mg, 0.020 mmol, 70 wt%) was added to the bicycle (5.0 mg, 0.014 mmol) and NaHCO<sub>3</sub> (3.4 mg, 0.041 mmol) in CH<sub>2</sub>Cl<sub>2</sub> (200 μL). The reaction mixture was stirred for 1 h at ambient temperature. The reaction mixture was diluted with EtOAc (1.0 mL). The organic phase was washed with a saturated Na<sub>2</sub>SO<sub>3(aq)</sub> solution, NaHCO<sub>3(aq)</sub>, brine, dried over MgSO<sub>4</sub> and concentrated under reduced pressure to afford epoxide **7.97**. <sup>1</sup>H NMR (500 MHz, CDCl<sub>3</sub>) δ 8.02 (dd, *J* = 5.2, 3.3 Hz, 2H), 7.62 – 7.57 (m, 1H), 7.49 – 7.46 (m, 2H), 5.73 (d, *J* = 16.8 Hz, 1H), 5.16 (d, *J* = 3.4 Hz, 1H), 5.12 (dd, *J* = 10.0, 2.0 Hz, 1H), 4.99 (dd, *J* = 16.7, 1.8 Hz, 1H), 4.85 (d, *J* = 12.4 Hz, 1H), 4.33 (d, *J* = 12.4 Hz, 1H), 3.28 (s, 1H), 2.77 (dd, *J* = 5.2, 3.4 Hz, 1H), 2.10 (dd, *J* = 10.7, 1.9 Hz, 1H), 1.82 – 1.80 (m, 3H), 1.38 (dd, *J* = 5.6, 2.2 Hz, 1H), 1.31 (d, *J* = 3.8 Hz, 3H), 1.02 (s, 3H), 0.90 (s, 3H). **HRMS** (ESI+) calcd for [C<sub>23</sub>H<sub>28</sub>O<sub>5</sub>Li]<sup>+</sup> (M-Li)<sup>+</sup>: *m/z* 391.2091, found 391.2094.



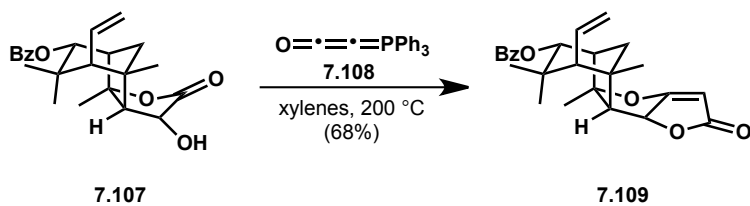
**$\alpha$ -Hydroxy ketone 7.103:** *m*-Chloroperbenzoic acid (12.8 mg, 0.0518 mmol, 70%) was added to a mixture of silyl enol ether **7.91** (16.6 mg, 0.0320 mmol) and NaHCO<sub>3</sub> (18.1 mg, 0.216 mmol) in CH<sub>2</sub>Cl<sub>2</sub> (500 μL) at -40 °C. The reaction was stirred as the cold bath gradually expired. After 2 h, 1 N HCl in MeOH was added. The mixture was stirred vigorously for 20 min, then diluted with EtOAc (2.0 mL). The organic layer was washed with a saturated Na<sub>2</sub>SO<sub>3(aq)</sub> solution, saturated NaHCO<sub>3(aq)</sub>, brine, dried over MgSO<sub>4</sub> and concentrated under reduced pressure to provide  $\alpha$ -hydroxy ketone **7.103** in 80% yield (8.3 mg, 0.25 mmol). <sup>1</sup>H NMR (600 MHz, CDCl<sub>3</sub>) δ 8.05 – 8.02 (m, 2H), 7.57 (dd, *J* = 10.5, 4.4 Hz, 1H), 7.48 – 7.43 (m, 2H), 5.93 – 5.85 (m, 1H), 5.18 (td, *J* = 4.2, 1.9 Hz, 2H), 5.03 (dd, *J* = 16.7, 1.7 Hz, 1H), 4.04 (d, *J* = 1.5 Hz, 1H), 2.75 (s, 1H), 2.19 (d, *J* = 10.9 Hz, 1H), 1.96 (s, 1H), 1.23 (s, 3H), 1.08 (s, 3H), 0.91 (s, 3H).



**Enal 7.78:** DMP (78.0 mg, 0.184 mmol) was added to a mixture of allylic alcohol **7.55** (30.0 mg, 0.0919 mmol) and NaHCO<sub>3</sub> (30.9 mg, 0.368 mmol) in CH<sub>2</sub>Cl<sub>2</sub> (900 μL). The reaction mixture was stirred at room temperature for 8 h. The reaction was quenched by the addition of a saturated Na<sub>2</sub>SO<sub>3(aq)</sub> solution (2.0 mL). The aqueous layer was extracted with Et<sub>2</sub>O (3 x 2.0 mL). The combined organic layers were washed with saturated NaHCO<sub>3(aq)</sub>, brine, dried over MgSO<sub>4</sub> and concentrated under reduced pressure to afford enal **7.78** as a white solid in 90% yield (26.7 mg, 0.0824 mmol). <sup>1</sup>H NMR (400 MHz, CDCl<sub>3</sub>) δ 9.63 (s, 1H), 8.34 – 8.30 (m, 2H), 7.12 (dd, *J* = 4.1, 2.5 Hz, 3H), 5.98 (s, 1H), 5.35 (d, *J* = 16.7 Hz, 1H), 5.23 (d, *J* = 3.1 Hz, 1H), 4.90 (dd, *J* = 10.0, 2.2 Hz, 1H), 4.72 (dd, *J* = 16.7, 2.0 Hz, 1H), 3.31 (dd, *J* = 5.5, 3.1 Hz, 1H), 1.65 (dd, *J* = 10.8, 1.8 Hz, 1H), 1.49 (d, *J* = 11.4 Hz, 1H), 1.28 (s, 1H), 1.05 (s, 3H), 0.84 (s, 3H), 0.73 (s, 3H); IR (film) ν<sub>max</sub> 2972, 1716, 1451, 1274 cm<sup>-1</sup>.

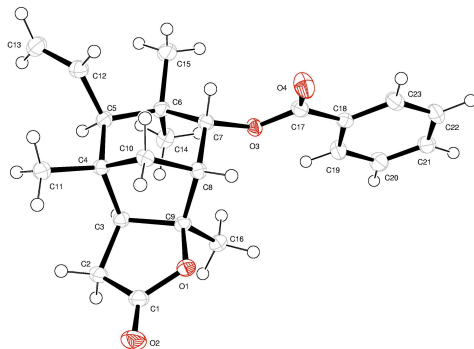


**α-Hydroxy lactone 7.107:** *n*-Butyllithium (59.0 μL, 0.147 mmol) was added to diisopropylamine (23.0 μL, 0.163 mmol) in THF (500 μL) at 0 °C. The mixture was stirred for 20 min at this temperature and then cooled to -78 °C. Lactone **7.70** (30.0 mg, 0.0814 mmol) in THF (200 μL) was added. After 30 min, Davis' oxaziridine (**7.106**, 42.5 mg, 0.163 mmol) in THF (200 μL) was added at -78 °C. The reaction mixture was stirred for 3.5 h as the cold bath gradually expired. The reaction was quenched with a saturated NH<sub>4</sub>Cl<sub>(aq)</sub> solution (1.0 mL). The aqueous layer was extracted with EtOAc (3 x 2.0 mL). The combined organic layer was washed with water, brine, dried over MgSO<sub>4</sub> and concentrated under reduced pressure to provide an oil. The crude oil was purified via flash chromatography (9:1 hexanes/EtOAc) to afford α-hydroxy lactone **7.107** in 75% yield (23.6 mg, 0.0614 mmol). <sup>1</sup>H NMR (400 MHz, CDCl<sub>3</sub>) δ 8.09 – 8.03 (m, 2H), 7.60 (t, *J* = 7.4 Hz, 1H), 7.48 (t, *J* = 7.7 Hz, 2H), 5.85 – 5.73 (m, 1H), 5.28 (d, *J* = 4.2 Hz, 1H), 5.11 (dd, *J* = 10.1, 1.9 Hz, 1H), 4.99 – 4.91 (m, 1H), 4.47 (s, 1H), 3.11 (dt, *J* = 12.7, 6.4 Hz, 1H), 2.84 (s, 1H), 2.60 (t, *J* = 4.6 Hz, 1H), 2.22 – 2.15 (m, 1H), 2.04 (d, *J* = 3.8 Hz, 1H), 1.94 (s, 3H), 1.73 (d, *J* = 13.2 Hz, 1H), 1.63 (dd, *J* = 11.0, 7.6 Hz, 1H), 1.56 (ddd, *J* = 13.2, 5.3, 2.0 Hz, 1H), 1.50 – 1.43 (m, 3H), 1.10 (d, *J* = 6.4 Hz, 3H), 0.96 (d, *J* = 7.4 Hz, 3H), 0.93 – 0.90 (m, 3H); <sup>13</sup>C NMR (151 MHz, CDCl<sub>3</sub>) δ 176.4, 165.7, 138.0, 133.2, 129.6, 128.6, 128.3, 117.5, 97.6, 79.6, 72.8, 63.7, 58.5, 48.6, 44.1, 37.2, 36.7, 32.6, 29.2, 23.6, 22.9; IR (film) ν<sub>max</sub> 3444, 2976, 1755, 1718, 1266 cm<sup>-1</sup>; HRMS (EI+) calcd for [C<sub>23</sub>H<sub>28</sub>O<sub>5</sub>]: *m/z* 384.1937, found 384.1942.



**Tetracycle 7.109:** A solution of  $\alpha$ -hydroxy lactone **7.107** (2.0 mg, 0.0052 mmol) and **7.108** (3.9 mg, 0.013 mmol) in *m*-xylenes (200  $\mu\text{L}$ ) was heated to 210 °C in a sand bath. After 2 h, the reaction mixture was cooled to room temperature and concentrated under reduced pressure to afford a crude product. Purification via flash chromatography (9:1 hexanes/EtOAc) afforded tetracycle **7.109**.  $^1\text{H NMR}$  (500 MHz,  $\text{CDCl}_3$ )  $\delta$  8.07 – 8.04 (m, 3H), 7.63 – 7.59 (m, 2H), 7.48 (dd,  $J = 7.4, 4.2$  Hz, 4H), 5.67 (s, 2H), 5.34 (dd,  $J = 8.4, 1.7$  Hz, 1H), 5.24 (d,  $J = 4.3$  Hz, 1H), 5.11 (dd,  $J = 10.1, 1.9$  Hz, 1H), 4.95 (dd,  $J = 14.2, 2.4$  Hz, 2H), 3.20 (d,  $J = 8.3$  Hz, 1H), 2.73 (d,  $J = 3.9$  Hz, 2H), 2.19 (d,  $J = 11.0$  Hz, 1H), 2.05 (s, 2H), 1.89 (s, 3H), 1.79 (s, 1H), 1.72 (d,  $J = 2.2$  Hz, 2H), 1.65 (s, 1H), 1.46 (s, 3H), 0.95 (s, 3H), 0.91 (s, 3H).

## X-Ray Structure of 7.70:



**X-Ray Experimental Details:** A colorless needle 0.10 x 0.10 x 0.10 mm in size was mounted on a Cryoloop with Paratone oil. Data were collected in a nitrogen gas stream at 100(2) K using phi and omega scans. Crystal-to-detector distance was 60 mm and exposure time was 5 seconds per frame using a scan width of 1.0°. Data collection was 99.9% complete to 67.00° in  $\theta$ . A total of 30382 reflections were collected covering the indices,  $-9 \leq h \leq 9$ ,  $-24 \leq k \leq 24$ ,  $-12 \leq l \leq 14$ . 3537 reflections were found to be symmetry independent, with an  $R_{\text{int}}$  of 0.0149. Indexing and unit cell refinement indicated a primitive, monoclinic lattice. The space group was found to be P2(1)/c (No. 14). The data were integrated using the Bruker SAINT software program and scaled using the SADABS software program. Solution by direct methods (SIR-2004) produced a complete heavy-atom phasing model consistent with the proposed structure. All non-hydrogen atoms were refined anisotropically by full-matrix least-squares (SHELXL-97). All hydrogen atoms were placed using a riding model. Their positions were constrained relative to their parent atom using the appropriate HFIX command in SHELXL-97.

## X-Ray Data:

|                        |  |                  |
|------------------------|--|------------------|
| Empirical formula      | C <sub>23</sub> H <sub>28</sub> O <sub>4</sub> |                  |
| Formula weight         | 368.45   |                  |
| Temperature            | 100(2) K                                       |                  |
| Wavelength             | 1.54178 Å                                      |                  |
| Crystal system         | Monoclinic                                     |                  |
| Space group            | P2(1)/c  |                  |
| Unit cell dimensions   | a = 8.0005(6) Å                                | a = 90°.         |
|                        | b = 20.1915(16) Å                              | b = 104.753(4)°. |
|                        | c = 12.3959(10) Å                              | g = 90°.         |
| Volume                 | 1936.4(3) Å <sup>3</sup>                       |                  |
| Z                      | 4  |                  |
| Density (calculated)   | 1.264 Mg/m <sup>3</sup>                        |                  |
| Absorption coefficient | 0.682 mm <sup>-1</sup>                         |                  |
| F(000)                 | 792  |                  |
| Crystal size           | 0.10 x 0.10 x 0.10 mm <sup>3</sup>             |                  |

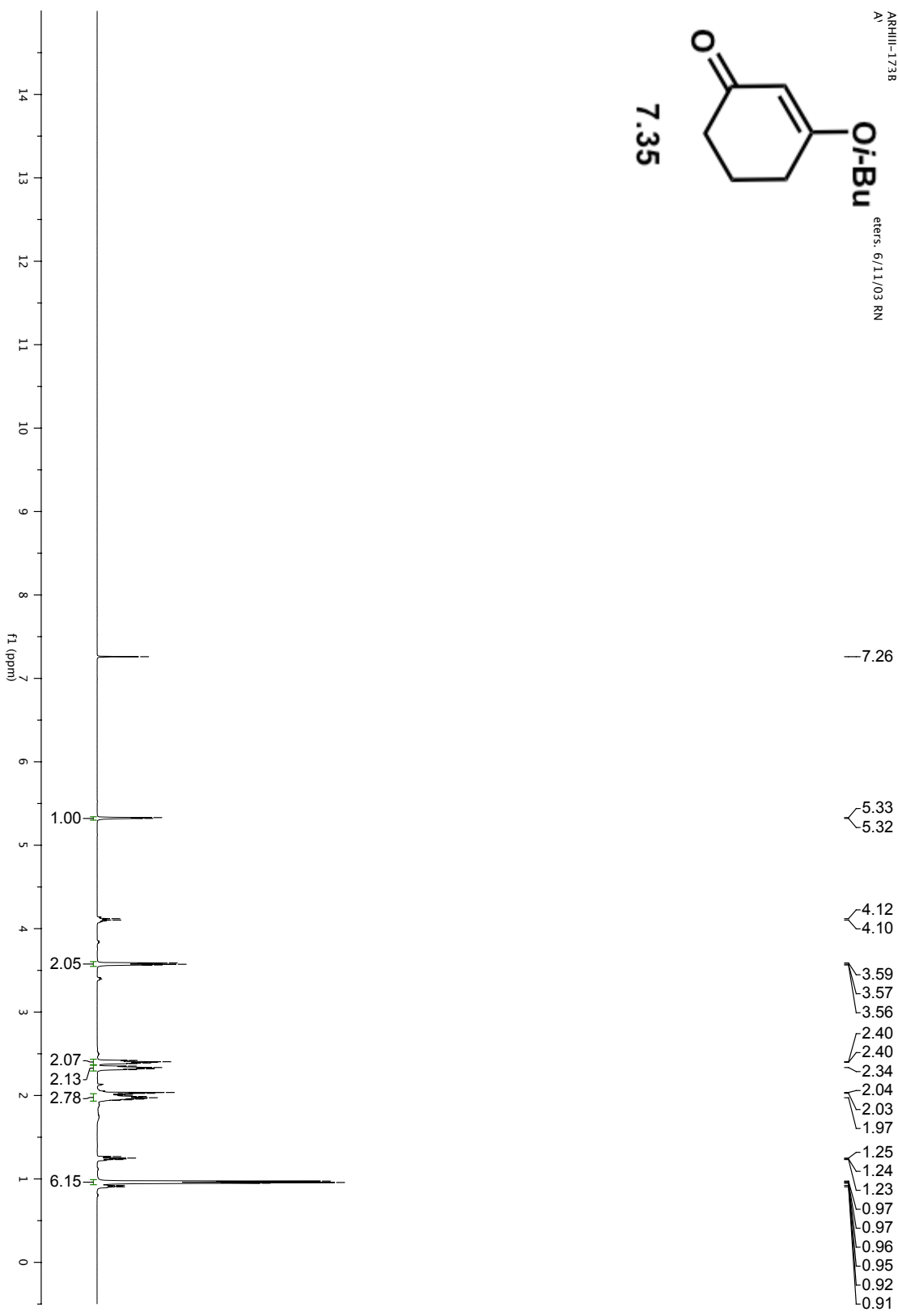
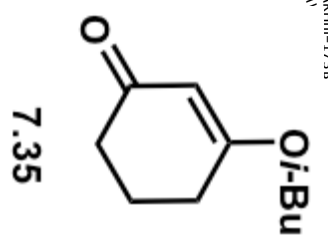
|                                   |   |
|-----------------------------------|---|
| Crystal color/habit               | colorless needle                            |
| Theta range for data collection   | 4.29 to 68.23°                              |
| Index ranges                      | -9<=h<=9, -24<=k<=24, -12<=l<=14            |
| Reflections collected             | 30382                                       |
| Independent reflections           | 3537 [R(int) = 0.0149]                      |
| Completeness to theta = 67.00°    | 99.9 %                                      |
| Absorption correction             | Semi-empirical from equivalents             |
| Max. and min. transmission        | 0.9349 and 0.9349                           |
| Refinement method                 | Full-matrix least-squares on F <sup>2</sup> |
| Data / restraints / parameters    | 3537 / 0 / 248                              |
| Goodness-of-fit on F <sup>2</sup> | 1.073                                       |
| Final R indices [I>2sigma(I)]     | R1 = 0.0397, wR2 = 0.0998                   |
| R indices (all data)              | R1 = 0.0414, wR2 = 0.1011                   |
| Largest diff. peak and hole       | 0.491 and -0.231 e.Å <sup>-3</sup>          |

### 7.10 References and Notes

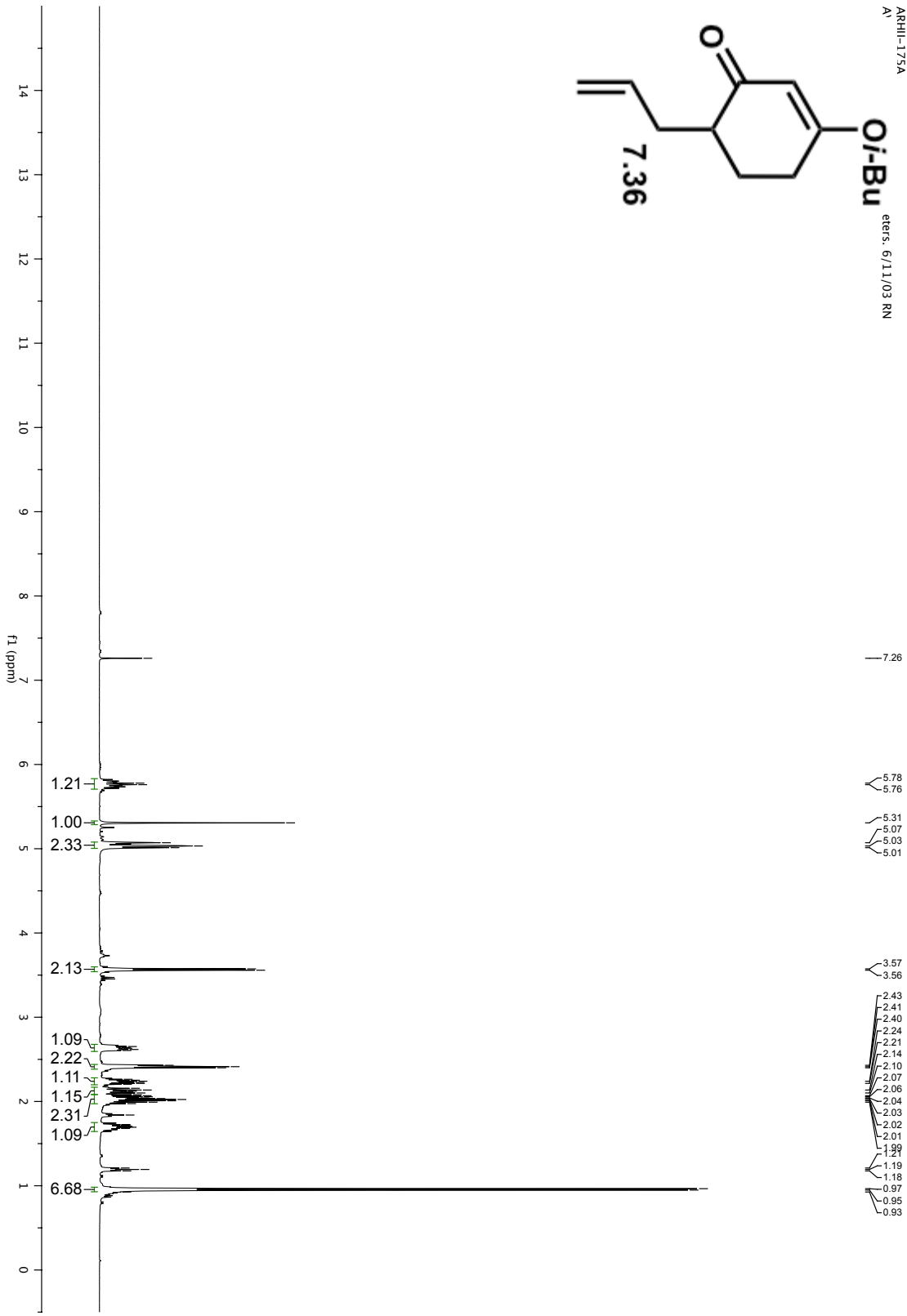
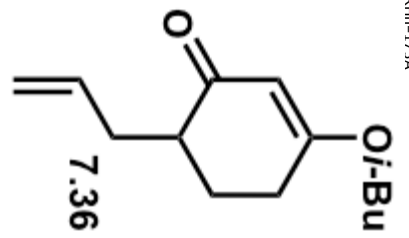
- (1) Dittmer, H. J. *Phylogeny and Form in the Plant Kingdom*; D. Van Nostrand Co.: Toronto, **1964**.
- (2) Toyota, M.; Saito, T.; Asakawa, Y. *Chem. Pharm. Bull.* **1998**, *46*, 178.
- (3) Wu, C. L.; Liu, H. J.; Uang, H. L. *Phytochemistry* **1994**, *35*, 822.
- (4) Liu, H. J.; Wu, C. L. *J. Asian Nat. Prod. Res.* **1999**, *1*, 177.
- (5) Peng, X. S.; Wong, H. N. C. *Chem. Asian J.* **2006**, *1*, 111.
- (6) Kende, A. S.; Roth, B.; Sanfilippo, P. J. *J. Am. Chem. Soc.* **1982**, *104*, 1784.
- (7) Staben, S. T.; Kennedy-Smith, J. J.; Huang, D.; Corkey, B. K.; LaLonde, R. L.; Toste, F. D. *Angew. Chem. Int. Ed.* **2006**, *45*, 5991.
- (8) Toyota, M.; Wada, T.; Fukumoto, K.; Ihara, M. *J. Am. Chem. Soc.* **1998**, *120*, 4916.
- (9) Felix, D.; Gschwend, K.; Wick, A. E.; Eschenmo. A *Helv. Chim. Acta* **1969**, *52*, 1030.
- (10) Culkin, D. A.; Hartwig, J. F. *Acc. Chem. Res.* **2003**, *36*, 234.
- (11) Lim, S. M.; Hill, N.; Myers, A. G. *J. Am. Chem. Soc.* **2009**, *131*, 5763.
- (12) Rubottom, G. M.; Vazquez, M. A.; Pelegrin D. *Tetrahedron Lett.* **1974**, 4319.

*Appendix Six:  
Spectra Relevant to Chapter 7*

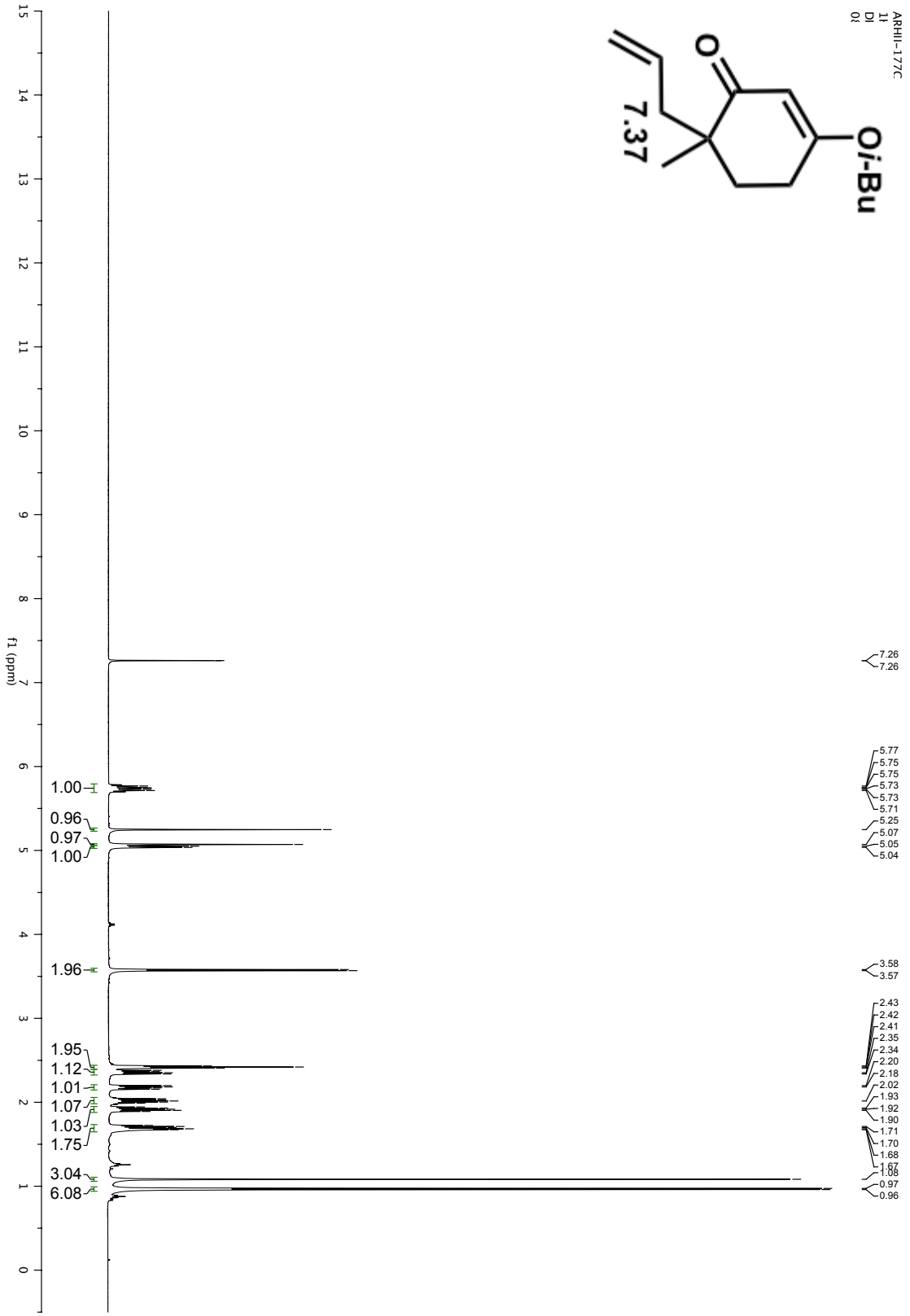
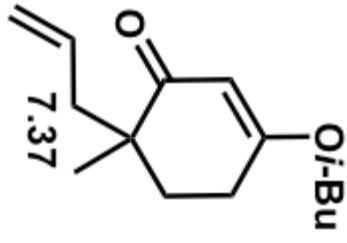
ARRHI-1738  
A1  
eters: 6/11/03 RN

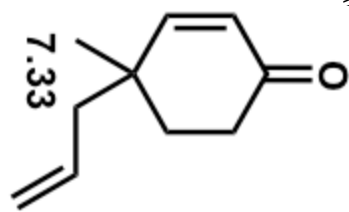




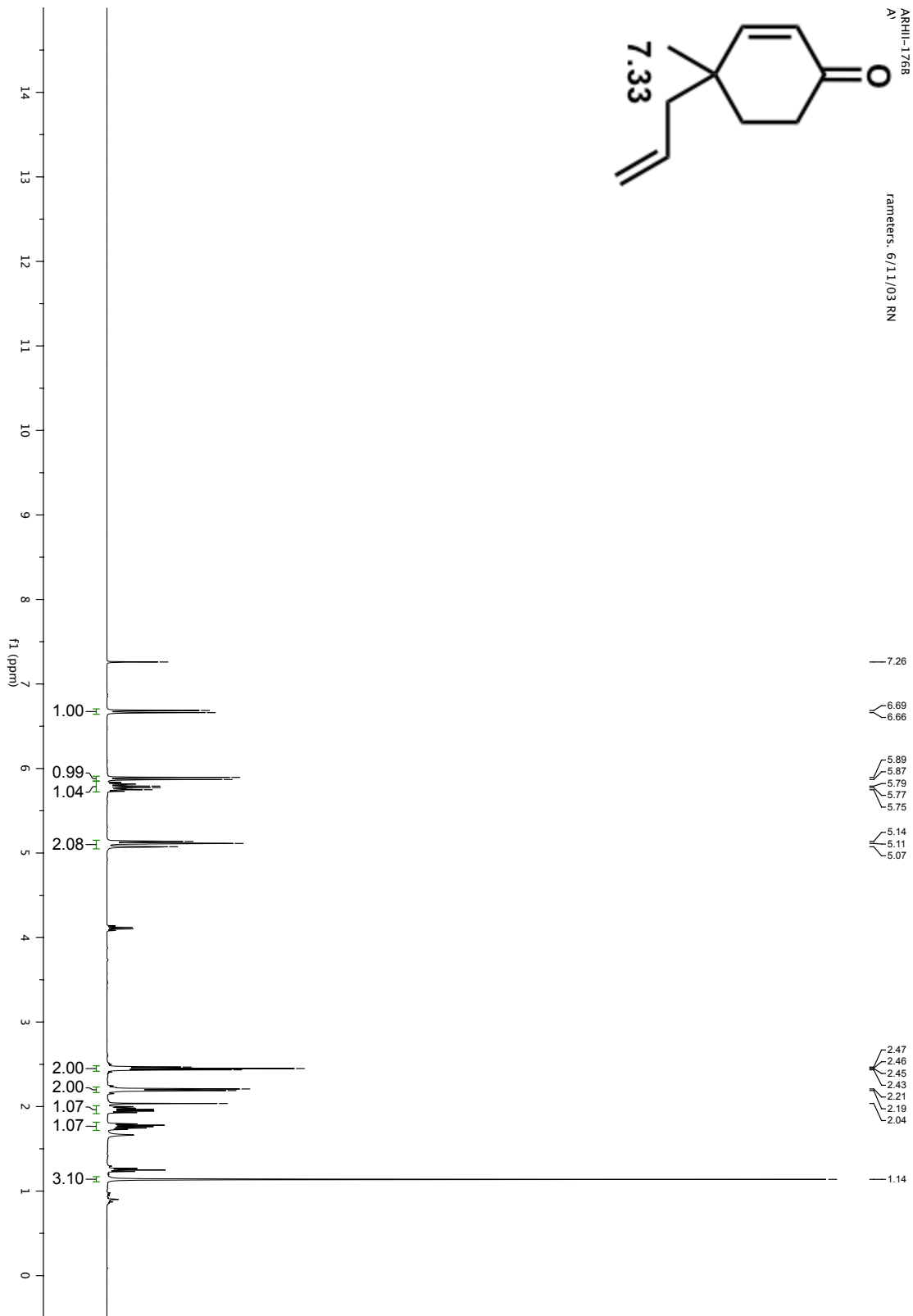


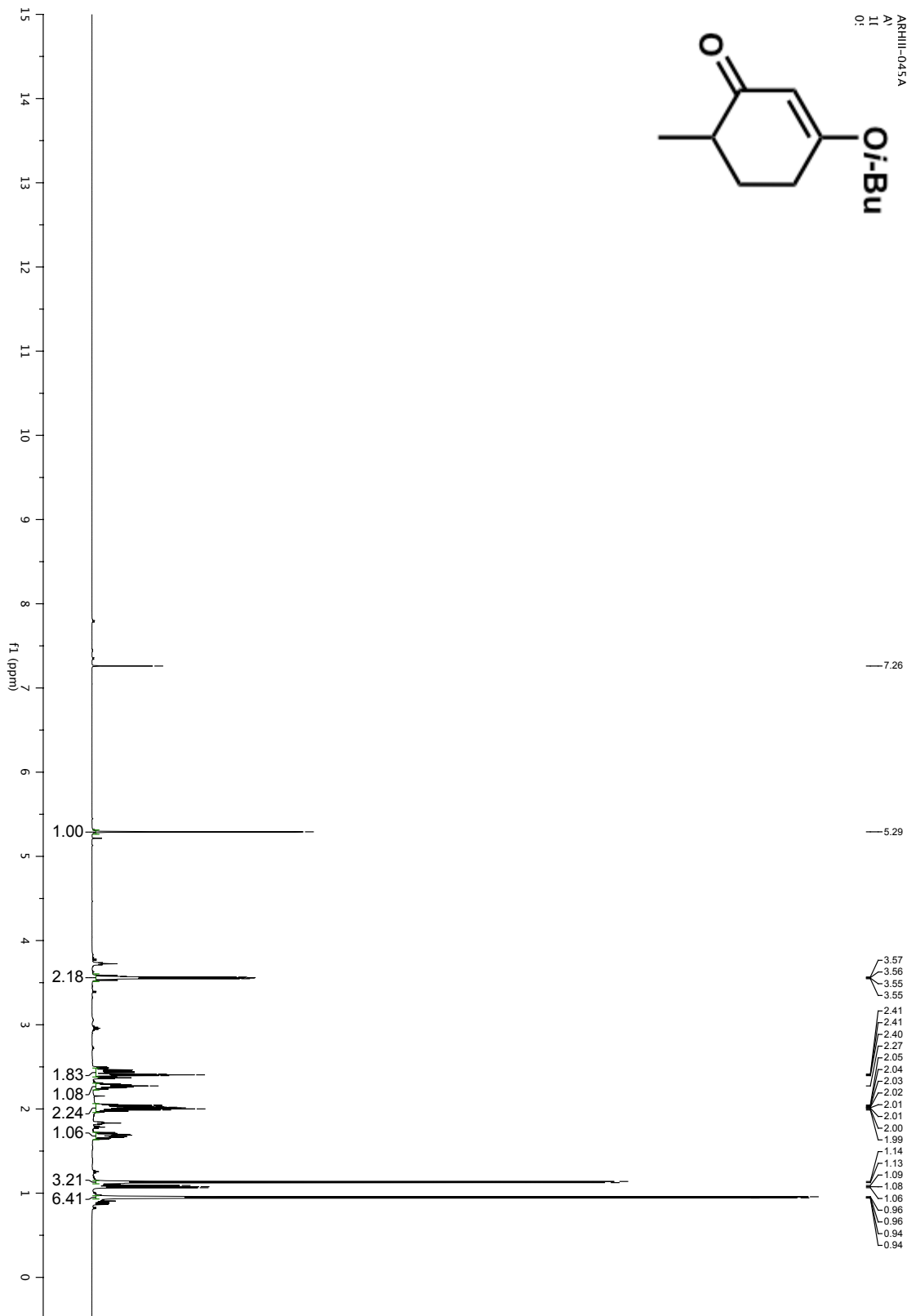
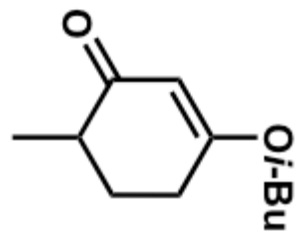
ARHII-177C  
11  
DI  
01



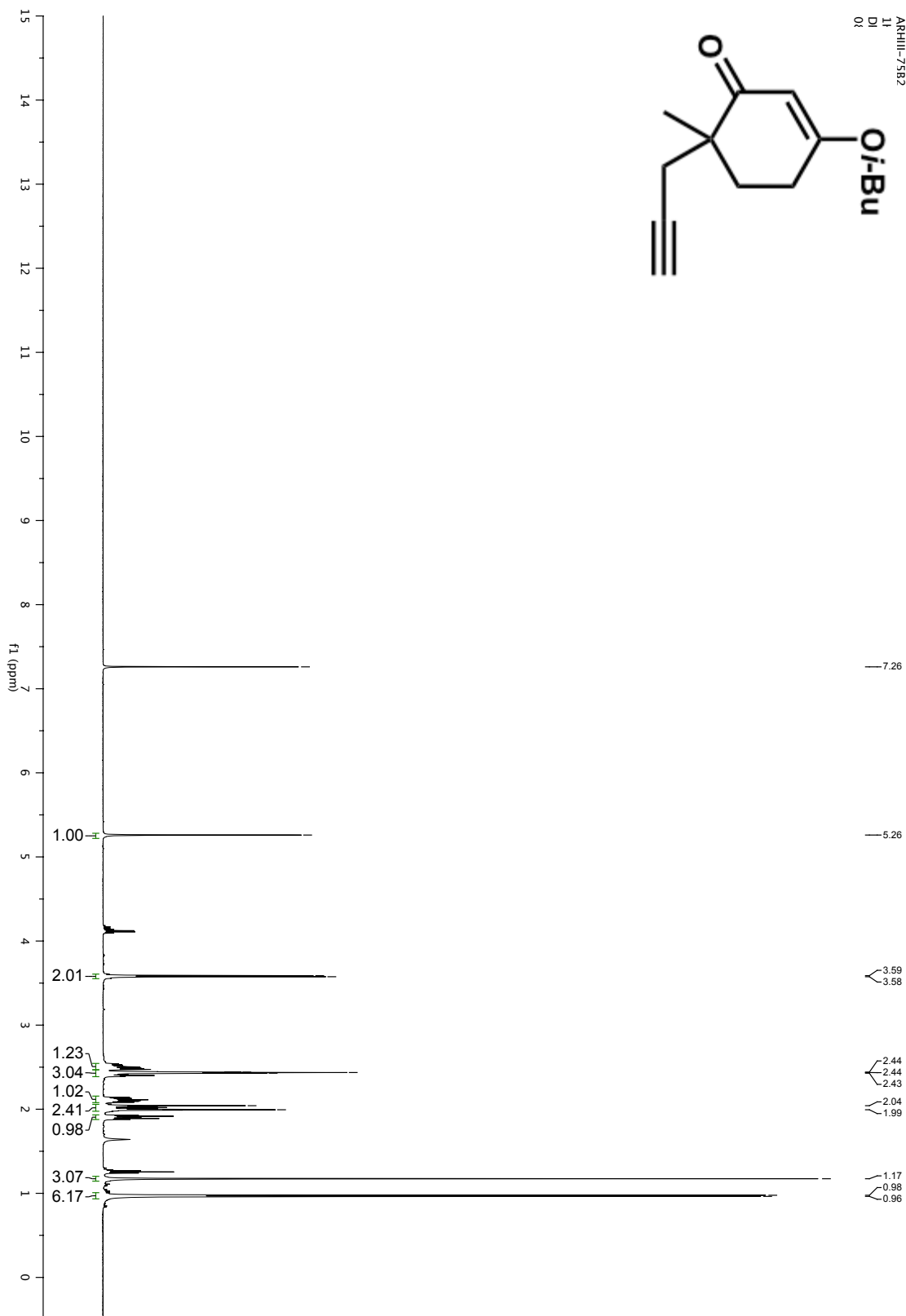
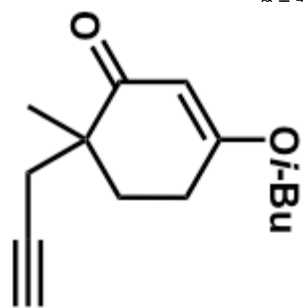


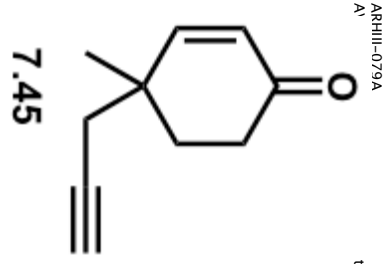
Parameters: 6/11/03 RN



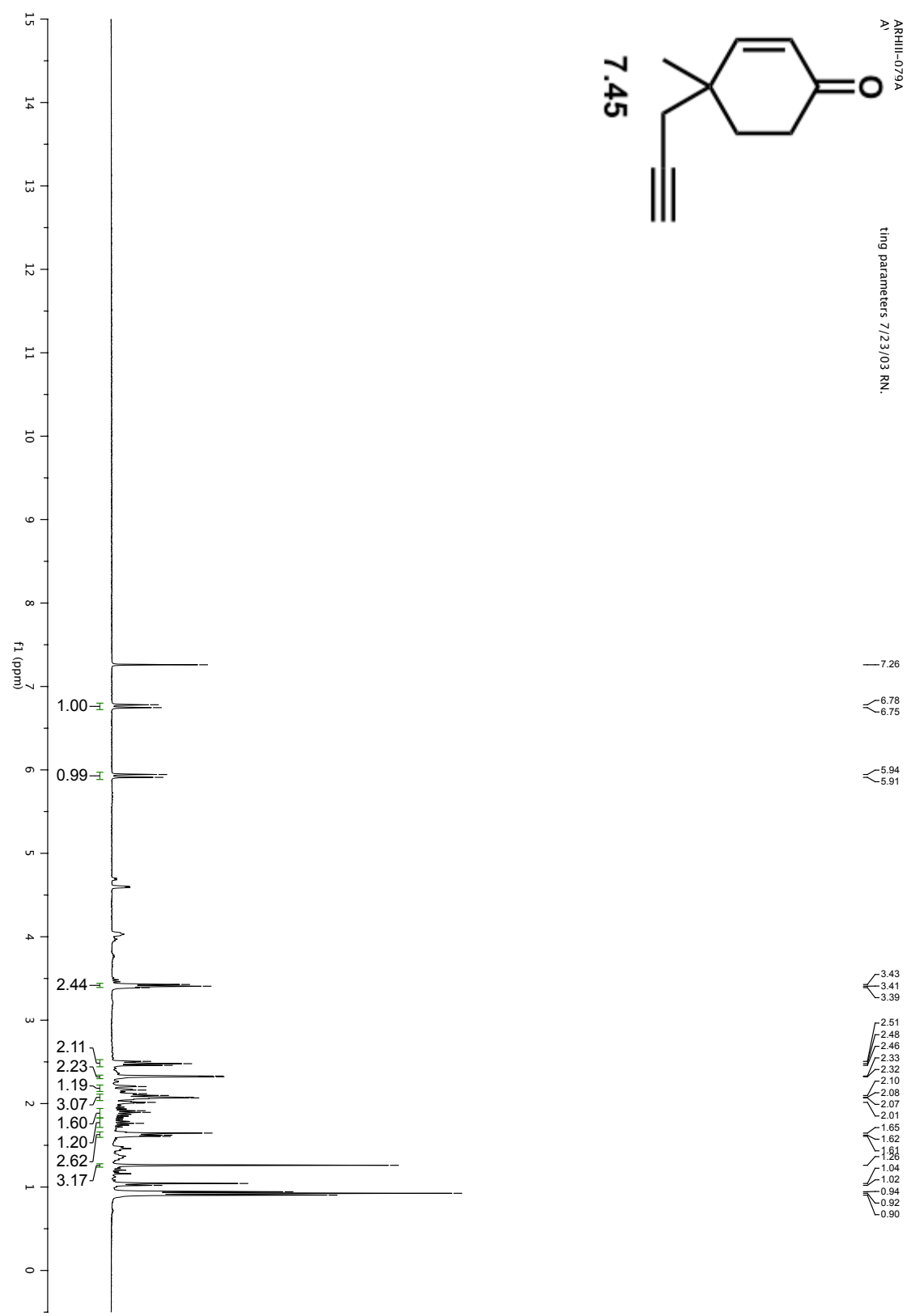


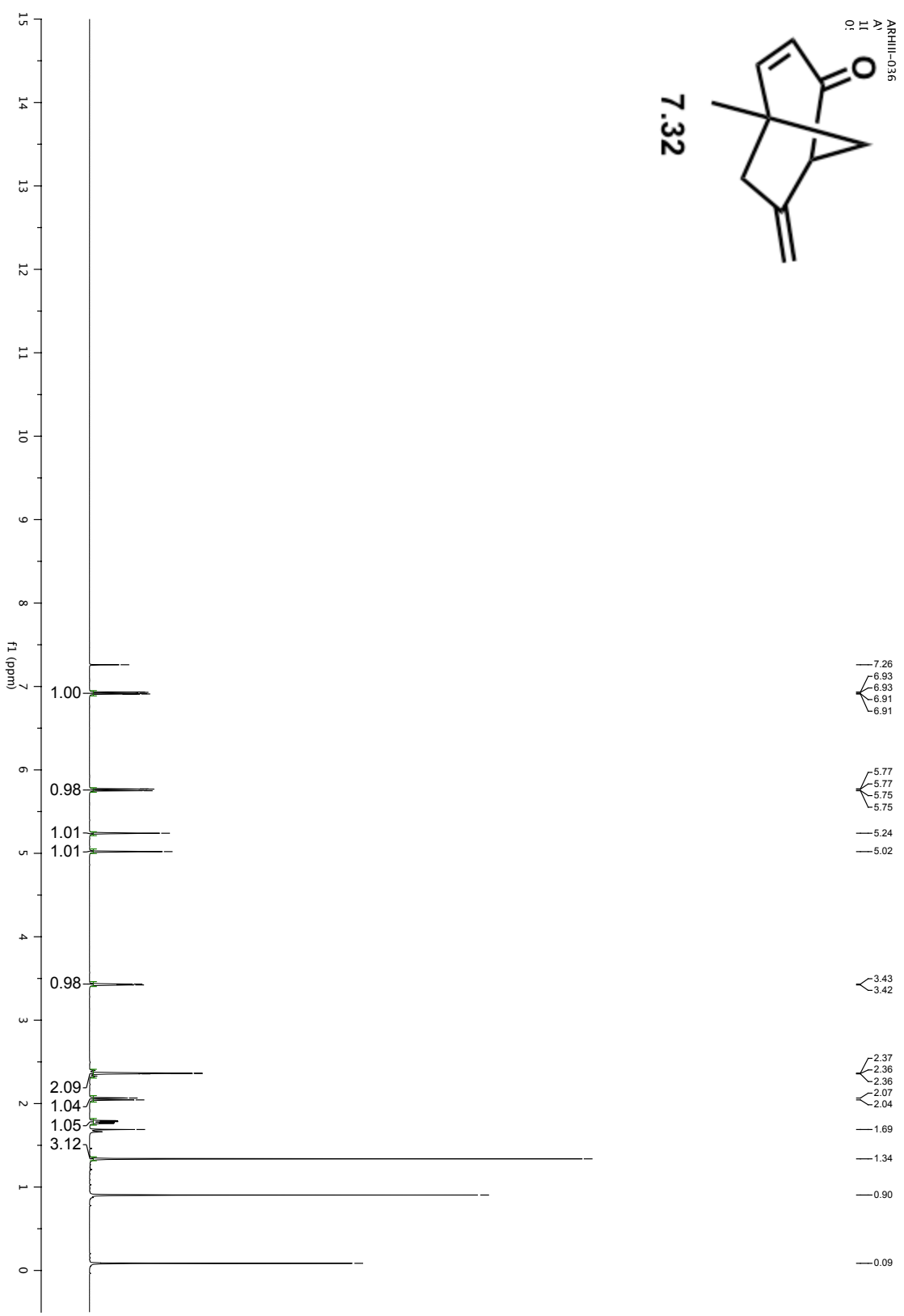
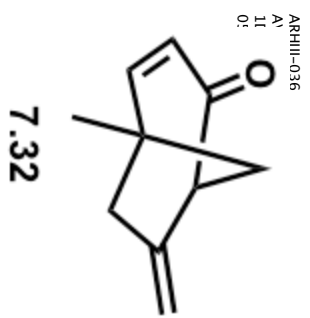
ARHHL-7582  
11  
DI  
01

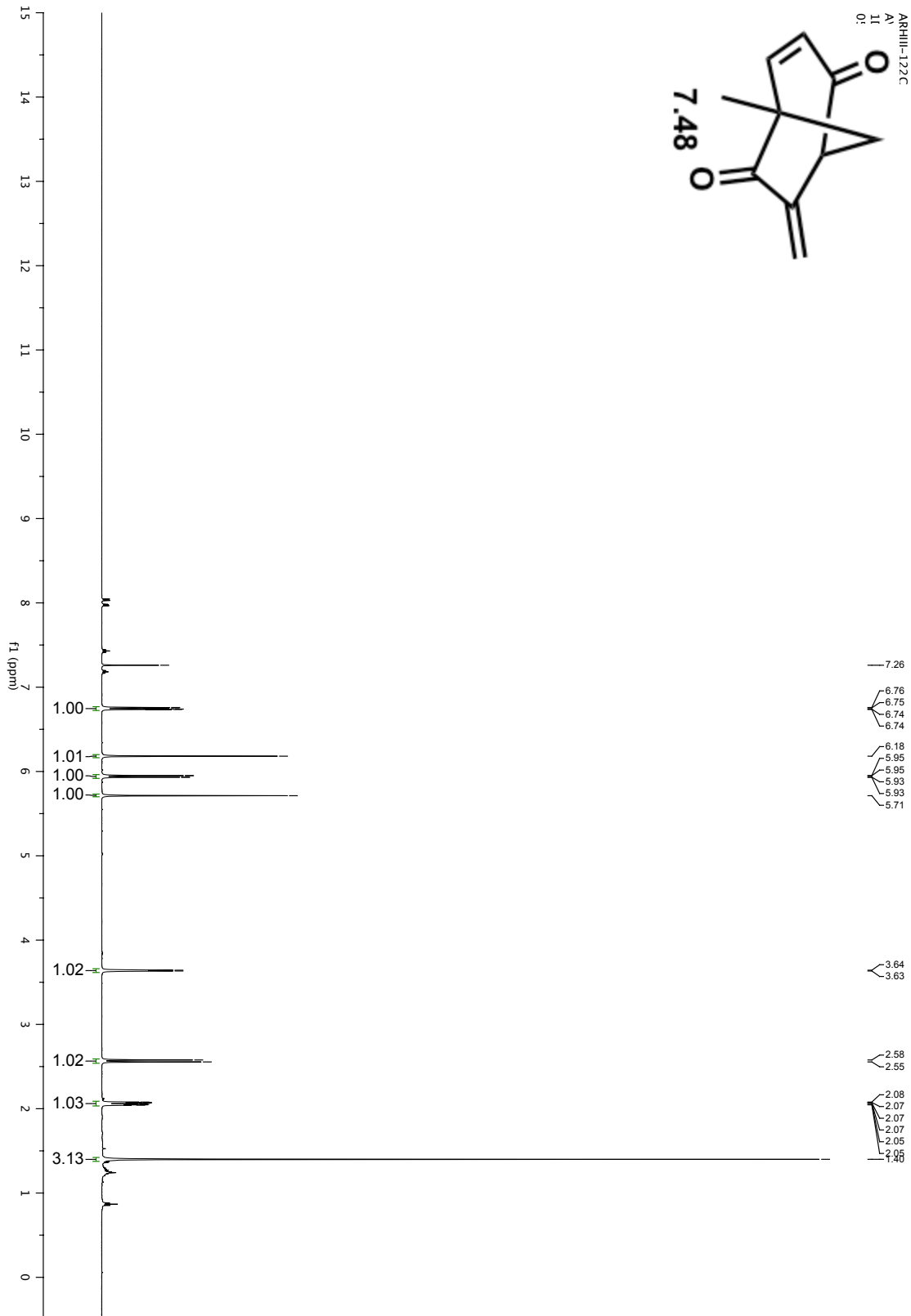
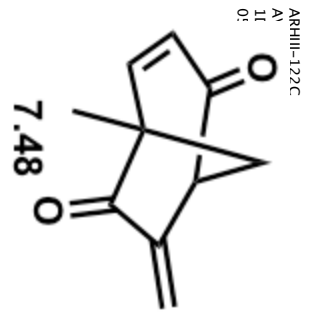




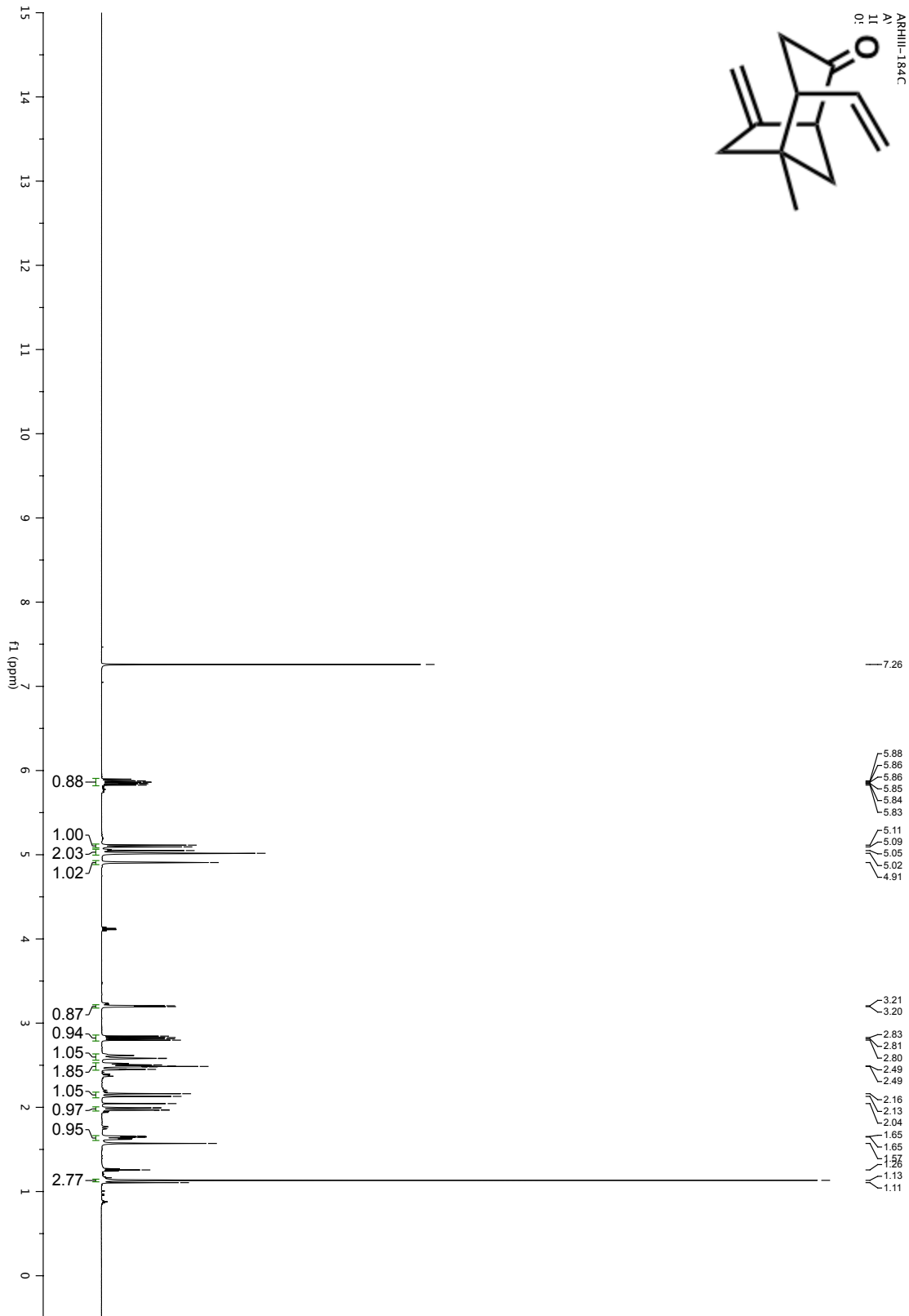
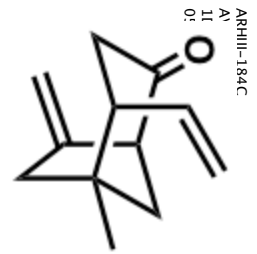
ting parameters 7/23/03 RN.

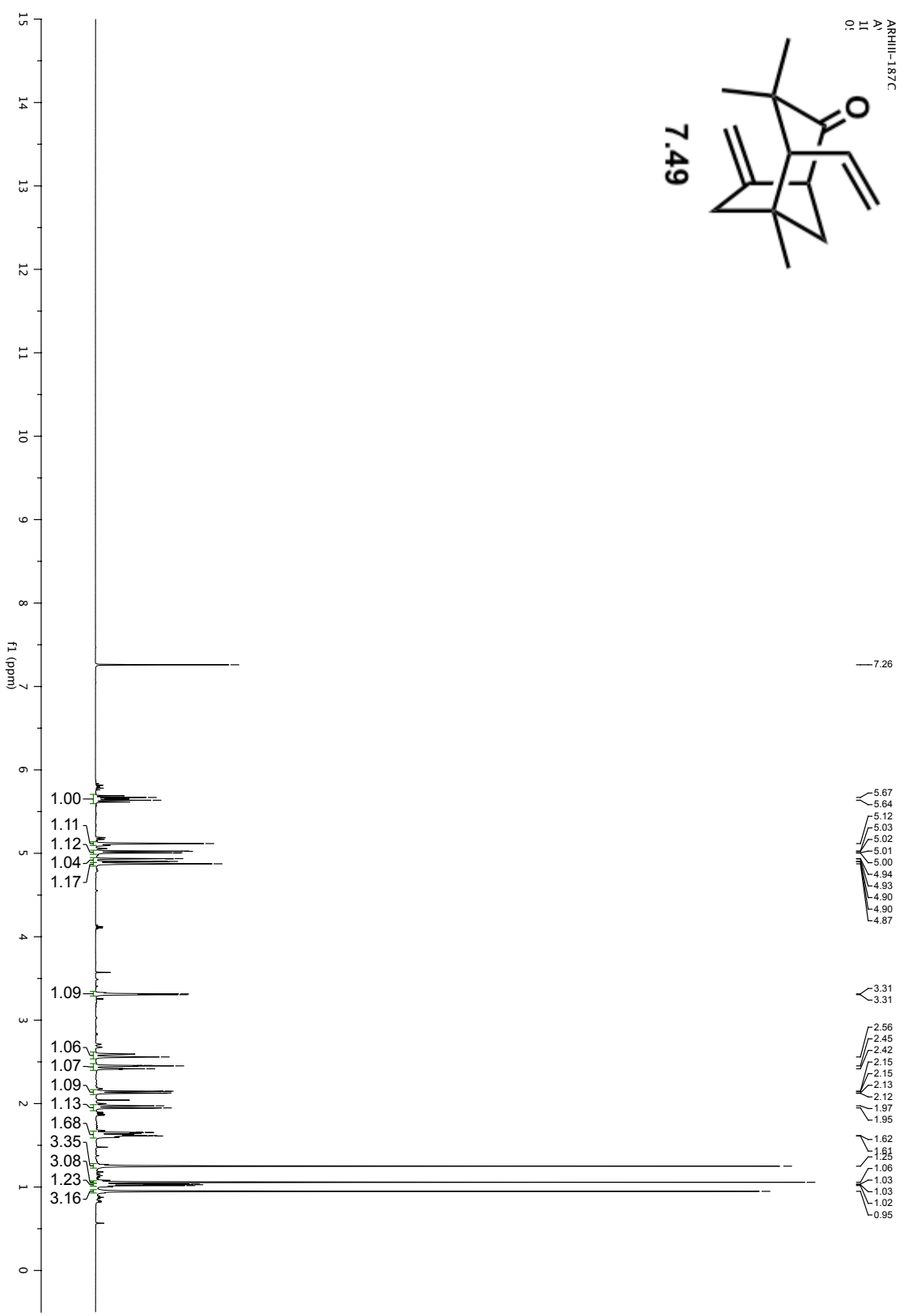
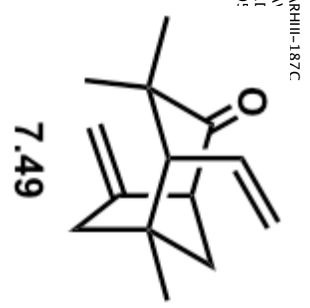


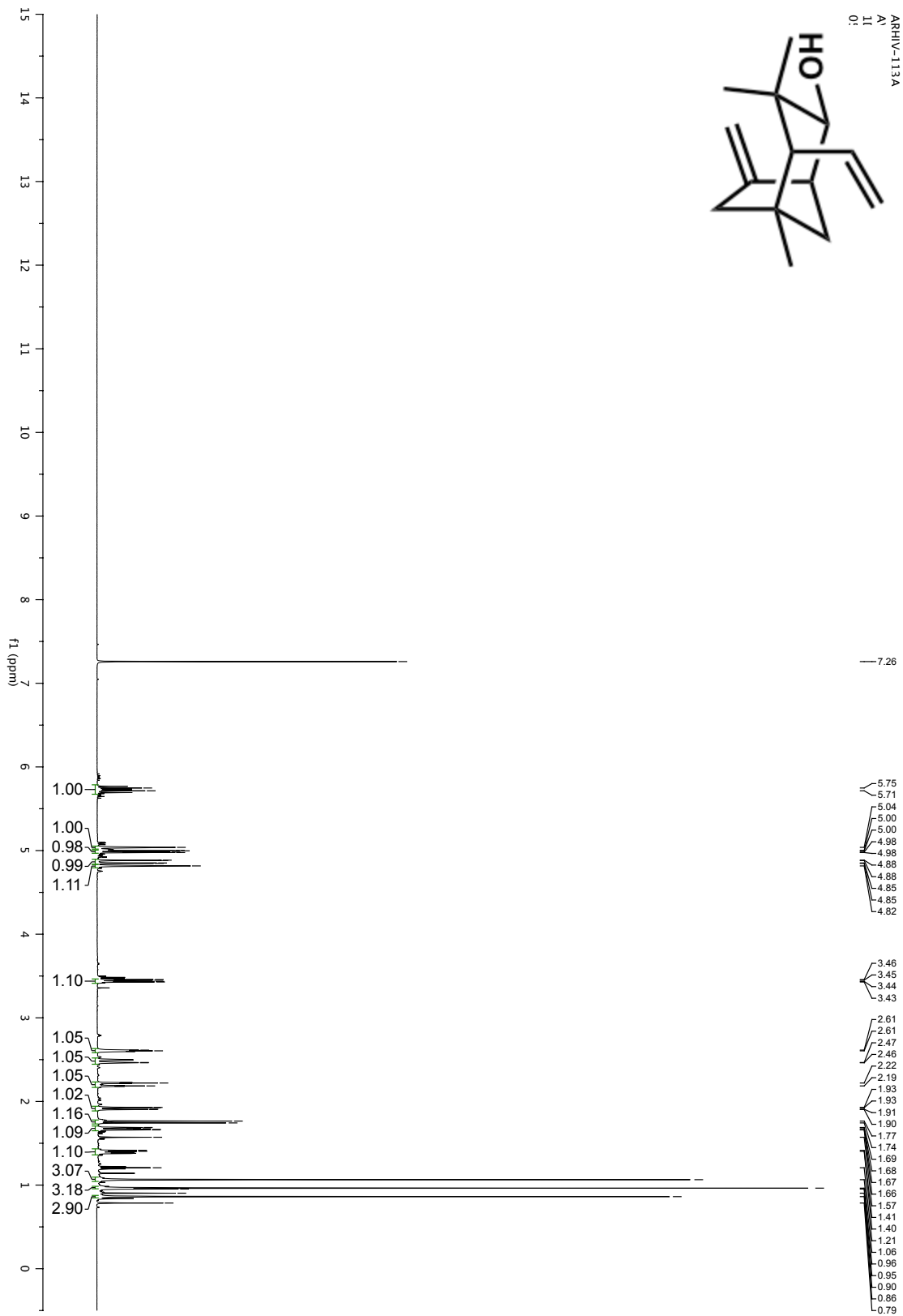




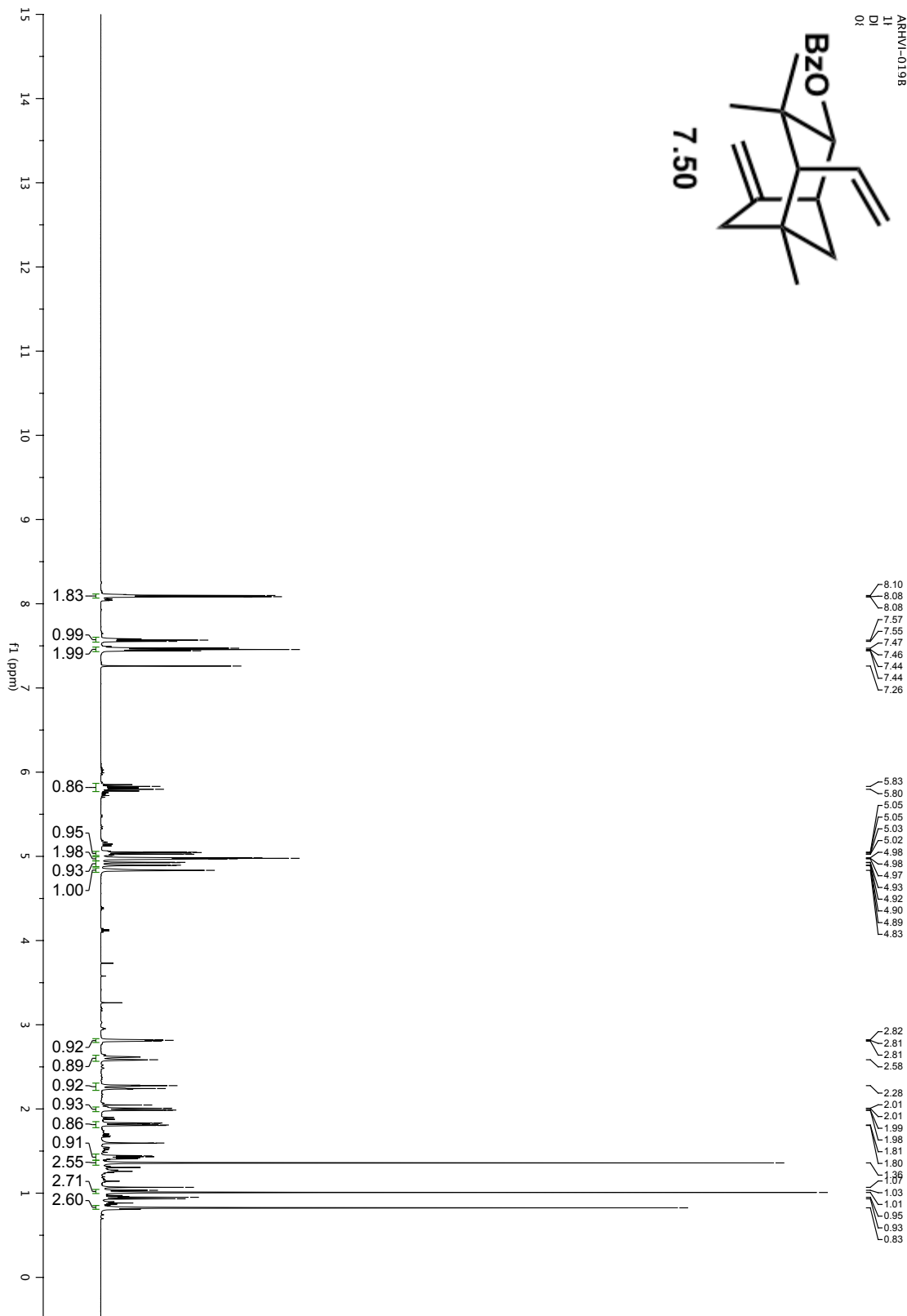
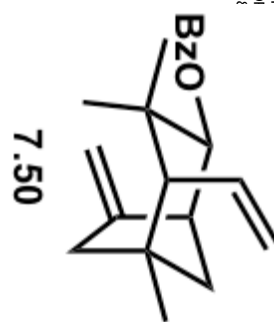


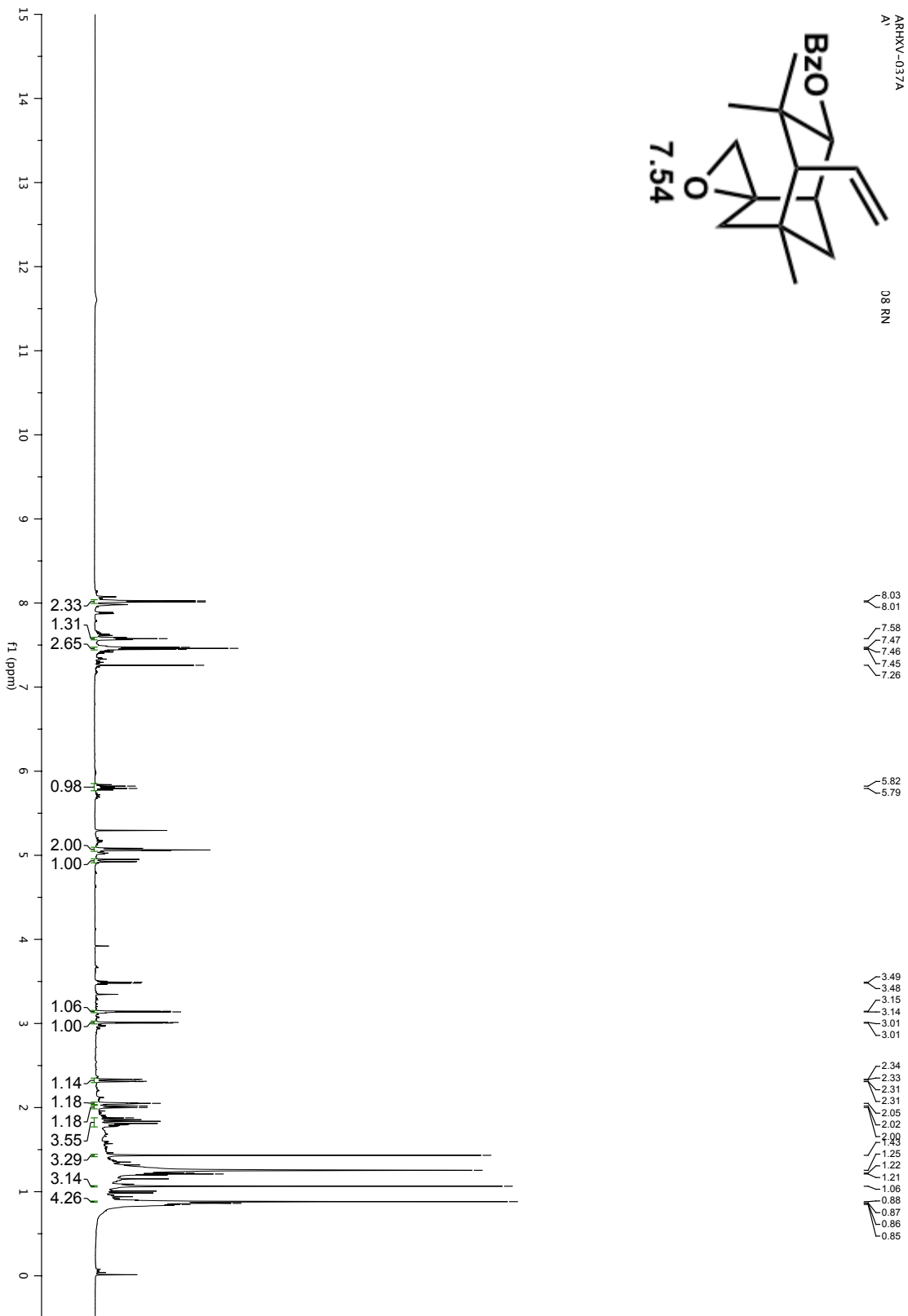


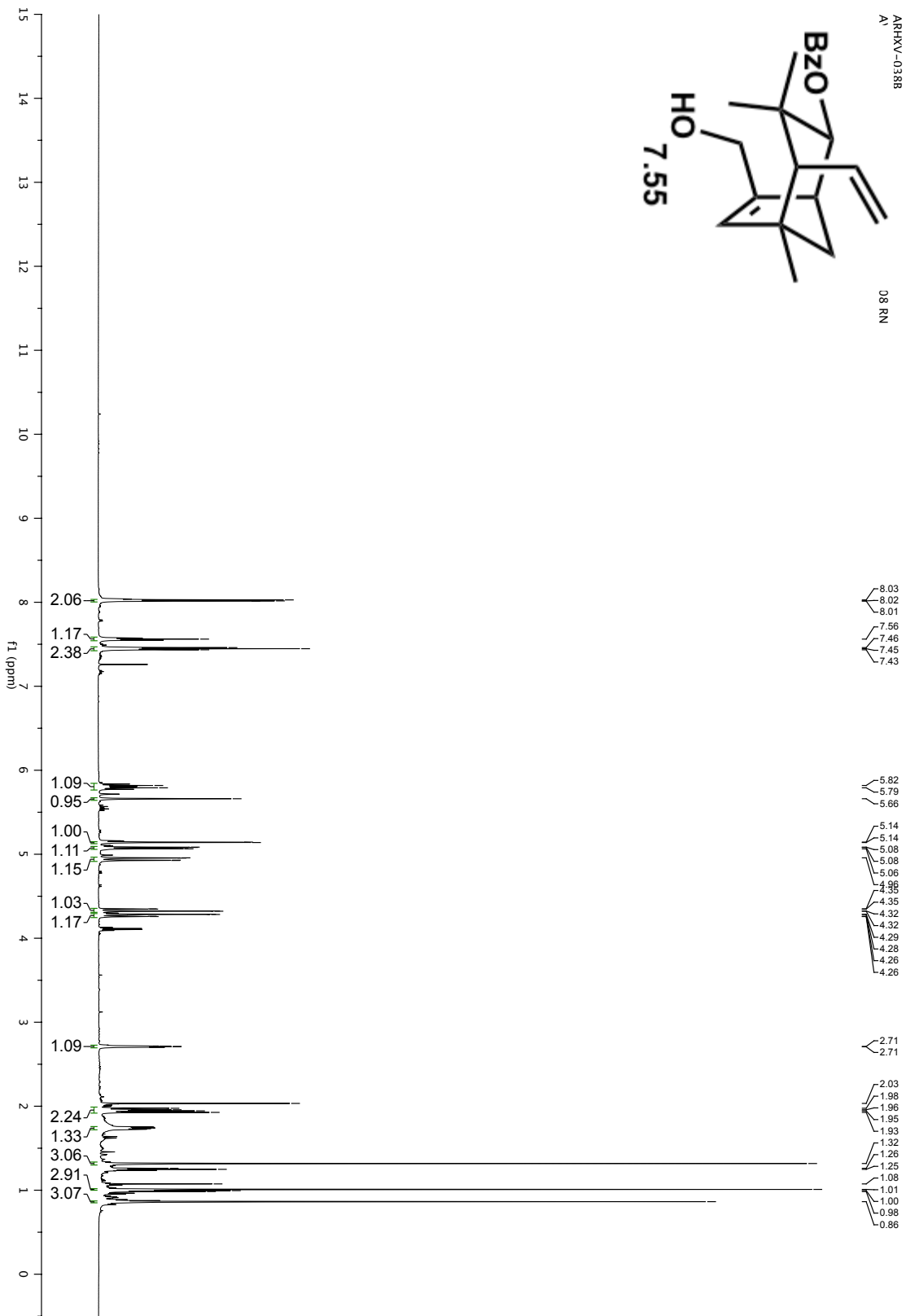


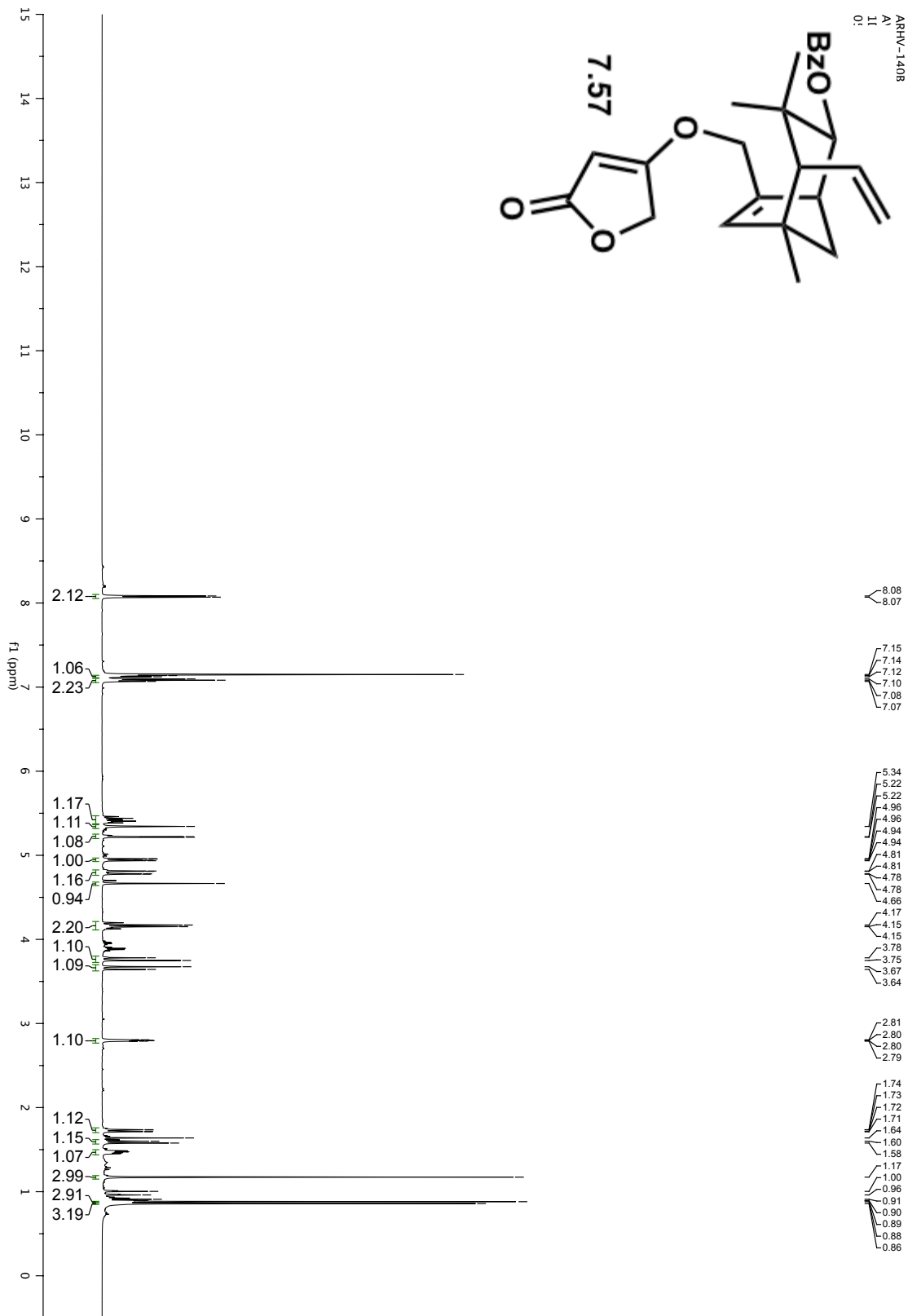


ARHVI-0198  
11  
DI  
01

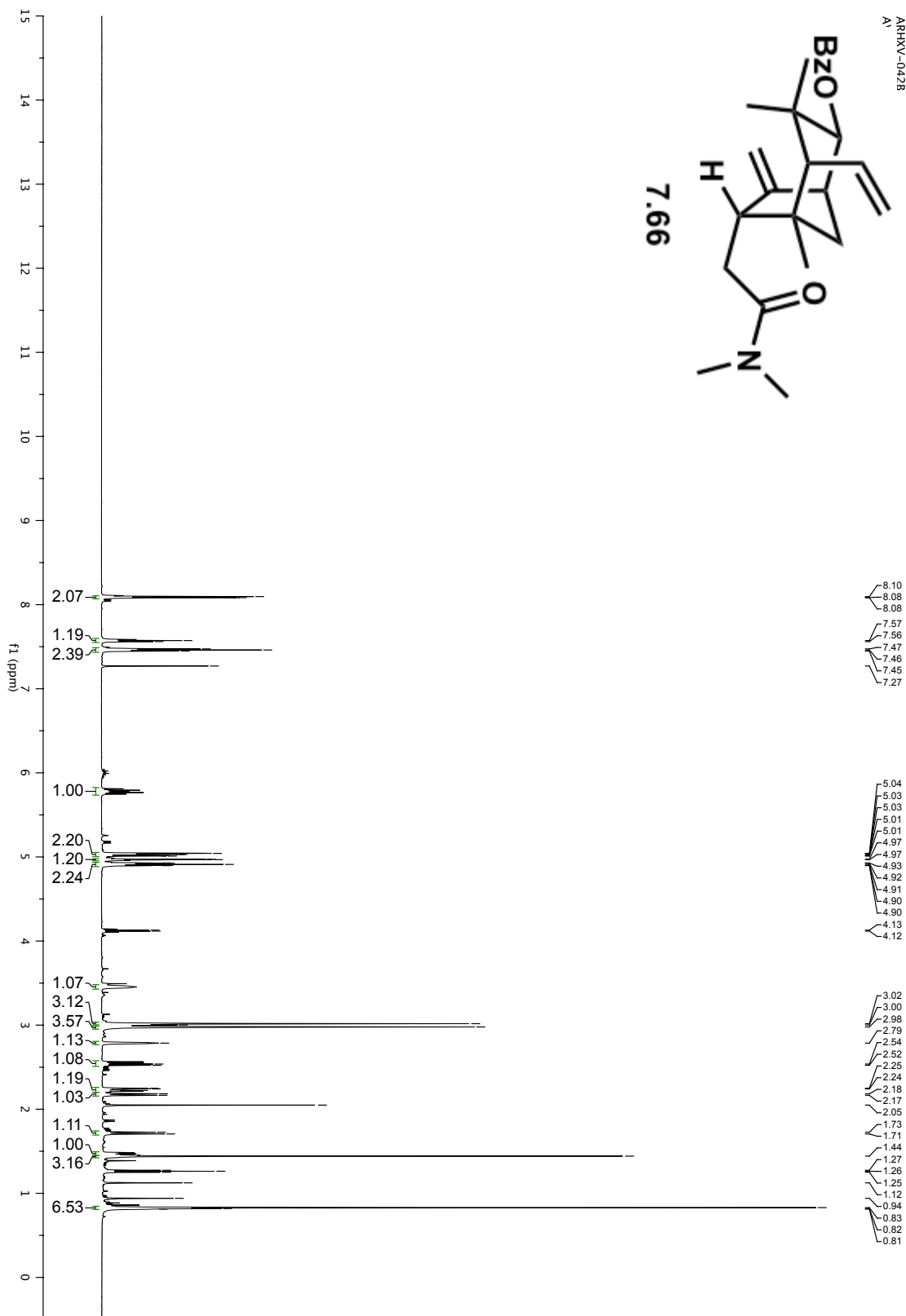
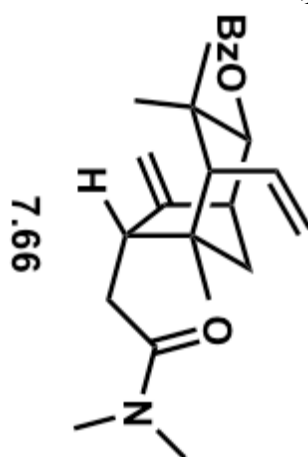






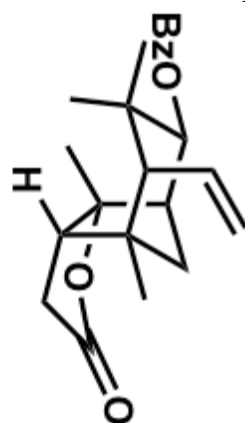


ARRXV-0428  
A'

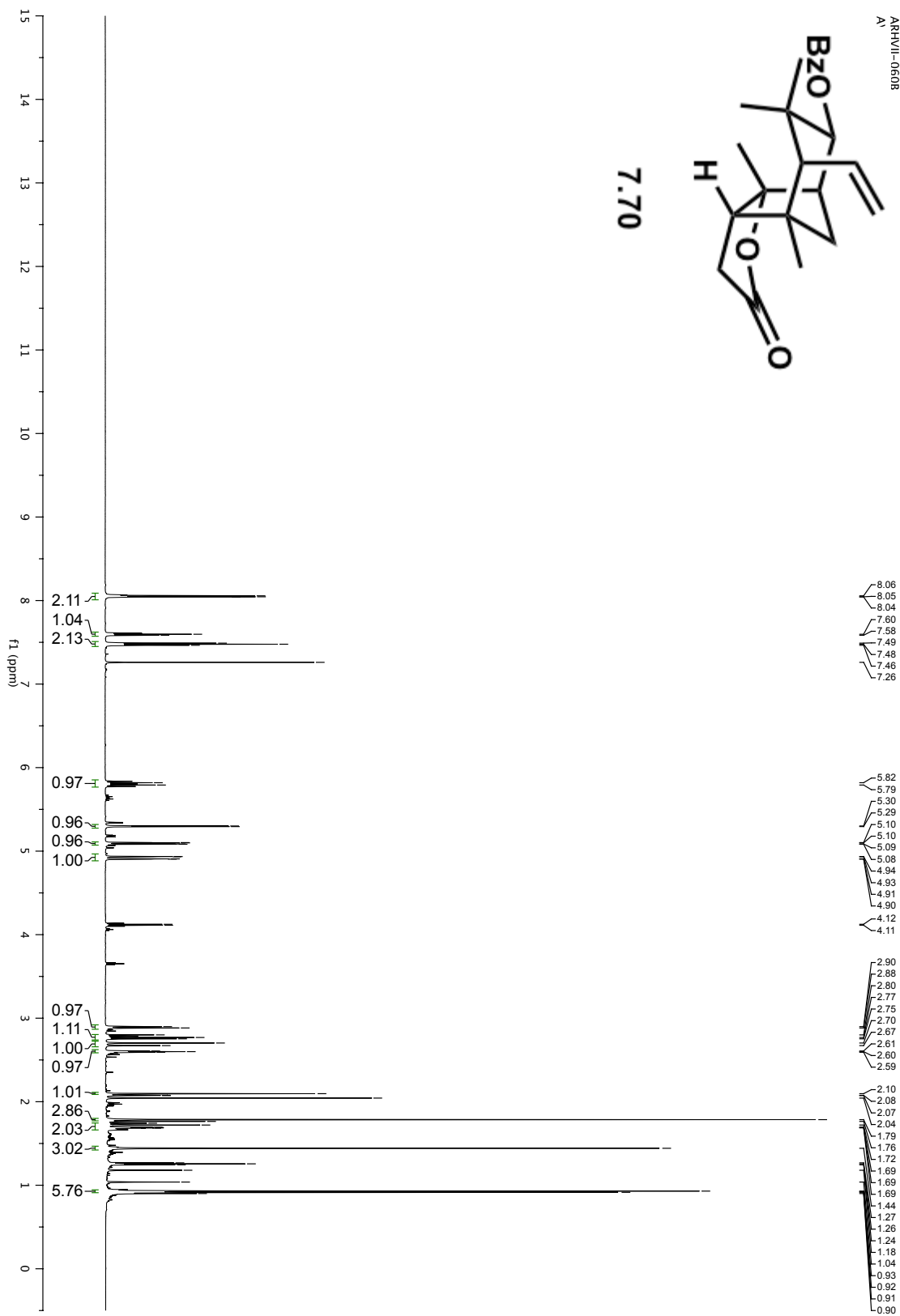




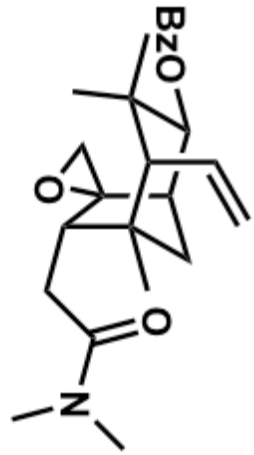
ARHVI-0608  
A'



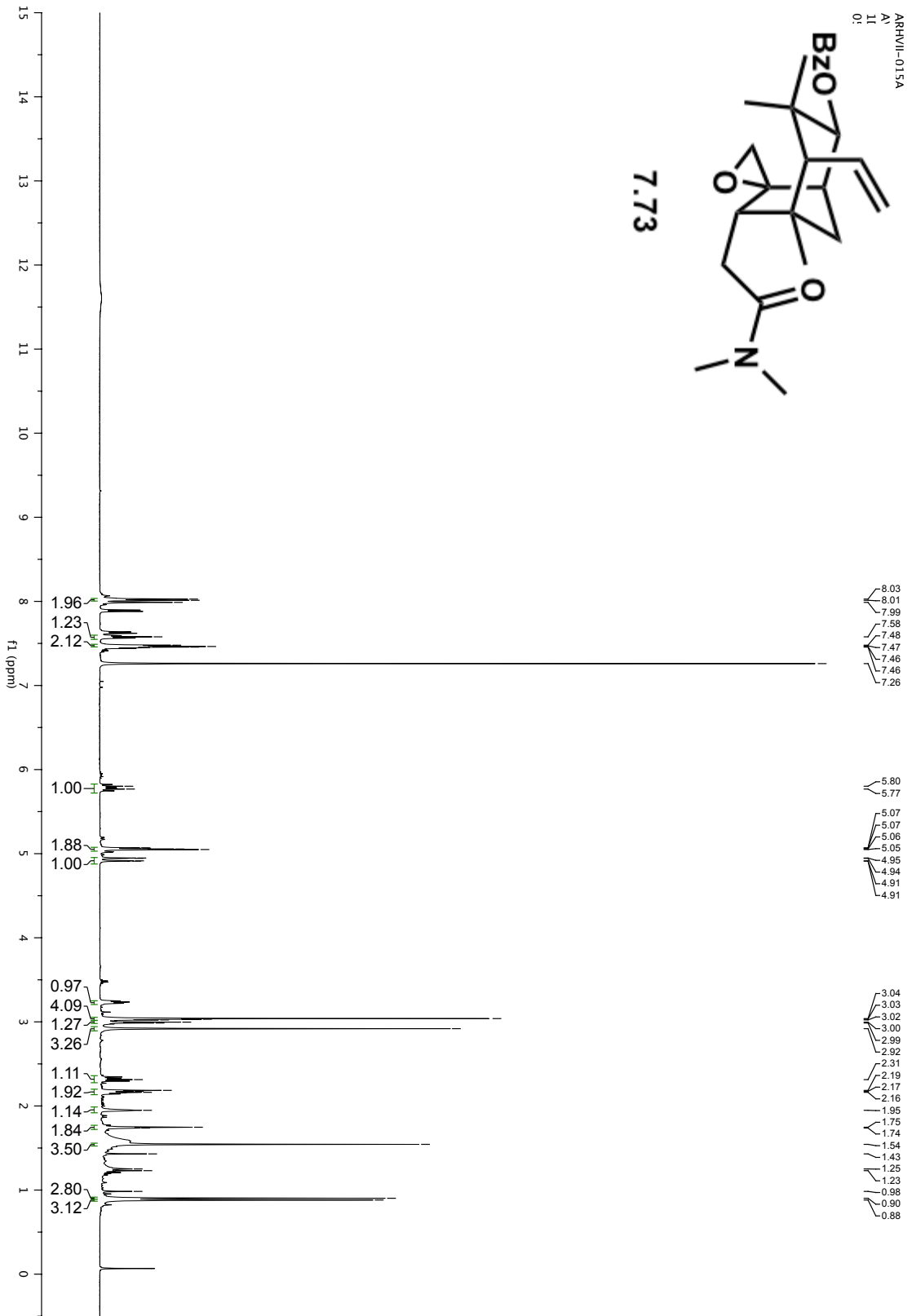
7.70

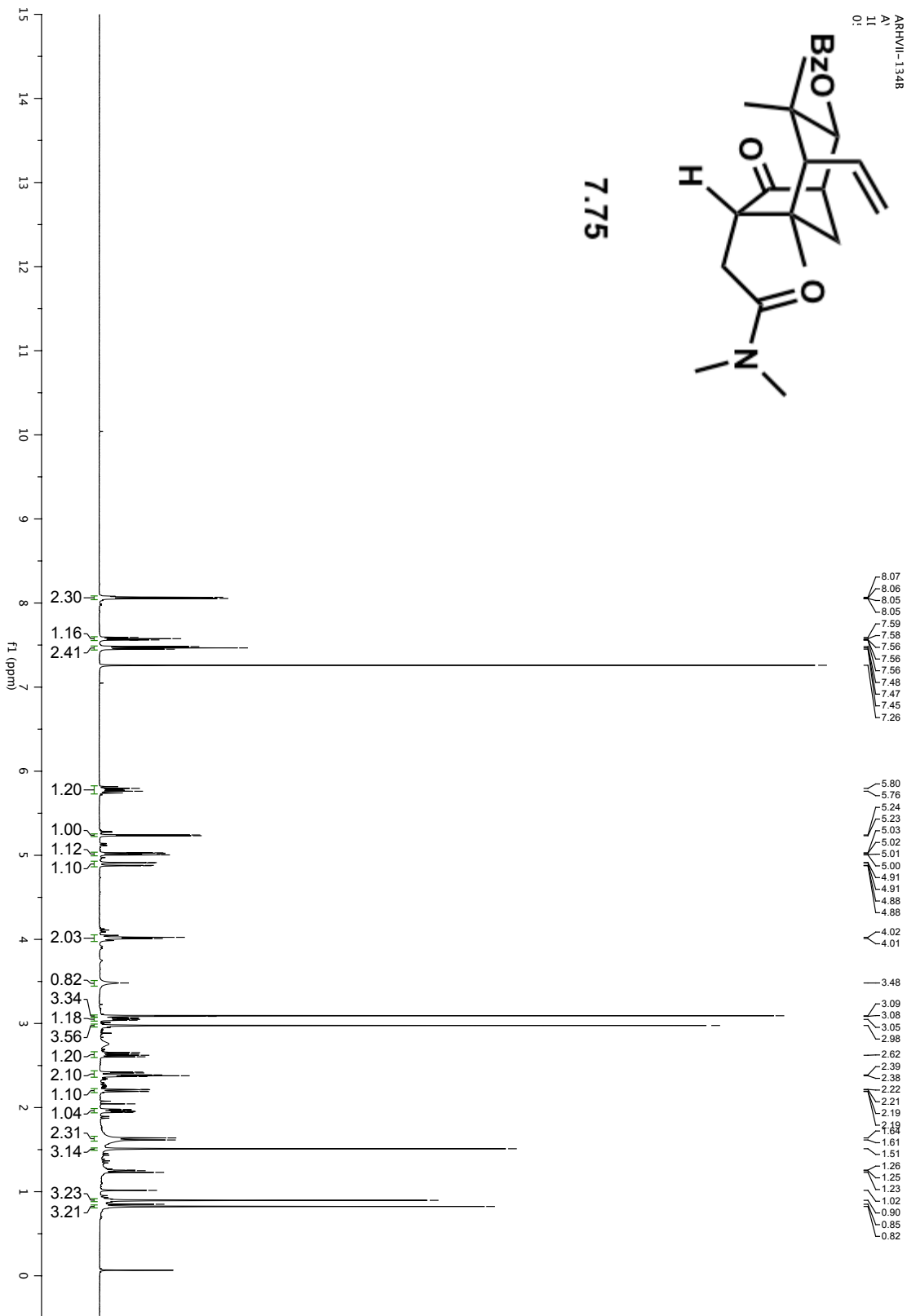


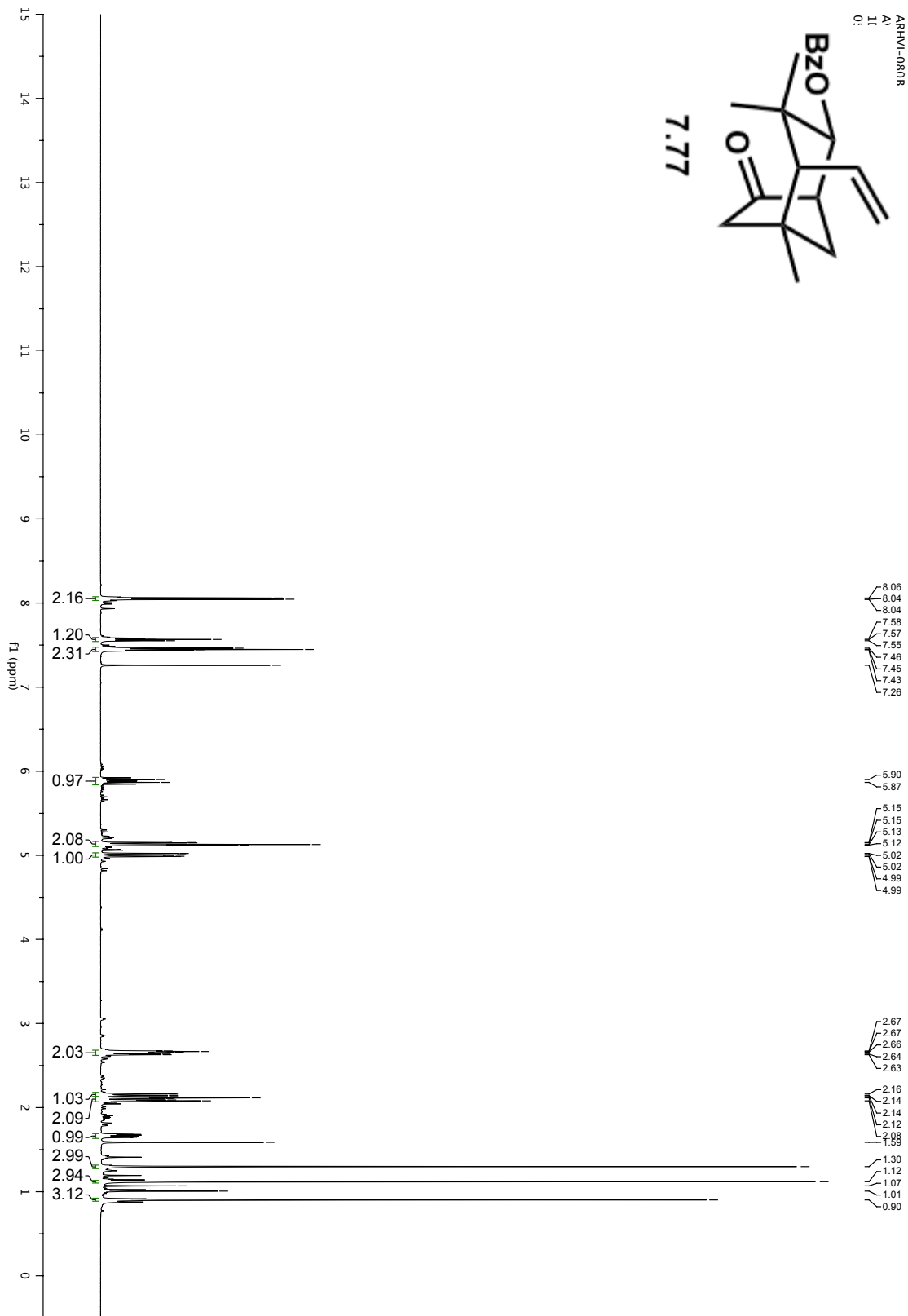
ARRVII-015A  
A:  
11  
O:



7.73





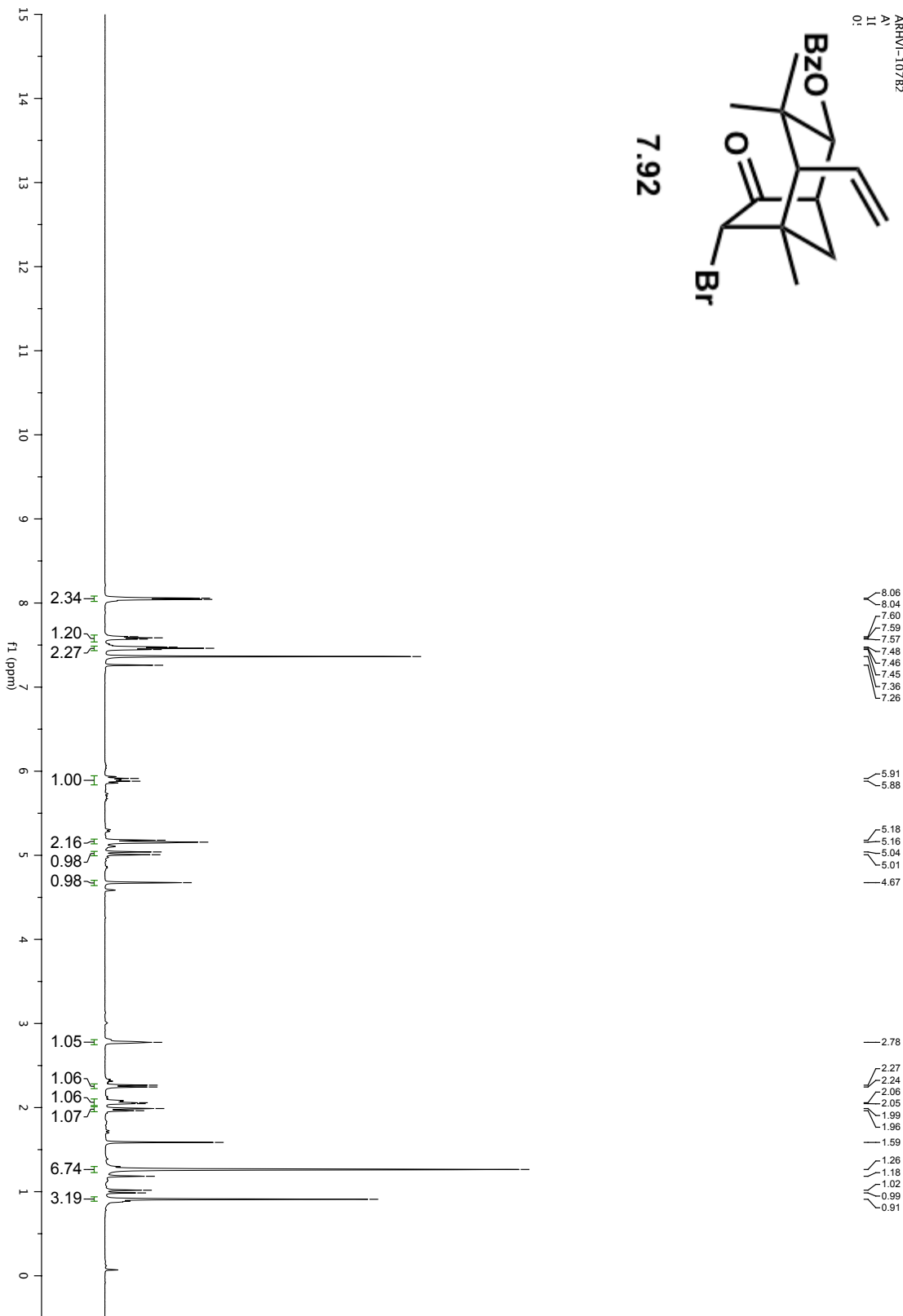


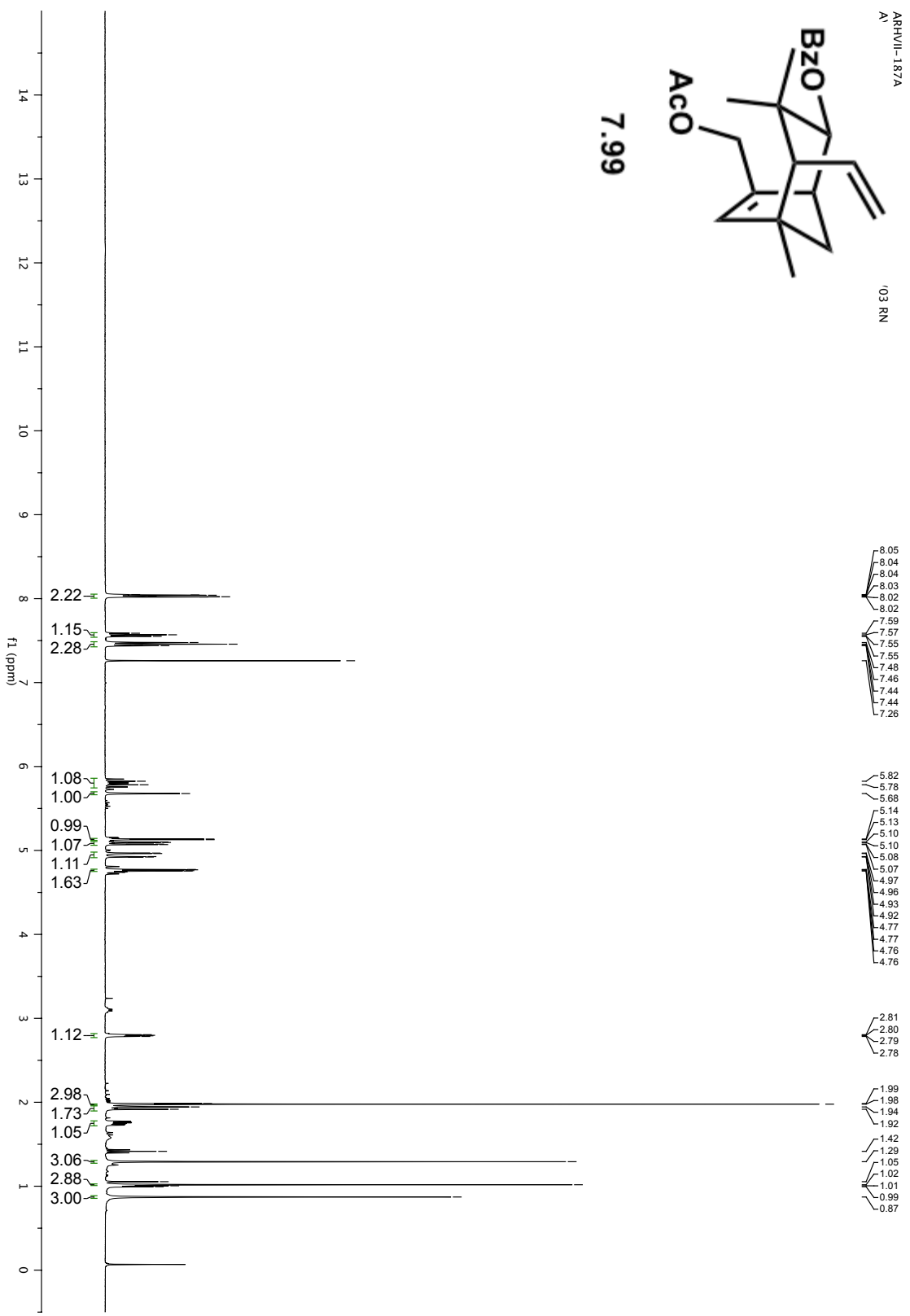
ARRHI-107B2

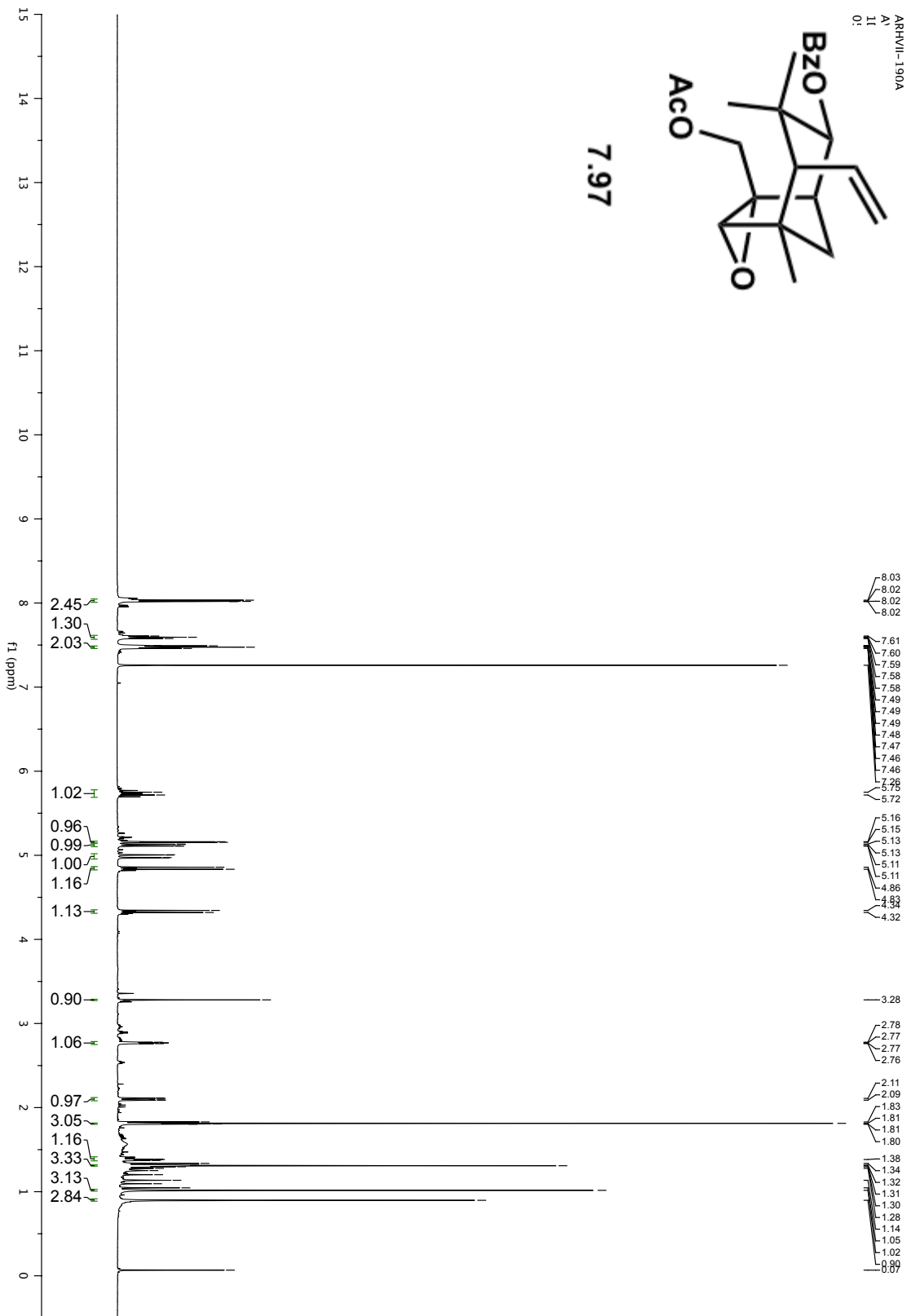
A:

11:

0:



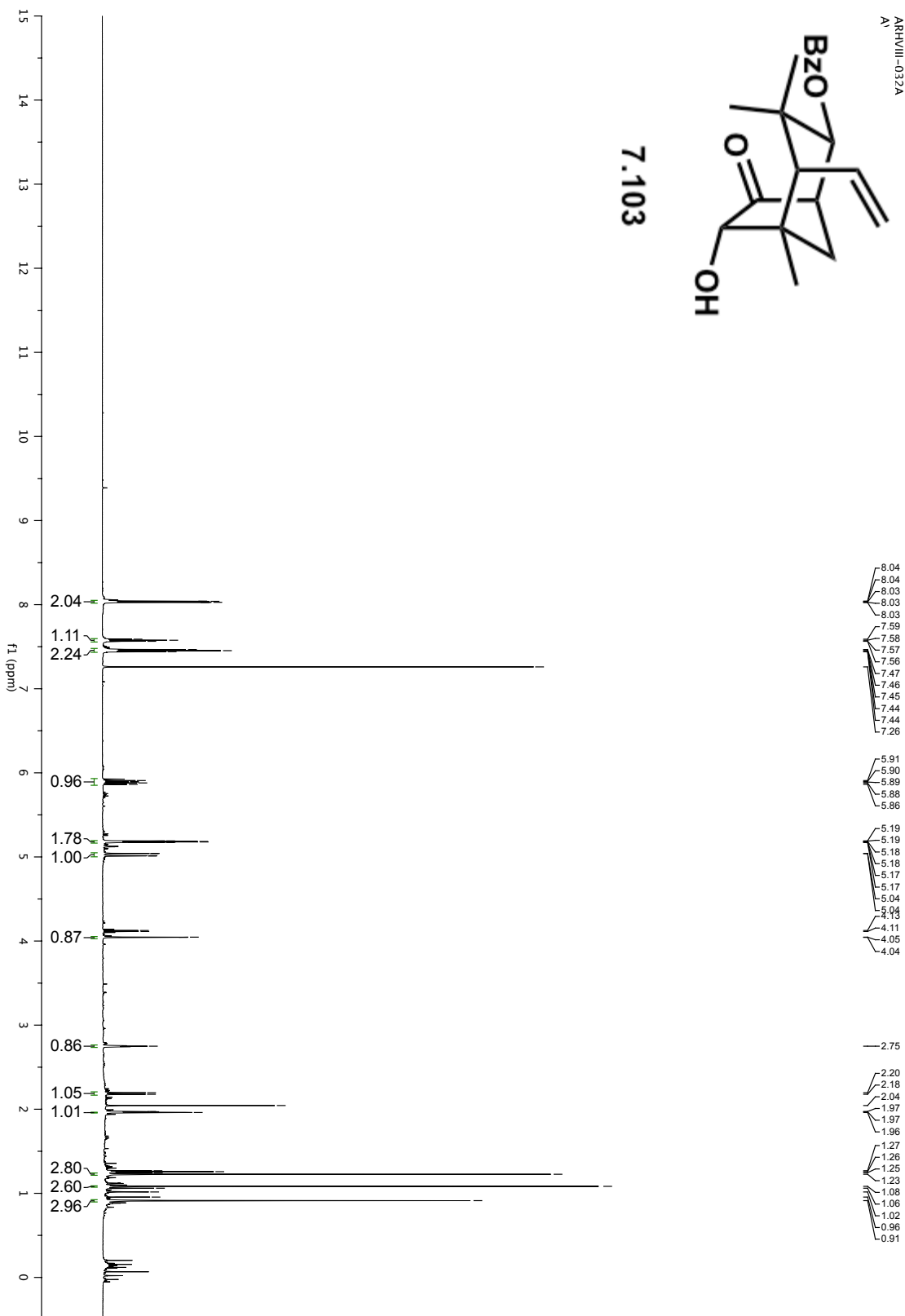




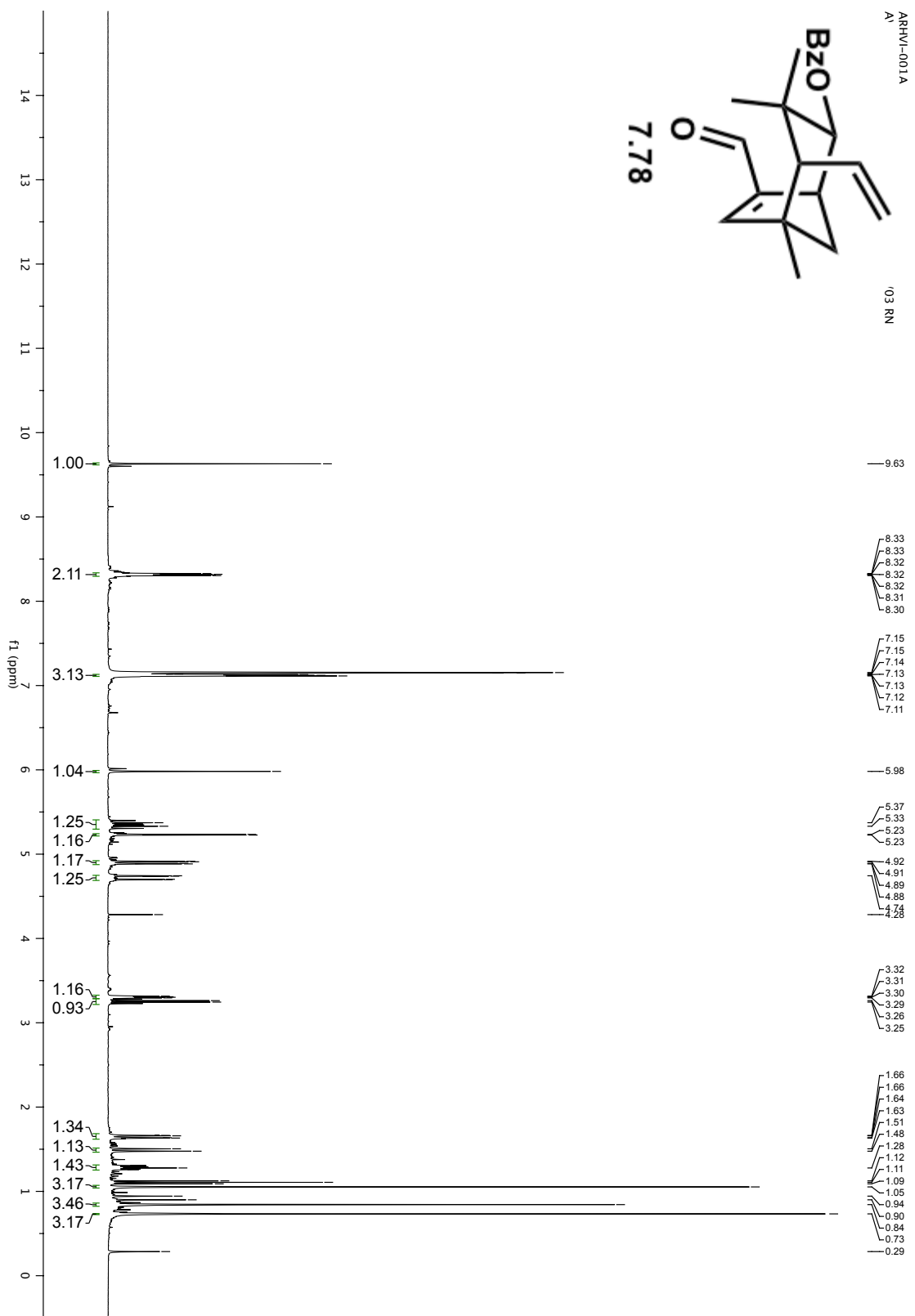
ARRVIII-032A  
A'



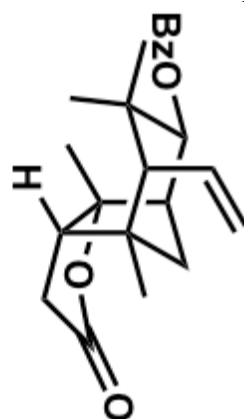
7.103







ARRXIII-0148  
A'



7.70

